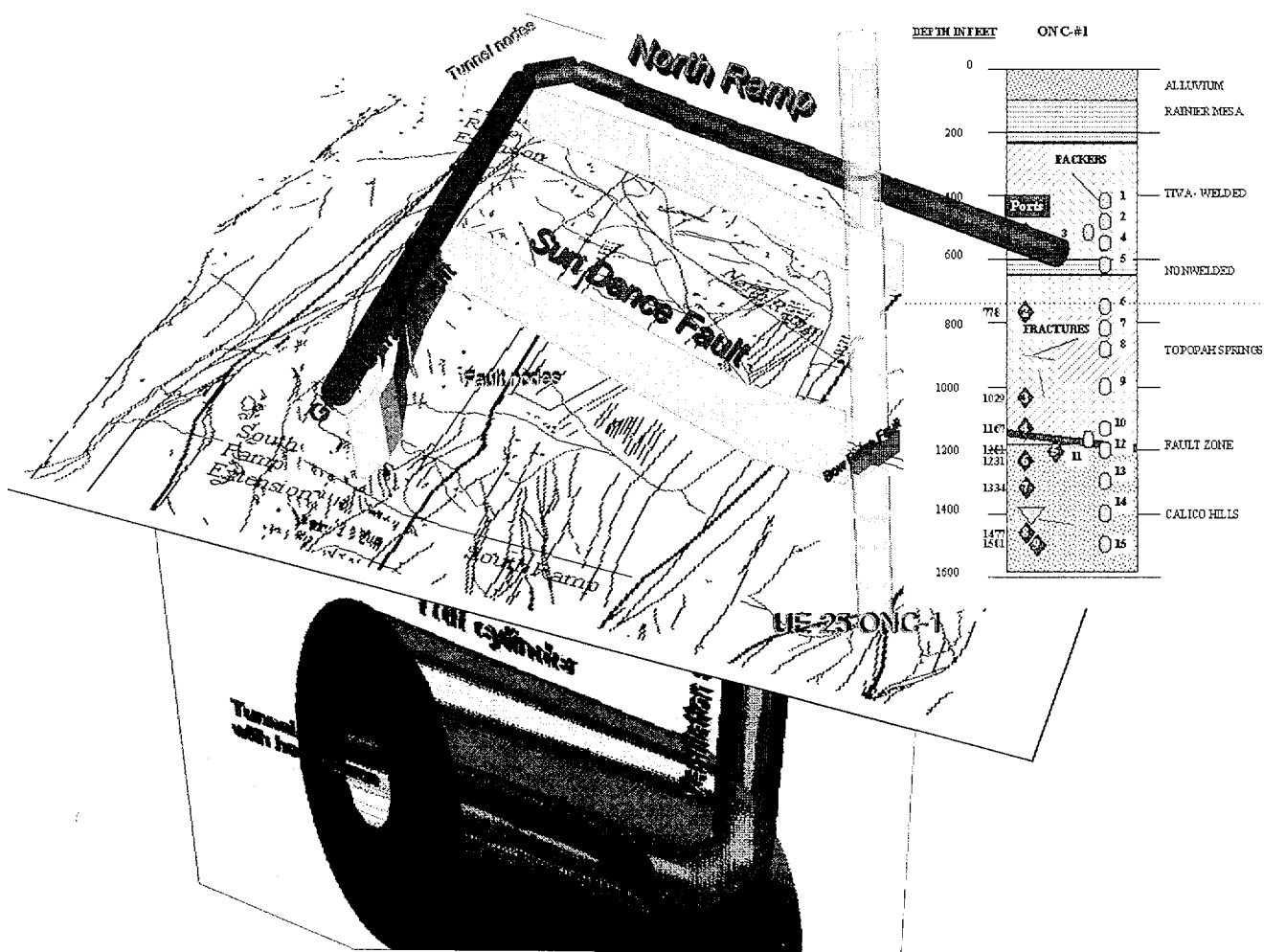


Rec'd with letter add 12/12/96

ANNUAL REPORT OF THE NYE COUNTY NUCLEAR WASTE REPOSITORY PROJECT OFFICE INDEPENDENT SCIENTIFIC INVESTIGATION PROGRAM

Prepared by:

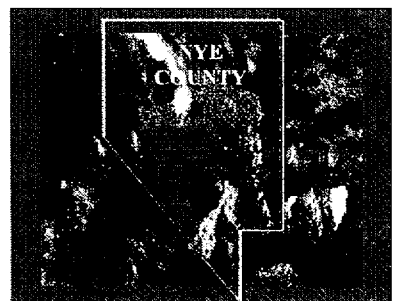
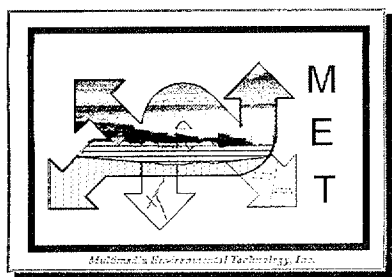
Multimedia Environmental Technology, Inc.
Newport Beach, California



9702140238 961212
PDR WASTE
WM-11

PDR

102-2
Volume I
October
1996



ANNUAL REPORT OF THE NYE COUNTY NUCLEAR WASTE REPOSITORY PROJECT OFFICE INDEPENDENT SCIENTIFIC INVESTIGATIONS PROGRAM

NYE COUNTY NUCLEAR WASTE REPOSITORY PROJECT OFFICE

Prepared By:

Multimedia Environmental Technology, Inc.

Newport Beach, California

October 1996

SIGNATURE AND DISCLAIMER PAGE

PREPARED AND REVIEWED BY:

Parviz Montazer

Teklu Hadgu

Ikram Haque

Michele Colbert

With Multimedia Environmental Technology, Newport Beach, California

REVIEWED BY:

Nick Stellavato

On-Site Geotechnical Representative, Nye County Nuclear Waste Repository Project Office, Nevada

Malachy R. Murphy

Repository Advisor, Nye County Nuclear Waste Repository Project Office, Nevada

Phil Niedzielski-Eichner

Policy and Projects Advisor, Governmental Dynamics, Inc.

DISCLAIMER

Although all data and work reported here have been performed under NWRPO QA program, this report is preliminary and has not been through MET QA Level-1 review. MET QA Level-1 report review requires verification of all numbers and figures included in a report. This exhaustive process is currently underway and any errors identified will be reported separately.

TABLE OF CONTENTS

VOLUME I

SIGNATURE AND DISCLAIMER PAGE.....	ii
PREPARED AND REVIEWED BY:.....	ii
REVIEWED BY:.....	ii
DISCLAIMER.....	ii
LIST OF FIGURES.....	v
LIST OF TABLES.....	ix
EXECUTIVE SUMMARY.....	x
1.0 INTRODUCTION	1
1.1 SCOPE AND ORGANIZATION OF REPORT	2
1.2 NYE COUNTY'S BOREHOLE AND TUNNEL MONITORING STUDIES	3
1.3 OTHER ACTIVITIES.....	4
1.4 PROPOSED FUTURE INVESTIGATIONS.....	5
2.0 INSTRUMENTATION AND MONITORING APPROACH.....	6
2.1 BOREHOLE DESCRIPTION.....	7
2.2 BOREHOLE INSTRUMENTATION	7
2.3 TUNNEL INSTRUMENTATION	8
2.4 CALIBRATION, DATA COLLECTION AND PROCESSING	9
3.0 SUMMARY OF PREVIOUS WORK	10
4.0 SUMMARY OF FIRST YEAR'S MONITORING RESULTS	13
4.1 BOREHOLE TEMPERATURE AND PRESSURE DATA	13
4.2 ESF TUNNEL TEMPERATURE, PRESSURE, AND HUMIDITY MONITORING DATA	15
5.0 CALCULATION OF AIR PERMEABILITIES FROM PRESSURE MONITORING DATA...	18
5.1 BOREHOLE PERMEABILITY CALCULATIONS.....	18
5.2 LARGE-SCALE PERMEABILITIES.....	22
6.0 MODELING VENTILATION EFFECTS ON MOISTURE IN REPOSITORY HOST ROCK	24

6.1 WASTE PACKAGE ISSUES.....	24
6.2 SHORT TERM SIMULATIONS OF EXISTING TUNNEL DATA.....	26
6.2.1 <i>SIMULATION SETUP</i>	27
6.3 LONG-TERM VENTILATION SIMULATIONS.....	31
6.3.1 <i>SIMULATION SETUP</i>	31
6.3.2 <i>RESULTS OF SIMULATIONS WITH FORCED VENTILATION (CASES 1 TO 6)</i>	33
6.3.3 <i>RESULTS OF SIMULATIONS WITH NATURAL VENTILATION (CASES 7, 8, 10,11)</i>	35
7.0 EVALUATION OF THE USE OF WATER IN THE TUNNEL.....	41
8.0 SUMMARY AND CONCLUSIONS	57
9.0 REFERENCES	60

VOLUME II

FIGURES

APPENDIX A

LIST OF FIGURES (INCLUDED IN VOLUME II)

- Figure 1-1 Location of Yucca Mountain Site in Nye County, Nevada
- Figure 1-2 Topography, location of selected boreholes, and ESF centerline at Yucca Mountain Site
- Figure 2-1 Schematic profile of instrumentation setup in UE-25 ONC#1 and USW NRG-4
- Figure 2-2 Location of humidity and temperature probes in ESF Tunnel
- Figure 2-3 Views of the ESF Tunnel
- Figure 4-1a-q Temperature fluctuation with time in UE-25 ONC#1
- Figure 4-2a-p Temperature fluctuation with time in USW NRG-4
- Figure 4-3a-q Pressure fluctuation with time in UE-25 ONC#1
- Figure 4-4a-p Pressure fluctuation with time in USW NRG-4
- Figure 4-5a-q Piezometric fluctuation with time in Probes 8 and 9 in UE-25 ONC#1
- Figure 4-6a-c Comparison of the pressure data versus depth for various unsaturated zone boreholes
- Figure 4-7a-c Comparison of the temperature data versus depth for various unsaturated zone boreholes
- Figure 4-8a-d Average pressure distribution comparison for selected months, 3-D
- Figure 4-9a-d Minimum pressure distribution comparison for selected months, 3-D
- Figure 4-10a-d Maximum pressure distribution comparison for selected months, 3-D
- Figure 4-11a-d Average temperature distribution comparison for selected months, 3-D
- Figure 4-12a-d Minimum temperature distribution comparison for selected months, 3-D
- Figure 4-13a-d Maximum temperature distribution comparison for selected months, 3-D
- Figure 4-14a-m Temperature fluctuation with time in ESF Tunnel
- Figure 4-15a-m Relative Humidity fluctuation with time in ESF Tunnel
- Figure 4-16a-m Pressure fluctuation with time in ESF Tunnel
- Figure 4-17 Temperature and humidity variation at Severe Wash meteorological station
- Figure 4-18 Pressure variation at Severe Wash meteorological station
- Figure 4-19 Temperature and humidity variation at NTS-60 meteorological station
- Figure 4-20 Pressure variation at NTS-60 meteorological station
- Figure 4-21 Wind speed variation at NTS-60 meteorological station
- Figure 5-1 Pressure fluctuation with time in NRG-4 during May 1995
- Figure 5-2 Pressure fluctuation with time in NRG-4 during June 1995
- Figure 5-3 One-dimensional grid and the results of permeability calculations for USW NRG-4
- Figure 5-4 Pressure fluctuation with time in ONC#1 during November 1995
- Figure 5-5 Pressure fluctuation with time in ONC#1 during January 1996

- Figure 5-6 Pressure fluctuation with time in ONC#1 during March 1996
- Figure 5-7 One-dimensional grid and the results of permeability calculations for UE-25 ONC#1
- Figure 5-8 Comparison of the simulated and observed barometric pressure responses in ONC#1 using 1-D vertical column of nodes in April 1996
- Figure 5-9 Detail map of UE-25 ONC#1
- Figure 5-10 Comparison of the simulated and observed barometric pressure responses in ONC#1 using tunnel and a 1-D mesh for April 1996
- Figure 6-1 Plan view of the axi-symmetric mesh used for simulations of tunnel ventilation
- Figure 6-2 Simulated humidity for one week of ventilation with measured humidity inset
- Figure 6-3 Simulated temperature for one week of ventilation with measured temperature inset
- Figure 6-4 Simulated distribution of capillary pressure around the tunnel at 11.4 days after start of ventilation
- Figure 6-4a Schematic diagram of flow through a tunnel (eddy diffusivity concept)
- Figure 6-5 Simulated pressures around the tunnel for various times, Case 1
- Figure 6-5a Pressure versus time plot for Case 1
- Figure 6-6 Simulated temperature around the tunnel for various times, Case 1
- Figure 6-6a Temperature versus time plot for Case 1
- Figure 6-7 Simulated capillary pressure around the tunnel for various times, Case 1
- Figure 6-7a Capillary pressure versus time plot for Case 1
- Figure 6-8 Simulated saturation around the tunnel for various times, Case 1
- Figure 6-8a Water saturation versus time plot for Case 1
- Figure 6-9 Simulated temperature around the tunnel for various times, Case 2
- Figure 6-9a Pressure versus time plot for Case 2
- Figure 6-9b Temperature versus time plot for Case 2
- Figure 6-10 Simulated capillary pressure around the tunnel for various times, Case 2
- Figure 6-10a Capillary pressure versus time plot for Case 2
- Figure 6-10b Water saturation versus time plot for Case 2
- Figure 6-11 Simulated temperature around the tunnel for various times, Case 3
- Figure 6-11a Temperature versus time plot for Case 3
- Figure 6-11b Pressure versus time plot for Case 3
- Figure 6-12 Simulated capillary pressure around the tunnel for various times, Case 3
- Figure 6-12a Capillary pressure versus time plot for Case 3
- Figure 6-12b Water saturation versus time plot for Case 3
- Figure 6-13 Simulated temperature around the tunnel for various times, Case 4
- Figure 6-13a Temperature versus time plot for Case 4

- Figure 6-13b Pressure versus time plot for Case 4
Figure 6-14 Simulated capillary pressure around the tunnel for various times, Case 4
Figure 6-14a Capillary pressure versus time plot for Case 4
Figure 6-14b Water saturation versus time plot for Case 4
Figure 6-15 Simulated temperature around the tunnel for various times, Case 5
Figure 6-15a Temperature versus time plot for Case 5
Figure 6-15b Pressure versus time plot for Case 5
Figure 6-16 Simulated capillary pressure around the tunnel for various times, Case 5
Figure 6-16a Capillary pressure versus time for Case 5
Figure 6-16b Water saturation versus time plot for Case 5
Figure 6-17 Simulated temperature around the tunnel for various times, Case 6
Figure 6-17a Temperature versus time plot for Case 6
Figure 6-17b Pressure versus time plot for Case 6
Figure 6-18 Simulated capillary pressure around the tunnel for various times, Case 6
Figure 6-18a Capillary pressure versus time plot for Case 6
Figure 6-18b Water saturation versus time plot for Case 6
Figure 6-19 Conceptual model of ventilation shafts relative to the ESF tunnel
Figure 6-19a Conceptualization of natural ventilation
Figure 6-19b Conceptualization of Tuff cylinder
Figure 6-19c Heat load per drift cylinder, Cases 7-9
Figure 6-20 Simulated pressure around the tunnel for various times, Case 7
Figure 6-20a Pressure versus time plot for Case 7
Figure 6-21 Simulated temperature around the tunnel for various times, Case 7
Figure 6-21a Temperature versus time plot for Case 7
Figure 6-22 Simulated capillary pressure around the tunnel for various times, Case 7
Figure 6-22a Capillary versus time plot for Case 7
Figure 6-23 Simulated water saturation around the tunnel for various times, Case 7
Figure 6-23a Water saturation versus time plot for Case 7
Figure 6-24 Simulated pressure around the tunnel for various times, Case 8
Figure 6-24a Pressure versus time plot for Case 8
Figure 6-25 Simulated temperature around the tunnel for various times, Case 8
Figure 6-25a Temperature versus time plot for Case 8
Figure 6-26 Simulated capillary pressure around the tunnel for various times, Case 8
Figure 6-26a Capillary pressure versus time plot for Case 8
Figure 6-27 Simulated water saturation around the tunnel for various times, Case 8
Figure 6-27a Water saturation versus time plot for Case 8

Note: Figures 6-28 through 6-31 (Case 9) have been intentionally removed

- Figure 6-32 Heat load per Gridblock, Cases 10 and 11
Figure 6-33 Simulated pressure around the tunnel for various times, Case 10
Figure 6-34 Simulated temperature around the tunnel for various times, Case 10
Figure 6-35 Simulated capillary pressure around the tunnel for various times, Case 10
Figure 6-36 Simulated saturation around the tunnel for various times, Case 10
Figure 6-37 Simulated variation of temperature versus time for Case 10
Figure 6-38 Simulated variation of saturation with time for Case 10
Figure 6-39 Simulated temperature around the tunnel for various times, Case 11
Figure 6-40 Simulated capillary pressure around the tunnel for various times, Case 11
Figure 6-41 Simulated variation of temperature with time for Case 11
Figure 6-42 Simulated variation of saturation with time for Case 11
Figure 7-1 Comparison of daily water usage with calculated ventilation-induced evaporation
Figure 7-2 Conceptual model of infiltration into a fractured zone exposed in a wet tunnel floor
Figure 7-3 Simulated saturation profile for a wet tunnel surface

LIST OF TABLES

- Table 6-1 Material properties used for simulation of ventilation effects
- Table 6-2 Summary of simulation setup for evaluation of natural ventilation effects
- Table 7-1 Estimated water usage in the ESF tunnel from March 25 to May 29, 1996.
- Table 7-2 Water usage history in the ESF tunnel

EXECUTIVE SUMMARY

Nye County Nuclear Waste Repository Project Office's Independent Scientific Investigation Program (ISIP) has identified several key scientific issues that may affect repository conceptual design and performance but are not currently being adequately addressed by the U.S. Department of Energy's (DOE) Yucca Mountain Program (YMP). These issues include:

- Adequate spatial characterization of pneumatic properties and pneumatic potential of the repository host rock.
- Potential geochemical disturbance of the repository host rock caused by site-characterization activities such as construction of the Exploratory Studies Facility (ESF) tunnel.
- Collection of pertinent information from the repository before it is disturbed by site characterization activities.
- Collecting data that could not be readily obtained after construction of the ESF.
- Characterization of hydraulic properties of the deep hydrogeologic units and understanding of the geologic and hydrogeologic system in these units.
- The nature of the steep groundwater gradients to the north and west of the repository.
- Potential alternative conceptual designs of the repository that can improve the performance of the repository, and the need for characterization of the pneumatic system in the repository block to help evaluate alternative conceptual designs.

- Understanding the western boundary of the repository block and, potentially, the interaction of the atmospheric processes with the repository horizon in the Solitario Canyon where the repository horizon is exposed.
- Radionuclide diffusion and dispersion investigations in the saturated zone.

The ISIP presently includes borehole and tunnel instrumentation, monitoring, data analysis, and numerical modeling activities to address the above concerns.

Nye County has installed and is currently monitoring pressure and temperature instruments in boreholes UE-25 ONC#1 and USW NRG-4 to evaluate the long-term pneumatic conditions at strategic depths in the subsurface both in response to fluctuations in atmospheric conditions and in response to other possible disturbances resulting from site characterization activities such as ESF tunnel construction. Nye County has also installed instruments to measure temperature, pressure, and humidity within the ESF tunnel to characterize the air being used to ventilate the tunnel which could potentially impact the performance of the repository. Finally, Nye County is conducting numerical modeling simulations to evaluate factors (including tunnel ventilation) which affect both short-term and long-term pneumatic and moisture conditions in the repository host rock .

A summary of activities undertaken by ISIP during the past year are as follows:

- Evaluation of critical data and information as it became available from the DOE's YMP Site Characterization Office.
- Observed water usage in the tunnel and its potential impact on the repository horizon and the scientific investigation results. Completed an analysis and a recommendation report and forwarded it to YMP Site Characterization Office.

- Prepared detailed review of procedures and methods used for in-situ air permeability tests and evaluated the results of some of these tests.
- Completed several letter reports to DOE on the interpretation of the results of the ^{36}Cl and other environmental and geological isotope studies. These communications have resulted in DOE giving more focused attention to the need for more detailed studies in the ESF tunnel, limiting the use of construction water, and enhanced interpretation of the results of the isotope sampling.
- Evaluated the saturated zone pumping tests that were performed in the C-Well complex during the past year.
- Monitored responses to these pumping tests in the ONC#1 saturated-zone instrumentation.

As a result of the evaluation of the ESF tunnel climatological data collected, Nye County concluded that substantial moisture was being removed from the rocks penetrated by the tunnel ventilation. In response to issues raised by Nye County, DOE assigned a task force to conduct observations in the ESF and perform numerical simulations for interpretation of the results in parallel with Nye County's effort. Nye County provided data, preliminary analytical and simulation results, and input for developing the proposal to this task force. Nye County data indicated that in addition to moisture, substantial amount of heat is being removed by the ventilation. Nye County performed additional simulations using A-TOUGH, a computer code designed to simulate coupled-open air with geologic formations and discovered that there is a tremendous potential for natural ventilation at the site due to its climate and its physiographic setting. Simplified simulations using A-TOUGH were performed to evaluate the potential of a naturally ventilated repository. One conclusion is that it is possible to design a repository that is naturally ventilated with peak rock temperatures of less than 30 degrees Celsius over a 10,000-year period. These simulations also showed that the

capillary pressure distribution would promote a strong gradient for water flow towards the emplacement tunnel during the entire 10,000 years. Nye County, believes that long-term waste containment implications of a naturally-ventilated repository warrants additional analysis.

Nye County is planning to perform several investigations in the near future to understand some of the issues that were outlined above, by installing new wells in both the saturated and unsaturated zones, testing and sampling these wells, and performing data analysis and modeling. These issues are related to the steep gradients in the saturated zone north and west of the site, the potential for dilution in the saturated zone as unsaturated zone moisture enters the saturated zone, the atmospheric and pneumatic boundaries in the Solitario Canyon that might impact the repository performance, and the large-scale transport properties of the fractured formations in both saturated and unsaturated zones.

1.0 INTRODUCTION

The Nuclear Waste Policy Act of 1982, as amended in 1987, (NWPA) designates Yucca Mountain in Nye County, Nevada, as the candidate site for the nation's first high-level radioactive waste repository. U.S. Department of Energy (DOE) plans to evaluate the geotechnical suitability of this site through both scientific site characterization and the evaluation of socioeconomic impacts related to the siting, construction and operation of a high-level nuclear waste repository. NWPA empowers Nye County, as an affected unit of local government, to provide oversight, including independent monitoring and testing of the activities, performed by DOE at the Yucca Mountain Site (YMS), by an on-site representative.

The Nye County Nuclear Waste Repository Project Office (Nye County NWRPO) is responsible for protecting the health and safety of the Nye County citizens. NWRPO's on-site representative is responsible for designing and implementing The Independent Scientific Investigation Program (ISIP). Major objectives of the ISIP include:

- Investigating key issues related to conceptual design and performance of the repository that can have major impact on human health, safety, and the environment.
- Identifying areas not being addressed adequately by DOE

Nye County has identified several key scientific issues of concern that may affect repository design and performance which are not currently being adequately addressed by DOE. These issues include:

- Adequate spatial characterization of pneumatic properties and pneumatic potential of the repository host rock.

- Potential hydrochemical disturbance of the repository host rock caused by characterization activities such as ESF tunneling.
- Collection of pertinent information from the repository before it is disturbed by site characterization activities.
- Collecting data that could not be readily obtained after construction of the ESF.
- Characterization of hydraulic properties of the deep hydrogeologic units and understanding of the geologic and hydrogeologic system in these units.
- The nature of the steep groundwater gradients to the north and west of the repository.
- Potential alternative designs of the repository that can improve the performance of the repository, and the need for characterization of the pneumatic system in the repository block to help evaluate alternative designs.
- Understanding the western boundary of the repository block and potentially, the interaction of the atmospheric processes with the repository horizon in the Solitario Canyon where the repository horizon is exposed.
- Radionuclide diffusion and dispersion investigations in the saturated zone.

The reader is referred to a previous report (NWRPO, 1995; MET, 1995) for a detailed explanation of these specific concerns.

1.1 SCOPE AND ORGANIZATION OF REPORT

This report is a preliminary document that summarizes the first year of monitoring data from two boreholes that were instrumented by Nye County in March and April of 1995, as well as the first 12 months of monitoring data from the Exploratory Study Facility (ESF) tunnel which is currently under construction. It

presents representative examples of observations, and limited and preliminary interpretations for the purpose of discussion. Further evaluations of these results may provide alternative interpretations. Therefore, these preliminary interpretations do not constitute and should not be considered as the official position of Nye County.

This report is organized as follows. Section 2.0 presents a brief description of Nye County instrumentation in boreholes and the ESF as well as methods used to monitor and process data. Section 3.0 gives a brief summary of the previously reported (NWRPO, 1995) initial three months of borehole monitoring results and preliminary modeling to examine several factors affecting pneumatic pressure responses in boreholes, including tunnel ventilation effects. Section 4.0 summarizes the entire first year of monitoring data from the two boreholes and 12 months of data collected from the ESF tunnel. Section 5.0 describes and evaluates repository formation permeability calculated from air pressure fluctuation data by inverse modeling methods, both within boreholes and between boreholes and the ESF tunnels. Section 6.0 discusses results of the simulations performed to evaluate the various tunnel ventilation scenarios and their effects on water potential, capillary pressure, saturation, temperature, and pressure of repository host rock. Section 7.0 presents evaluation of ESF water use. Summary and conclusions are presented in Section 8. References are listed in Section 9.0. Figures and Appendix A are presented in Volume II. Tables appear at the end of each section.

1.2 NYE COUNTY'S BOREHOLE AND TUNNEL MONITORING STUDIES

The ISIP presently includes borehole and tunnel instrumentation, monitoring, data analysis, and numerical modeling activities to address the above concerns.

Figure 1-1 shows the regional setting of the Yucca Mountain. Nye County has installed and is currently monitoring pressure and temperature instruments in boreholes UE-25 ONC#1 and USW NRG-4 (Figure 1-2) to evaluate the long-term pneumatic conditions at strategic depths in the subsurface both in response to fluctuations in atmospheric conditions and in response to other possible disturbances resulting from site characterization activities such as the ESF tunnel construction. Nye County has also installed instruments to measure temperature, pressure, and humidity within the ESF tunnel to characterize the air being used to ventilate the tunnel which could potentially impact the performance of the repository. Finally, Nye County is conducting numerical modeling simulations to evaluate factors (including tunnel ventilation) which affect both short-term and long-term pneumatic and moisture conditions in the repository host rock .

1.3 OTHER ACTIVITIES

Nye County has also been evaluating new critical data and information as it becomes available from the DOE's Yucca Mountain Project studies. In the past year, Nye County has observed water usage in the tunnel and its potential impact on the repository horizon and the scientific investigation results. The interpretation of the results of the ^{36}Cl and other environmental and geological isotope studies have been the focus of many meetings attended by Nye County which has resulted in several letter reports to DOE during the past year. Some of these communications have resulted in DOE's more focused attention to some of the issues raised by Nye County. Specifically, these issues related to the need for more detailed studies in the ESF tunnel, limiting the use of construction water, and enhanced interpretation of the results of the isotope sampling.

Nye County evaluated procedures and methods used by DOE to conduct air-permeability tests in the unsaturated zone of YMS. As a result of several interactions between Nye County and DOE, satisfactory procedures were

developed and used by DOE in more recent testing efforts. The results of these tests were analyzed and reported (Advance Resources International, 1995).

In addition, Nye County has evaluated the saturated zone pumping tests that were performed in the C-Well complex during the past year. Nye County has also been monitoring responses to these pumping tests in the ONC#1 saturated-zone instrumentation.

1.4 PROPOSED FUTURE INVESTIGATIONS

Nye County is planning to perform several investigations in the near future to clear some of the issues that were outlined above by installing new wells in both the saturated and unsaturated zones, testing and sampling these wells, and performing data analysis and modeling. These issues are related to the steep gradients in the saturated zone north and west of the site, the potential for dilution in the saturated zone as unsaturated zone moisture enters the saturated zone, the atmospheric and pneumatic boundaries in the Solitario Canyon that might impact the repository performance, and the large-scale transport properties of the fractured formations in both saturated and unsaturated zones. These plans are briefly discussed in this report.

2.0 INSTRUMENTATION AND MONITORING APPROACH

The ONC#1 borehole was drilled and both ONC#1 and NRG-4 boreholes were instrumented to support the following data collection activities:

1. To monitor the long-term variation of pressure and temperature in hydrogeologic units that may be impacted by the construction of the ESF.
2. To perform vacuum and/or injection pneumatic testing to evaluate the horizontal and, to some extent (unknown), vertical pneumatic conductivity values of the hydrogeologic units packed off by the Westbay Instruments.
3. To sample intervals isolated by packers for environmental isotopes to evaluate the residence time of the gases in the hydrogeologic formations.

Due to funding constraints, Nye County borehole data collection activities to date have been limited to monitoring and analyzing subsurface variations in temperature and pressure (Item 1.).

The tunnel was instrumented with temperature, pressure, and humidity sensors to monitor pneumatic parameters of the ventilation air necessary to:

1. Assess the impact of this air on the gas composition and water content of the repository formation rock.
2. Permit calculation of large scale bulk permeabilities of the repository host rock between the ESF tunnel and Nye County instrumented boreholes (UE-25 ONC#1 and USW NRG-4).

2.1 BOREHOLE DESCRIPTION

Nye County borehole locations were selected primarily to establish baseline conditions before penetration of the repository host rock by the ESF tunnel and to monitor the effects of the mine ventilation system used in the ESF tunnel on the ambient pneumatic and moisture conditions of the unsaturated zone in the vicinity of the north and south ramps of the ESF tunnel. UE-25 ONC#1 is situated southeast of the repository block and is in the path of the future South Ramp of the ESF tunnel (Figure 1-2). It was also strategically located to be along the main trace of the Bow Ridge Fault system and close enough to DOE's C Well Complex (approximately 800 meters) to serve as a monitoring well during aquifer testing. It was drilled by Nye County in late 1994 and early 1995 using dual wall reverse circulation technology to demonstrate an alternative drilling and sampling method to DOE (NWRPO, 1995).

USW NRG-4 is located northeast of the repository block (Figure 1-2) and is situated about 1100 m from the North Ramp (NR) portal of the ESF tunnel. It was previously drilled by DOE. The ESF tunnel passed within approximately 15 meters of USW NRG-4 in the middle of June 1995. The effects of the tunnel excavation on pneumatic conditions in this instrumented borehole, as well as in UE-25 ONC#1, will be discussed in the following sections.

2.2 BOREHOLE INSTRUMENTATION

Nye County instrumented UE-25 ONC#1 and USW NRG-4 in early 1995 with Westbay Corporation's MOSDAX MP55 system. The MP-55 is a multilevel monitoring device that consists of an access casing with multiple ports or valves that can be opened to the formation. A multilevel packer system integrated into the access tube serves to isolate access ports and retrievable temperature/pressure measurement probes that connect to these access ports. An above ground data logger is used to monitor the temperature/pressure probes. A complete

description of this downhole monitoring system and installation procedures in these boreholes are presented in NWRPO (1995).

Fifteen downhole packers were used to isolate major stratigraphic units, a fault zone, and two isolated zones below the water table in UE-25 ONC#1. Figure 2-1 shows the location of 15 packers and 31 measurement ports in relation to stratigraphic units, the Bow Ridge fault zone, and the water table. MOSDAX temperature/sensor probes were installed in 9 of the 31 measurement ports available. It should be noted that the two bottom-most probes in UE-25 ONC#1 are situated below the water table and are monitoring the piezometric potential.

Prior to August 1995, the upper six packers in ONC#1 were not set in this borehole due to an alignment problem with the MP55 access casing. As a result, data from the upper measurement ports (Probes 1 and 2) in this borehole may be invalid from April through September 1995. In August the upper packers were set, thereby effectively isolating the upper stratigraphic units and measurement ports.

Seven downhole packers and 7 measurement ports were strategically installed in major stratigraphic units in USW NRG-4 as shown in Figure 2-1. MOSDAX temperature/sensor probes were installed in all 7 measurement ports.

2.3 TUNNEL INSTRUMENTATION

An underground climatological monitoring station was installed in August 1995 behind the ESF tunnel boring machine to measure the temperature, pressure, and relative humidity of the ventilation air. Figure 2-2 is a schematic drawing that shows the relative position of the instruments. This monitoring station (Figure 2-3) moves with the tunnel boring machine frame. Several other measurement stations have been recently installed by DOE, following the recommendation of Nye County, along the main axis of the tunnel and in radial alcoves to characterize the spatial variation of these parameters in the underground tunnel system.

2.4 CALIBRATION, DATA COLLECTION AND PROCESSING

Nye County NWRPO Quality Assurance (QA) procedures document the detailed methods followed to calibrate instruments (laboratory and field methods), to collect field data and transfer data into a databases, and to analyze and evaluate data through computer programs, including numerical modeling codes. The specific NWRPO QA procedures controlling activities described in this report are as follows:

- *Instrument Calibration and Collection and Processing of Data from Boreholes, Revised Version 1.0* (Applicable to the initial collection and processing of data from April to August, 1995).
- *Instrument Calibration and Collection and Processing of Data from Boreholes, Revised Version 2.0* (Applicable to the collection and processing of data after August, 1995).
- *Instrument Calibration and Collection and Processing of Data from ESF Tunnels.*
- *Computer Modeling and Data Analysis Quality Assurance Procedure.*

3.0 SUMMARY OF PREVIOUS WORK

The results of initial pressure and temperature monitoring data collected from boreholes UE 25-ONC#1 and USW NRG-4 from April through June, 1995 were presented in an earlier report (NWRPO, 1995). Temperature profiles in both boreholes appear to be consistent with previous geothermal gradient data obtained from Yucca Mountain. Moreover, pneumatic pressure changes at depth in the lower portion of UE-25 ONC#1 and throughout USW NRG-4 exhibit trends that are expected in layered geologic media. That is, there is a general dampening of the magnitude as well as an increasing time-lag in the peaks and valleys of barometric pressure fluctuations as depth increases. During this initial monitoring period, the upper portion of the borehole (probes 1 and 2 above packer No.6) was opened directly to the atmosphere and pressure data obtained from this portion of the borehole was not representative of in situ conditions.

Computer simulations were performed using A-TOUGH to evaluate a number of factors affecting pneumatic pressure responses versus depth in instrumented boreholes. Factors evaluated include permeability variations versus depth, ventilation effects of the tunnel excavation, and boundary conditions. Relatively simple one-dimensional setups and simulations were first conducted to obtain preliminary estimates of the pneumatic conductivity of different hydrogeologic units penetrated by the boreholes. Two-dimensional (quasi three-dimensional) set-ups and simulations were conducted to permit evaluation of tunnel ventilation effects on borehole pressure responses at different depths. The effects of boundaries were examined in both the one- and two-dimensional simulations.

Substantial differences in the results of permeability calculations were found between one-dimensional and two-dimensional simulations. For example, permeability values calculated for the Tiva Canyon hydrogeologic unit in the two-dimensional case are two orders of magnitude smaller than those calculated in the one-dimensional case, but correspond to the range reported by Montazer et. al.

(1987) for this unit. Moreover, values calculated for the Paintbrush Tuff Nonwelded unit in the two dimensional model are two to three orders of magnitude less than permeabilities calculated by the one-dimensional model which fall within the range of values reported by Montazer et. al. (1987). These differences may in part be due to the lateral subsurface movement of air due to pressure fluctuations that are not in phase with atmospheric pressure fluctuations caused by subsurface heterogeneities.

The effect of the tunnel is clearly demonstrated both in the pressure monitoring data from the USW NRG-4 borehole (located approximately 15 meters from the tunnel) and the two-dimensional simulation results. Pressure effects resulting from the tunnel excavation are predicted to occur as far as 100 m away from the tunnel in the short time of the simulations (about 10 days). Simulation of the tunnel effects over a longer time period is expected to influence larger radii.

Because of the heterogeneity of the formations involved, the direction of the flow of air is variable and can be in any direction. Introduction of modern environmental tracers into fracture systems in the unsaturated repository block could introduce artifacts into future environmental tracer analyses and interpretations for both water and gas samples collected from fractures. Based on the potential for the tunnel excavation process to introduce artifacts into the environmental tracer record, it is recommended that areas in the path of the ESF that are not as yet affected by the tunnel (e.g. locations greater than 500 m away from the tunnel excavation face) be sampled as soon as possible.

Also, it is important to continuously monitor the pressure, temperature, and humidity in the tunnel. This information can be used in future simulations to calculate the permeability of the material penetrated, and will provide relatively inexpensive cross-hole testing data (e.g. between the tunnel and nearby instrumented boreholes).

Finally, the simulations presented in this report suffer from an inadequate number and distribution of constraining parameters. If more data concerning these parameters are collected in the tunnel on a regular basis, the accuracy of calculated permeabilities may improve significantly in future simulations.

4.0 SUMMARY OF FIRST YEAR'S MONITORING RESULTS

4.1 BOREHOLE TEMPERATURE AND PRESSURE DATA

The variation of temperature in UE-25 ONC#1 and USW NRG-4 over the 17 months time period is shown in Figures 4-1a through 4-1q and Figures 4-2a through 4-2p, respectively. Temperatures reported for all downhole instruments are fairly stable with occasional deviations from the norm. Data from UE-25 ONC#1 from April to August, 1995 (when the upper 800 feet of borehole was open to the atmosphere) does not differ significantly from data collected after August 1995, suggesting that packer inflation has had little effect on downhole temperatures. The atmospheric probe (Probe 0) in each borehole records a wide range of daily and seasonal temperature fluctuations typical of a desert environment. Comparison of the temperature data from atmospheric probes (Probe 0) in USW NRG-4 and UE-25 ONC#1 indicates very consistent atmospheric temperature patterns at the two sites.

Pressure fluctuations with time for UE-25 ONC#1 and USW NRG-4 are shown in Figures 4-3a through 4-3q and Figures 4-4a through 4-4p, respectively for the 17 months monitoring period. These graphs show that pressure responses exhibit trends versus depth that are expected in layered geologic media. That is, there is a general dampening of the magnitude as well as an increasing time-lag in the peaks and valleys of barometric pressure fluctuations as depth increases. The only exception to these trends are data collected from April to August 1995 in UE-25 ONC#1 when the upper portion of the borehole was opened to the atmosphere and in both boreholes after the tunnel penetrated the proposed repository horizon.

Two of the probes in UE-25 ONC#1 (Probes 8 and 9) are below the water table. These probes monitor variation of piezometric level with time and are plotted in Figures 4-5a through 4-5q.

Comparison of Probe-0 pressure responses at USW NRG-4 and UE-25 ONC#1 indicate nearly identical responses over time when corrected for elevation differences.

Nye County has also received data from U. S. Geological Survey's monitoring boreholes. The unsaturated-zone boreholes for which data has been received (in July 1996) are shown in Figure 1-2. Plots of pressure and temperature for these boreholes are presented in Appendix A (some versions of this report may not include this appendix).

In order to compare the data collected by the Yucca Mountain Project (U.S. Geological Survey) with those collected by Nye County, the pressure data for all the boreholes are plotted in Figures 4-6a through c. These graphs show that, despite the significant difference in the data collection techniques, there is a close agreement between the averages of the data. The slight differences in the trends and magnitudes are expected due to the position of the boreholes and the depth of the measuring instruments. Similarly, Figure 4-7a compares the temperature averages for these boreholes.

In order to visualize the pressure and temperature distribution in Yucca Mountain, data for four time periods were selected. Averages, minimum, and maximum values for each period were kriged. It should be noted that kriging introduces errors in representation of the data that are operator dependent. Care has been used to minimize these errors; however, sparseness of the distribution of the boreholes in plan view compared with the dense spacing of the instrument stations in the boreholes create anisotropy in the variograms that may be artificial. The results of these kriged visualizations are shown in Figure sets 4-8 through 4-13. Each set presents data from four periods of time as follows:

1. May 1 to May 10, 1995
2. June 6 to June 26, 1995
3. December 1 to December 10, 1995
4. May 4 to May 14, 1996

The first time period was chosen to represent data before the ESF tunnel penetrated the Paintbrush Nonwelded (Ptn) unit. The second period is during perturbation of the Topopah Springs Welded unit by ESF tunnel. The latter two are at various stages of advancements of the ESF tunnel (see Section 7 for the stages of ESF advancement)..

Figure 4-8a through 4-10a show pressure distribution for the first period. As an example of the error introduced by kriging, there are only four boreholes in this period that have pressure data. Kriging has resulted in a high pressure field in the southern portion of the site where ONC#1 is located. ONC#1 has the deepest pressure probes and, as a result, has the highest pressures at depth. Kriging has resulted in generation of the high pressure field in the south in this figure. In later periods (Figures 4-8d through 4-13d), all eight boreholes have recorded the pressure and temperature.

4.2 ESF TUNNEL TEMPERATURE, PRESSURE, AND HUMIDITY MONITORING DATA

Results of the Nye County's monitoring in the ESF are presented in a series of graphs in Figures 4-14, 4-15, and 4-16. Figure 4-14a through m present the temperature fluctuation data in the ESF tunnel during the 13 months of monitoring since August of 1995. Figures 4-15a through m show the relative humidity and Figures 4-16a through m show pressure fluctuations with time, respectively. Initially, until November 1995, only one set of probes were installed in the ESF

tunnel near the tunnel boring machine (TBM). In December of 1995, two additional monitoring stations were installed at the same location in approximately the same plane perpendicular to the tunnel axis but at different distances from the walls of the tunnel. The purpose of the separation of the three sets of probes was to obtain the thermal and vapor concentration gradients in the tunnel perpendicular to the axis of the tunnel. As will be discussed in later sections, these gradients are important in defining the direction and magnitude of the vapor and heat flux in the tunnel. Both temperature and relative humidity data show a period of almost chaotic perturbations followed by a smooth recovery. The perturbations coincide with the tunnel operating days (Monday through Friday). The smooth recoveries correspond to the weekends and holidays. It is noticeable that the values of the temperature and relative humidity of Probe 2, which is in the center of the tunnel, are almost always smaller than the values of the other two probes.

In order to compare the climatic conditions in the ESF tunnel with the atmospheric climatic conditions, data from two weather stations near the ESF portal were obtained from the U.S. Department of Energy and are plotted in Figures 4-17 through 4-21. The location of one of the stations (NTS-60) is shown in Figure 1-2. The Sever Wash meteorological station is about one mile east of the ESF tunnel portal (not shown in Figure 1-2).

Detailed correlation and analysis of these data are currently underway by Nye County. A portion of these data was used for preliminary calibration of the model that will be described in Section 6. A cursory review of the graphs indicate that during the first three month of observation, the tunnel temperature and humidity were slightly influenced by the atmospheric conditions. The pressure fluctuations in the tunnel on the other hand have always been synchronous with the atmospheric pressure fluctuations. There is no detectable delay (lag) between the atmospheric and tunnel pressure fluctuations regardless of whether the tunnel ventilation was operating or not. The relative humidity of the atmospheric air is generally between 10 to 15 percent. The relative humidity of the atmospheric air

increases generally as a result of decline in temperature. This indicates that the moisture content (or specific humidity) of the atmospheric air is almost always low. This means, regardless of the relative humidity value of the outside air, the atmospheric air that enters the tunnel has a great potential for removing moisture from the rock.

5.0 CALCULATION OF AIR PERMEABILITIES FROM PRESSURE MONITORING DATA

Simulation of the pressure responses before and after the tunnel has provided estimates of the air permeability of the units intersected by the tunnel. Several methods of calculating permeability from these barometric responses have been used. The simplest form was the assumption that before the tunnel influence, the barometric pressure waves travel vertically in a uniform front. This conceptual model has been used by Edwin Weeks of the U.S. Geological Survey at Yucca Mountain and various other sites. However, quasi three-dimensional simulations (MET, 1995) have indicated that substantial amounts of lateral flow air occurs as a result of complex boundary conditions and heterogeneity in the hydrogeologic formations at the site. Furthermore, the tunnel effects are obviously three-dimensional. Attempts to simulate responses in ONC#1, which is at least 1.5 miles away from the tunnel, with the one-dimensional approach has not been successful.

5.1 BOREHOLE PERMEABILITY CALCULATIONS

Calibration to permeability values alone does not always have a unique solution. It is the overall diffusivity of the system (the dynamic combination of permeability, porosity, saturation, and density) that dictates the responses to barometric fluctuations at any of the boundary conditions. However, in cases where the boundary is connected to the zone of interest (where the probes are situated) through equivalent porous media (such as the connection between the atmospheric boundary and the TCWU), the response is broad and distinctly resembles the fluctuations at the boundary. Where there is more than one connection; such as along faults, the responses to each can be isolated and identified. In some cases, because the response through faults is through a small diffusivity (because of the small effective porosity and large permeability) it produces small ripples

superimposed on the broad signals that result from relatively low permeability and large porosity equivalent porous media pathways.

Figure 5-1 shows the pressure fluctuations with time in NRG-4 borehole during the month of May 1995. In this figure, it is noticeable that the pressure response to atmospheric fluctuations is substantially damped in probes below the Ptn Unit (Probes 4 to 7). Probe 3 which is near the bottom of the Ptn, is only slightly damped. It appears that a majority of the dampening occurs in the bottom portion of the Ptn unit where it is believed to have a higher moisture content which results in lower air permeability. On or about May 22, 1995, the ESF tunnel began penetrating the Tiva Canyon vitric zone which is the upper-most part of the Ptn. There is no noticeable change in the response of the pressure probes in NRG-4 in this figure.

Figure 5-2 shows the pressure fluctuations in NRG-4 borehole during the month of June 1995. On June 16, deviation from normal trend is noticeable in probe 7 but is not clearly detectable until June 18 when all deep probes began responding almost synchronously to the atmospheric fluctuations as a result of direct pneumatic communication of the tunnel with the fractured Topopah Spring Welded Unit (TSWU). Probe 3 continued to maintain a lag in barometric response relative to the other probes. The reason for this lag is that Probe 3 is separated from the tunnel and other affected units by nonwelded tuff both horizontally and vertically. As of the latest data set retrieval, this lag has remained about the same (see Section 4 and Figures 4-4a through 4-4p).

Data from NRG-4 in April, before the tunnel interference in June 1995, were used to calculate the permeability of the units isolated by the packers. A one-dimensional model using A-TOUGH computer code was setup for these calculations. The results of the calibration were used to simulate the May 1995 data. It appeared that a one-dimensional simulation of the conditions before the tunnel penetrated the repository host rock was appropriate to estimate the vertical

air permeability values. Figure 5-3 is a summary of the results of permeability calculations in NRG-4 for this one dimensional case.

Figure 5-4 is a plot of the pressure fluctuation data for November 1995 for well ONC#1. During this month, the ESF tunnel entered the repository horizon and began turning to the south (see Figure 1-2). In this figure, the lag time between probe 1 and the atmospheric fluctuations is about 4 hours. The lag time between the atmosphere and the probe 2 responses is 14 hours. Probe 2 responses are almost synchronous with all the lower probes in the unsaturated zone. The inset in this figure is the location of the probes in this borehole relative to the hydrogeological units. Probes 1 and 2 are separated by a thin layer of the Ptn unit.

Figure 5-5 is a plot of the pressure fluctuation data from January 18 to February 21, 1996. During this period the ESF tunnel was in the repository horizon in the area of Yucca Ridge where several northwest-southeast trending structures have been mapped. This structure probably intersects the Ghost Dance Fault, and is probably pneumatically connected to the Sundance Fault system.

In this figure, the lag times on February first are shown. On this day, the lag time between the atmosphere and Probe 2 is 20 hours and that between atmosphere and Probe 1 is about 1 hour. However, fluctuations in Probe 2 are still synchronous with all the deeper probes. It is noticeable, however, that in late February, the deeper probes began to show small ripples in their fluctuations. In March 1996 data (Figure 5-6) these ripples clearly become stronger. What is most interesting in this figure is that the lag between Probe 2 and deeper probes have become negative. That is, the deeper probes, which are vertically closer to the fault zone intersect ONC#1 at a depth of about 1200 feet. The fault zone in this figure is drawn to indicate the probable interval where it exists in this borehole. The fault is believed to be at a steep angle (NWRPO, 1995). The apparently low angle in this figure is a result of horizontal exaggeration.

In Figure 5-6, it is also notable that probe 1 has maintained its 4 hour lag but probe 2 has a lag of 36 hours from the atmospheric fluctuation. This apparent longer lag is partly due to the long-term atmospheric pressure decline in early March but it could also be due to superposition of other sources of pressure. Closer examination of the data indicates that this negative lag between Probe 2 and the deeper probes has been reoccurring since October 1995. Atmospheric pressure signals are not very strong between July and October 1995. However, comparison of the same strength signal between June 1995 (Figure 4-3c) and October 1995 (Figure 4-3g) clearly indicates that the negative lag was developed sometime between June and October of 1995. This is the period that the ESF tunnel has been advancing closer to ONC#1 borehole in the fractured TSWU. Similar lags can be observed in other boreholes at Yucca Mountain (see Appendix A). In particular UZ-4 and UZ-5 in December 95 and May 1996 and NRG-7a in December 95 and May 96 distinctly show this negative lag in probes placed below the Ptn unit.

In order to evaluate the cause of these effects, a one dimensional simulation of the ONC#1 column was setup to calculate the permeability of the instrumented sections. Data from April 1996 were used for this simulation. The column used for this set of simulations is shown in Figure 5-7. The simulated pressures are compared with the measured pressures in Figure 5-8. It was not possible to match the trends for probes below probe 2. Probes 1 and 2 are matched very closely.

To evaluate the potential for influence of the tunnel on the responses, a three-dimensional configuration was setup as shown in figure 5-9. The one dimensional configuration is pictorially shown as a vertical column of cylindrical nodes at the ONC#1 location. The major fractures are shown by vertical planar nodes. The tunnel nodes are shown with horizontal cylindrical nodes. The atmospheric fluctuations are connected to the top of the ONC#1 column and to the beginning of the tunnel. Therefore, communication with the atmosphere is through both a vertical column of hydrogeologic units as well as through the tunnel, Ghost Dance

and Sundance Fault systems. Figure 5-10 is a comparison of the observed versus simulated pressures in April 1996. The match is almost perfect with the three-dimensional configuration. This simulation exercise demonstrates that deviation of the pressure from normal trends in the deeper probes in ONC#1 are very likely due to the disturbance of the pressures in the repository horizon by the ESF tunnel.

5.2 LARGE-SCALE PERMEABILITIES

Comparison of the calculated permeability values in Figures 5-3 and 5-7 reveals that the bulk vertical air permeability of the TCWU is slightly smaller at ONC#1 site than at the NRG-4 site. The Ptn unit forms a barrier to barometric pressure transmission in both boreholes. Its effectiveness appears to be largely due to the existence of a low permeability layer near the bottom of the unit. At the NRG-4 site, the Ptn unit is thicker than at the ONC#1 site. This lower air permeability of the bottom layer is probably due to the higher moisture content of the unit in both sites. This layer corresponds with the Topopah Spring crystal rich vitric zone.

The fault zone at the ONC#1 site has a slightly higher permeability than its host rocks. In Figure 5-7, the air permeability of the Sundance Fault from the three-dimensional model is also shown. In calibrating this model, it was realized that the equivalent effective porosity of this zone is very small ($\phi = 1 \times 10^{-5}$). This small effective porosity indicates that the pressure transmission occurs along a very distinct path. This path is probably partly through the Ghost Dance, Sundance, and Bow Ridge Faults. Evaluation of the responses in other boreholes at the site is underway by Nye County to better understand this phenomenon.

Comparison of the overall permeability measurements from borehole packer testing shows that the overall permeability values measured in boreholes can be one to two orders of magnitude smaller than those calculated from barometric fluctuations. There are several reasons for the difference. The size of the rock block that is influenced by barometric pressure is much larger than that influenced by borehole packer testing. However, extreme values from testing boreholes

should have been much larger than the bulk permeability values of the same hydrogeologic units obtained from barometric testing. Montazer (1982) demonstrated this by conducting experiments in boreholes at various sampling sizes. The reason for the difference is that, until the sampling size is large enough to be the representative elemental volume (REV), the permeability of the smaller sized samples vary about a mean that could be smaller or larger than the permeability of the REV. That is some of the smaller sampling sizes contain large fractures that contribute to flow much more significantly than the permeability of the REV allows. This has not been observed at Yucca Mountain. The fractures in most of the hydrogeologic units are nearly vertical and not very well sampled by the vertical boreholes. Barometric effects are through these vertical fractures. Therefore, there appears to be a large anisotropy in the system. However, packer testing in vertical boreholes does not adequately sample these fractures to enable quantification of the anisotropy. The ESF tunnel influence is a much better source of perturbation that can aid in quantifying anisotropy of the TSWU. Preliminary analysis of some of the data indicates that the horizontal directional permeability may be as much as two-orders of magnitude smaller than the vertical directional permeability.

6.0 MODELING VENTILATION EFFECTS ON MOISTURE IN REPOSITORY HOST ROCK

6.1 WASTE PACKAGE ISSUES

The two most important aspects of the Yucca Mountain project are radionuclide isolation and thermal stability of the repository. Current concepts are that the repository will be sealed with crushed tuff or similar material (TSPA 1995) after 100 years of repository pre-closure period. Although some considerations have been given to a no backfill design, the results have not been satisfactory due to high temperatures and humidities predicted by the simulations. The shortcoming in all the simulations and analysis has been that the media around the waste package have been assumed to be relatively stagnant, whether air or crushed tuff. Nye County has performed its own simulations based on the concept proposed by Roseboom (1983) and Montazer and Wilson (1984) that the dry and open environment of the repository should be taken advantage of in the design of the repository. Preliminary simulations have been made using simplifying assumptions and the material properties presented in TSPA 1995. The results of these simulations are presented in the following sections.

One of the factors that affects the waste package longevity is the relative humidity. Relative humidity is not indicative of the moisture content of the air. A low relative humidity value at a high temperature does not necessarily mean a drier condition. In fact, at 225 degrees Celsius, an air volume with relative humidity of 1 percent contains 50 times more water vapor than the same volume of air at room temperature with a relative humidity of 100 percent. Relative humidity is used in the TSPA as an indicator for the rate of the waste package canister corrosion. It is concluded in the TSPA that "the corrosion rate of the waste package is slower at smaller relative humidity". The temperature is not mentioned as a factor in this conclusion. Thus, it is inappropriate to compare relative humidity values at

different temperatures. For example, the corrosion rate may not be higher at 60 percent relative humidity at room temperature than at 40 percent relative humidity at 200 degrees assuming that the temperature and vapor pressure remains constant.

One of the factors that accelerates corrosion of the canister is the water-vapor concentration gradient in the vicinity of the canister and not the relative humidity. A cold body placed in a stagnant air with high relative humidity results in formation of dew on the cold body. The cold body causes a vapor concentration gradient toward the body. If the same body is warmer than the air, the vapor concentration gradient is away from that body and no dew formation occurs. Therefore, if the concentration gradient is away from the canister (warm body), the corrosion due to the presence of the water vapor is less likely than when the concentration gradient is toward the canister. It is this concentration gradient that dictates whether water vapor molecules condense on the canister or not. In case of a back-filled repository, the only time that the vapor concentration is toward the canister is during the cooling period when the surrounding rock is warmer than the canister. In a well ventilated drift, the concentration gradient is always away from the canister. Therefore, TSPA 95's (TRW, 1995) (and Buscheck et. al, 1995) goal of reducing the relative humidity without removing moisture from the air around the package may not guarantee reduced corrosion.

Ventilation is one of the key features that can be exploited to increase the safety of the Yucca Mountain Site as a potential repository. Ventilation can remove substantial amounts of moisture from the drift walls in a very short period of time. It has been demonstrated in various experiments (Such as Ed Week's observations at UZ-6, and Nye County's observations in the ESF tunnel) that substantial amounts of moisture can be removed from the rocks in the mountain by natural convection due to topographic relief and thermal gradients. In many hillside mines, natural ventilation is the only means of supplying large amounts of air to these mines. Therefore, by considering a naturally ventilated repository (after construction) and taking advantage of the thermal drive of the waste package, the

repository may be kept dry during at least the first 1000 years, if not longer. The amount of moisture removed from the rocks during this time will create a thick low-saturation skin around the drifts that will require thousands of years to re-saturate. Ventilation can also remove large amounts of heat generated by the waste canisters.

In case of the TSPA 95's proposed approach, there is very little moisture removal from the system and re-saturation can occur much more rapidly than the ventilated case. In an unventilated case (backfilled repository), the moisture is just forced away from the repository. It has no place to go except for a little atmospheric ventilation along the Solitario Canyon. The moisture is trapped under an umbrella that will eventually return and re-wet the repository.

Of course, there are many other issues that need to be considered in a naturally ventilated repository such as the repository security, seismic stability, etc. such aspects need to be studied carefully.

6.2 SHORT TERM SIMULATIONS OF EXISTING TUNNEL DATA

ESF tunnel climatological data have only been available since August 1995 and only from the Nye County's monitoring program. During the present analysis no ESF climatological data from the Yucca Mountain project was available. Data collection activities by DOE contractors is underway. Nye County is also planning to install additional instrument stations to obtain the necessary data.

The purpose of these data collection activities is to develop an understanding of the interaction of the tunnel atmosphere with the repository host rock. As will be discussed, parameters of primary importance are the eddy diffusivity of the tunnel atmosphere, the hydraulic and pneumatic properties of the host rock, and thermal properties of the host rock.

A good set of ventilation flow-rate data was not available for the analysis that are presented here. Estimated ventilation flow rates vary between 1700 to 2265 cubic meters per minute (60,000 to 80,000 cubic feet per minute). The simulations are further simplified by assuming a constant atmospheric temperature, pressure, and humidity outside the tunnel. Further simulations are underway that will take these variations into consideration.

6.2.1 SIMULATION SETUP

The purpose of the simplified simulations performed for this section was to evaluate the reasonableness of the parameters used and the conceptual settings of the model.

6.2.1.1 MESH

The mesh for the simulations is shown in Figure 6-1. It consists of an axi-symmetric arrangement of the nodes. The tunnel is in a horizontal direction. No gravity is used in this mesh; therefore, the fluid flows are due to pressure gradients only. Because of the strong influence of the ventilation flow, the error introduced by ignoring gravitational forces is negligible. However, gravitational effects are expected to enhance ventilation due to buoyancy. More realistic simulations will be performed which will require three-dimensional discretization of the mesh.

The axi-symmetric mesh consists of 16 row of nodes along the tunnel which add up to about 560 meters. Each node represents a cylinder with its axis along the center of the tunnel as shown in Figure 6-1. The mesh has 20 of these concentric cylinders. The first five concentric cylinders represent the tunnel. The rest of the cylinders represent the surrounding rock.

In the forced-ventilation simulation case, the last set of concentric cylinders (at 560 m from the portal) were set to represent the rock which simulates a dead-end tunnel. This special case evaluated an existing condition which was used for

comparison with the observed data collected by Nye County since August 1995. The mesh extends to a radius of 300 meters.

6.2.1.2 INPUT PARAMETERS

The tunnel nodes have atmospheric properties. Table 6-1 summarizes some of the important input parameters. It should be noted that A-TOUGH, unlike other TOUGH family of codes, does not allow liquid flow in the tunnel nodes or between the tunnel nodes and the rock. Only vapor and air flow are allowed in the tunnel nodes and between the tunnel nodes and the rock. The rock properties are set at an equivalent porous media with permeability of 1×10^{-15} m² and an effective porosity of 35 percent. The initial saturation of 0.95 was assumed for the rock. Initial pressures were set equal to 87470 pascals (12.7 psi) for all the nodes. The pressure in the atmosphere outside the tunnel was kept constant at this value. The initial temperature for all nodes was set at 19 degrees Celsius (66.2 degrees Fahrenheit). The temperature of the atmosphere outside the tunnel was varied for different simulation cases but was kept at an average constant value throughout all simulations. This is not a limitation of the model but a simplification. Future simulations will consider variation of the atmospheric parameters.

6.2.2.1 RESULTS OF THE SIMULATION

This simulation represents a calibration of the model; but because of the many simplifications used for this and other simulations discussed later, calibration is not an appropriate term in the strict sense. What is referred to as calibration simulation here is a simulation setup, in its simple form, which has best reproduced the observed data.

The results of the forced-ventilation simulation are presented in 6-2 through 6-4. Figure 6-2 is a plot of variation of relative humidity with time for one shift of the ESF operation. The ESF ventilation usually begins early on Monday mornings and is shut by late Friday afternoon or Saturday Morning. Ventilation is applied by

pulling air through a ventilation duct that is always open at the working faces. Most of the air is vacuumed from the TBM face where the Nye County climatological monitoring instruments are located. For comparison with the simulation results, data from April 1996 were selected and are shown at the bottom of Figure 6-2. The relative humidity is nearly 100 percent during weekends when the ventilation is not operating. During the operation of the ventilation relative humidity drops down to a level that is determined by several factors. The state of the atmospheric air that enters the tunnel at the portal as a result of the pressure lowering near the TBM face is one of the important factors. The distance of the TBM face from the portal and the moisture content of the veneer of the rock that is in contact with the tunnel air and is in the path of the inflowing air also affect the final humidity state of the air at the TBM face. Another important factor affecting the humidity is the amount and nature of the construction water used near the face. In Figure 6-2, the observed data show many fluctuations that are believed to be primarily due to variations in the ventilation air flow rates but could also be due to other factors.

The simulation results presented in Figure 6-2 show substantial reduction in relative humidity of the tunnel air that varies with distance from the portal. In this simulation (with eddy diffusivity of $0.01 \text{ m}^2/\text{s}$ and atmospheric air of 28 degrees Celsius) the nodes near the tunnel portal are significantly influenced by the atmospheric air entering the tunnel which has a relative humidity of 10 percent (representative of dry desert air in summer time). Near the face of the TBM, the relative humidity drops from 100 to about 80 percent in the first day and gradually increases to about 90 percent before the ventilation shut down. The reason for this gradual rise in humidity is thermal equilibration of the atmospheric air with the host rock. The magnitude of the humidity changes simulated by this model compare well with the observed values. Since eddy diffusivity affects both vapor and thermal fluxes, the results of temperature simulations also need to be examined.

Figure 6-3 shows the result of simulation of the temperature in the tunnel and comparison with the observed temperatures at the TBM. The results are shown for a period of 12 days which was intended to simulate a six-day shut-down period following a week of ventilation. The observed temperatures dropped by about six degrees C. The simulated temperatures show a temperature lowering of about 8 degrees C near the TBM face. The reason for the temperature drop is the latent heat exchange which occurs as the warm and dry air of the desert enters the tunnel and comes in contact with the rock. This process is basically similar to an evaporative cooling effect. Even though the temperature of the air that enters the tunnel is at 28 degrees Celsius and the rock temperature at 19 degrees Celsius, both the rock and air temperatures drop. Eddy diffusivity has a significant effect on this evaporation process. The larger the eddy diffusivity, the larger is the evaporation potential of the flowing air and the larger is the thermal flux. Eddy diffusivity is a parameter that changes with air velocity. In this and subsequent simulations discussed here, eddy diffusivity is kept constant. This is reasonable for the case where ventilation air is relatively constant. Simulations to calibrate for variable eddy diffusivity require accurate flow measurements which are not currently available. Experiments are planned by Nye County to accurately measure and calculate the eddy diffusivity in the ESF tunnel.

The results of the simulated rock capillary pressures for this case are shown in Figure 6-4. These values agree very well with limited measurement made by DOE contractors in the ESF tunnel. The short-term simulations were able to mimic the temperature and humidity changes during ventilation shutdown and startup. Simulated saturation changes extend to depths of more than 3 m in a relatively short period of time. Recent observations made in the ESF tunnel (informal communication with Yucca Mountain Project staff, December, 1995) indicated that a sharp drying front occurred after the ventilation was started. Observations indicated that in the Tiva Canyon Welded Unit, capillary pressures went from -1 bar to -100 bars at about 5 cm, to 50 bars at 10 cm, to 2 bars at 20 cm, and to 1.5

bars at 40 cm (probably background) following 500 hours of ventilation. This translates to a saturation change of 10 to 20 percent in about 20 days. In this unit, temperature dropped from about 20 to 16 degrees Celsius during the same period of time. The simulation predicted a temperature change of about 8 degrees and saturation changes of about 15% at a distance of 10 m from the face of the tunnel. The difference in the observed versus simulated results is due to simplifications made in the model and uncertainty in eddy diffusivity values. In general, it appears that the simplistic setup can reasonably simulate the thermodynamic processes that are involved in ventilation of the ESF.

In order to better conceptualize the eddy diffusivity phenomenon, a schematic drawing of the process is shown in Figure 6-4a. Stagnant air has a very low thermal conductivity. Its vapor diffusion is in the order of $2.13 \times 10^{-5} \text{ m}^2/\text{s}$. In flowing air, both vapor and heat are transferred mostly advectively. The mass and heat transfer perpendicular to the direction of flow of air occurs through mixing that is resulted from development of eddies, as shown in Figure 6-4a. This transfer is substantially greater than that of a stagnant air and is dependent on the velocity of the air and the state of turbulence. In chemical engineering and atmospheric sciences the transfer coefficient is referred to as eddy diffusivity. The principal of flow of both heat and vapor is the same as the Fick's Law but with a dynamic diffusivity coefficient.

6.3 LONG-TERM VENTILATION SIMULATIONS

6.3.1 SIMULATION SETUP

The purpose of the simplified simulations performed for this section was to demonstrate the importance of the natural- and forced-ventilation in controlling the thermodynamic processes in a tunnel. Also, the sensitivity of the results to the magnitude of the eddy diffusivity is evaluated.

Table 6-2 presents a summary of the simulations performed for this task. A total of 11 simulation cases were made using the above described mesh setup. The first six simulations were designed to evaluate the sensitivity of the results of the model to variation of the eddy diffusivity and the atmospheric air temperature. These six cases differ only in the value of eddy diffusivity and the temperature of the atmospheric air entering the tunnel. In these six cases forced-ventilation is used similar to the short-term simulation described above.

Simulation cases seven through nine were performed to evaluate the effect of heat as would be applied by the waste package. However, as a demonstration simulation, an equivalent heat that would be provided by 42 waste packages with a spacing of six meters was considered. In these latter three simulations, a ventilation shaft is used instead of forced-ventilation. The shaft node is the only node that has gravitational forces present. The atmospheric pressure and temperature at both the tunnel portal and the top of the shaft are kept at the same constant value. Therefore, the driving forces for the air movement in the tunnel and along the shaft are the buoyancy caused by the temperature of the waste package, the host rock temperature, and the pressure caused by the weight of the column of air in the shaft (opposing buoyancy). These conditions simulate atmospheric conditions that promote air suction in the wells.

The average temperature of 15 degrees is used, which is conservatively high compared to the average annual temperature at Yucca Mountain. Lower atmospheric air temperature would result in a larger air flow and cooler temperature in the waste area. The atmospheric air was assumed to have an average relative humidity of 10 percent.

Figure 6-19c is a plot of the decaying heat load used for each of the waste nodes. This curve is based on the values presented in the TSPA 95. The values used are for six waste packages; however as noted above, the waste packages are more closely spaced than in the current TSPA design.

Simulation cases 10 and 11 are different from cases 7 through 9 only in the pressure at the top of the shaft that promotes outflow in the shaft (helping the buoyancy). Only two cases of 0.01 and 0.001 eddy diffusivity are used in this case. Thermal load in the tunnel is increased in these two cases by increasing the number of nodes (or grid blocks) with thermal load to 10 instead of six.

6.3.2 RESULTS OF SIMULATIONS WITH FORCED VENTILATION (CASES 1 TO 6)

6.3.2.1 SIMULATIONS

The results of Case 1 with atmospheric air temperature of 15 degrees Celsius are presented in Figures 6-5 through 6-8. The cause of the slight pressure drop in the host rock during the 100-year simulation is the constant forced ventilation at the end of the tunnel. Pressure in the host rock drops by about 25 pascals (approximately 0.004 psi) within the first 25 m radius in about 11 days. Such changes have already been observed in NRG-4 as presented earlier. After 100 years, the pressure in the entire 300-m radial distance is affected by about 225 pa (0.0331 psi). This is not unreasonable, considering the observations and simulations presented for the ESF tunnel-ONC #1 interactions. Pressure results for the next five cases are similar and will not be presented.

Temperature effects are shown in Figure 6-6. The temperature in the entire first 25 m radius of the model drops by at least one degree Celsius. Comparison of the April 1995 with August 1996 temperature data in NRG-4 indicates that probes 4 and 5 which are at the tunnel level have dropped by about one degree Celsius, whereas probes above and below show only about 0.1 to 0.2 degrees decline in temperature. Although these changes in temperature measurements could be due to drift in transducer calibrations, the coincidental trend is unlikely.

The capillary pressure distribution for this case is shown in Figure 6-7. It should be noted that in this figure and in all subsequent plots of capillary pressure, a presentation error is present near the tunnel nodes which is an artifact of the interpolation routine used by the post processor. As was noted earlier, A-TOUGH does not allow liquid flow between the tunnel elements and the host rock. In simulations, the capillary pressure value of the tunnel nodes is reported by the model as zero (an arbitrary value). The post processor uses this value. For this reason the nodes near the center of the tunnel appear wet. The capillary pressures are also presented in a plot of capillary pressure versus time for a set of nodes that are perpendicular to the tunnel and are midway between the portal and the end of the tunnel (Figure 6-7a). It should also be noted that in these simulations the equivalent porous media representation of the host rock is used. Therefore, the capillary pressure and other results represent the variables for a fractured rock system and not the matrix of the rock. The effect of the matrix will be to slow down the drying process. Therefore, the capillary pressures may correspond to slightly wetter conditions than showed by these simulations.

Figure 6-8 presents distribution of the saturation for various times. Corresponding water saturation results are presented in Figure 6-8a. Results of other cases for forced ventilation are shown in Figures 6-9 through 6-18.

In summary, comparison of these six cases indicates that in the long-term, higher outside temperature and larger eddy diffusivity result in an increase in both heat and mass transfer between the host rock and the tunnel air, i.e., a cooler and dryer host rock. The direction of the flow could be different depending on the relative magnitude of the temperature of the two media.

6.3.3 RESULTS OF SIMULATIONS WITH NATURAL VENTILATION (CASES 7, 8, 10, AND 11)

Figure 6-19a and 6-19b conceptually show the condition that these simulation represent. A naturally ventilated repository would have a more complex set of shafts and tunnels that would be designed to optimize the flow of air. In figure 6-19a, simplified equations are used to conceptually show the pressure differences at the entrance and at the bottom of the shaft. The more accurate equations are in integral forms because the density of air changes with elevation. In these three cases, however, the pressure at the top of the shaft (P_{atm}) was set equal to the pressure at the entrance (P_2). Figure 6-19c shows the heat load used for this set of simulations.

The results of these simulations are shown in Figures 6-20 Through 6-27. Comparison of pressure distribution for the heated cases in Figures 6-20 and 6-24 indicates that the pressure distribution is similar between the three cases. An increase in pressure at the end of the tunnel near the shaft (lower left corner of the graphs) is due to the column of air in the shaft. Because the pressure at the top of the shaft is set at the same pressure as the atmosphere at the tunnel portal.

Figures 6-21 and 6-25 show the temperature distribution for Cases 7 and 8. Case 9 produces higher temperatures similar to the TSPA 95 cases and the results are not presented here. In both Cases 7 and 8, the temperature of the repository approaches that of the atmospheric temperature of 15 °C after 10,000 years. Significant differences are noted in the first 10 years. In Case 7 the eddy diffusivity of 0.01 (m²/s) results in a much faster cooling effect than in the other two cases. The hot spot (temperatures in the rock nodes adjacent to tunnel; see Figures 6-21a and 6-25a) reaches about 20 °C in Case 7 and 22.5 °C in Case 8. The flow rate through the shaft in all these cases is about 1130 m³/min (40,000 cfm). In the worst case, the temperature of the air near the canister reaches 130 °C and drops to 45 °C after 100 years. However, these simulations predict that the temperature

of the air in the tunnel near the rock remains within 15 to 20 °C. In these three cases, radiation heat flux is not considered. In Cases 10 and 11, radiative heat flux is included in the simulations.

Figures 6-22, 6-22a, 6-26, and 6-26a are plots of the absolute values of the capillary pressure with time for Cases 7 and 8. In all cases, absolute values of the capillary pressure increase with time. More importantly, the gradients of the capillary pressure are such that the flow of water is towards the tunnel. These gradients are strongest for Case 7 with eddy diffusivity of 0.01 m²/s and decline as the smaller eddy diffusivity is used for simulations.

Saturation values (Figures 6-23, 6-23a, 6-27, and 6-27a) follow the capillary pressure trends, as expected. Saturation values decline to about 60 percent after 10,000 years in case 7 and to about 70 percent for Case 8. It is noticeable that in Case 7, the rock nodes near the tunnel become dry after 1000 years.

Figure 6-32 is a plot of the thermal load for the Cases 10 and 11. As noted earlier, in these two cases, the outside pressures are set to correspond to natural atmospheric pressures. That is the pressure at the top of the shaft is smaller than the pressure at the tunnel portal. The pressure difference was calculated by considering the elevation difference of the two points and the density of the air at 15 °C temperature. In these cases eddy diffusivities of 0.01 and 0.001 were used.

Simulated pressure results are shown in Figure 6-33. Pressure distribution is about the same for both cases. In these cases, a lower pressure at the end of the tunnel (bottom of the shaft) is noticed. This is due to lower density of air in the shaft that is carrying a warmer air to the surface. Pressure distribution after 10,000 years represents a steady state condition that is equilibrated between the outside pressure and the pressure in the tunnels. At this time, the pressure at the bottom of the shaft is influenced by the temperature distribution in the tuff cylinder.

The temperature distribution for Case 10 is shown in Figure 6-34 for various times. A temperature gradient is still present after 10,000 years when the temperature in the tuff cylinder has begun to equilibrate with the atmospheric temperature of 15 °C. The hot spot in the tunnel near the waste package reaches a maximum of 33 °C. The rock temperature near the tunnel continues to drop below 10 °C until after about 2 years when it rises back to approach 15 °C (see figure 6-37). The reason for continued drop of the rock temperature is the air current that is caused by the presence of the heat source (waste canisters). As the heat source weakens, the air current in the tunnel also declines in rate. As a result, there is less evaporative cooling and the rock temperature climbs to equilibrate with the atmospheric temperature. This pattern can also be observed in the saturation curve in Figures 6-36 and 6-38. Capillary pressure gradients remain directed towards the tunnel at all times (Figure 6-35).

Results of Case 11 are shown in Figures 6-39 through 6-42. As expected, temperature values rise to a higher level in this case (Figure 6-39). The air in the vicinity of the tunnel reaches a maximum temperature value of 75 °C and declines slowly to about 62 °C in the first 20 years (Figure 6-41). From then, it declines to a temperature of about 16 °C. The rock node in the vicinity of the tunnel drops down from 19 °C (initial conditions) to about 6 °C and then rises to approach an equilibrium temperature of 15 °C. Saturation of the rock (Figure 6-42) in the vicinity of the tunnel drops down to a dry state at 2000 years and remains dry for the duration of the 10,000-year simulation.

In summary, the data collected from the ESF tunnel indicate that there is substantial temperature and moisture loss from the rock surface as a result of ventilation air. Simulation of the existing conditions suggest that an eddy diffusivity value of between 0.001 and 0.01 m²/s is an appropriate value for flow rates between 1132 and 2830 m³/min (40,000 and 100,000 cfm). Long-term simulations and calibration with the data from NRG-4 provided thermal

conductivity and air permeability values that were needed for simulation of the heated conditions. Strong air currents may be produced by natural ventilation. Application of the natural ventilation aided by the heat source may provide a cool and dry host rock with a moisture gradient that will be toward the emplacement tunnels during the first 10,000 years.

It is realized that these simulations are very simplistic and many other factors need to be considered. No infiltration was used in these simulations. The amount of bulk infiltration is negligible compared to the amount of moisture that is removed by the natural ventilation. However, pulse infiltration at fault zones and areas near Ptn may result in more water inflow into the tunnel than can be handled by the natural infiltration. Engineering of an open repository will be complicated and need special study.

The presentation of the results of these simulations is intended to generate interest in this potential alternative waste emplacement. The results should not be used as any design criteria or for any decision making about the waste disposal.

Table 6-1 Material Properties Used For Simulation of Ventilation Effects

Material Name	Density (kg/m ³)	Porosity	Saturated Viscosity (m ² /s)	Saturated Conductivity (W/m°C)	Saturated Heat (W/m°C)	Compressibility (1/K)	Expansion Coefficient (1/K)	Contraction Factor	Heat Capacity (J/kg°C)	Latent Heat (J/kg)	Viscosity (Pa)	Prandtl Number	Slope
ROCK1	2650	0.342	10 ⁻¹⁵	2.4	1255	0	0	0.66	0.4438	0.08	5.67 × 10 ⁷	10 ⁷	1.001
ATMOS	-	0.99	5 × 10 ⁻⁶	0.021	1000	10 ⁻⁵	0	0	-	-	-	-	-

Table 6-2 - Summary of simulation setup for evaluation of natural ventilation effects

CASE	Eddy Diffusivity/Air-to-ground Ratio (m ² /s)	Airspeed at Ground (m/s)	Initial Heat Load (kW)	Total Run Time (Seconds)	Initial Rock Temp. (°C)
1	0.01	15	0	100	19
2	0.01	28	0	100	19
3	0.001	15	0	100	19
4	0.001	28	0	100	19
5	0.0001	15	0	100	19
6	0.0001	28	0	100	19
7	0.01	15	360	10000	19
8	0.001	15	360	10000	19
9	0.0001	15	360	10000	19
10	0.01	15	445	10000	19
11	0.001	15	445	10000	19

7.0 EVALUATION OF THE USE OF WATER IN THE TUNNEL

Recently, Nye County's Nuclear Waste Repository Project team visited the Exploratory Studies Facility (ESF) tunnel. One of the observations made by the team was related to the water usage in the tunnel. Nye County has observed on several occasions standing water throughout the entire length of the tunnel boring machine (TBM) and its attachments. Also it has noted that water spraying with a high pressure hose is routinely being used by the miners to wash the walk ways and other seemingly unnecessary areas. Furthermore, recent evaluation of the report on chlorine 36 has revealed that majority of the samples were contaminated with the J-13 water (tagged with lithium bromide) which is the main source of the ESF tunnel water. It is noteworthy that these samples have been taken at least 10 cm into the rock and from the walls of the tunnel which are not subjected to standing water and are only sprayed for cleaning purposes. Nye County has recently performed preliminary mass balance calculations to evaluate the water usage in the tunnel. These calculations augment previous Nye County work on the impact of ventilation on water removal from the ESF.

Daily water usage from March through June 1996 has been provided by the ESF personnel. Nye County has been continuously monitoring pressure, temperature, and humidity near the TBM through the instrumentation installed by the County.

Comparison of the water usage and water removed from the tunnel is graphically depicted in Figure 7-1. The total amount of water used between March 25 and May 29 is shown in Table 7-1 along with the calculated amount of water removed by ventilation.

Table 1 - Estimated water usage in the ESF tunnel from March 25 to May 29, 1996. All values in gallons.

Total water used	Total water estimated to be removed by ventilation	Amount of water unaccounted for	Error due to unknown working days
2,117,325	628,537	1,488,788	-16,926

It is evident that about 1.5 million gallons of water is not accounted for by ventilation. Unknown amounts of water are being removed by the "muck"; however, the fact that there is always standing water in the tunnel indicates that ventilation and mucking lead to incomplete water removal. It is conceivable that with time the standing water behind the TBM will dry up; however, until this standing water is totally evaporated, the downward infiltration potential is great. Infiltration occurs as a result of the head of the standing water and by the change in the capillary-pressure differential on the rock surface. The TSWU in its natural state has a capillary pressure of a few tens of bars. Changing the capillary pressure of the surface of the rock to zero (by wetting), can induce substantial capillary pressure differential which will lead to infiltration of water into the host rock. Of most concern is the water that enters the fracture system. The water that enters the fracture system, may flow beyond depths that neither evaporation nor the heat of the waste could retrieve in a short period of time. Such fluxes may need to be considered in the pre-waste emplacement travel time calculations from the disturbed zone to the accessible environment. Aside from regulatory implications, such flows can have impact on the radionuclide transport.

Assume that only 10 percent of the water unaccounted for penetrates the rock. This is about 150,000 gallons. In the 65 days, assume that 1300 ft of tunnel is excavated. Therefore, for a width of 10 feet of the bottom of the tunnel, this water

is applied to a 13000 ft² area. Simple calculations show that approximately 1.5 ft of water infiltrates the rock. That is equivalent to an infiltration rate in excess of 2000 mm/yr. It is evident that even if it is assumed that only 0.1 percent of the unaccounted water (1500 gallons) has infiltrated the rock, it equates to a 20 mm/yr infiltration rate. The mountain has never seen such infiltration rates based on the analyses that have been documented by the DOE contractors.

In order to demonstrate the significance of the wet surfaces in the tunnel, a simple conceptual numerical model of the situation was setup. The conceptual model was 5 meters wide by 25 meters deep as shown in Figure 7-2. A vertical fracture zone of about 0.5 meter thickness was placed in the middle of the model. The properties of this fracture zone are equivalent to a broken Topopah Springs Welded Unit. The surrounding rock has the properties of the matrix of this unit. The floor of the tunnel was kept wet (at a 95% saturation) for the entire duration of simulation. Evaporation equivalent to that induced by the ventilation was imposed at the tunnel floor. The rock matrix was initially set at 65% saturation and that of the fracture zone was set at 20% saturation (to simulate a drained fracture). The wetting (saturation) front in the fracture travels a distance of 10 m (30 ft) in about 0.003 days (4 minutes, Figure 7-3). After this time, the wetting front travels at a relatively slower rate. However, after 8 days it reaches the lower boundary of this model which is at 20 meters (66 feet) below the floor of the tunnel.

Although this model is very simplified, it demonstrates the potential for propagation of even a slight wetness in a fractured zone.

Table 7-2 Water usage history in the ESF tunnel.

DATE	BEGIN STATION	END STATION	END STATION	STRATIGRAPHY	ADVANCE	ADVANCE	Cumulative ESF Advancement	DAILY WATER	CUMULATIVE WATER USAGE TO DATE	COMMENTS
	(METERS)	(FEET)	(METERS)		(METERS)	(FEET)	(FEET)	USAGE (GALLONS)	1000s of gal	
1-Jan-95	1 + 01.4	1 + 01.4		Tiva Canyon crystal poor middle nonlithophysal zone	0	0	0		0	
2-Jan-95	1 + 01.4	1 + 01.4		Tiva Canyon crystal poor middle nonlithophysal zone	0	0	0		0	
3-Jan-95	1 + 01.4	1 + 06.9		Tiva Canyon crystal poor middle nonlithophysal zone			0		0	
4-Jan-95	1 + 06.9	1 + 08.2		Tiva Canyon crystal poor middle nonlithophysal zone	1.3	4.3	4.3		0	
5-Jan-95	1 + 08.2	1 + 16.9		Tiva Canyon crystal poor middle nonlithophysal zone	8.7	28.5	32.8		0	
6-Jan-95	1 + 16.9	1 + 23.9	406.5	Tiva Canyon crystal poor middle nonlithophysal zone	2.3	7.7	40.5		0	
7-Jan-95	1 + 23.9	1 + 23.9	406.5	Tiva Canyon crystal poor middle nonlithophysal zone	0	0	40.5		0	
8-Jan-95	1 + 23.9	1 + 23.9	406.5	Tiva Canyon crystal poor middle nonlithophysal zone	0	0	40.5		0	
9-Jan-95	1 + 23.9	1 + 31.7	432.1	Tiva Canyon crystal poor middle nonlithophysal zone	2.6	8.5	49		0	
10-Jan-95	1 + 31.7	1 + 35.2	443.6	Tiva Canyon crystal poor middle nonlithophysal zone	3.4	11.2	60.2		0	
11-Jan-95	1 + 35.2	1 + 36.5	447.8	Tiva Canyon crystal poor middle nonlithophysal zone	1.3	4.3	64.5		0	
12-Jan-95	1 + 36.5	1 + 36.5	447.8	Tiva Canyon crystal poor middle nonlithophysal zone	0	0	64.5		0	
13-Jan-95	1 + 36.5	1 + 36.5	447.8	Tiva Canyon crystal poor middle nonlithophysal zone	0	0	64.5		0	
14-Jan-95	1 + 36.5	1 + 36.5	447.8	Tiva Canyon crystal poor middle nonlithophysal zone	0	0	64.5		0	
15-Jan-95	1 + 36.5	1 + 36.5	447.8	Tiva Canyon crystal poor middle nonlithophysal zone	0	0	64.5		0	
16-Jan-95	1 + 36.5	1 + 36.5	447.8	Tiva Canyon crystal poor middle nonlithophysal zone	0	0	64.5		0	
17-Jan-95	1 + 36.5	1 + 44.8	475.1	Tiva Canyon crystal poor middle nonlithophysal zone	8.3	27.2	91.7		0	
18-Jan-95	1 + 44.8	1 + 51.3	496.4	Tiva Canyon crystal poor middle nonlithophysal zone	6.5	21.3	113		0	
19-Jan-95	1 + 51.3	1 + 55.3	509.5	Tiva Canyon crystal poor middle nonlithophysal zone	2	6.6	119.6		0	
20-Jan-95	1 + 55.3	1 + 66.2	545.3	Tiva Canyon crystal poor middle nonlithophysal zone	3.6	11.9	131.5		0	
21-Jan-95	1 + 66.2	1 + 66.2	545.3	Tiva Canyon crystal poor middle nonlithophysal zone	0	0	131.5		0	
22-Jan-95	1 + 66.2	1 + 66.2	545.3	Tiva Canyon crystal poor middle nonlithophysal zone	0	0	131.5		0	
23-Jan-95	1 + 66.2	1 + 74.9	573.8	Tiva Canyon crystal poor middle nonlithophysal zone	8.7	28.5	160		0	
24-Jan-95	1 + 74.9	1 + 82.5	598.8	Tiva Canyon crystal poor middle nonlithophysal zone	7.6	24.9	184.9		0	
25-Jan-95	1 + 82.5	1 + 87.1	613.8	Tiva Canyon crystal poor middle nonlithophysal zone	4.6	15.1	200		0	
26-Jan-95	1 + 87.1	1 + 88.9	619.8	Tiva Canyon crystal poor middle nonlithophysal zone	1.8	5.9	205.9		0	
27-Jan-95	1 + 88.9	1 + 88.9	619.8	Tiva Canyon crystal poor middle nonlithophysal zone	0	0	205.9		0	
28-Jan-95	1 + 88.9	1 + 88.9	619.8	Tiva Canyon crystal poor middle nonlithophysal zone	0	0	205.9		0	
29-Jan-95	1 + 88.9	1 + 88.9	619.8	Tiva Canyon crystal poor middle nonlithophysal zone	0	0	205.9		0	
30-Jan-95	1 + 88.9	1 + 98.0	649.6	Tiva Canyon crystal poor lower lithophysal zone	9.1	29.8	235.7		0	
31-Jan-95	1 + 98.0	1 + 98.0	649.6	Tiva Canyon crystal poor lower lithophysal zone	0	0	235.7		0	BOW RIDGE FAULT
1-Feb-95	1 + 98.0	1 + 98.0	649.6	Tiva Canyon crystal poor lower lithophysal zone	0	0	235.7		0	CONCRETE BOW RIDGE FAULT VOID
2-Feb-95	1 + 98.0	1 + 98.0	649.6	Tiva Canyon crystal poor lower lithophysal zone	0	0	235.7		0	CONCRETE BOW RIDGE FAULT VOID
3-Feb-95	1 + 98.0	1 + 98.0	649.6	Tiva Canyon crystal poor lower lithophysal zone	0	0	235.7		0	CONCRETE BOW RIDGE FAULT VOID
4-Feb-95	1 + 98.0	1 + 98.0	649.6	Tiva Canyon crystal poor lower lithophysal zone	0	0	235.7		0	
5-Feb-95	1 + 98.0	1 + 98.0	649.6	Tiva Canyon crystal poor lower lithophysal zone	0	0	235.7		0	
6-Feb-95	1 + 98.0	2 + 01.9	662.4	Bow Ridge fault zone	3.9	12.8	248.5		0	
7-Feb-95	2 + 01.9	2 + 01.9	662.4	Bow Ridge fault zone	0	0	248.5		0	SHOTCRETE VOIDS/BEARING SURFACE
8-Feb-95	2 + 01.9	2 + 04.9	672.2	pre-Ranier Mesa Tuff	3	9.8	258.3		0	
9-Feb-95	2 + 04.9	2 + 06.0	675.8	pre-Ranier Mesa Tuff	1.1	3.6	261.9		0	
10-Feb-95	2 + 06.0	"	"	pre-Ranier Mesa Tuff			261.9		0	WEEKEND REPORT
11-Feb-95	"	2 + 11.6	694.2	pre-Ranier Mesa Tuff	5.6	18.4	280.3		0	WEEKEND REPORT
12-Feb-95	2 + 11.6	2 + 11.6	694.2	pre-Ranier Mesa Tuff			280.3		0	
13-Feb-95	2 + 11.6	2 + 15.9	709.3	pre-Ranier Mesa Tuff	4.3	14.1	294.4		0	THRU BOW RIDGE FAULT
14-Feb-95	2 + 15.9	2 + 26.8	744.1	pre-Ranier Mesa Tuff	10.9	35.8	330.2		0	
15-Feb-95	2 + 26.8	2 + 38.8	?	pre-Ranier Mesa Tuff	12	39.4	369.6		0	
16-Feb-95	2 + 38.8	2 + 50.0	762.2	pre-Ranier Mesa Tuff	11.2	36.7	406.3		0	
17-Feb-95	2 + 50.9	"	"	pre-Ranier Mesa Tuff			406.3		0	N/REPORT

Table 7-2 Water usage history in the ESF tunnel.

DATE	BEGIN STATION	END STATION	END STATION	STRATIGRAPHY	ADVANCE	ADVANCE	CUMMULATIVE ESF ADVANCEMENT	DAILY WATER	CUMULATIVE WATER USAGE TO DATE	COMMENTS
18-Feb-95	**	2 + 70.9	826	Tuff "X"	20	0	406.3		0	
19-Feb-95	2 + 70.9	2 + 70.9	826	Tuff "X"	0	0	406.3		0	
20-Feb-95	2 + 70.9	2 + 73.0	895.7	Tuff "X"	2.1	6.9	413.2		0	
21-Feb-95	2 + 73.0	2 + 82.8	927.8	Tuff "X"	9.8	32.1	445.3		0	
22-Feb-95	2 + 82.8	2 + 93.5	962.9	Tuff "X"	10.7	35.1	480.4		0	
23-Feb-95	2 + 93.5	3 + 12.2	1024.3	Tuff "X"	18.7	61.4	541.8		0	
24-Feb-95	3 + 12.2	3 + 20.2	1050.5	Tuff "X"	8	26.2	568		0	
25-Feb-95	3 + 20.2	3 + 20.2	1050.5	Tuff "X"	0	0	568		0	
26-Feb-95	3 + 20.2	3 + 20.2	1050.5	Tuff "X"	0	0	568		0	
27-Feb-95	3 + 20.2	3 + 38.1	1109.3	pre-Tuff "X"	17.9	58.7	626.7		0	
28-Feb-95	3 + 38.1	3 + 49.1	1148.4	pre-Tuff "X"	11	36.1	662.8		0	
1-Mar-95	3 + 49.1	3 + 56.4	1169.3	Tiva Canyon vitric zone	7.3	23.9	686.7		0	
2-Mar-95	3 + 56.4	3 + 67.8	1206.7	Tiva Canyon crystal rich nonlithophysal zone	11.4	37.4	724.1		0	
3-Mar-95	3 + 67.8	3 + 67.8	1206.7	Tiva Canyon crystal rich nonlithophysal zone	0	0	724.1		0	NO TBM OPERATION - MECH. FAIL
4-Mar-95	3 + 67.8	3 + 67.8	1206.7	Tiva Canyon crystal rich nonlithophysal zone	0	0	724.1		0	NO TBM OPERATION - MECH. FAIL
5-Mar-95	3 + 67.8	3 + 67.8	1206.7	Tiva Canyon crystal rich nonlithophysal zone	0	0	724.1		0	NO TBM OPERATION - MECH. FAIL
6-Mar-95	3 + 67.8	3 + 67.8	1206.7	Tiva Canyon crystal rich nonlithophysal zone	0	0	724.1		0	NO TBM OPERATION - MECH. FAIL
7-Mar-95	3 + 67.8	3 + 71.6	1219.2	Tiva Canyon crystal rich nonlithophysal zone	3.8	12.6	736.7		0	
8-Mar-95	3 + 71.6	3 + 77.1	1237.2	Tiva Canyon crystal rich nonlithophysal zone	5.5	18	754.7		0	
9-Mar-95	3 + 77.1	3 + 94.6	1294.6	Tiva Canyon crystal rich nonlithophysal zone	17.5	57.4	812.1		0	
10-Mar-95	3 + 94.6	4 + 10.8	1347.8	Tiva Canyon crystal rich nonlithophysal zone	16.2	53.1	865.2		0	
11-Mar-95	4 + 10.8	4 + 10.8	1347.8	Tiva Canyon crystal rich nonlithophysal zone	0	0	865.2		0	
12-Mar-95	4 + 10.8	4 + 10.8	1347.8	Tiva Canyon crystal rich nonlithophysal zone	0	0	865.2		0	HIGH WATER AT FORTY MILE WASH
13-Mar-95	4 + 10.8	4 + 26.8	1400.3	Tiva Canyon crystal rich nonlithophysal zone	16	52.5	917.7		0	
14-Mar-95	4 + 26.8	4 + 37.6	1435.7	Tiva Canyon crystal rich lithophysal zone	10.8	35.4	953.1		0	
15-Mar-95	4 + 37.6	4 + 44.6	1458.7	Tiva Canyon crystal poor upper lithophysal zone	7	23	976.1		0	
16-Mar-95	4 + 44.6	4 + 51.9	1482.6	Tiva Canyon crystal poor upper lithophysal zone	7.3	24	1000.1		0	
17-Mar-95	4 + 51.9	4 + 63.8	1521.7	Tiva Canyon crystal poor upper lithophysal zone	11.9	39	1039.1		0	
18-Mar-95	4 + 63.8	4 + 63.8	1521.7	Tiva Canyon crystal poor upper lithophysal zone	0	0	1039.1		0	
19-Mar-95	4 + 63.8	4 + 63.8	1521.7	Tiva Canyon crystal poor upper lithophysal zone	0	0	1039.1		0	
20-Mar-95	4 + 63.8	4 + 77.4	1566.3	Tiva Canyon crystal poor upper lithophysal zone	13.6	44.6	1083.7		0	
21-Mar-95	4 + 77.4	4 + 91.4	1612.2	Tiva Canyon crystal poor upper lithophysal zone	4.7	15.3	1099		0	
22-Mar-95	4 + 91.4	4 + 93.7	1619.8	Tiva Canyon crystal poor upper lithophysal zone	2.3	7.5	1106.5		0	
23-Mar-95	4 + 93.7	5 + 06.4	1661.4	Tiva Canyon crystal poor upper lithophysal zone	12.7	41.7	1148.2		0	
24-Mar-95	5 + 06.4	5 + 15.7	1691.9	Tiva Canyon crystal poor upper lithophysal zone	9.3	30.5	1178.7		0	
25-Mar-95	5 + 15.7	5 + 15.7	1691.9	Tiva Canyon crystal poor upper lithophysal zone	0	0	1178.7		0	
26-Mar-95	5 + 15.7	5 + 15.7	1691.9	Tiva Canyon crystal poor upper lithophysal zone	0	0	1178.7		0	
27-Mar-95	5 + 15.7	5 + 30.4	1740.2	Tiva Canyon crystal poor upper lithophysal zone	14.7	48.2	1226.9		0	
28-Mar-95	5 + 30.4	5 + 38.9	1768	Tiva Canyon crystal poor upper lithophysal zone	8.5	27.9	1254.8		0	
29-Mar-95	5 + 38.9	5 + 46.0	1791.3	Tiva Canyon crystal poor upper lithophysal zone	3.6	11.6	1266.4		0	
30-Mar-95	5 + 46.0	5 + 48.6	1799.9	Tiva Canyon crystal poor upper lithophysal zone	2.6	8.5	1274.9		0	
31-Mar-95	5 + 48.6	5 + 49.4	1802	Tiva Canyon crystal poor upper lithophysal zone	0.8	2.6	1277.5		0	
1-Apr-95	5 + 49.4	5 + 49.4	1802	Tiva Canyon crystal poor upper lithophysal zone	0	0	1277.5		0	
2-Apr-95	5 + 49.4	5 + 49.4	1802	Tiva Canyon crystal poor upper lithophysal zone	0	0	1277.5		0	
3-Apr-95	5 + 49.4	5 + 51.7	1810	Tiva Canyon crystal poor upper lithophysal zone	2.3	7.5	1285		0	
4-Apr-95	5 + 51.7	5 + 52.2	1811.7	Tiva Canyon crystal poor upper lithophysal zone	0.5	1.6	1286.6		0	
5-Apr-95	5 + 52.2	5 + 52.2	1811.7	Tiva Canyon crystal poor upper lithophysal zone	0	0	1286.6		0	
6-Apr-95	5 + 52.2	5 + 53.5	1815.9	Tiva Canyon crystal poor middle nonlithophysal zone	1.3	4.3	1290.9		0	
7-Apr-95	5 + 53.5	5 + 53.5	1817.3	Tiva Canyon crystal poor middle nonlithophysal zone	0.4	1.3	1292.2		0	
8-Apr-95	5 + 53.5	5 + 53.5	1817.3	Tiva Canyon crystal poor middle nonlithophysal zone	0	0	1292.2		0	

Table 7-2 Water usage history in the ESF tunnel.

DATE	BEGIN STATION	END STATION	STRATIGRAPHY	ADVANCE	ADVANCE	Cumulative ESF Advancement	DAILY WATER	CUMULATIVE WATER USAGE TO DATE	COMMENTS
9-Apr-95	5 + 53.5	5 + 53.9	Tiva Canyon crystal poor middle non lithophysal zone	0	0	1292.2		0	
10-Apr-95	5 + 53.9	5 + 54.2	Tiva Canyon crystal poor middle non lithophysal zone	0.3	1	1293.2	0	0	
11-Apr-95	5 + 54.2	5 + 54.2	Tiva Canyon crystal poor middle non lithophysal zone	0	0	1293.2	2,750	3	
12-Apr-95	5 + 54.2	5 + 54.2	Tiva Canyon crystal poor middle non lithophysal zone	0	0	1293.2	4,010	7	
13-Apr-95	5 + 54.2	5 + 54.2	Tiva Canyon crystal poor middle non lithophysal zone	0	0	1293.2	1,040	8	
14-Apr-95	5 + 54.2	5 + 54.2	Tiva Canyon crystal poor middle non lithophysal zone	0	0	1293.2	2,910	11	72 HR REPORT - WEEKEND
15-Apr-95	5 + 54.2	5 + 54.2	Tiva Canyon crystal poor middle non lithophysal zone	0	0	1293.2	40	11	72 HR REPORT - WEEKEND
16-Apr-95	5 + 54.2	5 + 54.2	Tiva Canyon crystal poor middle non lithophysal zone	0	0	1293.2	0	11	72 HR REPORT - WEEKEND
17-Apr-95	5 + 54.2	5 + 55.9	Tiva Canyon crystal poor middle non lithophysal zone	1.7	5.5	1298.7	1,700	12	
18-Apr-95	5 + 55.9	5 + 57.8	Tiva Canyon crystal poor middle non lithophysal zone	1.9	6.2	1304.9	1,410	14	
19-Apr-95	5 + 57.8	5 + 61.7	Tiva Canyon crystal poor middle non lithophysal zone	3.9	12.8	1317.7	3,220	17	
20-Apr-95	5 + 61.7	5 + 66.9	Tiva Canyon crystal poor middle non lithophysal zone	5.2	17.1	1334.8	3,630	21	
21-Apr-95	5 + 66.9	5 + 76.6	Tiva Canyon crystal poor middle non lithophysal zone	9.7	31.8	1366.6	4,300	25	
22-Apr-95	5 + 76.6	5 + 76.6	Tiva Canyon crystal poor middle non lithophysal zone	0	0	1366.6	0	25	
23-Apr-95	5 + 76.6	5 + 76.6	Tiva Canyon crystal poor middle non lithophysal zone	0	0	1366.6	0	25	
24-Apr-95	5 + 76.6	5 + 86.0	Tiva Canyon crystal poor middle non lithophysal zone	9.4	30.8	1397.4	6,420	31	
25-Apr-95	5 + 86.0	5 + 97.2	Tiva Canyon crystal poor lower lithophysal zone	11.2	36.7	1434.1	6,400	38	
26-Apr-95	5 + 97.2	6 + 09.2	Tiva Canyon crystal poor lower lithophysal zone	12	39.4	1473.5	6,080	44	
27-Apr-95	6 + 09.2	6 + 21.2	Tiva Canyon crystal poor lower lithophysal zone	12	39.4	1512.9	3,920	48	
28-Apr-95	6 + 21.2	6 + 33.9	Tiva Canyon crystal poor lower lithophysal zone	12.7	41.7	1554.6	3,870	52	
29-Apr-95	6 + 33.9	6 + 33.9	Tiva Canyon crystal poor lower lithophysal zone	0	0	1554.6	340	52	
30-Apr-95	6 + 33.9	6 + 33.9	Tiva Canyon crystal poor lower lithophysal zone	0	0	1554.6	0	52	
1-May-95	6 + 33.9	6 + 48.1	Tiva Canyon crystal poor lower lithophysal zone	14.2	46.6	1601.2	6,550	59	
2-May-95	6 + 48.1	6 + 55.2	Tiva Canyon crystal poor lower lithophysal zone	7.1	23.3	1624.5	4,490	63	
3-May-95	6 + 55.2	6 + 64.6	Tiva Canyon crystal poor lower lithophysal zone	9.4	30.8	1655.3	5,580	69	
4-May-95	6 + 64.6	6 + 73.9	Tiva Canyon crystal poor lower lithophysal zone	9.3	30.5	1685.8	5,100	74	
5-May-95	6 + 73.9	6 + 80.6	Tiva Canyon crystal poor lower lithophysal zone	6.7	22	1707.8	3,265	77	
6-May-95	6 + 80.6	6 + 80.6	Tiva Canyon crystal poor lower lithophysal zone	0	0	1707.8	11,585	89	
7-May-95	6 + 80.6	6 + 80.6	Tiva Canyon crystal poor lower lithophysal zone	0	0	1707.8	0	89	
8-May-95	6 + 80.6	6 + 87.3	Tiva Canyon crystal poor lower lithophysal zone	6.7	22	1729.8	3,170	92	
9-May-95	6 + 87.3	6 + 97.1	Tiva Canyon crystal poor lower lithophysal zone	9.9	32.5	1762.3	5,160	97	
10-May-95	6 + 97.1	7 + 09.4	Tiva Canyon crystal poor lower non lithophysal zone	12.3	40.4	1802.7	5,130	102	
11-May-95	7 + 09.4	7 + 24.2	Tiva Canyon crystal poor lower non lithophysal zone	14.8	48.6	1851.3	5,730	108	
12-May-95	7 + 24.2	7 + 41.5	Tiva Canyon crystal poor lower non lithophysal zone	17.3	56.8	1908.1	5,730	114	
13-May-95	7 + 41.5	7 + 41.5	Tiva Canyon crystal poor lower non lithophysal zone	0	0	1908.1	14,410	128	
14-May-95	7 + 41.5	7 + 41.5	Tiva Canyon crystal poor lower non lithophysal zone	0	0	1908.1	0	128	
15-May-95	7 + 41.5	7 + 50.9	Tiva Canyon crystal poor lower non lithophysal zone	9.4	30.8	1938.9	3,810	132	
16-May-95	7 + 50.9	7 + 62.7	Tiva Canyon crystal poor lower non lithophysal zone	11.8	38.7	1977.6	4,310	136	
17-May-95	7 + 62.7	7 + 74.5	Tiva Canyon crystal poor lower non lithophysal zone	11.8	38.7	2016.3	3,400	139	
18-May-95	7 + 74.5	7 + 74.5	Tiva Canyon crystal poor lower non lithophysal zone	0	0	2016.3	5,600	145	
19-May-95	7 + 74.5	7 + 74.5	Tiva Canyon crystal poor lower non lithophysal zone	0	0	2016.3	9,300	154	
20-May-95	7 + 74.5	7 + 74.5	Tiva Canyon crystal poor lower non lithophysal zone	0	0	2016.3	0	154	
21-May-95	7 + 74.5	7 + 74.5	Tiva Canyon crystal poor lower non lithophysal zone	0	0	2016.3	0	154	
22-May-95	7 + 74.5	7 + 88.2	Tiva Canyon crystal poor vitric zone	13		2016.3	5,550	160	
23-May-95	7 + 88.2	8 + 05.7	Tiva Canyon crystal poor vitric zone	17.5	57.4	2073.7	5,710	166	
24-May-95	8 + 05.7	8 + 19.2	Tiva Canyon crystal poor vitric zone	13.5	44.3	2118	5,056	171	
25-May-95	8 + 19.2	8 + 35.5	Tiva Canyon crystal poor vitric zone	16.3	53.5	2171.5	6,520	177	
26-May-95	8 + 35.5	8 + 48.4	Tiva Canyon crystal poor vitric zone	12.9	42.3	2213.8	3,520	181	
27-May-95	8 + 48.4	8 + 48.4	Tiva Canyon crystal poor vitric zone	0	0	2213.8		181	
28-May-95	8 + 48.4	2783.5	Tiva Canyon crystal poor vitric zone	0	0	2213.8		181	

Table 7-2 Water usage history in the ESF tunnel.

DATE	BEGIN STATION	END STATION	END STATION	STRATIGRAPHY	ADVANCE	ADVANCE	Cumulative ESF Advancement	DAILY WATER	CUMULATIVE WATER USAGE TO DATE	COMMENTS
29-May-95	8 + 48.4	8 + 48.4	2783.5	Tiva Canyon crystal poor vitric zone	0	0	2213.8		181	
30-May-95	8 + 48.4	8 + 64.0	2834.6	Tiva Canyon crystal poor vitric zone	15.6	51.2	2265	3,921	185	
31-May-95	8 + 64.0	8 + 79.6	2885.8	Bedded Tufts (including thin Yucca Mtn member)	15.6	51.2	2316.2	7,161	192	
1-Jun-95	8 + 79.6	9 + 03.2	2963.3	Bedded Tufts (including thin Yucca Mtn member)	23.6	77.4	2393.6	7,683	199	
2-Jun-95	9 + 03.2	9 + 14.6	3000.7	Pah Canyon Member	11.4	37.4	2431	4,377	204	72 HR REPORT - WEEKEND
3-Jun-95	9 + 14.6	9 + 14.6	3000.7	Pah Canyon Member	0	0	2431	566	204	72 HR REPORT - WEEKEND
4-Jun-95	9 + 14.6	9 + 14.6	3000.7	Pah Canyon Member	0	0	2431	0	204	72 HR REPORT - WEEKEND
5-Jun-95	9 + 14.6	9 + 25.7	3037.1	Pah Canyon Member	11.1	36.4	2467.4	4,494	209	
6-Jun-95	9 + 25.7	9 + 36.4	3072.2	Pah Canyon Member	10.7	35.1	2502.5	3,891	213	
7-Jun-95	9 + 36.4	9 + 58.6	3145	Pah Canyon Member	22.2	72.8	2575.3	10,158	223	
8-Jun-95	9 + 58.6	9 + 72.2	3189.6	Pah Canyon Member	13.6	44.6	2619.9	7,900	231	
9-Jun-95	9 + 72.2	9 + 72.2	3189.6	Pah Canyon Member	0	0	2619.9	2,849	234	72 HR REPORT - WEEKEND
10-Jun-95	9 + 72.2	9 + 72.2	3189.6	Pah Canyon Member	0	0	2619.9	2,140	236	72 HR REPORT - WEEKEND
11-Jun-95	9 + 72.2	9 + 72.2	3189.6	Pah Canyon Member	0	0	2619.9	0	236	72 HR REPORT - WEEKEND
12-Jun-95	9 + 72.2	9 + 93.1	3258.2	Pah Canyon Member	20.9	68.6	2688.5	10,561	246	
13-Jun-95	9 + 93.1	10 + 14.4	3328.1	Pah Canyon Member	21.3	69.9	2758.4	11,266	258	
14-Jun-95	10 + 14.4	10 + 32.2	3386.5	Pre-Pah Canyon tufts	17.8	58.4	2816.8	8,503	266	
15-Jun-95	10 + 32.2	10 + 50.6	3446.9	Pre-Pah Canyon tufts	18.4	60.4	2877.2	13,009	279	
16-Jun-95	10 + 50.6	10 + 68.3	3504.9	Topopah Spring crystal rich vitric zone	17.7	58.1	2935.3	13,834	293	72 HR REPORT - WEEKEND
17-Jun-95	10 + 68.3	10 + 68.3	3504.9	Topopah Spring crystal rich vitric zone	0	0	2935.3	1,677	295	72 HR REPORT - WEEKEND
18-Jun-95	10 + 68.3	10 + 68.3	3504.9	Topopah Spring crystal rich vitric zone	0	0	2935.3	0	295	72 HR REPORT - WEEKEND
19-Jun-95	10 + 68.3	10 + 85.1	3560	Topopah Spring crystal rich vitric zone	16.8	55.1	2990.4	10,000	305	
20-Jun-95	10 + 85.1	11 + 01.2	3612.9	Topopah Spring crystal rich vitric zone	16.1	52.8	3043.2	9,722	314	
21-Jun-95	11 + 01.2	11 + 11.2	3645.7	Topopah Spring crystal rich vitric zone	10	32.8	3076	7,146	322	
22-Jun-95	11 + 11.2	11 + 16.7	3663.7	Topopah Spring crystal rich vitric zone	5.5	18	3094	4,715	326	
23-Jun-95	11 + 16.7	"	"	Topopah Spring crystal rich vitric zone			3094	9,378	336	72 HR REPORT - WEEKEND
24-Jun-95	"	"	"	Topopah Spring crystal rich vitric zone			3094	12,574	348	72 HR REPORT - WEEKEND
25-Jun-95	"	11 + 25.9	3693.9	Topopah Spring crystal rich vitric zone	9.2	30.2	3124.2	0	348	72 HR REPORT - WEEKEND
26-Jun-95	11 + 25.9	11 + 30.2	3708	Topopah Spring crystal rich vitric zone	4.3	14.1	3138.3	12,278	361	
27-Jun-95	11 + 30.2	11 + 35.8	3726.4	Topopah Spring crystal rich vitric zone	5.6	18.4	3156.7	6,303	367	
28-Jun-95	11 + 35.8	11 + 37.9	3733.3	Topopah Spring crystal rich vitric zone	2.1	6.9	3163.6	3,288	370	
29-Jun-95	11 + 37.9	11 + 37.9	3733.3	Topopah Spring crystal rich vitric zone	0	0	3163.6	2,089	372	
30-Jun-95	11 + 37.9	11 + 37.9	3733.3	Topopah Spring crystal rich vitric zone	0	0	3163.6	8,026	380	CONVEYOR INSTALLATION
1-Jul-95	11 + 37.9	11 + 37.9	3733.3	Topopah Spring crystal rich vitric zone	0	0	3163.6	2,136	382	CONVEYOR INSTALLATION
2-Jul-95	11 + 37.9	11 + 37.9	3733.3	Topopah Spring crystal rich vitric zone	0	0	3163.6		382	
3-Jul-95	11 + 37.9	11 + 37.9	3733.3	Topopah Spring crystal rich vitric zone	0	0	3163.6		382	
4-Jul-95	11 + 37.9	11 + 37.9	3733.3	Topopah Spring crystal rich vitric zone	0	0	3163.6		382	
5-Jul-95	11 + 37.9	11 + 37.9	3733.3	Topopah Spring crystal rich vitric zone	0	0	3163.6		385	
6-Jul-95	11 + 37.9	11 + 37.9	3733.3	Topopah Spring crystal rich vitric zone	0	0	3163.6	1,995	387	
7-Jul-95	11 + 37.9	11 + 37.9	3733.3	Topopah Spring crystal rich vitric zone	0	0	3163.6	3,115	390	
8-Jul-95	11 + 37.9	11 + 37.9	3733.3	Topopah Spring crystal rich vitric zone	0	0	3163.6	2,695	393	
9-Jul-95	11 + 37.9	11 + 37.9	3733.3	Topopah Spring crystal rich vitric zone	0	0	3163.6	1,130	394	
10-Jul-95	11 + 37.9	11 + 37.9	3733.3	Topopah Spring crystal rich vitric zone	0	0	3163.6	3,275	397	
11-Jul-95	11 + 37.9	11 + 37.9	3733.3	Topopah Spring crystal rich vitric zone	0	0	3163.6	2,943	400	
12-Jul-95	11 + 37.9	11 + 37.9	3733.3	Topopah Spring crystal rich vitric zone	0	0	3163.6	1,920	402	
13-Jul-95	11 + 37.9	11 + 38.2	3734.3	Topopah Spring crystal rich vitric zone	0.3	1	3164.6	3,186	405	
14-Jul-95	11 + 38.2	11 + 38.2	3734.3	Topopah Spring crystal rich vitric zone	0	0	3164.6	3,579	409	
15-Jul-95	11 + 38.2	11 + 38.2	3734.3	Topopah Spring crystal rich vitric zone	0	0	3164.6	3,168	412	
16-Jul-95	11 + 38.2	11 + 38.2	3734.3	Topopah Spring crystal rich vitric zone	0	0	3164.6		412	
17-Jul-95	11 + 38.2	11 + 49.0	3769.5	Topopah Spring crystal rich vitric zone	10.8	35.4	3200	7,386	419	

Table 7-2 Water usage history in the ESF tunnel.

DATE	BEGIN STATION	END STATION	END STATION	STRATIGRAPHY	ADVANCE	ADVANCE	CUMMULATIVE ESF ADVANCEMENT	DAILY WATER	CUMULATIVE WATER USAGE TO DATE	COMMENTS
18-Jul-95	11 + 49.0	11 + 54.9	3789	Topopah Spring crystal rich vitric zone	5.9	19.4	3219.4	6,005	425	
19-Jul-95	11 + 54.9	11 + 59.1	3802.3	Topopah Spring crystal rich vitric zone	4.2	13.8	3233.2	4,751	430	
20-Jul-95	11 + 59.1	11 + 62.8	3815	Topopah Spring crystal rich vitric zone	3.7	12.1	3245.3	6,643	437	
21-Jul-95	11 + 62.8	11 + 64.4	3820.2	Topopah Spring crystal rich vitric zone	1.6	5.2	3250.5	6,917	444	
22-Jul-95	11 + 64.4	11 + 64.4	3820.2	Topopah Spring crystal rich vitric zone	0	0	3250.5	2,210	446	
23-Jul-95	11 + 64.4	11 + 64.4	3820.2	Topopah Spring crystal rich vitric zone	0	0	3250.5		446	
24-Jul-95	11 + 64.4	11 + 68.2	3832.7	Topopah Spring crystal rich vitric zone	3.8	12.5	3263		446	
25-Jul-95	11 + 68.2	11 + 71.9	3844.8	Topopah Spring crystal rich vitric zone	3.7	12.1	3275.1		446	
26-Jul-95	11 + 71.9	11 + 74.0	3851.7	Topopah Spring crystal rich vitric zone	2.1	6.9	3282		446	
27-Jul-95	11 + 74.0	11 + 74.0	3851.7	Topopah Spring crystal rich vitric zone	0	0	3282		446	
28-Jul-95	11 + 74.0	11 + 74.0	3851.7	Topopah Spring crystal rich vitric zone	0	0	3282		446	
29-Jul-95	11 + 74.0	11 + 74.0	3851.7	Topopah Spring crystal rich vitric zone	0	0	3282		446	
30-Jul-95	11 + 74.0	11 + 74.0	3851.7	Topopah Spring crystal rich vitric zone	0	0	3282		446	
31-Jul-95	11 + 74.0	11 + 77.6	3863.5	Topopah Spring crystal rich vitric zone	3.6	11.8	3293.8	6,045	452	
1-Aug-95	11 + 77.6	11 + 80.6	3873.4	Topopah Spring crystal rich vitric zone	3	9.8	3303.6	6,460	458	
2-Aug-95	11 + 80.6	11 + 83.2	3881.9	Topopah Spring crystal rich vitric zone	2.6	8.5	3312.1	15,020	473	
3-Aug-95	11 + 83.2	11 + 87.6	3896.3	Topopah Spring crystal rich vitric zone	4.4	14.4	3326.5	16,850	490	
4-Aug-95	11 + 87.6	11 + 91.2	3908.1	Topopah Spring crystal rich vitric zone	3.6	11.8	3338.3	6,680	497	72 HR REPORT - WEEKEND
5-Aug-95	11 + 91.2	11 + 91.2	3908.1	Topopah Spring crystal rich vitric zone	0	0	3338.3	460	497	
6-Aug-95	11 + 91.2	11 + 91.2	3908.1	Topopah Spring crystal rich vitric zone	0	0	3338.3		497	
7-Aug-95	11 + 91.2	12 + 15.1	3986.5	Topopah Spring crystal rich nonlithophysal zone	23.9	78.4	3416.7	22,990	520	Began using UG conveyor system
8-Aug-95	12 + 15.1	12 + 34.6	4050.5	Topopah Spring crystal rich nonlithophysal zone	19.5	64	3480.7	25,325	546	
9-Aug-95	12 + 34.6	12 + 61.0	4137.1	Topopah Spring crystal rich nonlithophysal zone	26.1	85.6	3566.3	33,585	579	
10-Aug-95	12 + 60.7	12 + 61.7	4139.4	Topopah Spring crystal rich nonlithophysal zone	1	3.3	3569.6	4,677	584	TBM backed up for maintenance
11-Aug-95	12 + 61.7	12 + 61.7	4139.4	Topopah Spring crystal rich nonlithophysal zone	0	0	3569.6	1,328	585	
12-Aug-95	12 + 61.7	12 + 61.7	4139.4	Topopah Spring crystal rich nonlithophysal zone	0	0	3569.6	437	586	
13-Aug-95	12 + 61.7	12 + 61.7	4139.4	Topopah Spring crystal rich nonlithophysal zone	0	0	3569.6		586	
14-Aug-95	12 + 61.7	12 + 61.7	4139.4	Topopah Spring crystal rich nonlithophysal zone	0	0	3569.6	290	586	
15-Aug-95	12 + 61.7	12 + 61.7	4139.4	Topopah Spring crystal rich nonlithophysal zone	0	0	3569.6	3	586	
16-Aug-95	12 + 61.7	12 + 61.7	4139.4	Topopah Spring crystal rich nonlithophysal zone	0	0	3569.6	265	586	
17-Aug-95	12 + 61.7	12 + 61.7	4139.4	Topopah Spring crystal rich nonlithophysal zone	0	0	3569.6	1,215	588	
18-Aug-95	12 + 61.7	12 + 61.7	4139.4	Topopah Spring crystal rich nonlithophysal zone	0	0	3569.6	1,277	589	
19-Aug-95	12 + 61.7	12 + 61.7	4139.4	Topopah Spring crystal rich nonlithophysal zone	0	0	3569.6	2,014	591	
20-Aug-95	12 + 61.7	12 + 61.7	4139.4	Topopah Spring crystal rich nonlithophysal zone	0	0	3569.6		591	
21-Aug-95	12 + 61.7	12 + 80.3	4200.5	Topopah Spring crystal rich nonlithophysal zone	18.6	61	3630.6	26,105	617	
22-Aug-95	12 + 80.3	12 + 90.9	4235.2	Topopah Spring crystal rich nonlithophysal zone	10.6	34.8	3665.4	23,035	640	
23-Aug-95	12 + 90.9	13 + 02.0	4271.7	Topopah Spring crystal rich nonlithophysal zone	11.1	36.4	3701.8	21,480	661	
24-Aug-95	13 + 02.0	13 + 07.2	4288.7	Topopah Spring crystal rich nonlithophysal zone	5.2	17.1	3718.9	20,830	682	
25-Aug-95	13 + 07.2	13 + 18.6	4326.1	Topopah Spring crystal rich nonlithophysal zone	11.4	37.4	3756.3	28,390	711	
26-Aug-95	13 + 18.6	13 + 18.6	4326.1	Topopah Spring crystal rich nonlithophysal zone	0	0	3756.3	0	711	
27-Aug-95	13 + 18.6	13 + 18.6	4326.1	Topopah Spring crystal rich nonlithophysal zone	0	0	3756.3		711	
28-Aug-95	13 + 18.6	13 + 30.9	4366.5	Topopah Spring crystal rich nonlithophysal zone	12.3	40.4	3796.7	19,950	731	
29-Aug-95	13 + 30.9	13 + 48.3		Topopah Spring crystal rich nonlithophysal zone			3796.7	25,191	756	
30-Aug-95	13 + 48.3	13 + 69.0	4491.5	Topopah Spring crystal rich nonlithophysal zone	20.7	67.9	3864.6	26,939	783	
31-Aug-95	13 + 69.0	14 + 14.8	4641.7	Topopah Spring crystal rich nonlithophysal zone	45.8	150.3	4014.9	48,100	831	
1-Sep-95	14 + 14.8	14 + 51.6	4762.5	Topopah Spring crystal rich nonlithophysal zone	36.8	120.7	4135.6	48,117	879	
2-Sep-95	14 + 51.6	14 + 51.6	4762.5	Topopah Spring crystal rich nonlithophysal zone	0	0	4135.6	0	879	
3-Sep-95	14 + 51.6	14 + 51.6	4762.5	Topopah Spring crystal rich nonlithophysal zone	0	0	4135.6		879	
4-Sep-95	14 + 51.6	14 + 51.6	4762.5	Topopah Spring crystal rich nonlithophysal zone	0	0	4135.6	0	879	
5-Sep-95	14 + 51.6	14 + 95.8	4907.5	Topopah Spring crystal rich nonlithophysal zone	44.2	145	4280.6	49,323	928	

Table 7-2 Water usage history in the ESF tunnel.

DATE	BEGIN STATION	END STATION	END STATION	STRATIGRAPHY	ADVANCE	ADVANCE	Cumulative ESF Advancement	DAILY WATER	CUMULATIVE WATER USAGE TO DATE	COMMENTS
6-Sep-95	14 + 95.8	15 + 26.1	5006.9	Topopah Spring crystal rich nonlithophysal zone	30.3	99.4	4380	48,690	977	
7-Sep-95	14 + 26.1	15 + 60.5	5119.8	Topopah Spring crystal rich nonlithophysal zone	34.4	113	4493	43,190	1,020	
8-Sep-95	15 + 60.5	15 + 60.5	5119.8	Topopah Spring crystal rich nonlithophysal zone	0	0	4493	1,322	1,022	
9-Sep-95	15 + 60.5	15 + 60.5	5119.8	Topopah Spring crystal rich nonlithophysal zone	0	0	4493	198	1,022	
10-Sep-95	15 + 60.5	15 + 60.5	5119.8	Topopah Spring crystal rich nonlithophysal zone	0	0	4493		1,022	
11-Sep-95	15 + 60.5	15 + 87.4	5208	Topopah Spring crystal rich nonlithophysal zone	26.9	88.3	4581.3	31,060	1,053	
12-Sep-95	15 + 87.4	16 + 21.1	5318.6	Topopah Spring crystal rich nonlithophysal zone	33.7	110.6	4691.9	36,930	1,090	
13-Sep-95	16 + 21.1	16 + 51.2	5417.3	Topopah Spring crystal rich nonlithophysal zone	30.1	98.8	4790.7	41,070	1,131	
14-Sep-95	16 + 51.2	16 + 78.2	5505.9	Topopah Spring crystal rich nonlithophysal zone	27	88.6	4879.3	36,765	1,168	
15-Sep-95	16 + 78.2	17 + 03.9	5590.2	Topopah Spring crystal rich nonlithophysal zone	25.7	84.3	4963.6	30,380	1,198	
16-Sep-95	17 + 03.9	17 + 03.9	5590.2	Topopah Spring crystal rich nonlithophysal zone	0	0	4963.6	0	1,198	
17-Sep-95	17 + 03.9	17 + 03.9	5590.2	Topopah Spring crystal rich nonlithophysal zone	0	0	4963.6		1,198	
18-Sep-95	17 + 03.9	17 + 14.8	5626	Topopah Spring crystal rich nonlithophysal zone	10.9	35.8	4999.4	13,605	1,212	
19-Sep-95	17 + 14.8	17 + 48.8	5737.5	Topopah Spring crystal rich lithophysal zone	34	111.5	5110.9	33,350	1,245	
20-Sep-95	17 + 48.8	17 + 86.4	5860.9	Topopah Spring crystal rich lithophysal zone	37.6	123.4	5234.3	39,300	1,284	
21-Sep-95	17 + 86.4	18 + 18.9	5967.5	Topopah Spring crystal poor upper lithophysal zone	32.5	106.6	5340.9	35,800	1,320	
22-Sep-95	18 + 18.9	18 + 52.7	6078.4	Topopah Spring crystal poor upper lithophysal zone	33.8	110.9	5451.8	39,426	1,359	
23-Sep-95	18 + 52.7	18 + 52.7	6078.4	Topopah Spring crystal poor upper lithophysal zone	0	0	5451.8	19,274	1,379	
24-Sep-95	18 + 52.7	18 + 52.7	6078.4	Topopah Spring crystal poor upper lithophysal zone	0	0	5451.8		1,379	
25-Sep-95	18 + 52.7	18 + 67.6	6127.3	Topopah Spring crystal poor upper lithophysal zone	14.9	48.9	5500.7	20,641	1,399	
25-Sep-95	18 + 67.6	18 + 98.7	4072.2	Topopah Spring crystal poor upper lithophysal zone	10.4	34	5534.7	34,333	1,434	
27-Sep-95	18 + 98.7	19 + 24.3	6313.3	Topopah Spring crystal poor upper lithophysal zone	25.6	28	5562.7	32,450	1,466	
28-Sep-95	19 + 24.3	19 + 52.1	6404.5	Topopah Spring crystal poor upper lithophysal zone	27.8	91.2	5653.9	34,550	1,501	
29-Sep-95	19 + 52.1	20 + 02.1	6568.6	Topopah Spring crystal poor upper lithophysal zone	50	164	5817.9	45,085	1,546	
30-Sep-95	20 + 02.1	20 + 02.1	6568.6	Topopah Spring crystal poor upper lithophysal zone	0	0	5817.9		1,546	
1-Oct-95	20 + 02.1	20 + 02.1	6568.6	Topopah Spring crystal poor upper lithophysal zone	0	0	5817.9		1,546	
2-Oct-95	20 + 02.1	20 + 40.3	6693.9	Topopah Spring crystal poor upper lithophysal zone	38.2	125.3	5943.2	38,150	1,584	
3-Oct-95	20 + 40.3	20 + 82.7	6833	Topopah Spring crystal poor upper lithophysal zone	42.4	139.1	6082.3	34,965	1,619	
4-Oct-95	20 + 82.7	21 + 21.5	6960.3	Topopah Spring crystal poor upper lithophysal zone	12.9	42.4	6124.7	34,240	1,653	
5-Oct-95	21 + 21.5	21 + 21.5	6960.3	Topopah Spring crystal poor upper lithophysal zone	0	0	6124.7		1,654	
6-Oct-95	21 + 21.5	21 + 21.5	6960.3	Topopah Spring crystal poor upper lithophysal zone	0	0	6124.7	1,330	1,654	
7-Oct-95	21 + 21.5	21 + 21.5	6960.3	Topopah Spring crystal poor upper lithophysal zone	0	0	6124.7	1,542	1,656	
8-Oct-95	21 + 21.5	21 + 21.5	6960.3	Topopah Spring crystal poor upper lithophysal zone	0	0	6124.7	120	1,656	
9-Oct-95	21 + 21.5	21 + 52.3	7061.4	Topopah Spring crystal poor upper lithophysal zone	10.3	33.7	6158.4	33,143	1,689	
10-Oct-95	21 + 52.3	21 + 74.8	7135.2	Topopah Spring crystal poor upper lithophysal zone	22.5	73.8	6232.2	25,075	1,714	
11-Oct-95	21 + 74.8	21 + 99.9	7217.5	Topopah Spring crystal poor upper lithophysal zone	25.1	82.3	6314.5	24,550	1,739	
12-Oct-95	21 + 99.9	22 + 14.4	7265.1	Topopah Spring crystal poor upper lithophysal zone	14.5	47.6	6362.1	27,450	1,766	
13-Oct-95	22 + 14.4	22 + 36.8	7338.6	Topopah Spring crystal poor upper lithophysal zone	22.4	73.5	6435.6	36,046	1,802	
14-Oct-95	22 + 36.8	22 + 36.8	7388.6	Topopah Spring crystal poor upper lithophysal zone	0	0	6435.6	1,679	1,804	
15-Oct-95	22 + 36.8	22 + 36.8	7388.6	Topopah Spring crystal poor upper lithophysal zone	0	0	6435.6		1,804	
16-Oct-95	22 + 36.8	22 + 62.3	7422.2	Topopah Spring crystal poor upper lithophysal zone	25.5	83.7	6519.3	37,705	1,842	
17-Oct-95	22 + 62.3	22 + 89.0	7509.8	Topopah Spring crystal poor upper lithophysal zone	28.7	87.6	6606.9	35,150	1,877	
18-Oct-95	22 + 89.0	23 + 03.8	?????	Topopah Spring crystal poor upper lithophysal zone	4.9	16.2	6623.1	25,993	1,903	
19-Oct-95	23 + 03.8	23 + 23.6	7623.4	Topopah Spring crystal poor upper lithophysal zone	19.8	64	6687.1	32,581	1,935	
20-Oct-95	23 + 23.6	23 + 46.8	7699.5	Topopah Spring crystal poor upper lithophysal zone	23.2	76.1	6763.2	28,858	1,964	
21-Oct-95	23 + 46.8	23 + 46.8	7699.5	Topopah Spring crystal poor upper lithophysal zone	0	0	6763.2	484	1,965	
22-Oct-95	23 + 46.8	23 + 46.8	7699.5	Topopah Spring crystal poor upper lithophysal zone	0	0	6763.2		1,965	
23-Oct-95	23 + 46.8	23 + 74.8	7791.3	Topopah Spring crystal poor upper lithophysal zone	28	91.9	6855.1	29,214	1,994	
24-Oct-95	23 + 74.8	24 + 06.9	7896.7	Topopah Spring crystal poor upper lithophysal zone	32.1	105.3	6960.4	31,340	2,025	
25-Oct-95	24 + 06.9	24 + 28.0	7965.9	Topopah Spring crystal poor upper lithophysal zone	21.1	69.2	7029.6	28,100	2,053	

Table 7-2 Water usage history in the ESF tunnel.

DATE	BEGIN STATION	END STATION	END STATION	STRATIGRAPHY	ADVANCE	ADVANCE	Cumulative ESF Advancement	DAILY WATER	CUMULATIVE WATER USAGE TO DATE	COMMENTS
21-Aug-96	62 + 38.3	62 + 45.7	20491.1	Topopah Spring crystal poor middle nonlithophysal zone	7.4	24.3	18229.4		8,686	
22-Aug-96	62 + 45.7	62 + 64.0	20551.2	Topopah Spring crystal poor middle nonlithophysal zone	18.3	60	18289.4		8,686	
23-Aug-96	62 + 64.0	62 + 81.6	20608.9	Topopah Spring crystal poor middle nonlithophysal zone	17.6	57.7	18347.1		8,686	
24-Aug-96	62 + 81.6	62 + 81.6	20608.9	Topopah Spring crystal poor middle nonlithophysal zone	0	0	18347.1		8,686	
25-Aug-96	62 + 81.6	62 + 81.6	20608.9	Topopah Spring crystal poor middle nonlithophysal zone	0	0	18347.1		8,686	
26-Aug-96	62 + 81.6	62 + 93.7	20648.6	Topopah Spring crystal poor middle nonlithophysal zone	12.1	39.7	18386.8		8,686	
27-Aug-96	62 + 93.7	63 + 06.3	20590	Topopah Spring crystal poor middle nonlithophysal zone	12.6	41.3	18428.1		8,686	
28-Aug-96	63 + 06.3	63 + 25.0	20751.3	Topopah Spring crystal poor middle nonlithophysal zone	18.7	61.4	18489.5		8,686	
29-Aug-96	63 + 25.0	63 + 47.1	20823.8	Topopah Spring crystal poor middle nonlithophysal zone	22.1	72.5	18562		8,686	
30-Aug-96	63 + 47.1	63 + 47.1	20823.8	Topopah Spring crystal poor middle nonlithophysal zone	0	0	18562		8,686	TBM shut down for ventilation
31-Aug-96	63 + 47.1	63 + 47.1	20823.8	Topopah Spring crystal poor middle nonlithophysal zone	0	0	18562		8,686	TBM shut down for ventilation
1-Sep-96	63 + 47.1	63 + 47.1	20823.8	Topopah Spring crystal poor middle nonlithophysal zone	0	0	18562		8,686	TBM shut down for ventilation
2-Sep-96	63 + 47.1	63 + 47.1	20823.8	Topopah Spring crystal poor middle nonlithophysal zone	0	0	18562		8,686	TBM shut down for ventilation
3-Sep-96	63 + 47.1	63 + 47.1	20823.8	Topopah Spring crystal poor middle nonlithophysal zone	0	0	18562		8,686	TBM shut down for ventilation
Note: Unless otherwise noted Date is beginning of a three shift day starting at 8:00 a.m. and ending 8:00 a.m.					189.3				8,686	
						Max			8,686	

8.0 SUMMARY AND CONCLUSIONS

Nye County Nuclear Waste Repository Project Office's (NWRPO) Investigation Program (ISIP) is concerned with several key scientific issues that may impact the repository design and performance. The ISIP presently includes borehole and tunnel instrumentation, monitoring, data analysis, and numerical modeling activities to address some of these concerns.

Nye County has installed and is currently monitoring pressure and temperature instruments in boreholes UE-25 ONC#1 and USW NRG-4 to evaluate the long-term pneumatic conditions at strategic depths in the subsurface both in response to fluctuations in atmospheric conditions and in response to other possible disturbances resulting from site characterization activities such as ESF tunnel construction. Nye County has also installed instruments to measure temperature, pressure, and humidity within the ESF tunnel to characterize the air being used to ventilate the tunnel which could potentially impact the performance of the repository. Finally, Nye County is conducting numerical modeling simulations to evaluate factors (including tunnel ventilation) which affect both short-term and long-term pneumatic and moisture conditions in the repository host rock .

A summary of activities undertaken by ISIP during the past year are as follows:

- Evaluation of critical data and information as it became available from the DOE's YMP Site Characterization Office.
- Observed water usage in the tunnel and its potential impact on the repository horizon and the scientific investigation results. Completed an analysis and a recommendation report and forwarded it to YMP Site Characterization Office.

- Prepared detailed review of procedures and methods used for in-situ air permeability tests and evaluated the results of some of these tests.
- Completed several letter reports to DOE on the interpretation of the results of the ^{36}Cl and other environmental and geological isotope studies. These communications have resulted in DOE giving more focused attention to the need for more detailed studies in the ESF tunnel, limiting the use of construction water, and enhanced interpretation of the results of the isotope sampling.
- Evaluated the saturated zone pumping tests that were performed in the C-Well complex during the past year.
- Monitored responses to these pumping tests in the ONC#1 saturated-zone instrumentation.

As a result of the evaluation of the ESF tunnel climatalogical data collected, Nye County concluded that substantial moisture was being removed from the rocks penetrated by the tunnel ventilation. In response to issues raised by Nye County, DOE assigned a task force to conduct observations in the ESF and perform numerical simulations for interpretation of the results in parallel with Nye County's effort. Nye County provided data, preliminary analytical and simulation results, and input for developing the proposal to this task force. Nye County data indicated that in addition to moisture, substantial amount of heat is being removed by the ventilation. Nye County performed additional simulations using A-TOUGH, a computer code designed to simulate coupled-open air with geologic formations and discovered that there is a tremendous potential for natural ventilation at the site due to its climate and its physiographic setting. Simplified simulations using A-TOUGH were performed to evaluate the potential of a naturally ventilated repository. One conclusion is that it is possible to design a repository that is naturally ventilated with peak rock temperatures of less than 30

degrees Celsius over a 10,000-year period. These simulations also showed that the capillary pressure distribution would promote a strong gradient for water flow towards the emplacement tunnels during the entire 10,000 years. Nye County, believes that long-term waste containment implications of a naturally-ventilated repository warrants additional analysis.

Nye County is planning to perform several investigations in the near future to understand some of the issues that were outlined above, by installing new wells in both the saturated and unsaturated zones, testing and sampling these wells, and performing data analysis and modeling. These issues are related to the steep gradients in the saturated zone north and west of the site, the potential for dilution in the saturated zone as unsaturated zone moisture enters the saturated zone, the atmospheric and pneumatic boundaries in the Solitario Canyon that might impact the repository performance, and the large-scale transport properties of the fractured formations in both saturated and unsaturated zones.

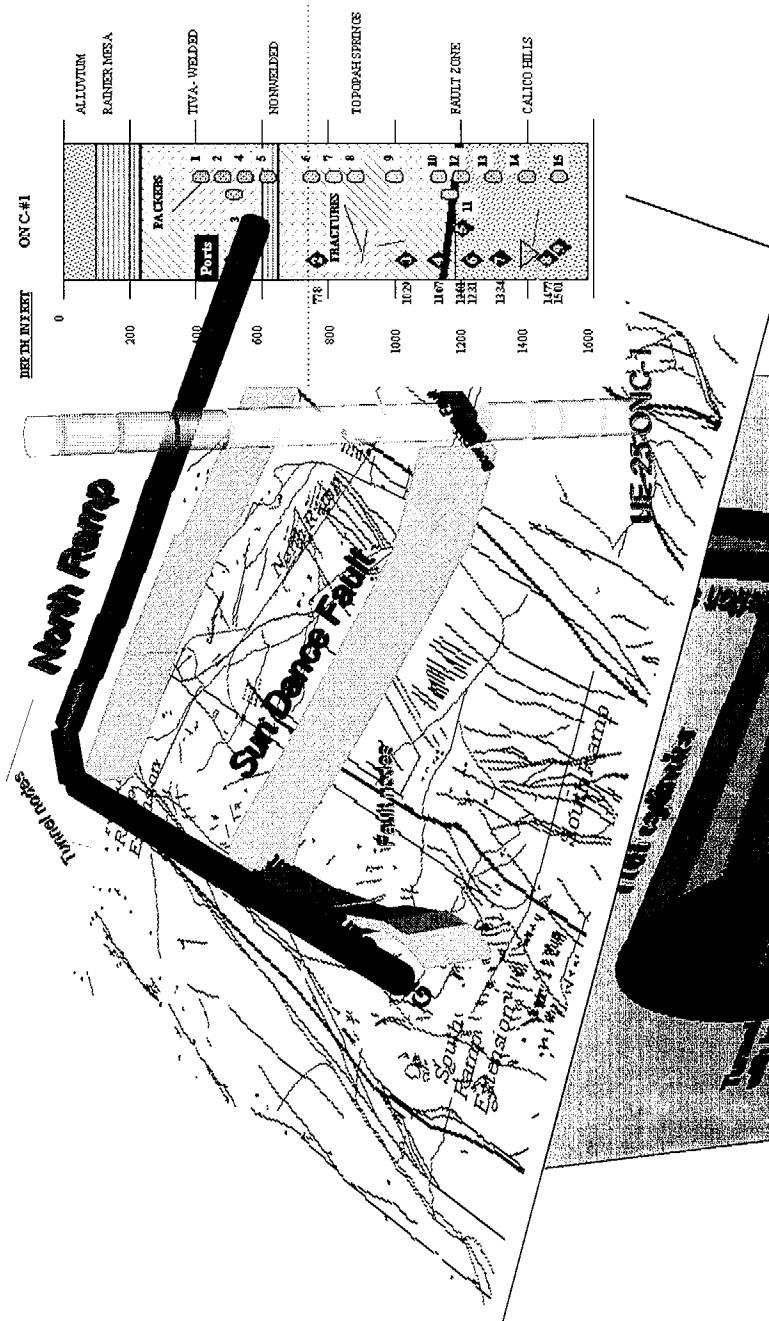
9.0 REFERENCES

- Advance Resources International, 1995, Analysis of Permeability Tests at Yucca Mountain, Nevada.
- Buscheck, T.A., J.J. Nitao, and L. Ramspot, 1995, Localized Dry-out: An Approach for managing the Thermo-hydrological Effects of Decay Heat at Yucca Mountain, Material Research Society Symposium on Scientific Basis for Nuclear Waste Management, 1995 Fall Meeting, Boston, Massachusetts.
- Multimedia Environmental Technology, Inc., 1995, Interim Report On Results Of Instrumentation And Monitoring Of UE-25 UE-25 Onc#1 And USW Nrg-4 Boreholes, Yucca Mountain, Nevada, Nye County Nuclear Waste Repository Office, Nye County, Nevada.
- Montazer, P., and W.E. Wilson, 1984, Conceptual hydrologic model of flow in the unsaturated zone, Yucca Mountain, Nevada, U.S. Geological Survey, Water Resources Investigation Report 84-4345.
- Montazer et. Al. 1987, Characterization of Unsaturated Flow Through Fractured Rocks, Groundwater Monitoring Review.
- Montazer, Parviz and Stellavato, Nick, 1996, Simulation and observation of ESF tunnel effects on barometric conditions, International High-Level Radioactive Waste Conference, April1996, Las Vegas, Nevada.
- Montazer, Parviz and Stellavato, Nick, 1996, Moisture Removal From The Repository By Ventilation And Impacts on Design, International High-Level Radioactive Waste Conference, April1996, Las Vegas, Nevada.
- Montazer, P., 1982, Permeability of unsaturated fractured metamorphic rocks near an underground opening: Golden, Colorado School of Mines, Ph.D. Thesis, 630 p.
- NWRPO, 1995. Borehole UE-25 ONC#1 and USW NRG-4 drilling and instrumentation report, Yucca Mountain, Nevada. Prepared by the Nuclear Waste Repository Project Office, Nye County Nuclear Waste Repository Program. September 1, 1995.
- Roseboom, E.H., 1983, Disposal of high-level nuclear waste above the water table in arid regions: U.S. Geological Survey Circular 903, 21p.
- TRW, 1995, Total System Performance Assessment -1995, An evaluation of the Potential Yucca Mountain Repository.

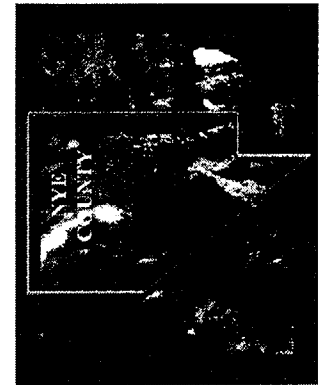
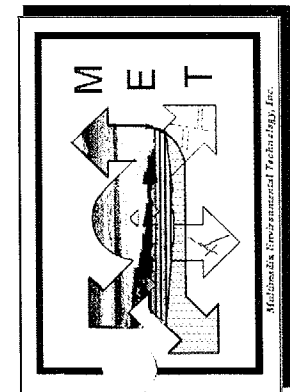
**ANNUAL REPORT OF THE NYE COUNTY NUCLEAR WASTE
REPOSITORY PROJECT OFFICE INDEPENDENT SCIENTIFIC
INVESTIGATION PROGRAM**

Prepared by:

**Multimedia Environmental Technology, Inc.
Newport Beach, California**



**Volume II
October
1996**



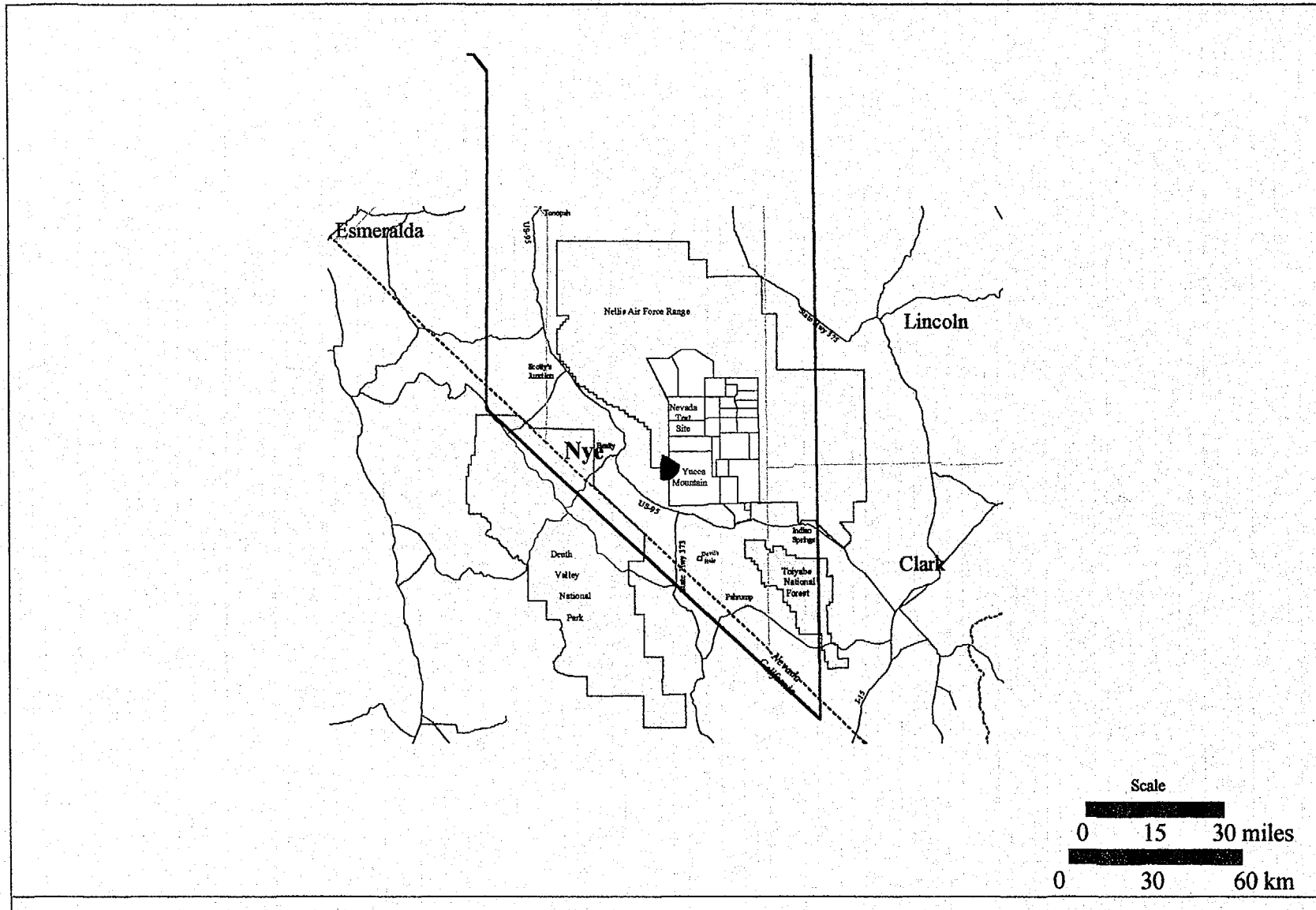
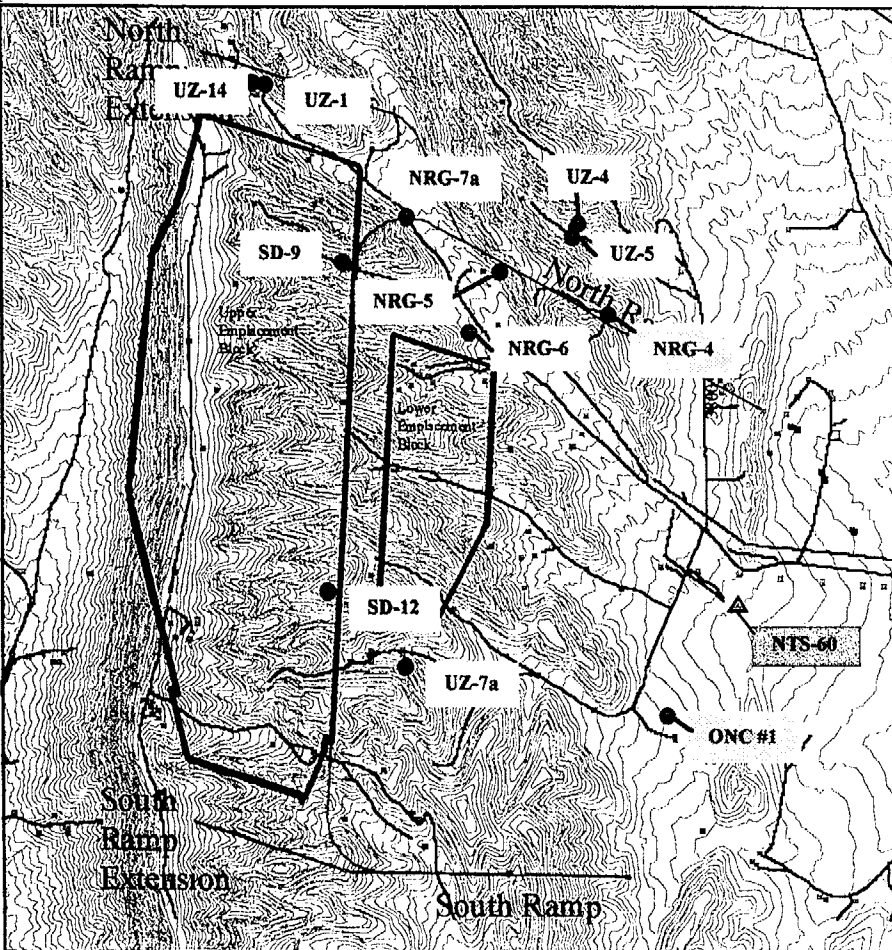


Figure 1-1 - Location of Yucca Mountain Site in Nye County, Nevada.

August 24, 1996
P266::D:\user\projects\Nye\county\annrep96\figures

Prepared for:
Nye County Nuclear Waste Repository Project Office

Prepared by:
Multimedia Environmental Technology, Inc.
Newport Beach, CA



EXPLANATION

- Exploratory Studies Facility (ESF) center line
 - UZ-14 Borehole location
 - Other borehole (existing and planned)
 - Roads
 - 20-ft contour line
- 0 2000 4000 6000 8000 10,000 Feet
- SCALE

Figure 1-2 - Topography, location of selected boreholes, and ESF centerline at Yucca Mountain Site.

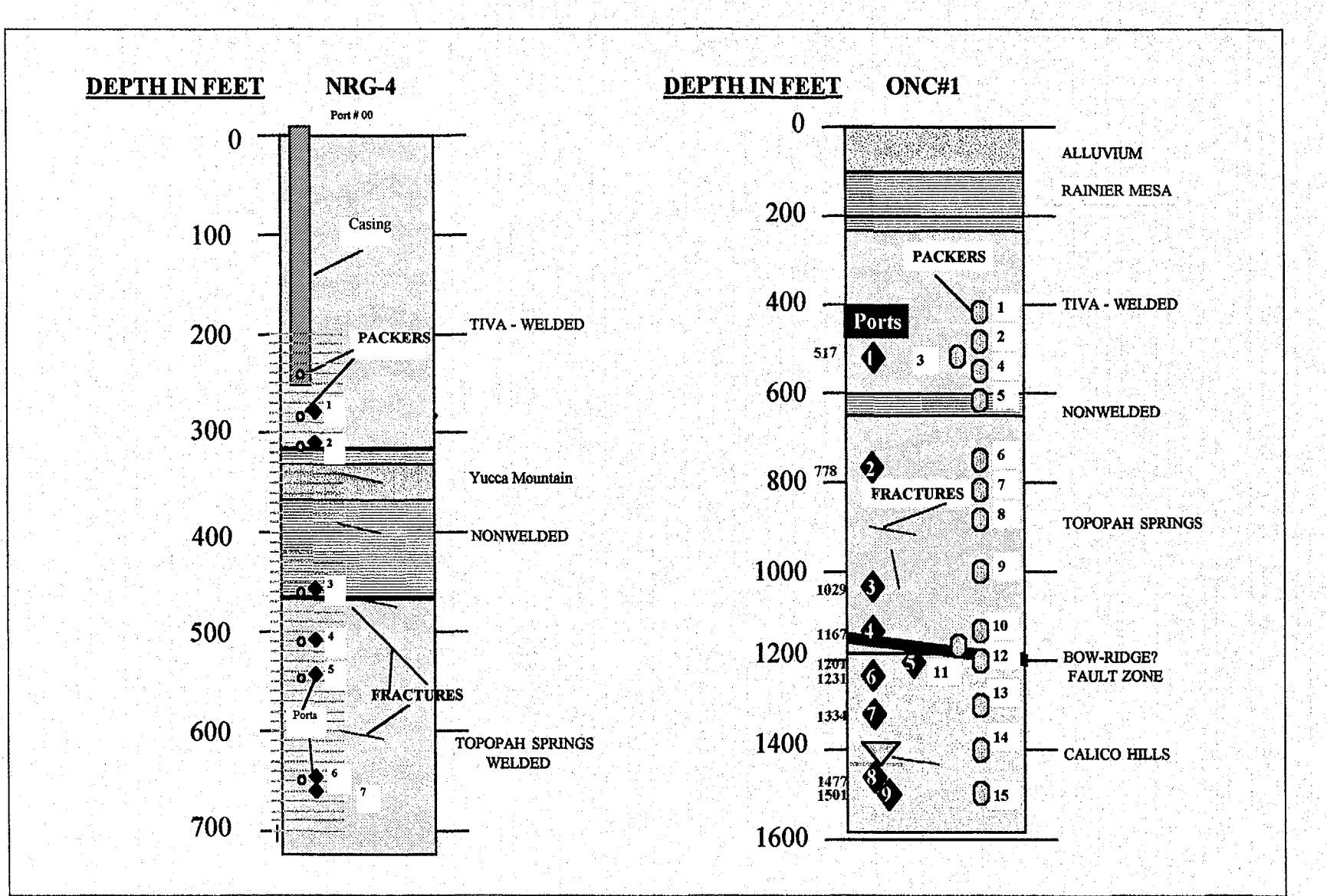
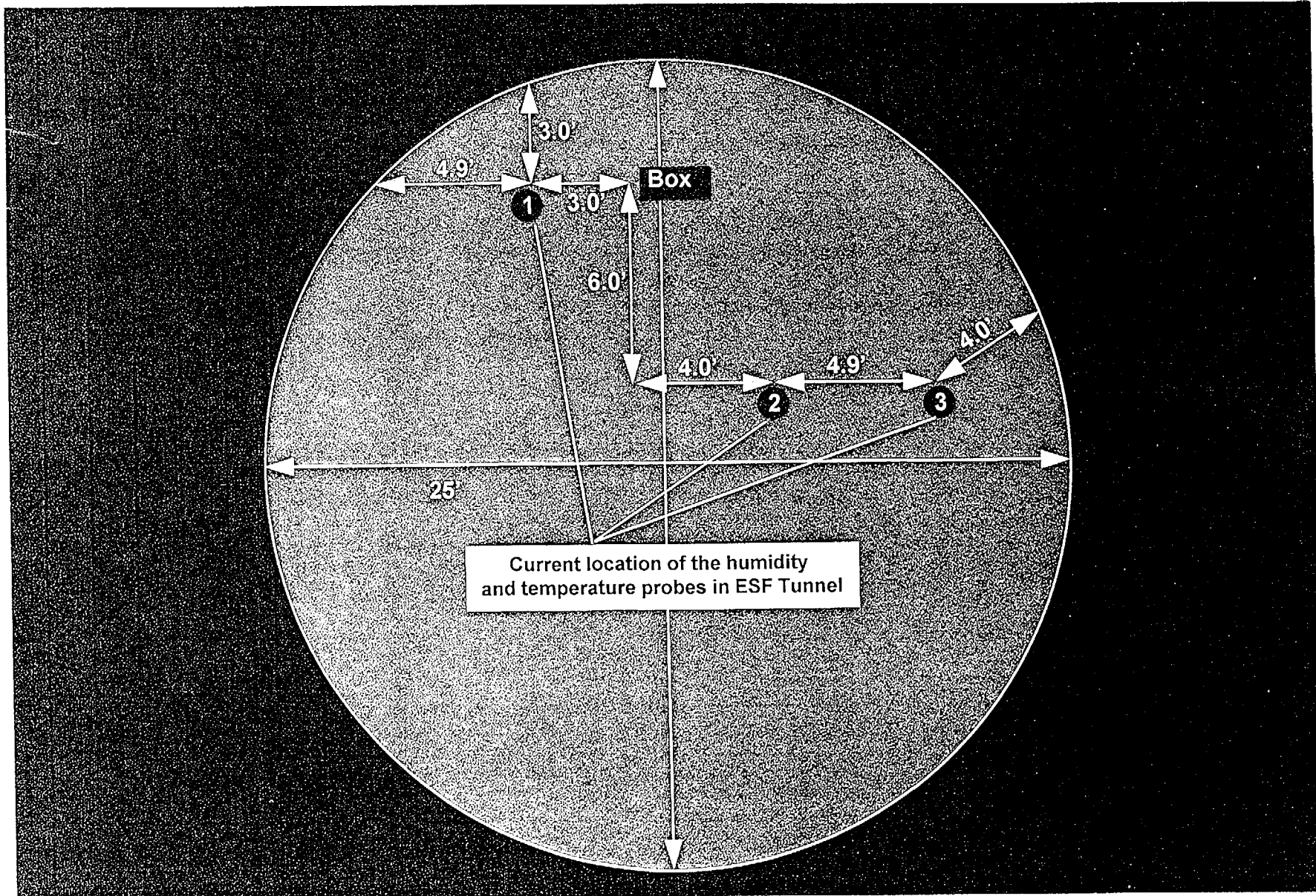
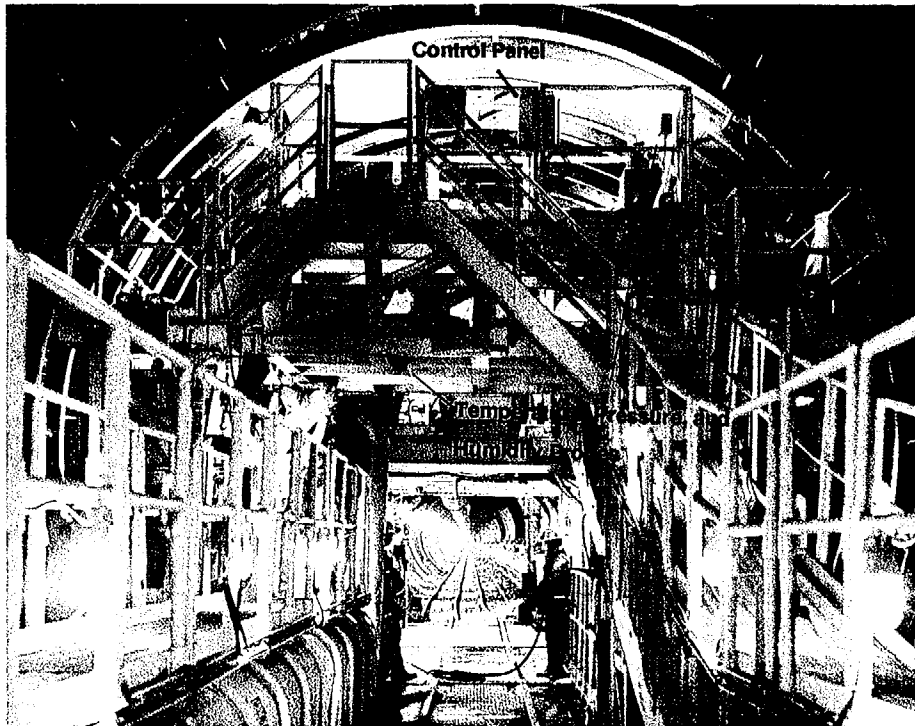


Figure 2-1 - Schematic profile of instrumentation setup in UE-25 ONC# 1 and USW NRG-4





a) View of tunnel with the location of two of the three climatological instrument stations.



b) View of tunnel in same direction, but at farther distance away.

APRIL 1995

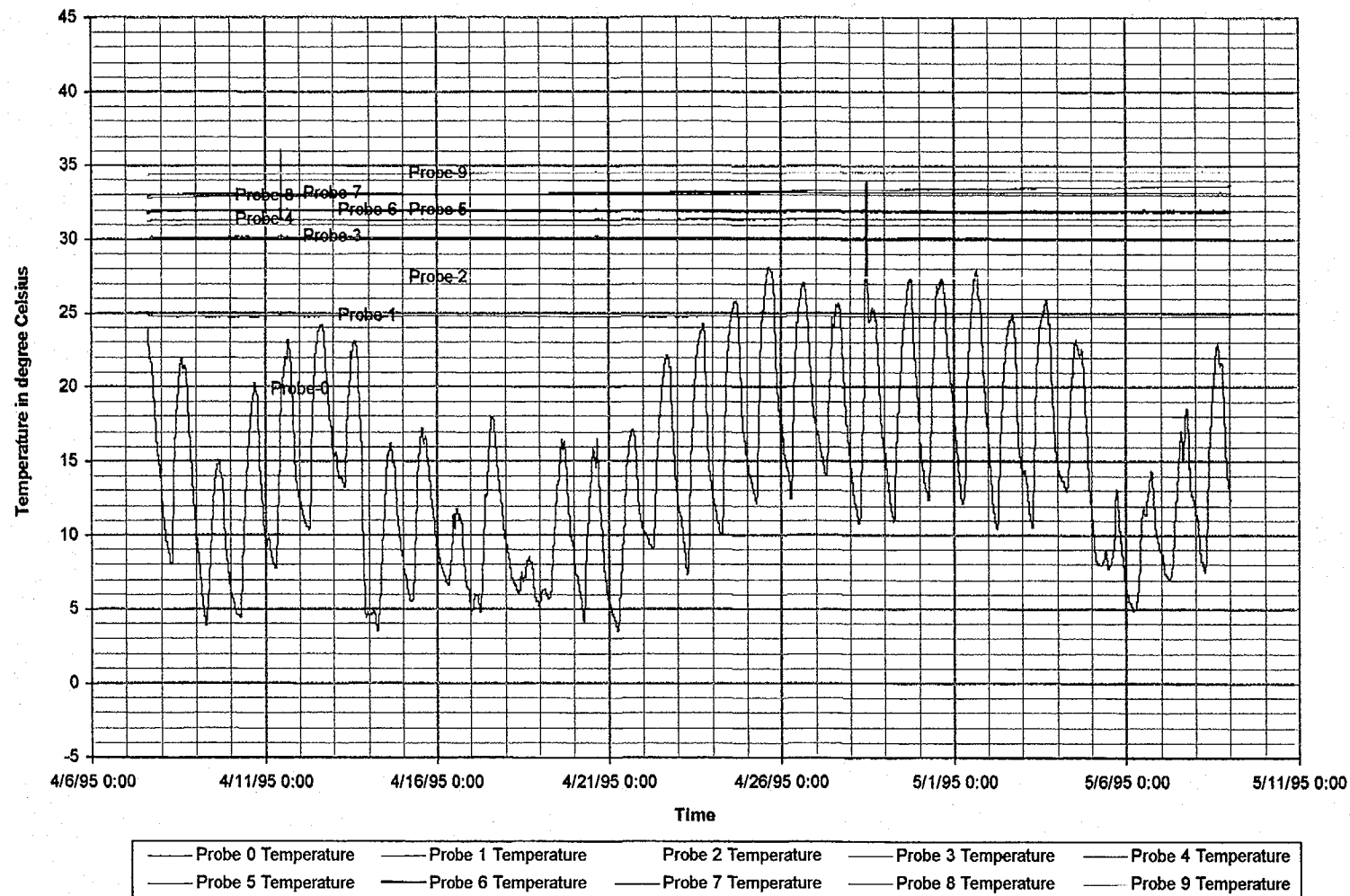


Figure 4-1a Temperature fluctuation with time in ONC-1

MAY 1995

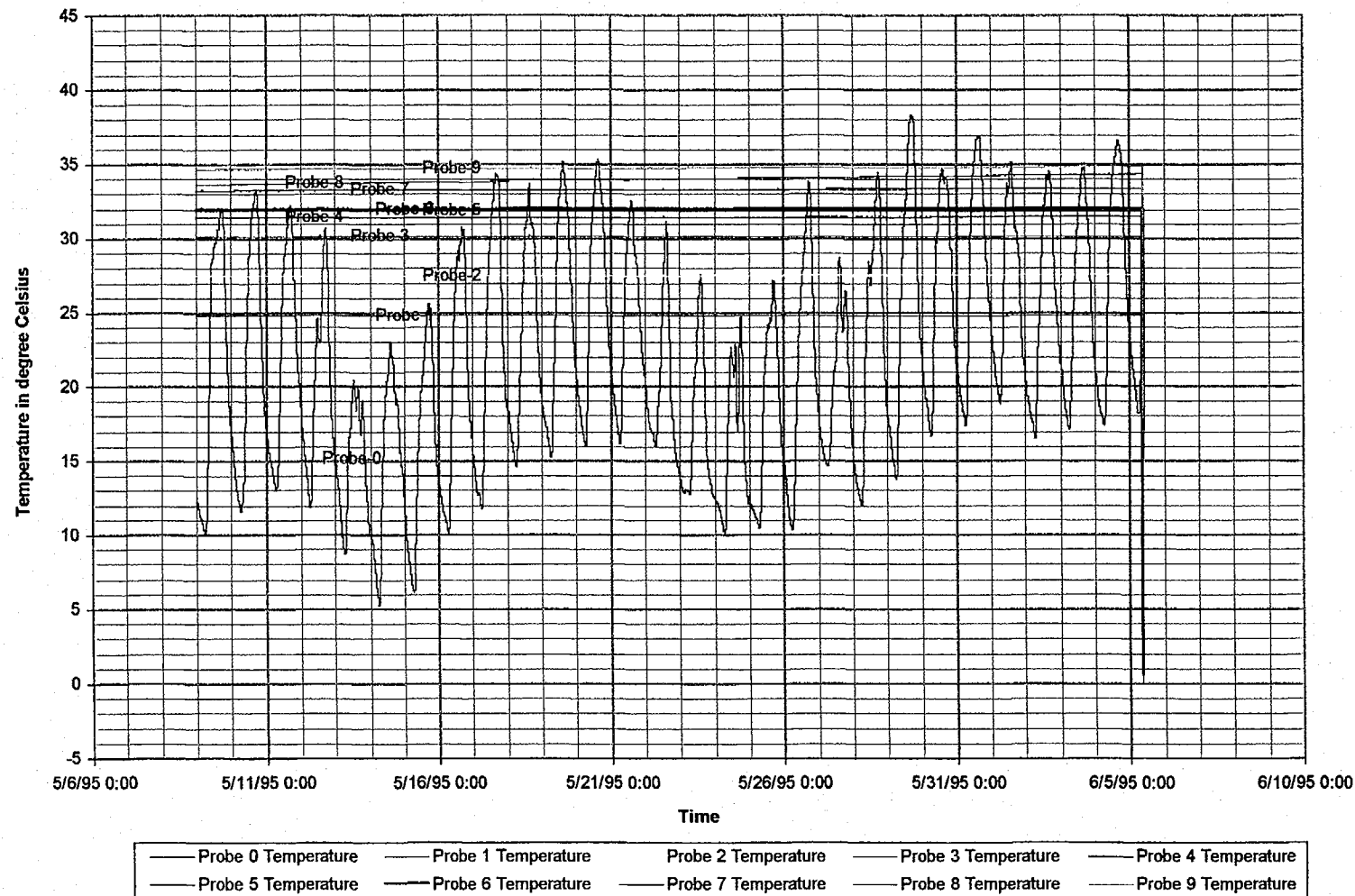


Figure 4-1b Temperature fluctuation with time in ONC-1

August 24, 1996
P266:D:\user\projects\Nye county\unrep96\figures

Prepared for:
Nye County Nuclear Waste Repository Project Office

Prepared by:
Multimedia Environmental Technology, Inc.
Newport Beach, CA

JUNE 1995

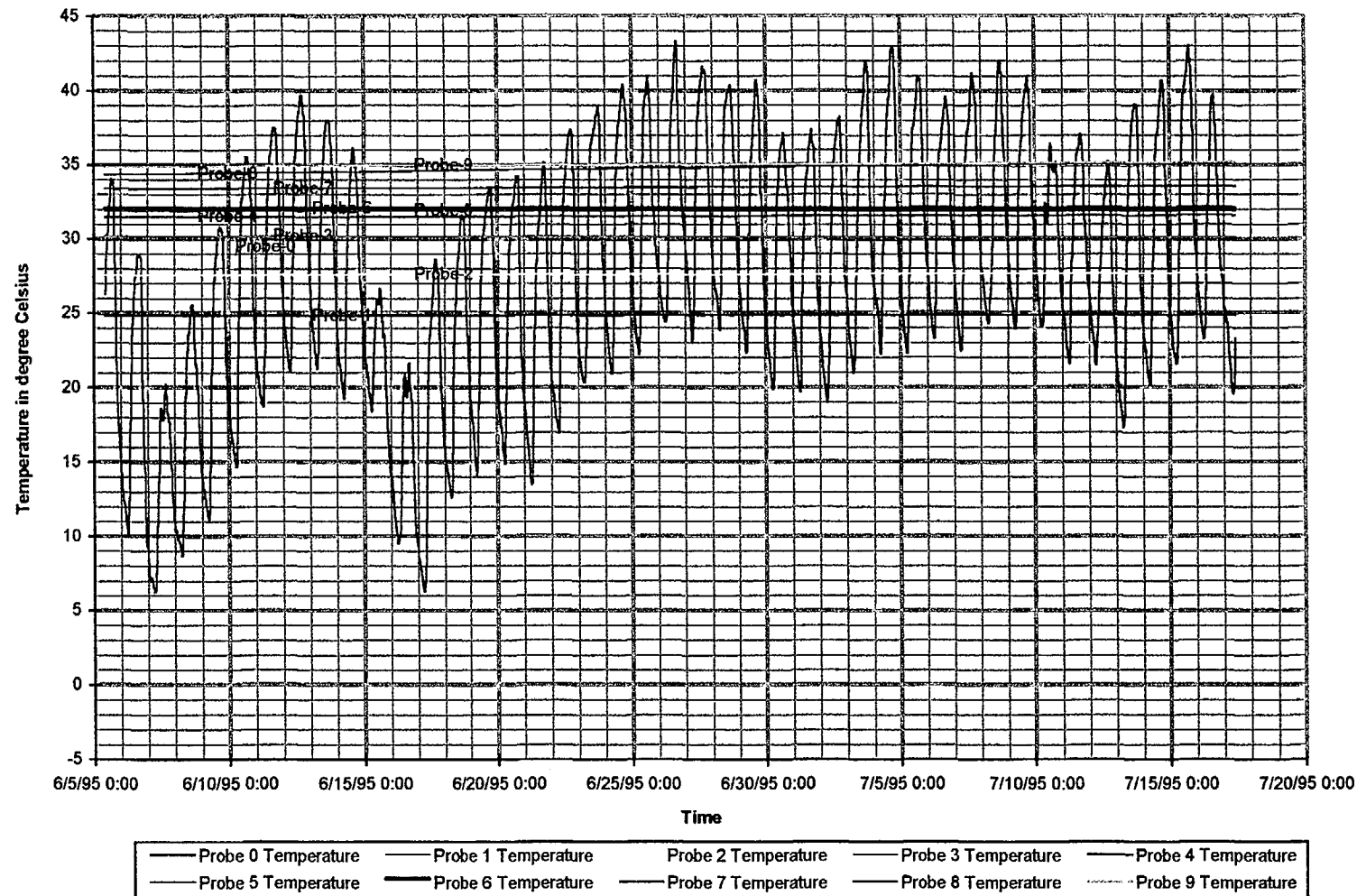


Figure 4-1c Temperature fluctuation with time in ONC-1

JULY 1995

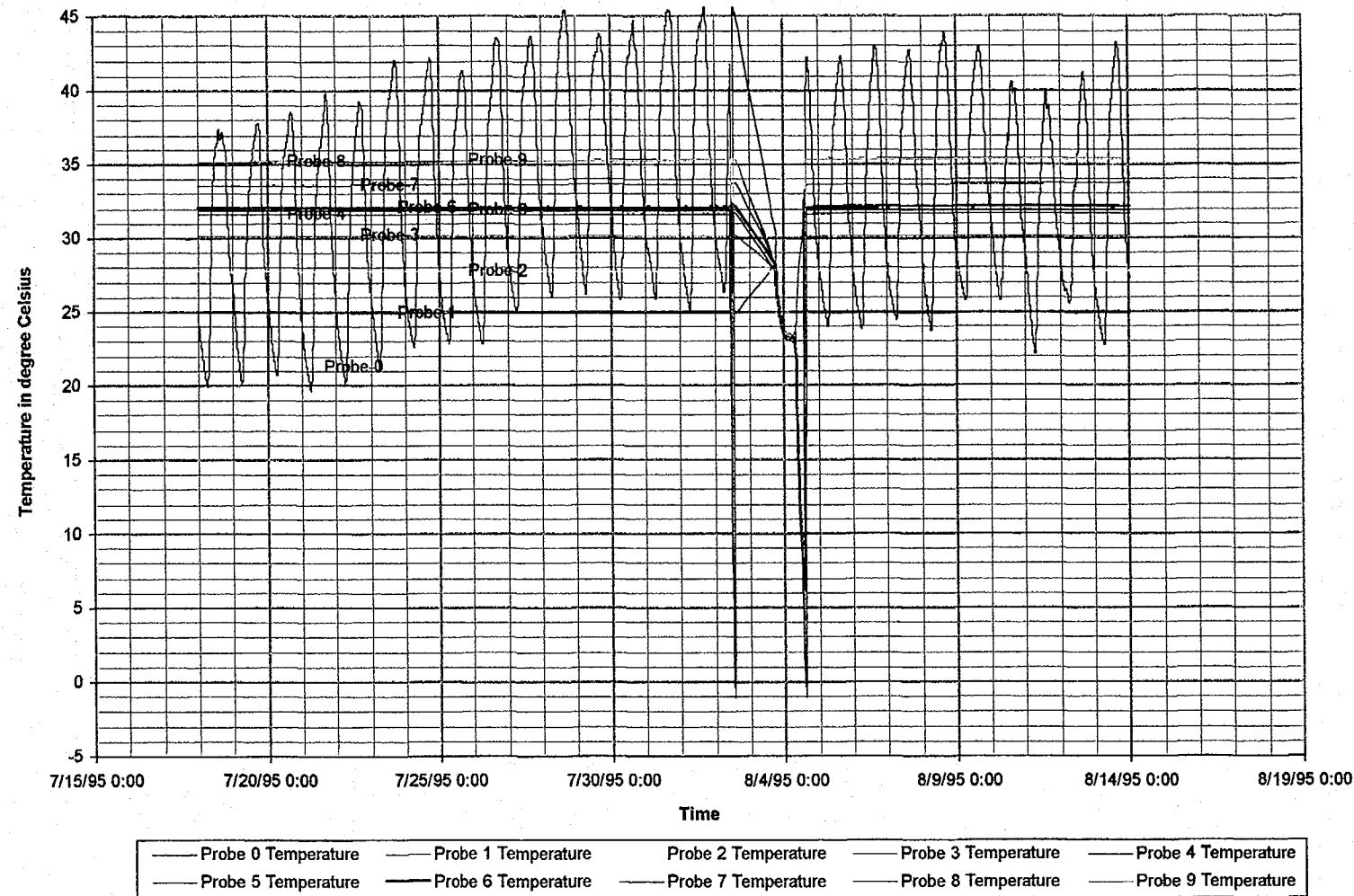


Figure 4-1d Temperature fluctuation with time in ONC-1

August 24, 1996
P266:D:\user\project\Nye\county\annrep96\figures

Prepared for:
Nye County Nuclear Waste Repository Project Office

Prepared by:
Multimedia Environmental Technology, Inc.
Newport Beach, CA

AUGUST 1995

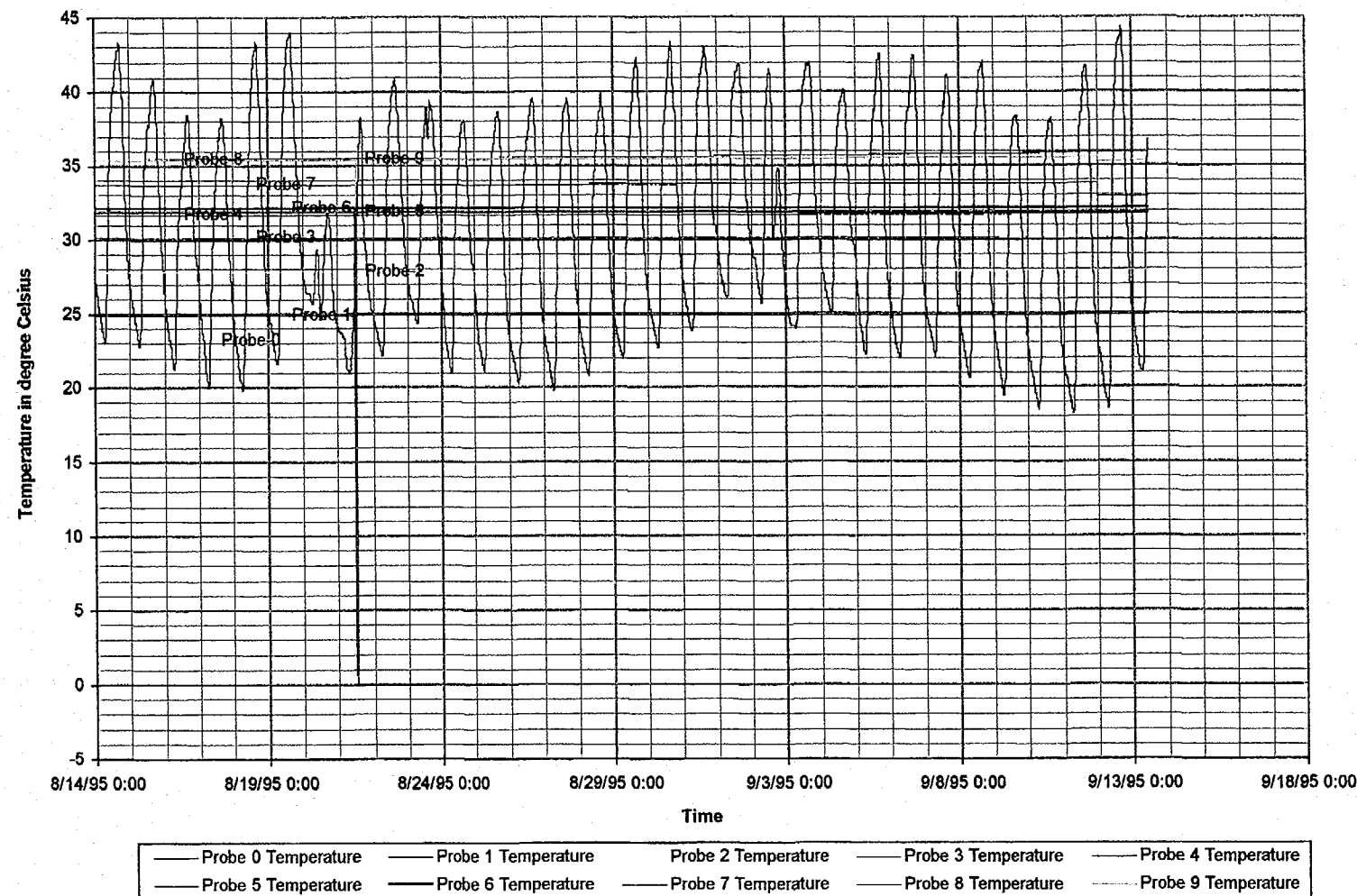


Figure 4-1e Temperature fluctuation with time in ONC-1

August 24, 1996
P266:D:\user\projects\NyeCounty\annrep96\figures

Prepared for:
Nye County Nuclear Waste Repository Project Office

Prepared by:
Multimedia Environmental Technology, Inc.
Newport Beach, CA

SEPT. 1995

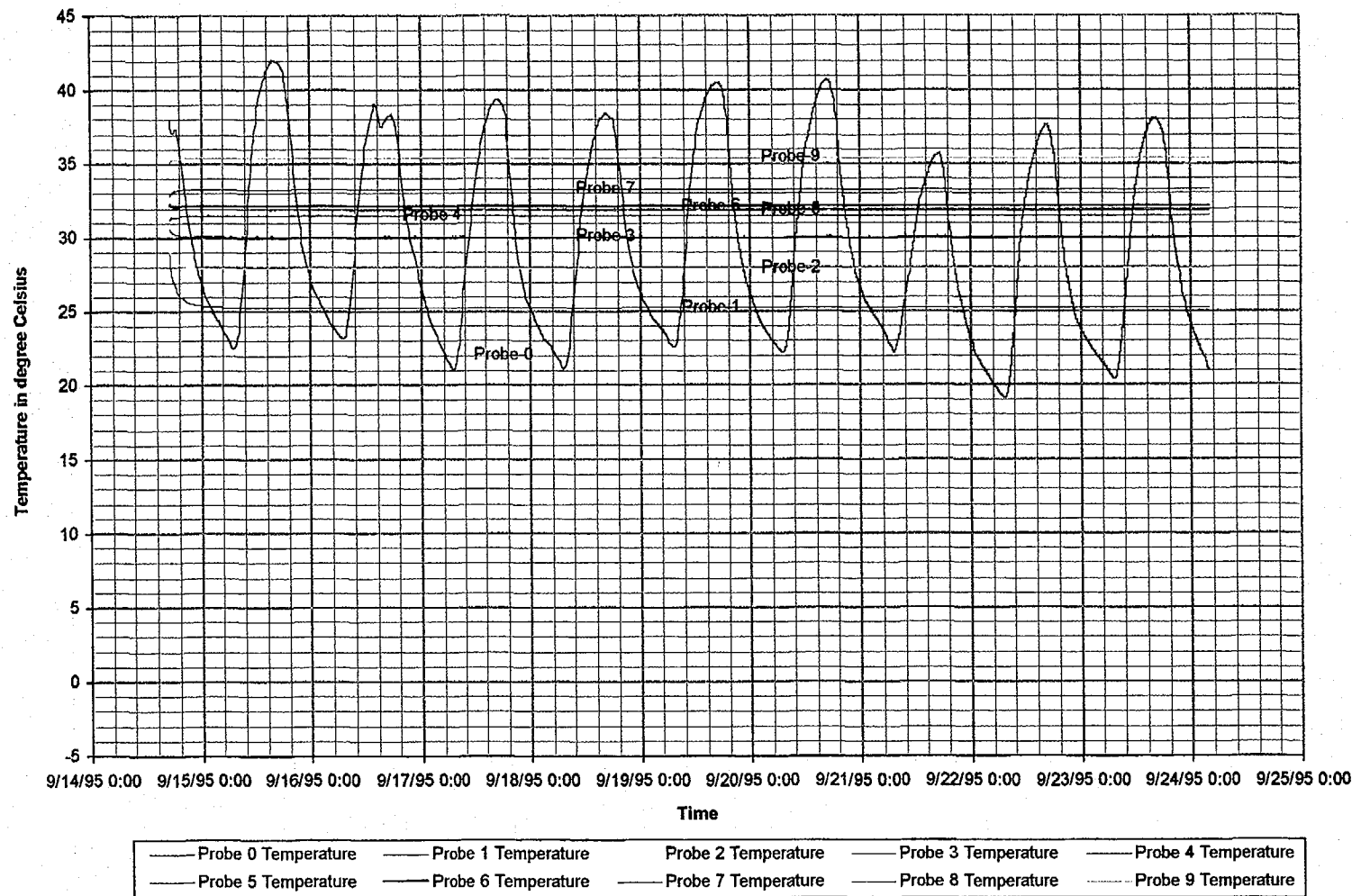


Figure 4-1f Temperature fluctuation with time in ONC-1

OCT. 1995

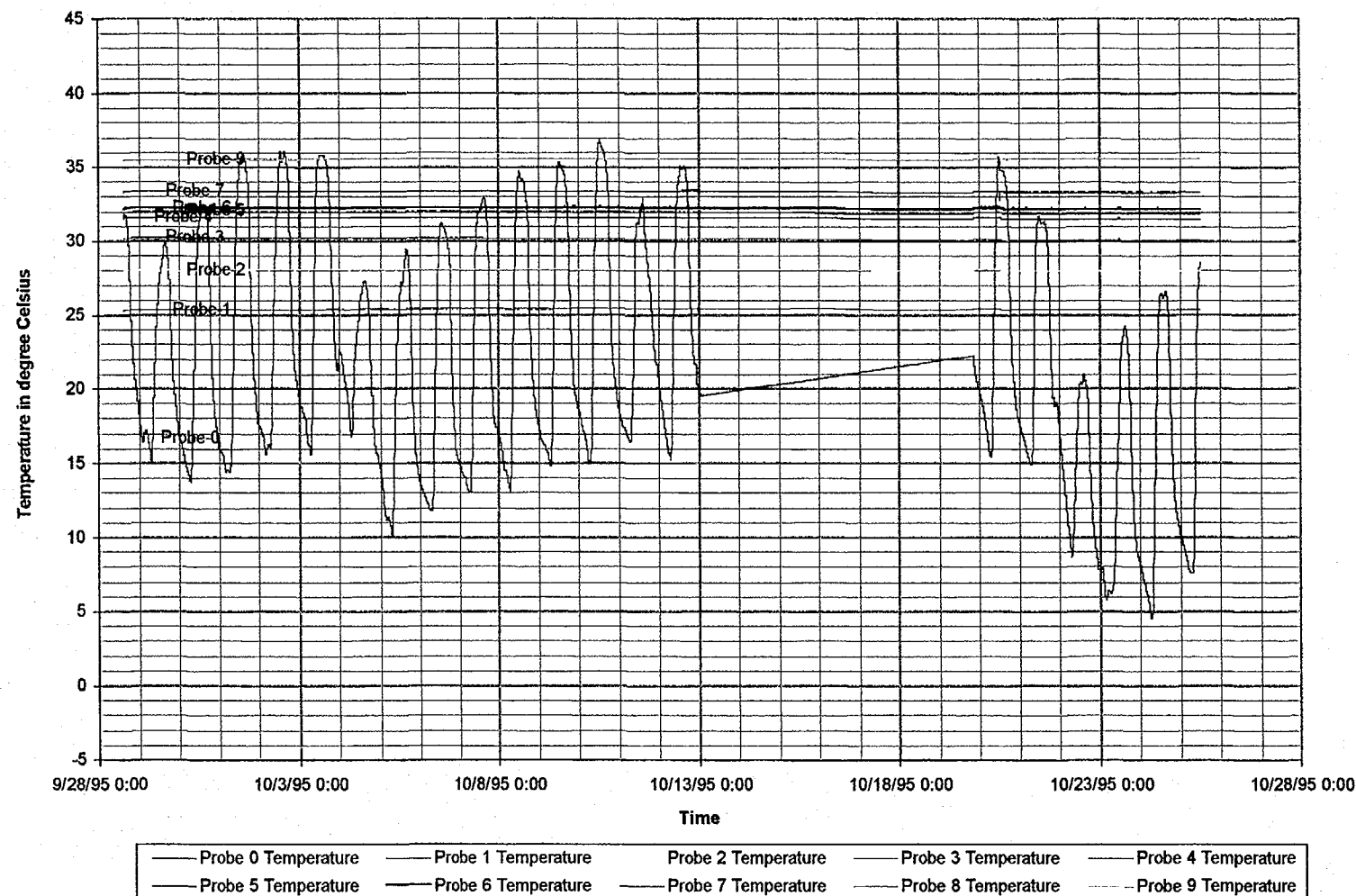


Figure 4-1g Temperature fluctuation with time in ONC-1

November 1995

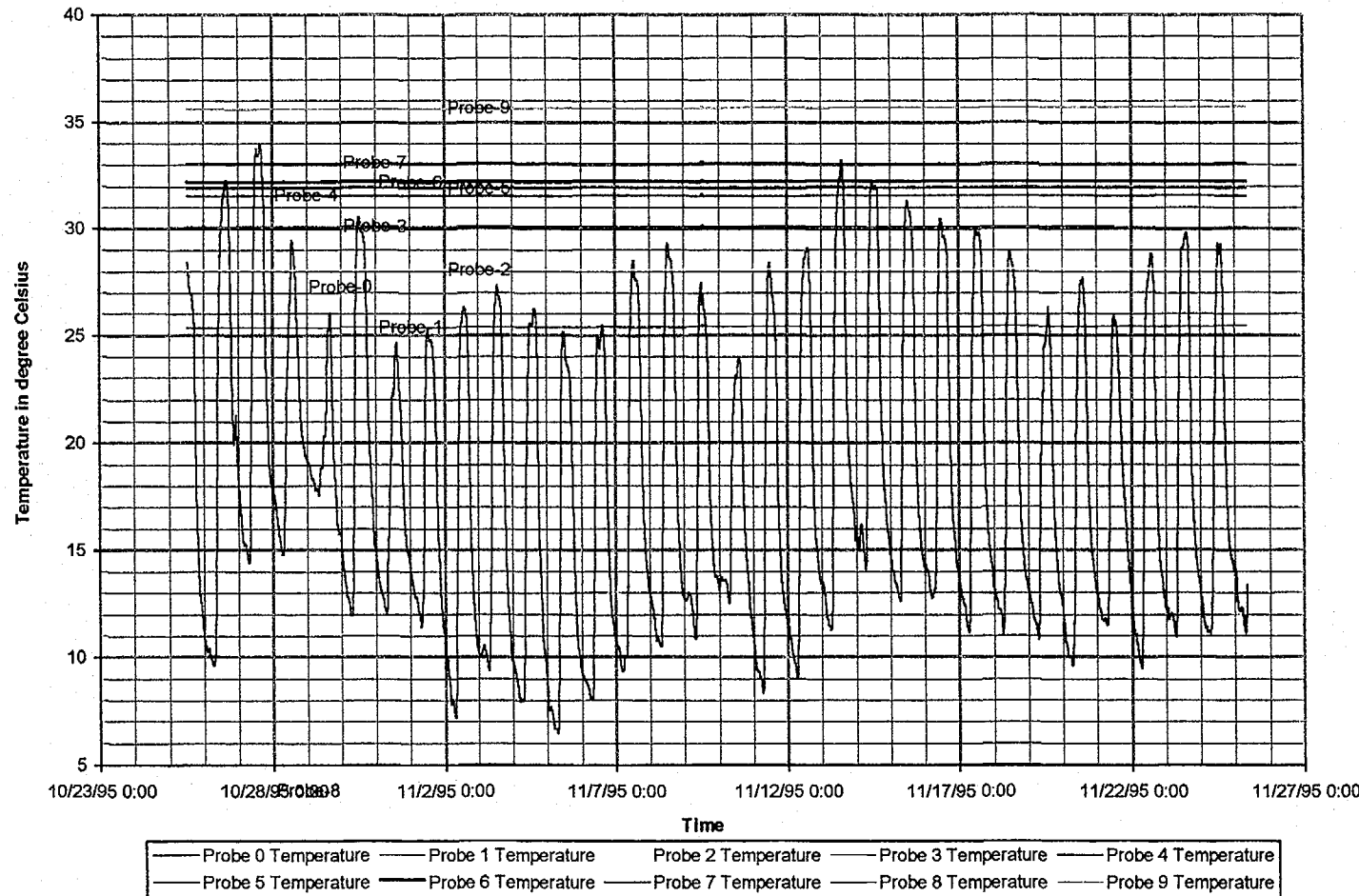


Figure 4-1h Temperature fluctuation with time in ONC-1

August 24, 1996
P2663:32 PMD:\user\projects\NyeCounty\annrep96\figures

Prepared for:
Nye County Nuclear Waste Repository Project Office

Prepared by:
Multimedia Environmental Technology, Inc.
Newport Beach, CA

December 1995

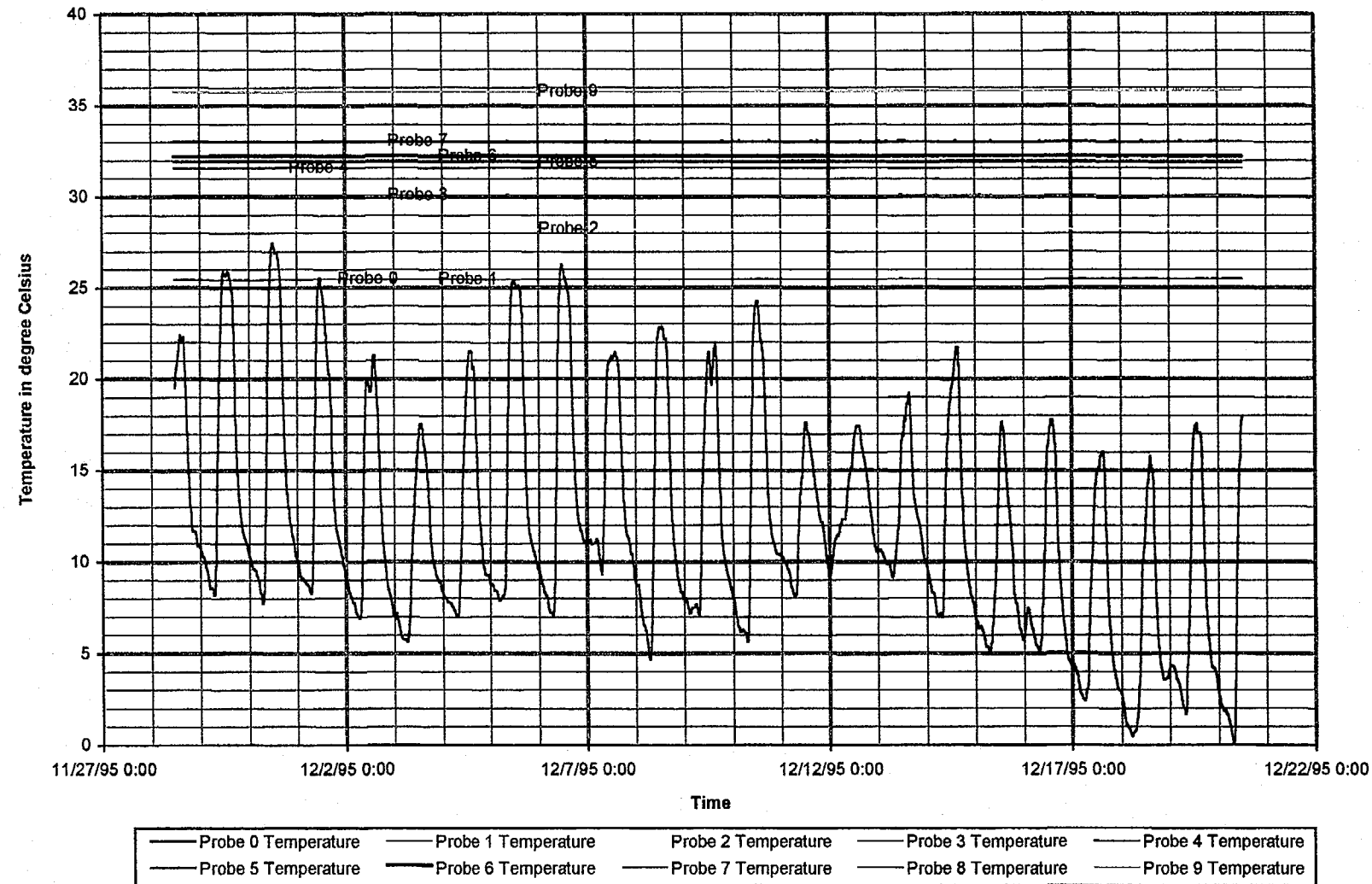


Figure 4-1I Temperature fluctuation with time in ONC-1

January 1996

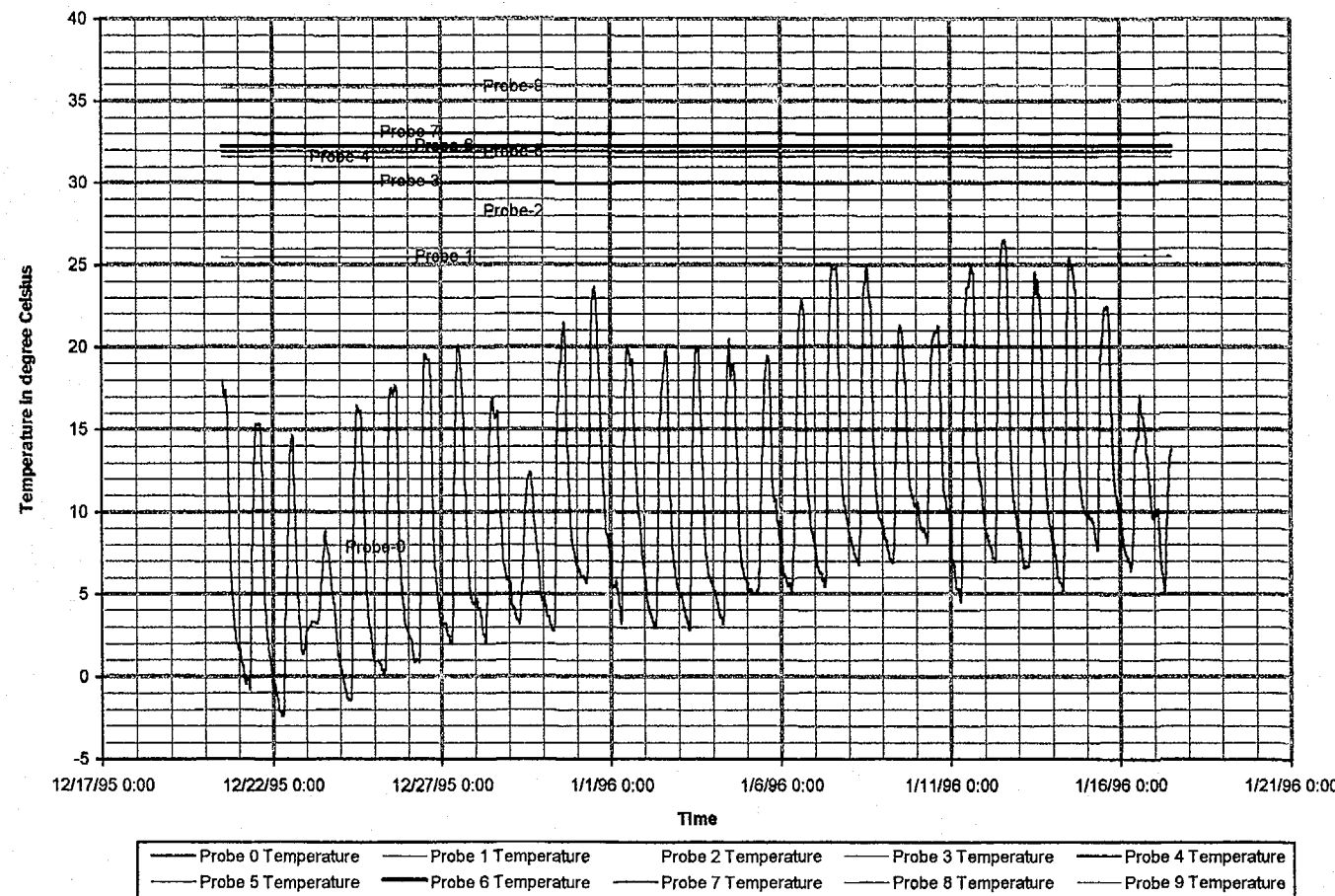


Figure 4-1j Temperature fluctuation with time in ONC-1

August 24, 1996
P2664:05 PMD:\user\projects\Nye county\unrop96\figures

Prepared for:
Nye County Nuclear Waste Repository Project Office

Prepared by:
Multimedia Environmental Technology, Inc.
Newport Beach, CA

February 1996

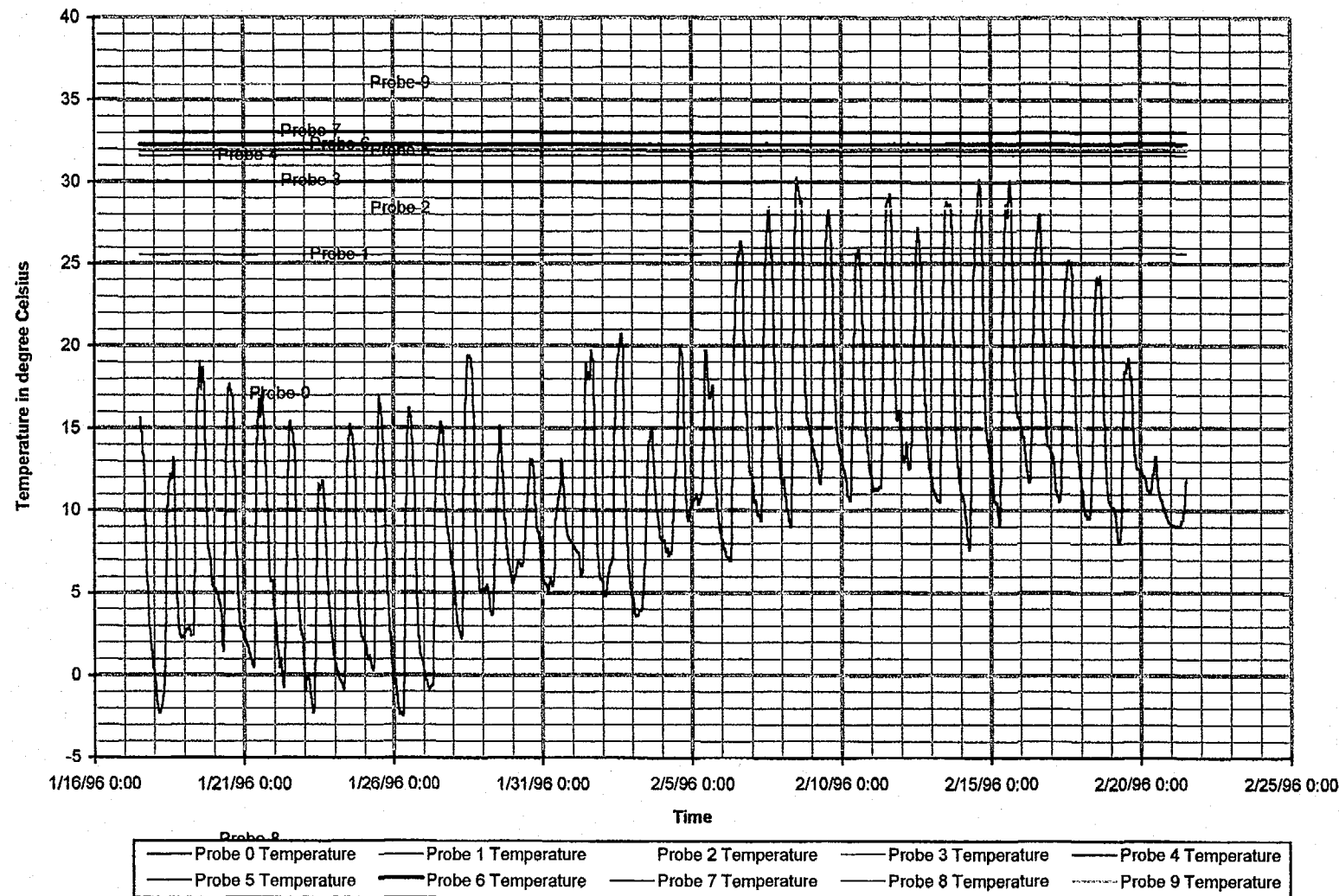


Figure 4-1k Temperature fluctuation with time in ONC-1

MARCH 1996

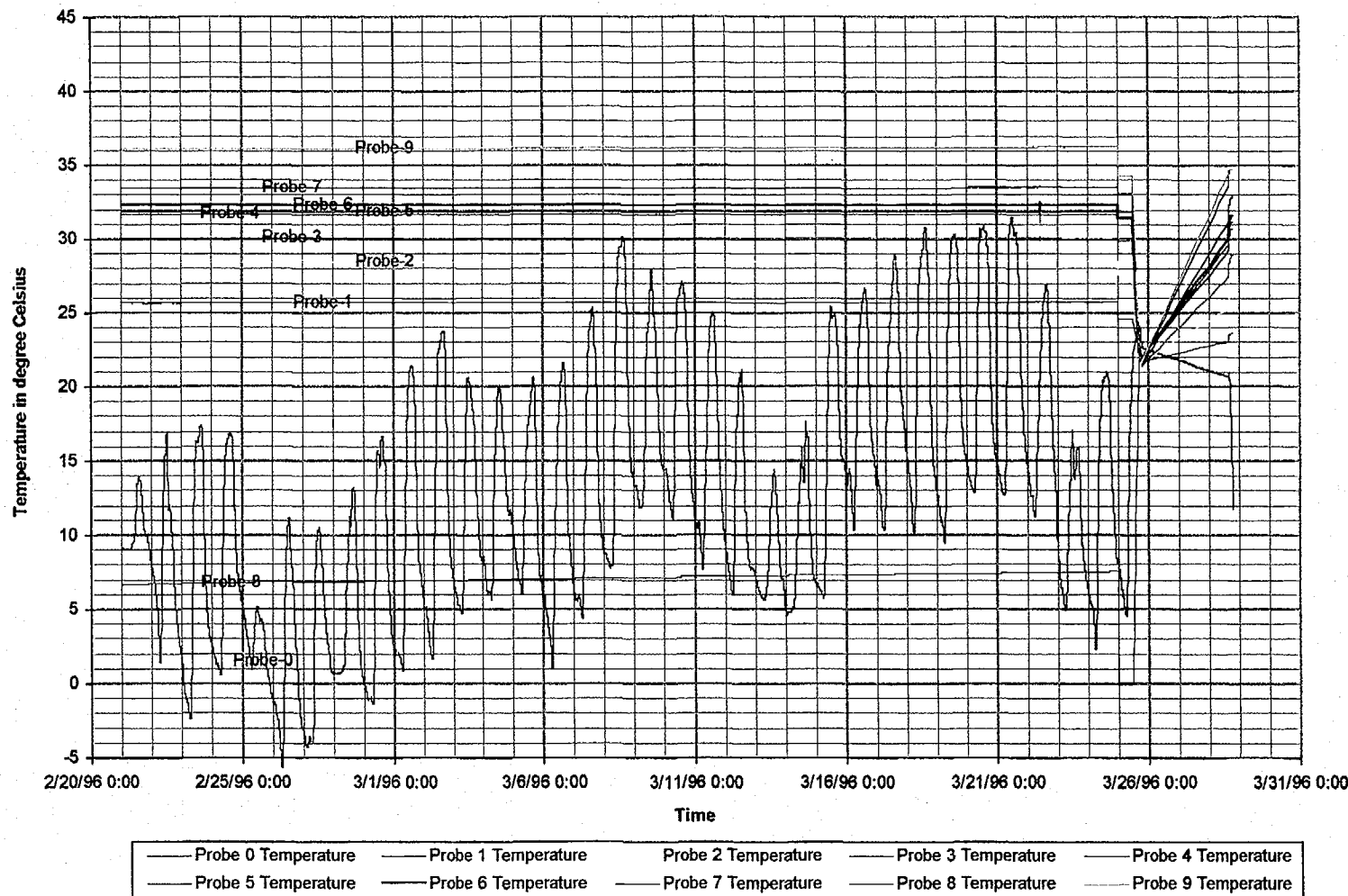


Figure 4-1L Temperature fluctuation with time in ONC-1

APRIL 1996

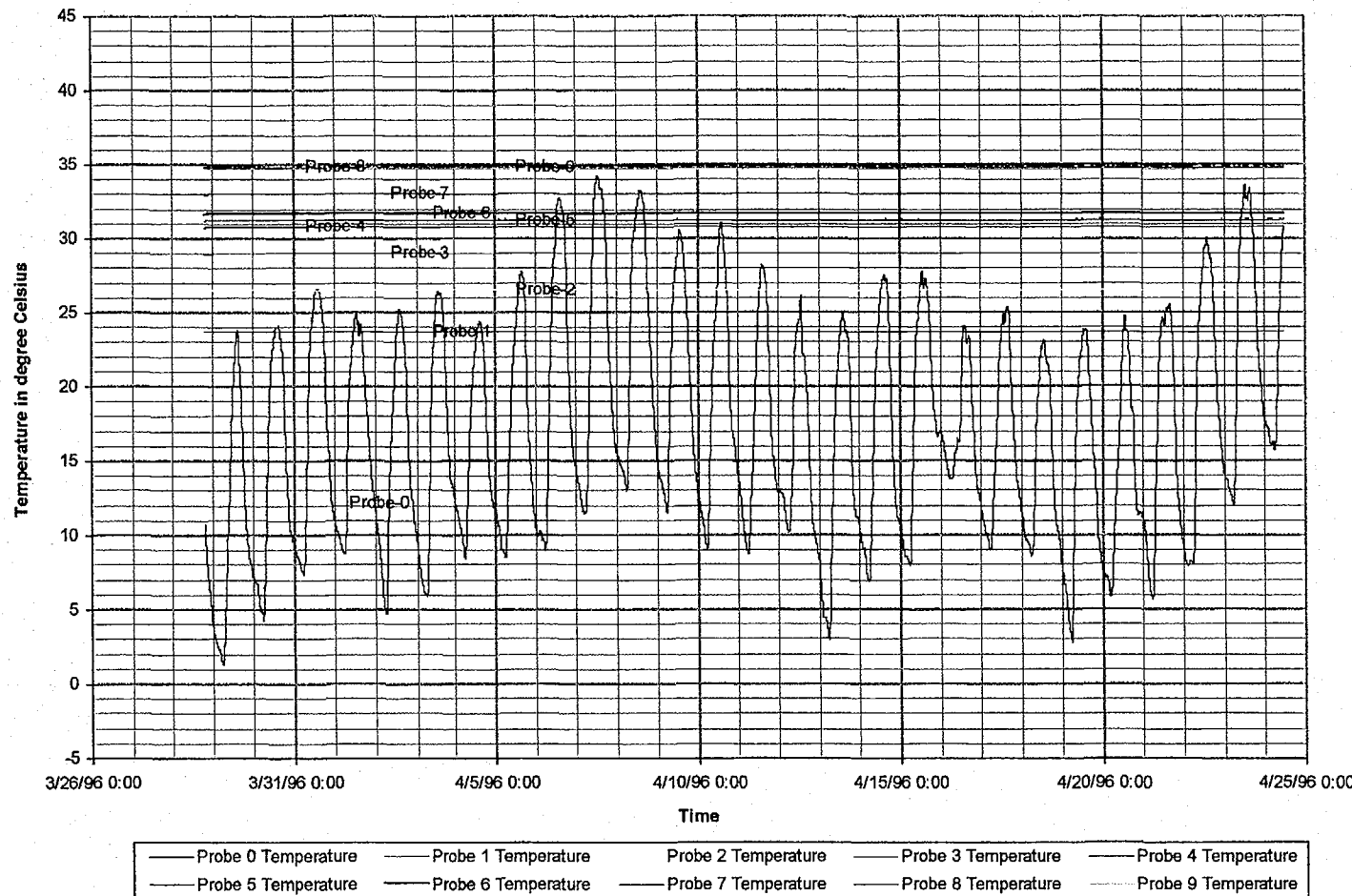


Figure 4-1m Temperature fluctuation with time in ONC-1

August 24, 1996
P266:D:\user\projects\NyeCounty\annrep96\figures

Prepared for:
Nye County Nuclear Waste Repository Project Office

Prepared by:
Multimedia Environmental Technology, Inc.
Newport Beach, CA

MAY 1996

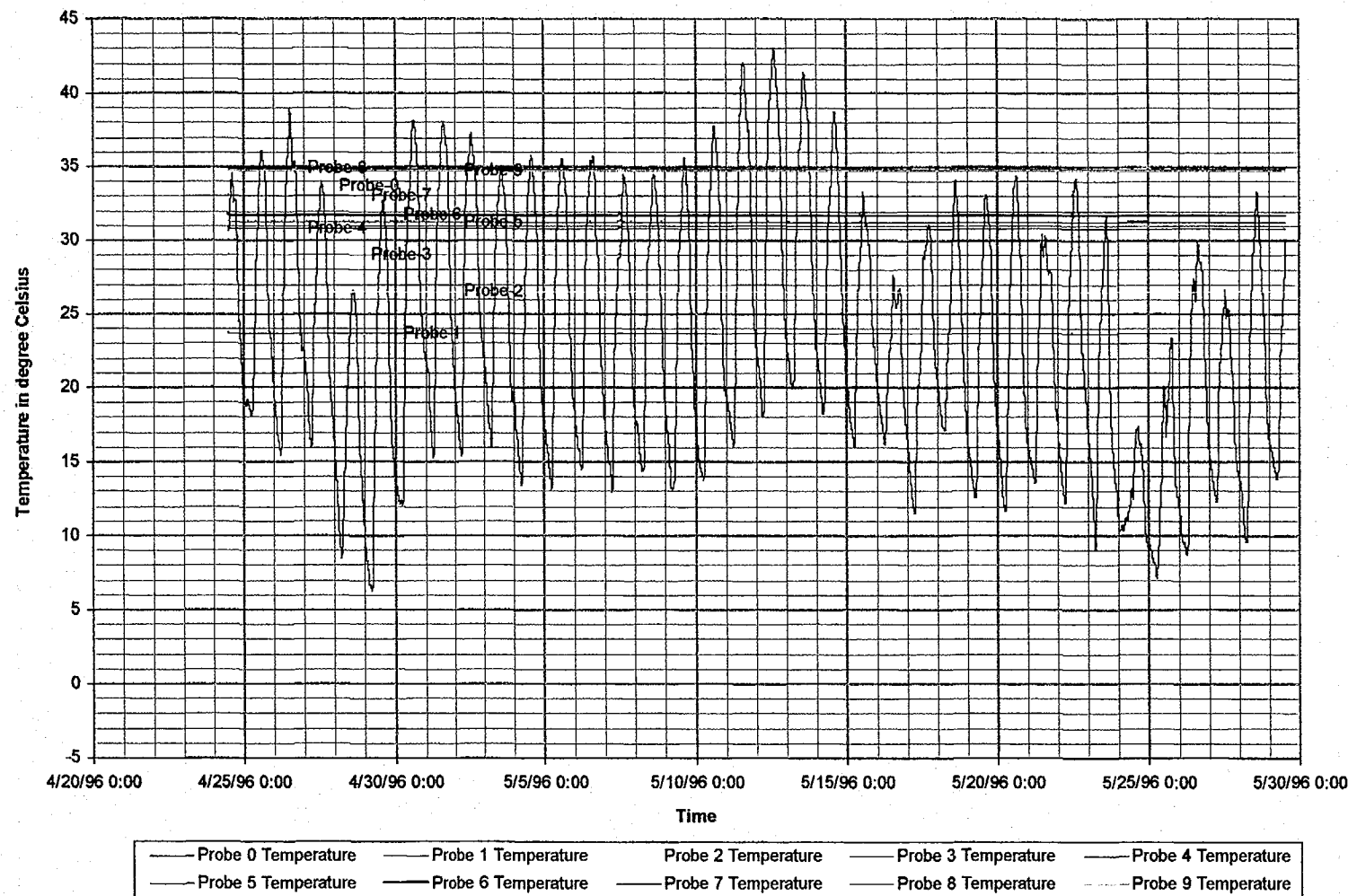


Figure 4-1n Temperature fluctuation with time in ONC-1

August 24, 1996
P266:D:\user\projects\NyeCounty\annrep96\figures

Prepared for:
Nye County Nuclear Waste Repository Project Office

Prepared by:
Multimedia Environmental Technology, Inc.
Newport Beach, CA

JUNE 1996

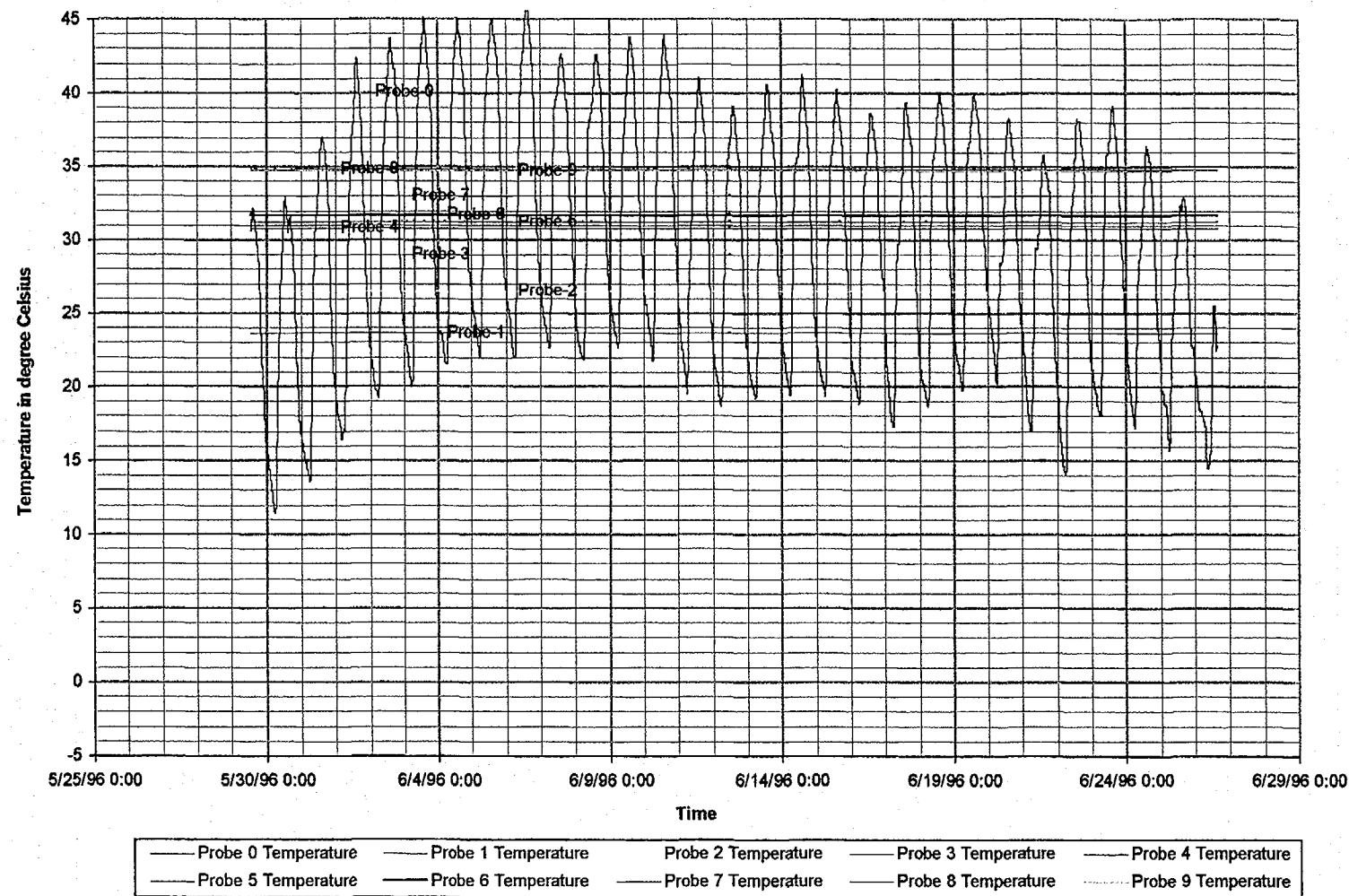


Figure 4-10 Temperature fluctuation with time in ONC-1

August 24, 1996
P266:D:\user\projects\NyeCounty\annrep96\figures

Prepared for:
Nye County Nuclear Waste Repository Project Office

Prepared by:
Multimedia Environmental Technology, Inc.
Newport Beach, CA

JULY 1996

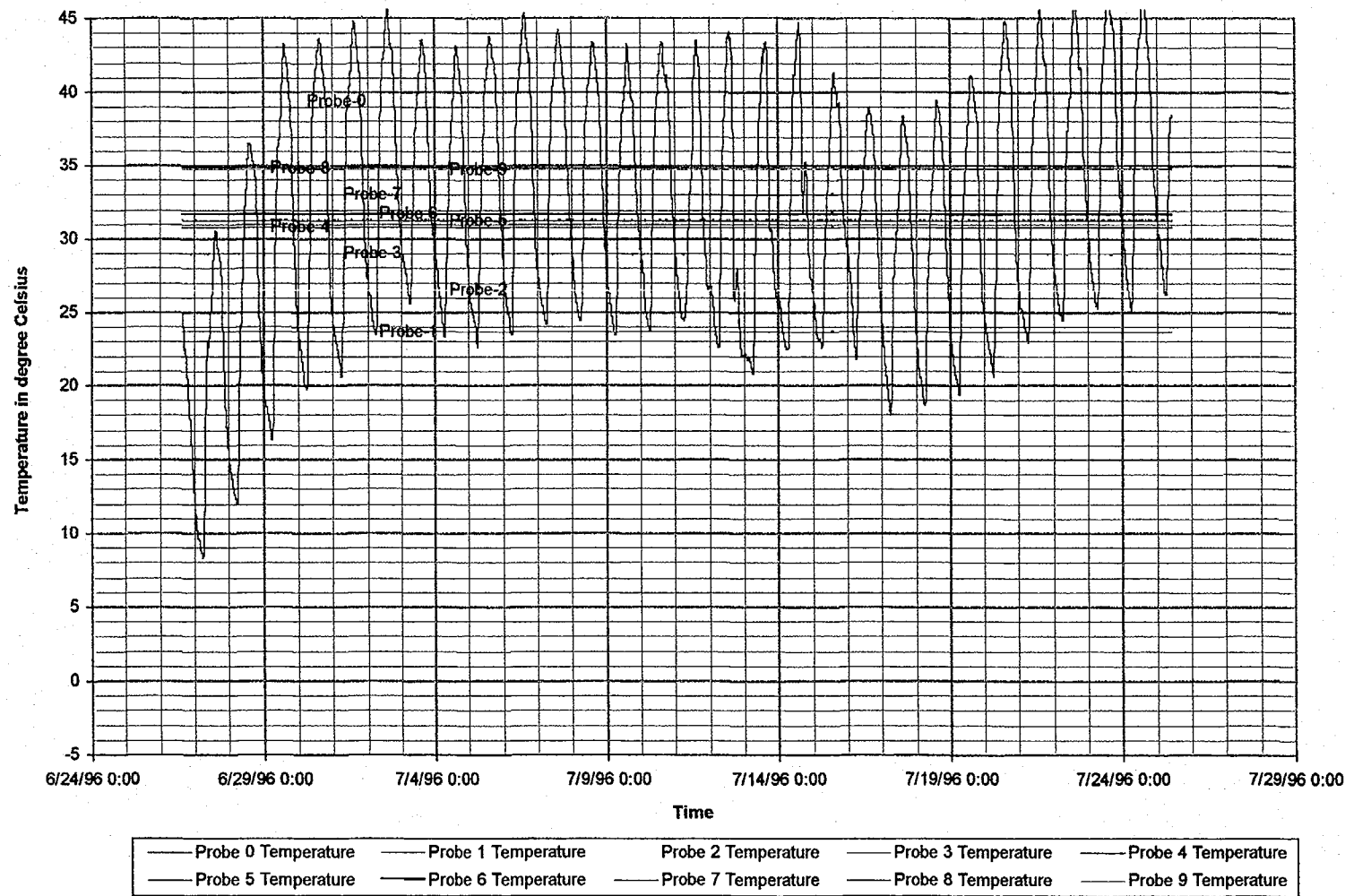


Figure 4-1p Temperature fluctuation with time in ONC-1

August 1996

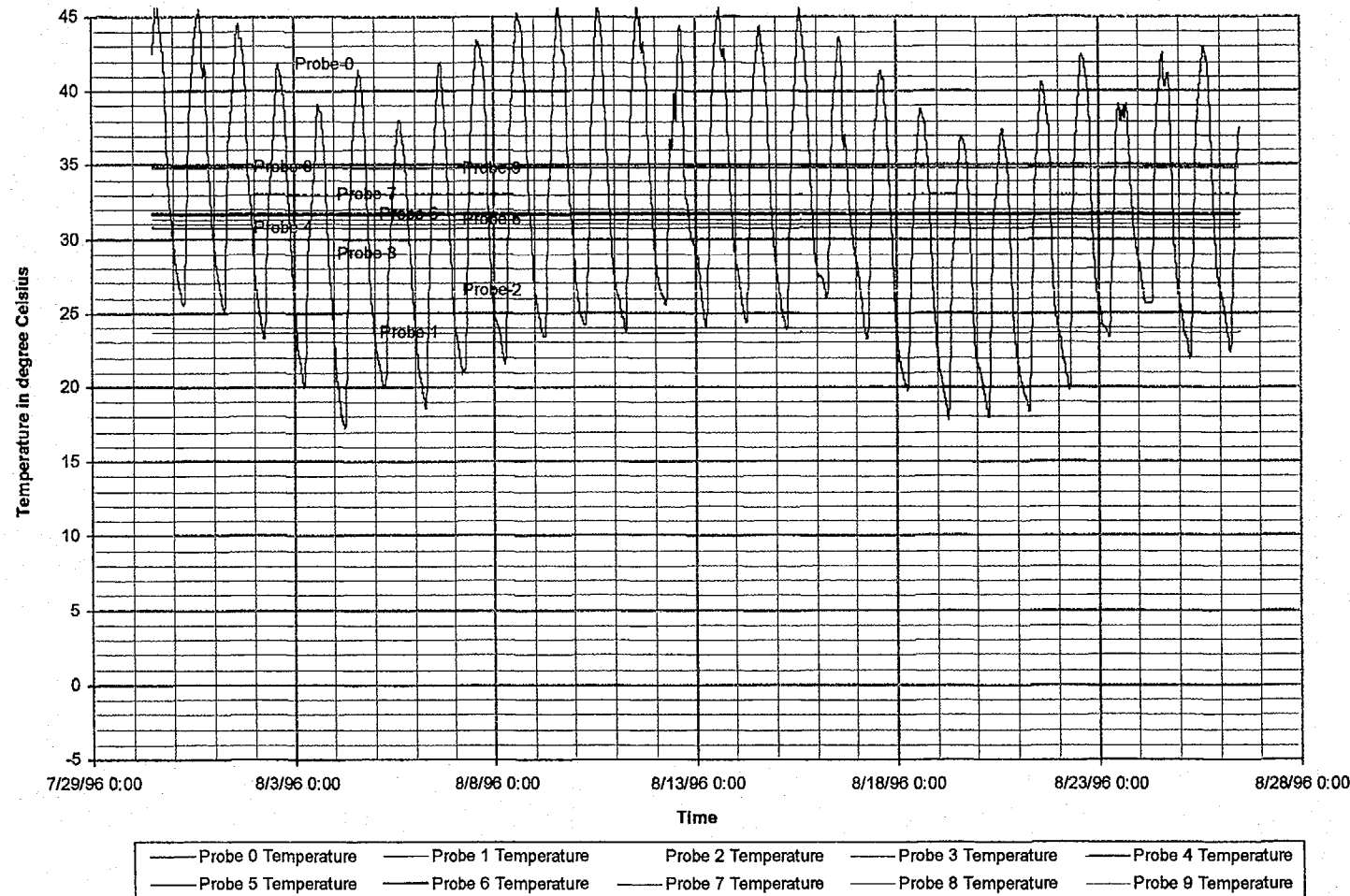


Figure 4-1q Temperature fluctuation with time in ONC-1

April 1995

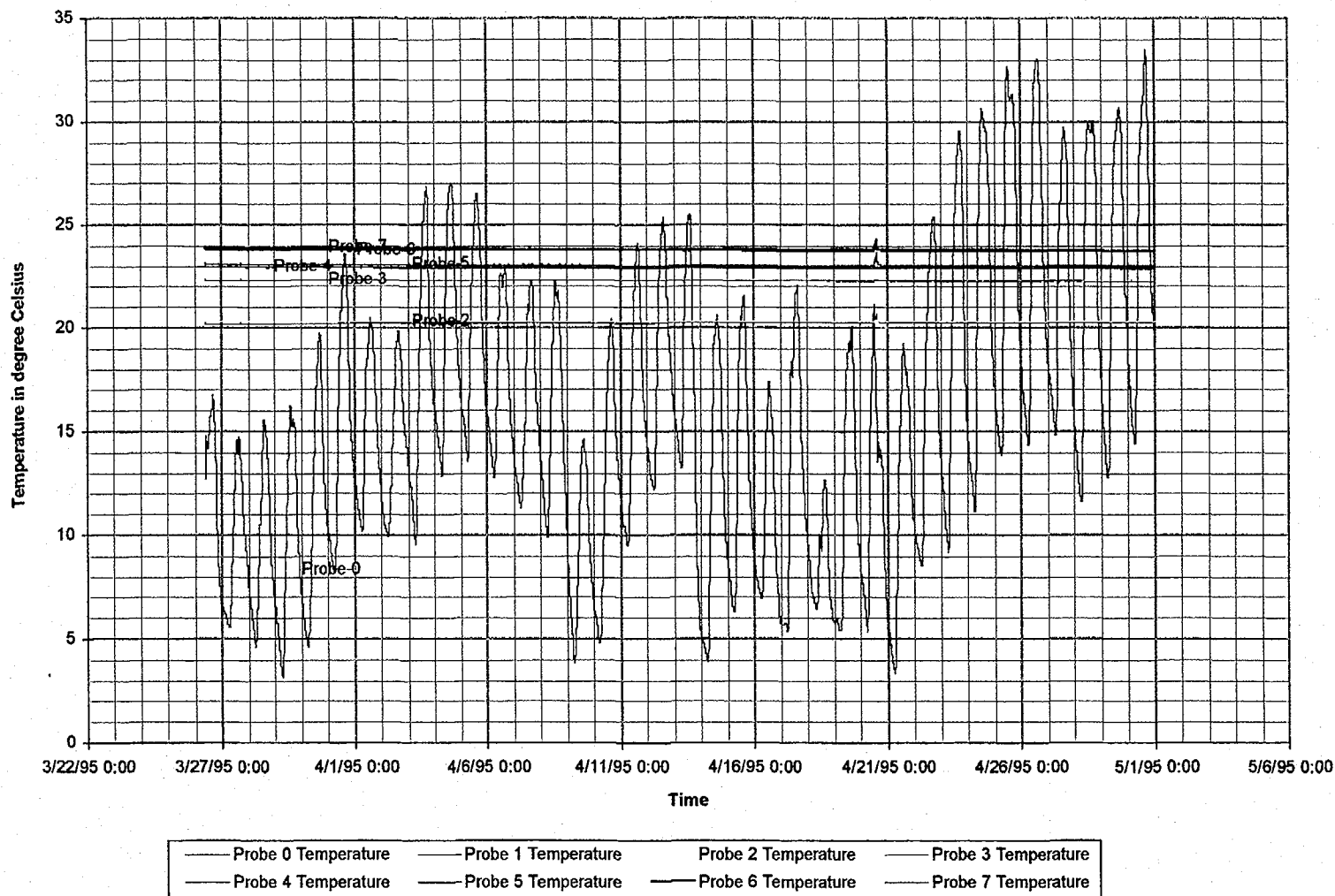


Figure 4-2a Temperature fluctuation with time in NRG-4

MAY 1995

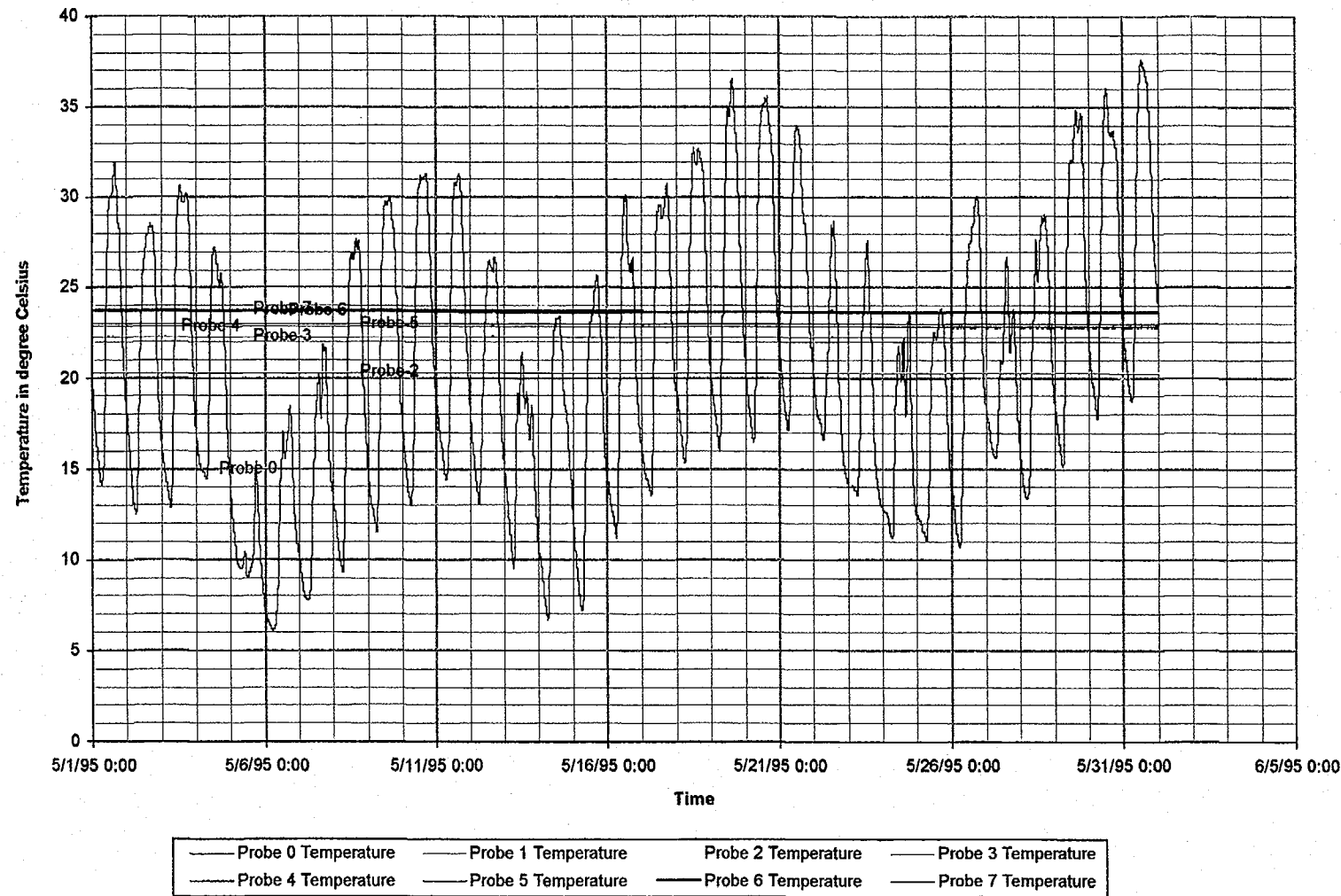


Figure 4-2b Temperature fluctuation with time in NRG-4

JUNE 1995

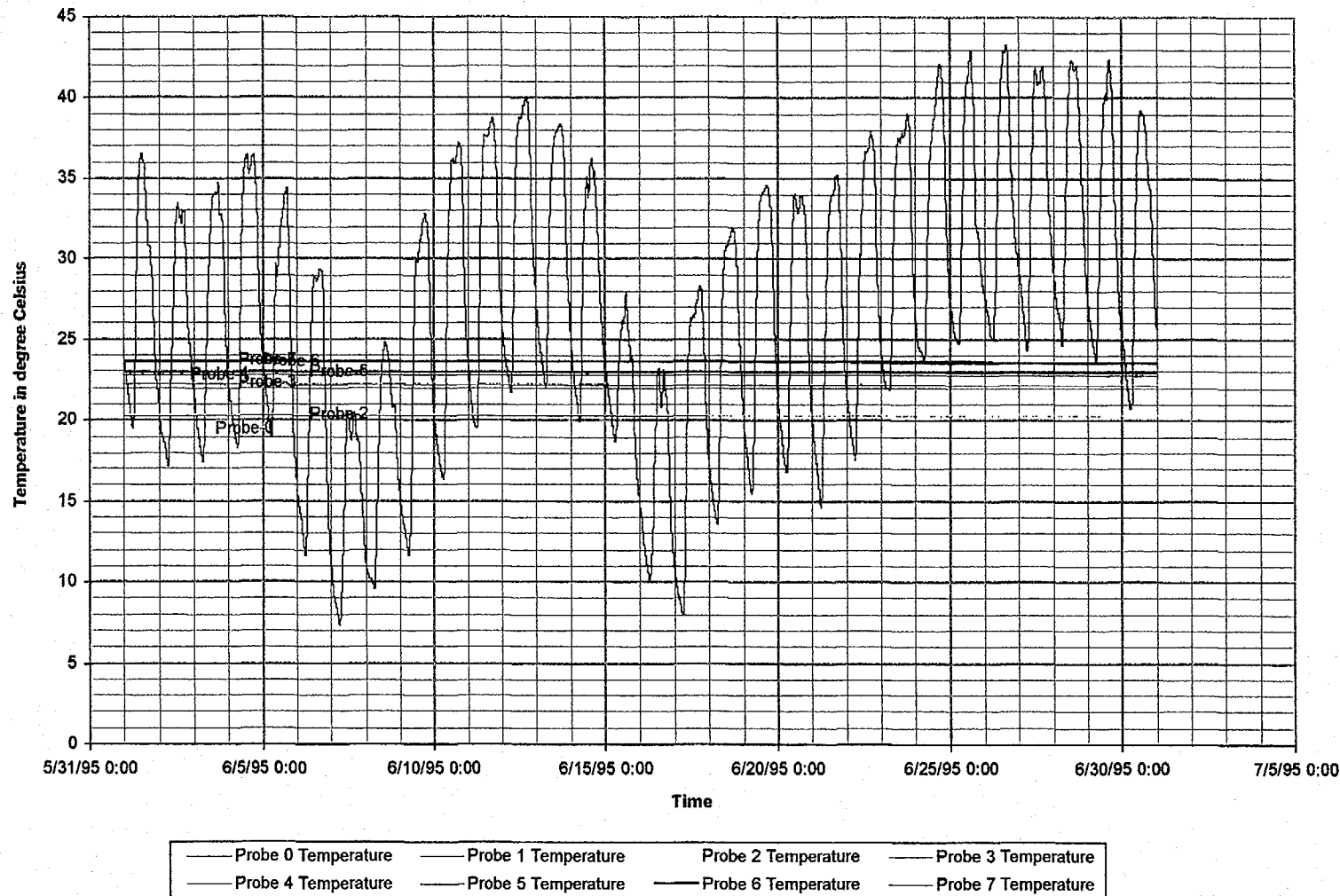


Figure 4-2c Temperature fluctuation with time in NRG-4

JULY 1995

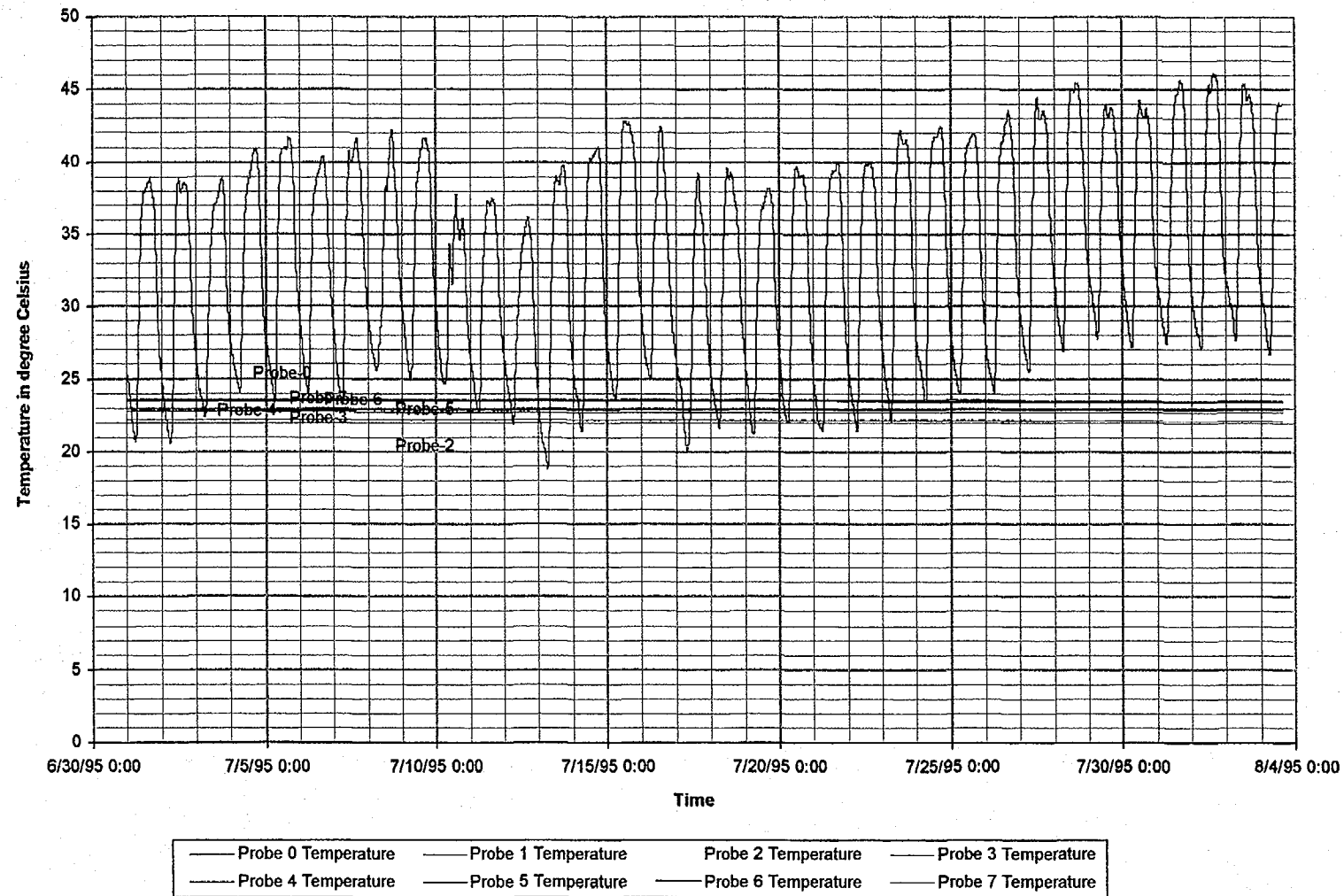


Figure 4-2d Temperature fluctuation with time in NRG-4

SEPT. 1995

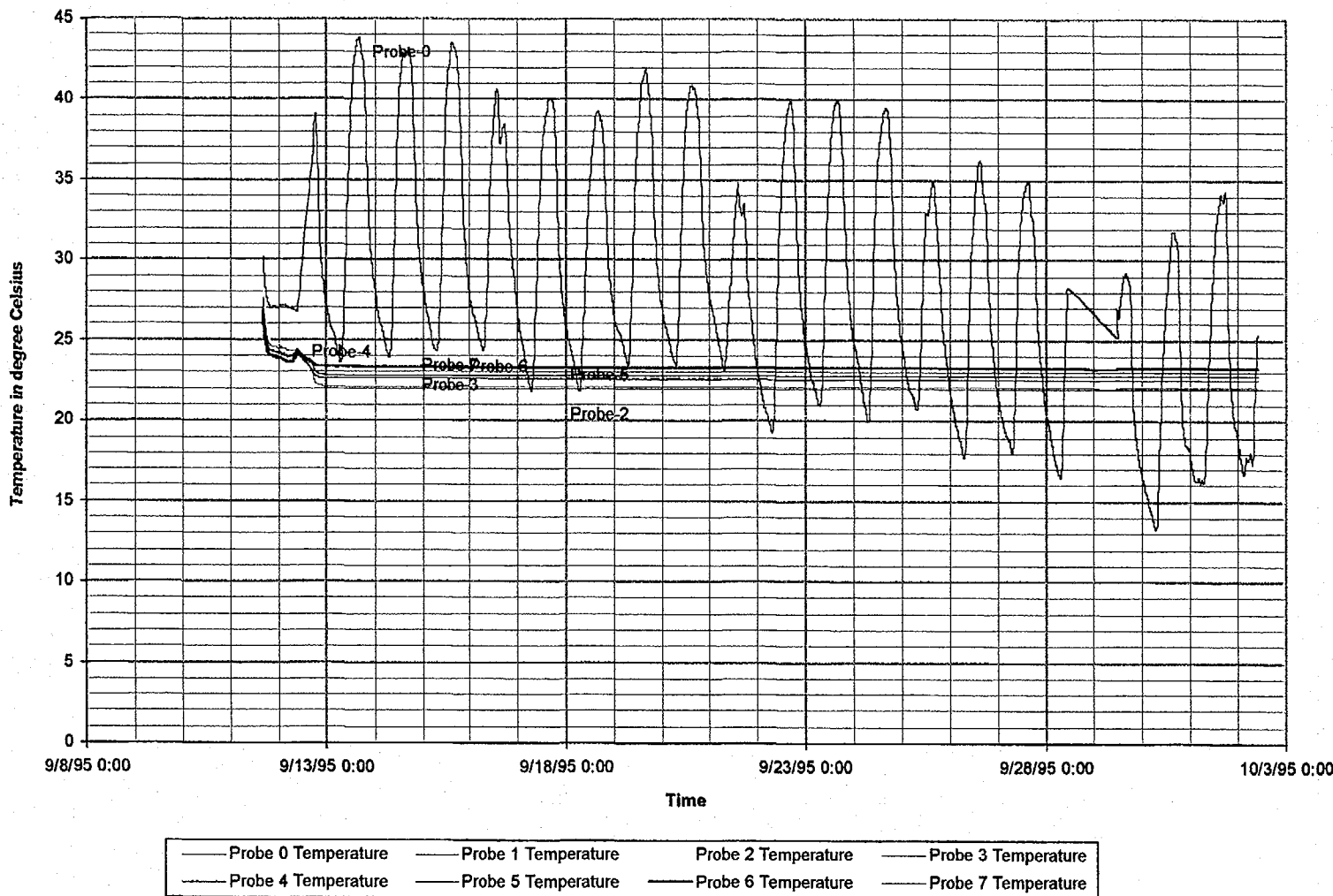


Figure 4-2e Temperature fluctuation with time in NRG-4

OCT. 1995

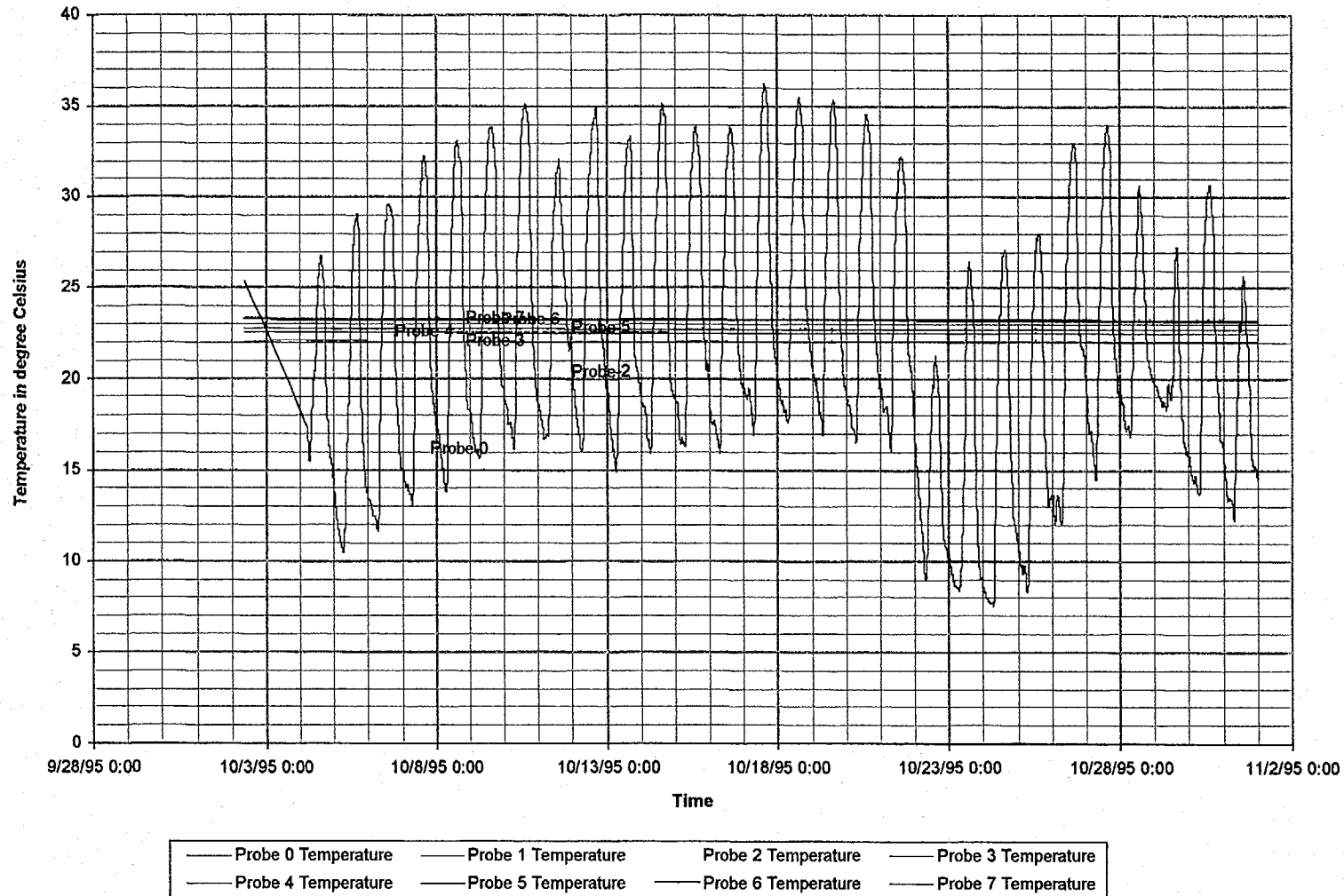


Figure 4-2f Temperature fluctuation with time in NRG-4

November 1995

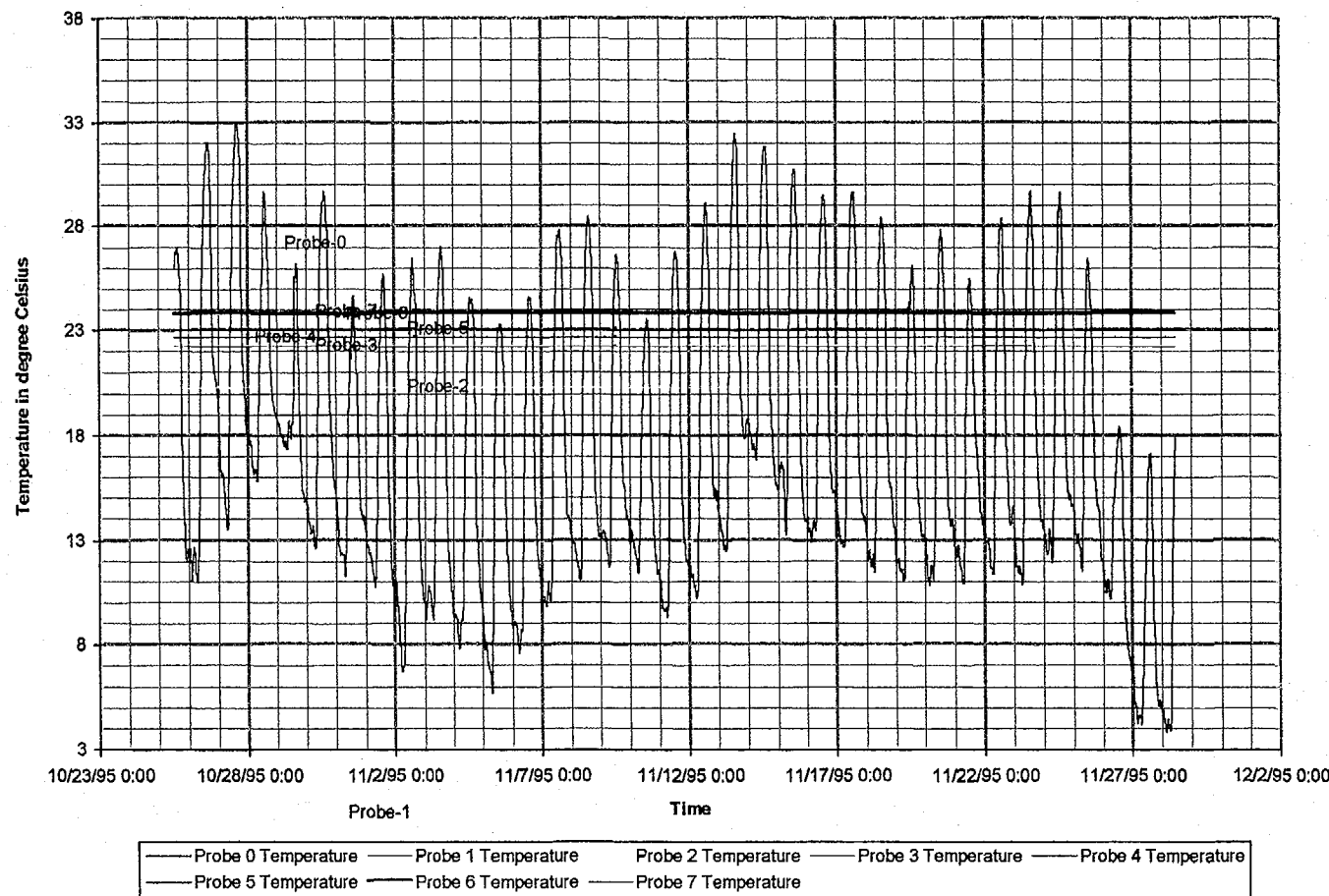


Figure 4-2g Temperature fluctuation with time in NRG-4

August 24, 1996
P2663:16 PMD:\user\projects\NyeCounty\mnrep96\figures

Prepared for:
Nye County Nuclear Waste Repository Project Office

Prepared by:
Multimedia Environmental Technology, Inc.
Newport Beach, CA

December 1995

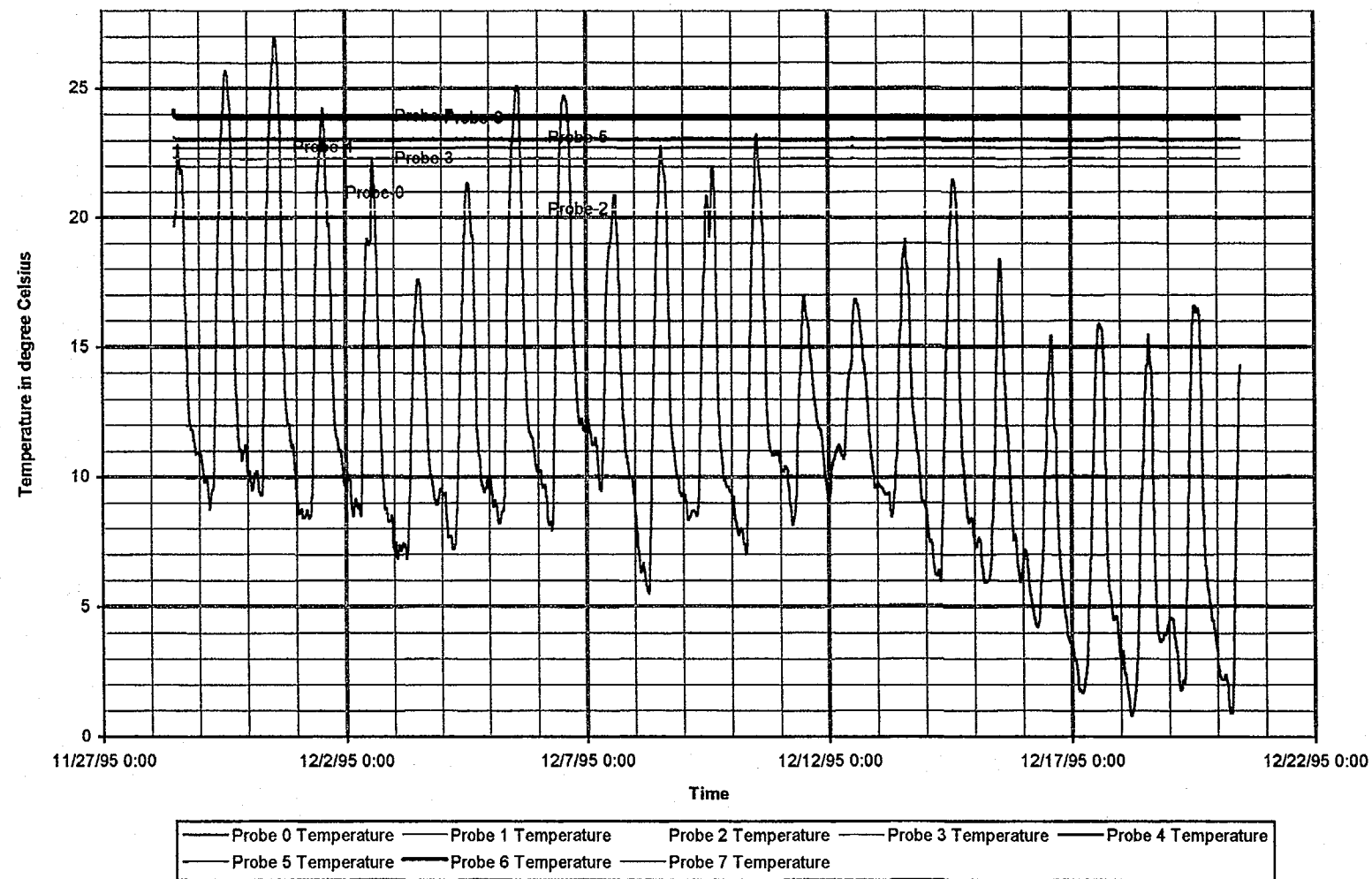


Figure 4-2h Temperature fluctuation with time in NRG-4

January 1996

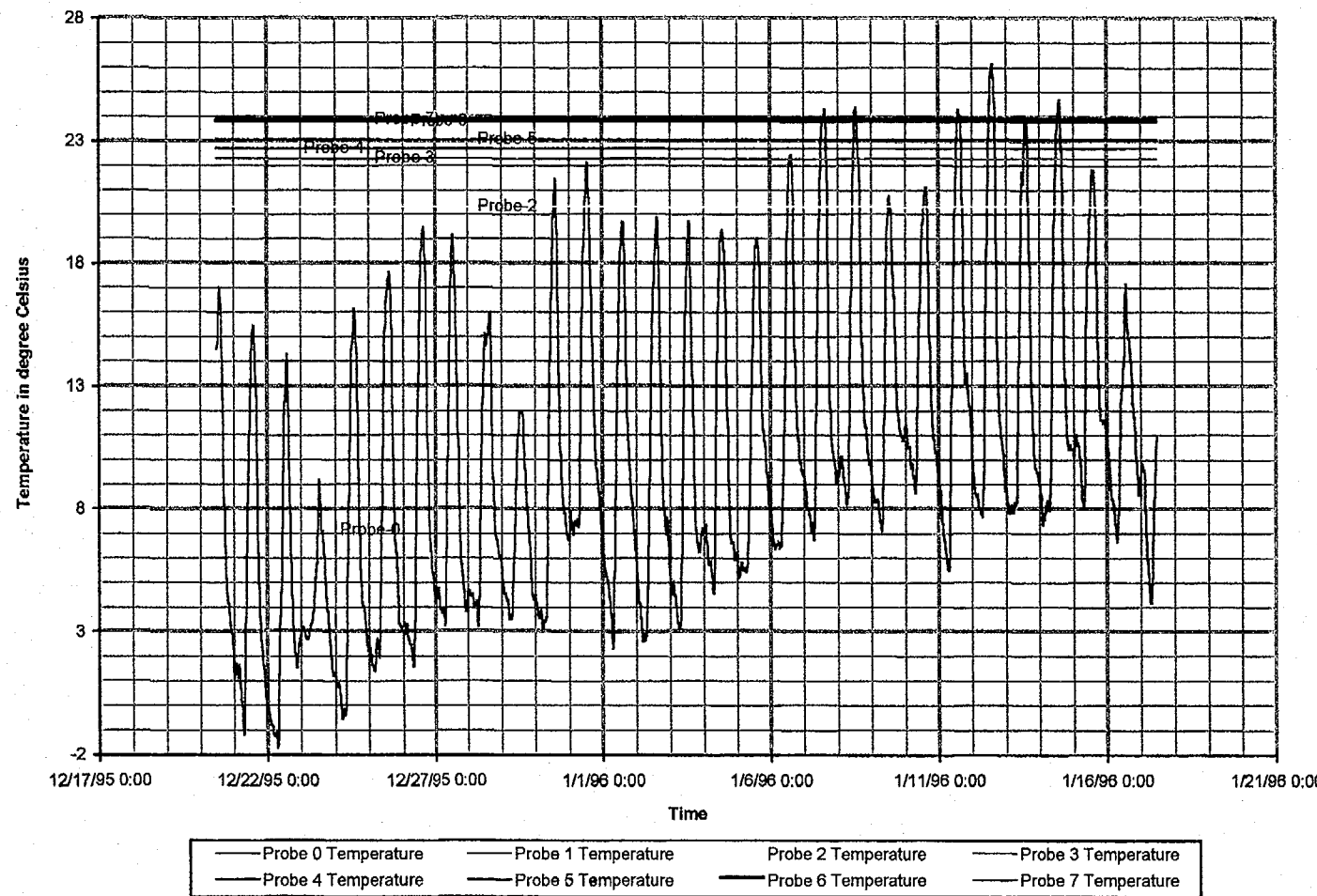


Figure 4-2i Temperature fluctuation with time in NRG-4

February 1996

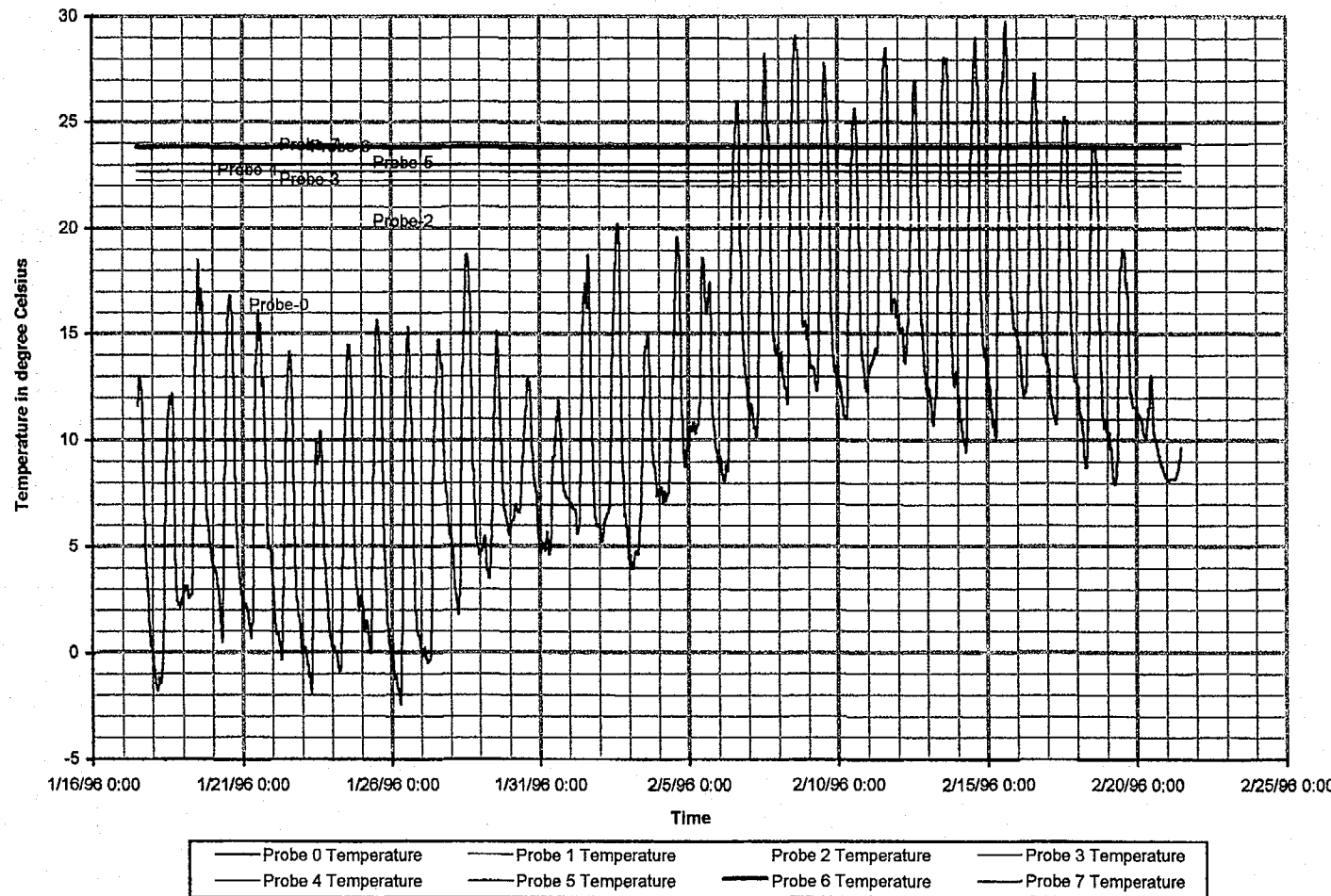


Figure 4-2j Temperature fluctuation with time in NRG-4

August 24, 1996

P2668:01 AMD:\user\projctas\Nyecounty\enarop96\figures

Prepared for:
Nye County Nuclear Waste Repository Project Office

Prepared by:
Multimedia Environmental Technology, Inc.
Newport Beach, CA

March 1996

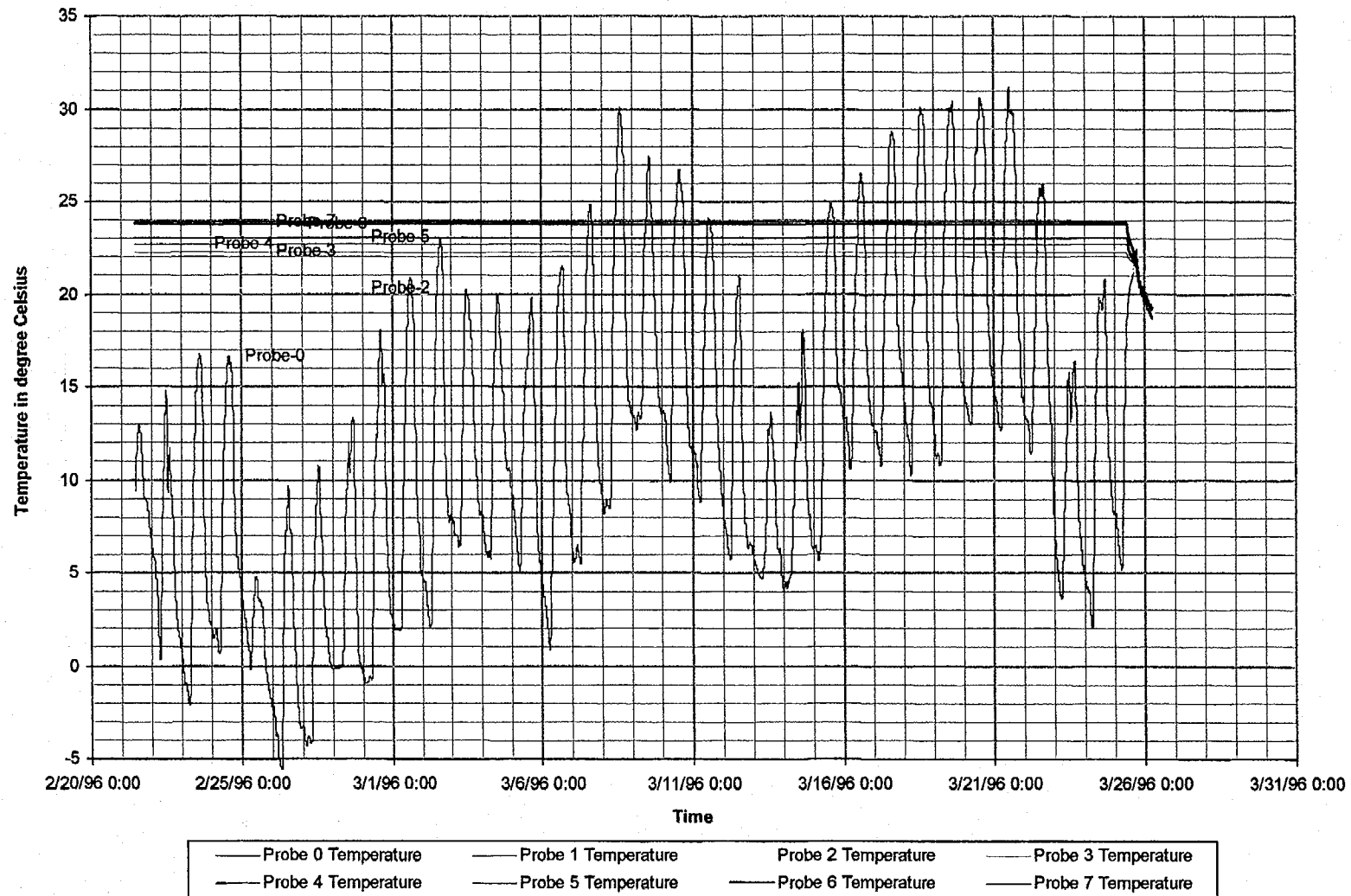


Figure 4-2k Temperature fluctuation with time in NRG-4

April 1996

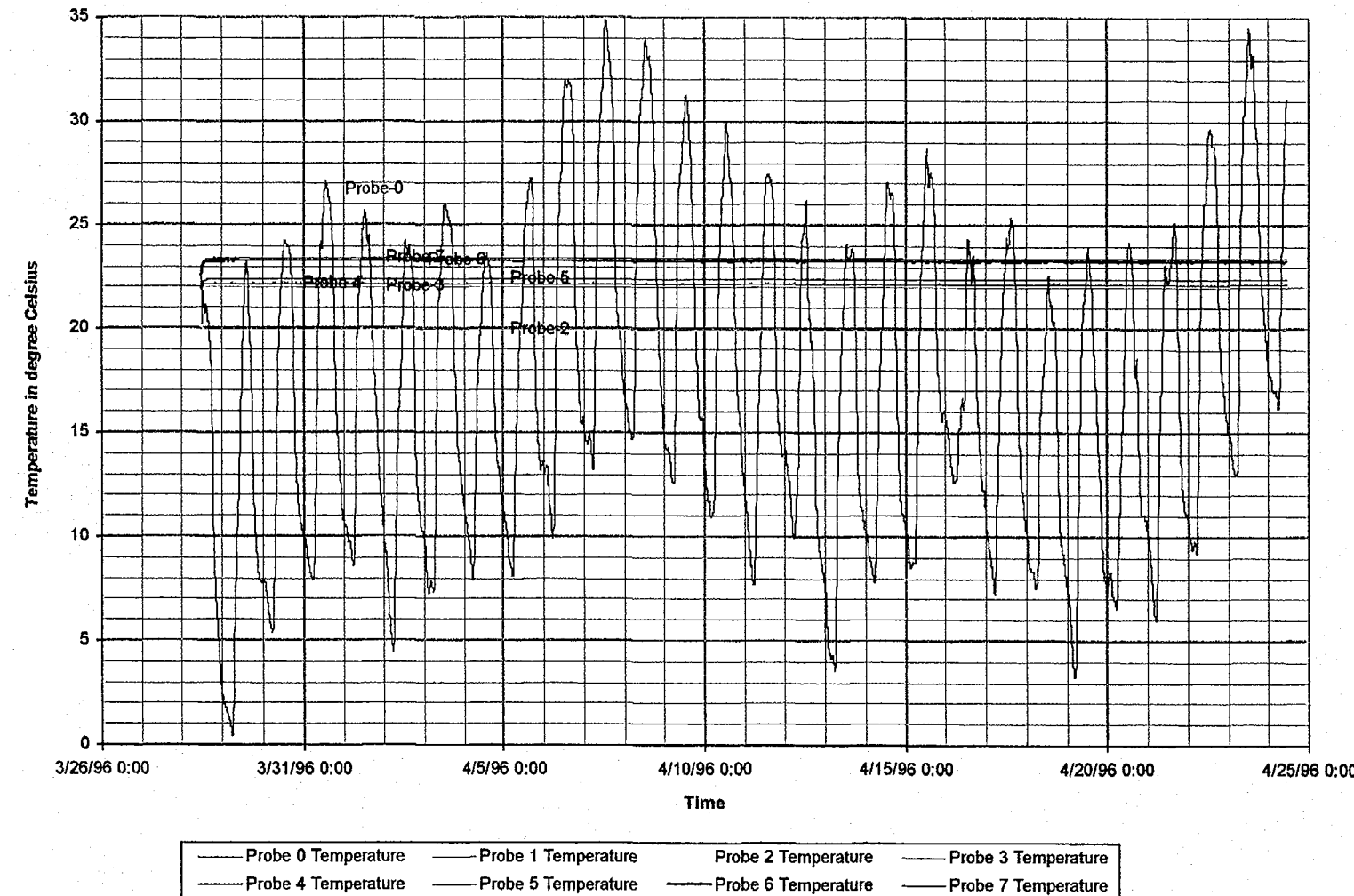


Figure 4-2L Temperature fluctuation with time in NRG-4

MAY 1996

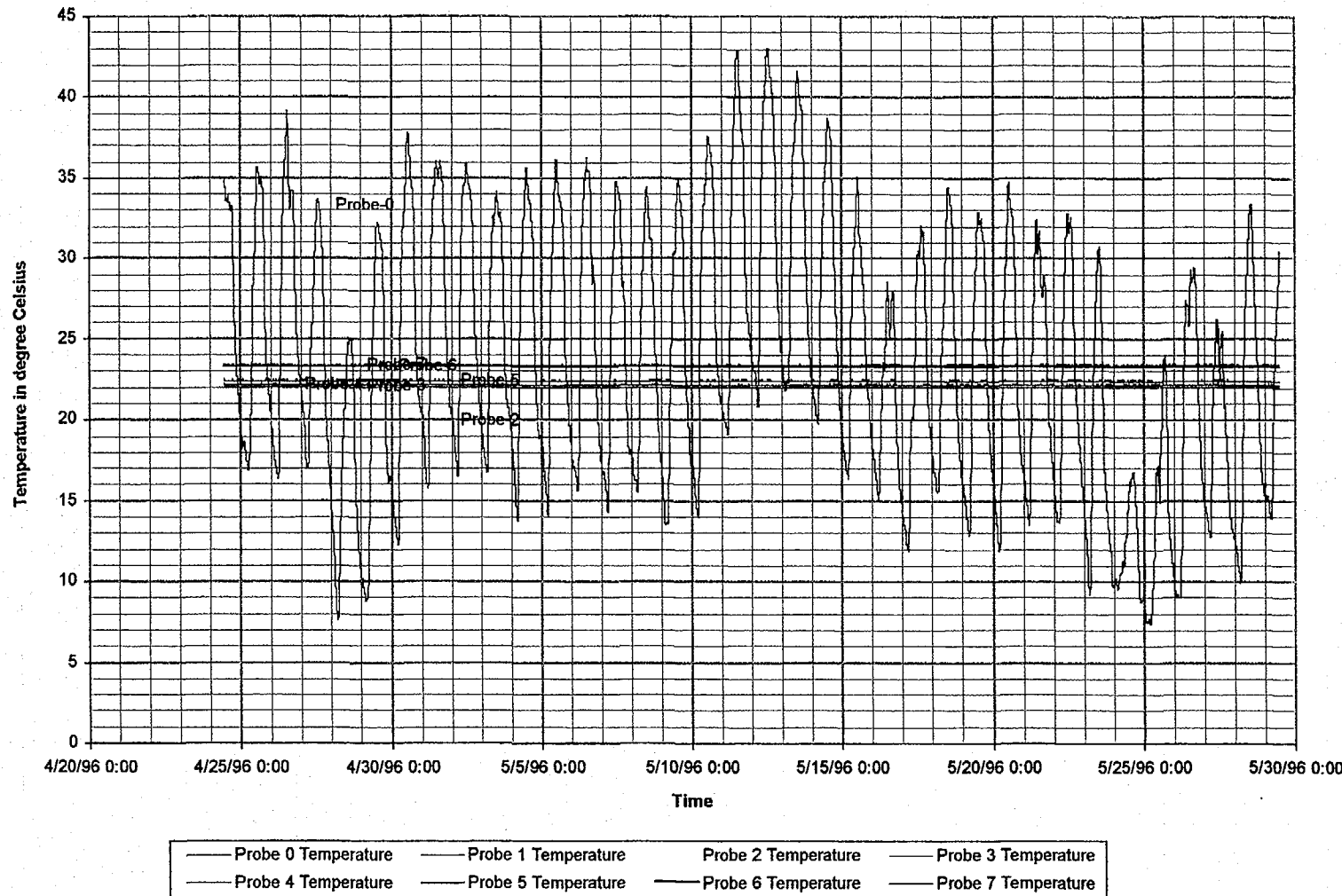


Figure 4-2m Temperature fluctuation with time in NRG-4

JUNE 1996

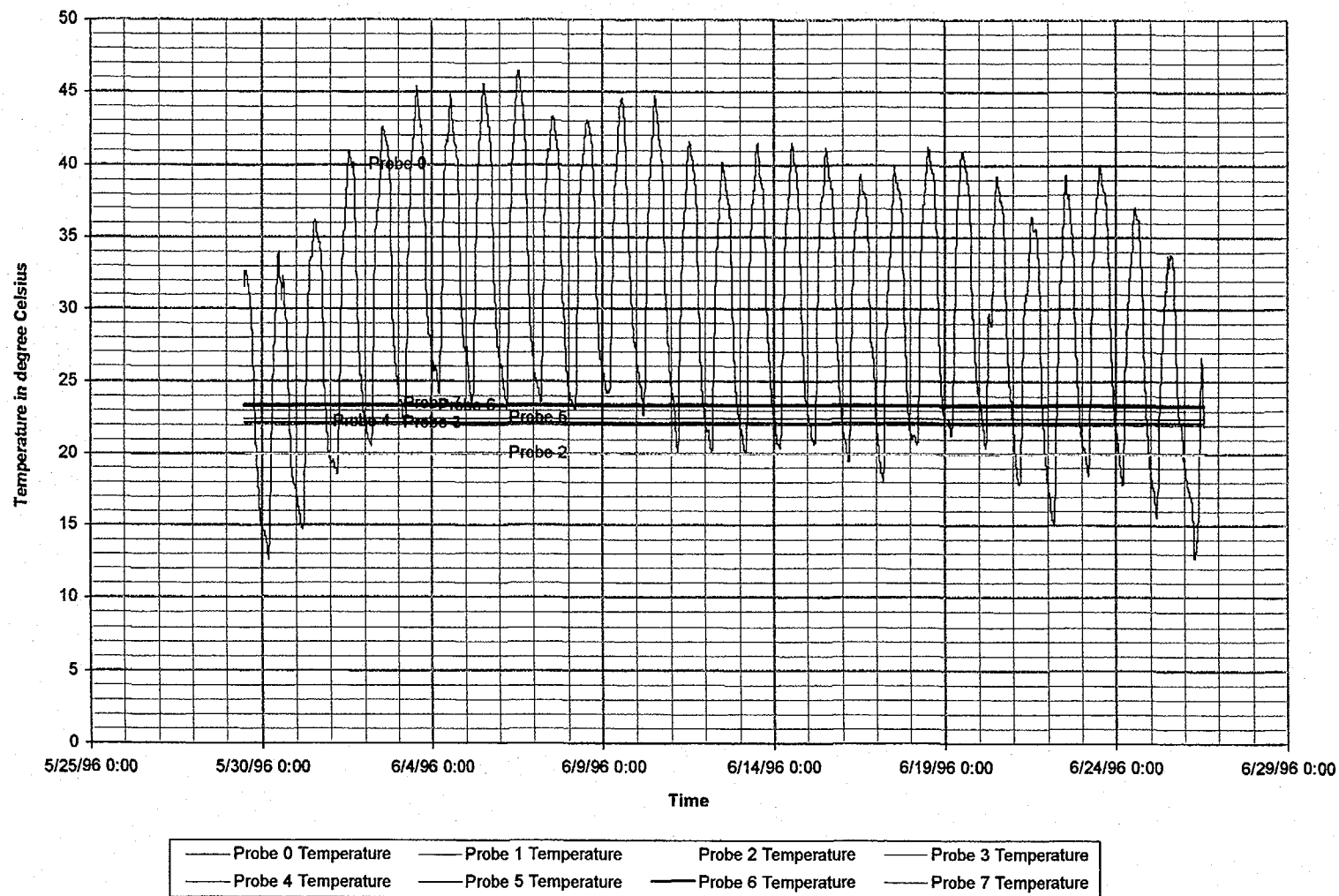


Figure 4-2n Temperature fluctuation with time in NRG-4

August 24, 1996
P266:D:\user\projects\NyeCounty\anurop96\figures

Prepared for:
Nye County Nuclear Waste Repository Project Office

Prepared by:
Multimedia Environmental Technology, Inc.
Newport Beach, CA

JULY 1996

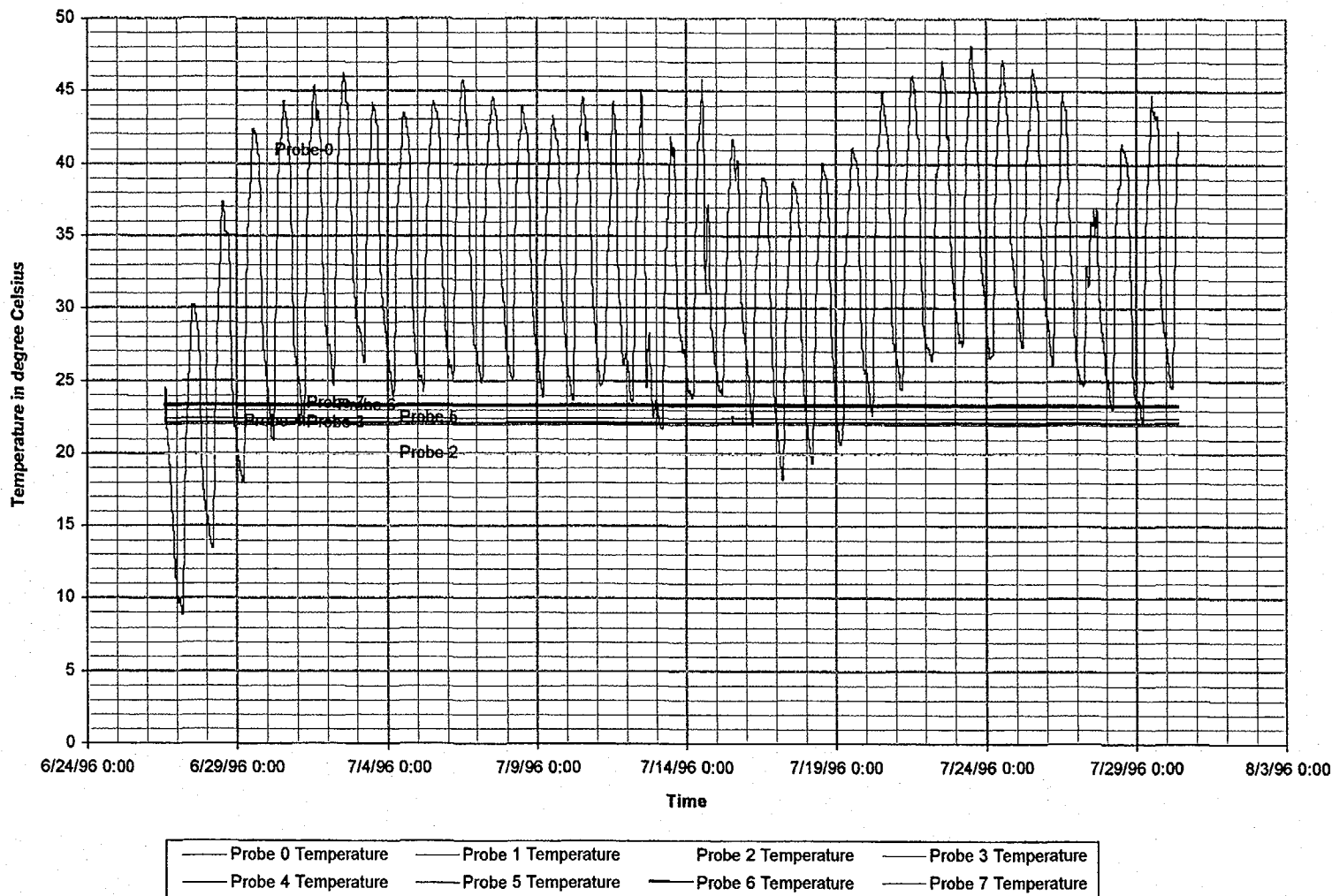


Figure 4-2o Temperature fluctuation with time in NRG-4

August 24, 1996
P266:D:\user\projects\NyeCounty\anrcp96\figures

Prepared for:
Nye County Nuclear Waste Repository Project Office

Prepared by:
Multimedia Environmental Technology, Inc.
Newport Beach, CA

August 1996

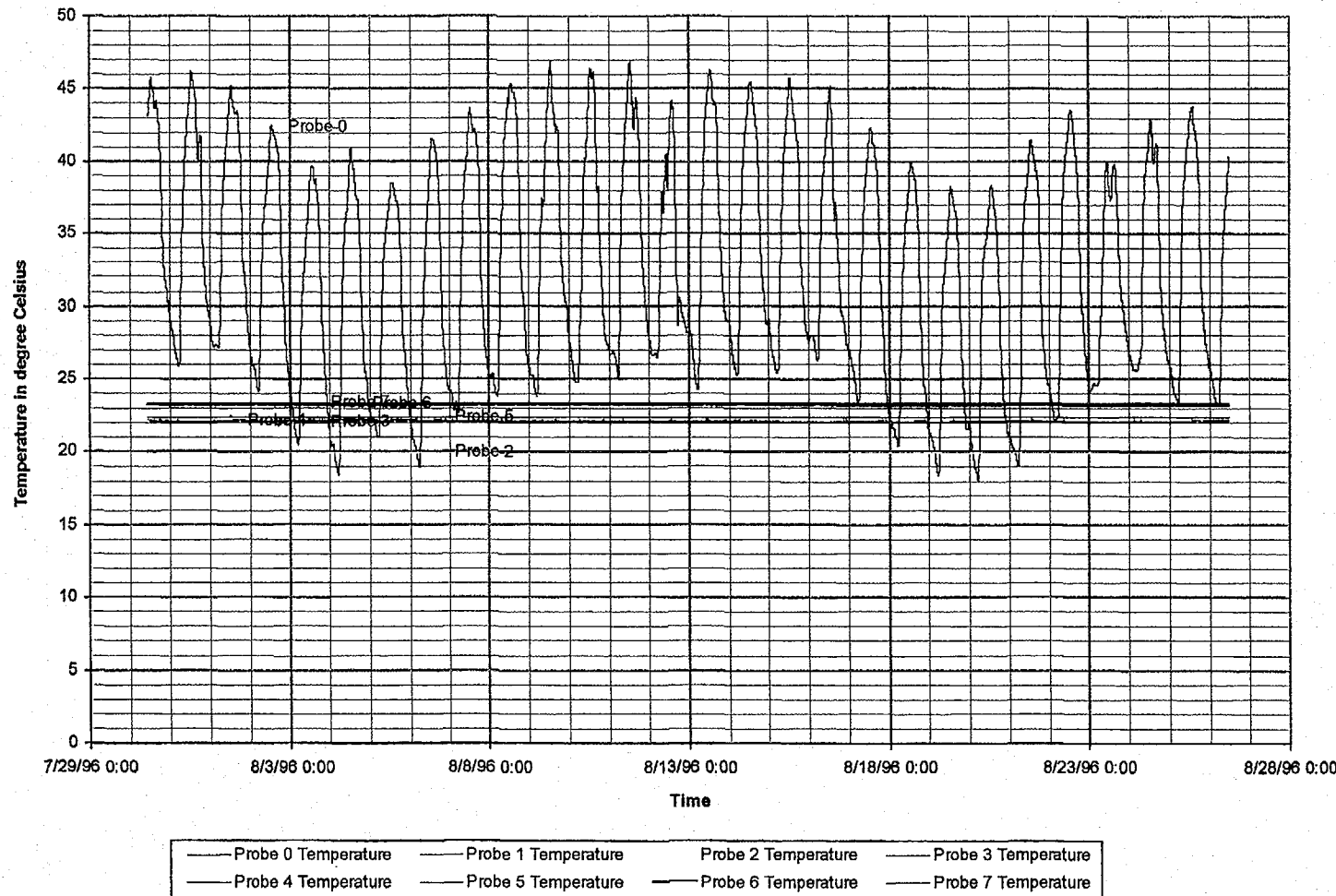


Figure 4-2p Temperature fluctuation with time in NRG-4

April 1995

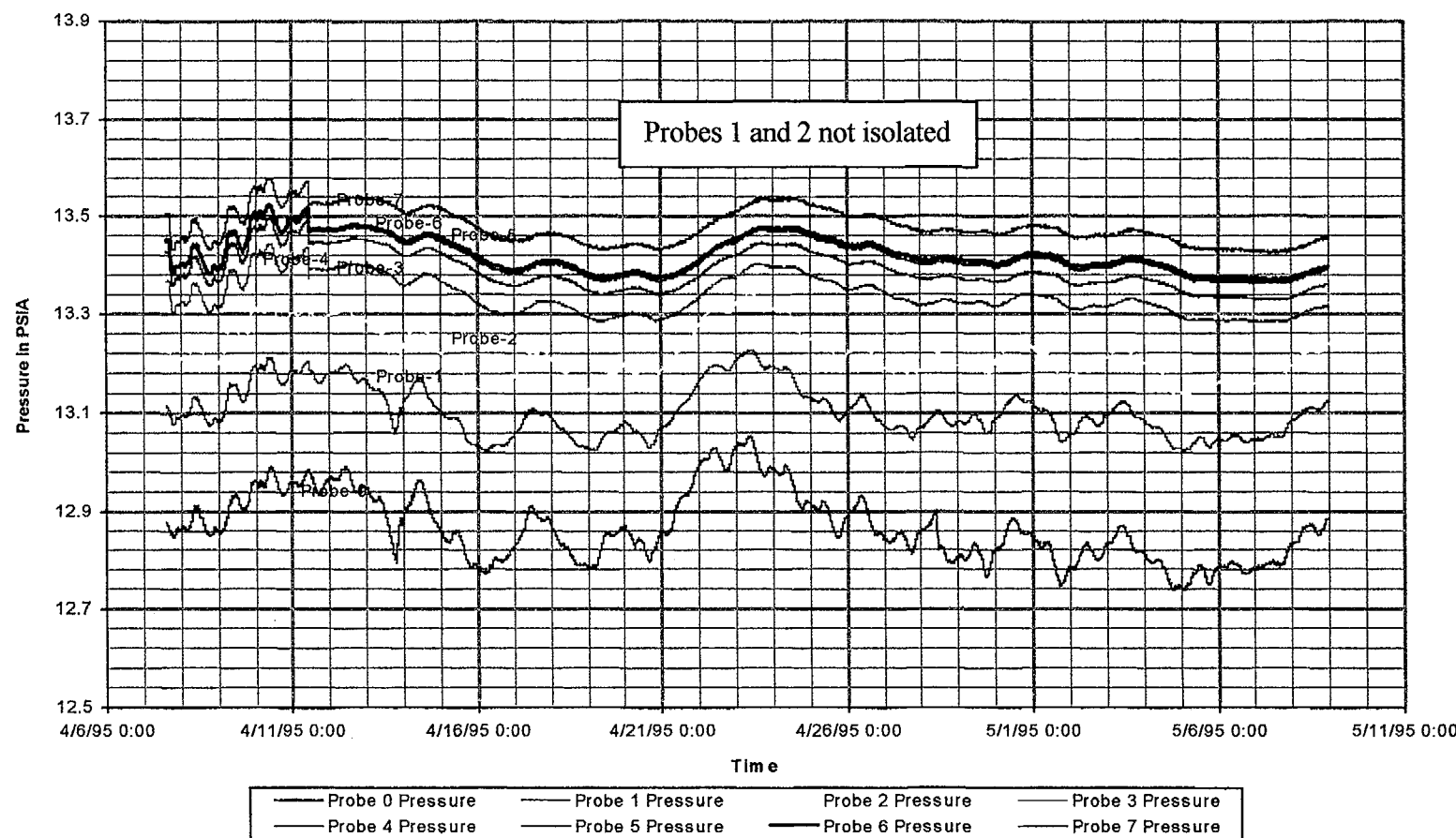


Figure 4-3a Pressure fluctuation with time in ONC-1

May 1995

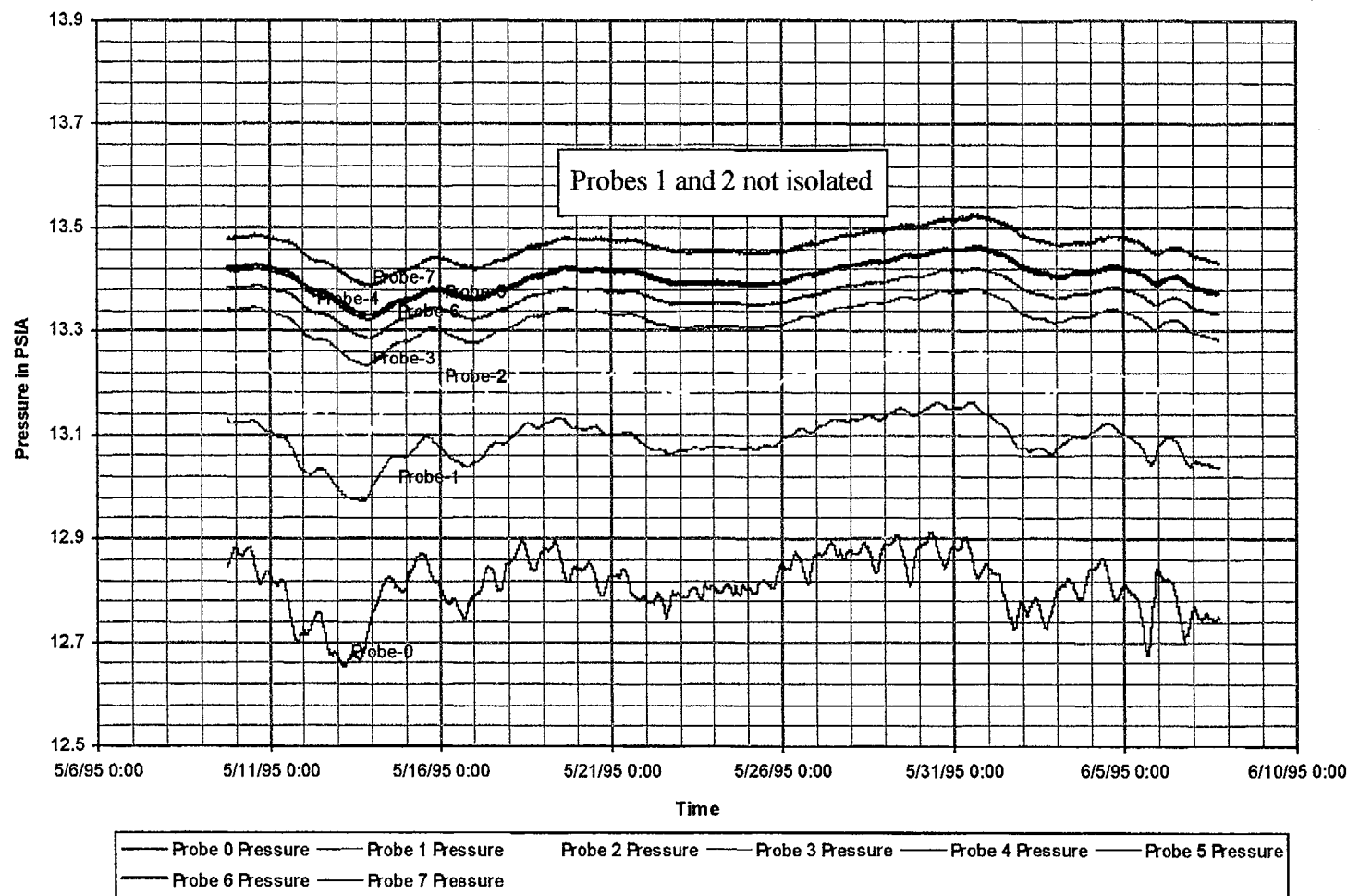


Figure 4-3b Pressure fluctuation with time in ONC-1

June 1995

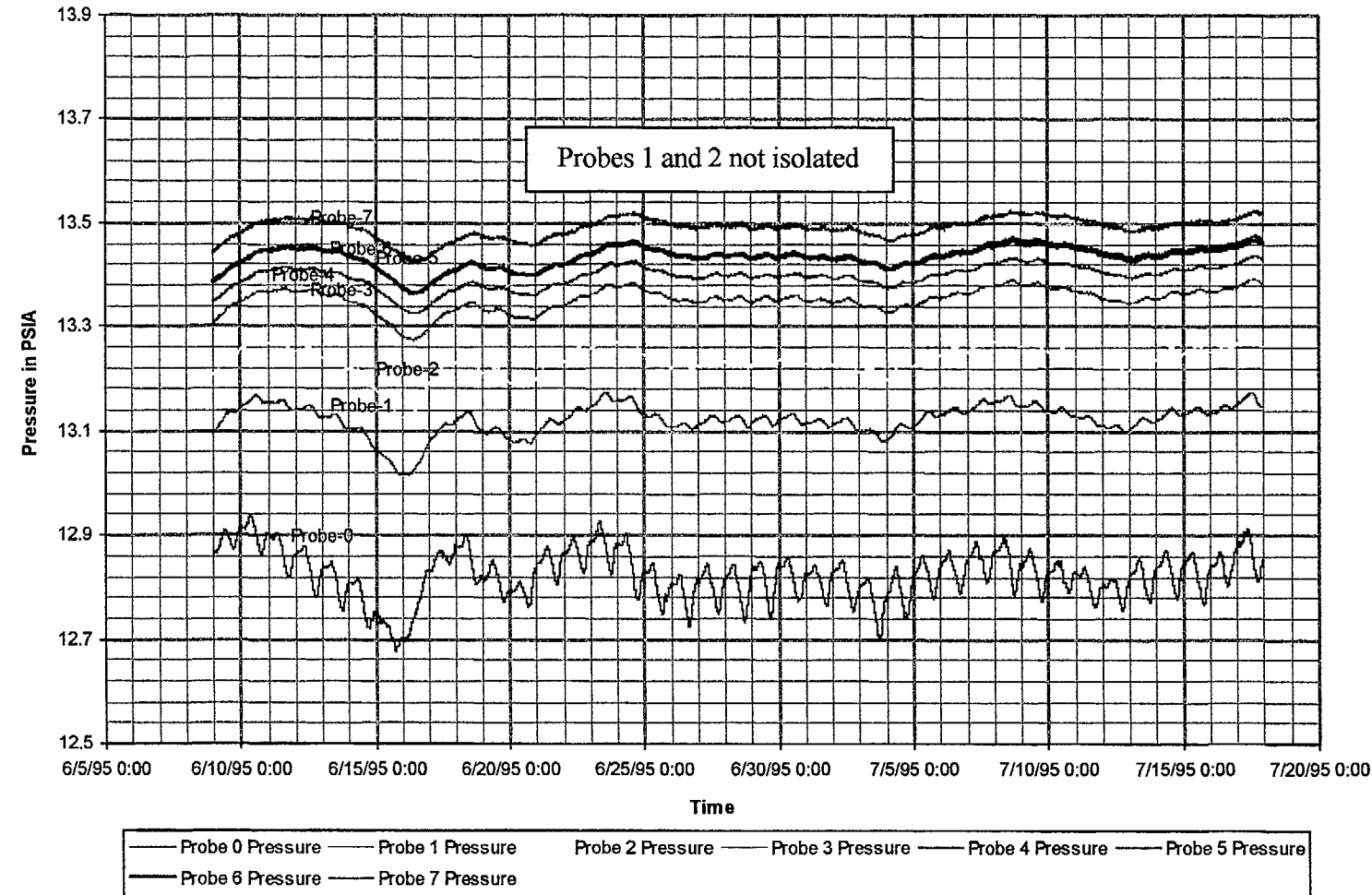


Figure 4-3c Pressure fluctuation with time in ONC-1

July 1995

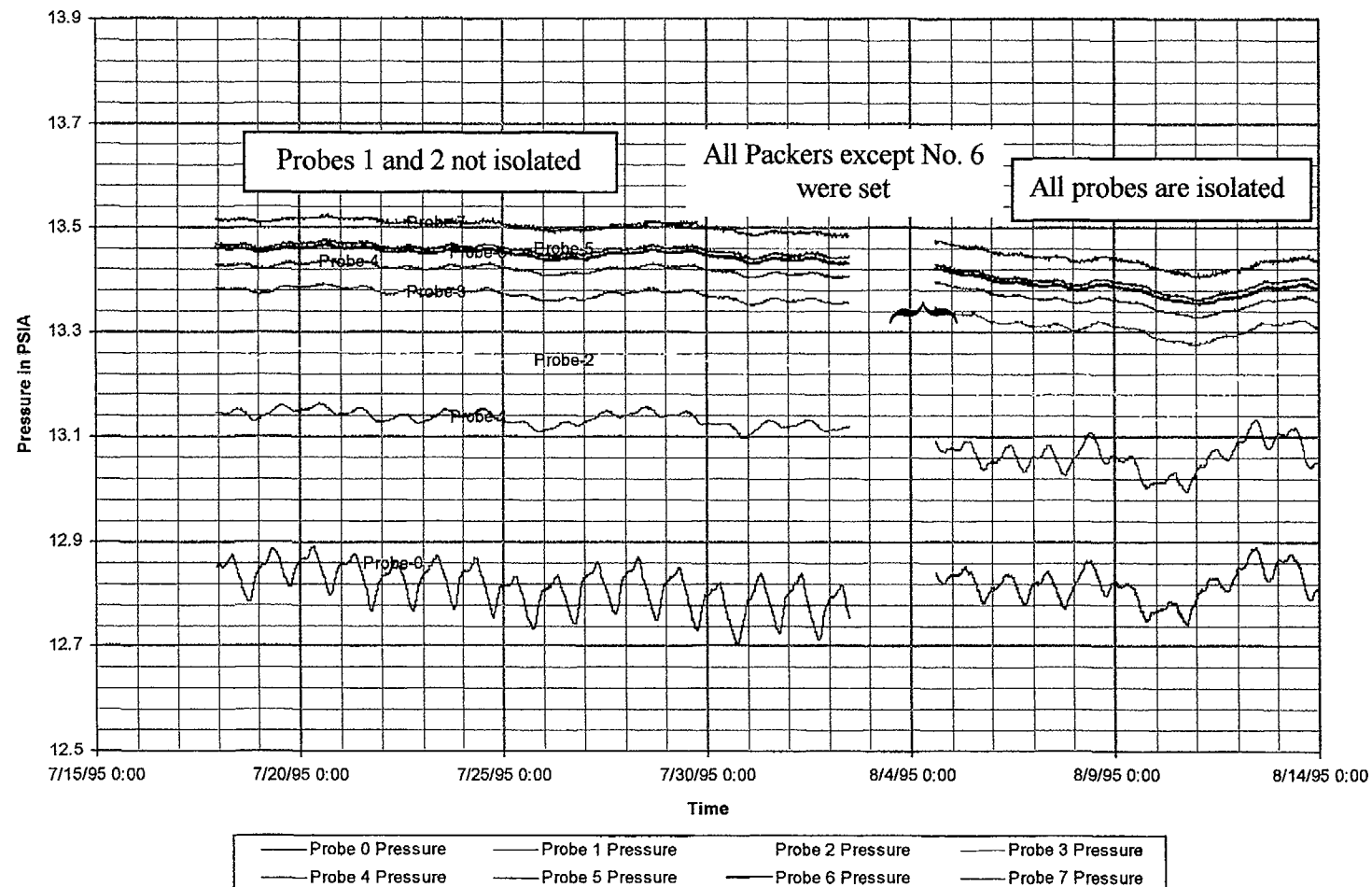


Figure 4-3d Pressure fluctuation with time in ONC-1

August 1995

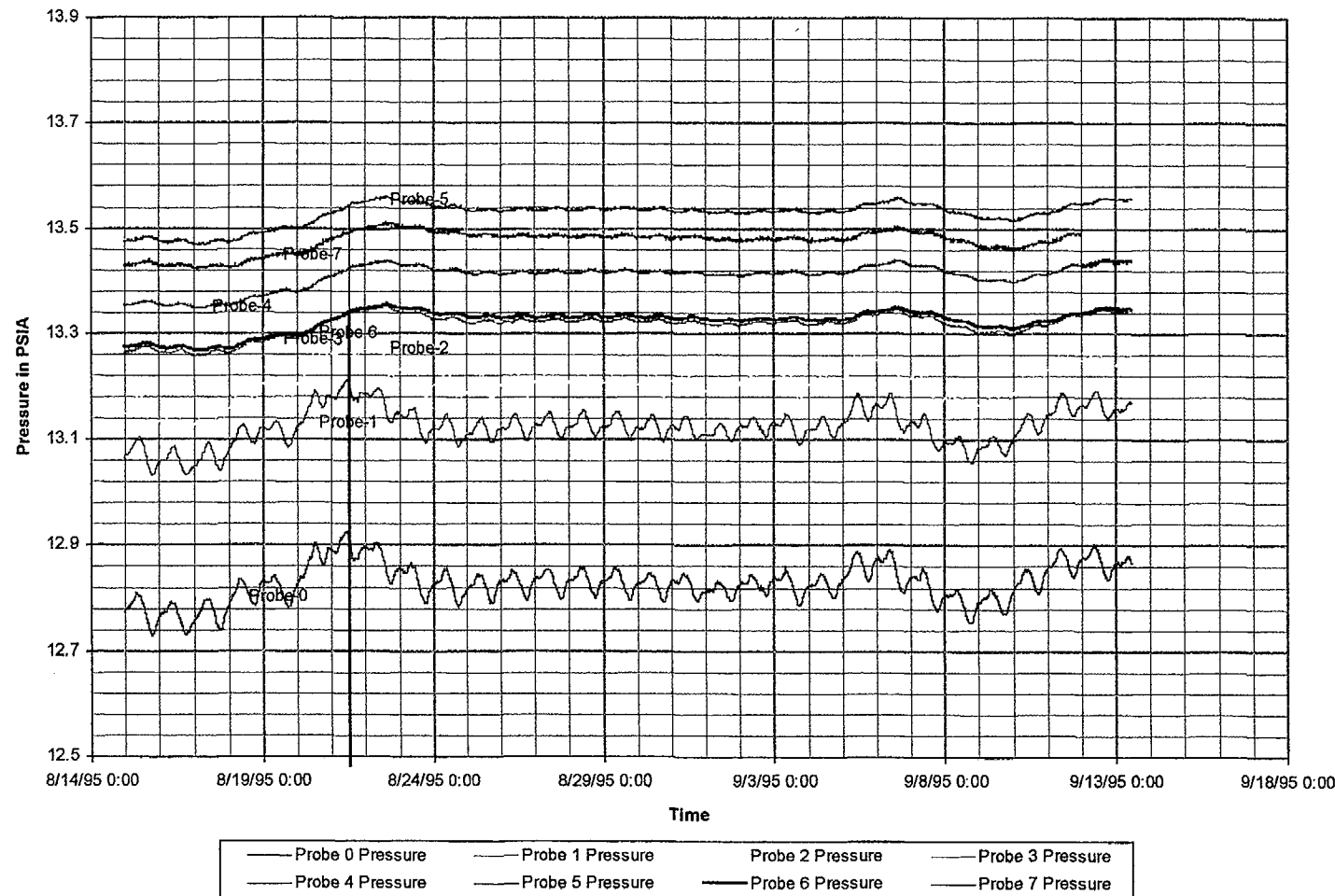


Figure 4-3e Pressure fluctuation with time in ONC-1

August 24, 1996
P2662:01 PMD:\user\projects\NyeCounty\manrep96\figures

Prepared for:
Nye County Nuclear Waste Repository Project Office

Prepared by:
Multimedia Environmental Technology, Inc.
Newport Beach, CA

September 1995

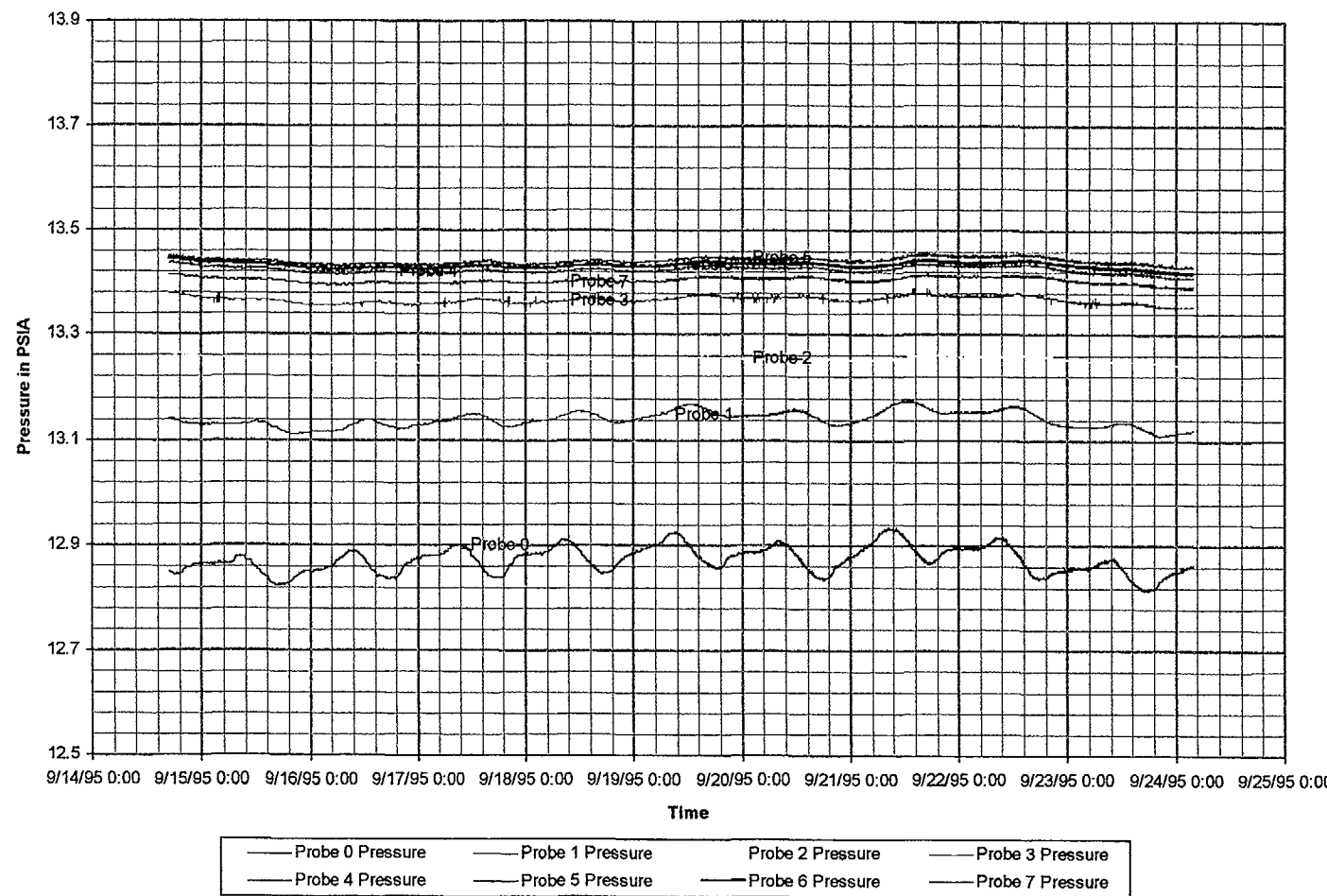


Figure 4-3f Pressure fluctuation with time in ONC-1

October 1995

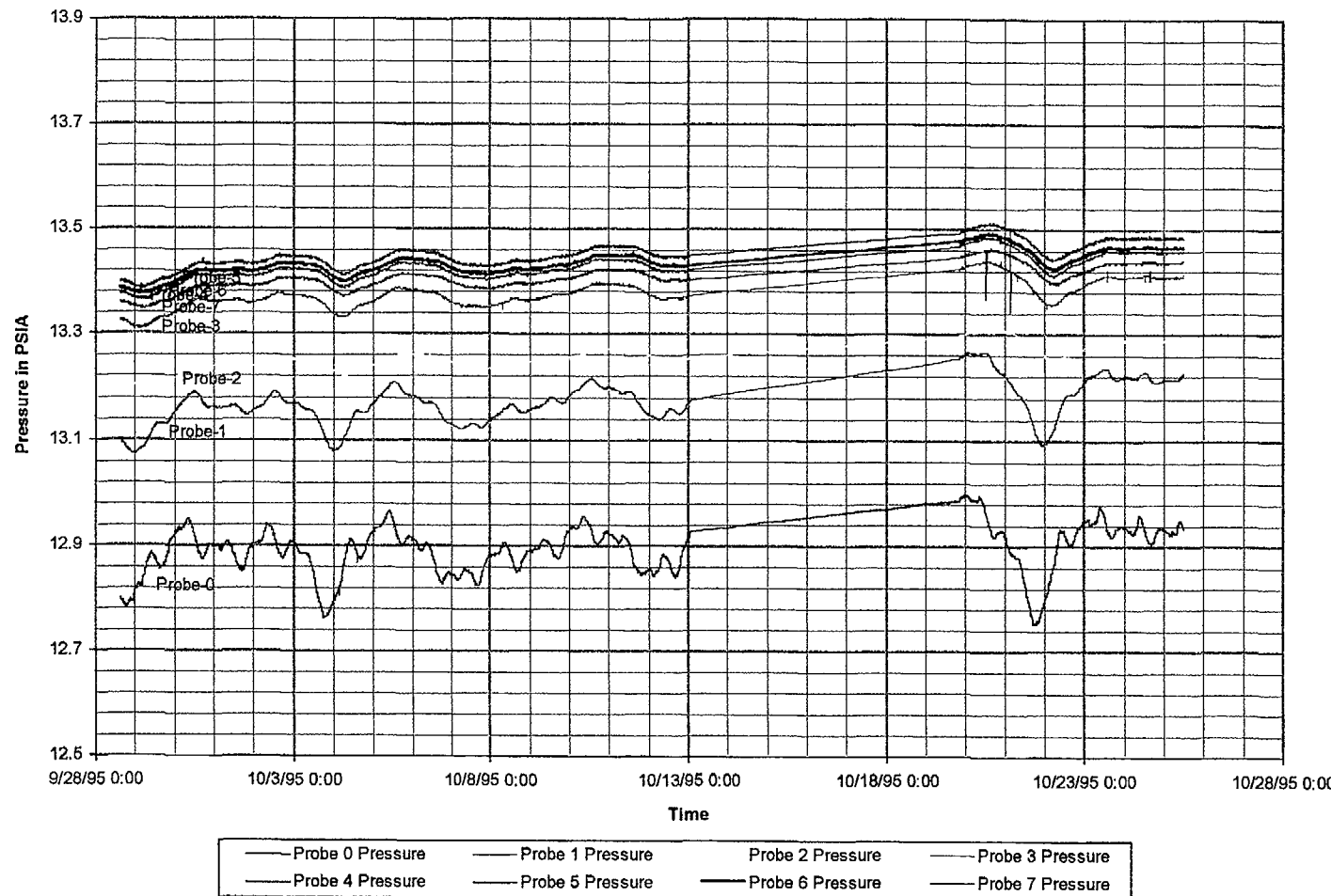


Figure 4-3g Pressure fluctuation with time in ONC-1

November 1995

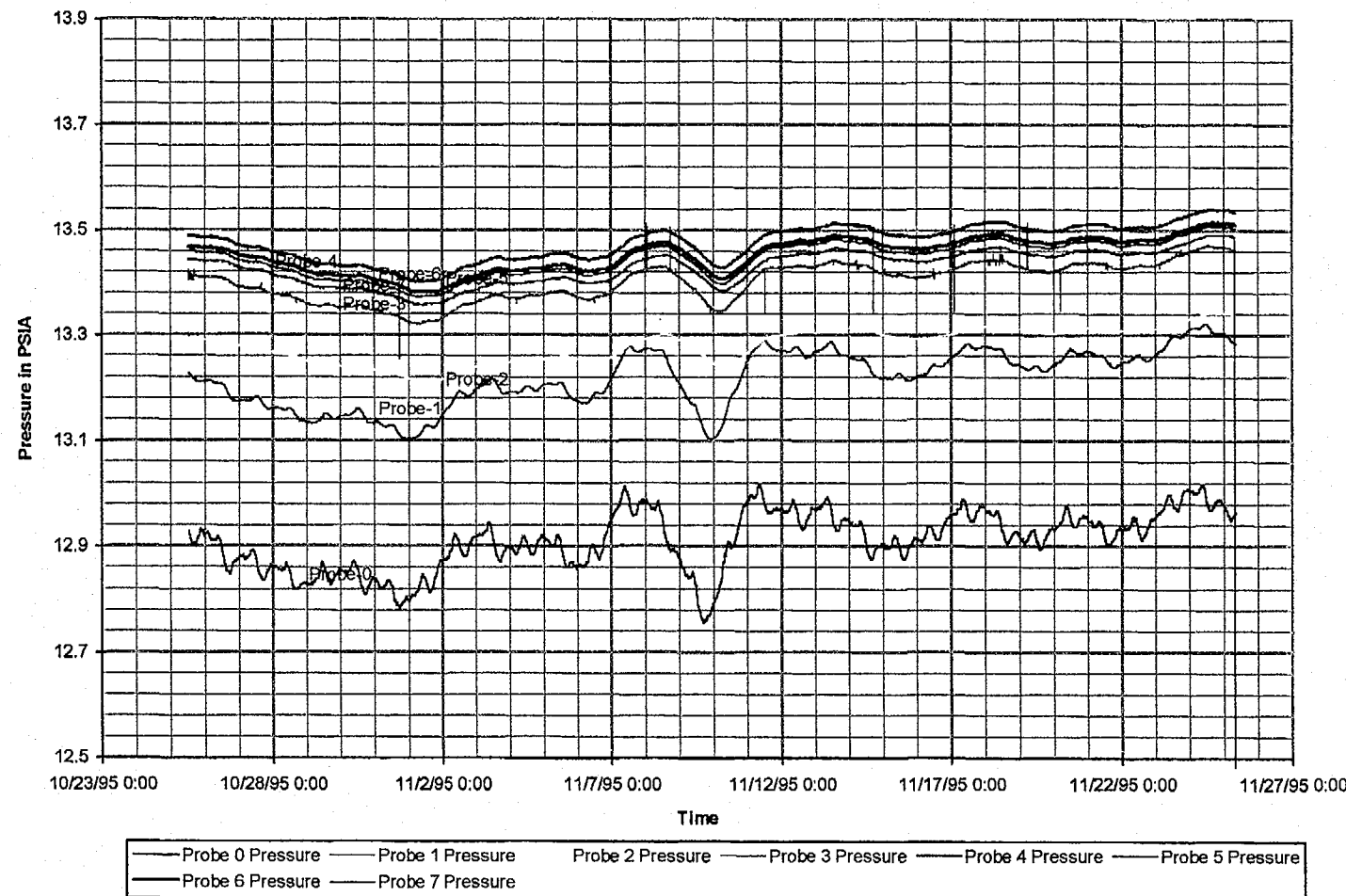


Figure 4-3h Pressure fluctuation with time in ONC-1

December 1995

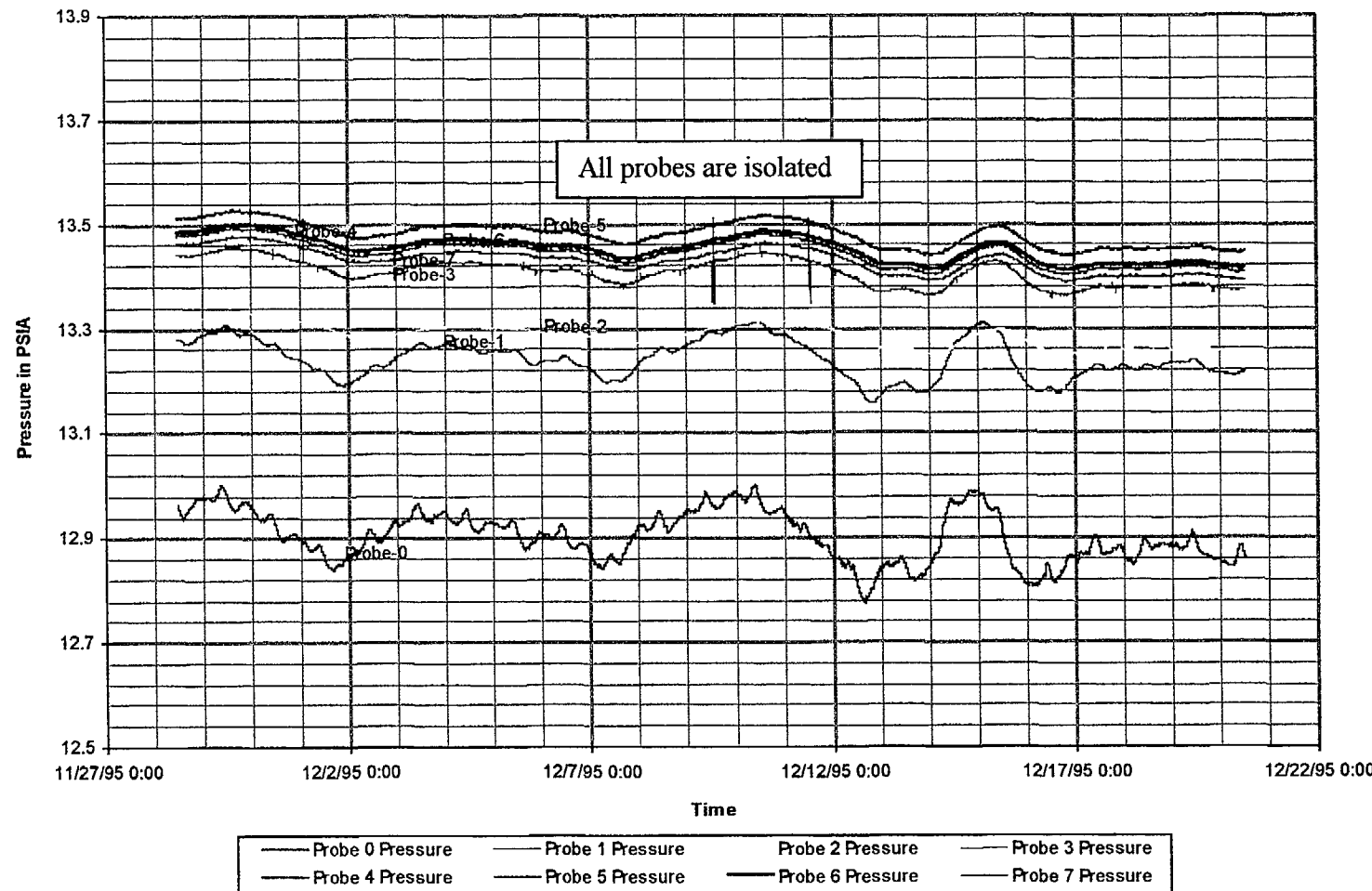


Figure 4-3i Pressure fluctuation with time in ONC-1

January 1996

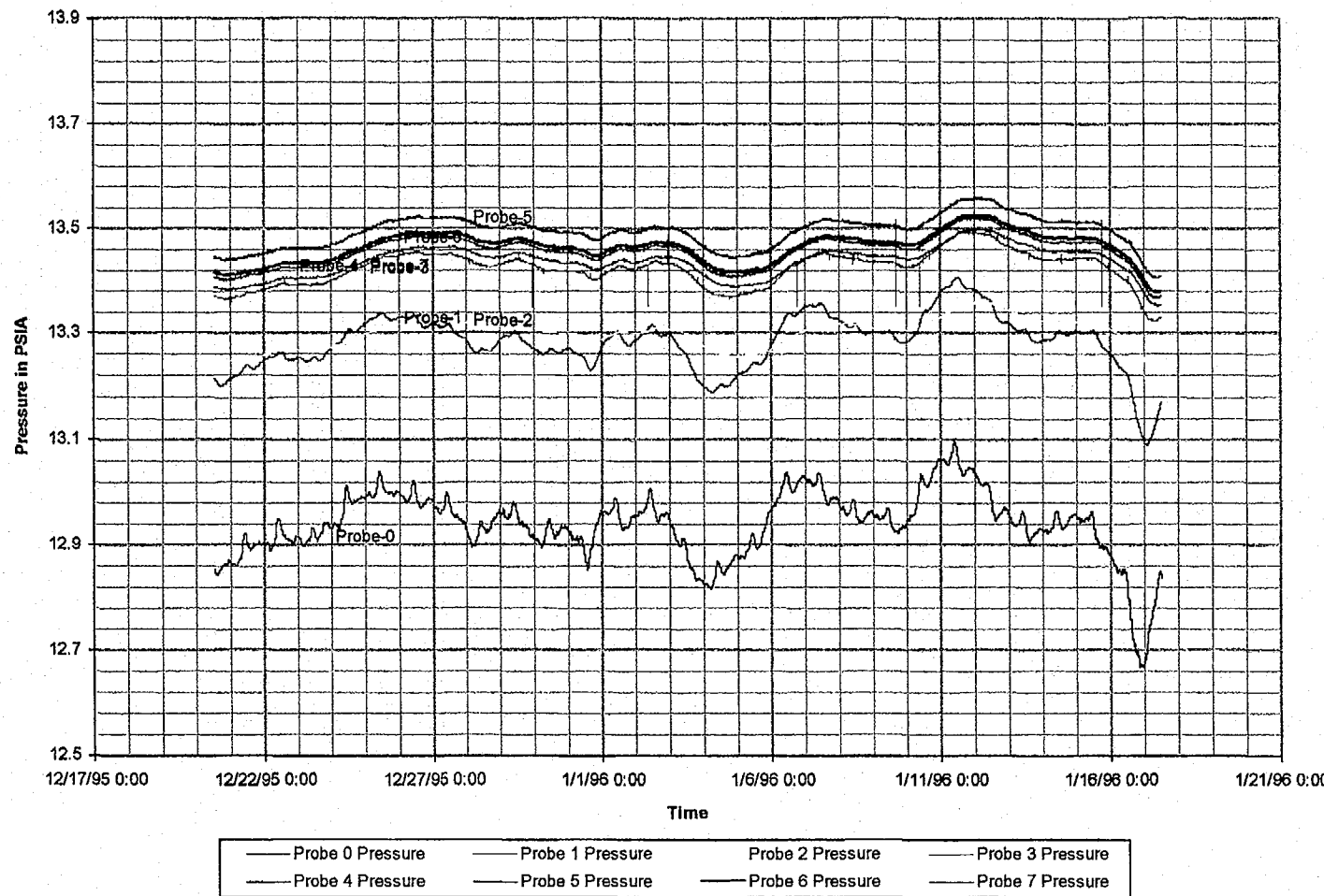


Figure 4-3j

Pressure fluctuation with time in ONC-1

February 1996

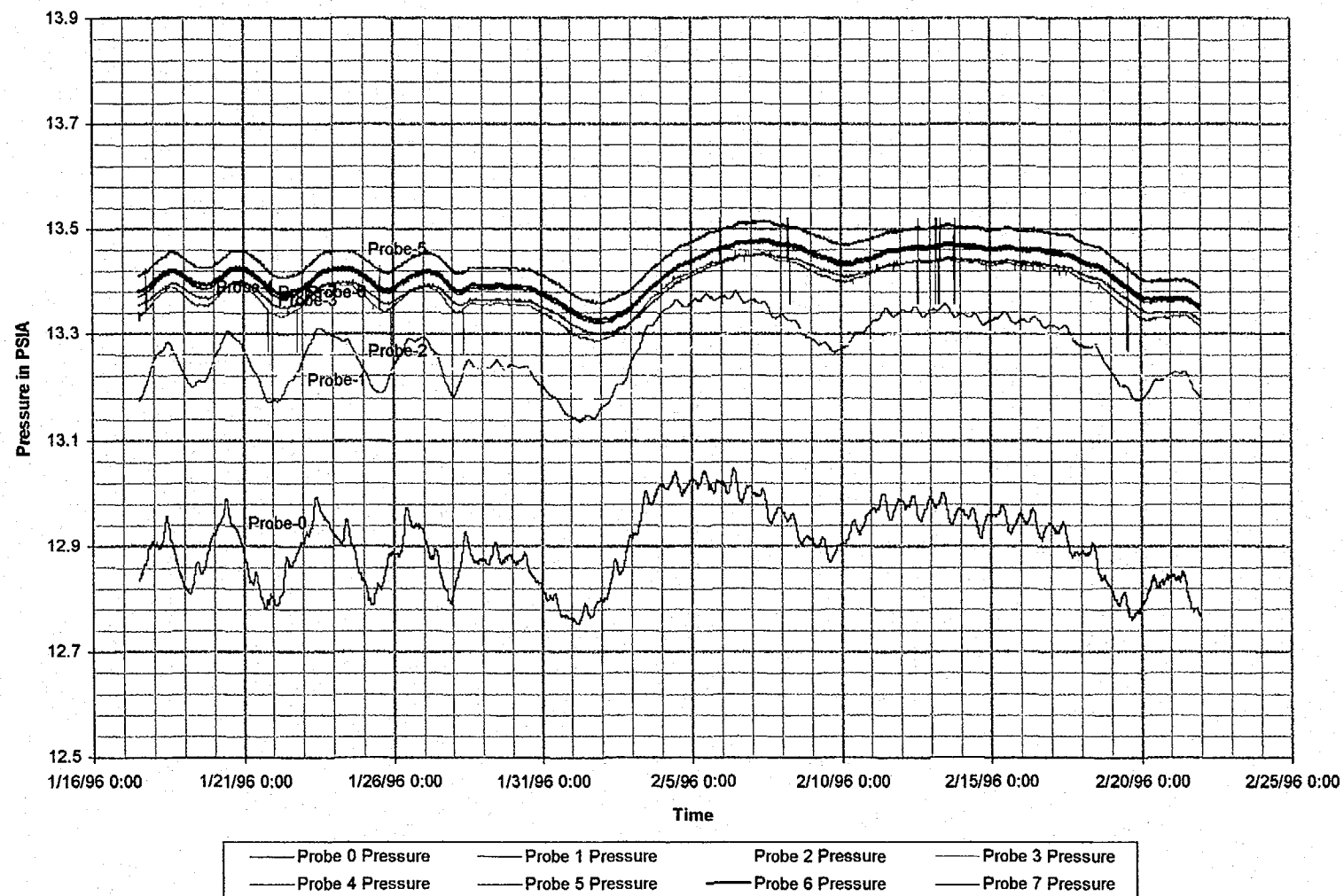


Figure 4-3k Pressure fluctuation with time in ONC-1

MARCH 1996

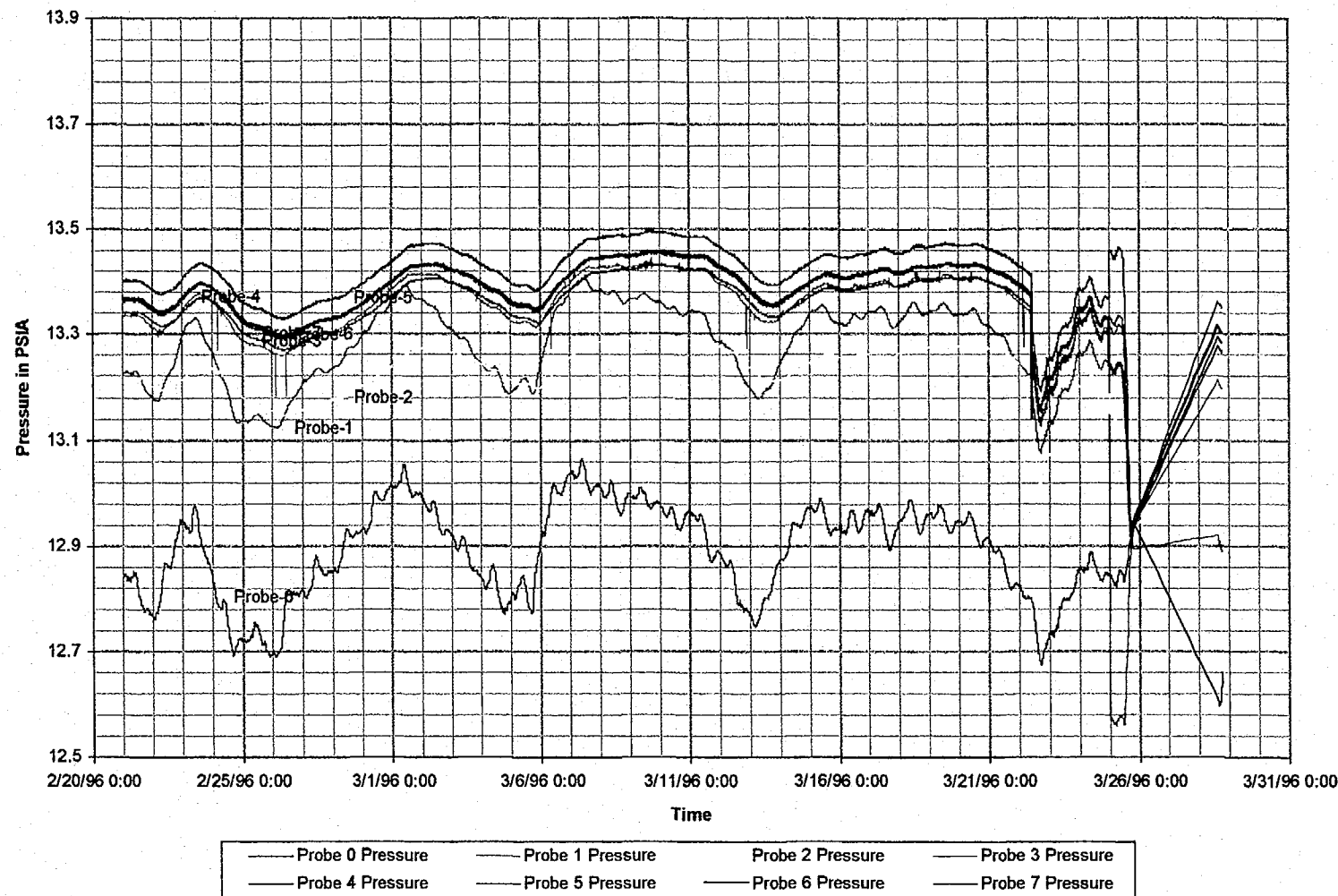


Figure 4-3L Pressure fluctuation with time in ONC-1

APRIL 1996

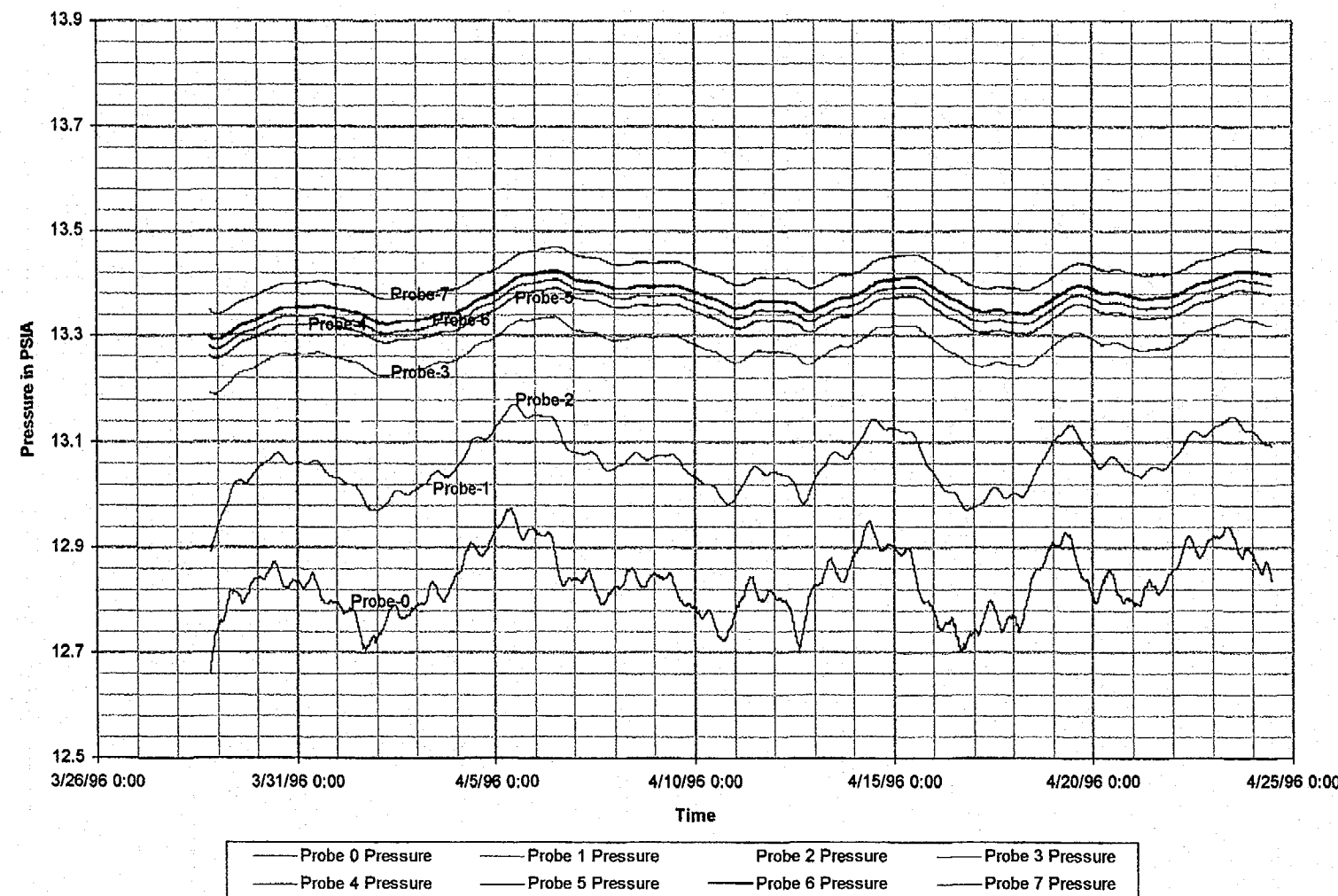


Figure 4-3m Pressure fluctuation with time in ONC-1

August 24, 1996
P266:D:\user\projects\Nyecounty\annrep96\figures

Prepared for:
Nye County Nuclear Waste Repository Project Office

Prepared by:
Multimedia Environmental Technology, Inc.
Newport Beach, CA

MAY 1996

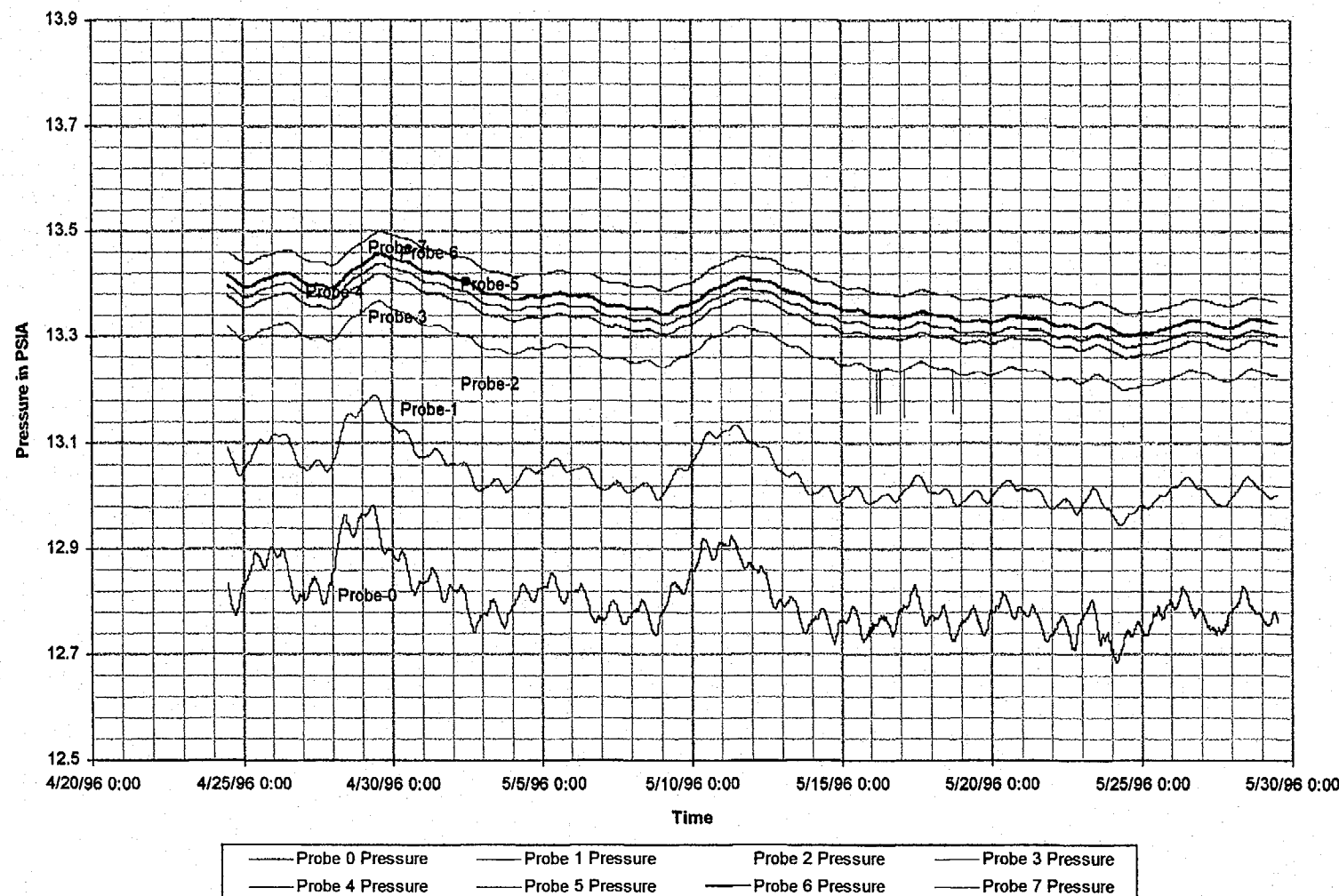


Figure 4-3n Pressure fluctuation with time in ONC-1

JUNE 1996

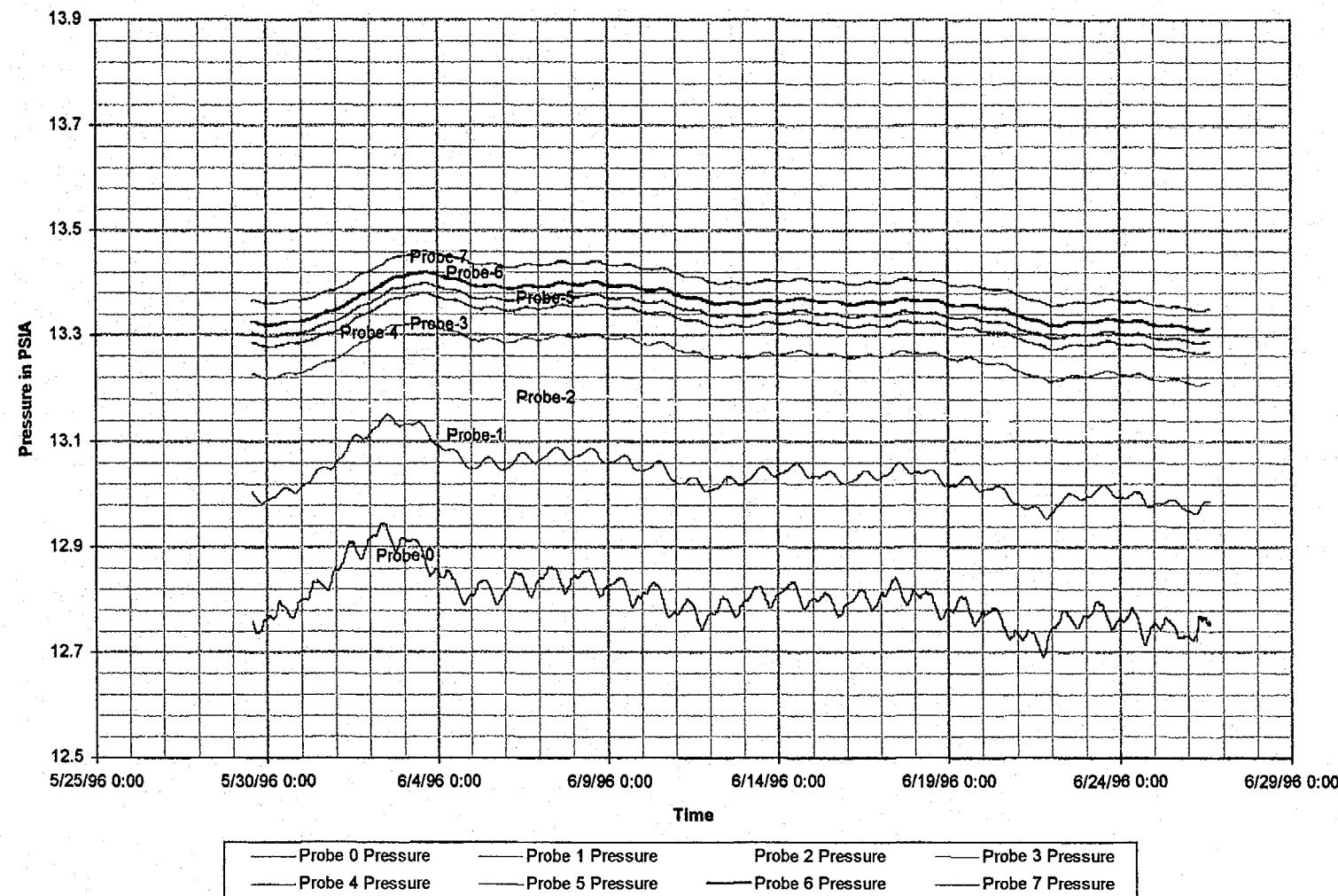


Figure 4-3o Pressure fluctuation with time in ONC-1

JULY 1996

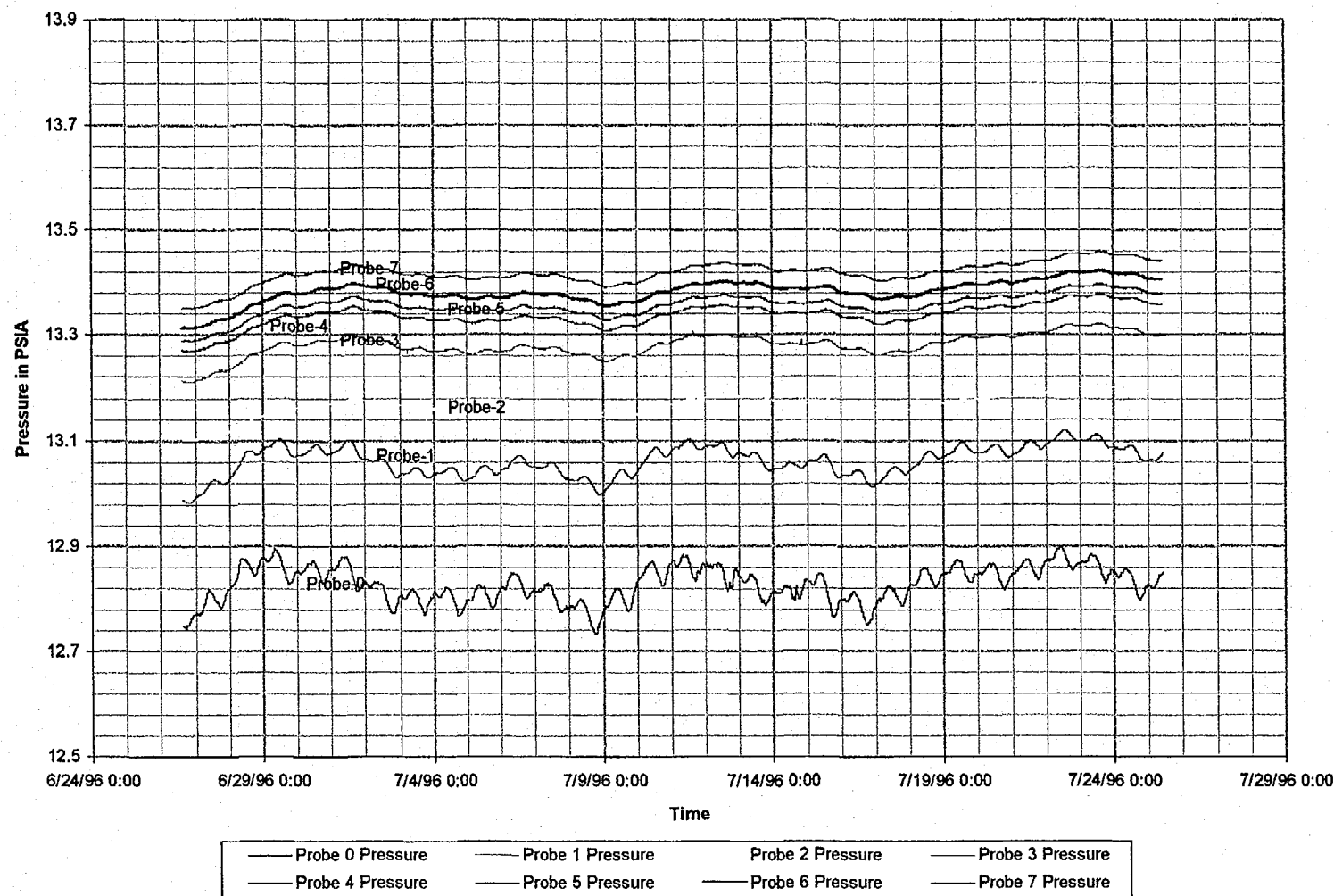


Figure 4-3p Pressure fluctuation with time in ONC-1

August 24, 1996
P266:D:\user\projects\NyeCounty\annrep96\figures

Prepared for:
Nye County Nuclear Waste Repository Project Office

Prepared by:
Multimedia Environmental Technology, Inc.
Newport Beach, CA

August 1996

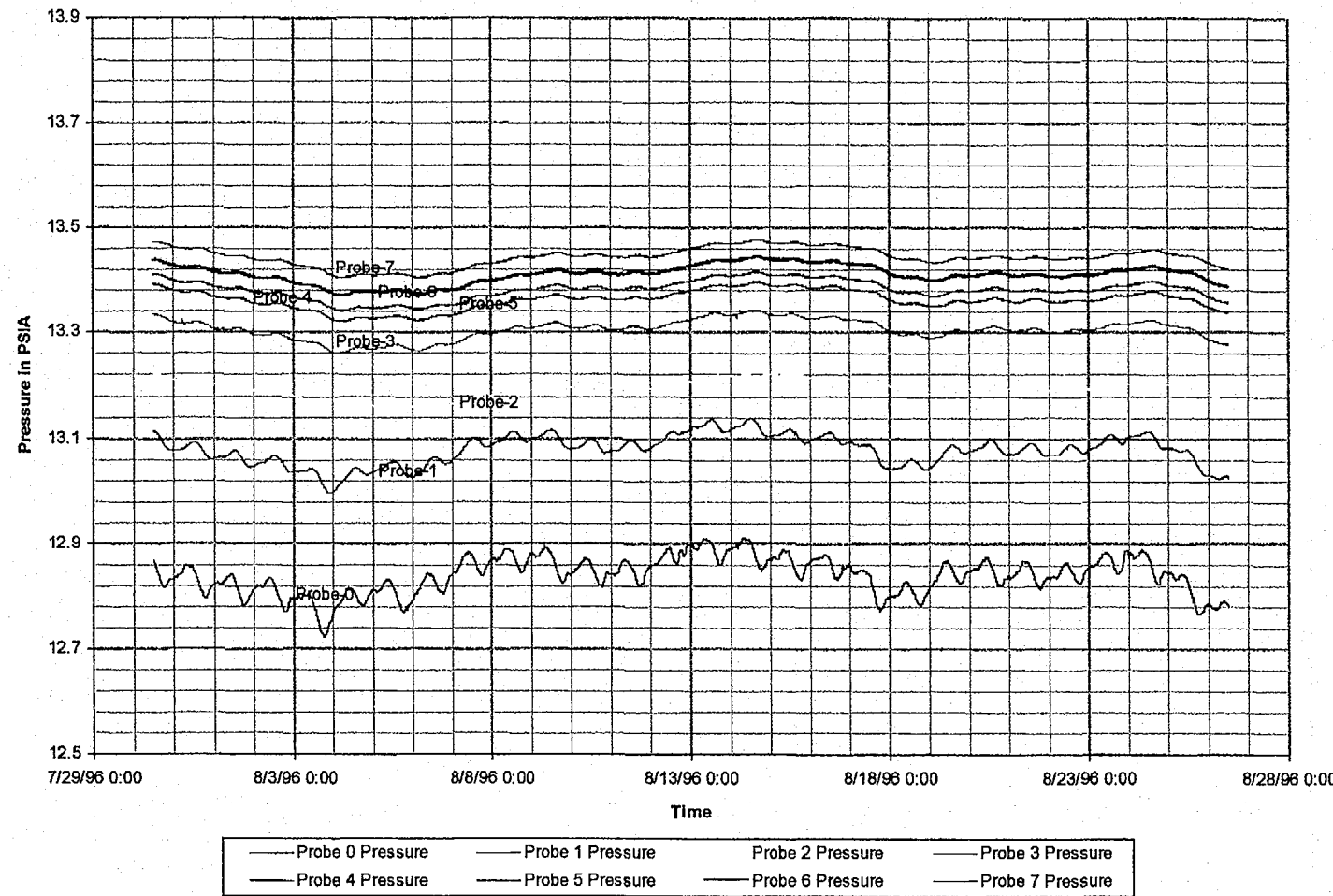


Figure 4-3q Pressure fluctuation with time in ONC-1

April 1995

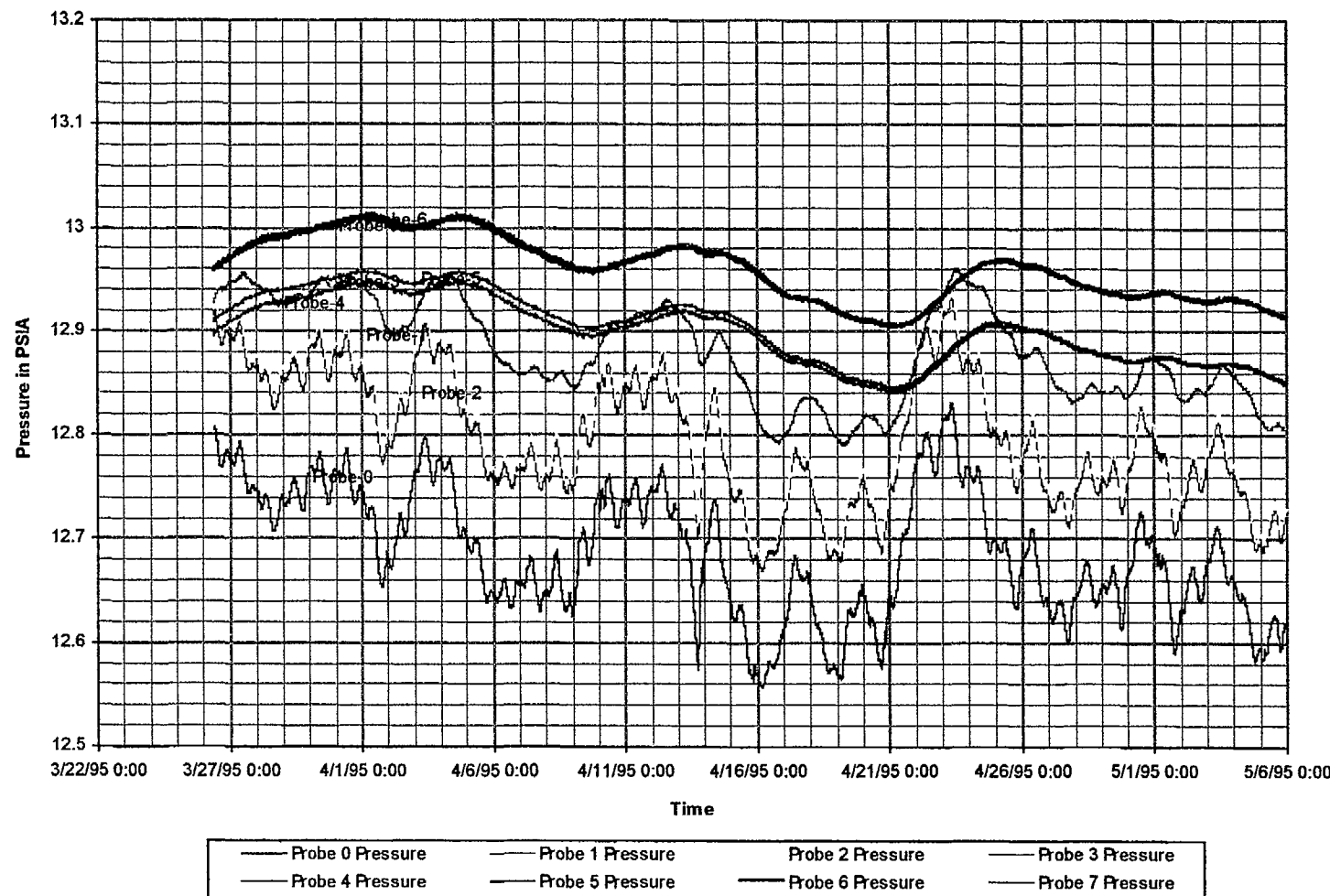


Figure 4-4a Pressure fluctuation with time in NRG-4

May 1995

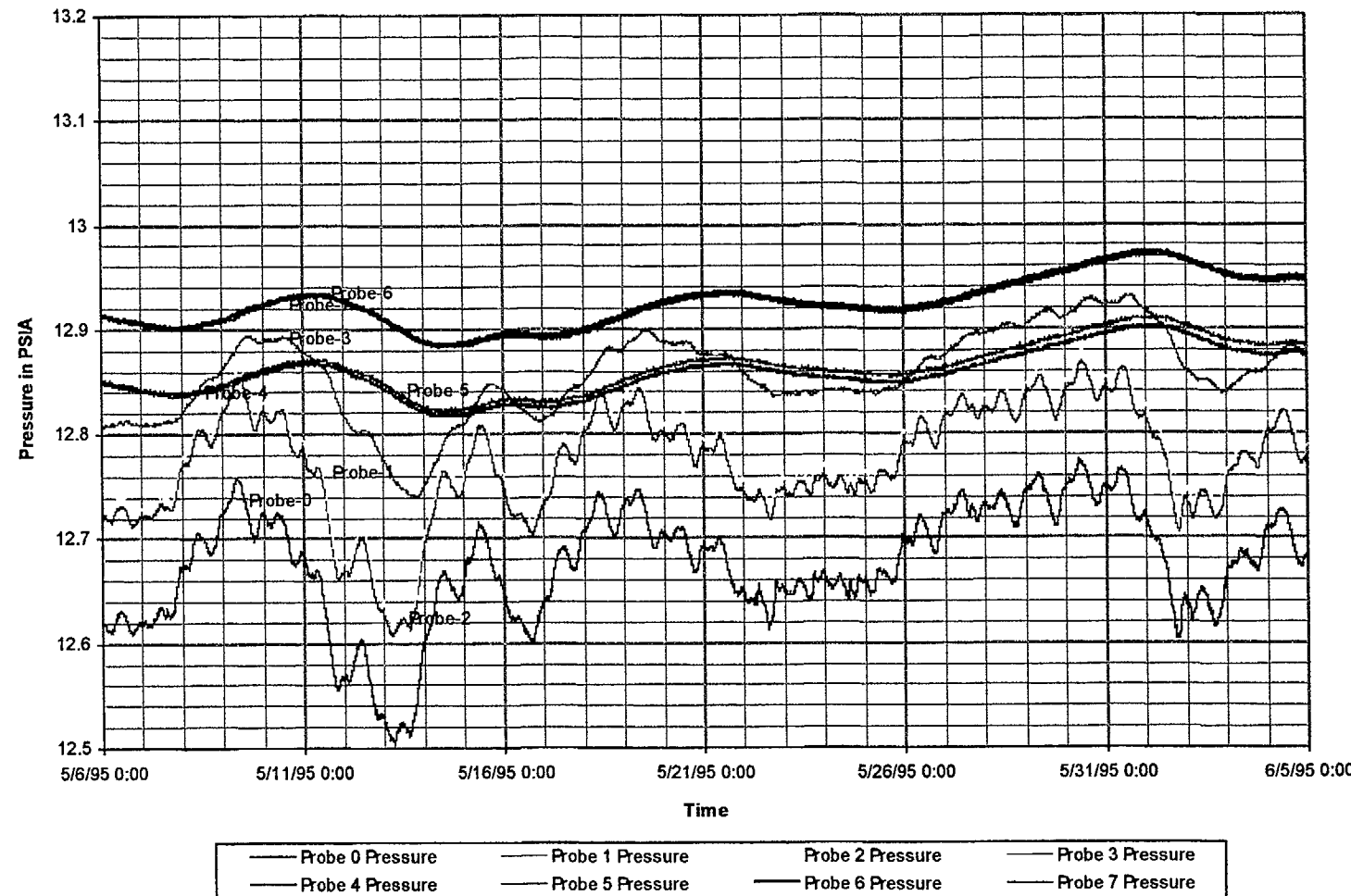


Figure 4-4b Pressure fluctuation with time in NRG-4

June 1995

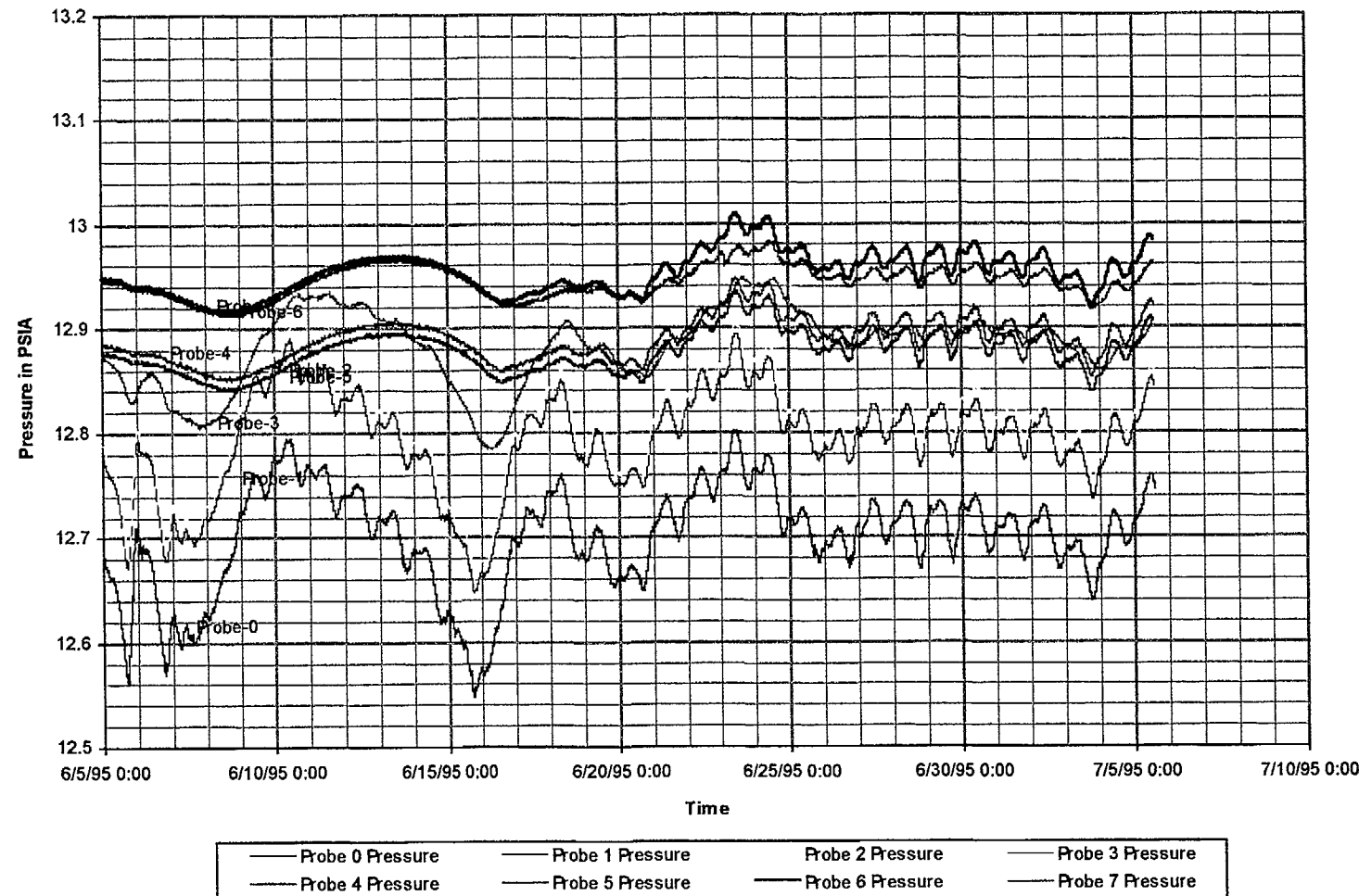


Figure 4-4c Pressure fluctuation with time in NRG-4

July 1995

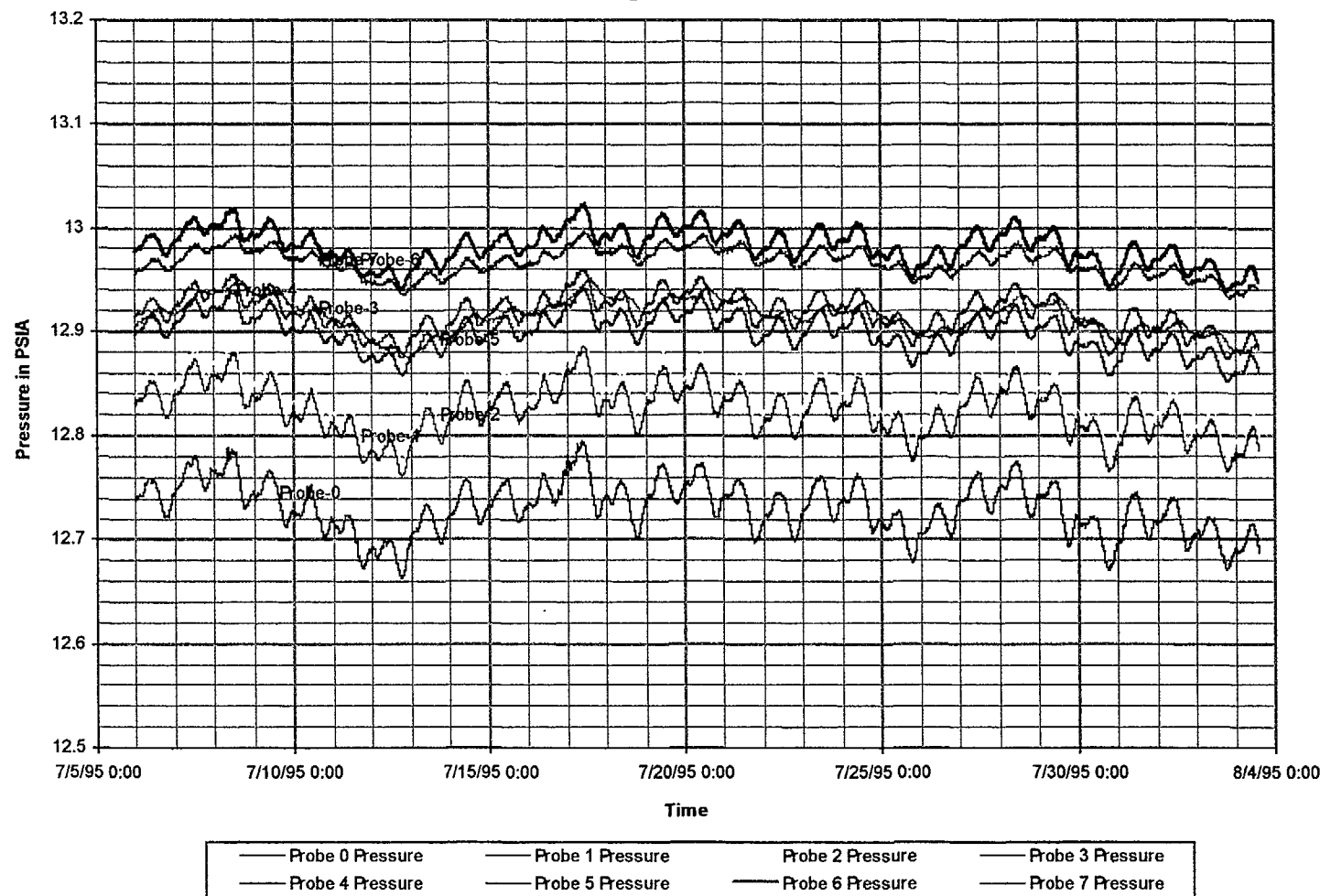


Figure 4-4d Pressure fluctuation with time in NRG-4

September 1995

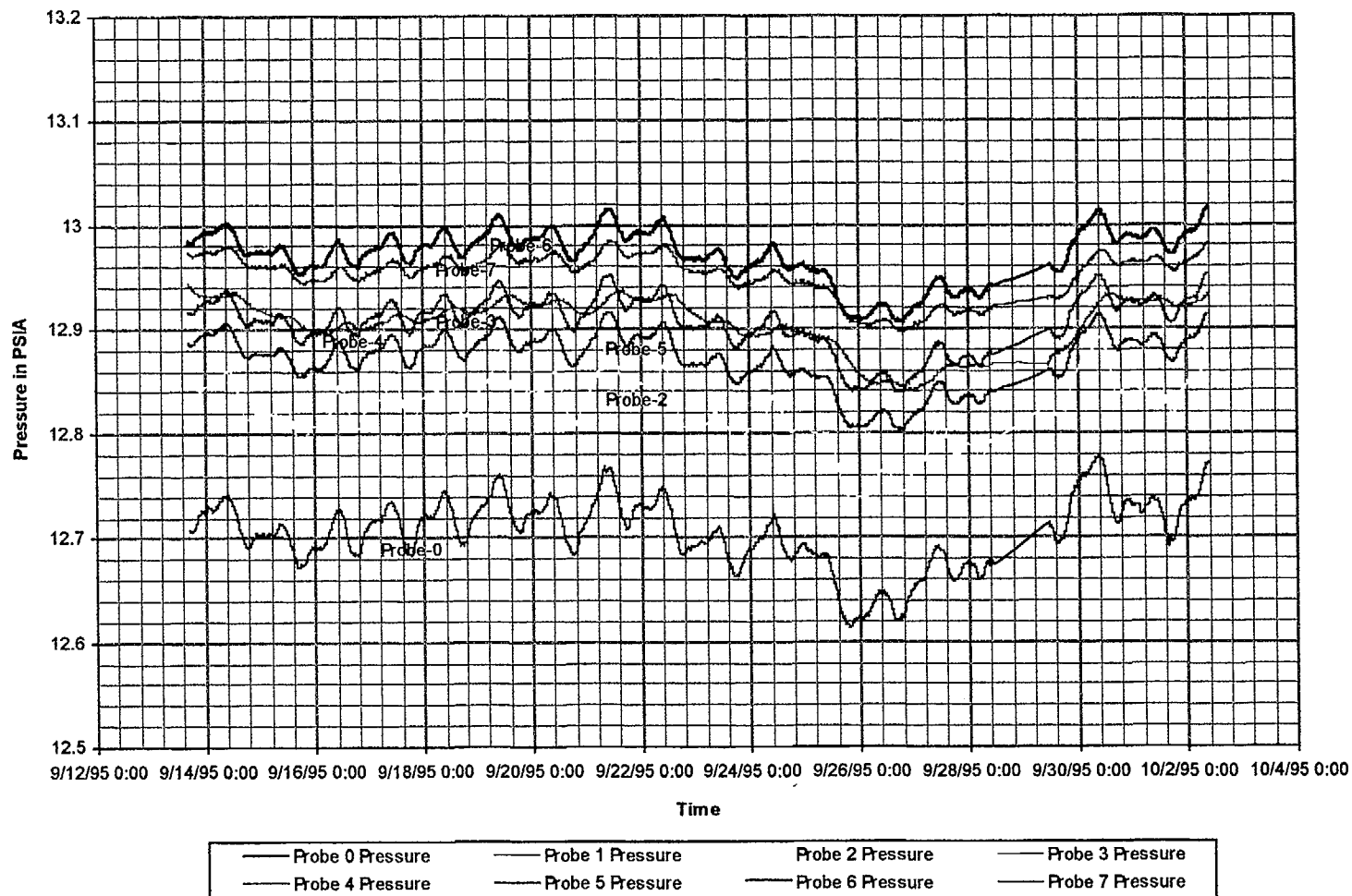


Figure 4-4e Pressure fluctuation with time in NRG-4

October 1995

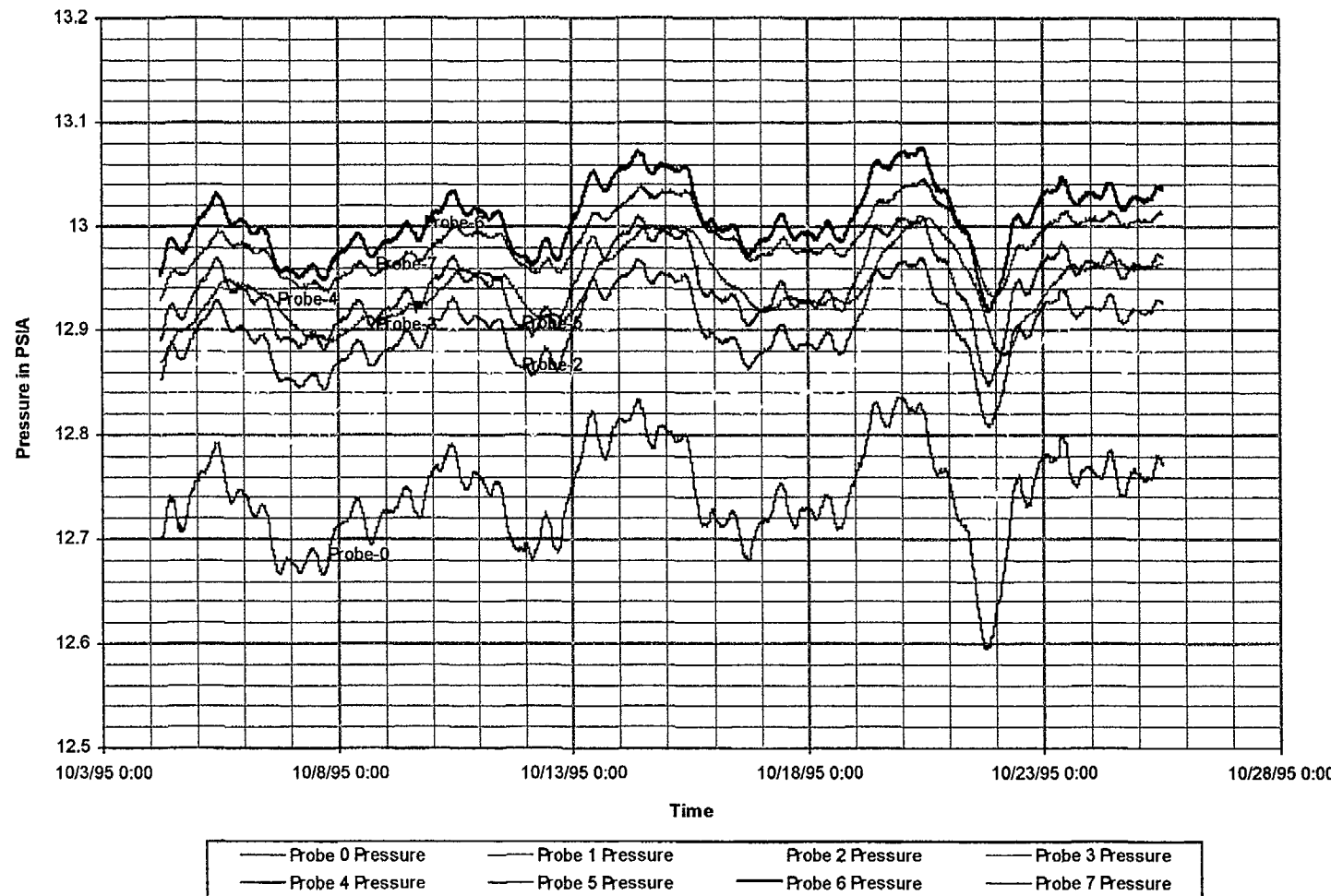


Figure 4-4f Pressure fluctuation with time in NRG-4

November 1995

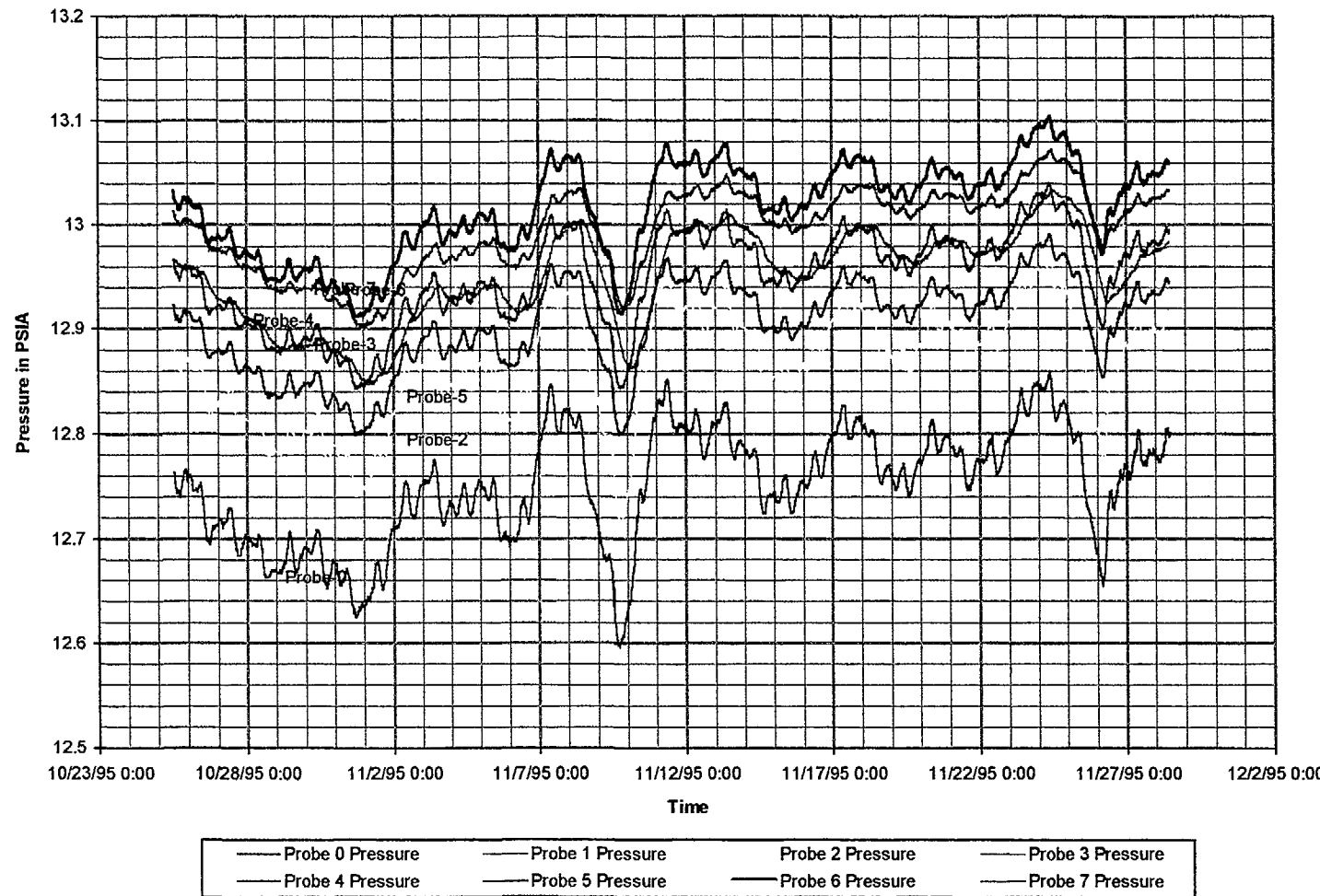


Figure 4-4g Pressure fluctuation with time in NRG-4

December 1995

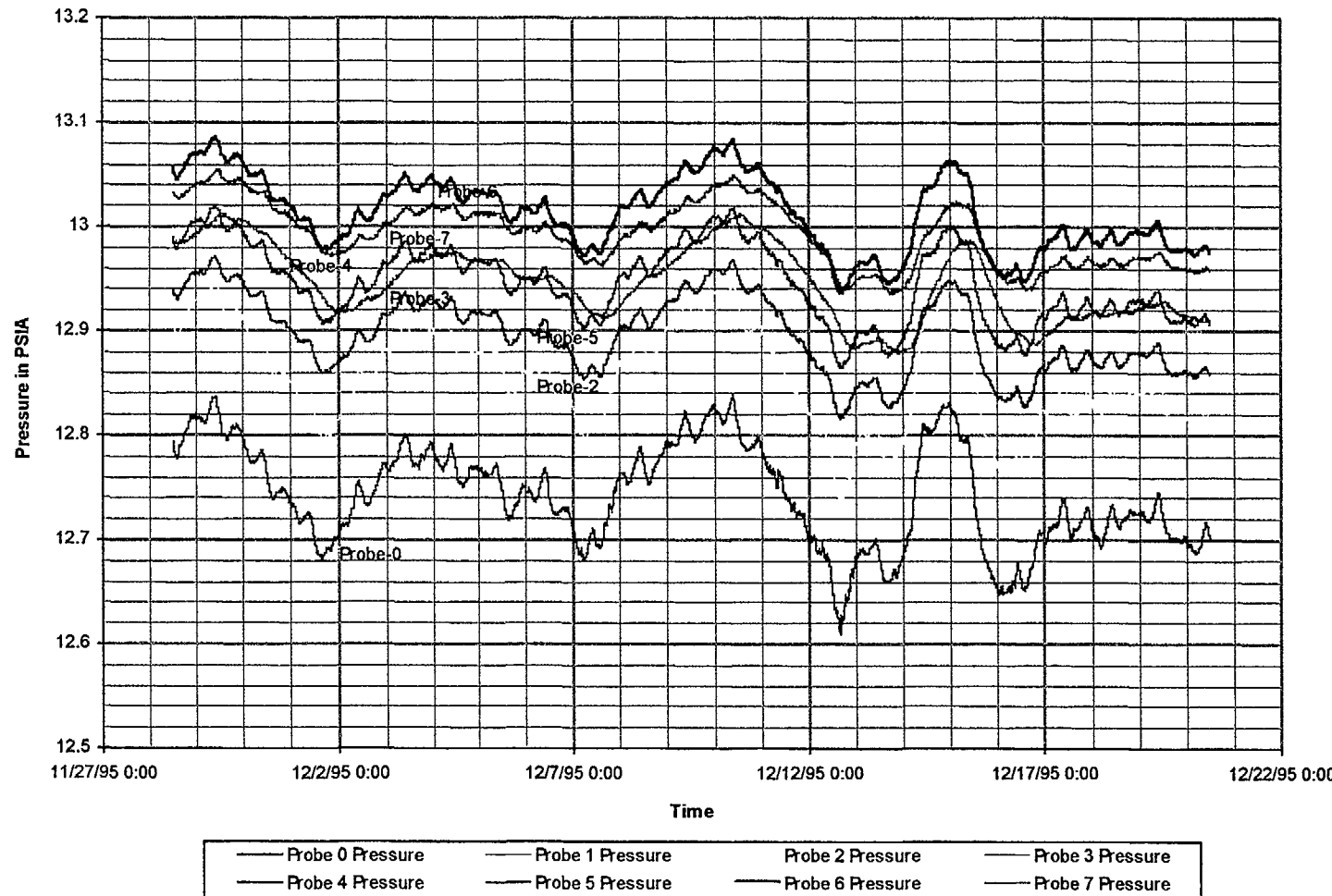


Figure 4-4h Pressure fluctuation with time in NRG-4

August 24, 1996
P26611:06 AMD:user\projects\Nyecounty\unrep96\figures

Prepared for:
Nye County Nuclear Waste Repository Project Office

Prepared by:
Multimedia Environmental Technology, Inc.
Newport Beach, CA

January 1996

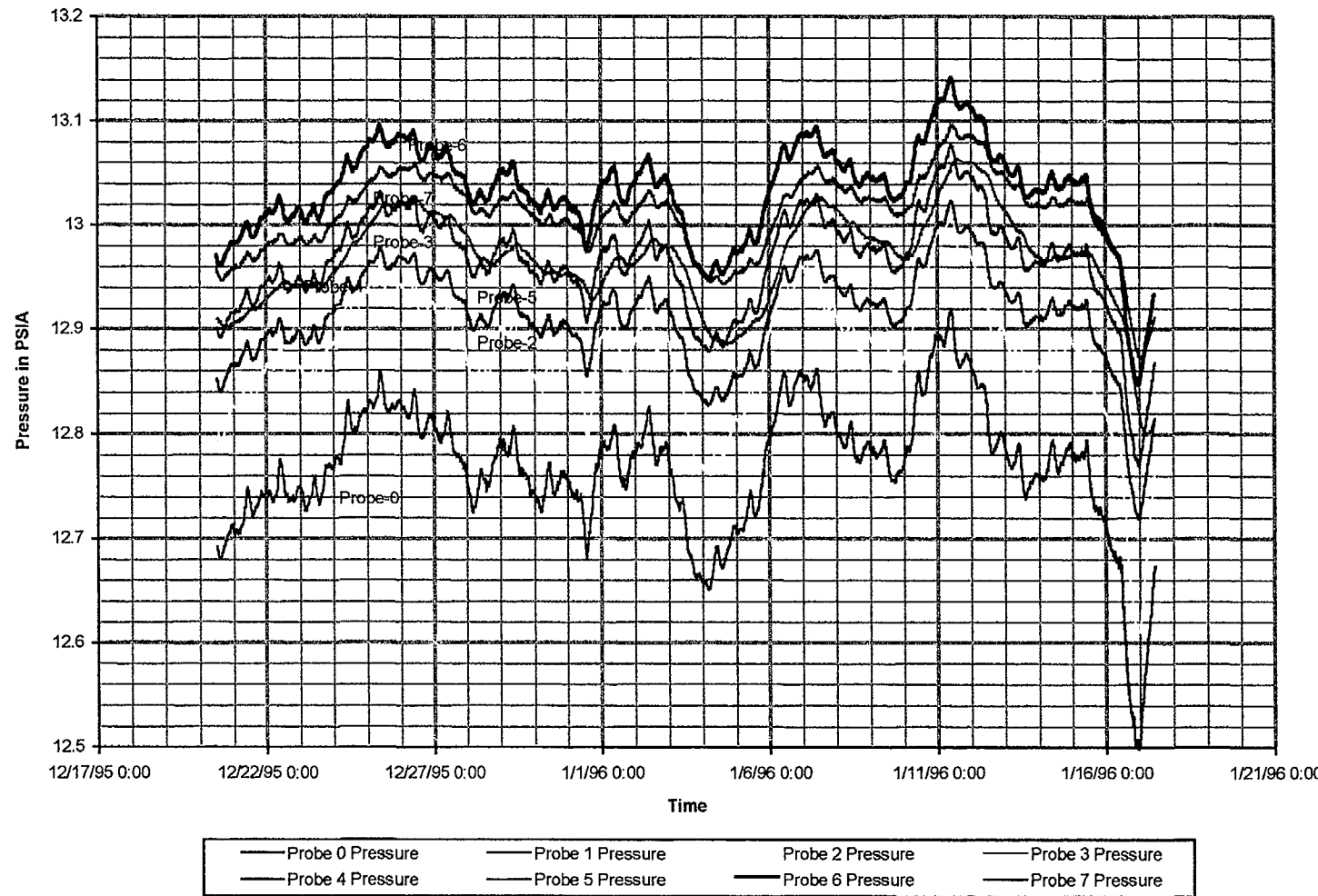


Figure 4-4i Pressure fluctuation with time in NRG-4

February 1996

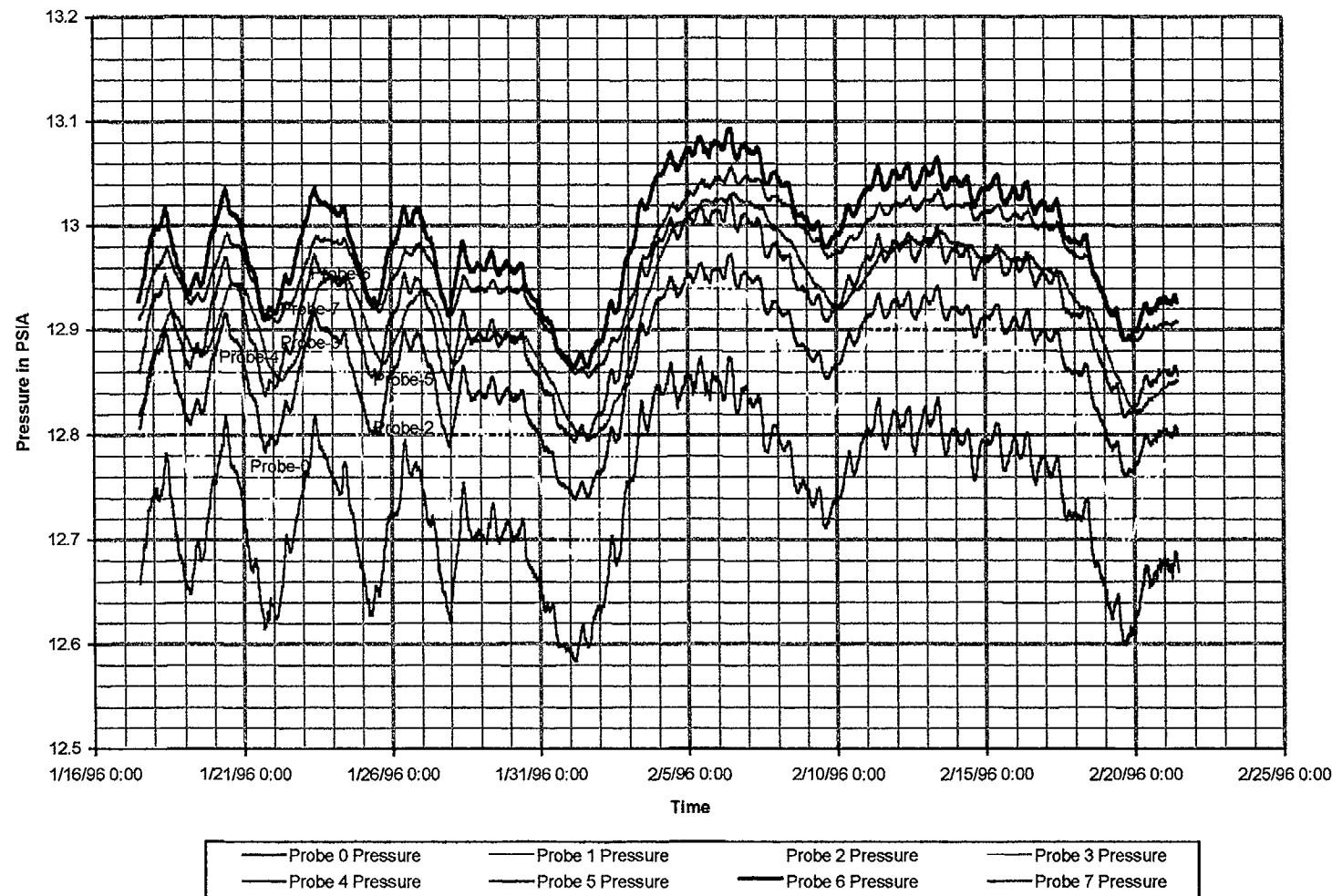


Figure 4-4j Pressure fluctuation with time in NRG-4

March 1996

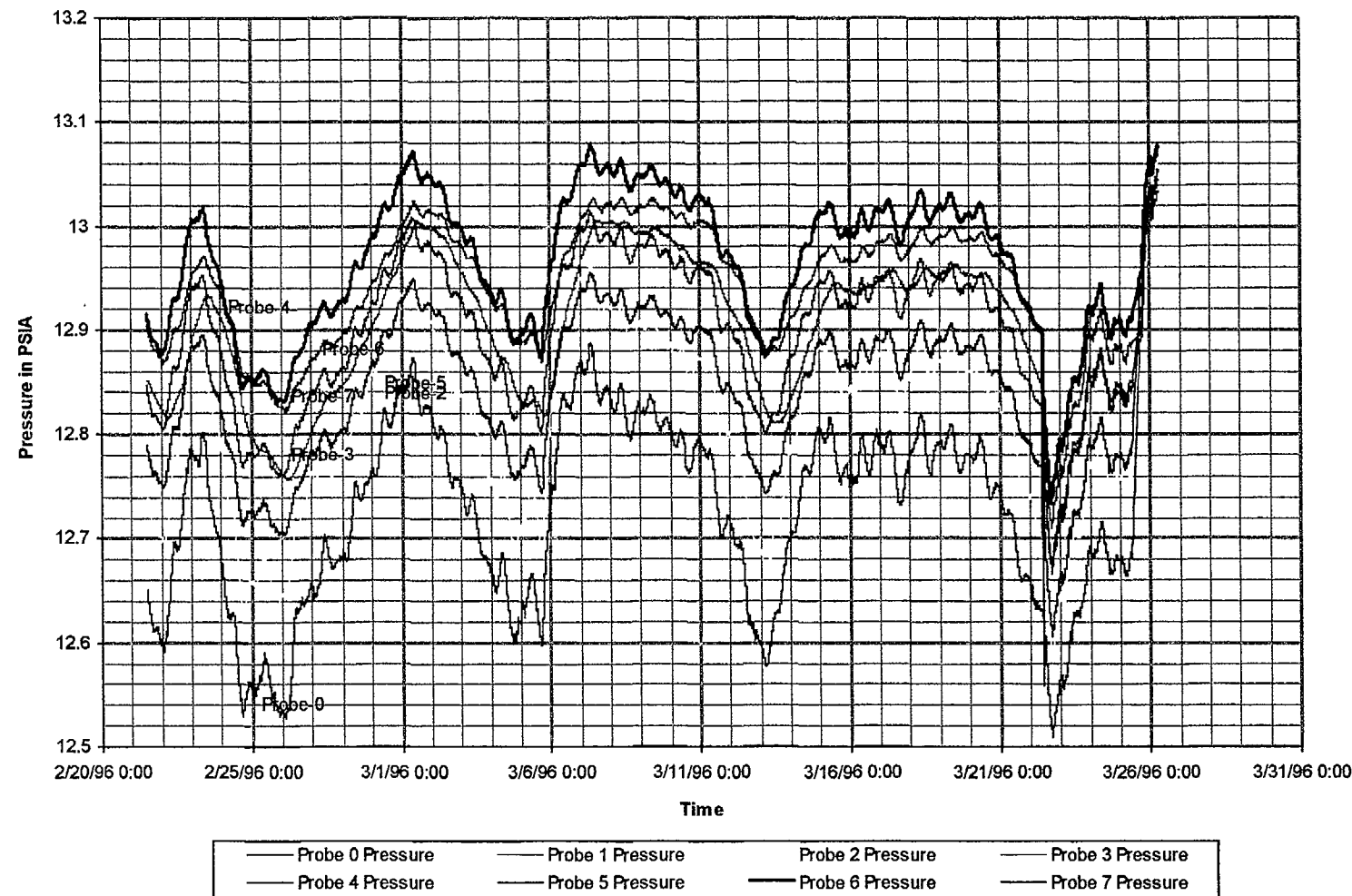


Figure 4-4k Pressure fluctuation with time in NRG-4

April 1996

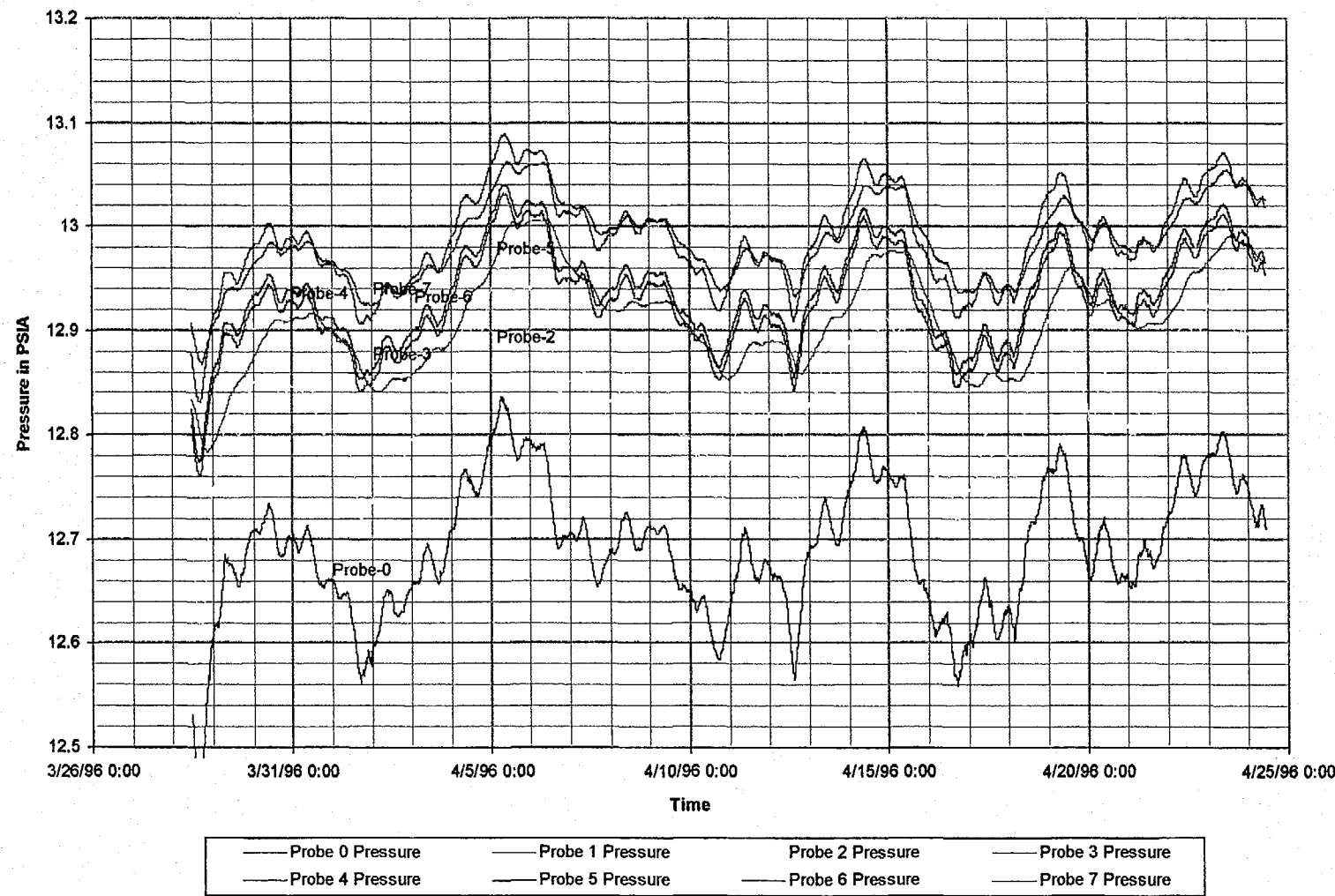


Figure 4-4L Pressure fluctuation with time in NRG-4

August 24, 1996
P266:D:\user\projects\Nye county\annrep96\figures

Prepared for:
Nye County Nuclear Waste Repository Project Office

Prepared by:
Multimedia Environmental Technology, Inc.
Newport Beach, CA

MAY 1996

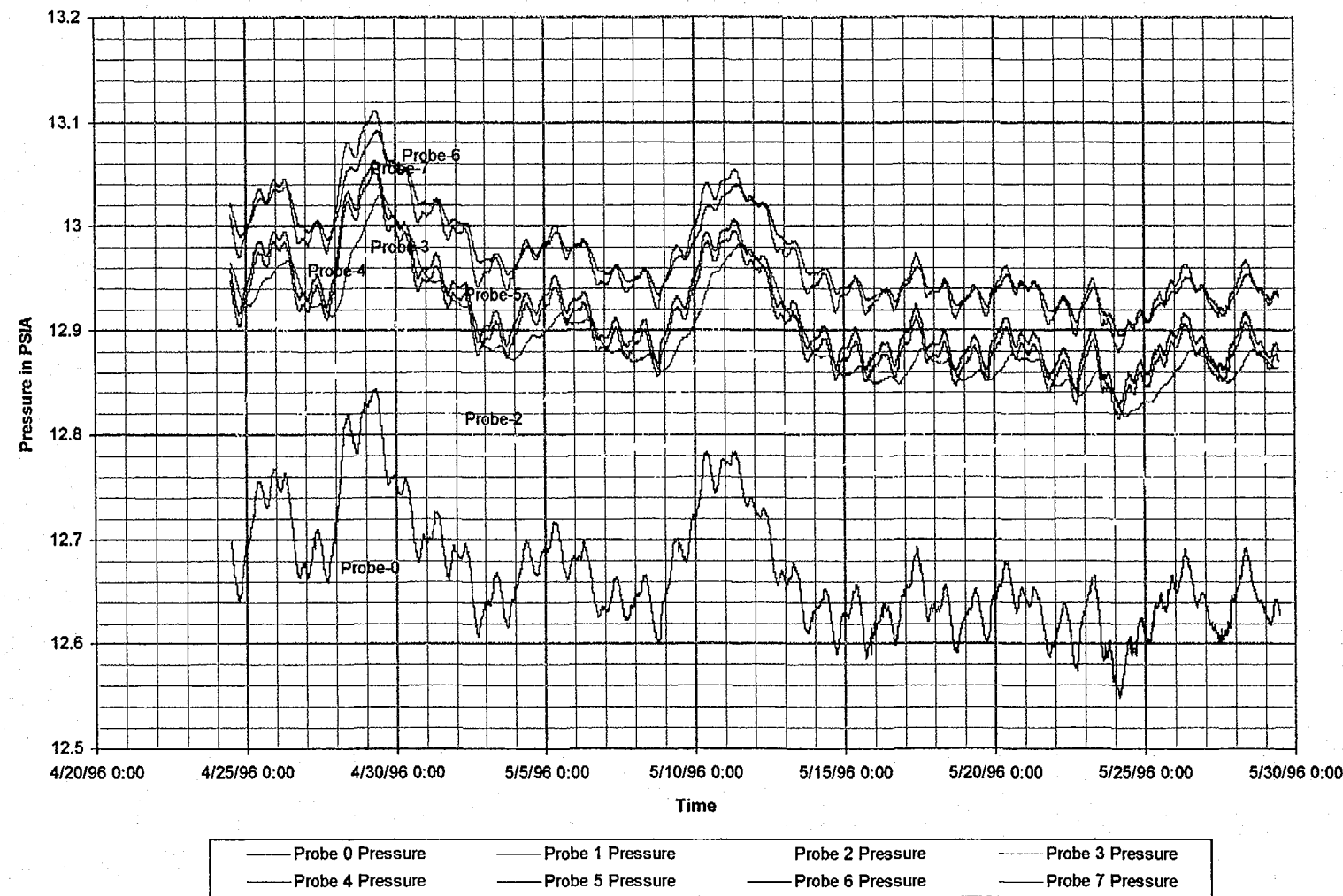


Figure 4-4m Pressure fluctuation with time in NRG-4

JUNE 1996

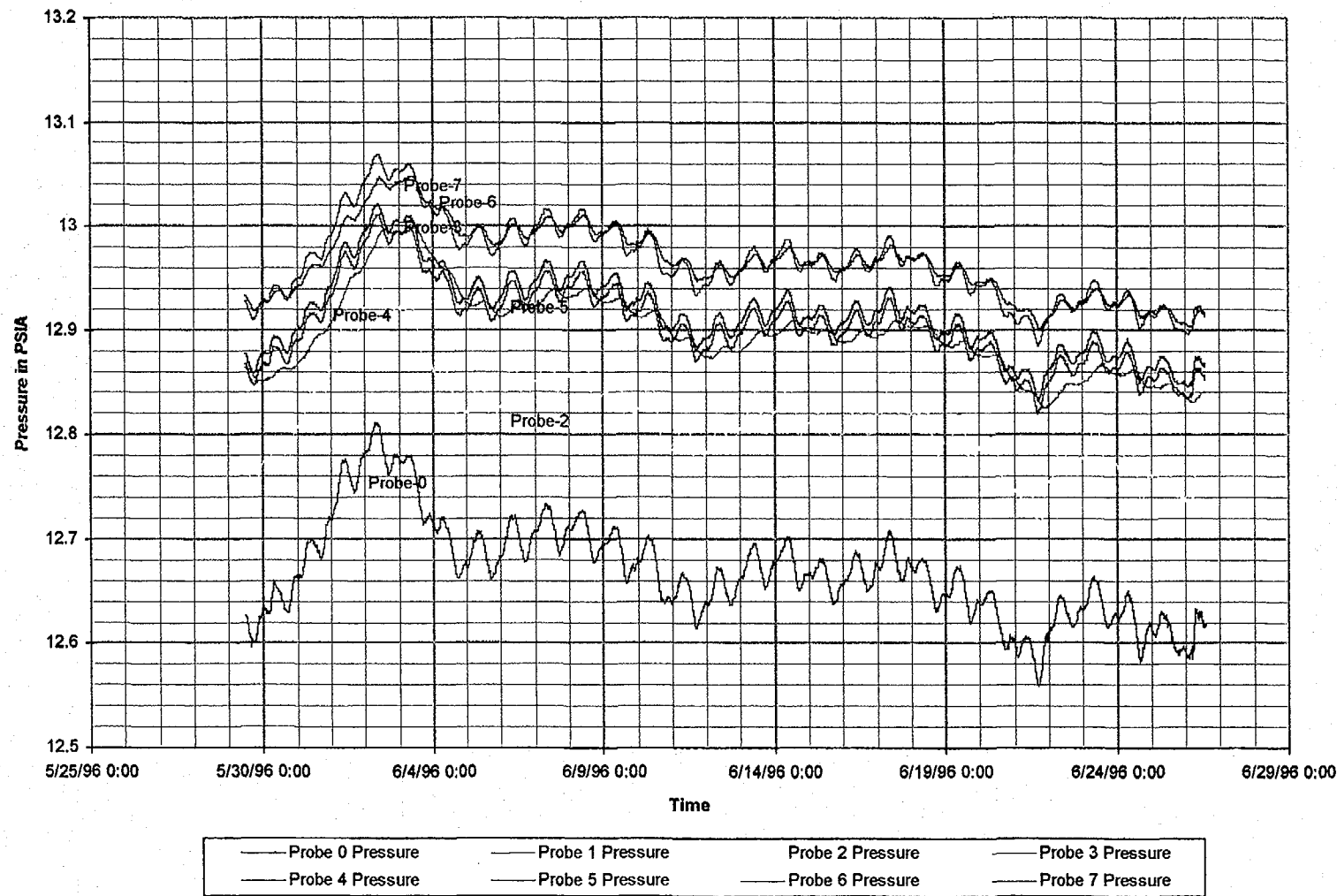


Figure 4-4n Pressure fluctuation with time in NRG-4

August 24, 1996
P266:D:\user\projetc\Nyecounty\annrep96\figures

Prepared for:
Nye County Nuclear Waste Repository Project Office

Prepared by:
Multimedia Environmental Technology, Inc.
Newport Beach, CA

JULY 1996

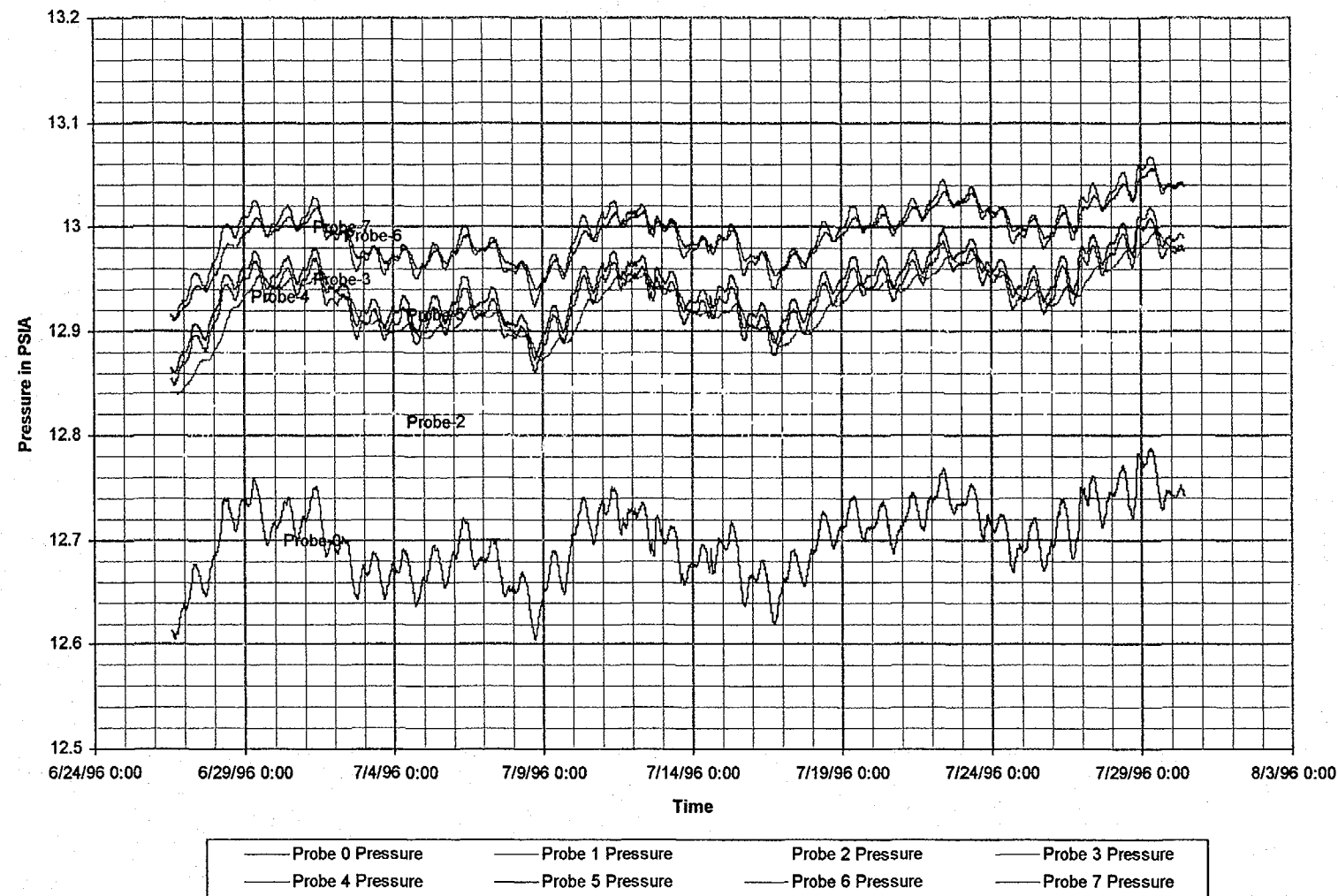


Figure 4-4o Pressure fluctuation with time in NRG-4

August 1996

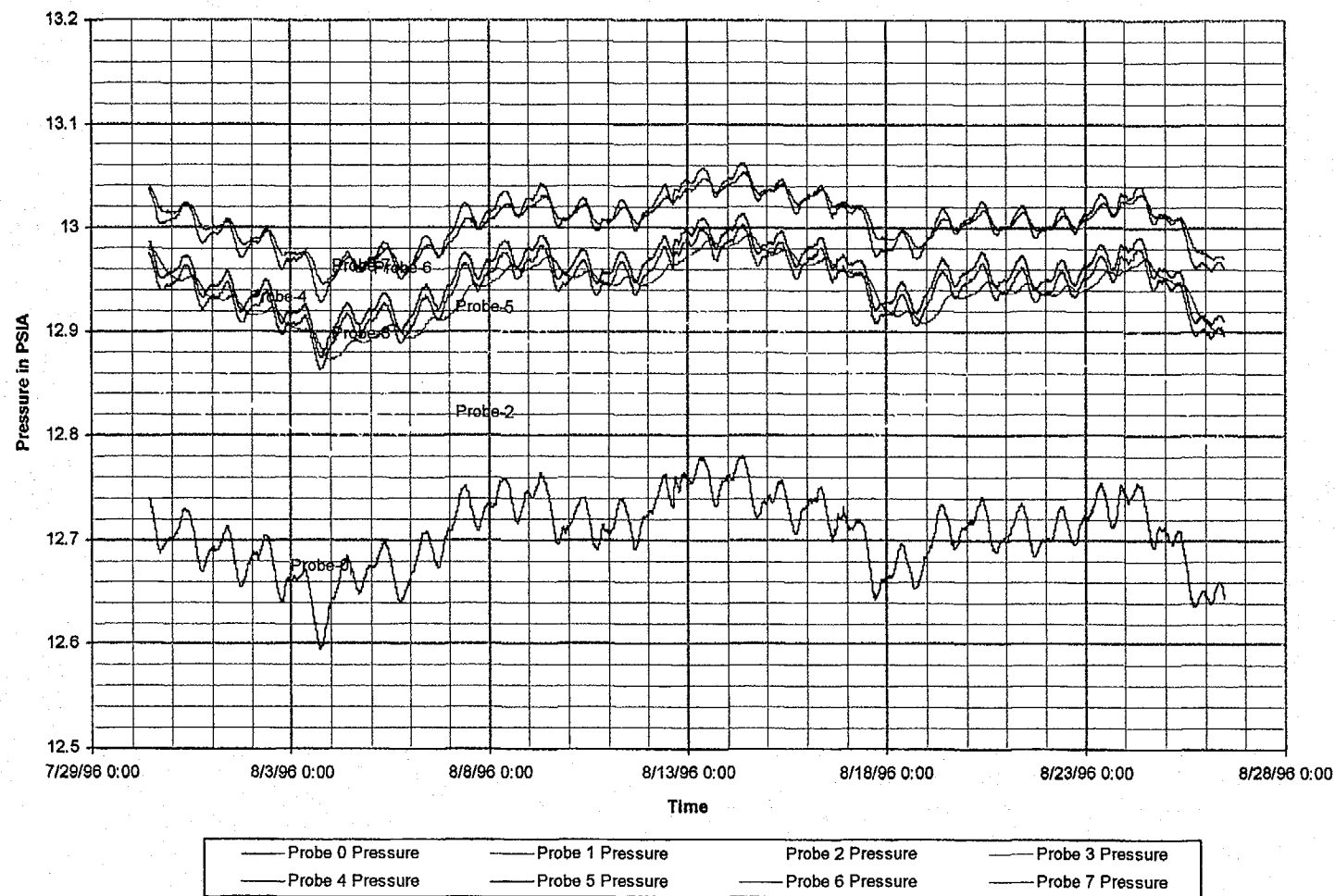


Figure 4-4p Pressure fluctuation with time in NRG-4

April 1995

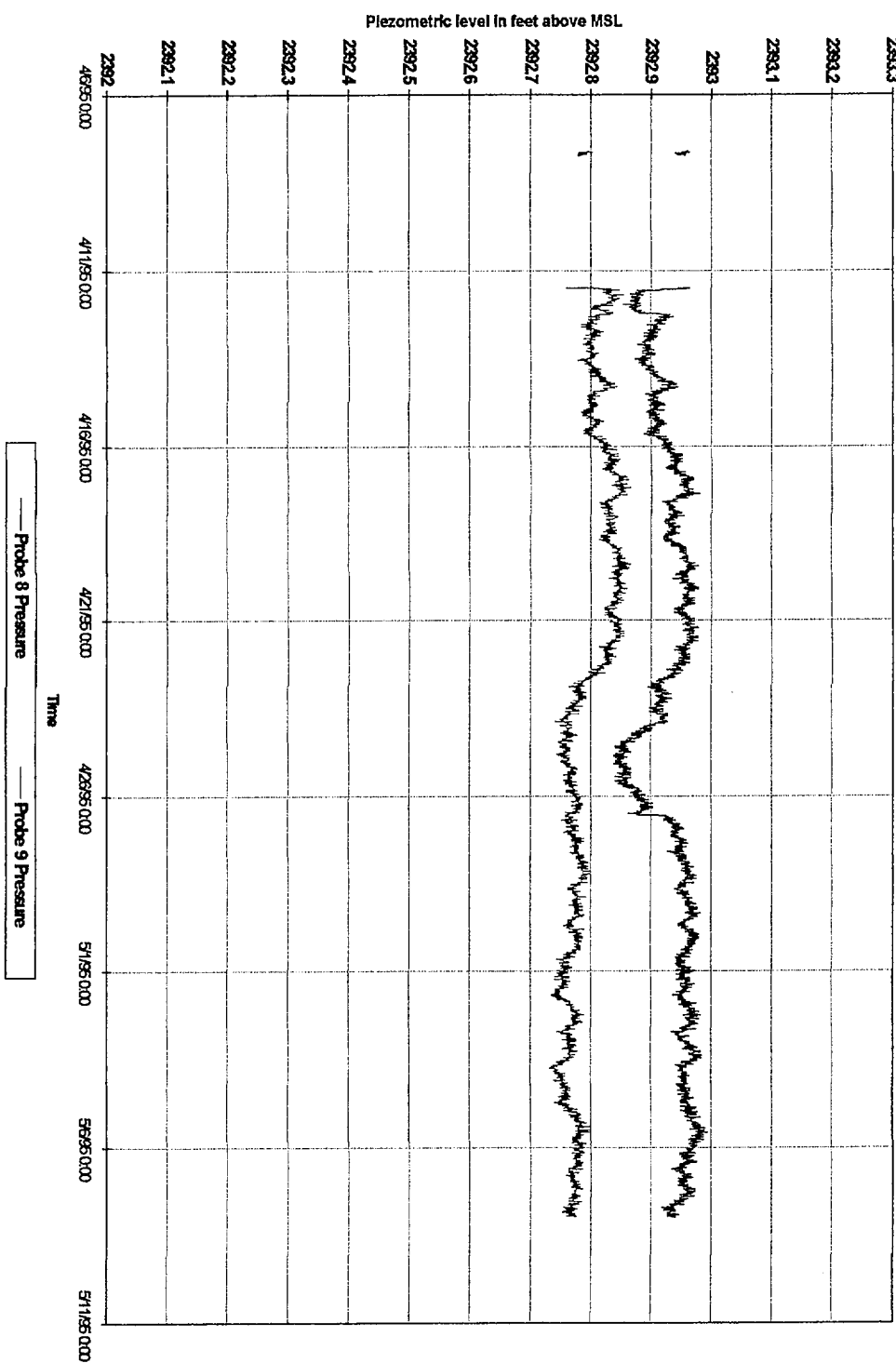


Figure 4-5a Piezometric fluctuation with time in ONC-1

August 24, 1996
P2659.00 AMD\user\project\NyeCounty\ammp\95\figures

Prepared for:
Nye County Nuclear Waste Repository Project Office

Prepared by:
Multimedia Environmental Technology, Inc.
Newport Beach, CA

May 1995

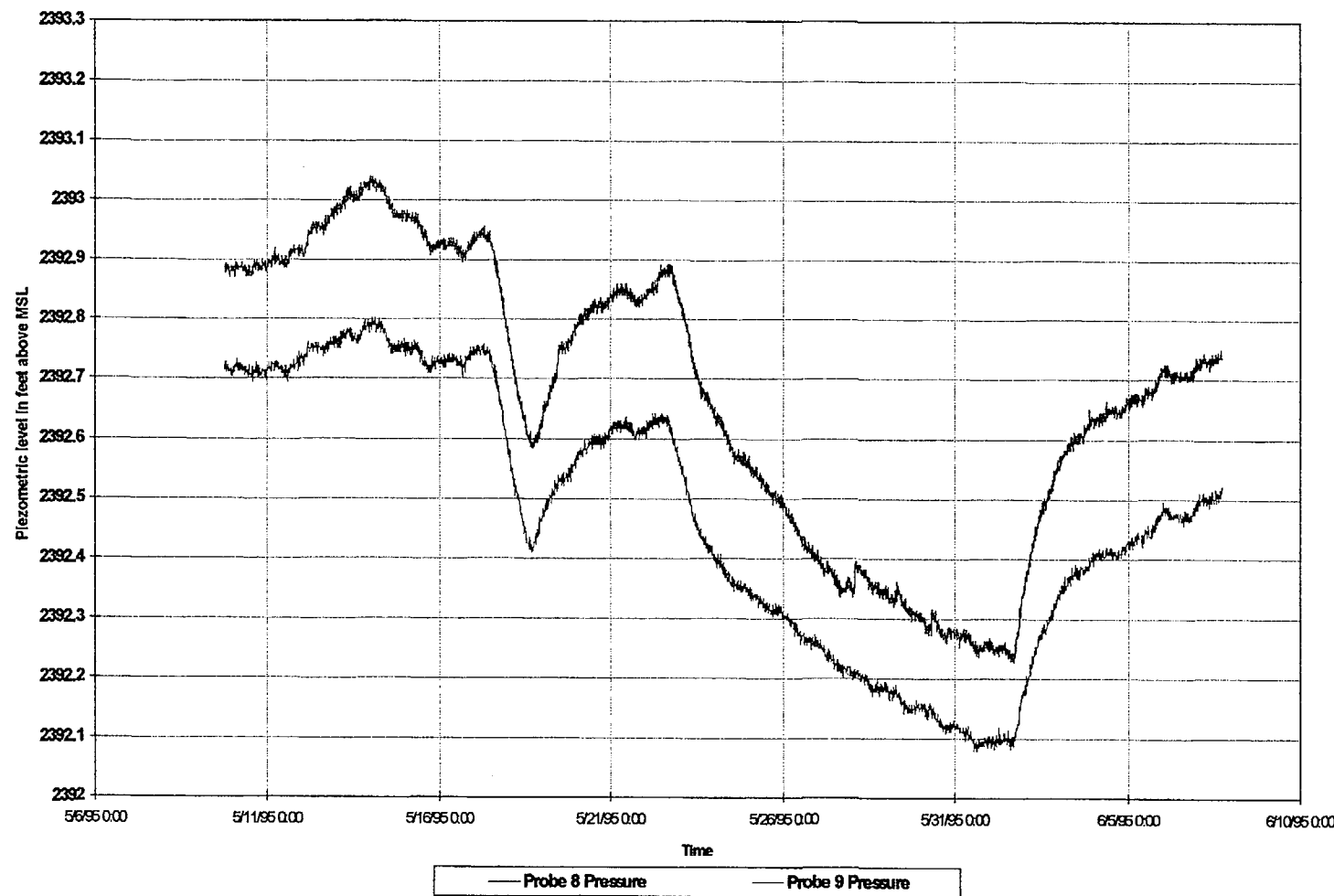


Figure 4-5b Piezometric fluctuation with time in ONC-1

June 1995

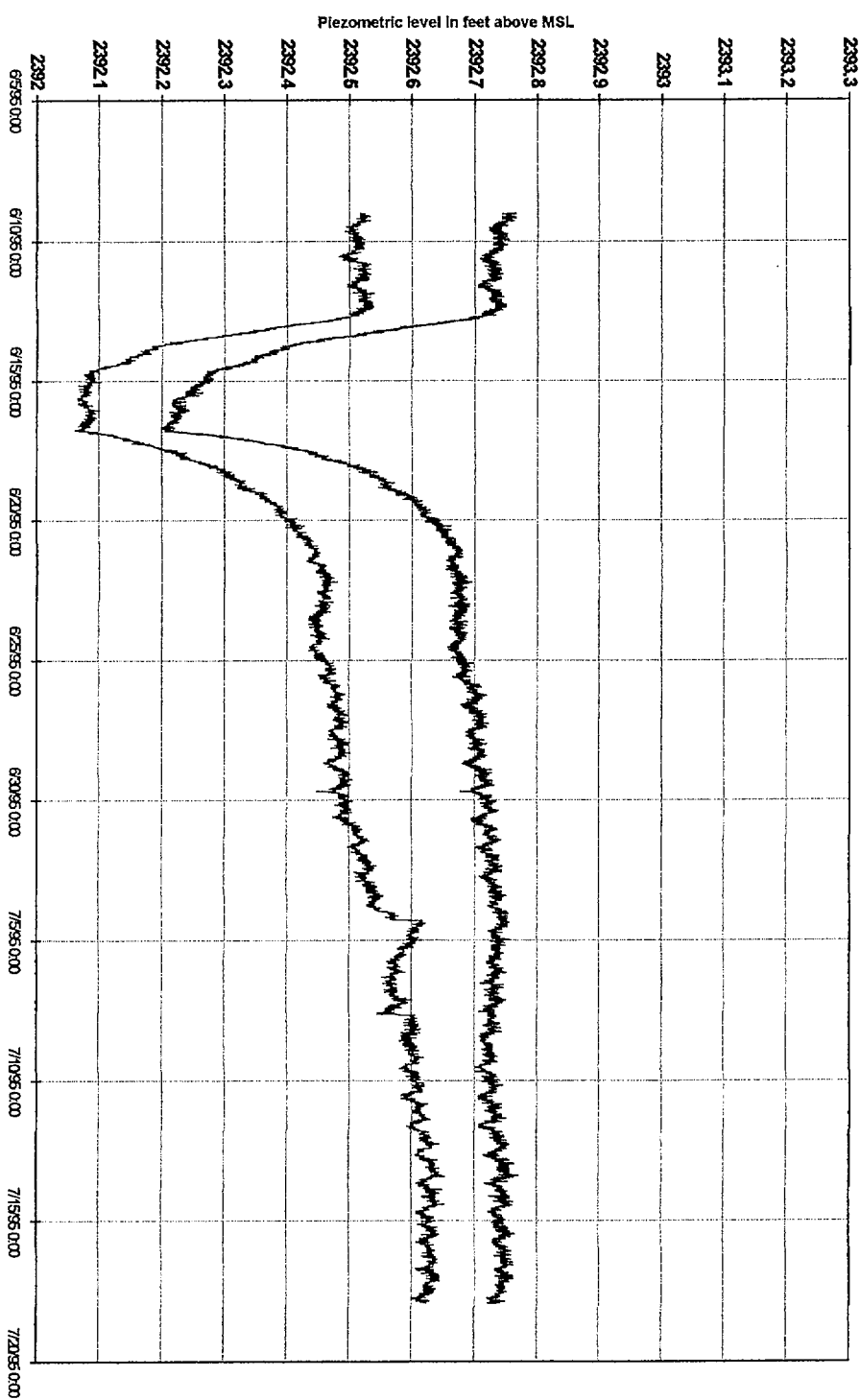


Figure 4-5c Piezometric fluctuation with time in ONC-1

August 24, 1995
P2669-10 AWD:jwm\project\Nyecont\June95\figures

Prepared for:
Nye County Nuclear Waste Repository Project Office

Prepared by:
Multimedia Environmental Technology, Inc.
Newport Beach, CA

July 1995

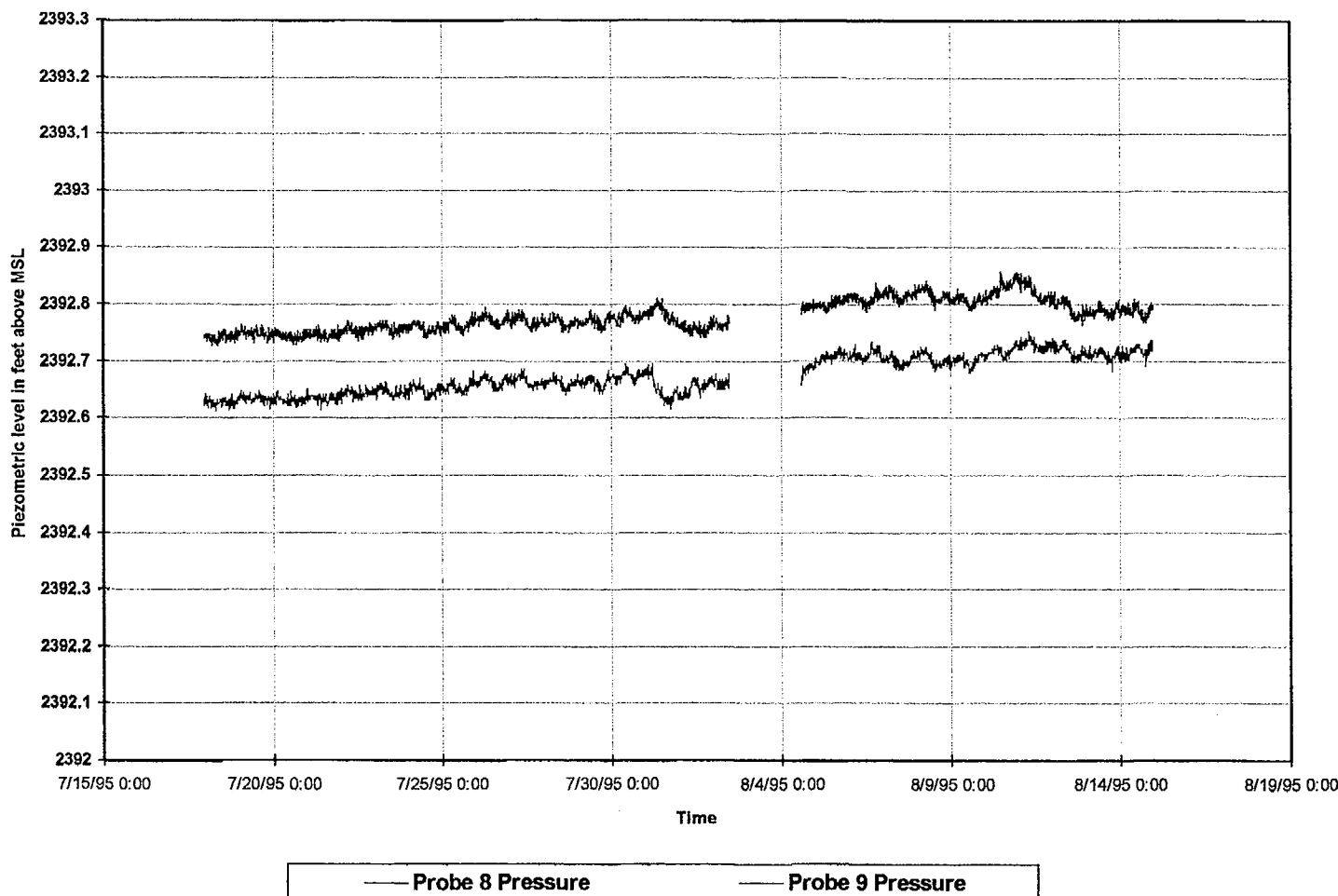


Figure 4-5d Piezometric fluctuation with time in ONC-1

August 1995

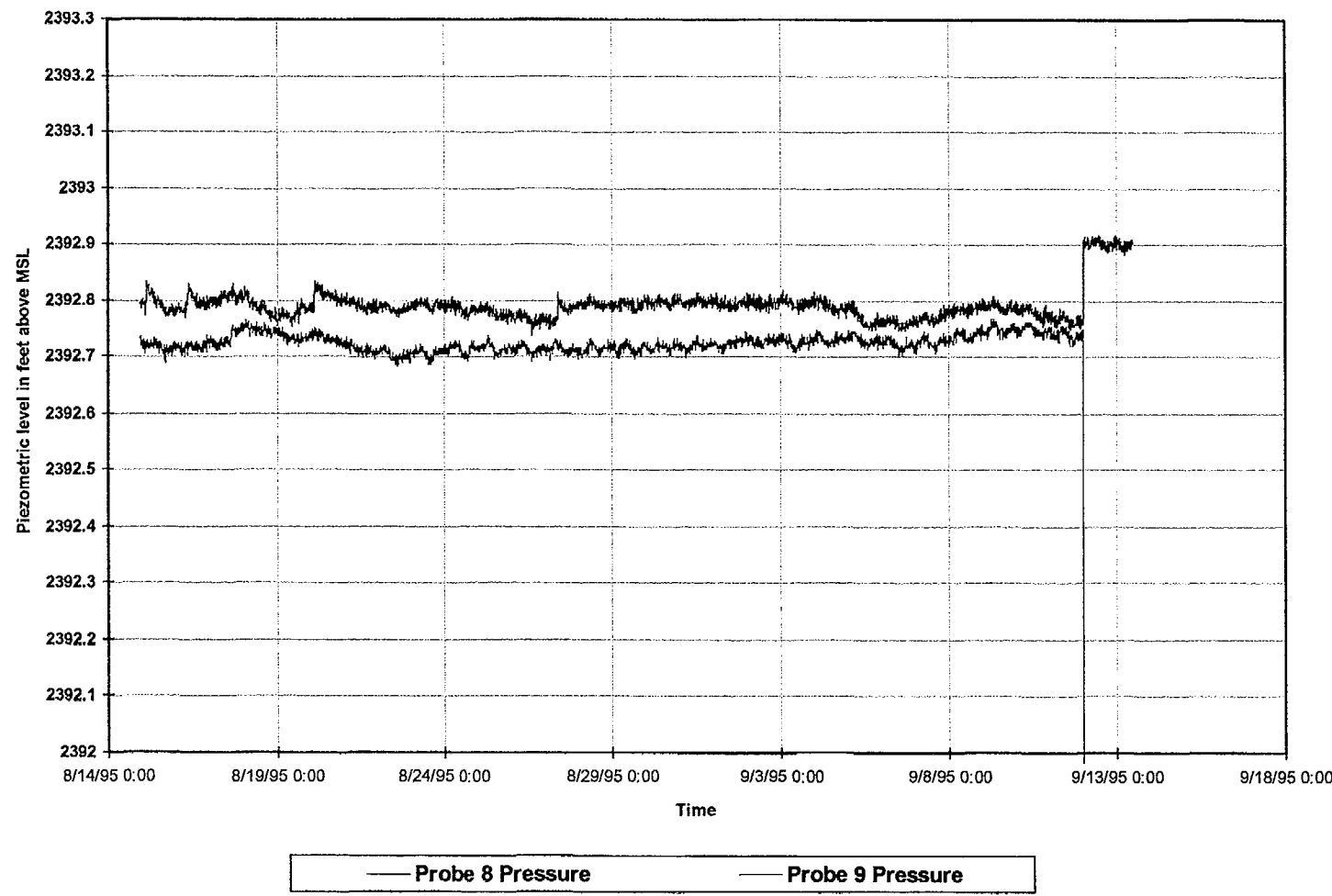


Figure 4-5e Piezometric fluctuation with time in ONC-1

September 1995

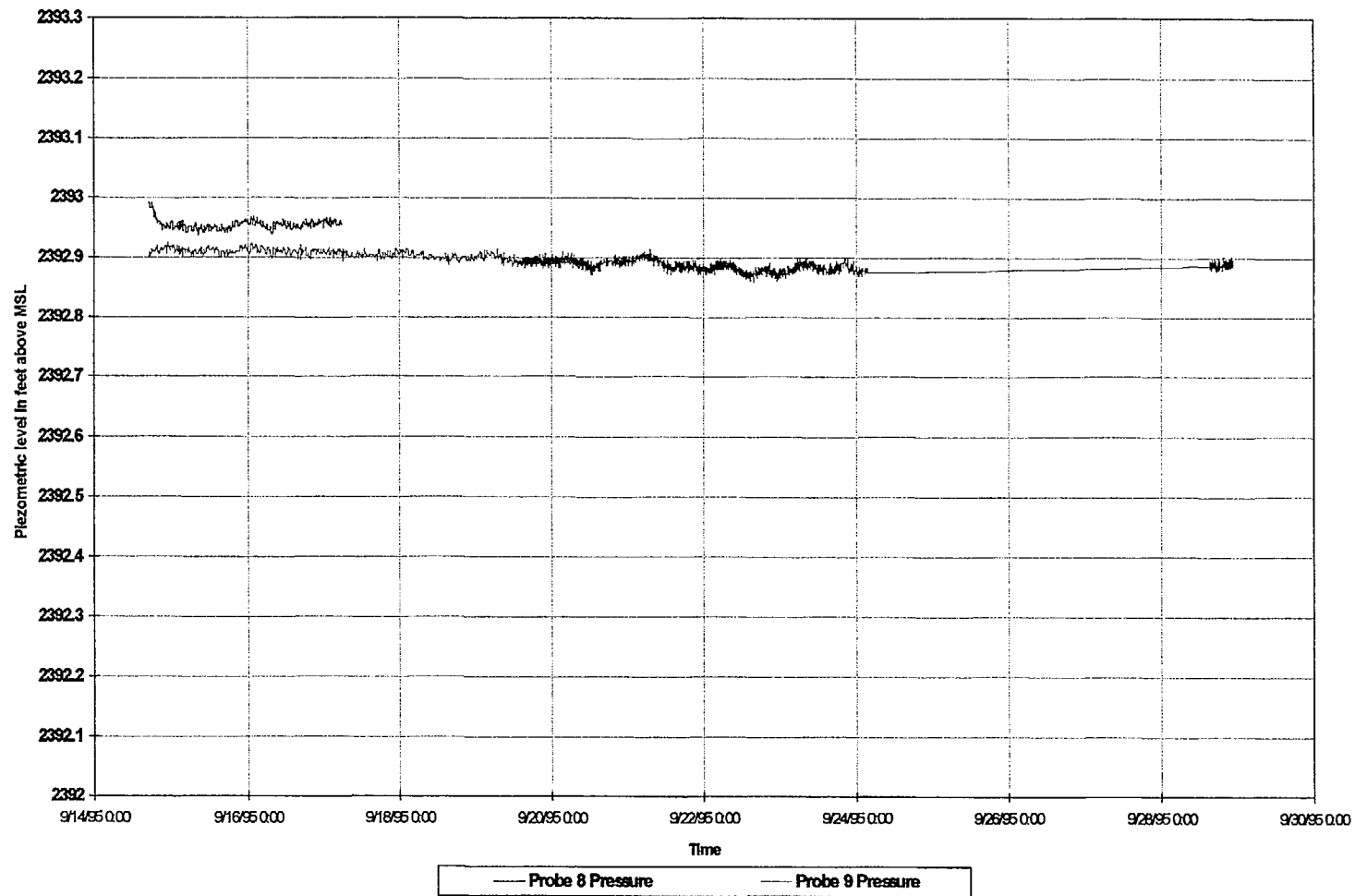


Figure 4-5f

Piezometric fluctuation with time in ONC-1

August 24, 1996
P2669.23 AMD:\user\projects\NyeCounty\enrcp96\figures

Prepared for:
Nye County Nuclear Waste Repository Project Office

Prepared by:
Multimedia Environmental Technology, Inc.
Newport Beach, CA

October 1995

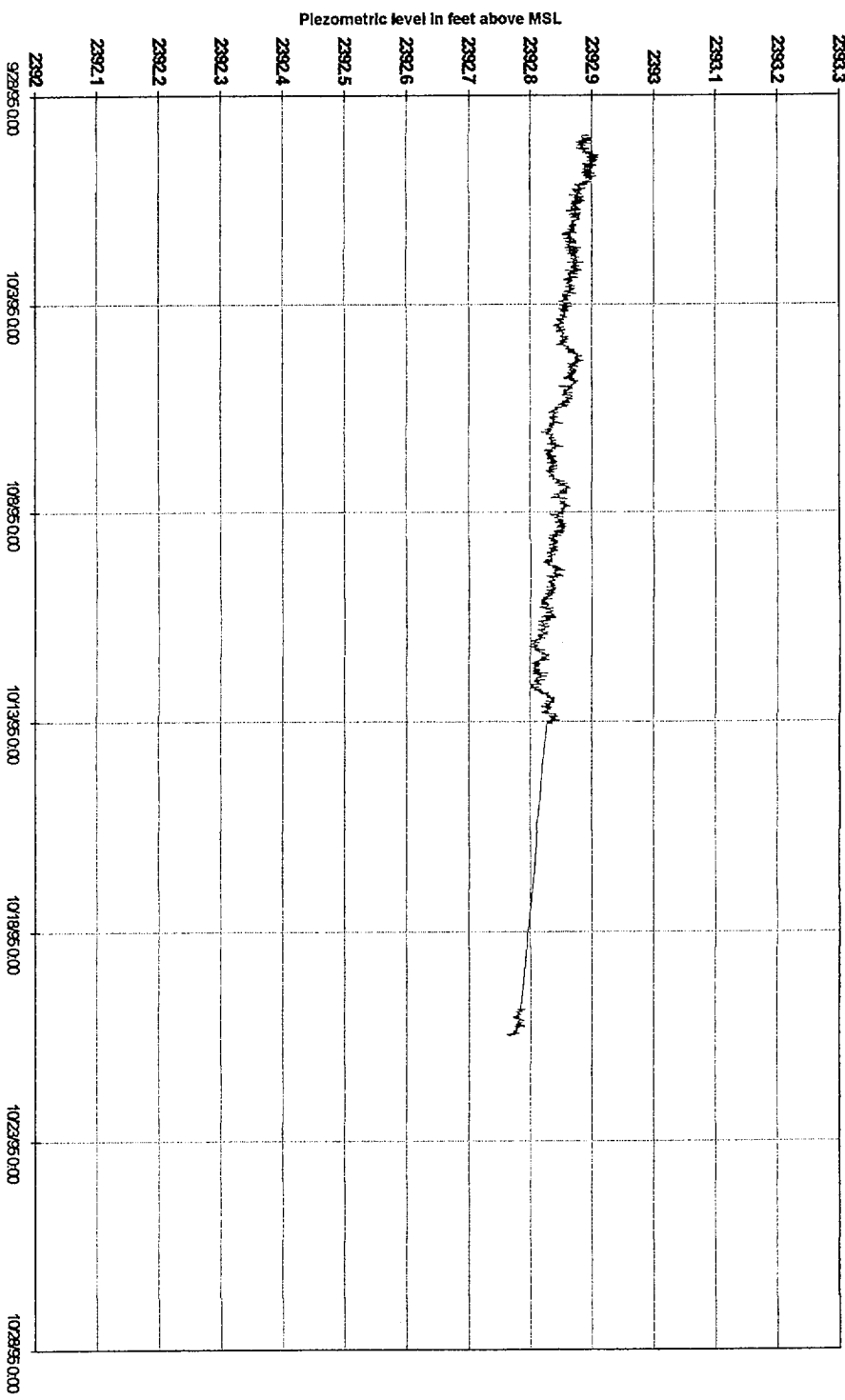


Figure 4-5g Piezometric fluctuation with time in ONC-1

August 24, 1996
P2669:23 AMD:usw:projects\NyeCounty\amrep96\figures

Prepared for:
Nye County Nuclear Waste Repository Project Office

Prepared by:
Multimedia Environmental Technology, Inc.
Newport Beach, CA

November 1995

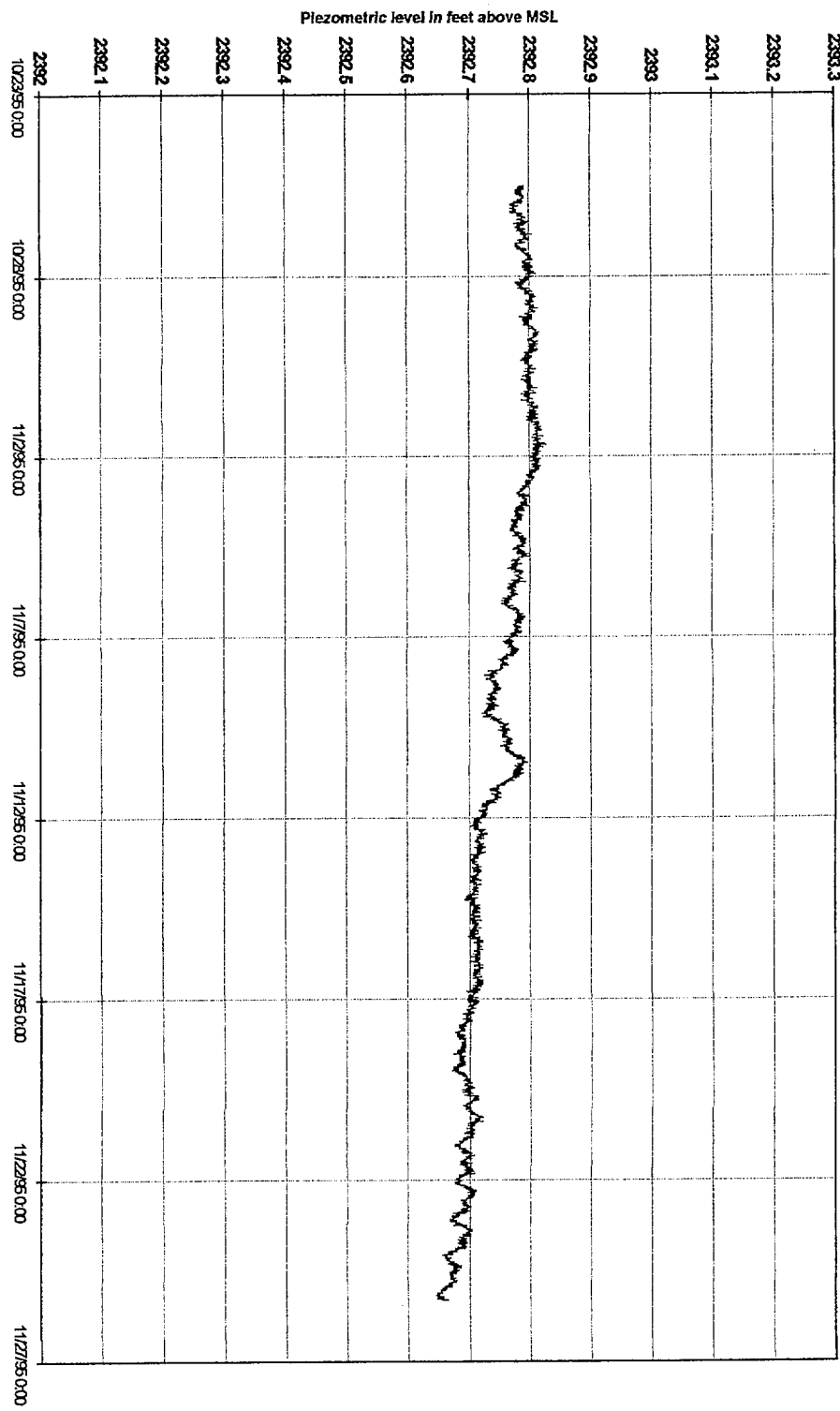


Figure 4-5h Piezometric fluctuation with time in ONC-1

August 24, 1995
P265923 AMD/underground/NyeCounty/summary96/figures

Prepared for:
Nye County Nuclear Waste Repository Project Office

Prepared by:
Multimedia Environmental Technology, Inc.
Newport Beach, CA

December 1995

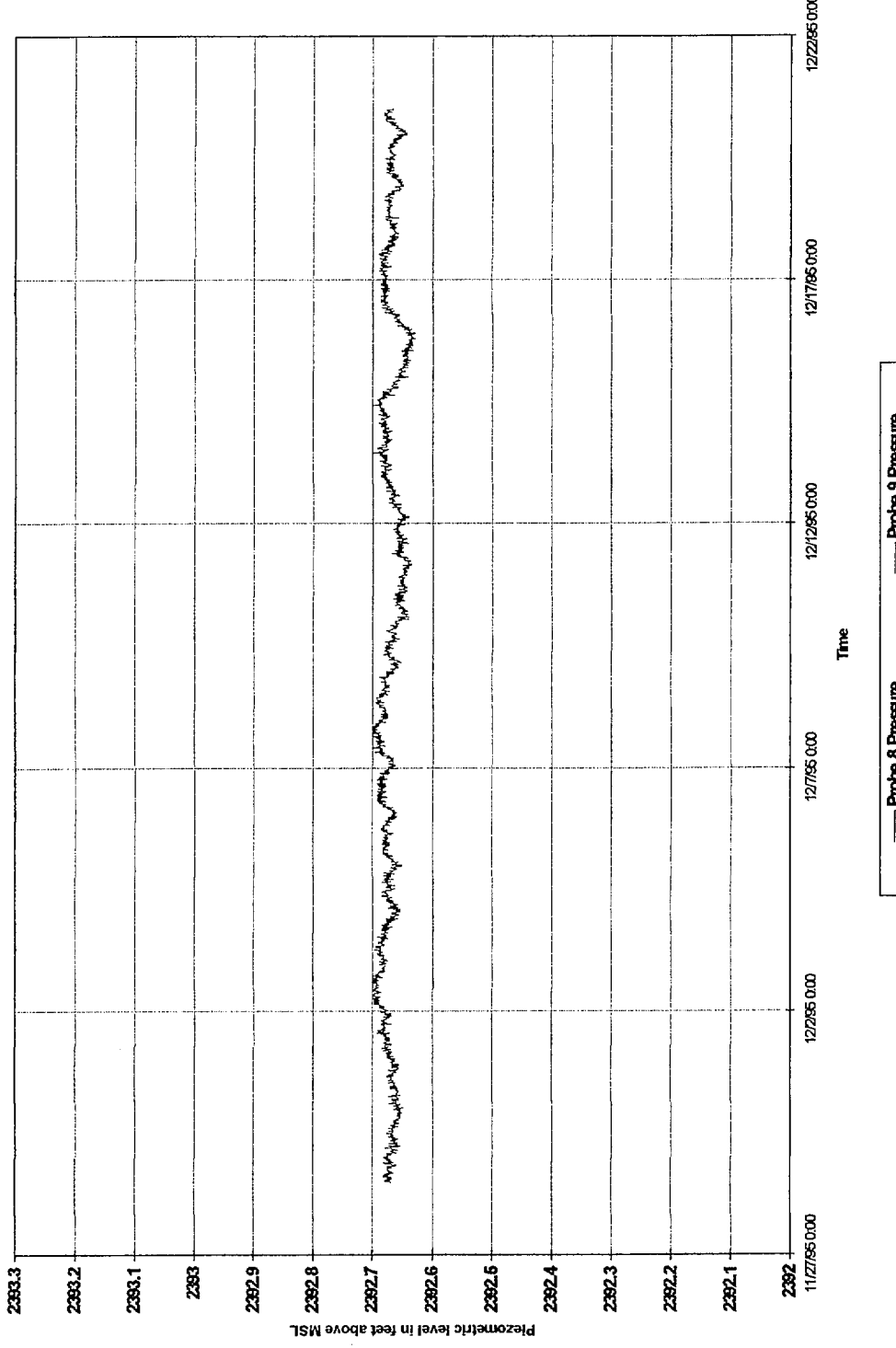


Figure 4-5i Piezometric fluctuation with time in ONC-1

August 24, 1996
P266923 AWD:usw:projecl:NyeCounty:unmap90figures

Prepared for:
Nye County Nuclear Waste Repository Project Office

Prepared by:
Multimedia Environmental Technology, Inc.
Newport Beach, CA

January 1996

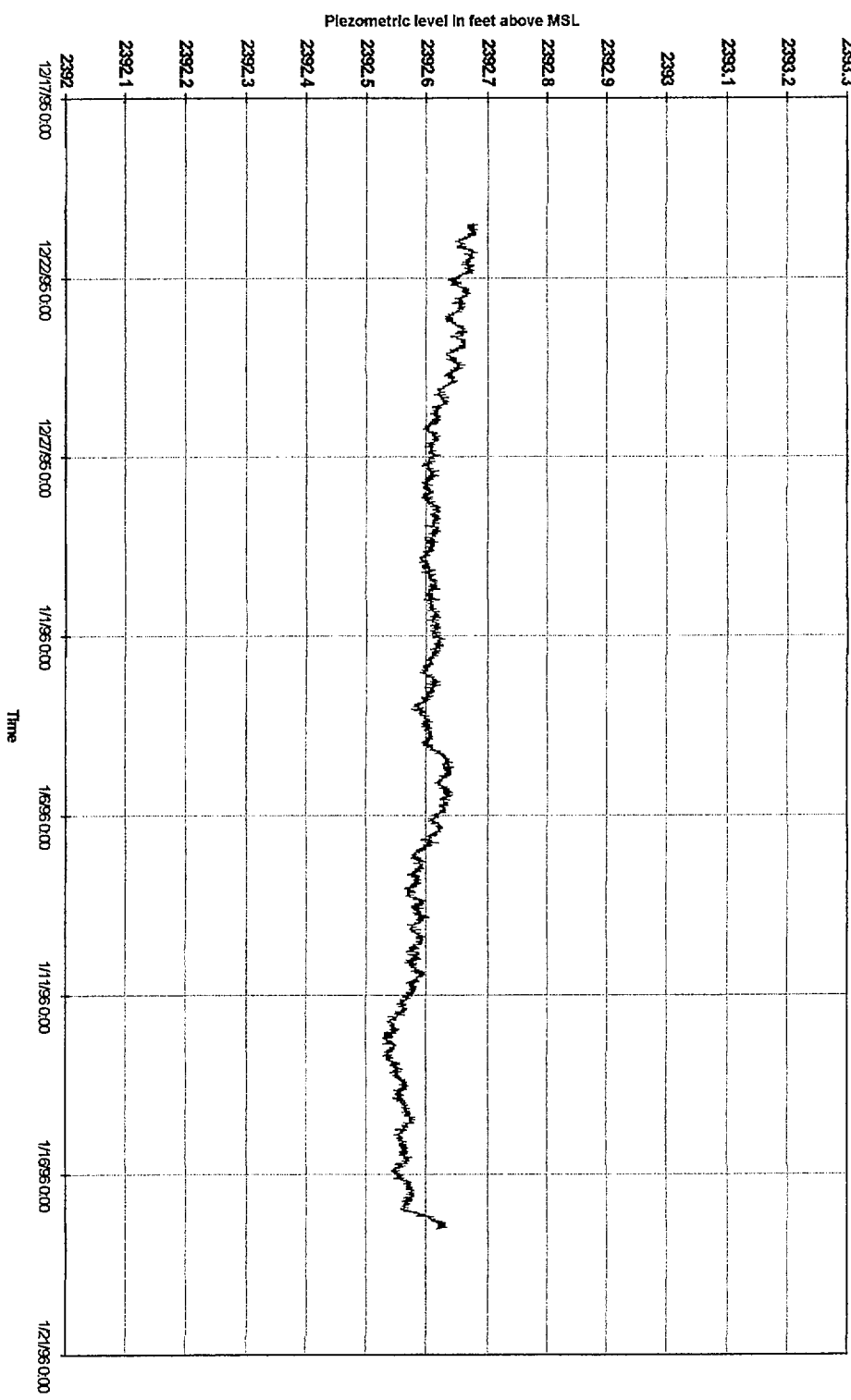


Figure 4-5j Piezometric fluctuation with time in ONC-1

August 24, 1996
P2669123 AMD:unproj01\NyeCounty\unproj06\figures

Prepared for:
Nye County Nuclear Waste Repository Project Office

Prepared by:
Multimedia Environmental Technologies, Inc.
Newport Beach, CA

February 1996

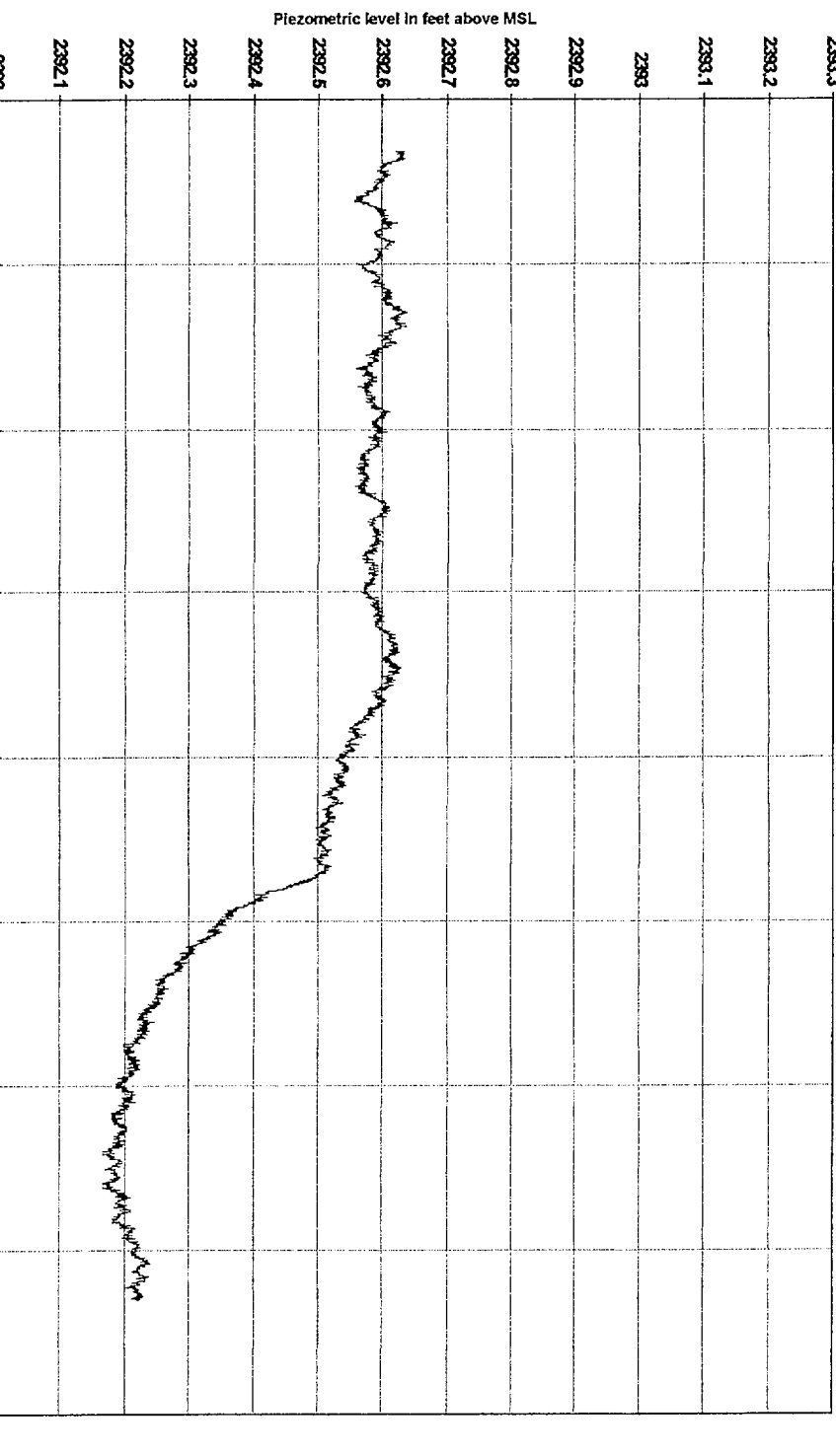


Figure 4-5k Piezometric fluctuation with time in ONC-1

August 24, 1996
P665923 AMD\waterprojec\Nyecounty\waterrep96\figures

Prepared for:
Nye County Nuclear Waste Repository Project Office

Multimedia Environmental Technology, Inc.
Newport Beach, CA

March 1996

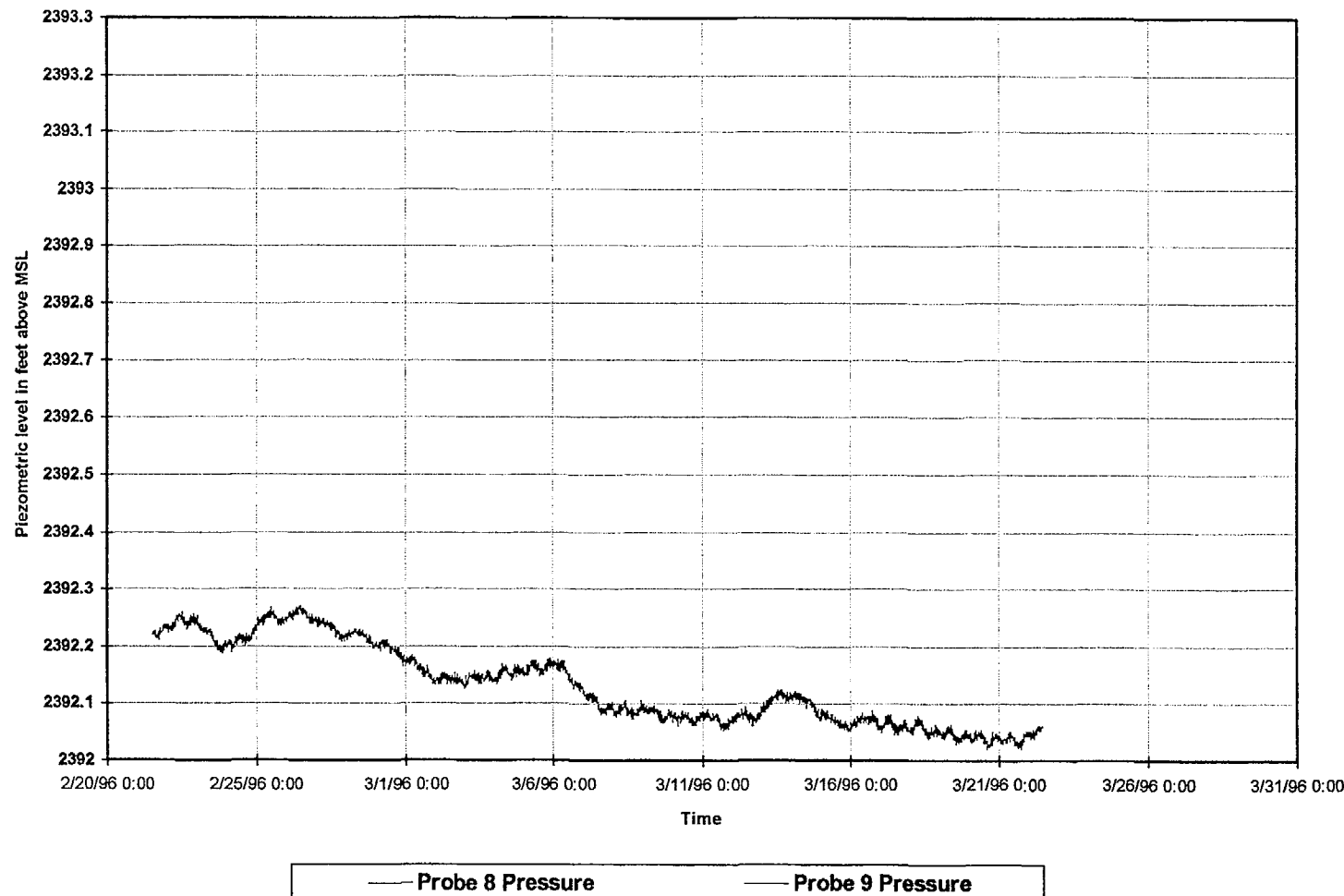


Figure 4-5L Piezometric fluctuation with time in ONC-1

August 24, 1996
P26612:31 PMD:\user\projects\Nyecounty\annrep96\figures

Prepared for:
Nye County Nuclear Waste Repository Project Office

Prepared by:
Multimedia Environmental Technology, Inc.
Newport Beach, CA

April 1996

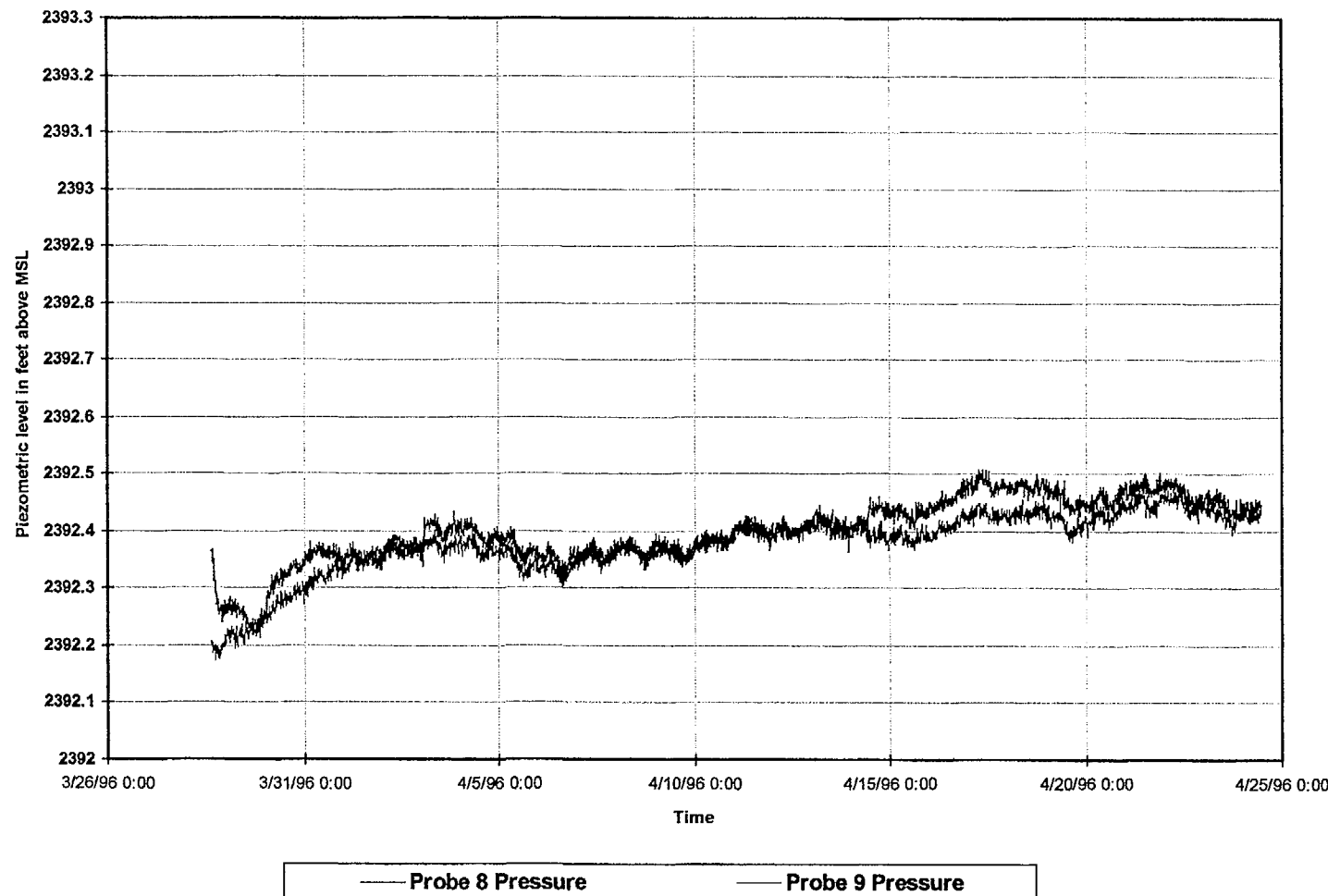


Figure 4-5m Piezometric fluctuation with time in ONC-1

May 1996

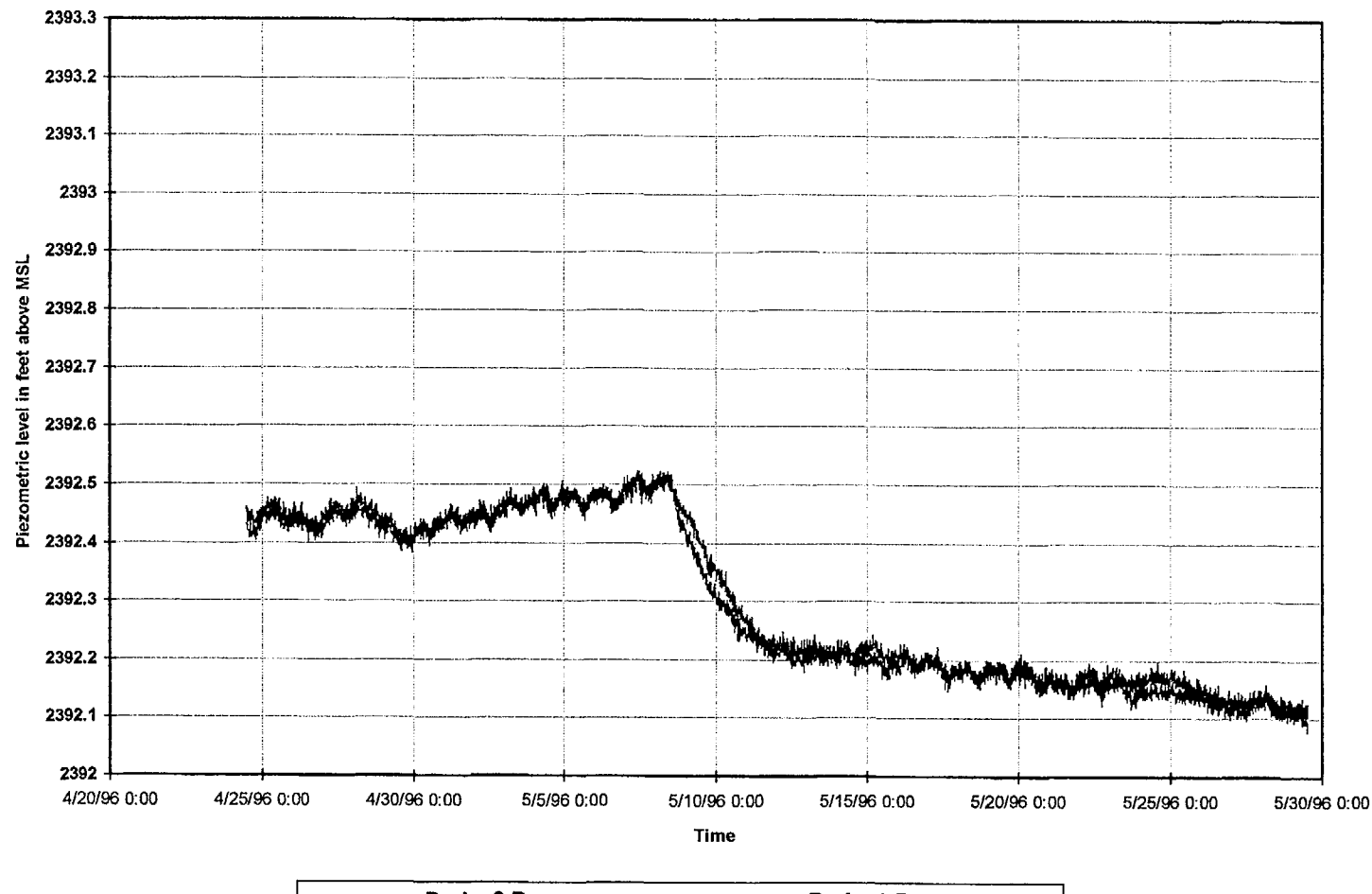


Figure 4-5n Piezometric fluctuation with time in ONC-1

June 1996

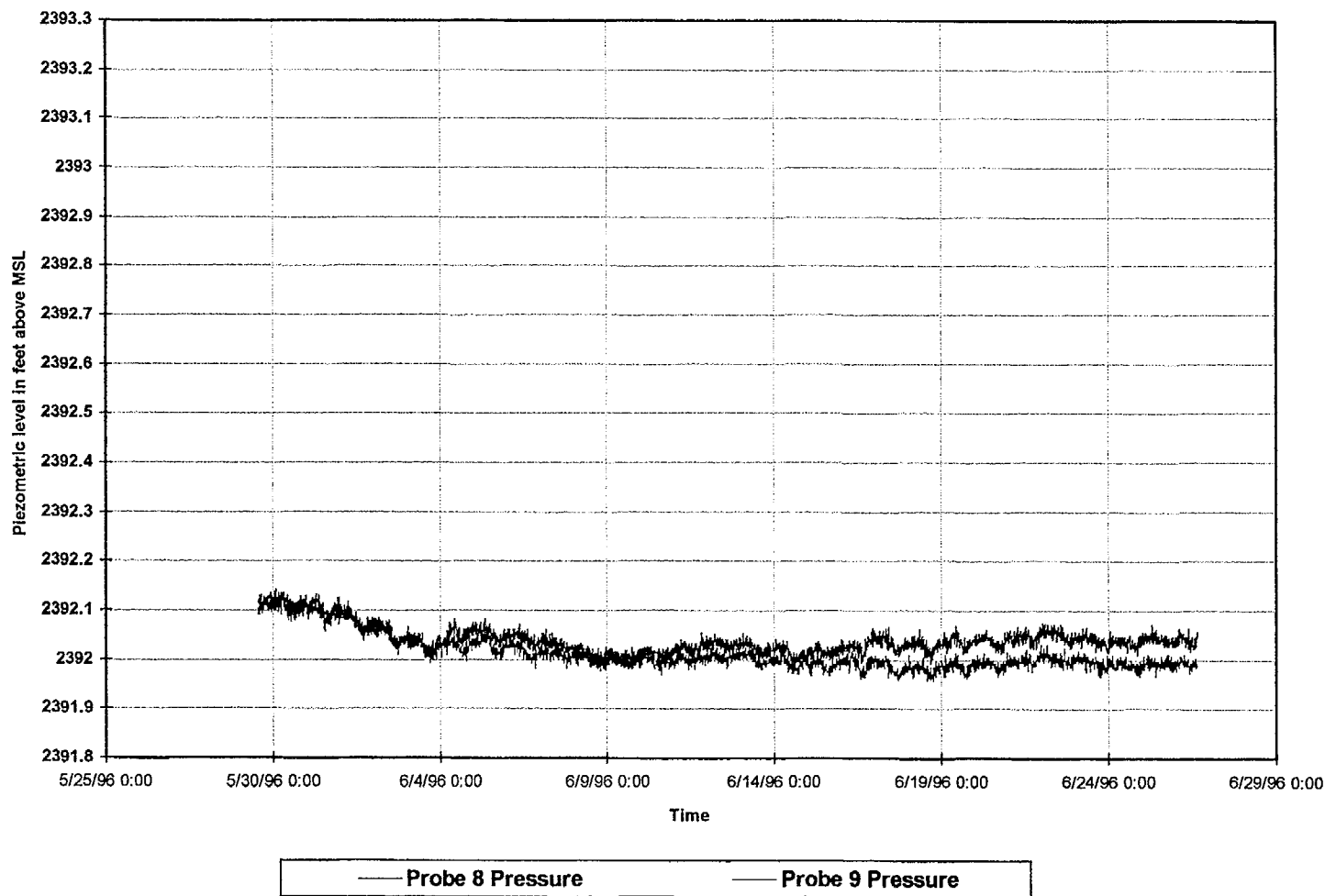


Figure 4-5o Piezometric fluctuation with time in ONC-1

July 1996

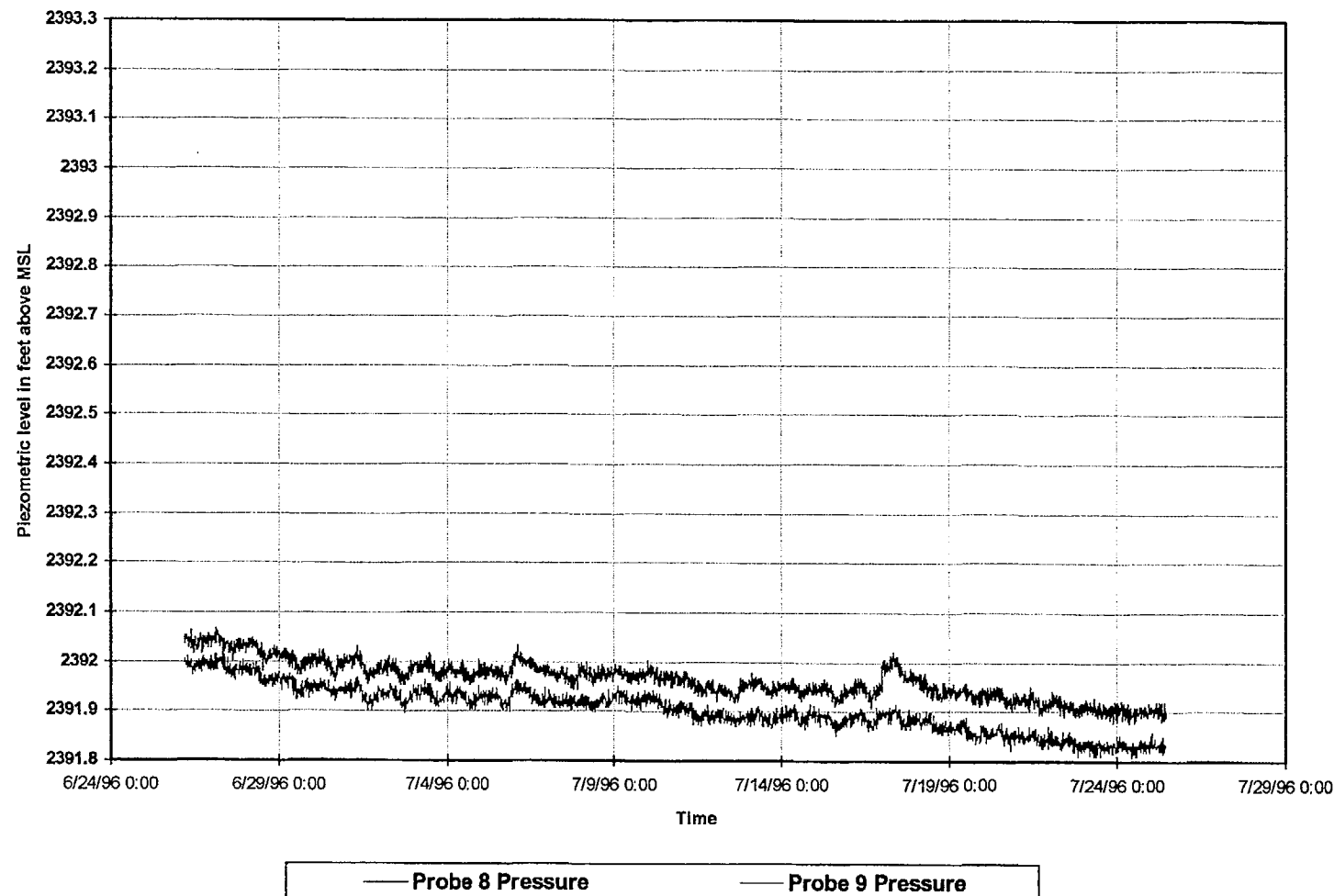


Figure 4-5p Piezometric fluctuation with time in ONC-1

August 1996

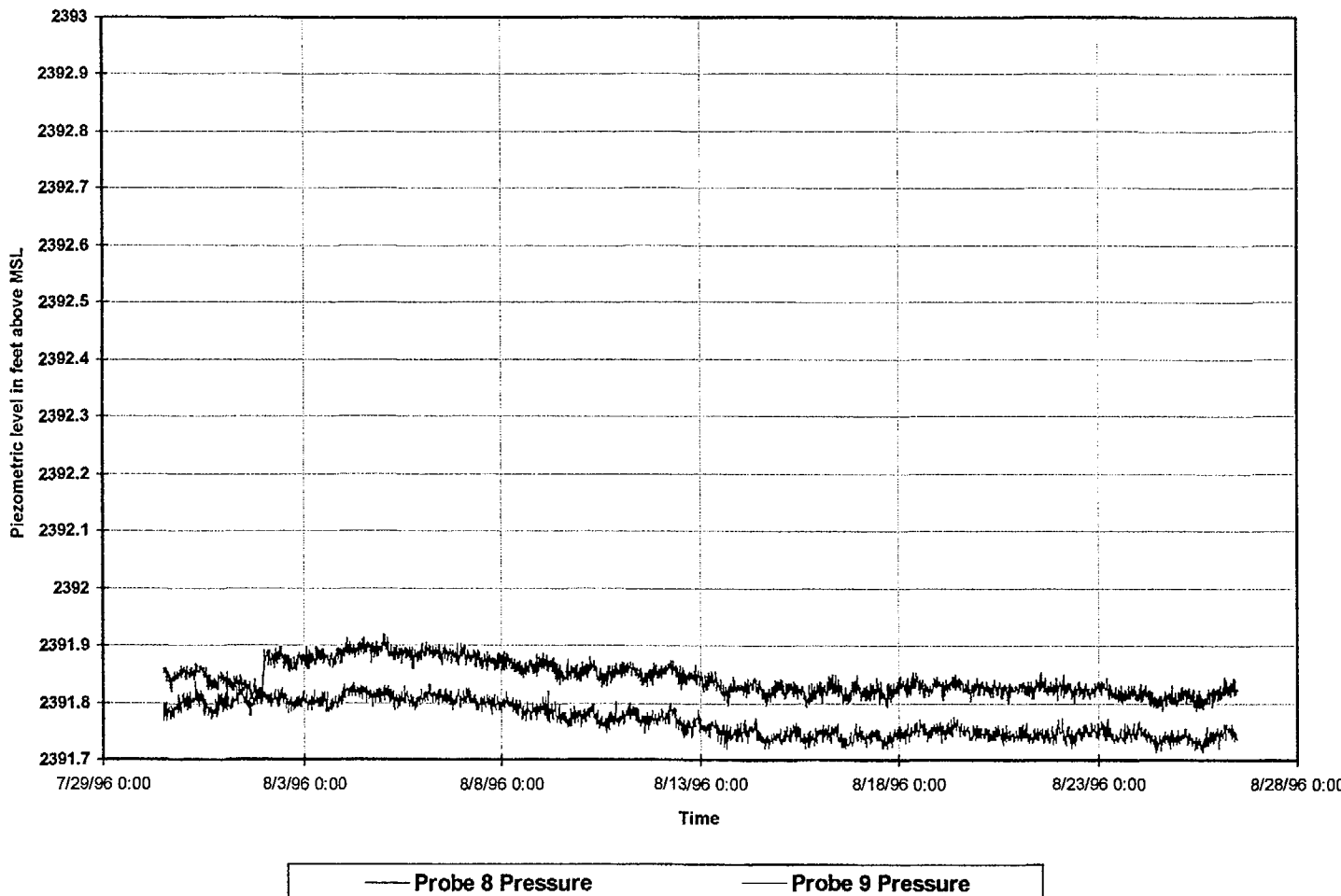
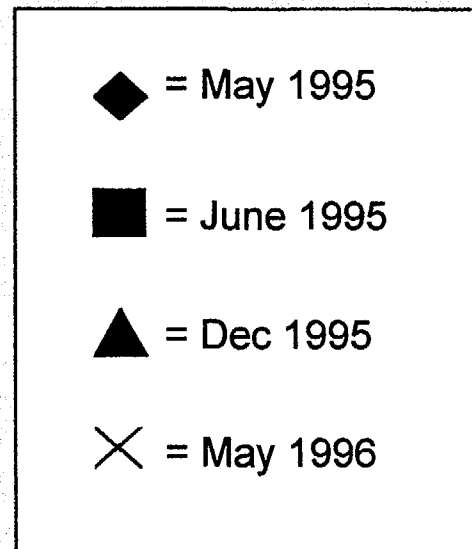


Figure 4-5q Piezometric fluctuation with time in ONC-1

Symbol Convention for Figures 4-6 and 4-7



Comparison of average pressure data versus depth for various unsaturated zone boreholes

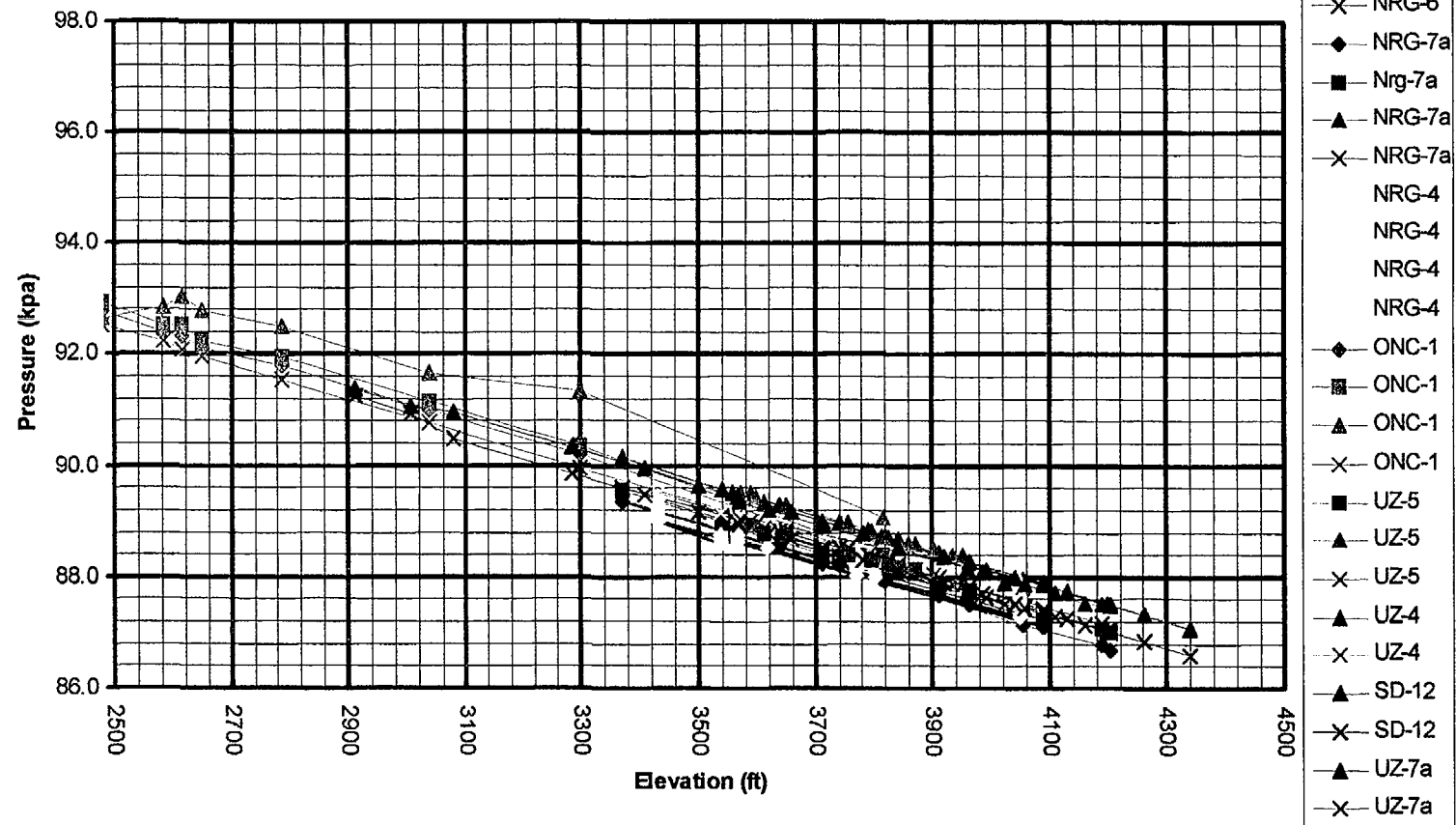


Figure 4-6a

Comparison of minimum pressure data versus depth for various unsaturated zone boreholes

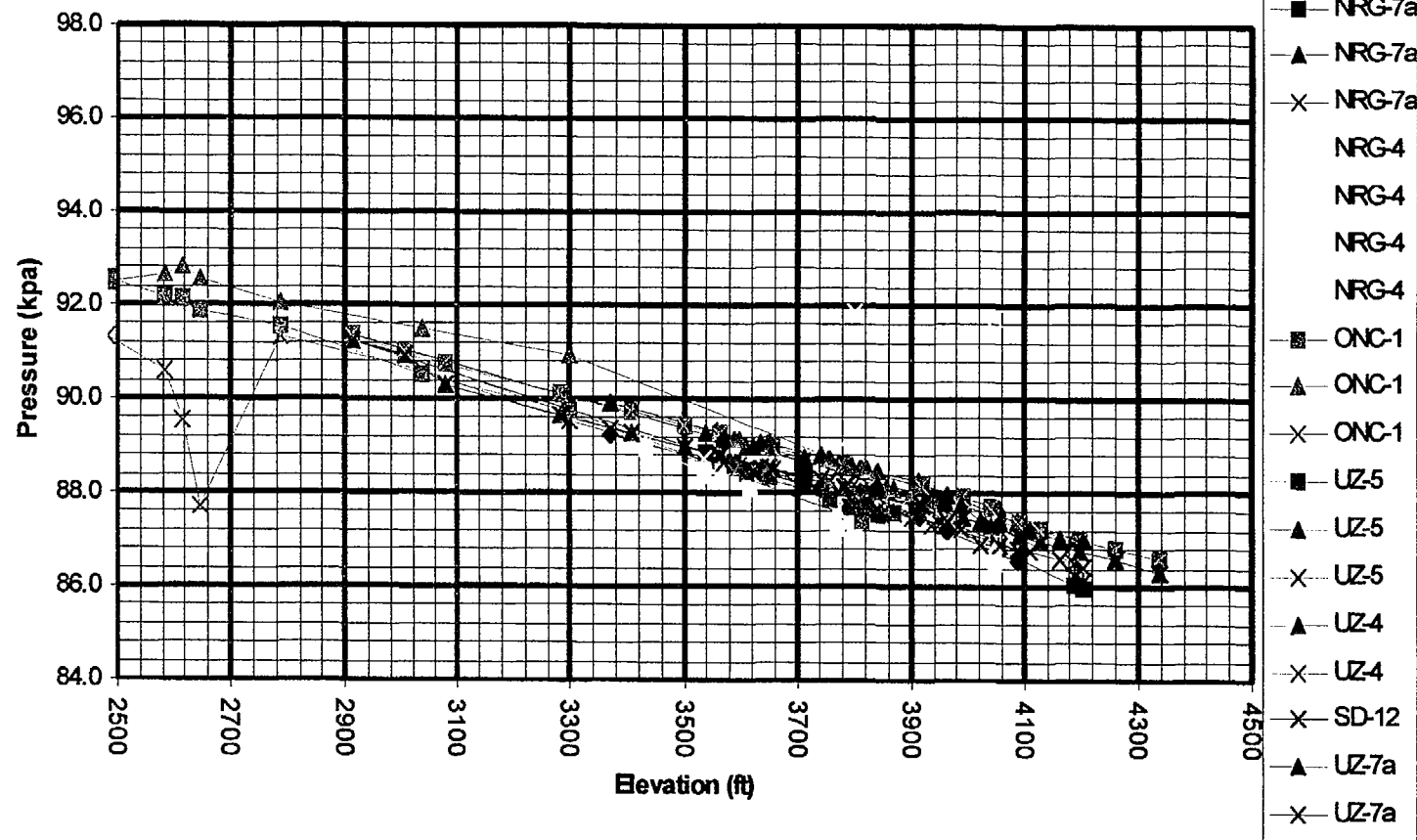


Figure 4-6b

August 24, 1996
P26609:41 AMD:\user\projects\Nye County\unrcp96\figures

Prepared for:
Nye County Nuclear Waste Repository Project Office

Prepared by:
Multimedia Environmental Technology, Inc.
Newport Beach, CA

Comparison of maximum pressure data versus depth for various unsaturated zone boreholes

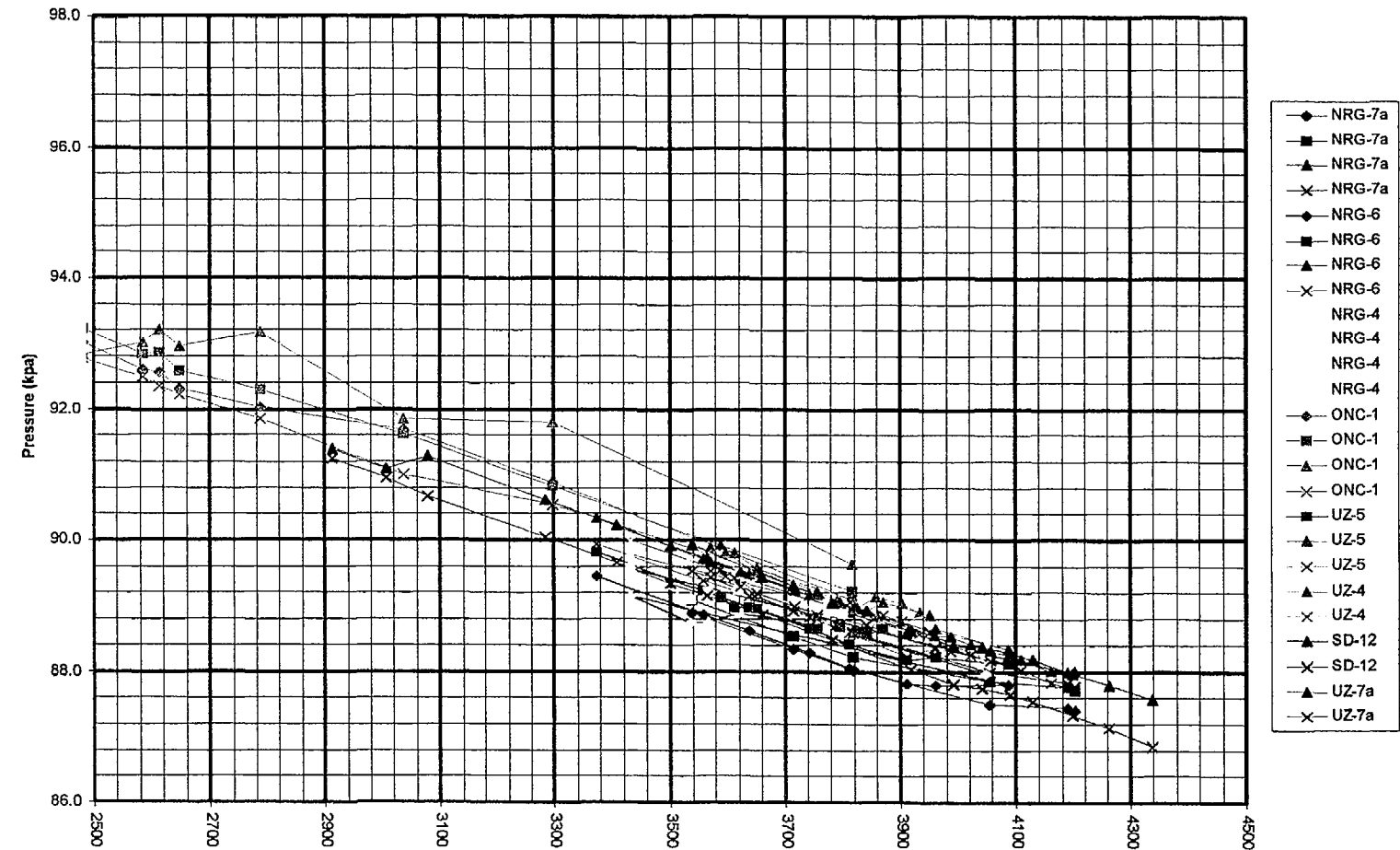


Figure 4-6c

August 24, 1996
P26609:41 AMD:\user\projects\NyeCounty\amrep96\figures

Prepared for:
Nye County Nuclear Waste Repository Project Office

Prepared by:
Multimedien Environmental Technology, Inc.
Newport Beach, CA

Comparison of average temperature data versus depth for various unsaturated zone boreholes

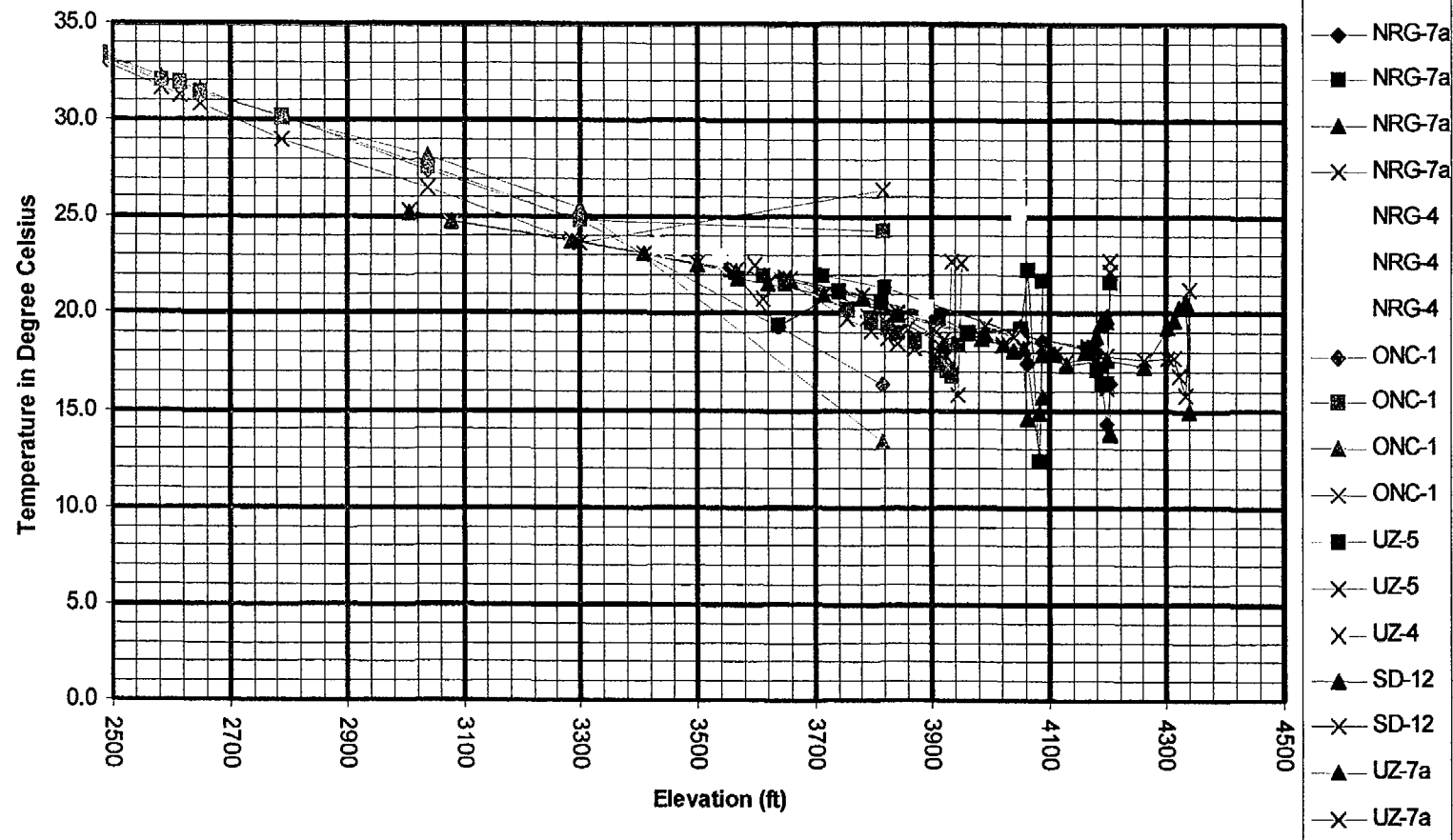


Figure 4-7a

Comparison of minimum temperature data versus depth for various unsaturated zone boreholes

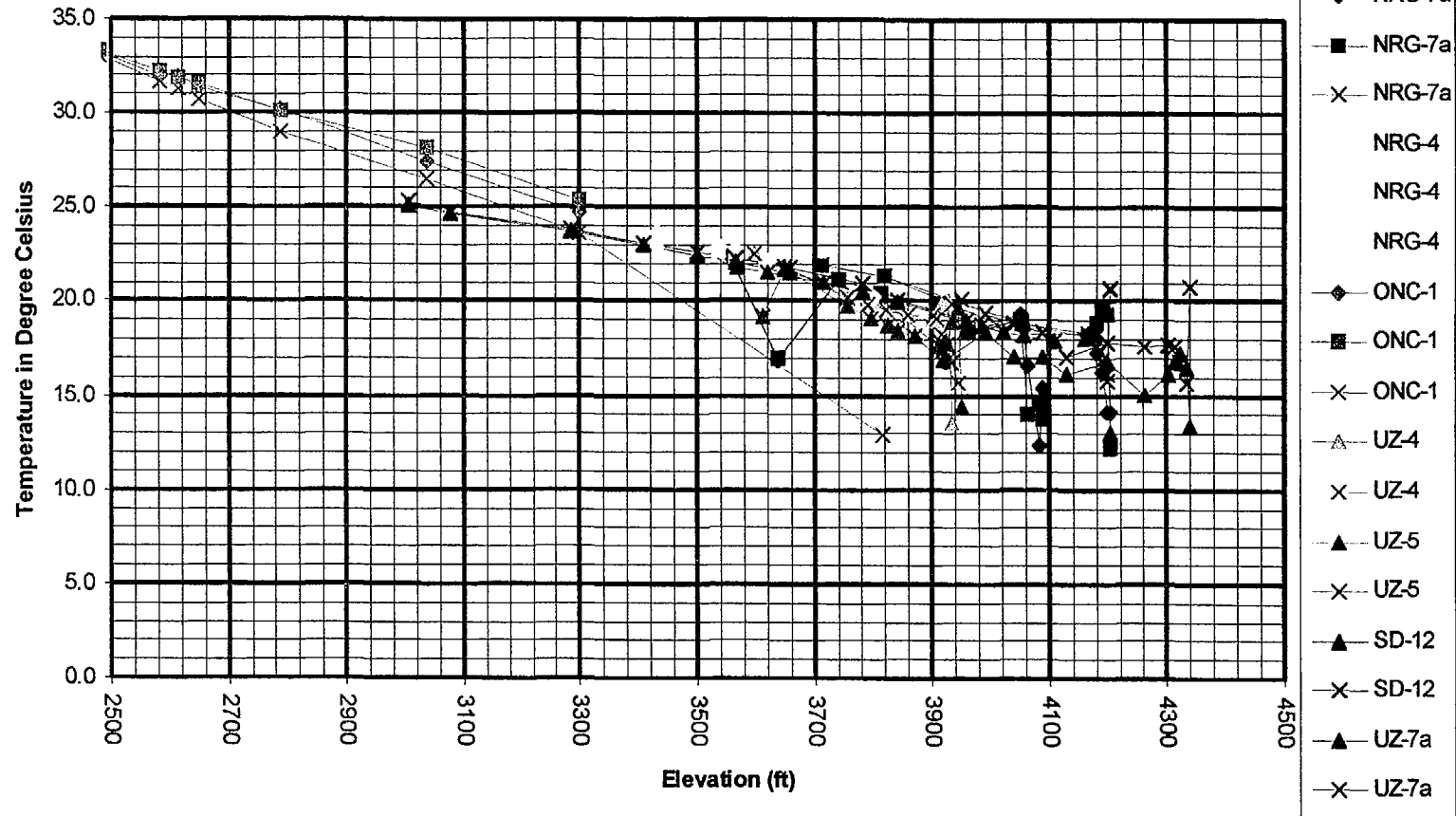


Figure 4-7b

Comparison of maximum temperature data versus depth for various unsaturated zone boreholes

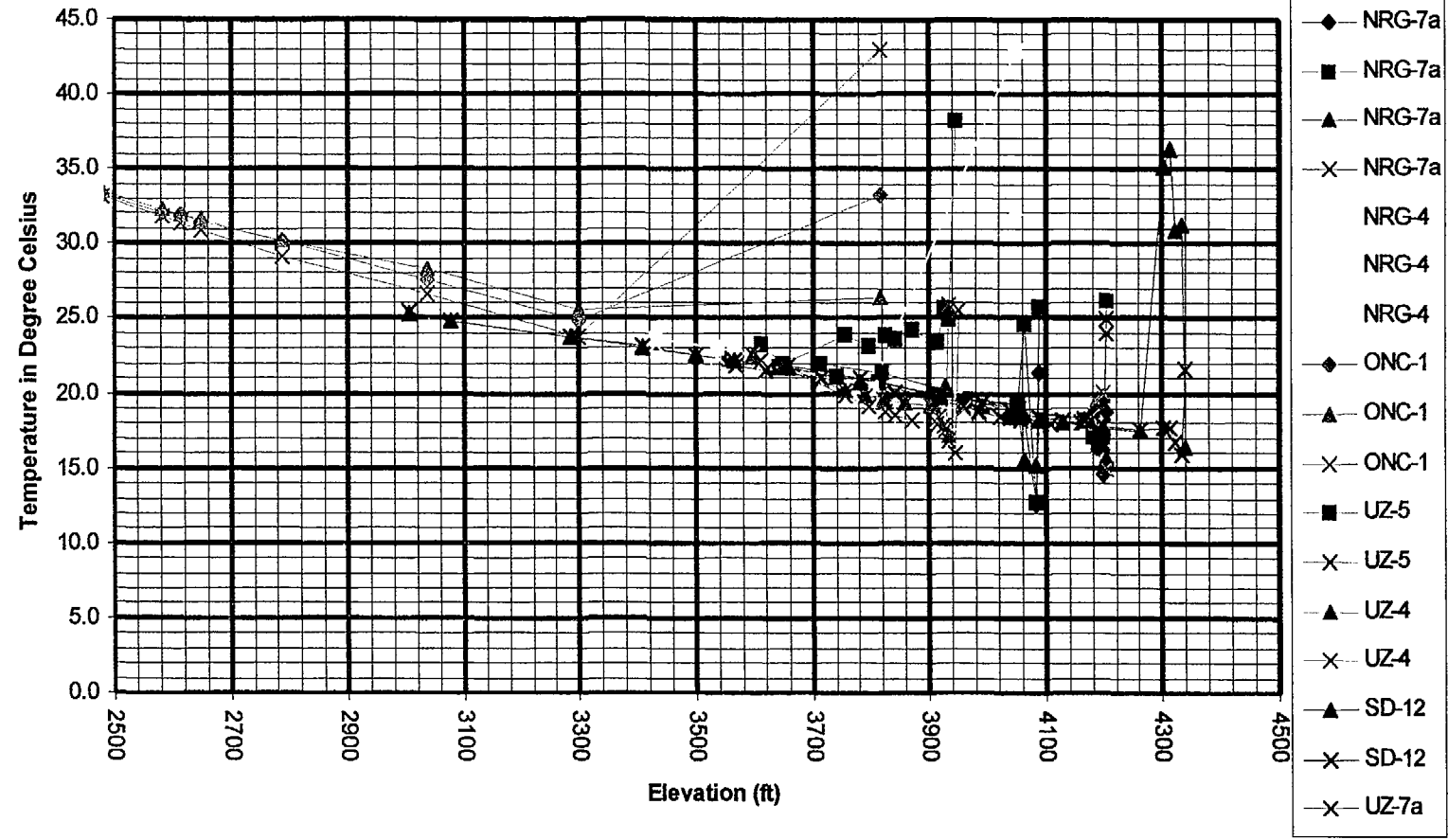
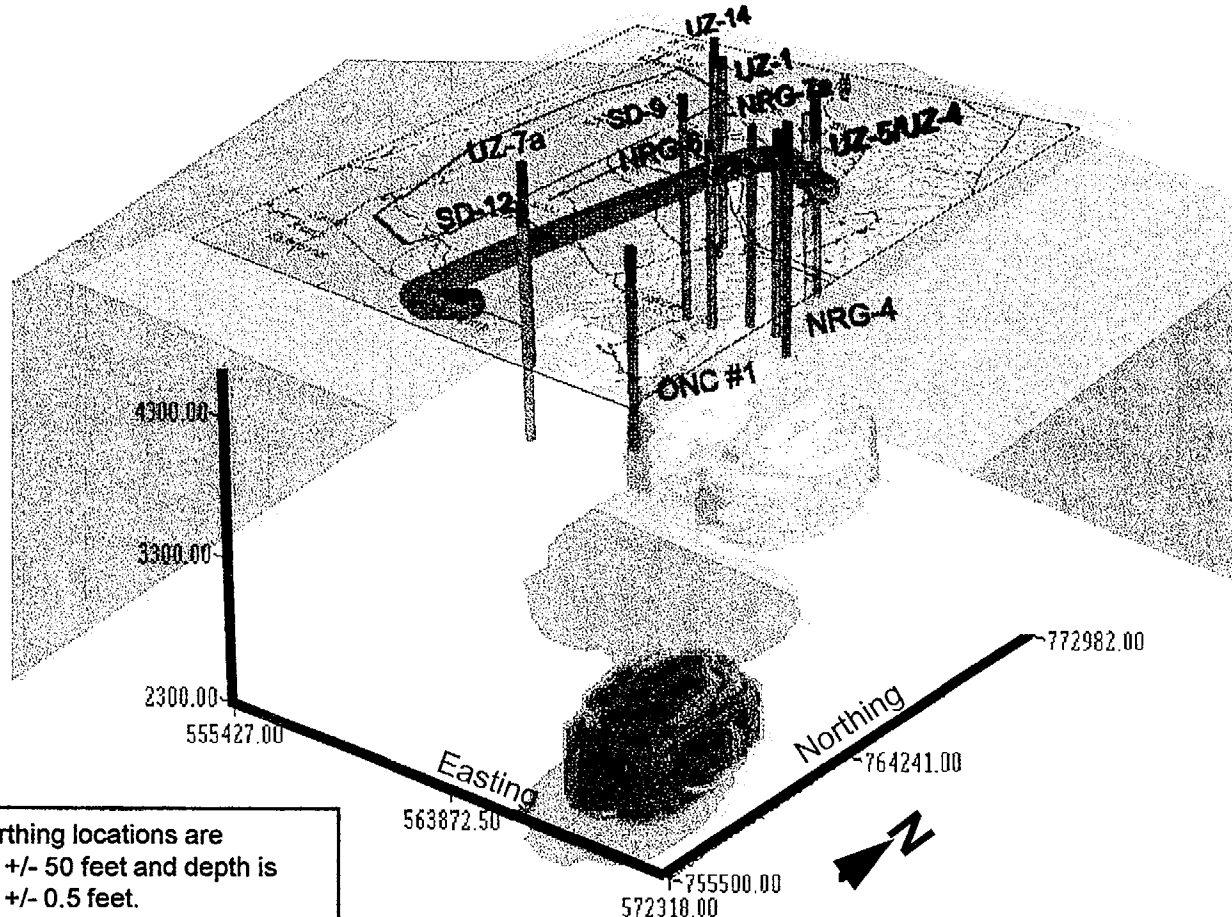
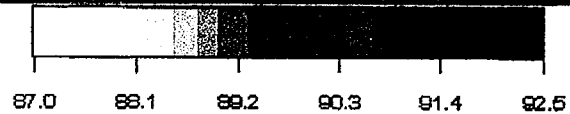
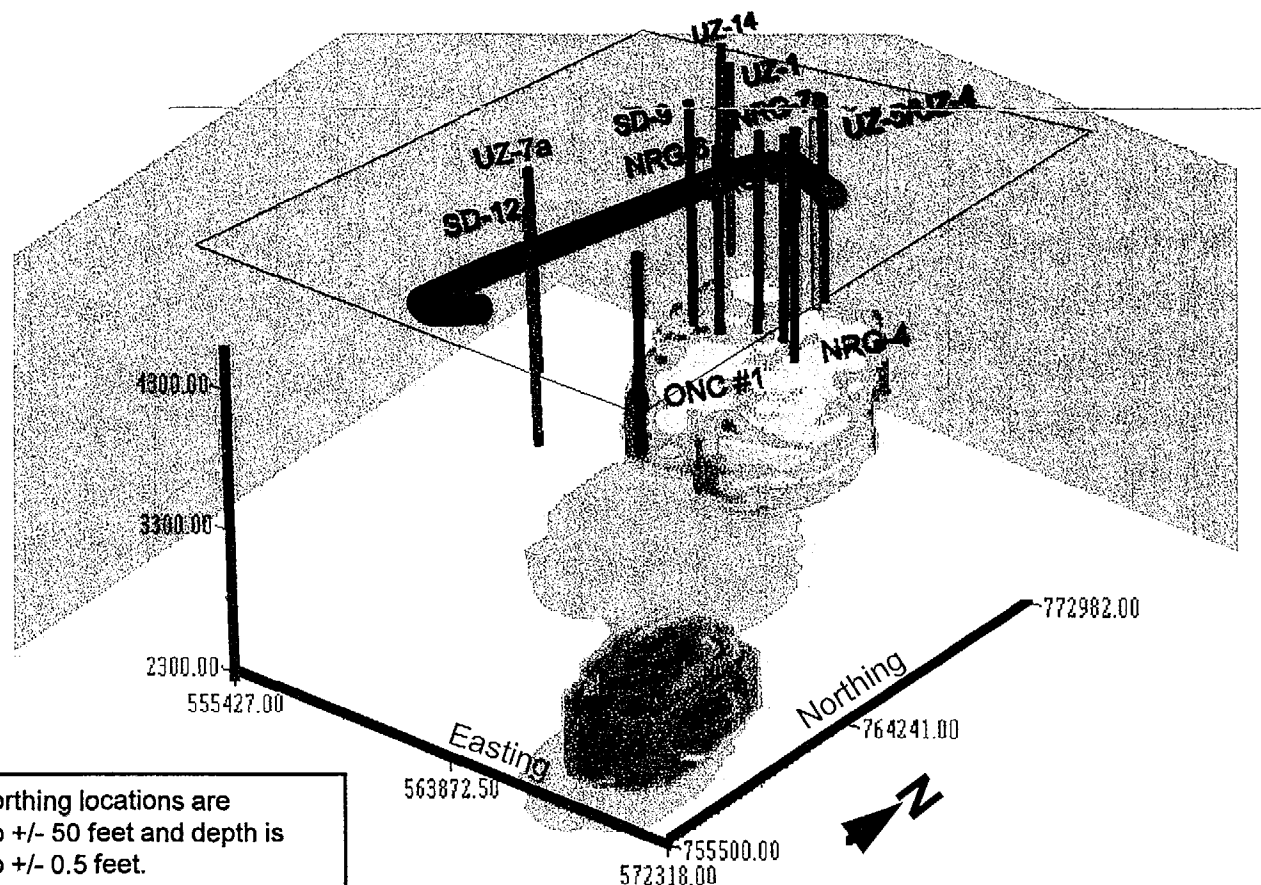


Figure 4-7c



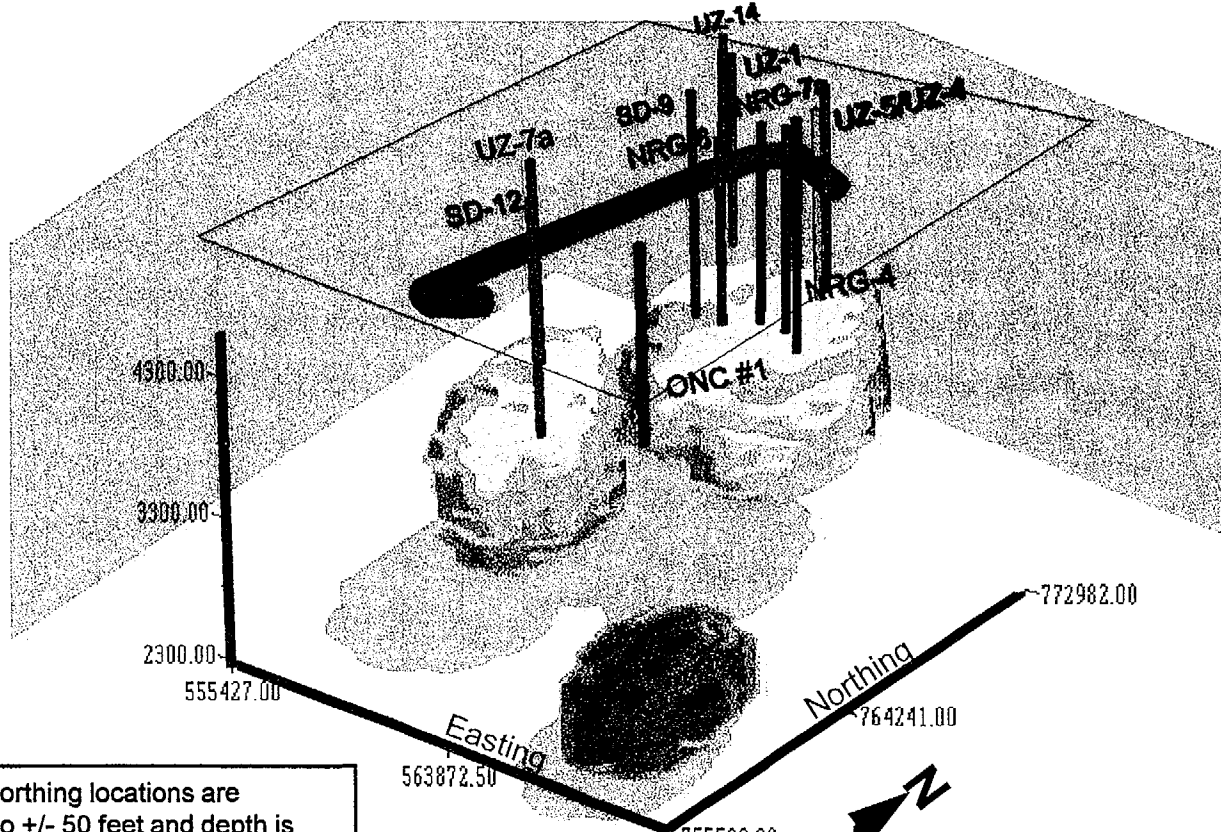
Average pressure distribution in kPa (May 1995)





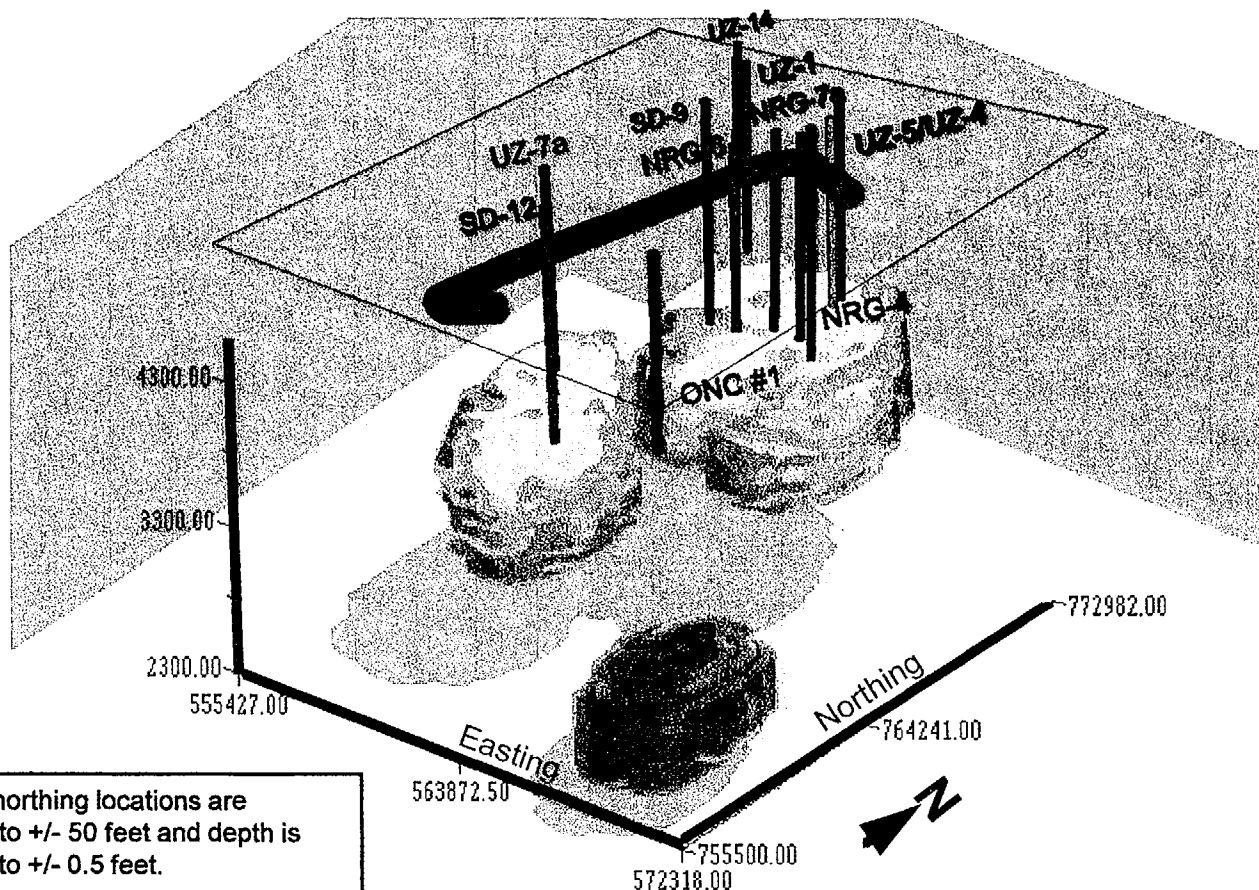
Average pressure distribution in kPa (June 1995)



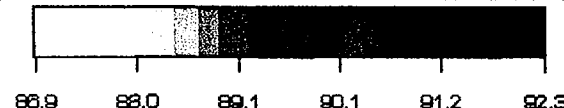


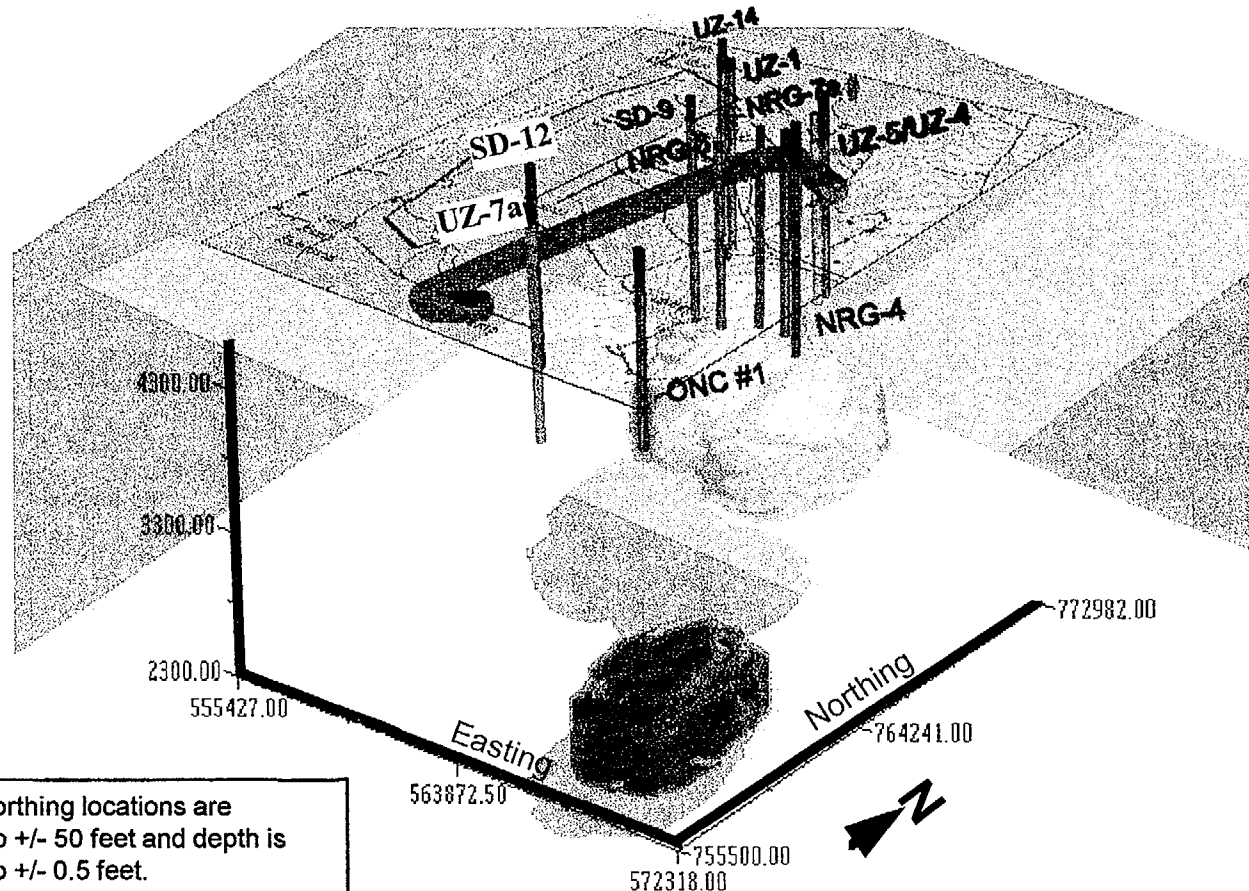
Average pressure distribution in kPa (Dec 1995)



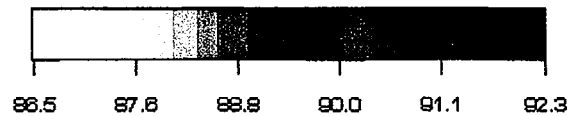


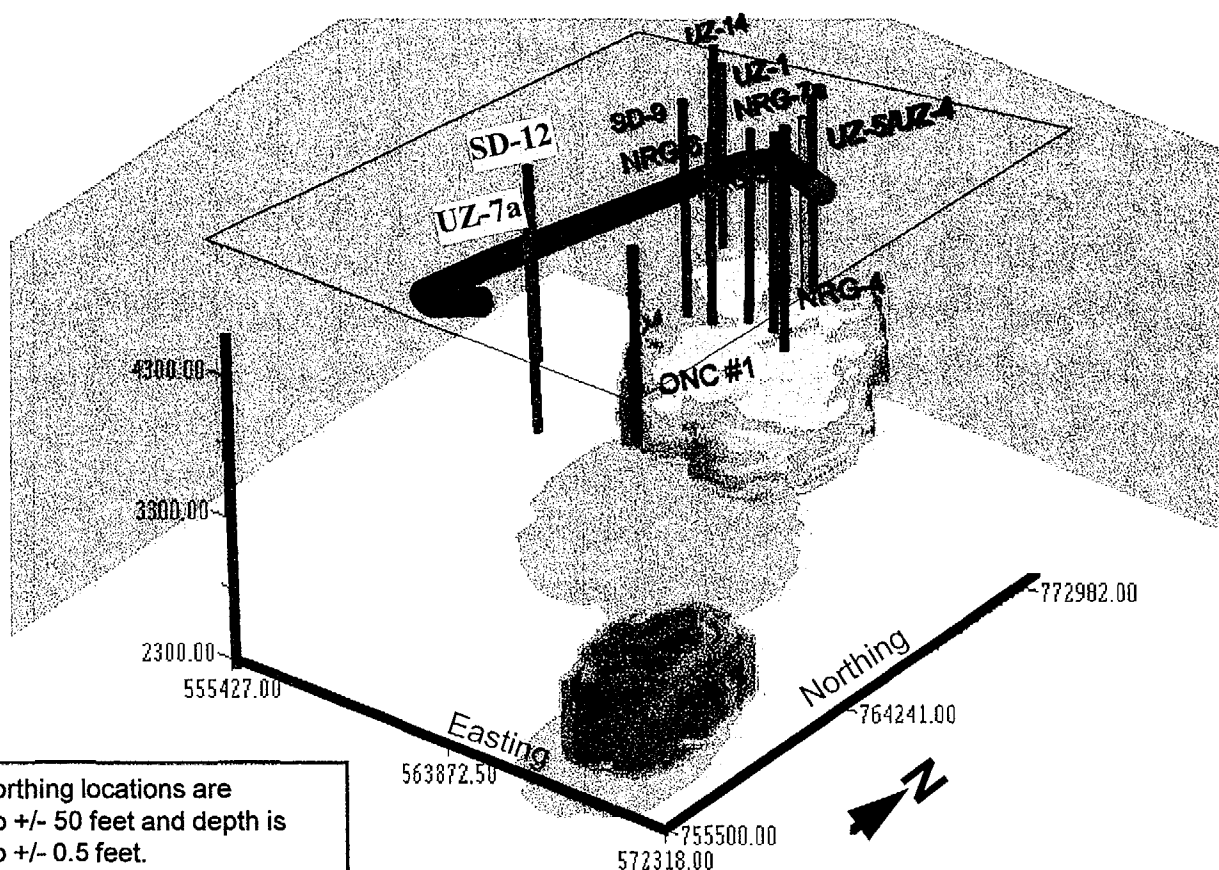
Average pressure distribution in kPa (May 1996)





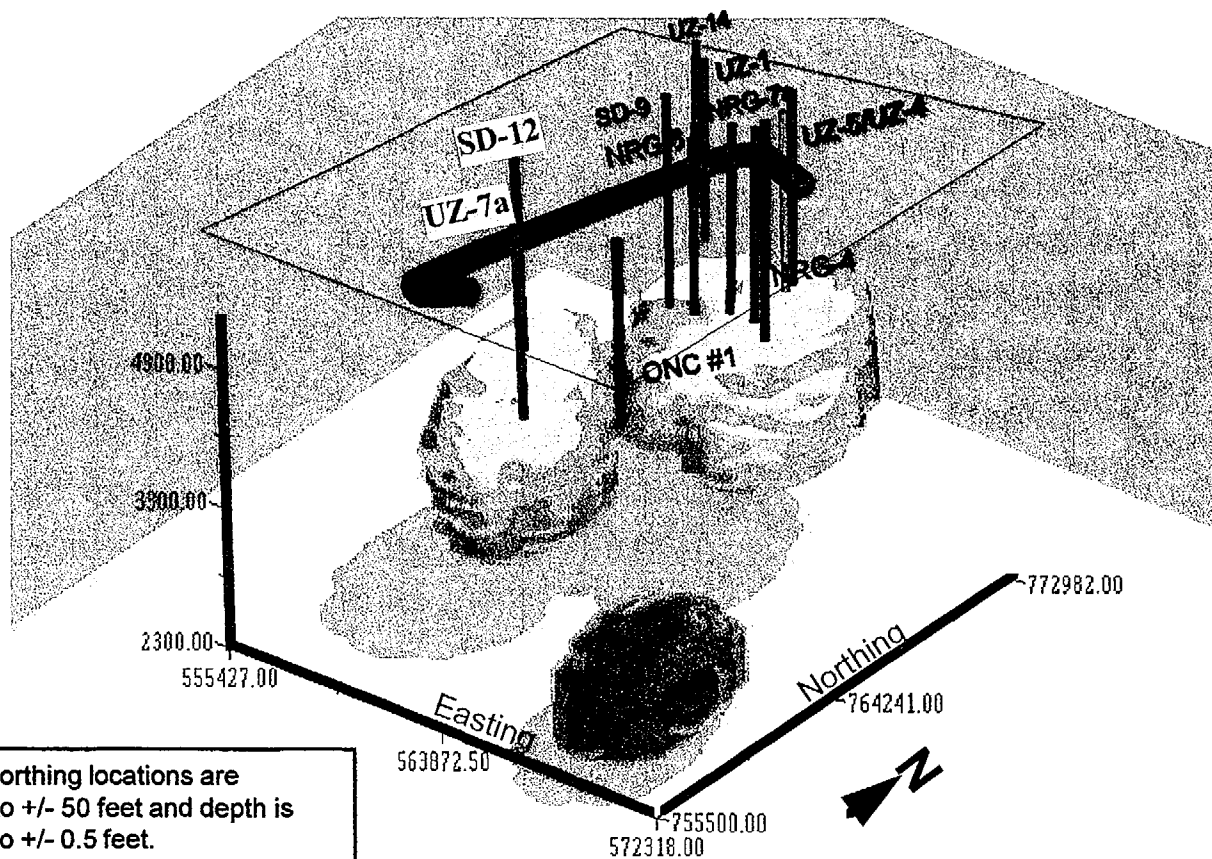
Minimum pressure distribution in kPa (May 1995)



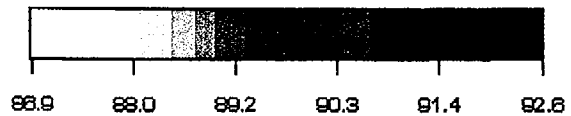


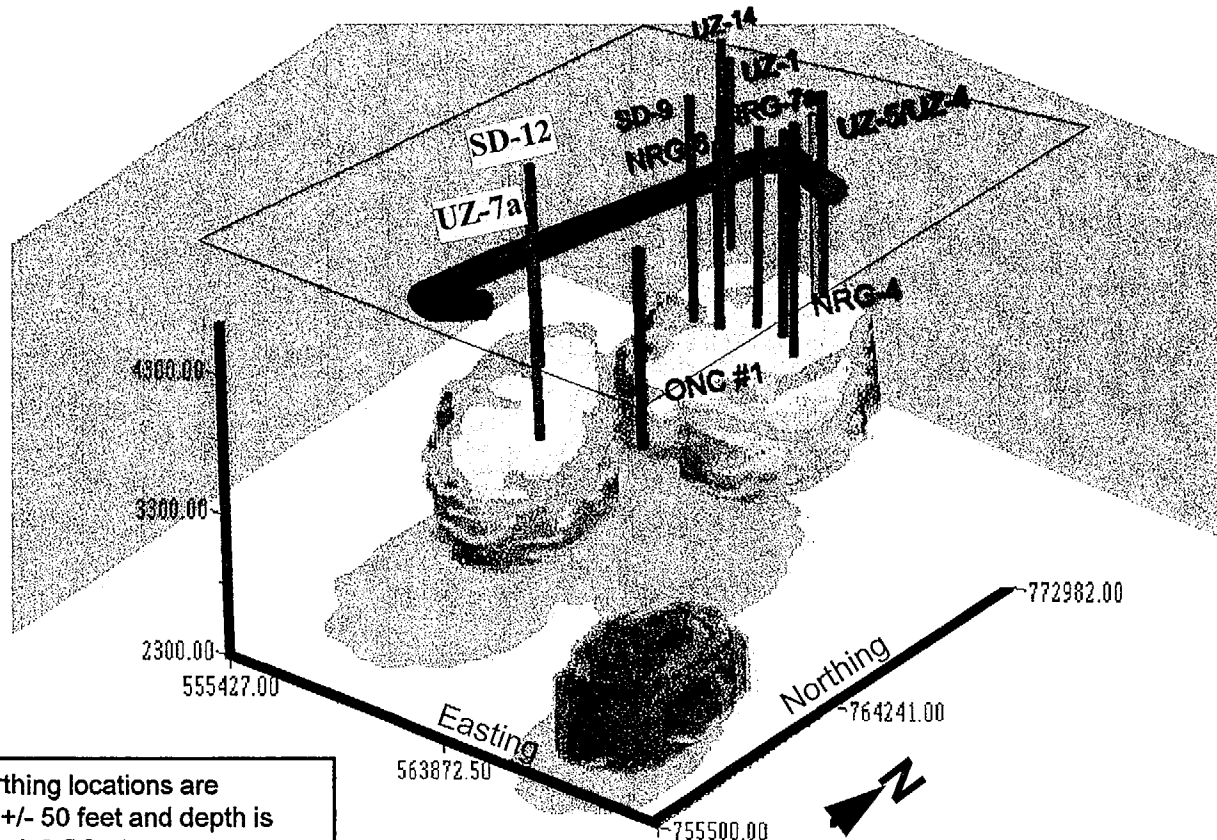
Minimum pressure distribution in kPa (June 1995)





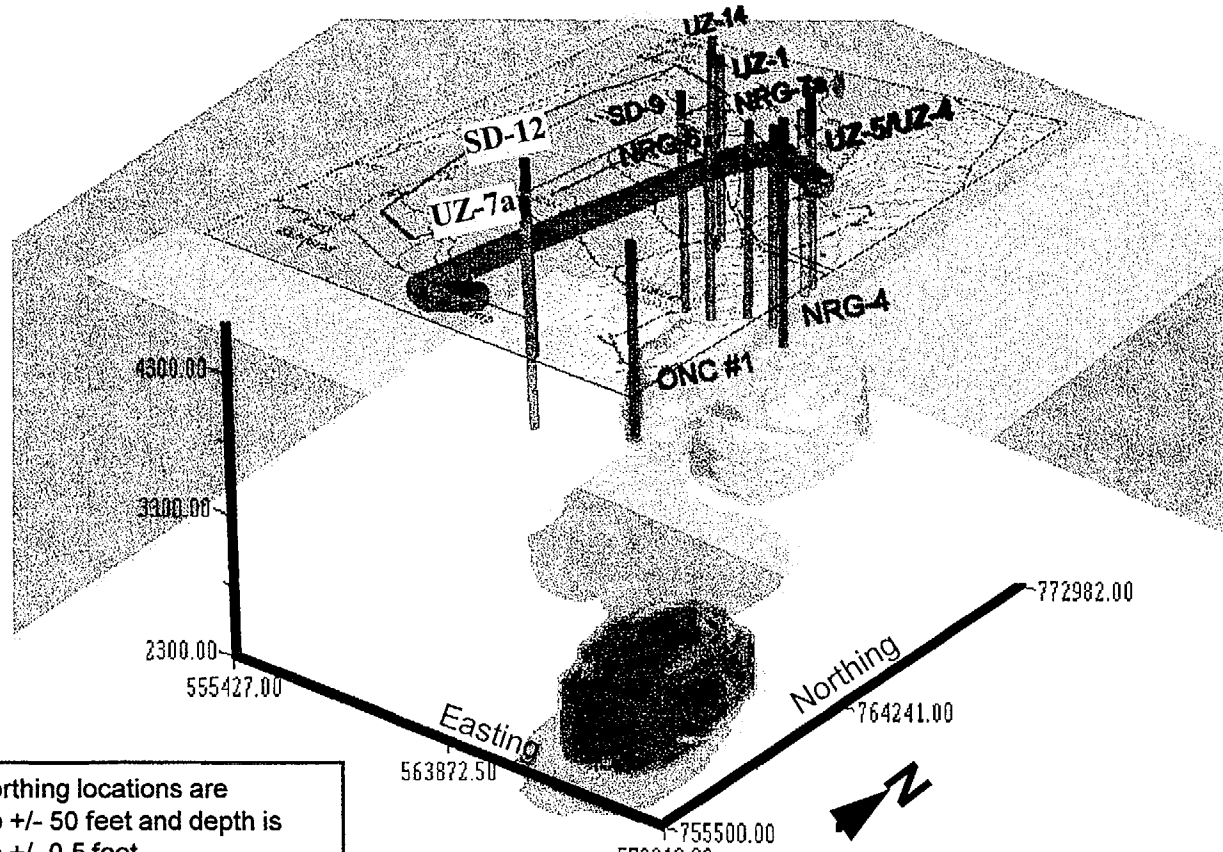
Minimum pressure distribution in kPa (Dec 1995)





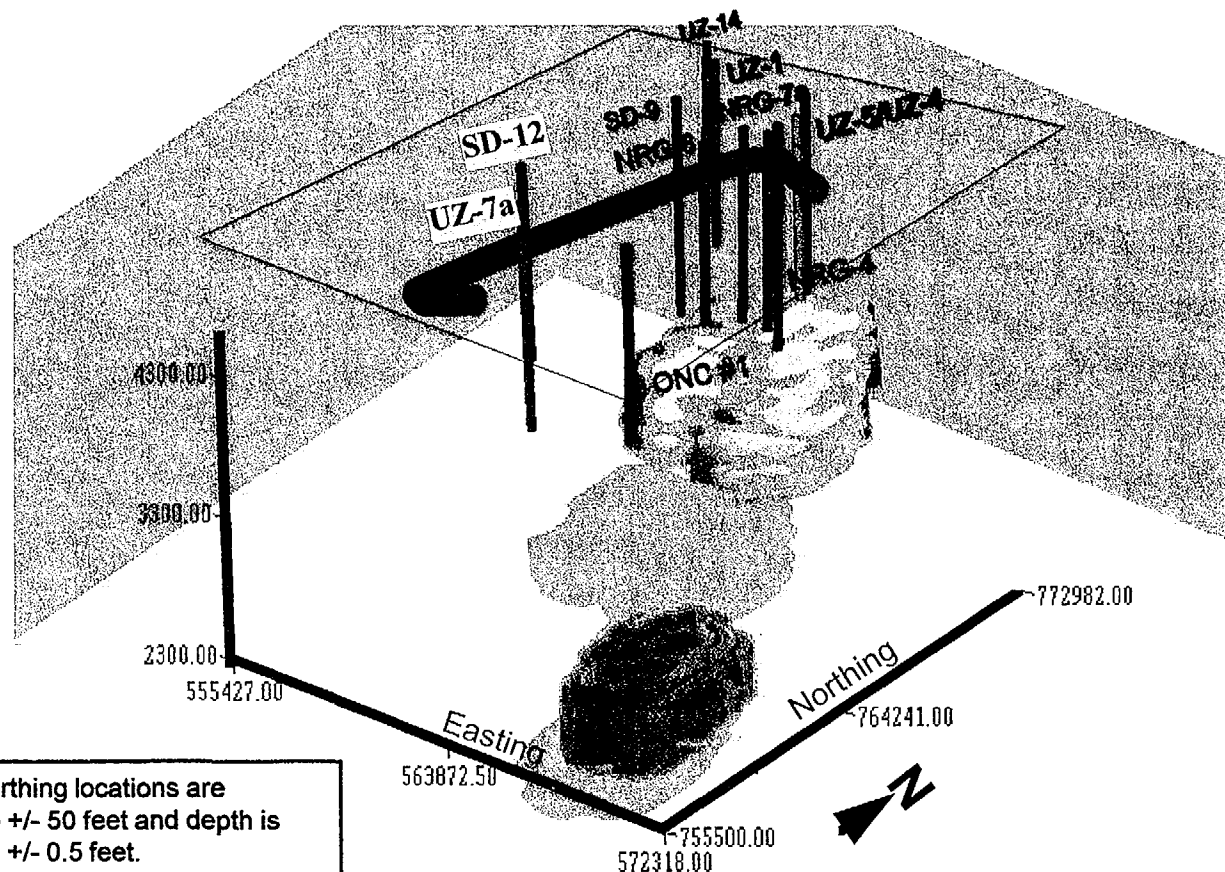
Minimum pressure distribution in kPa (May 1996)





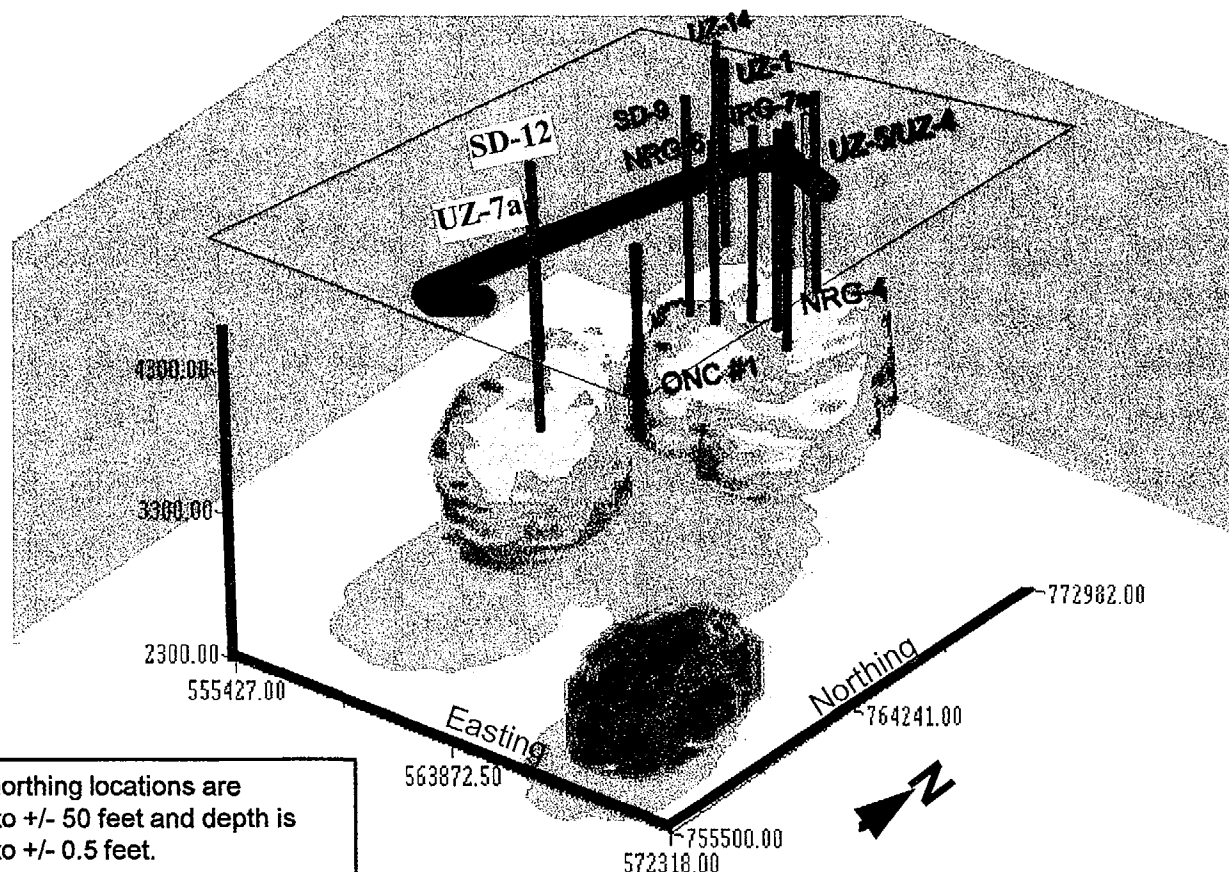
Maximum pressure distribution in kPa (May 1995)





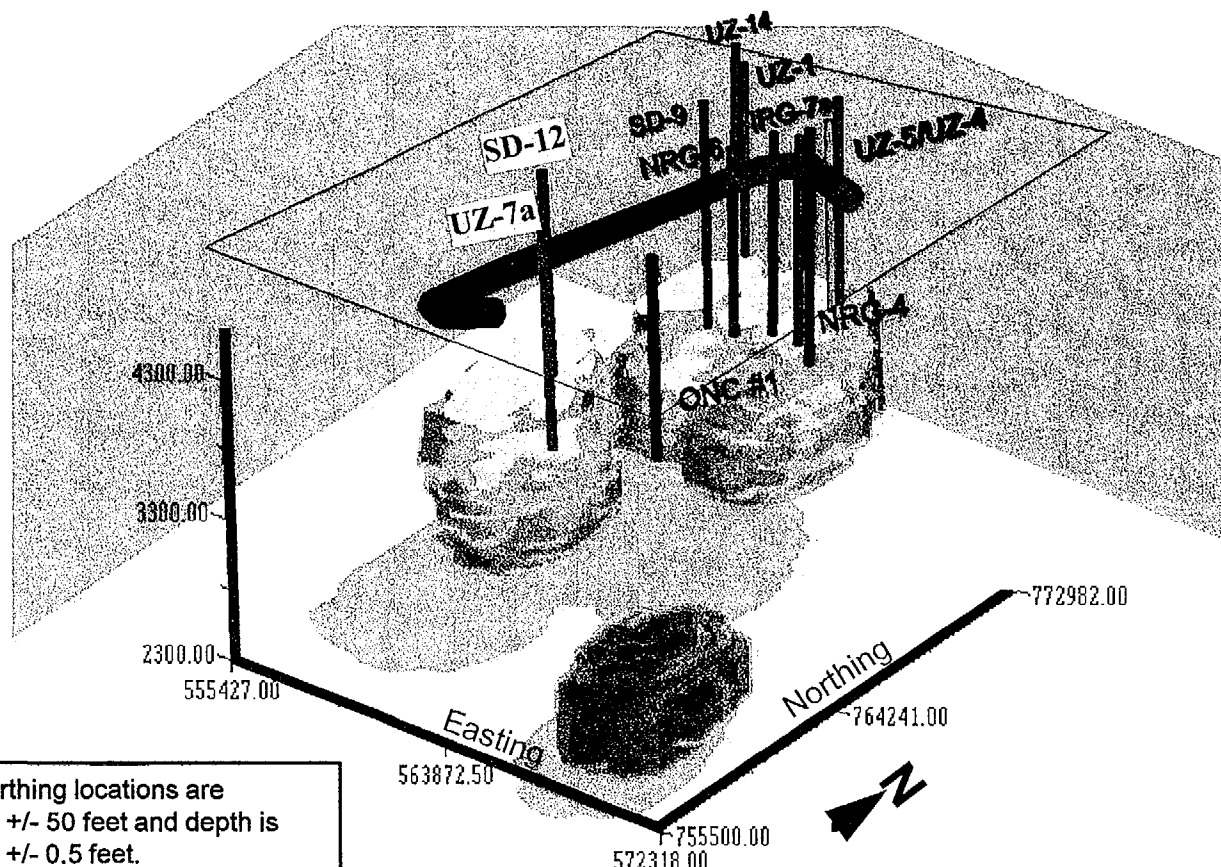
Maximum pressure distribution in kPa (June 1995)



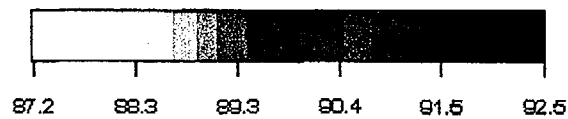


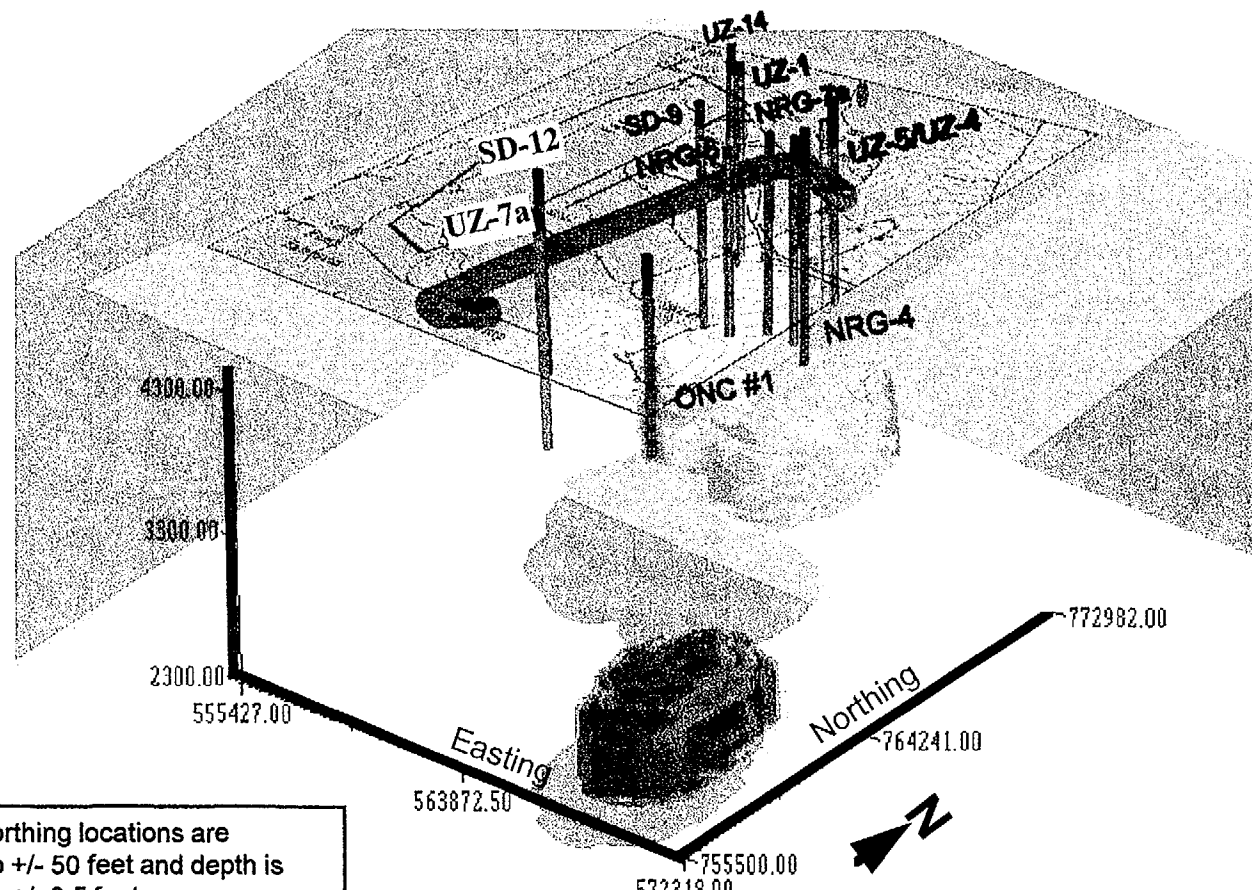
Maximum pressure distribution in kPa (Dec 1995)





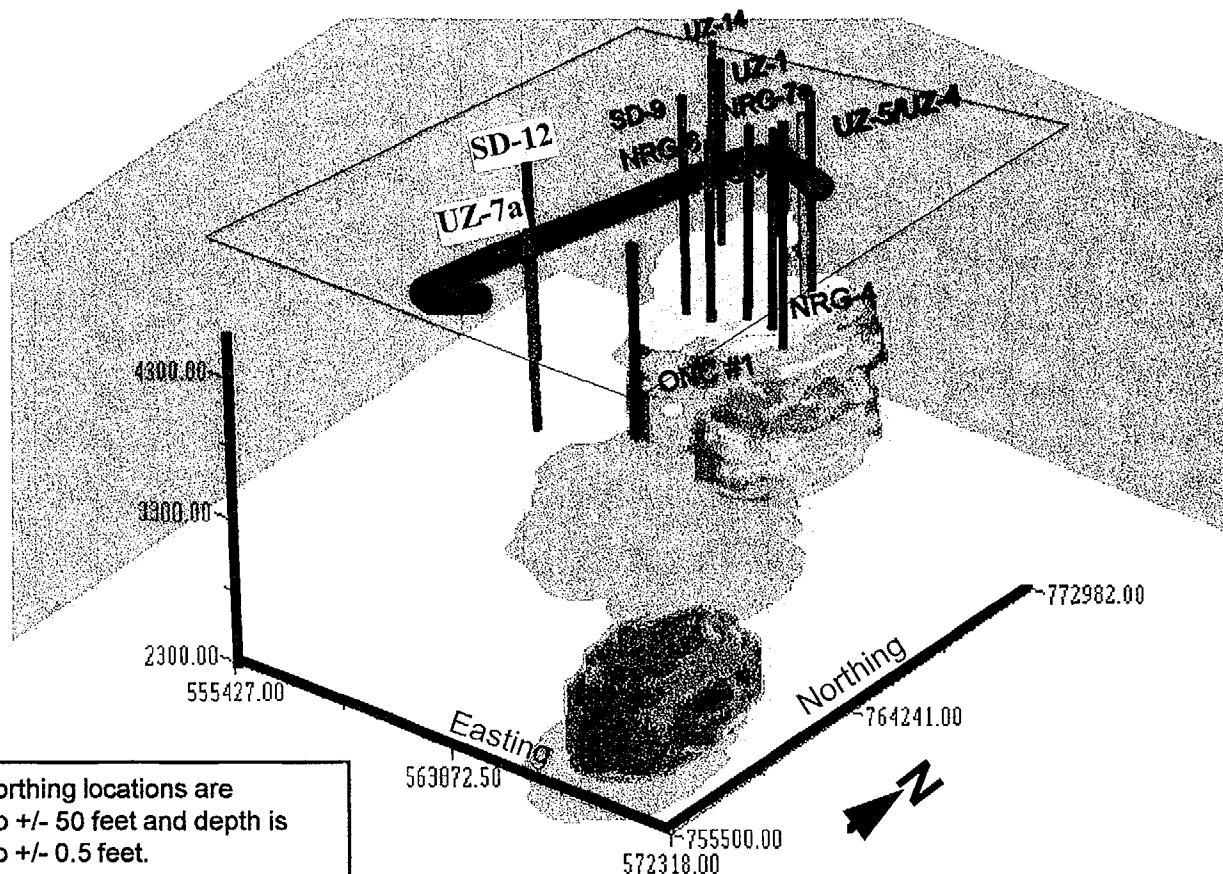
Maximum pressure distribution in kPa (May 1996)



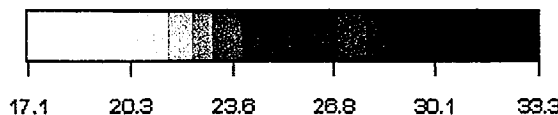


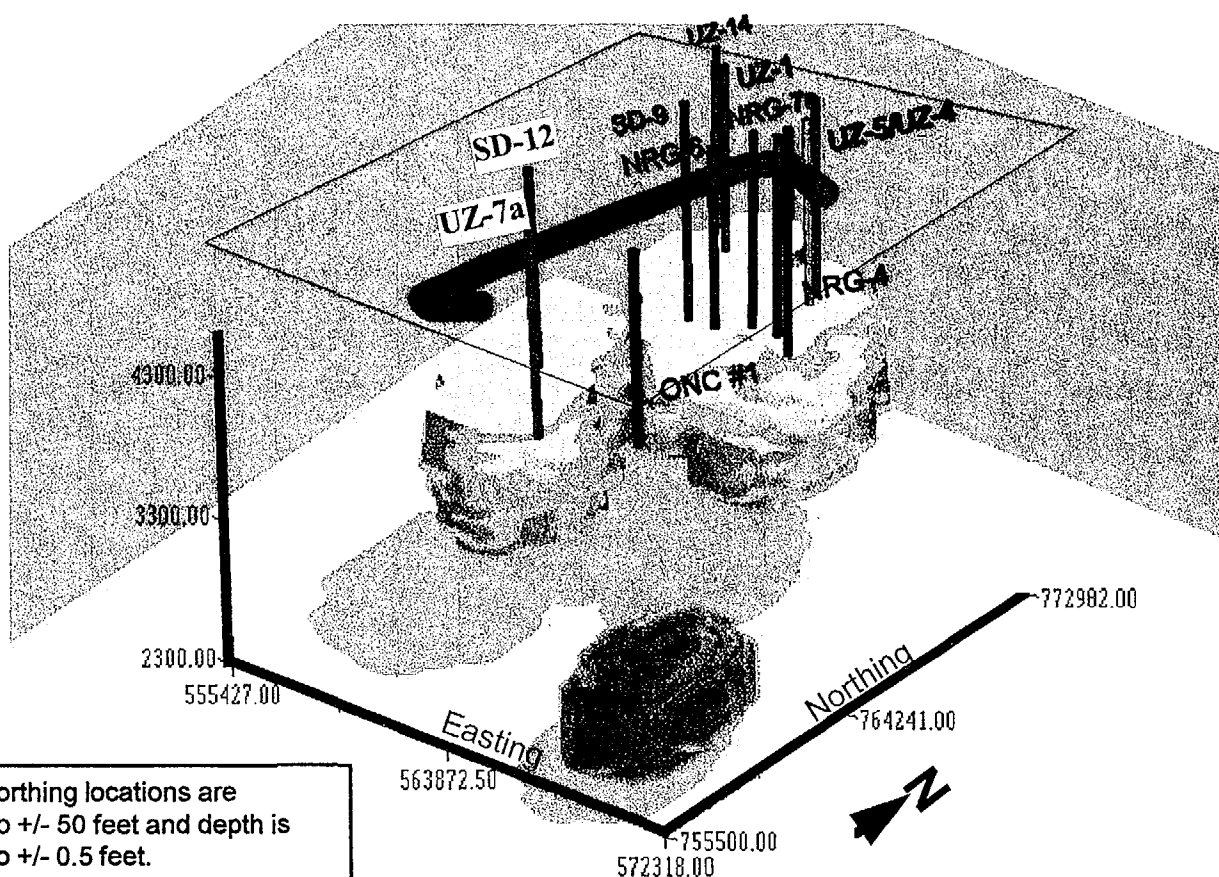
Average temperature distribution in deg. Celsius (May 1995)





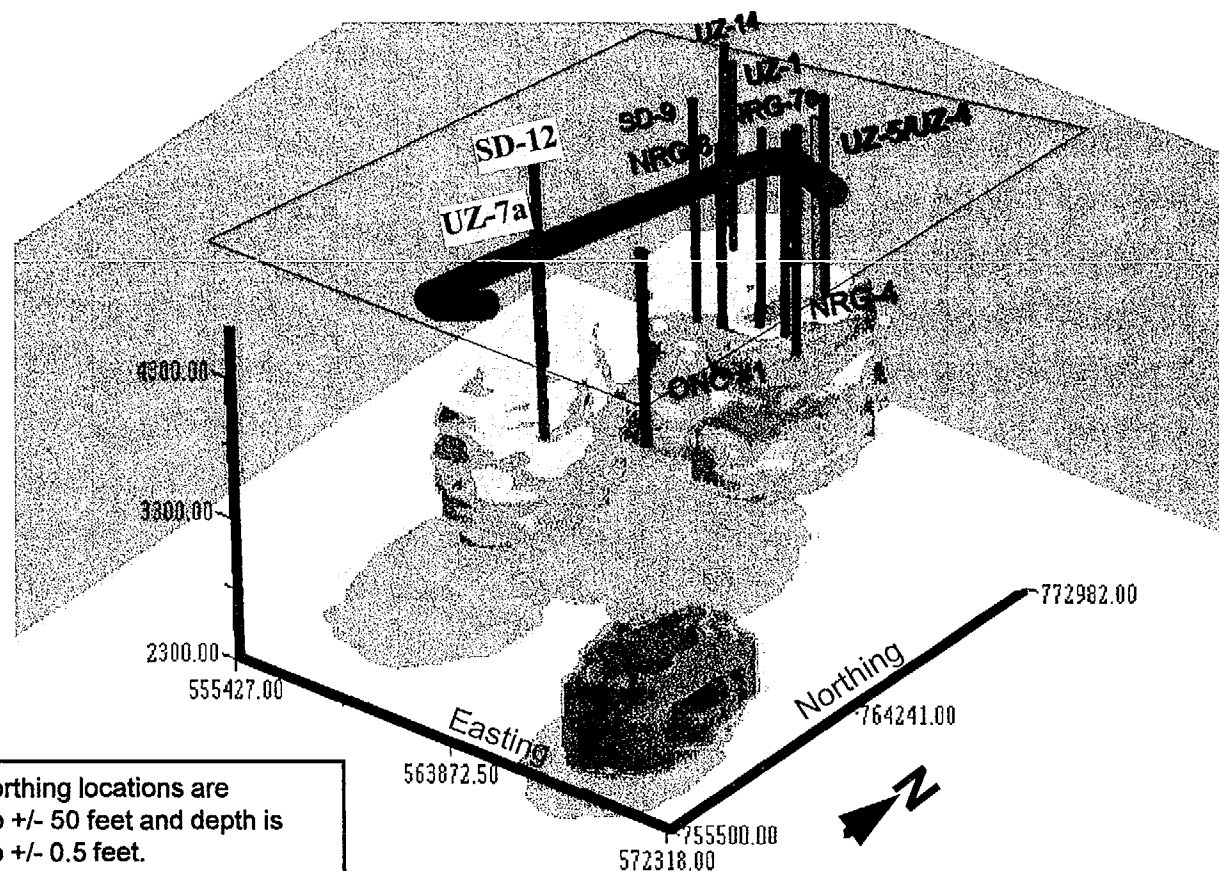
Average temperature distribution in deg. Celsius (June 1995)





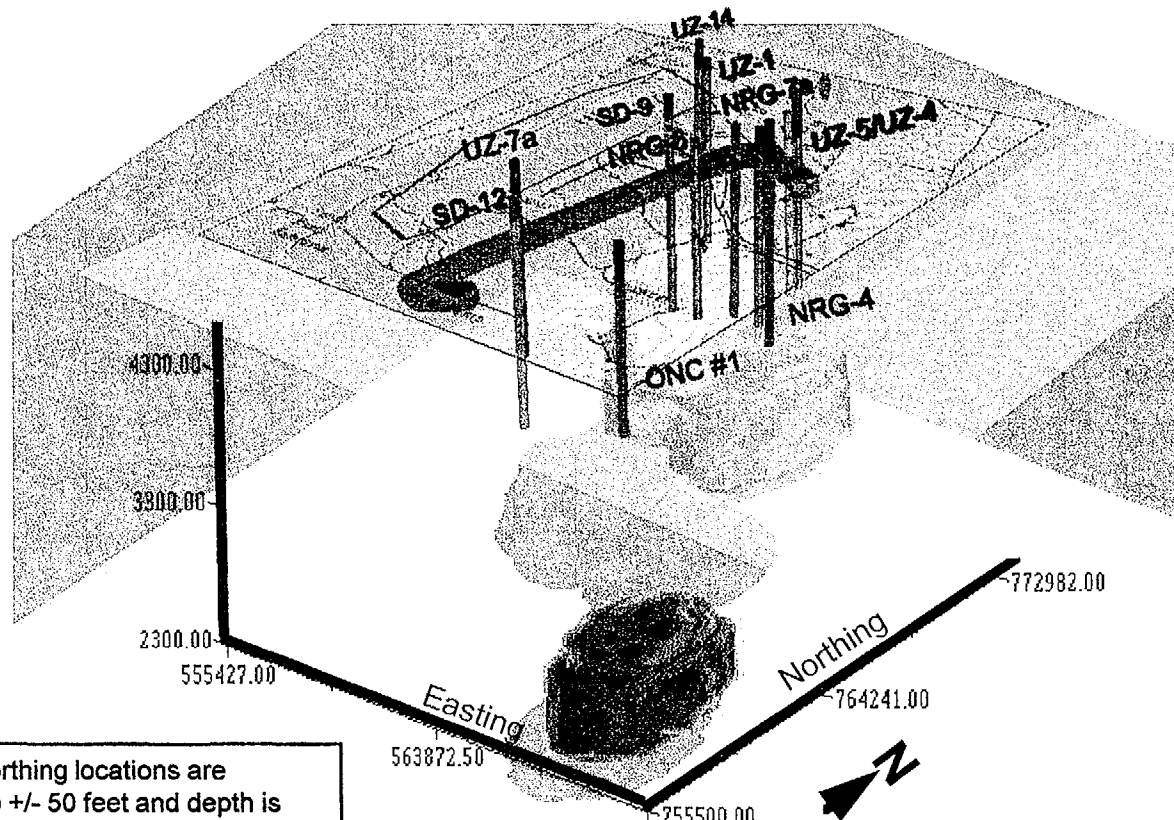
Average temperature distribution in deg. Celsius (Dec 1995)





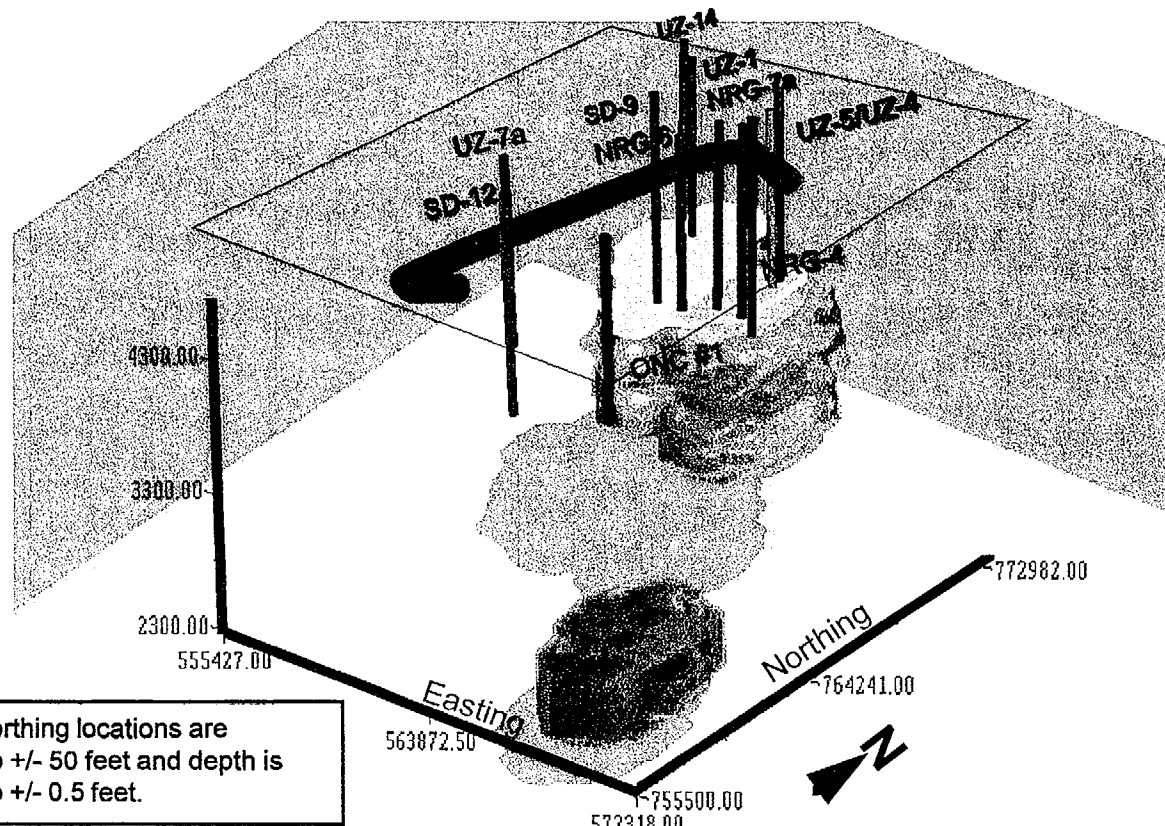
Average temperature distribution in deg. Celsius (May 1996)



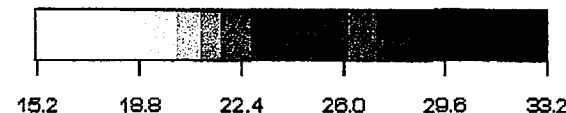


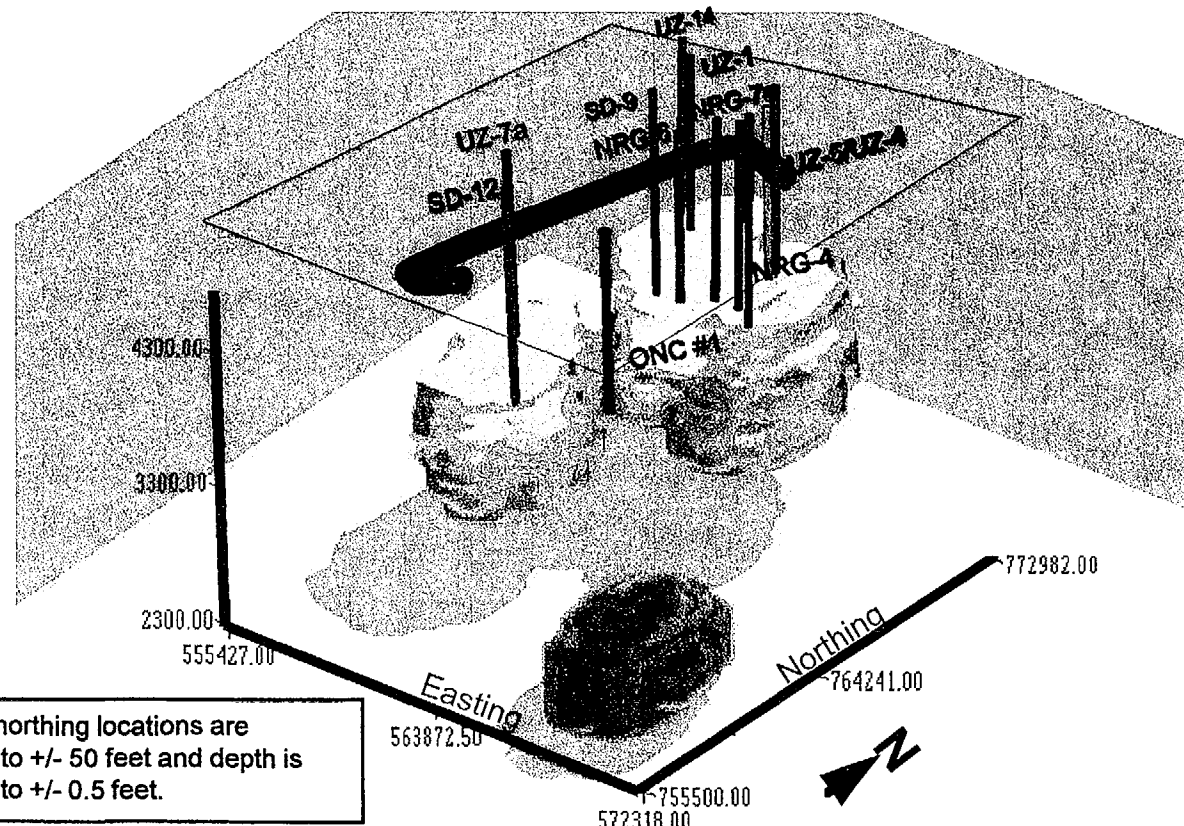
Minimum temperature distribution in deg. Celsius (May 1995)



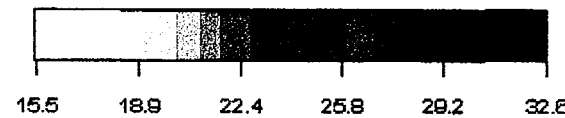


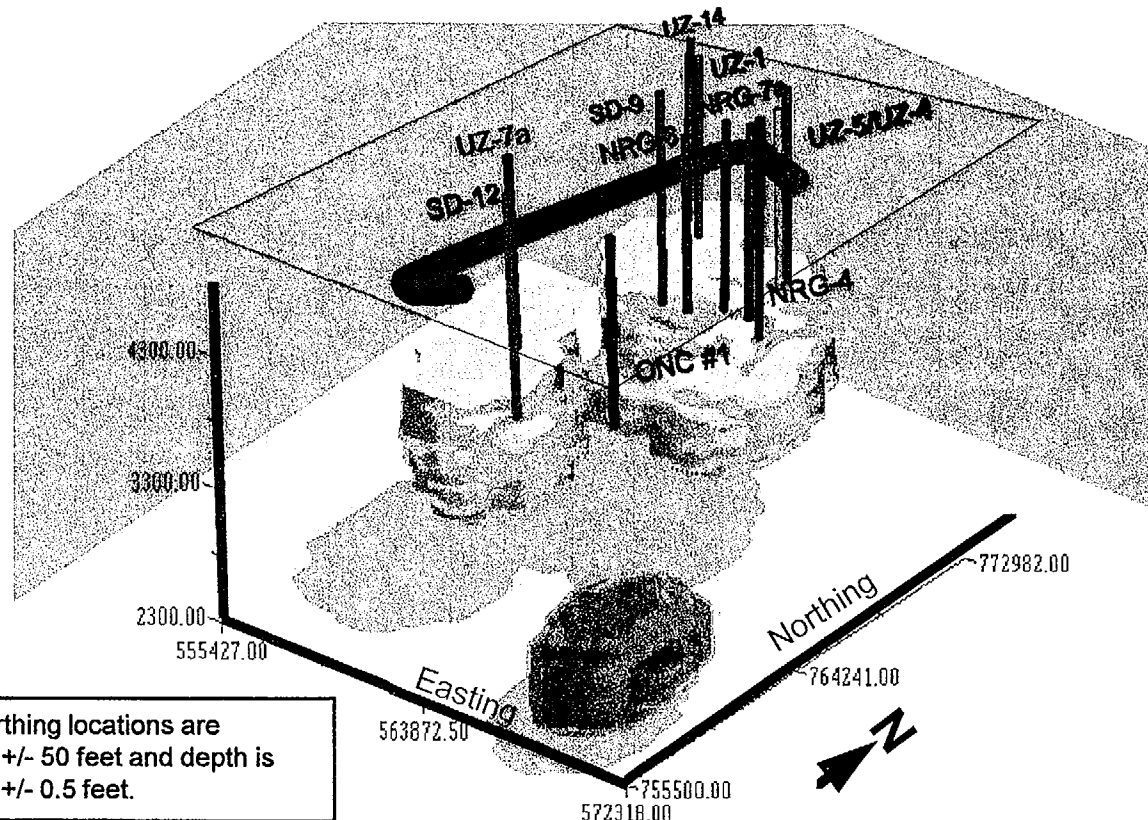
Minimum temperature distribution in deg. Celsius (June 1995)



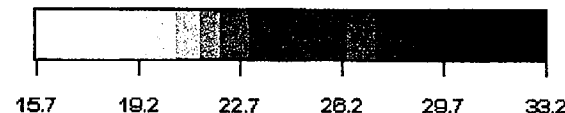


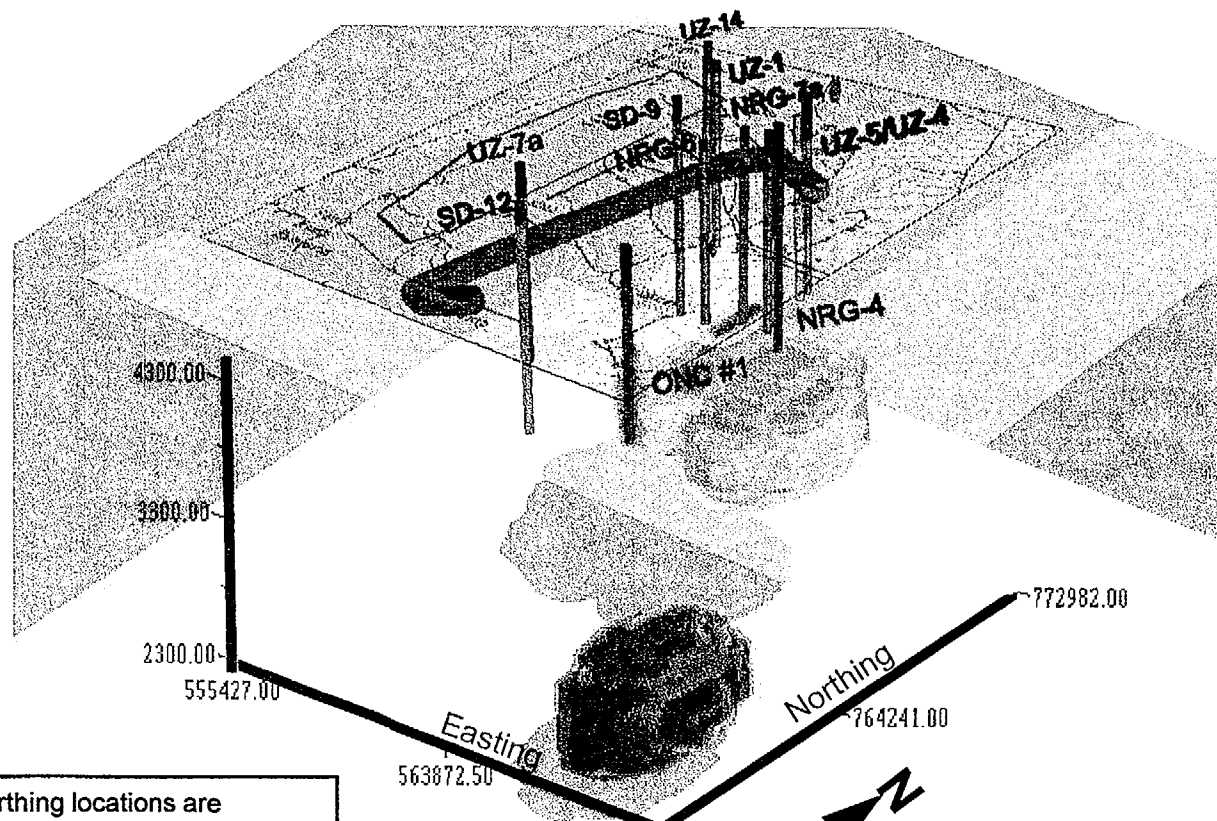
Minimum temperature distribution in deg. Celsius (Dec 1995)





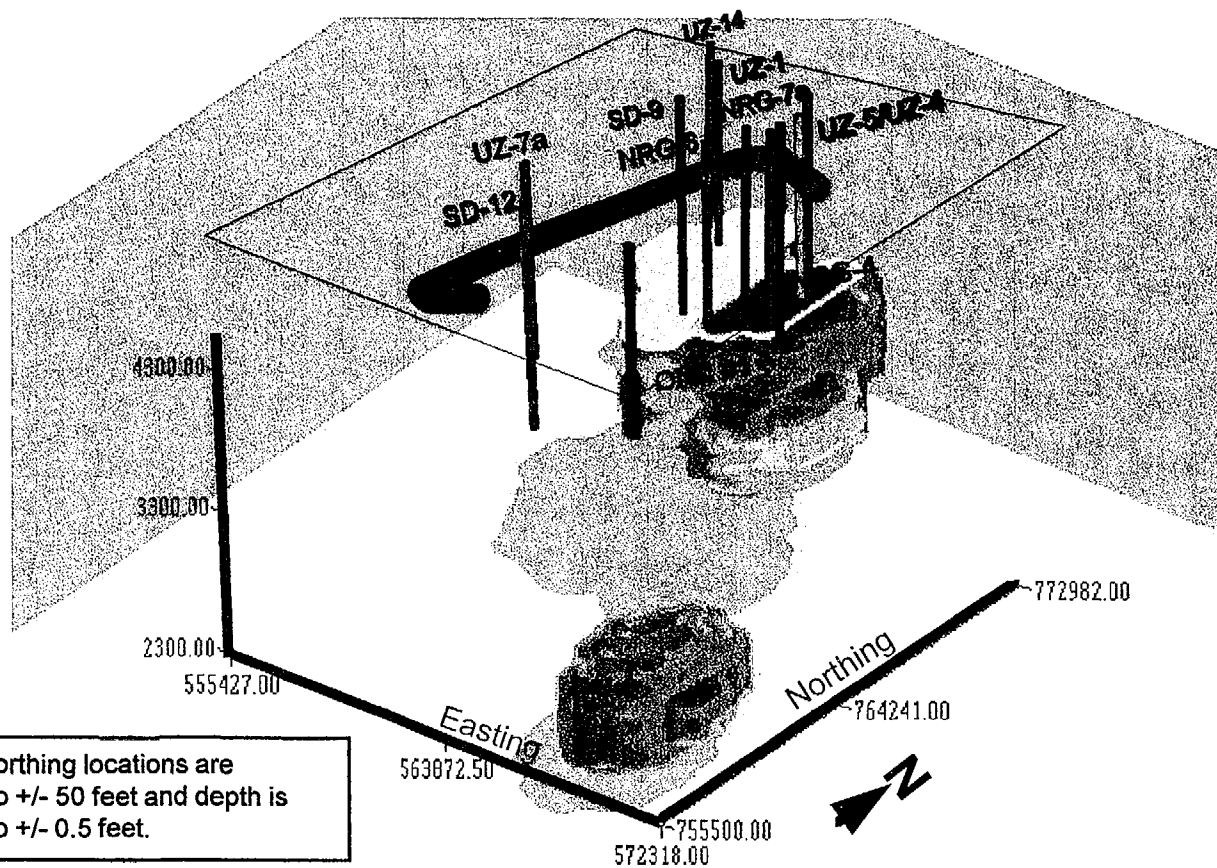
Minimum temperature distribution in deg. Celsius (May 1996)





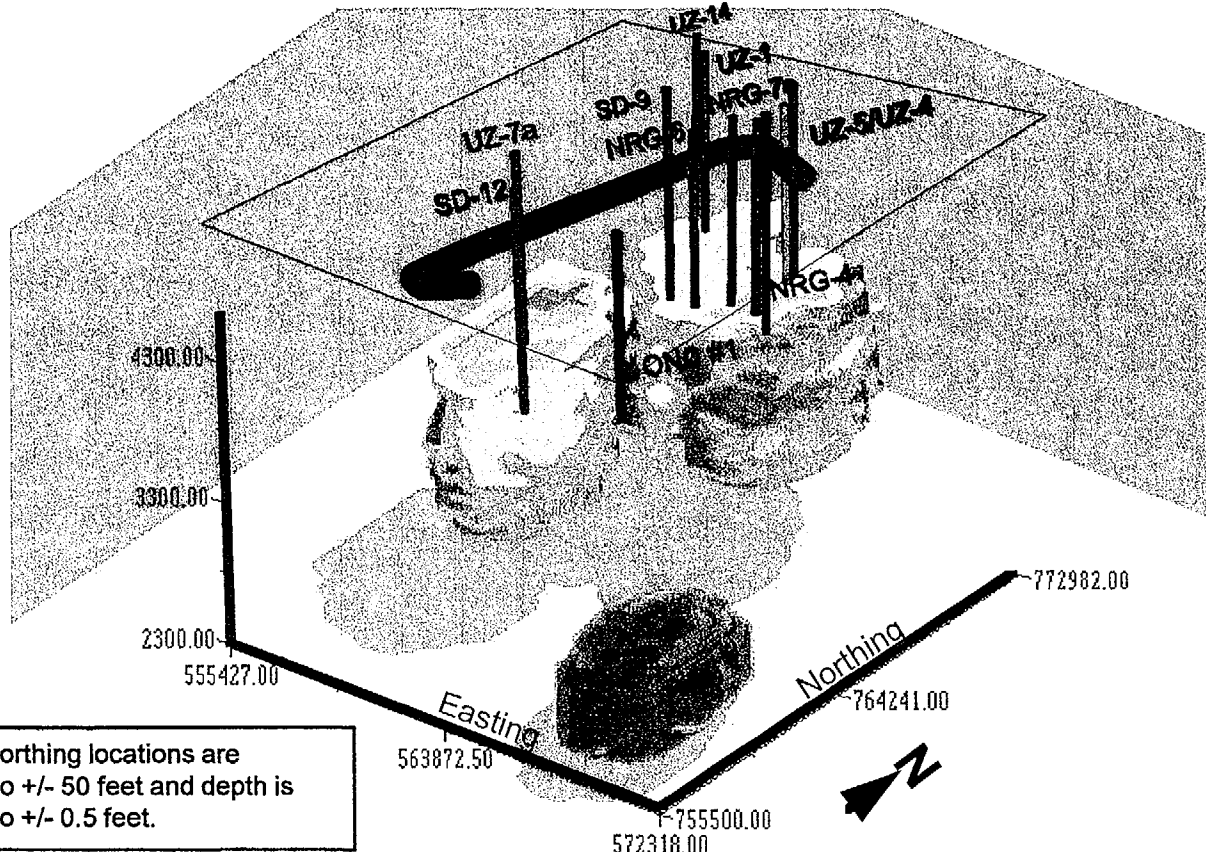
Maximum temperature distribution in deg. Celsius (May 1995)



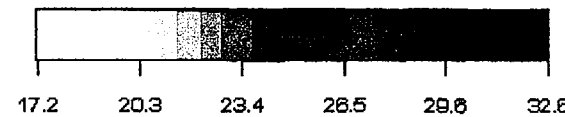


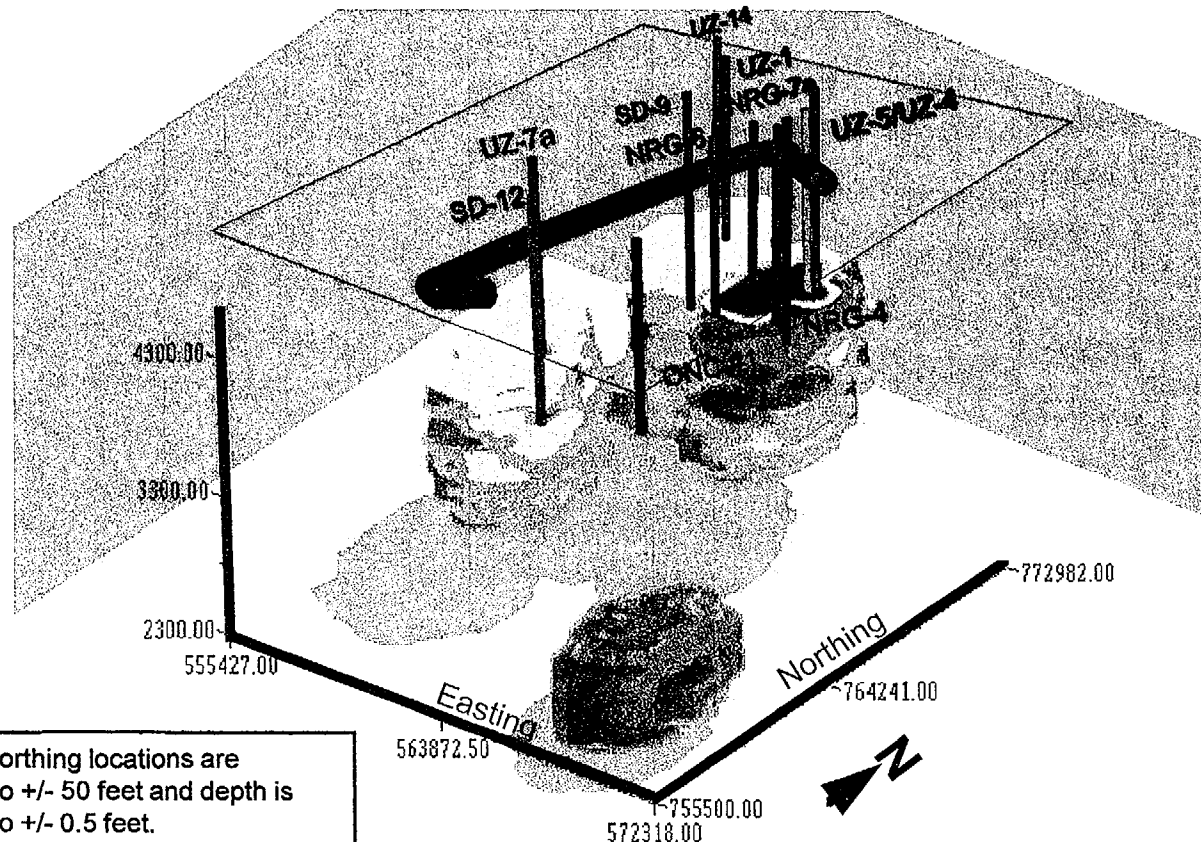
Maximum temperature distribution in deg. Celsius (June 1995)





Maximum temperature distribution in deg. Celsius (Dec 1995)





Maximum temperature distribution in deg. Celsius (May 1996)



August 1995

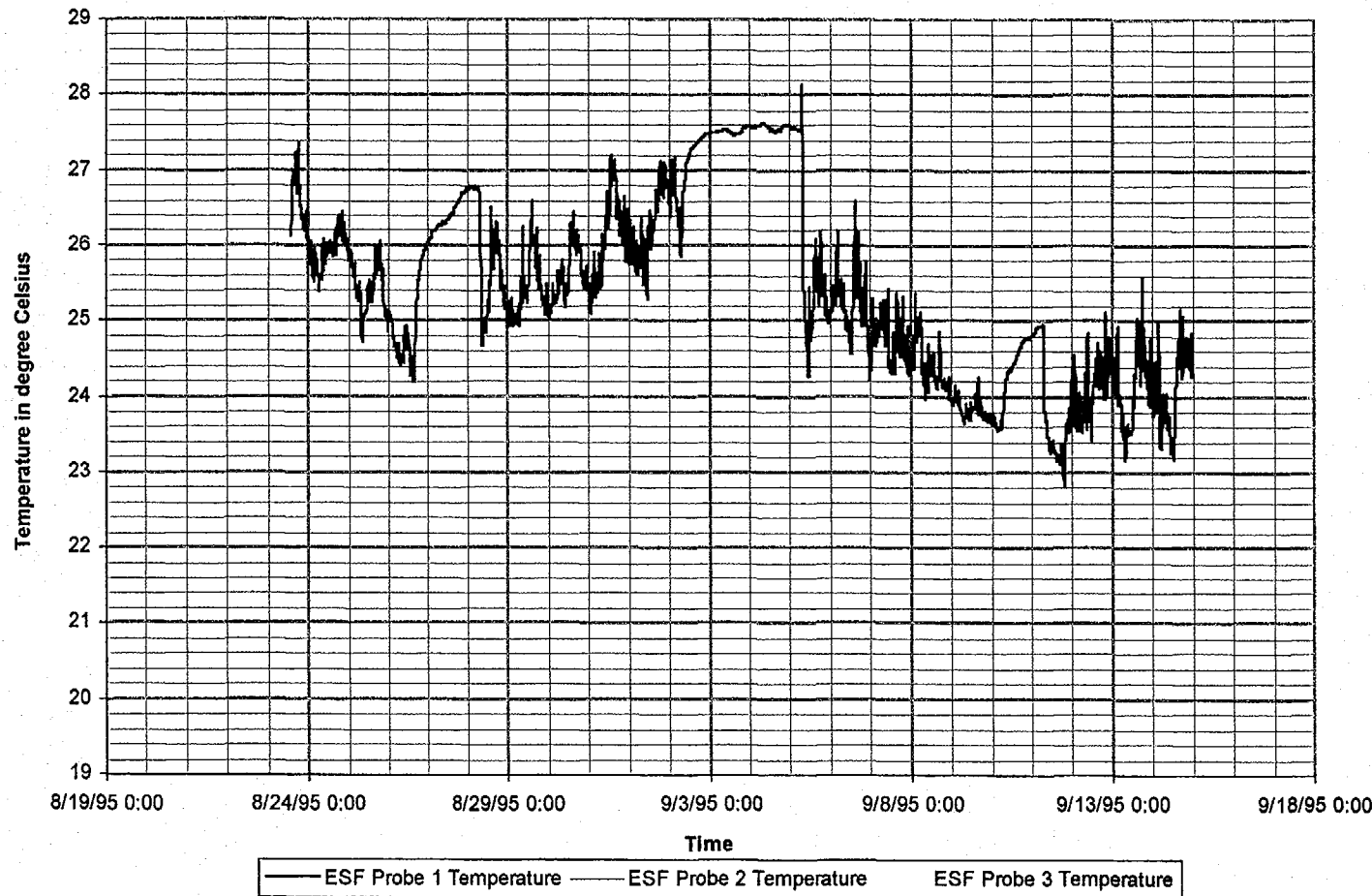


Figure 4-14a Temperature fluctuation with time in ESF Tunnel

August 24, 1996
P2666.24 PMD:\user\projects\Nyecounty\annrep96\figures

Prepared for:
Nye County Nuclear Waste Repository Project Office

Prepared by:
Multimedia Environmental Technology, Inc.
Newport Beach, CA

September 1995

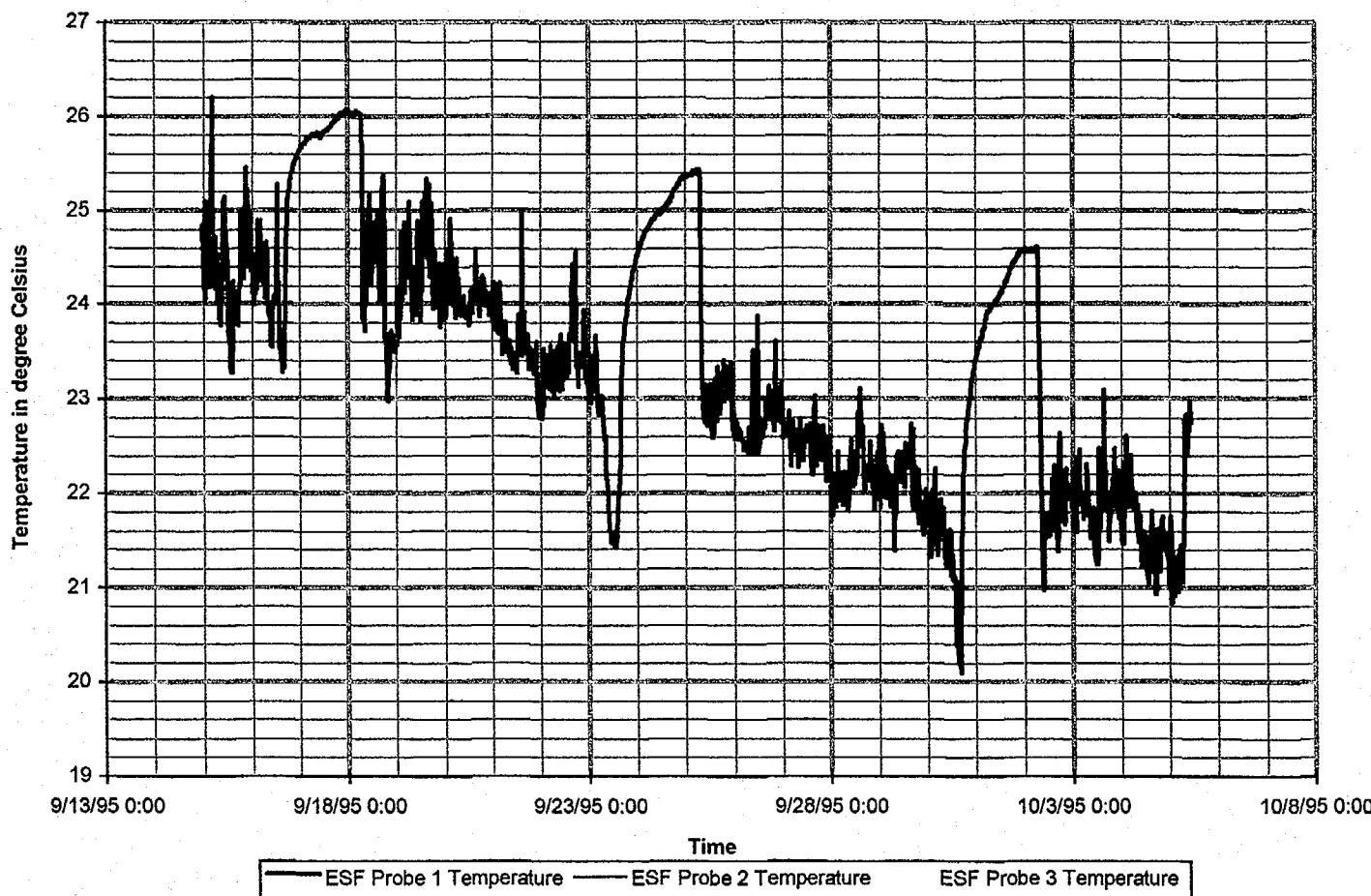


Figure 4-14b Temperature fluctuation with time in ESF Tunnel

October 1995

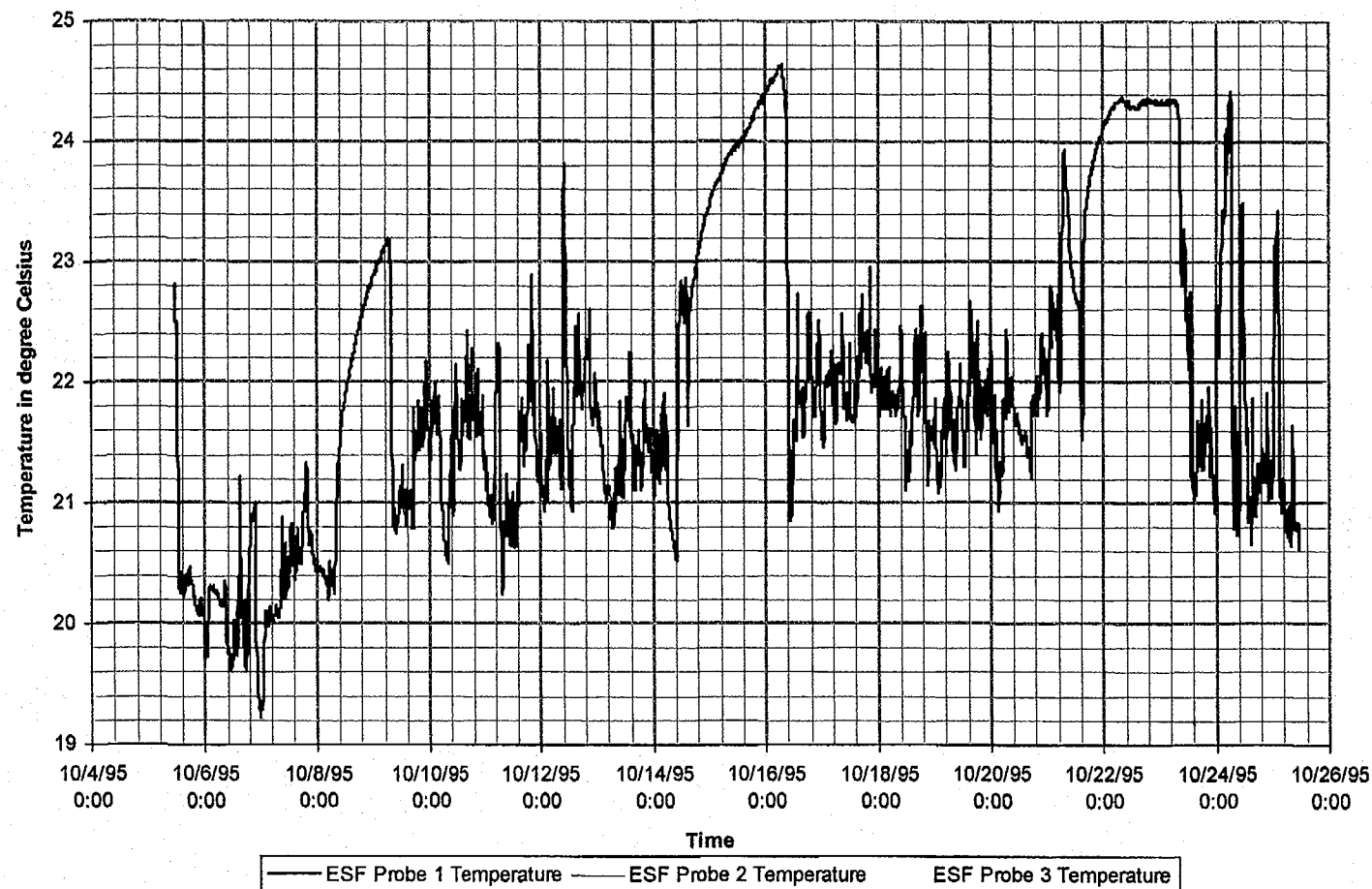


Figure 4-14c Temperature fluctuation with time in ESF Tunnel

November 1995

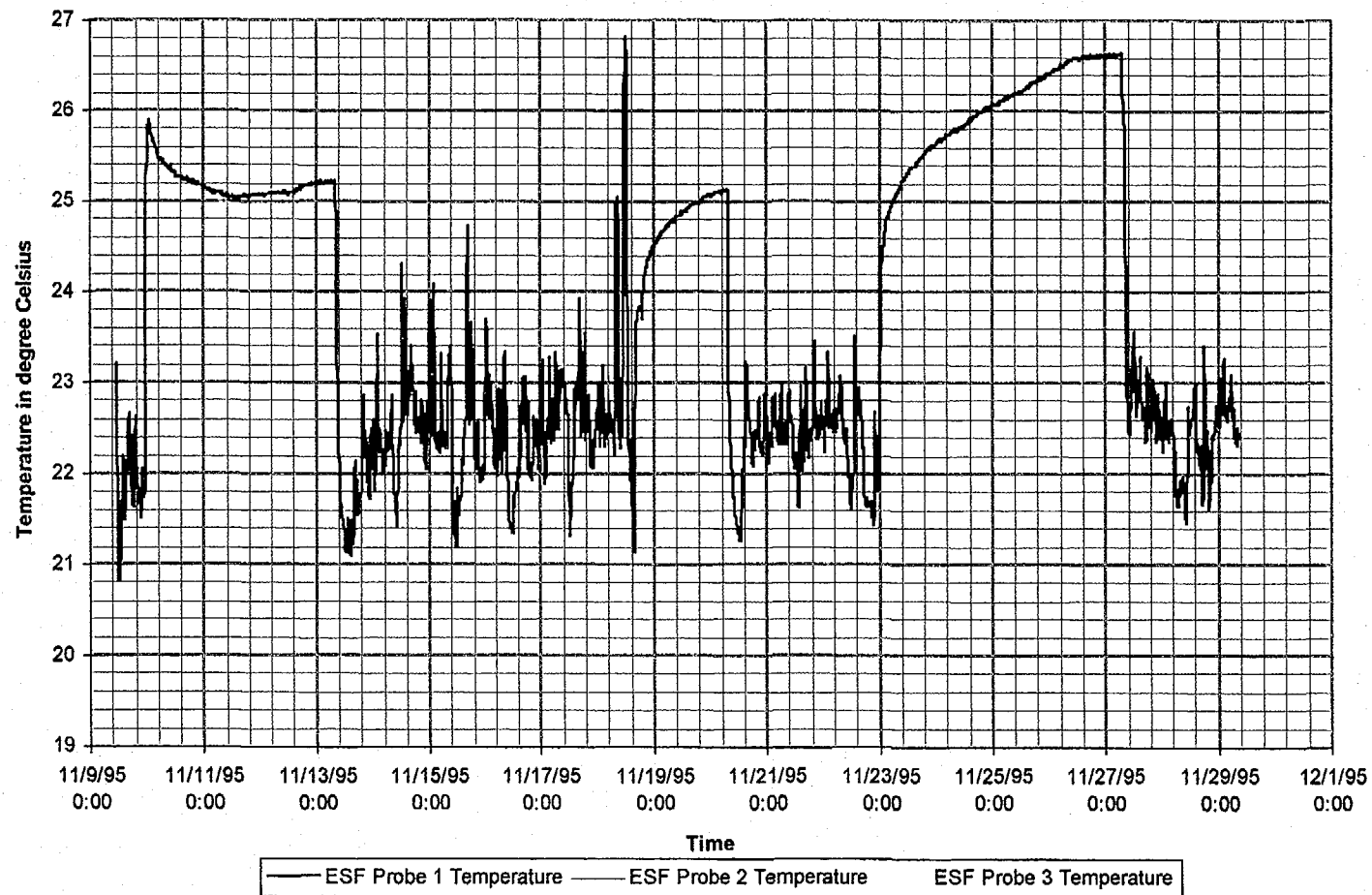


Figure 4-14d Temperature fluctuation with time in ESF Tunnel

December 1995

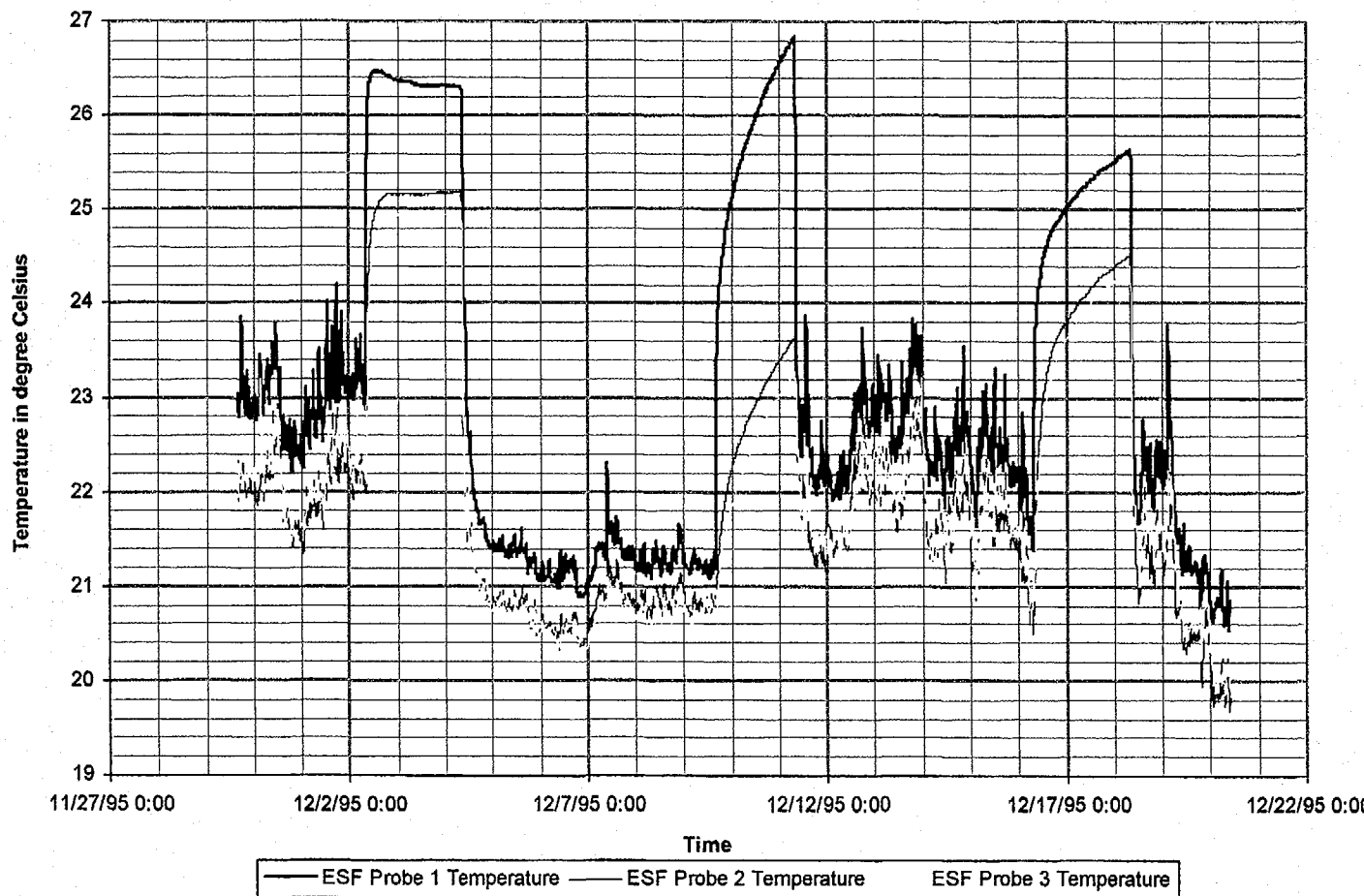


Figure 4-14e Temperature fluctuation with time in ESF Tunnel

January 1996

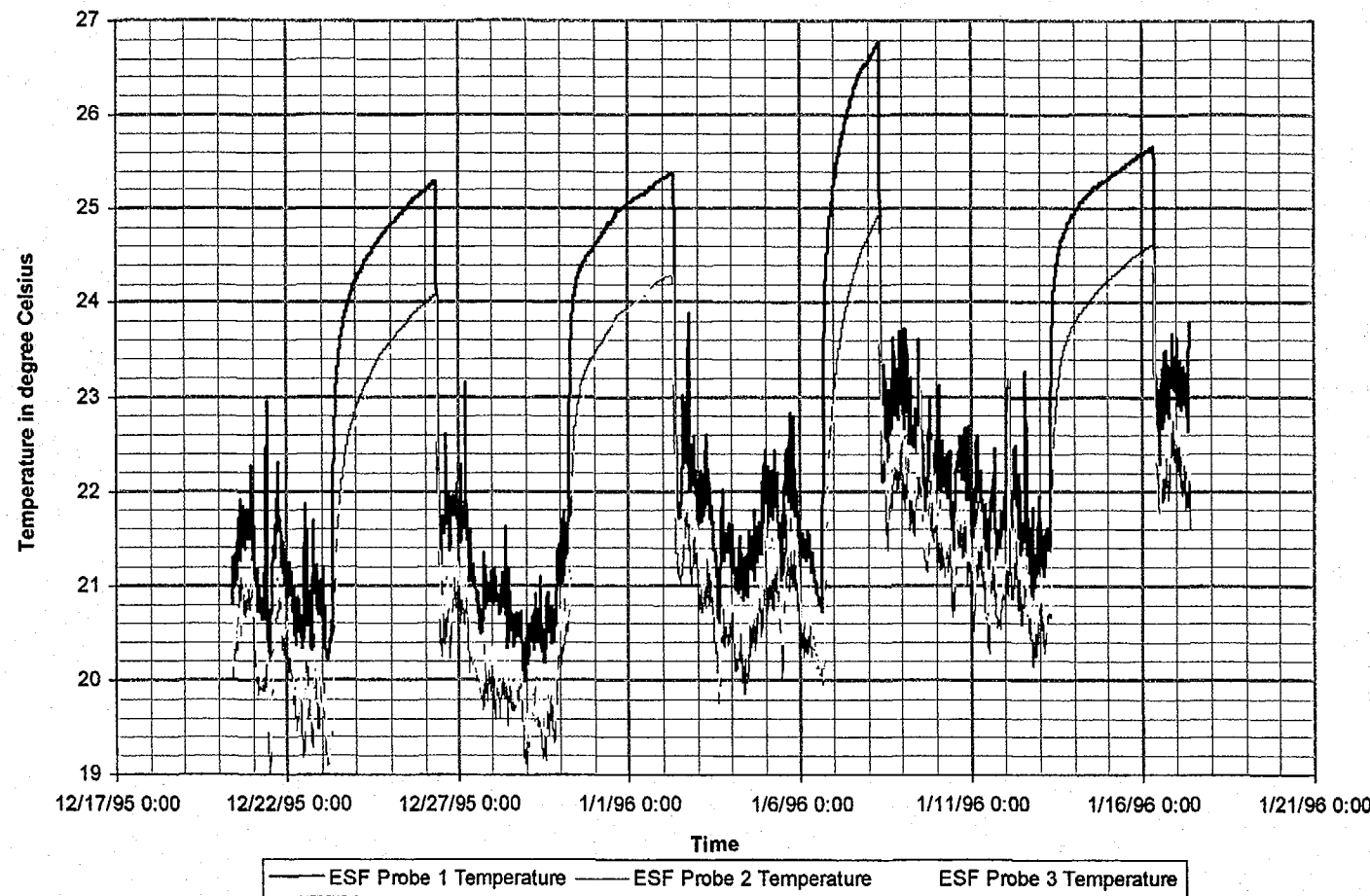


Figure 4-14f Temperature fluctuation with time in ESF Tunnel

August 24, 1996
P2666:24 PMD:\user\projects\Nye County\enrep96\figures

Prepared for:
Nye County Nuclear Waste Repository Project Office

Prepared by:
Multimedia Environmental Technology, Inc.
Newport Beach, CA

February 1996

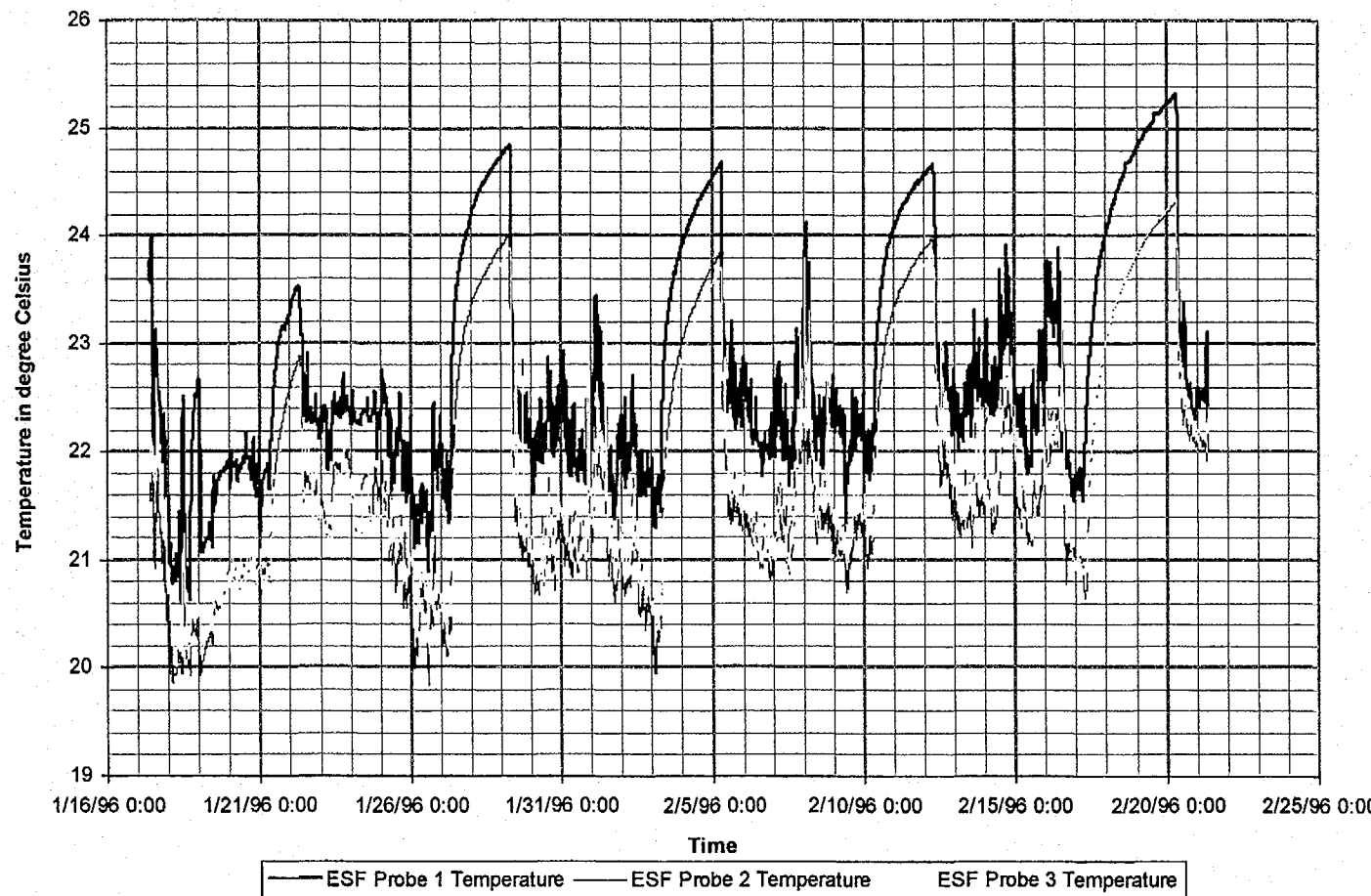


Figure 4-14g Temperature fluctuation with time in ESF Tunnel

March 1996

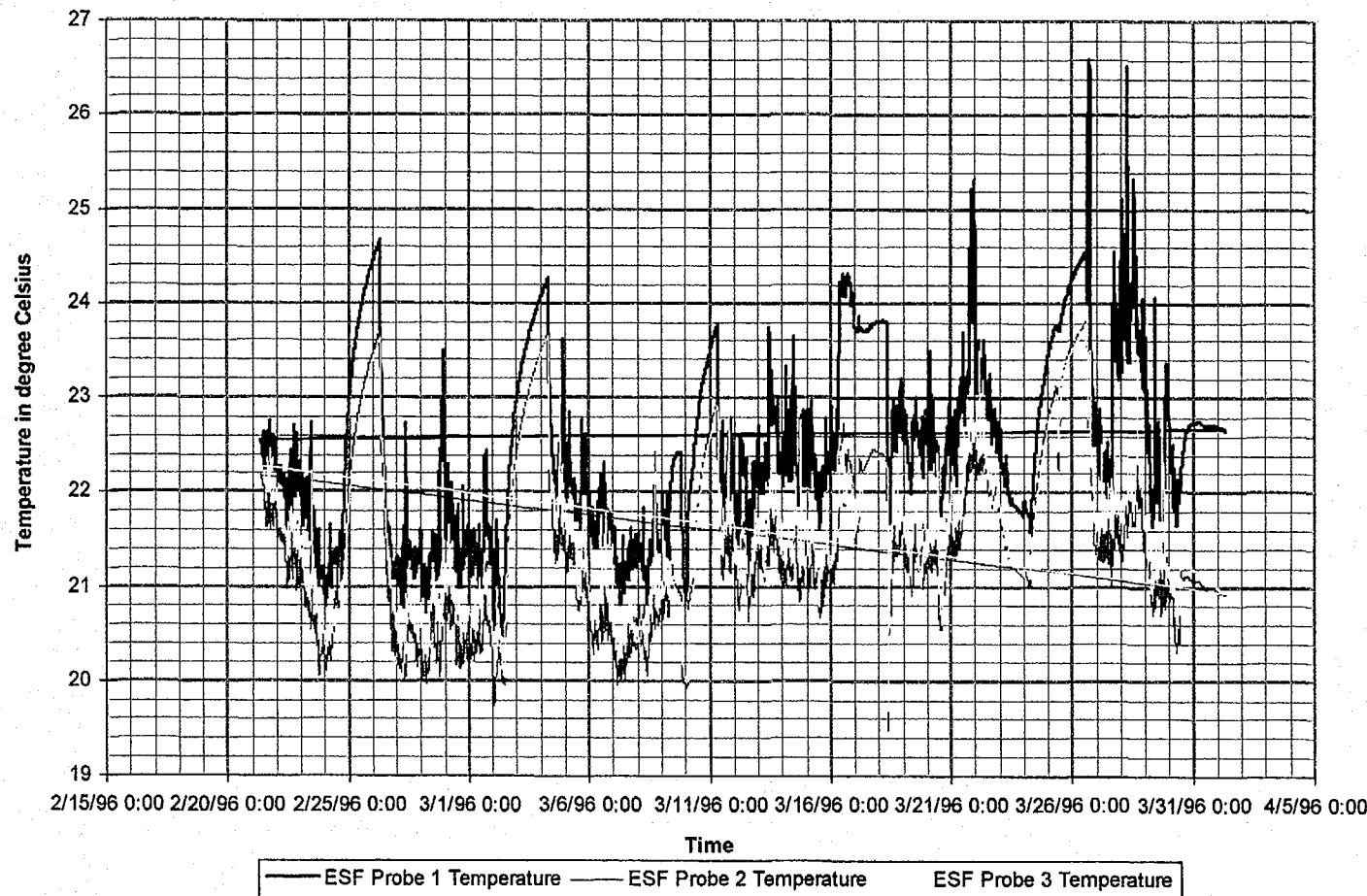


Figure 4-14h Temperature fluctuation with time in ESF Tunnel

APRIL 1996

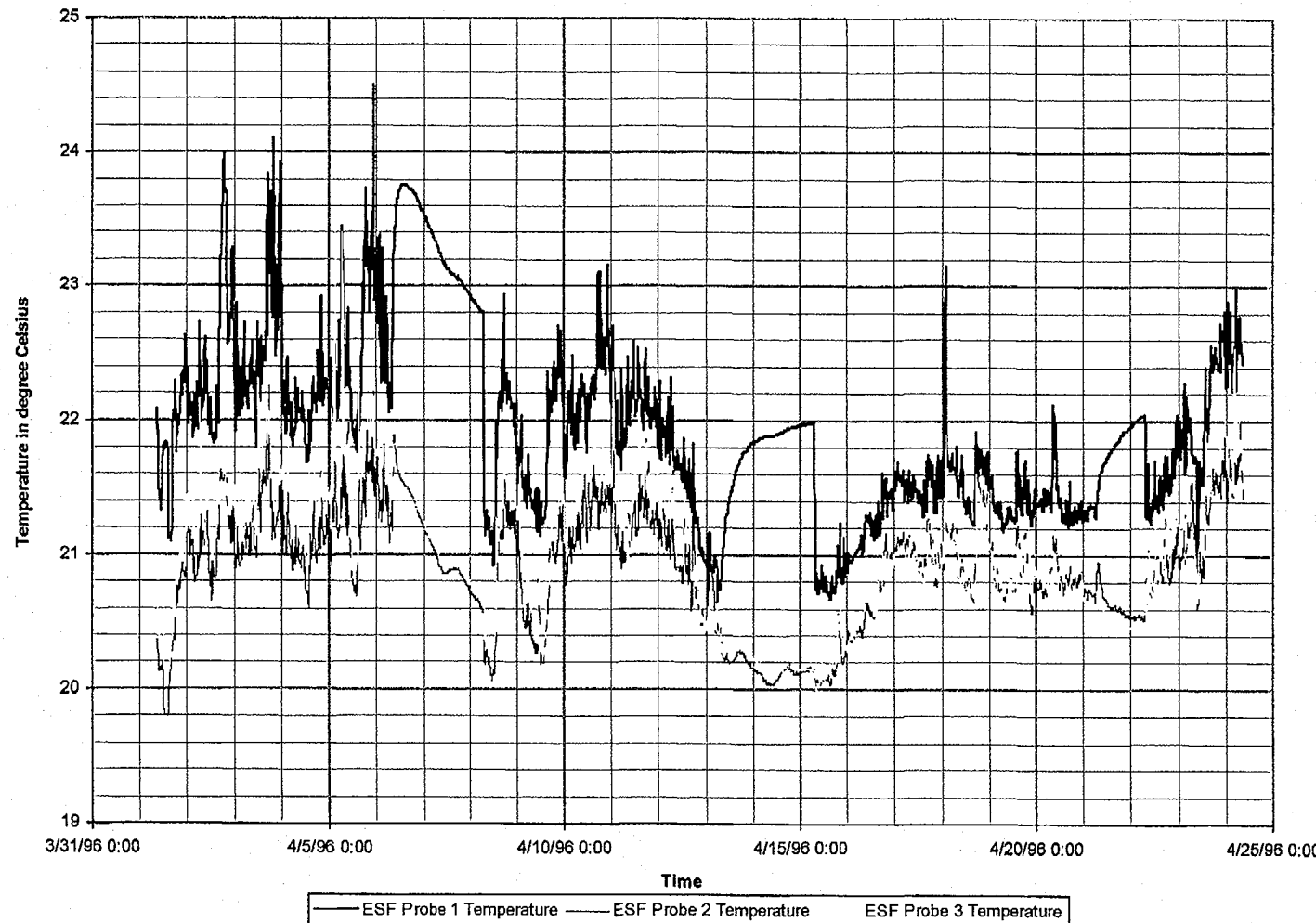


Figure 4-14i Temperature fluctuation with time in ESF Tunnel

MAY 1996

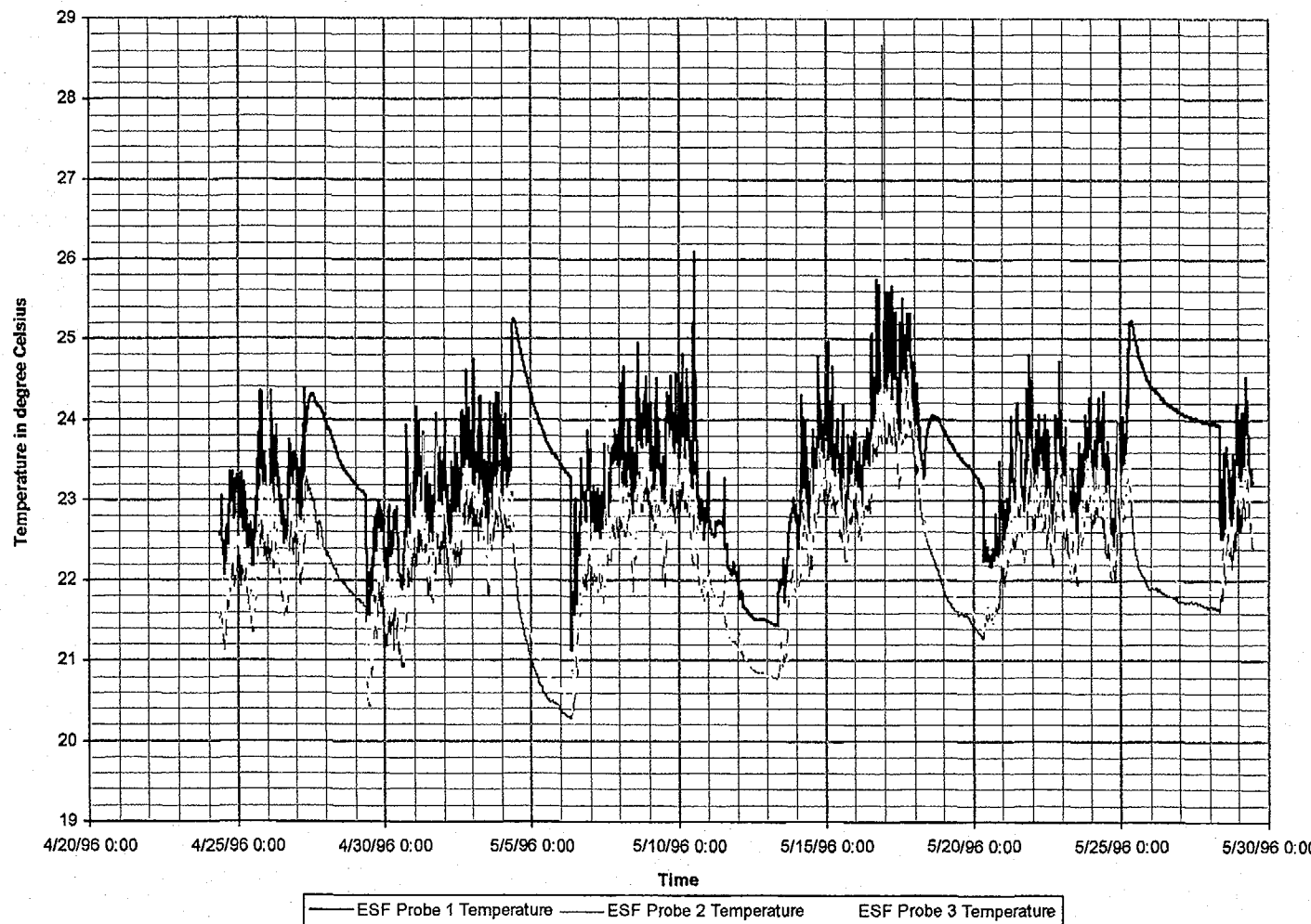


Figure 4-14j Temperature fluctuation with time in ESF Tunnel

August 24, 1996
P266:D:\user\projetc\Nye\county\annrap96\figures

Prepared for:
Nye County Nuclear Waste Repository Project Office

Prepared by:
Multimedia Environmental Technology, Inc.
Newport Beach, CA

JUNE 1996

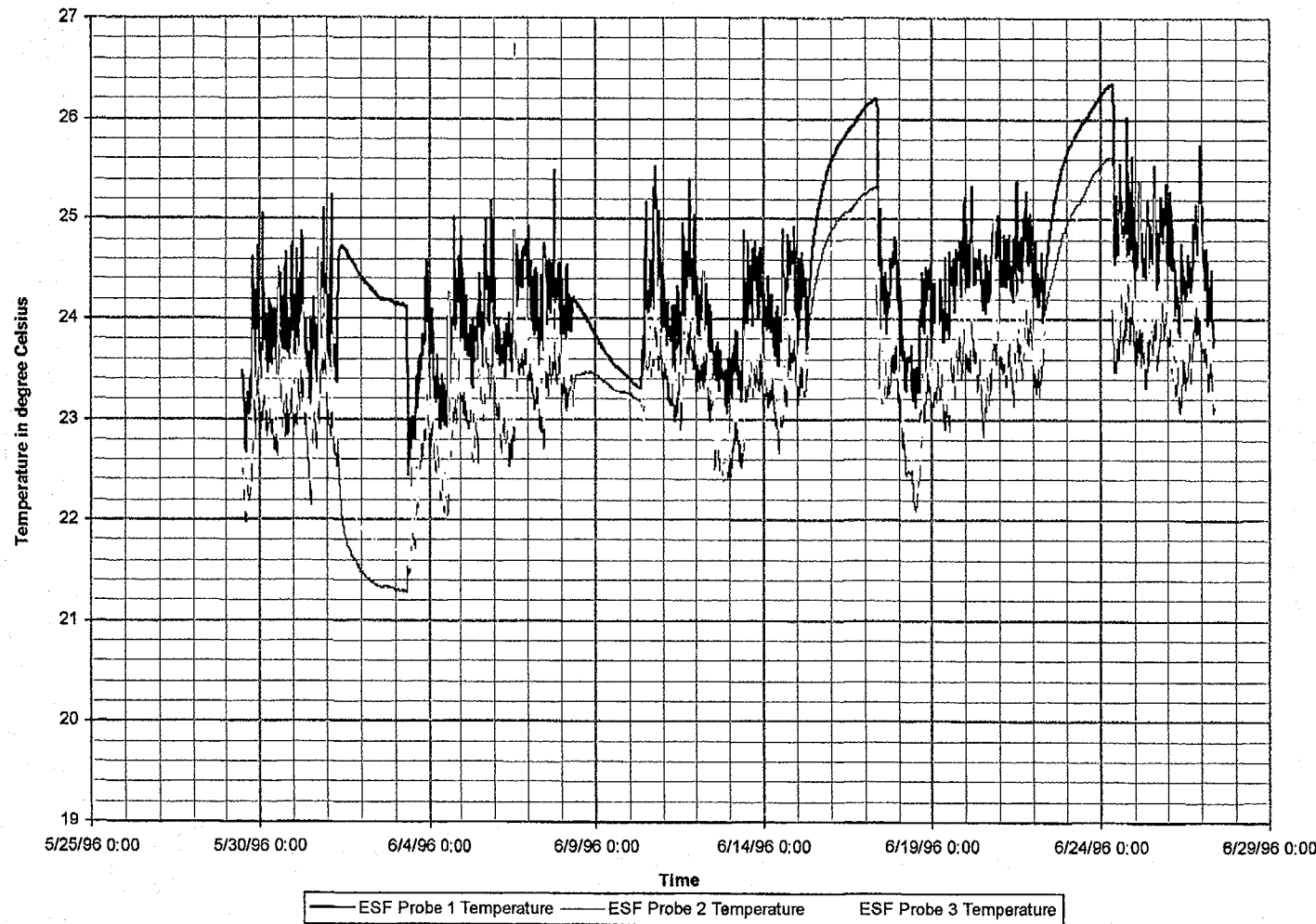


Figure 4-14k Temperature fluctuation with time in ESF Tunnel

August 24, 1996
P266:D:\user\projects\NyeCounty\annrep96\figures

Prepared for:
Nye County Nuclear Waste Repository Project Office

Prepared by:
Multimedia Environmental Technology, Inc.
Newport Beach, CA

JULY 1996

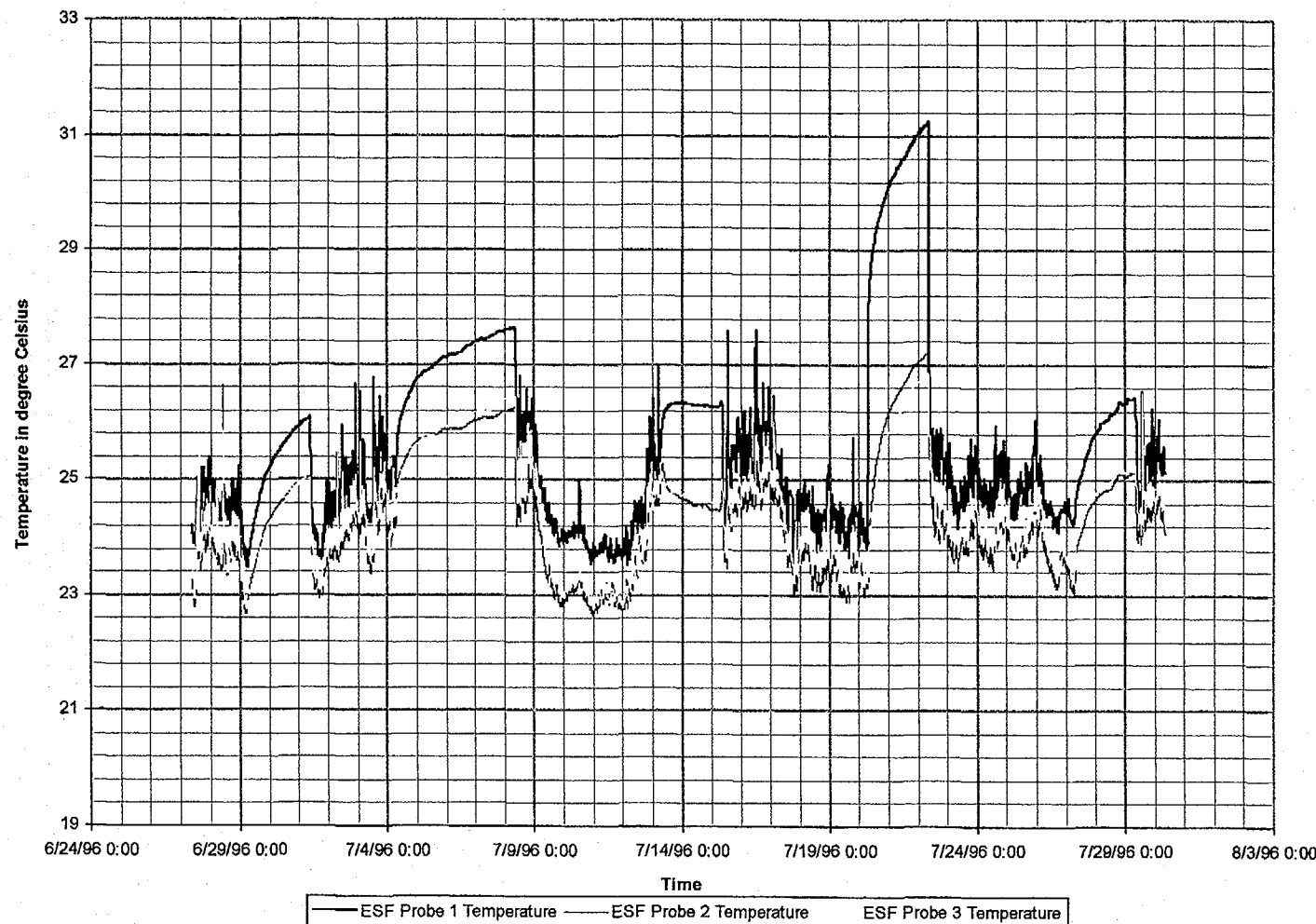


Figure 4-14L Temperature fluctuation with time in ESF Tunnel

August 1996

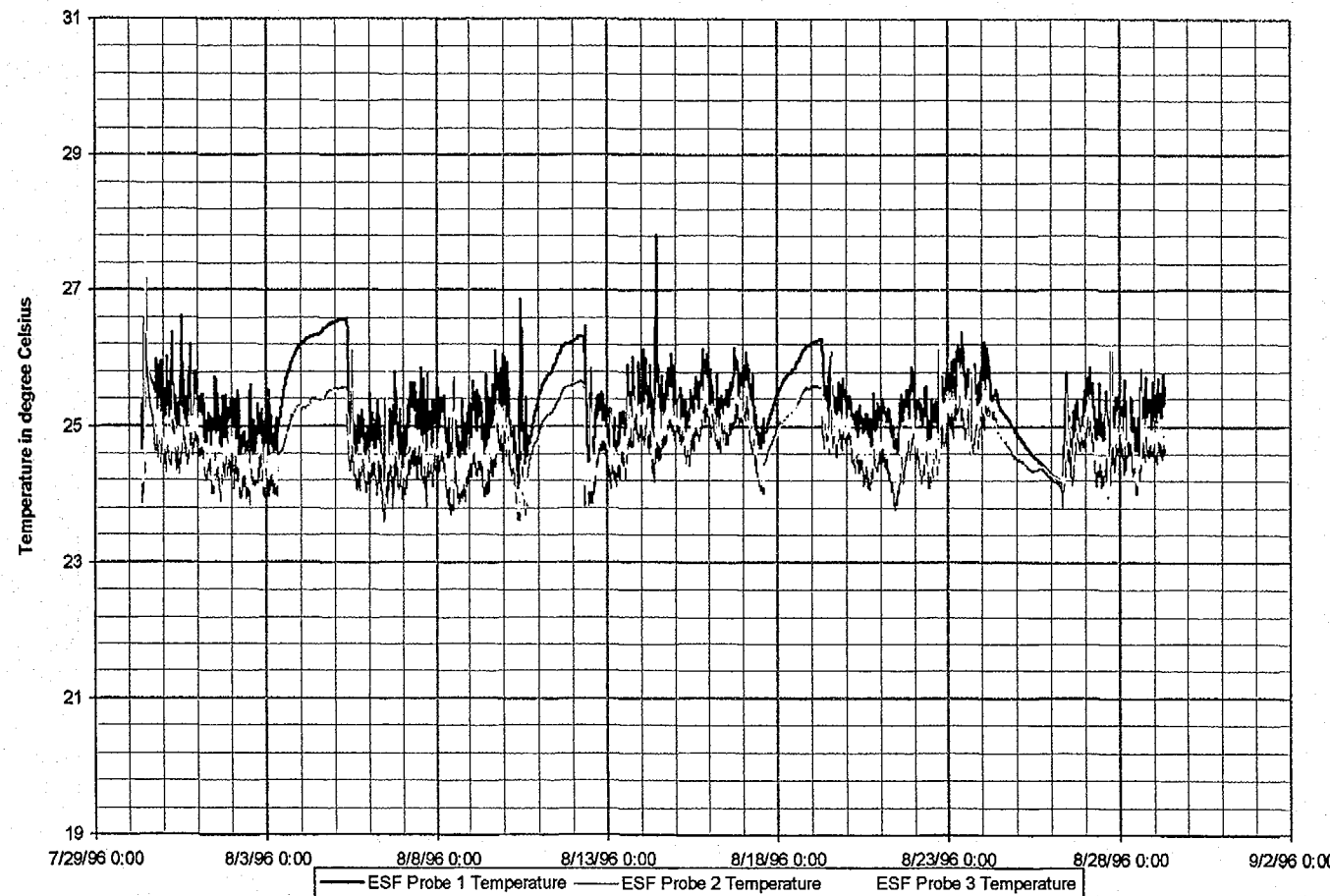


Figure 4-14m Temperature fluctuation with time in ESF Tunnel

August 24, 1996
P2667:59 AMD:\user\projects\NyeCounty\enrep96\figures

Prepared for:
Nye County Nuclear Waste Repository Project Office

Prepared by:
Multimedia Environmental Technology, Inc.
Newport Beach, CA

August 1995

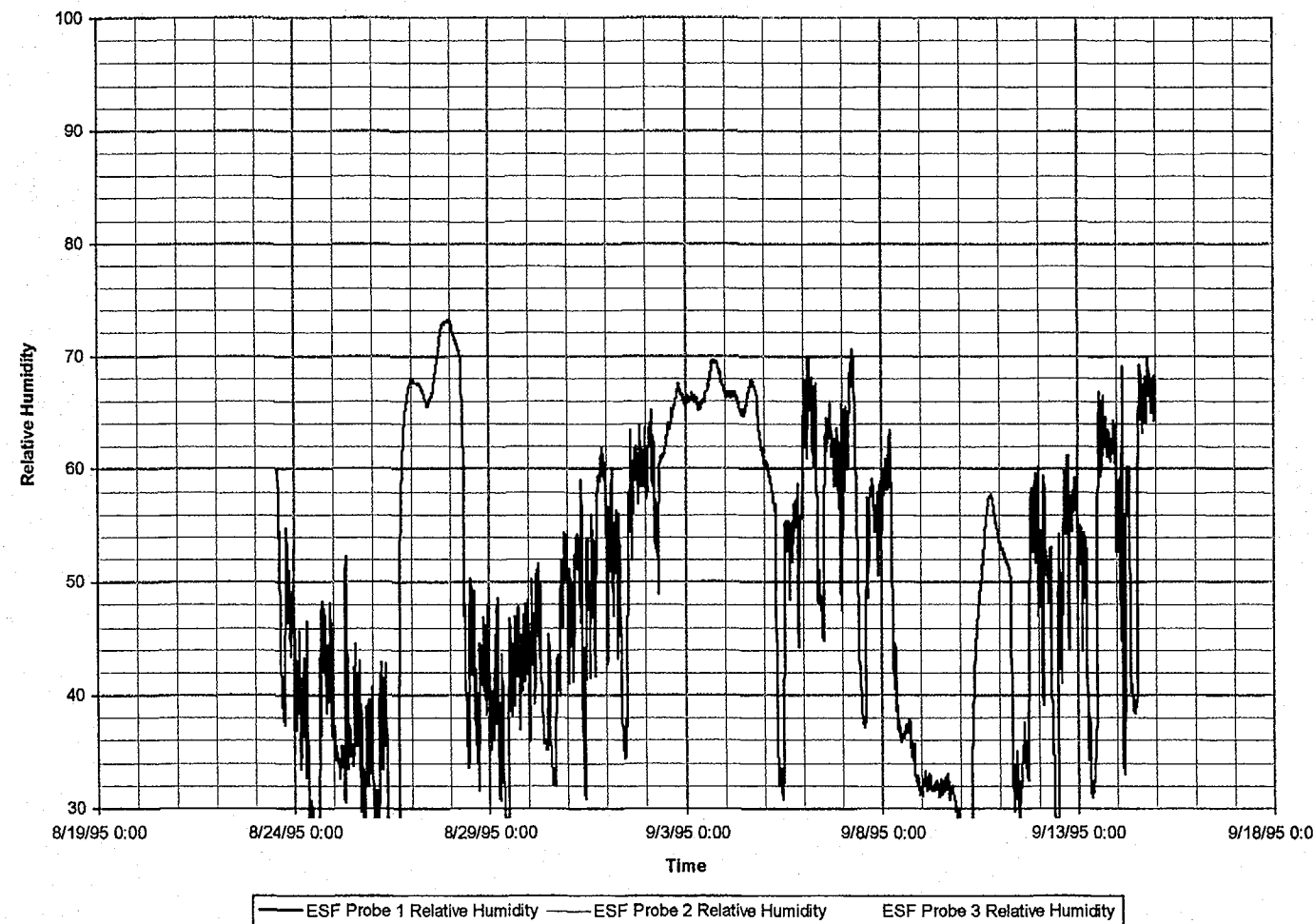


Figure 4-15a Relative Humidity fluctuation with time in ESF Tunnel

August 24, 1996
P2666:24 PMD:\user\projects\Nyecounty\annrop96\figures

Prepared for:
Nye County Nuclear Waste Repository Project Office

Prepared by:
Multimedia Environmental Technology, Inc.
Newport Beach, CA

September 1995

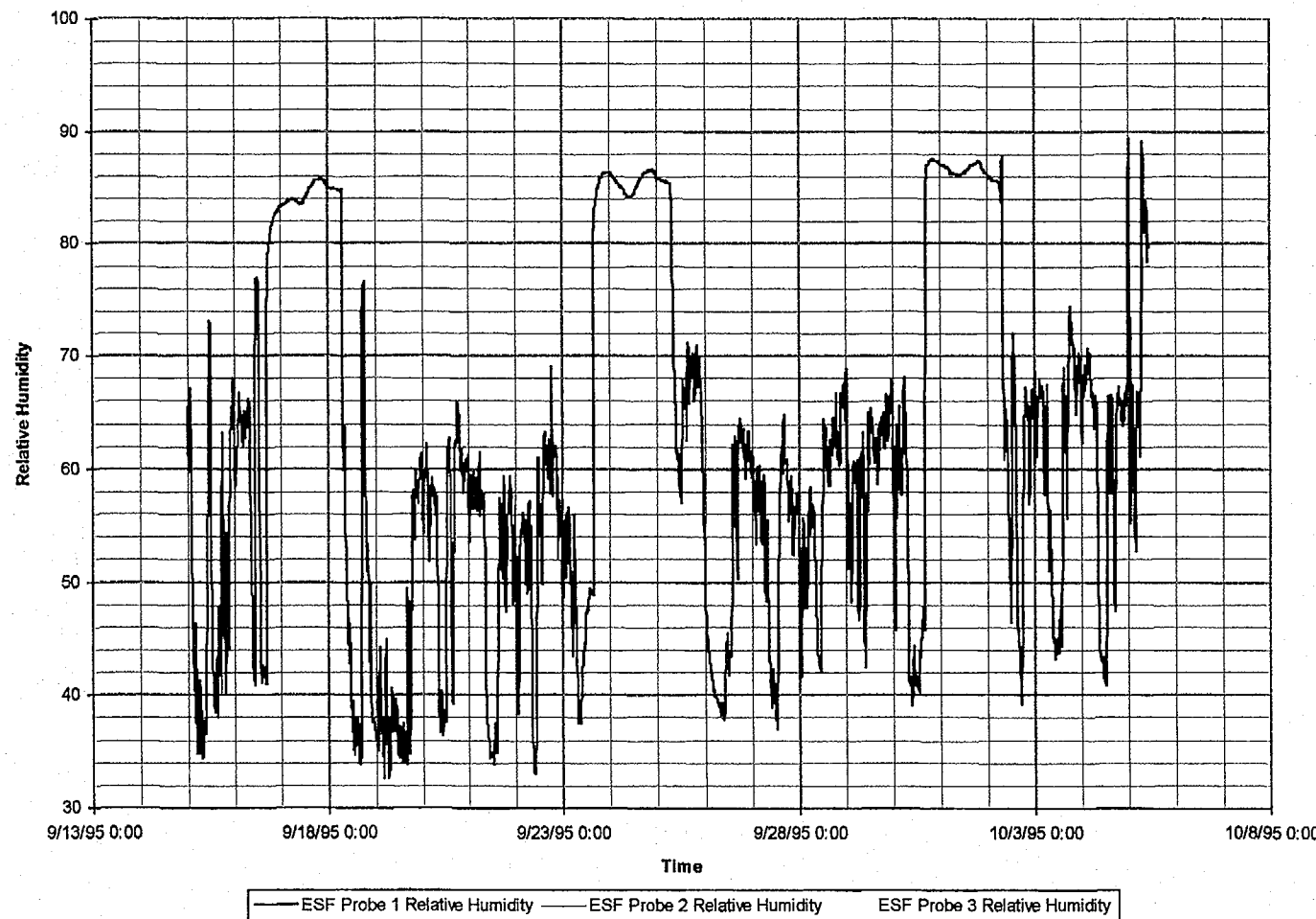


Figure 4-15b Relative Humidity fluctuation with time in ESF Tunnel

October 1995

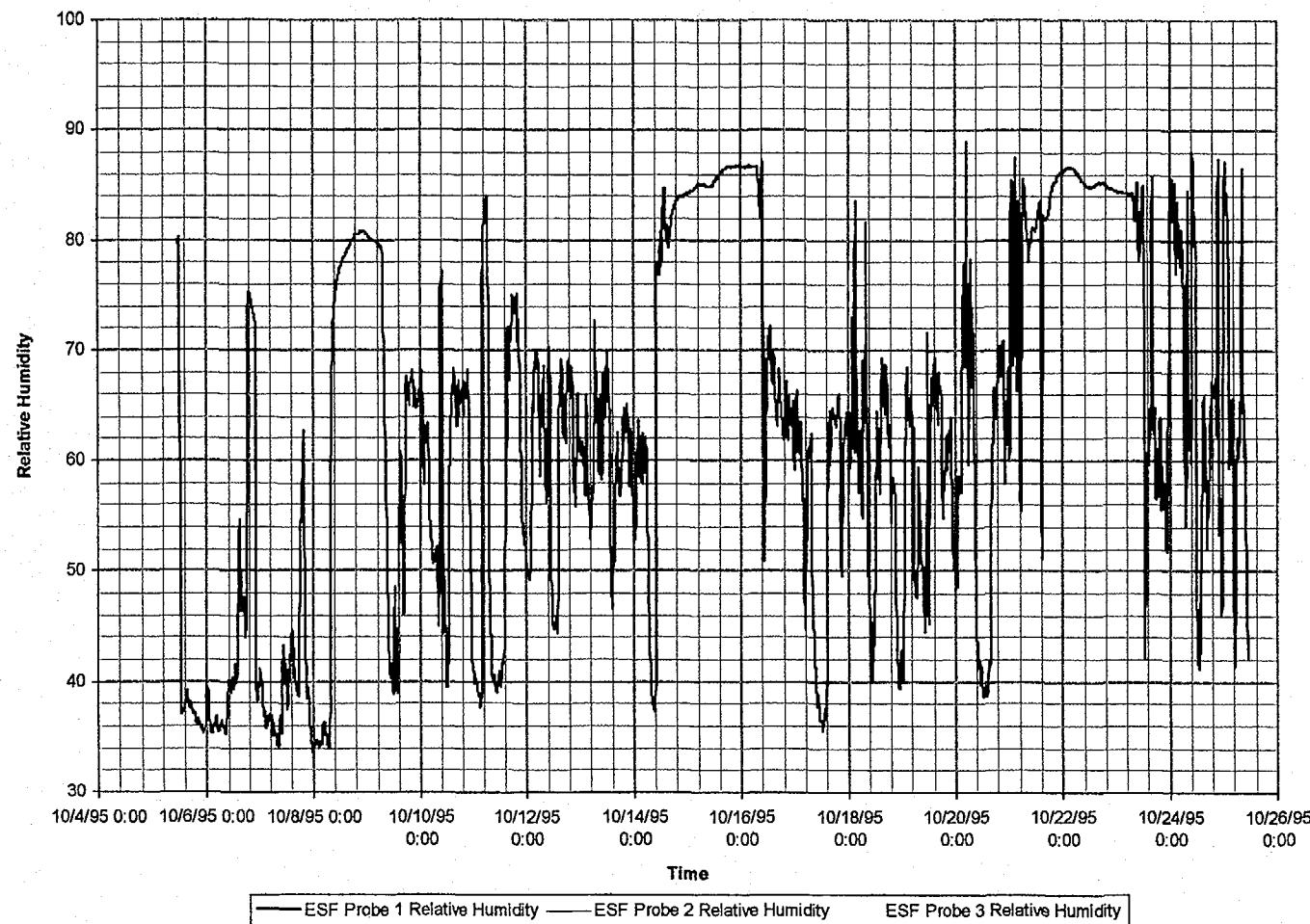


Figure 4-15c Relative Humidity fluctuation with time in ESF Tunnel

August 24, 1996
P266624 PMD:\user\projects\NyeCounty\amrep96\figures

Prepared for:
Nye County Nuclear Waste Repository Project Office

Prepared by:
Multimedia Environmental Technology, Inc.
Newport Beach, CA

November 1995

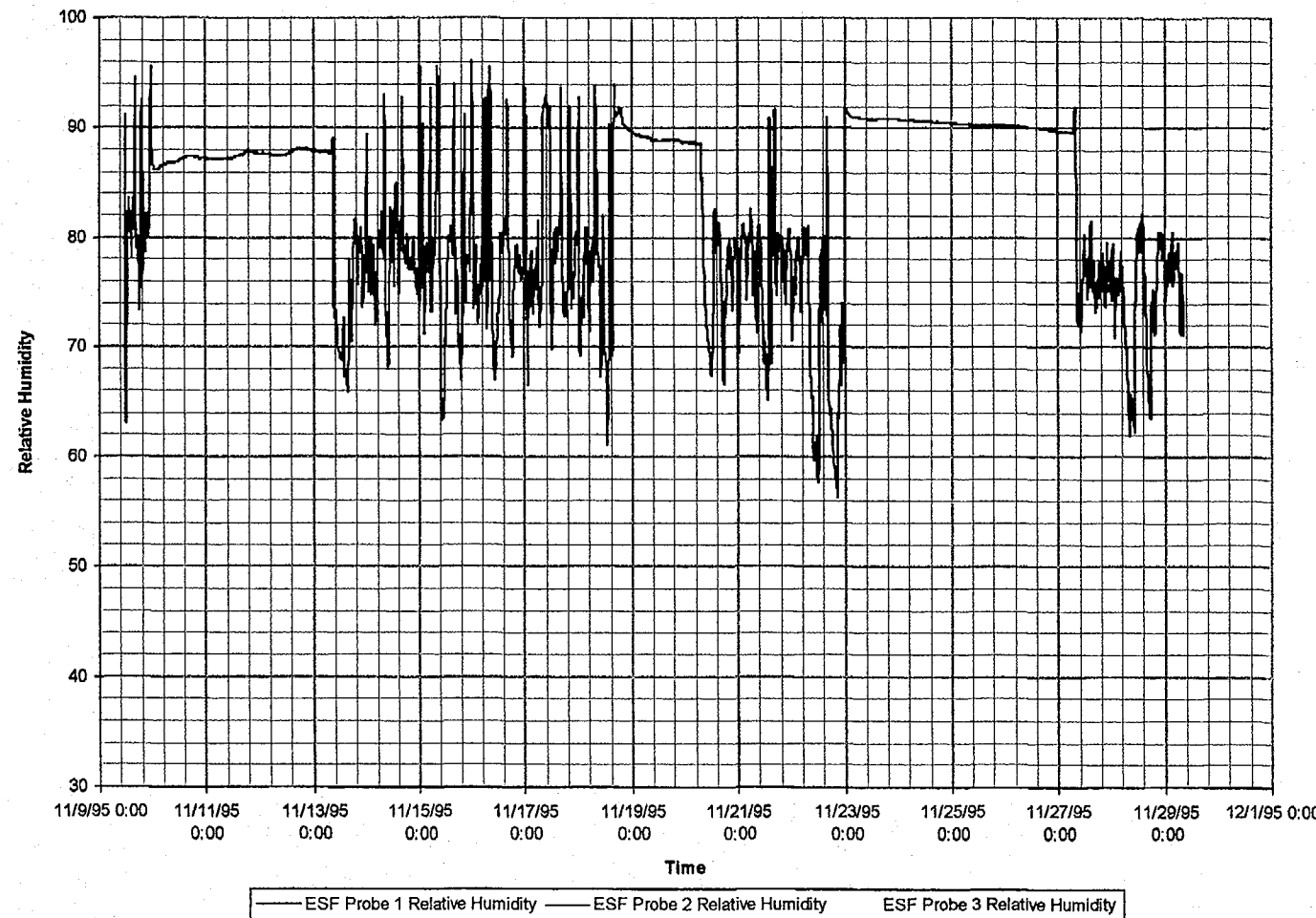


Figure 4-15d Relative Humidity fluctuation with time in ESF Tunnel

December 1995

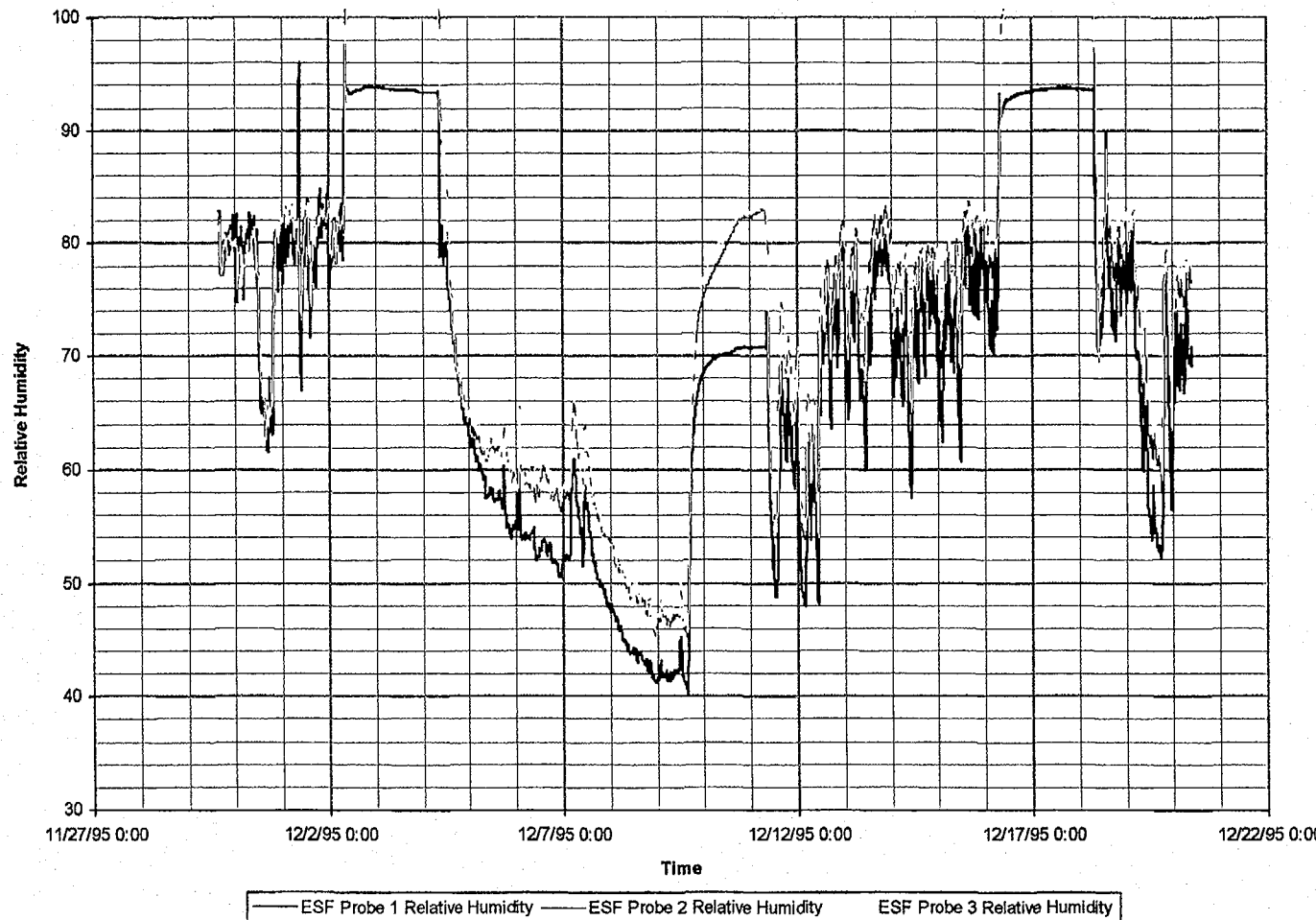


Figure 4-15e Relative Humidity fluctuation with time in ESF Tunnel

January 1996

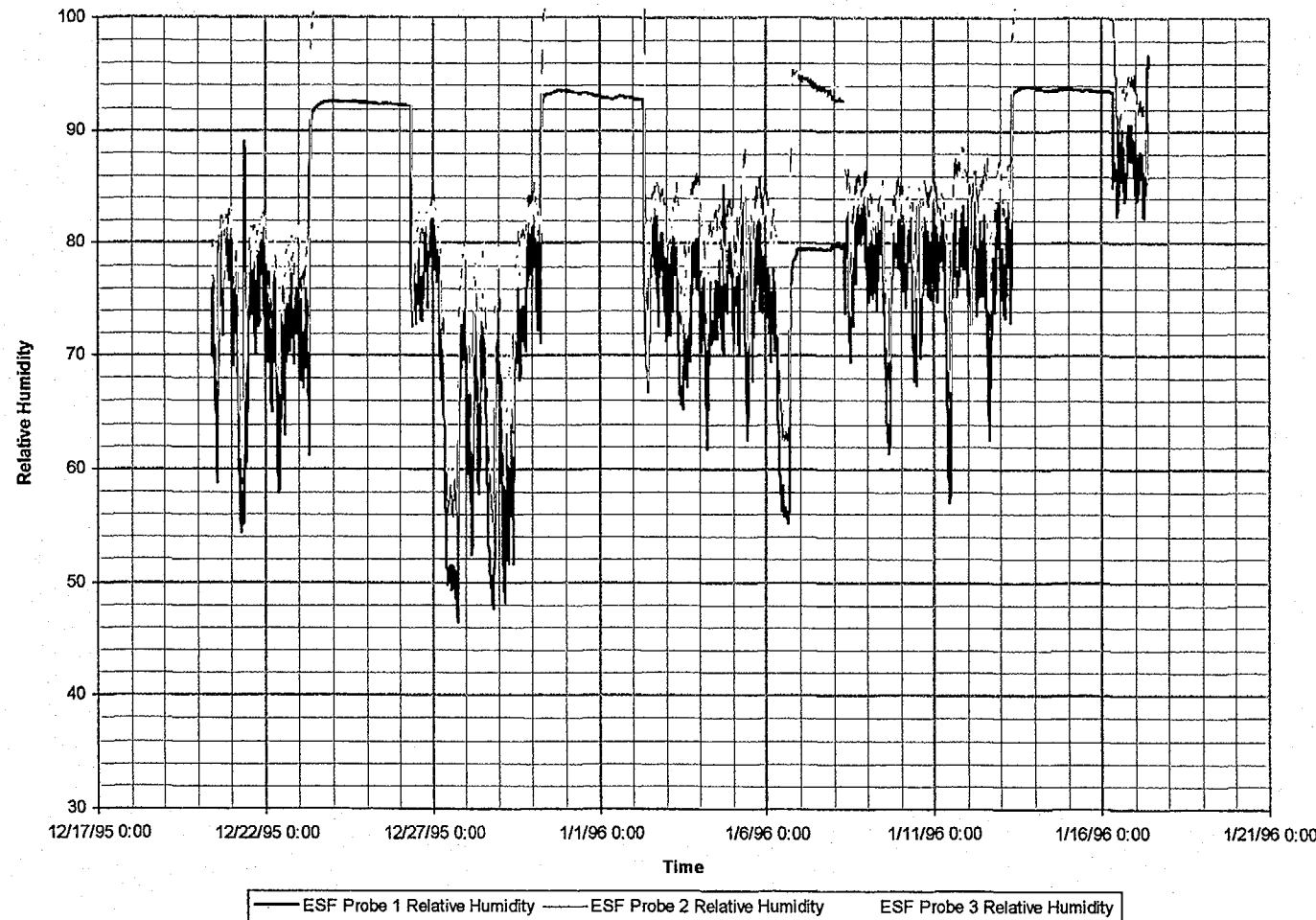


Figure 4-15f Relative Humidity fluctuation with time in ESF Tunnel

February 1996

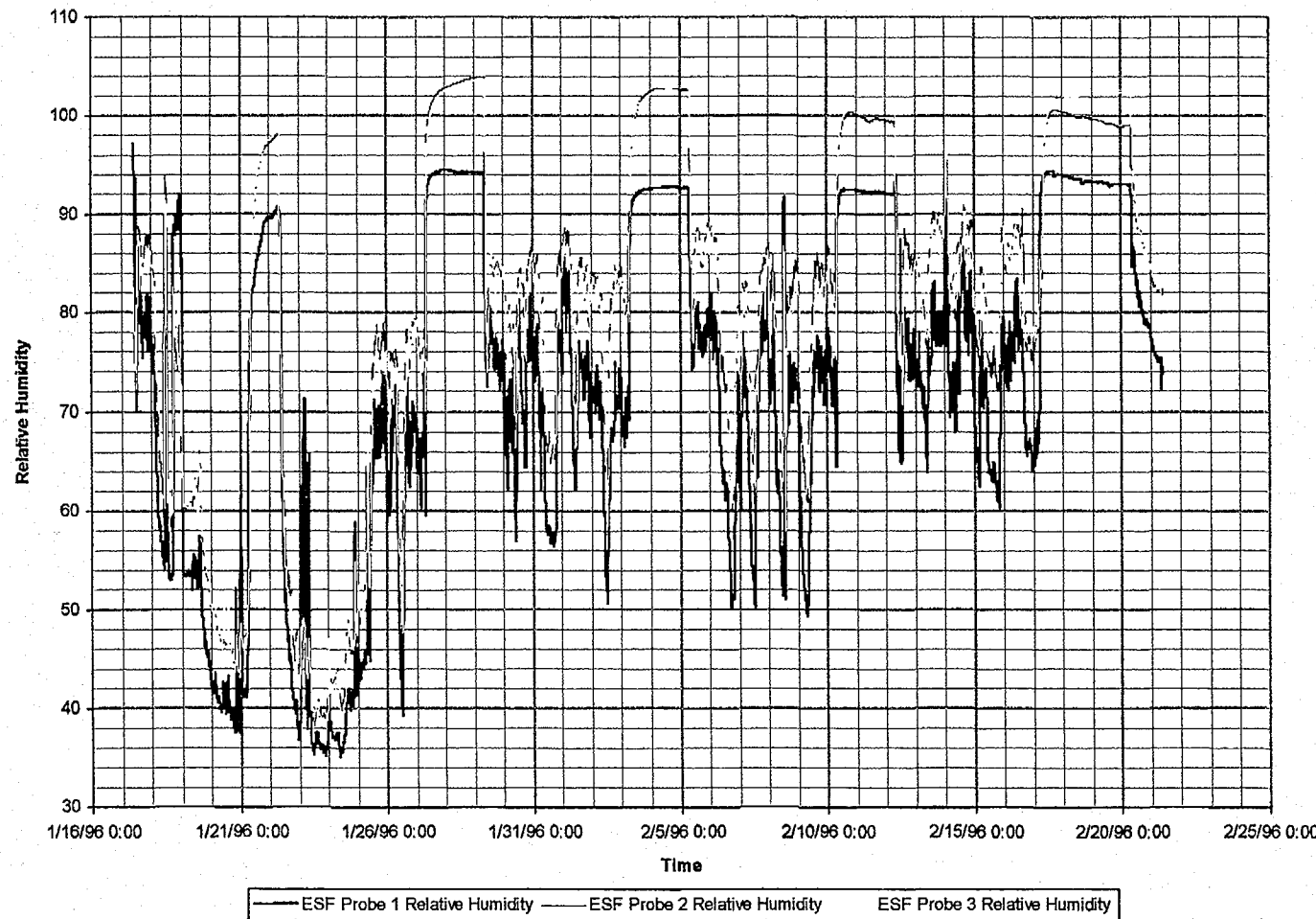


Figure 4-15g Relative Humidity fluctuation with time in ESF Tunnel

August 24, 1996
P2666:24 PMD:\user\projects\NyeCounty\anrep96\figures

Prepared for:
Nye County Nuclear Waste Repository Project Office

Prepared by:
Multimedia Environmental Technology, Inc.
Newport Beach, CA

March 1996

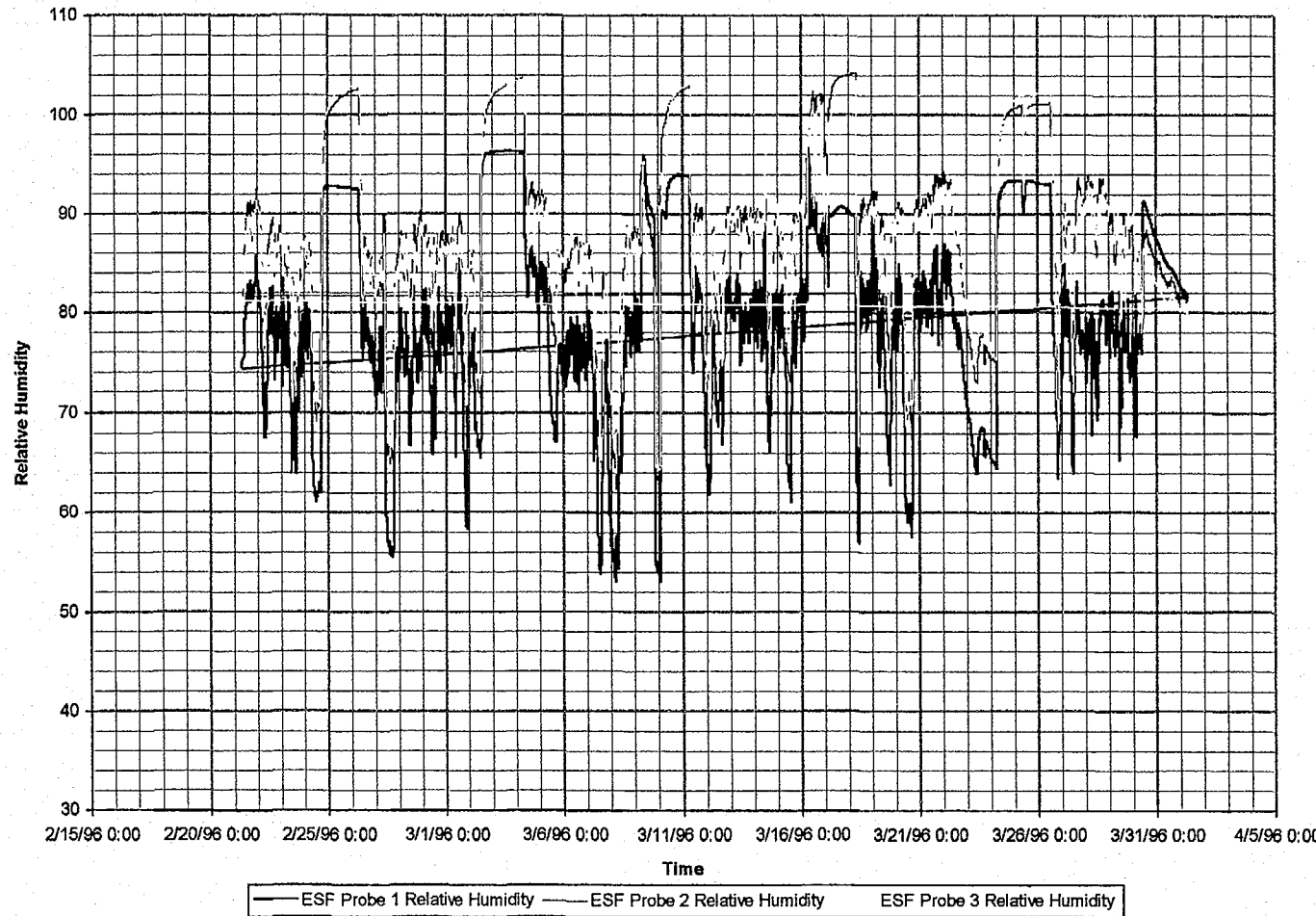


Figure 4-15h Relative Humidity fluctuation with time in ESF Tunnel

APRIL 1996

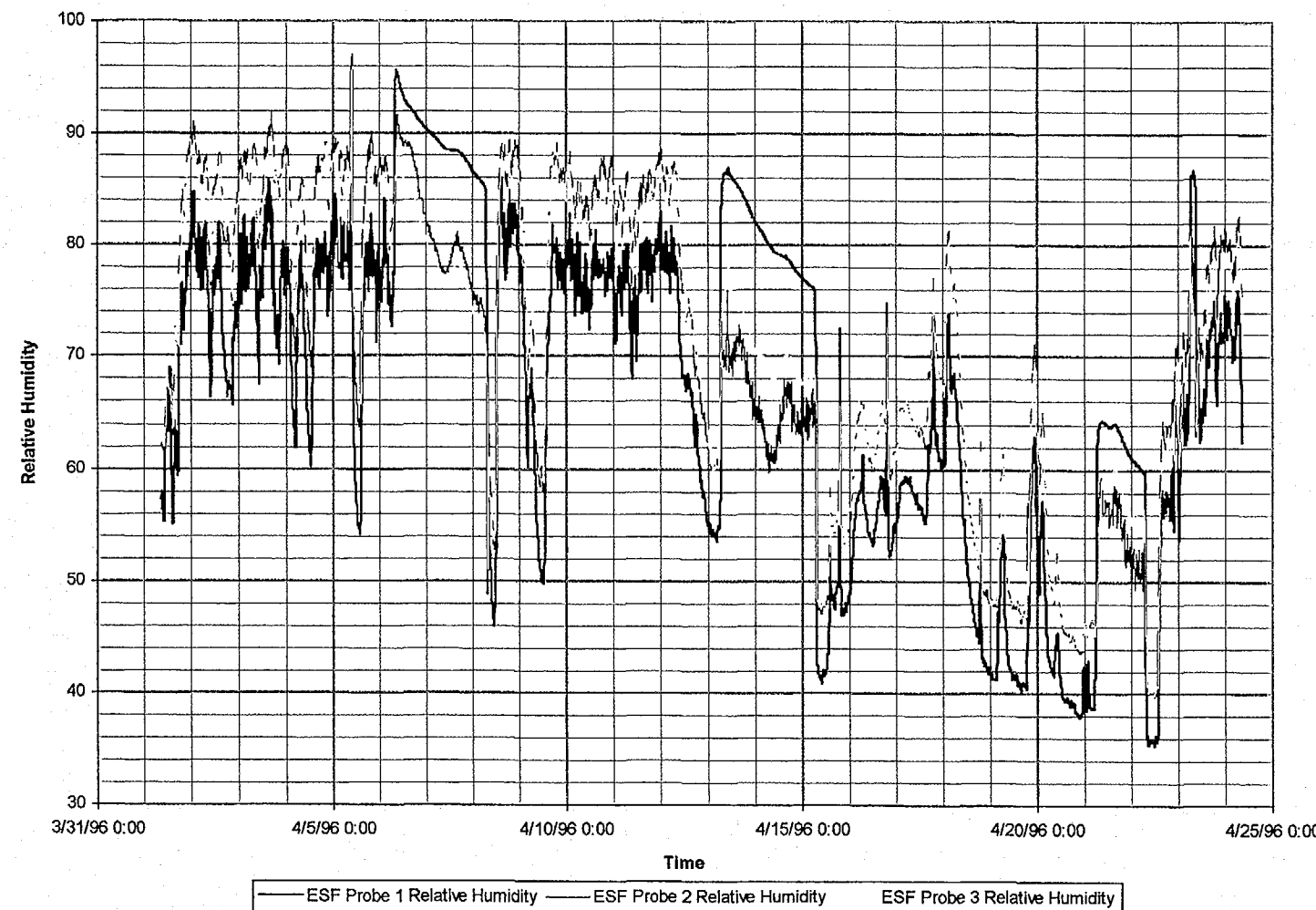


Figure 4-15i Relative Humidity fluctuation with time in ESF Tunnel

MAY 1996

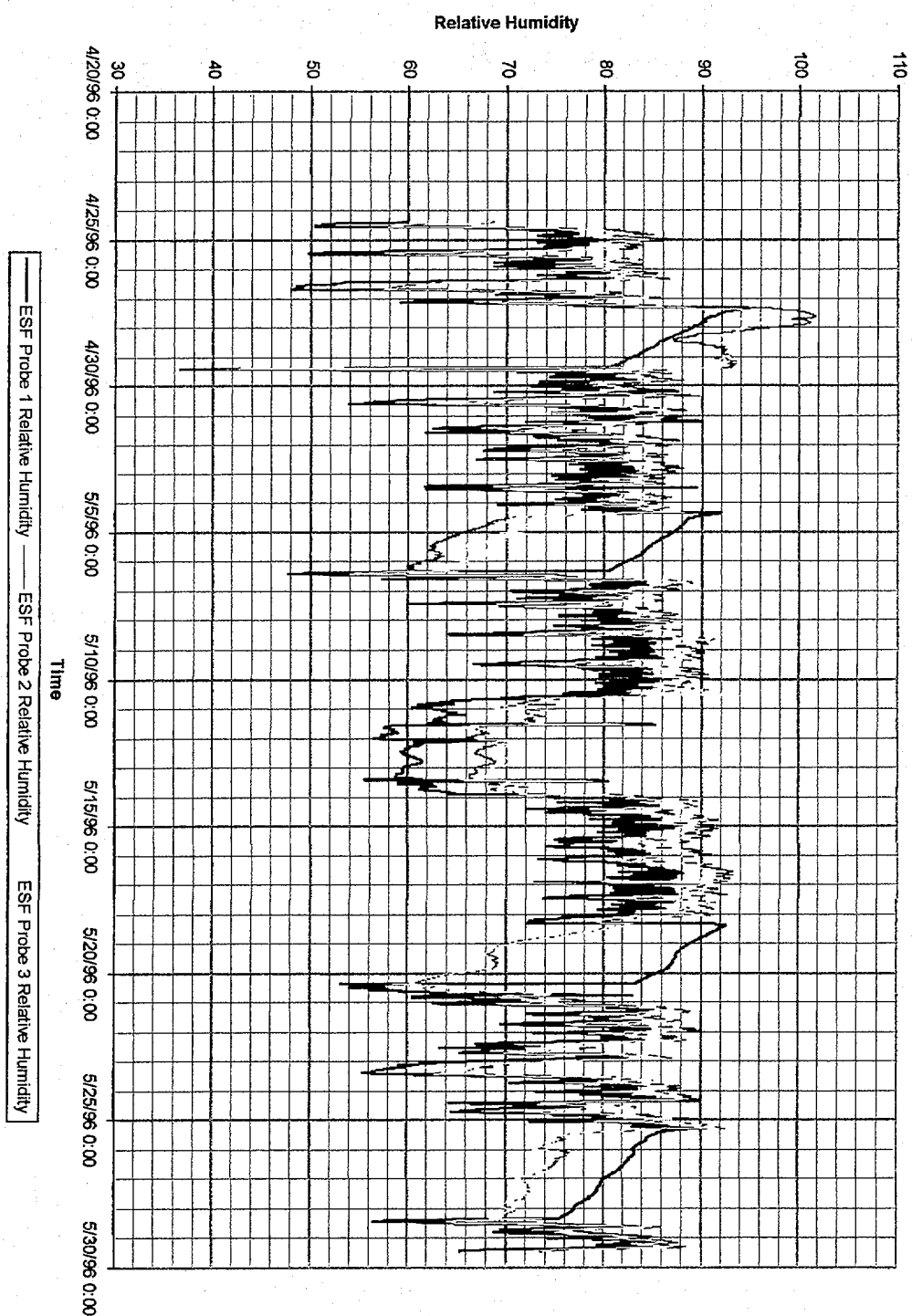


Figure 4-15j Relative Humidity fluctuation with time in ESF Tunnel

August 24, 1996
P266.D:\user\proj\wyoming\mrap\figures

Prepared for:
Nye County Nuclear Waste Repository Project Office

Prepared by:
Multimodal Environmental Technology, Inc.
Newport Beach, CA

JUNE 1996

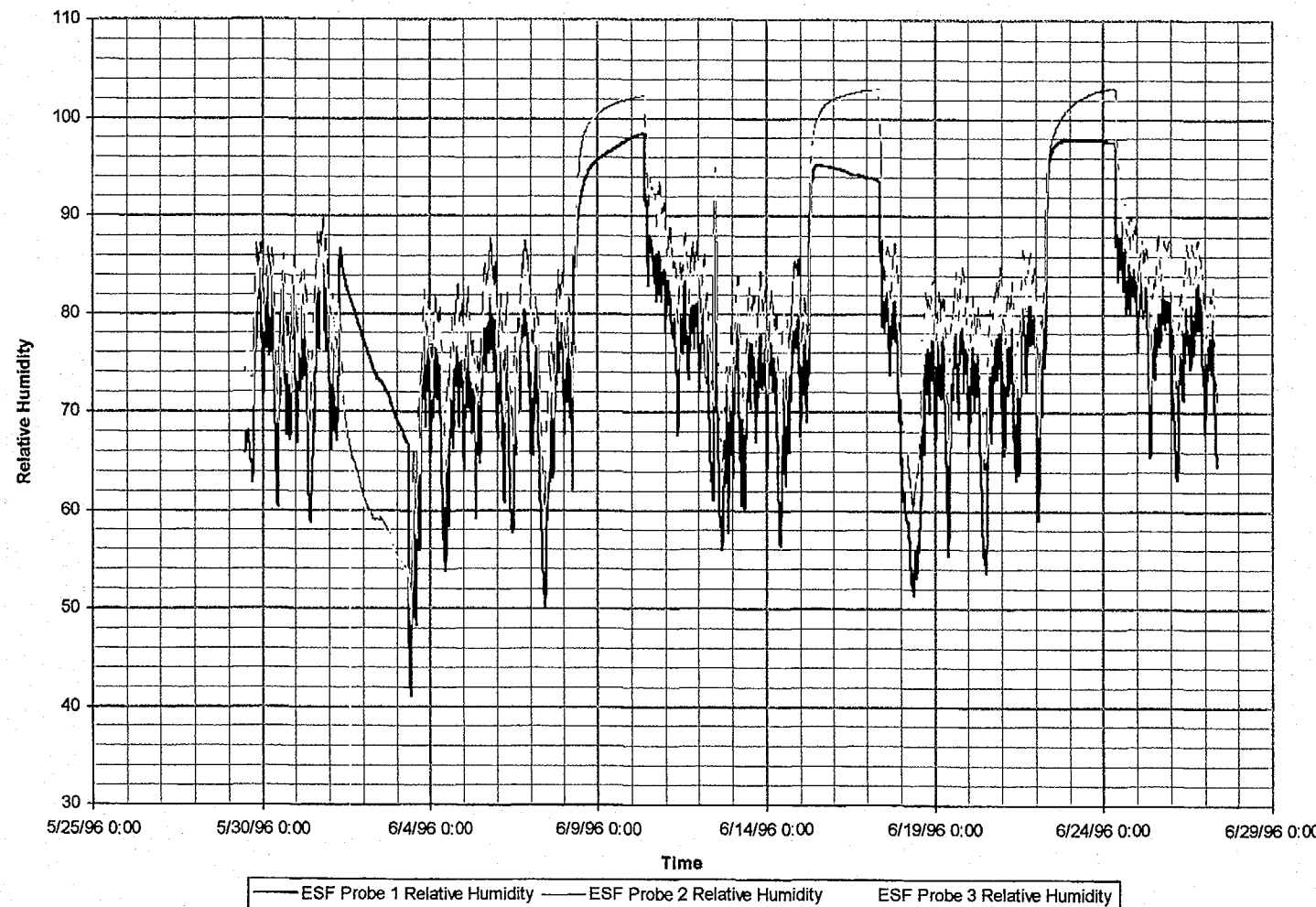


Figure 4-15k Relative Humidity fluctuation with time in ESF Tunnel

August 24, 1996
P266:D:\user\projects\Nye county\annrep96\figures

Prepared for:
Nye County Nuclear Waste Repository Project Office

Prepared by:
Multimedia Environmental Technology, Inc.
Newport Beach, CA

JULY 1996

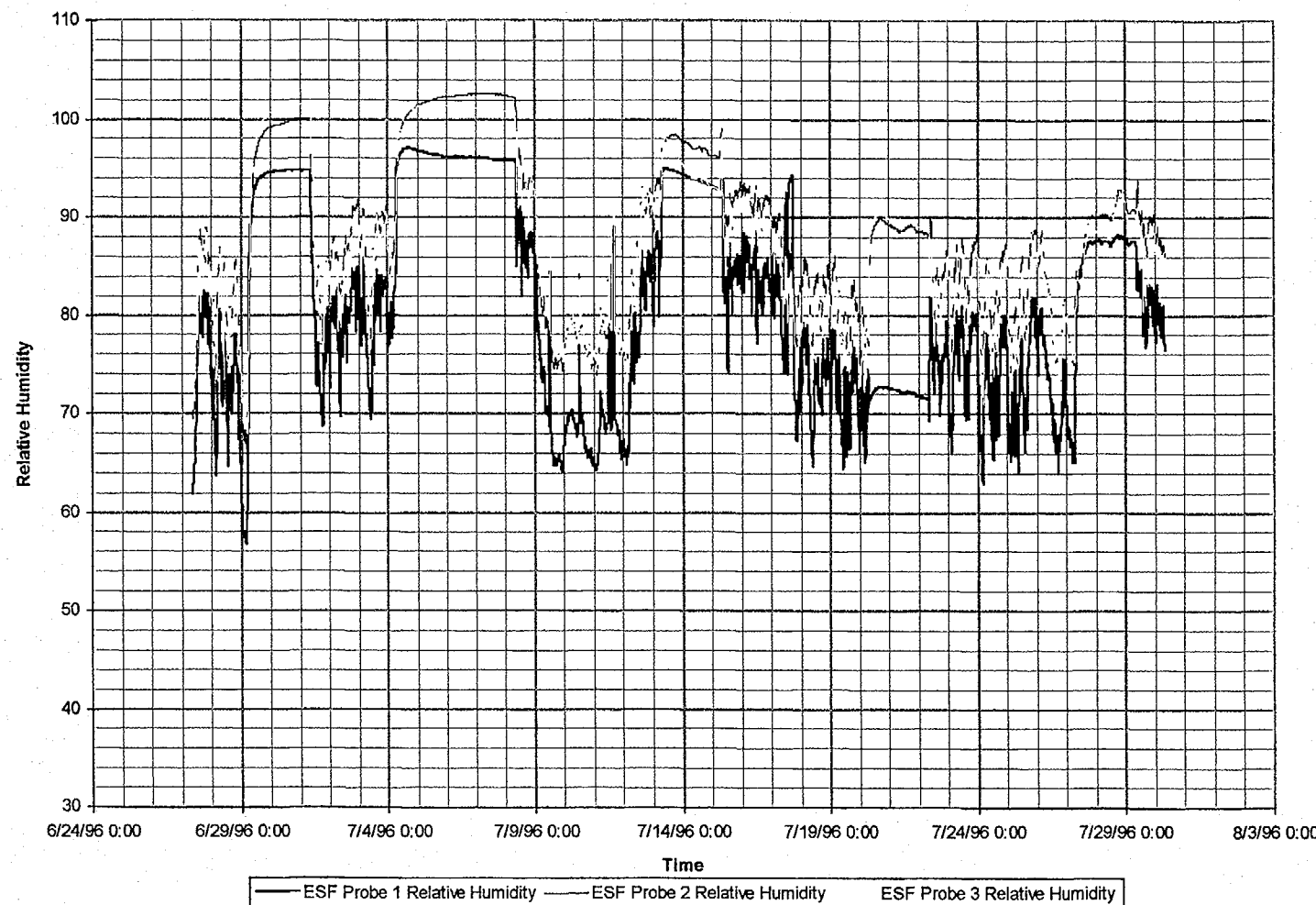


Figure 4-15L Relative Humidity fluctuation with time in ESF Tunnel

August 24, 1996
P266:D:\user\projects\NyeCounty\annrep96\figures

Prepared for:
Nye County Nuclear Waste Repository Project Office

Prepared by:
Multimedia Environmental Technology, Inc.
Newport Beach, CA

August 1996

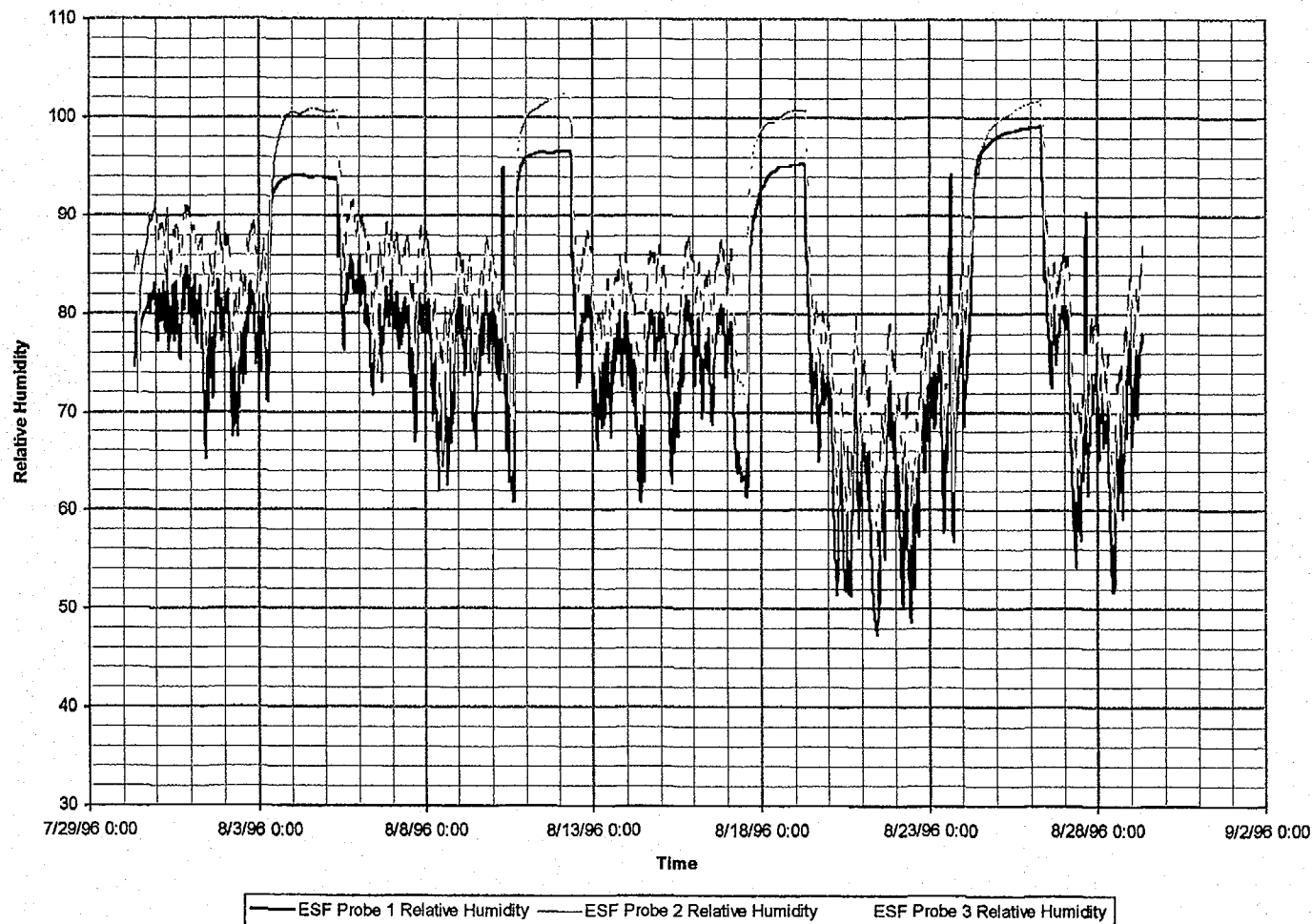


Figure 4-15m Relative Humidity fluctuation with time in ESF Tunnel

August 24, 1996
P2667:39 AMD:\user\projects\Nye County\unrep96\figures

Prepared for:
Nye County Nuclear Waste Repository Project Office

Prepared by:
Multimedia Environmental Technology, Inc.
Newport Beach, CA

AUGUST 1995

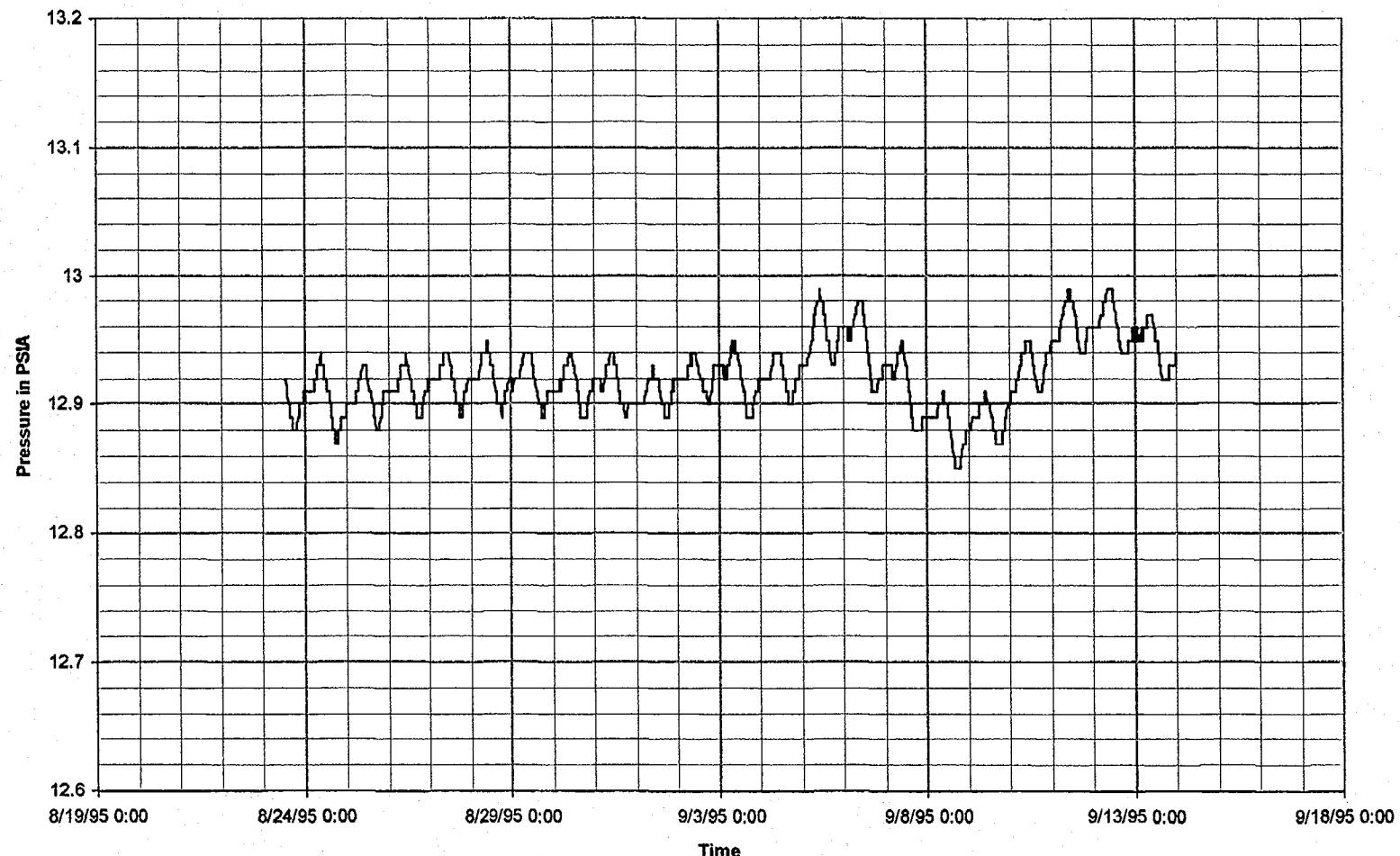


Figure 4-16a Pressure fluctuation with time in ESF Tunnel

August 24, 1996
P266:D:\user\projects\Nye\count\annrep96\figures

Prepared for:
Nye County Nuclear Waste Repository Project Office

Prepared by:
Multimedia Environmental Technology, Inc.
Newport Beach, CA

SEPTEMBER 1995

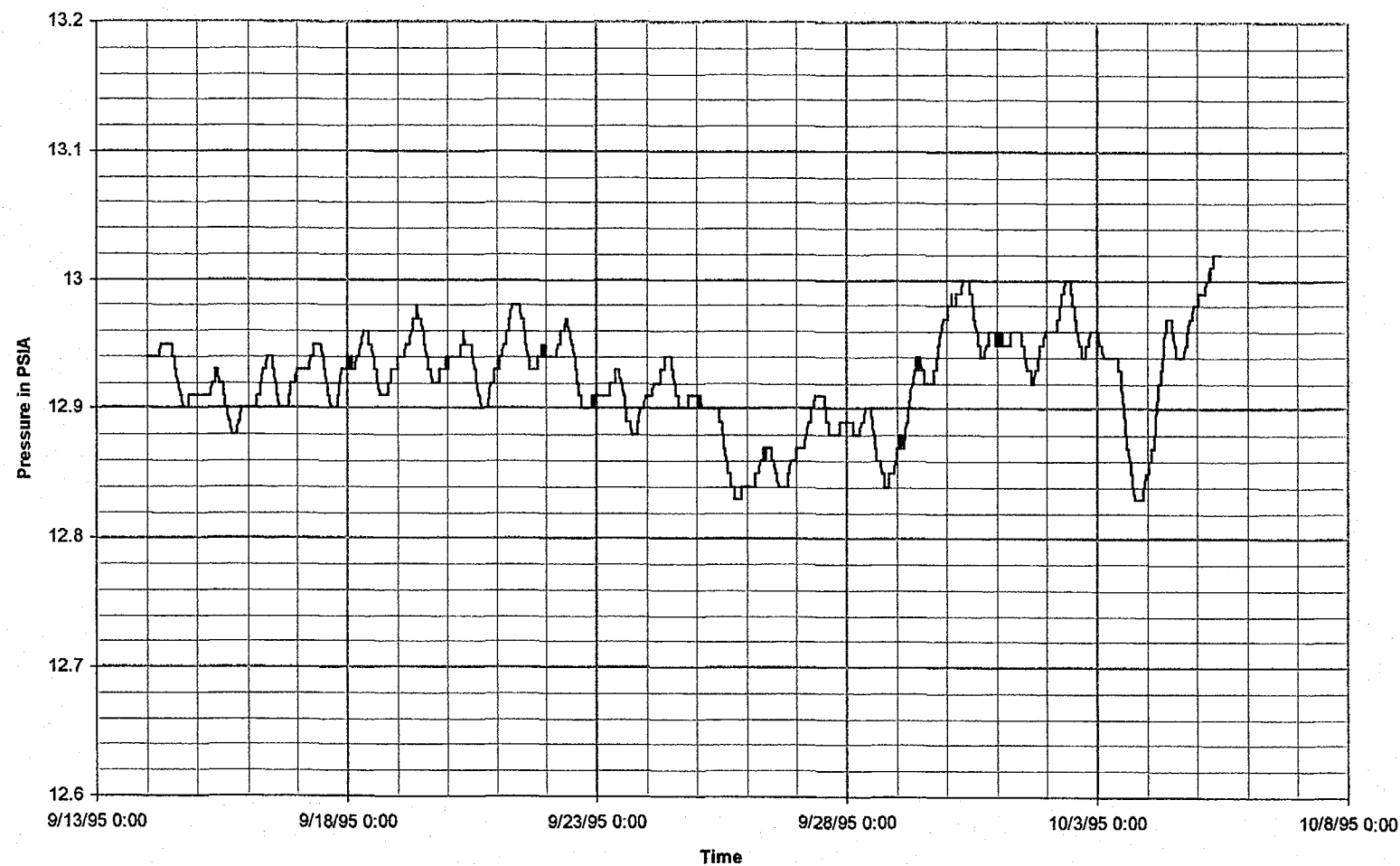


Figure 4-16b Pressure fluctuation with time in ESF Tunnel

August 24, 1996
P266:D:\user\projects\Nyecounty\annrep96\figures

Prepared for:
Nye County Nuclear Waste Repository Project Office

Prepared by:
Multimedia Environmental Technology, Inc.
Newport Beach, CA

OCTOBER 1995

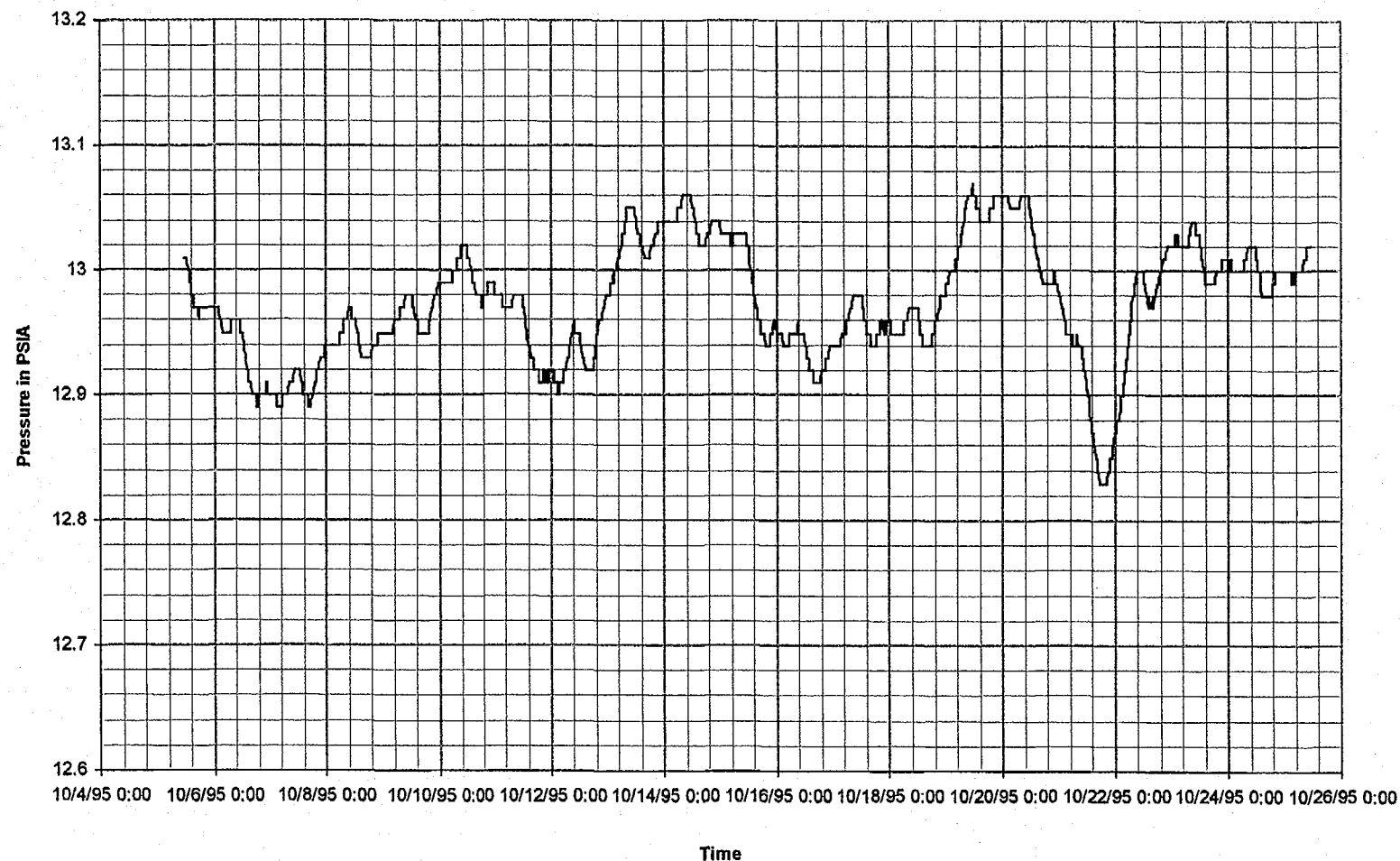


Figure 4-16c Pressure fluctuation with time in ESF Tunnel

NOVEMBER 1995

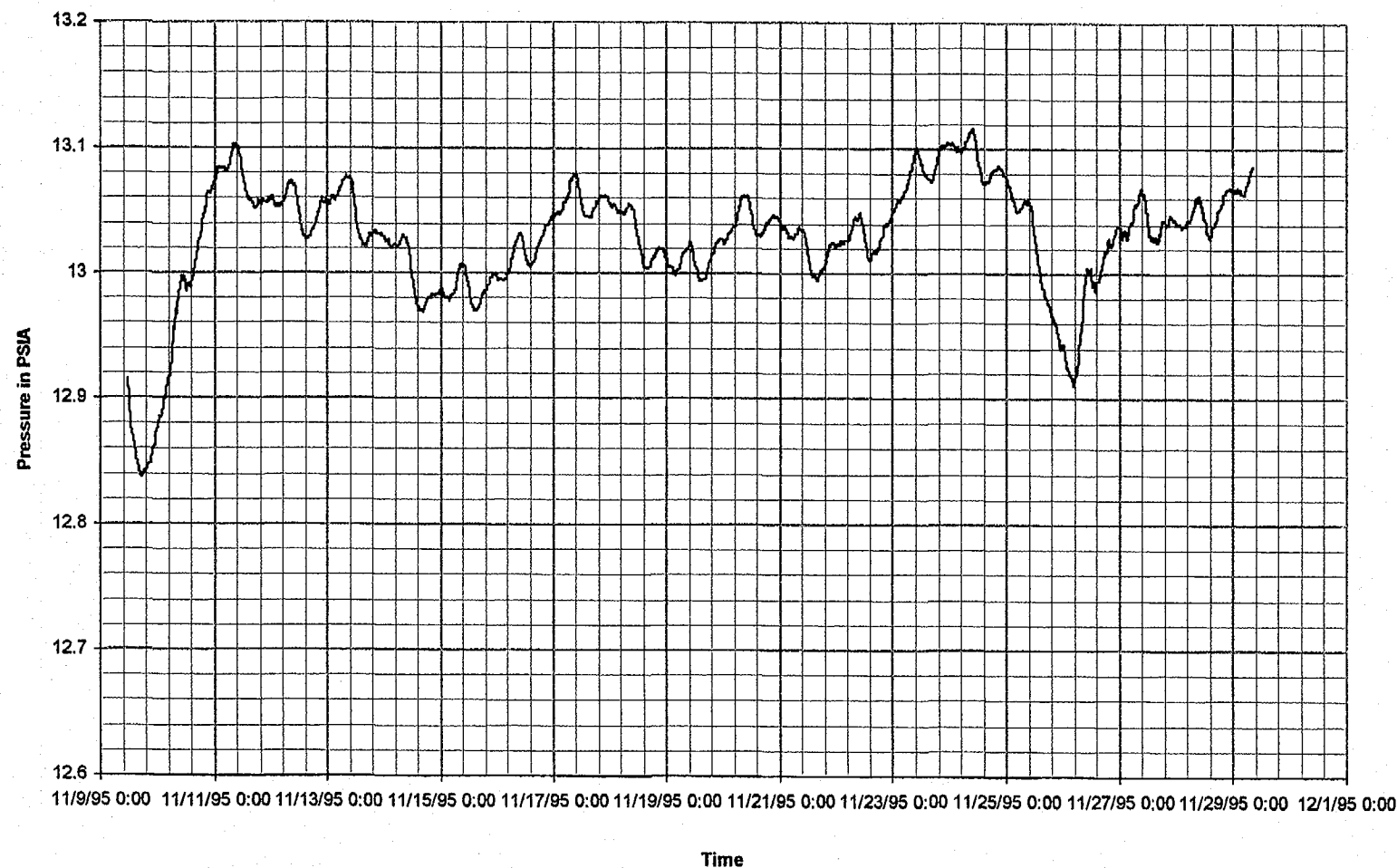


Figure 4-16d Pressure fluctuation with time in ESF Tunnel

August 24, 1996
P266:D:\user\project\Nye\county\annrep96\figures

Prepared for:
Nye County Nuclear Waste Repository Project Office

Prepared by:
Multimedia Environmental Technology, Inc.
Newport Beach, CA

DECEMBER 1995

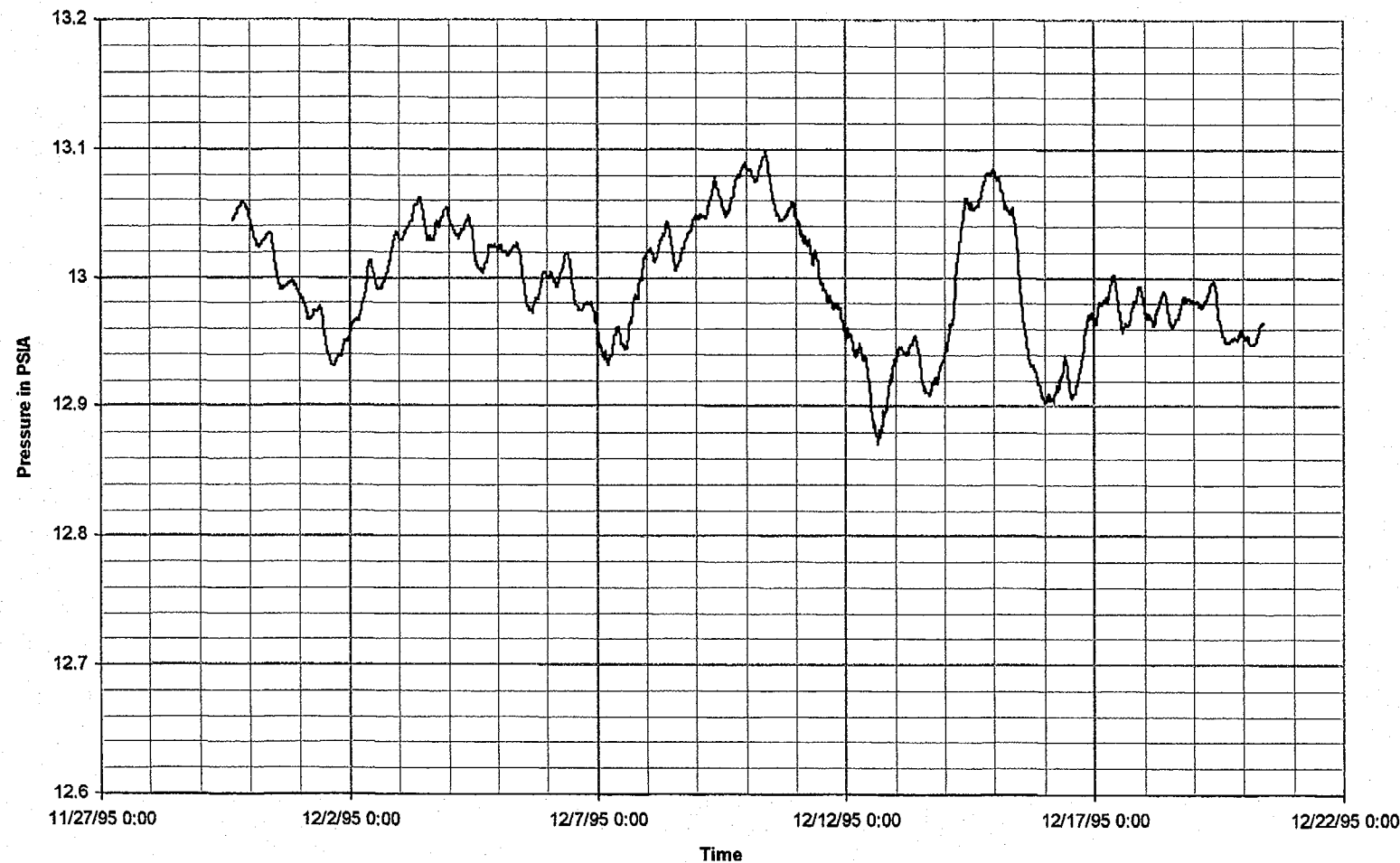


Figure 4-16e Pressure fluctuation with time in ESF Tunnel

August 24, 1996
P266:D:\user\projects\Nyecounty\annrep96\figures

Prepared for:
Nye County Nuclear Waste Repository Project Office

Prepared by:
Multimedia Environmental Technology, Inc.
Newport Beach, CA

JANUARY 1996

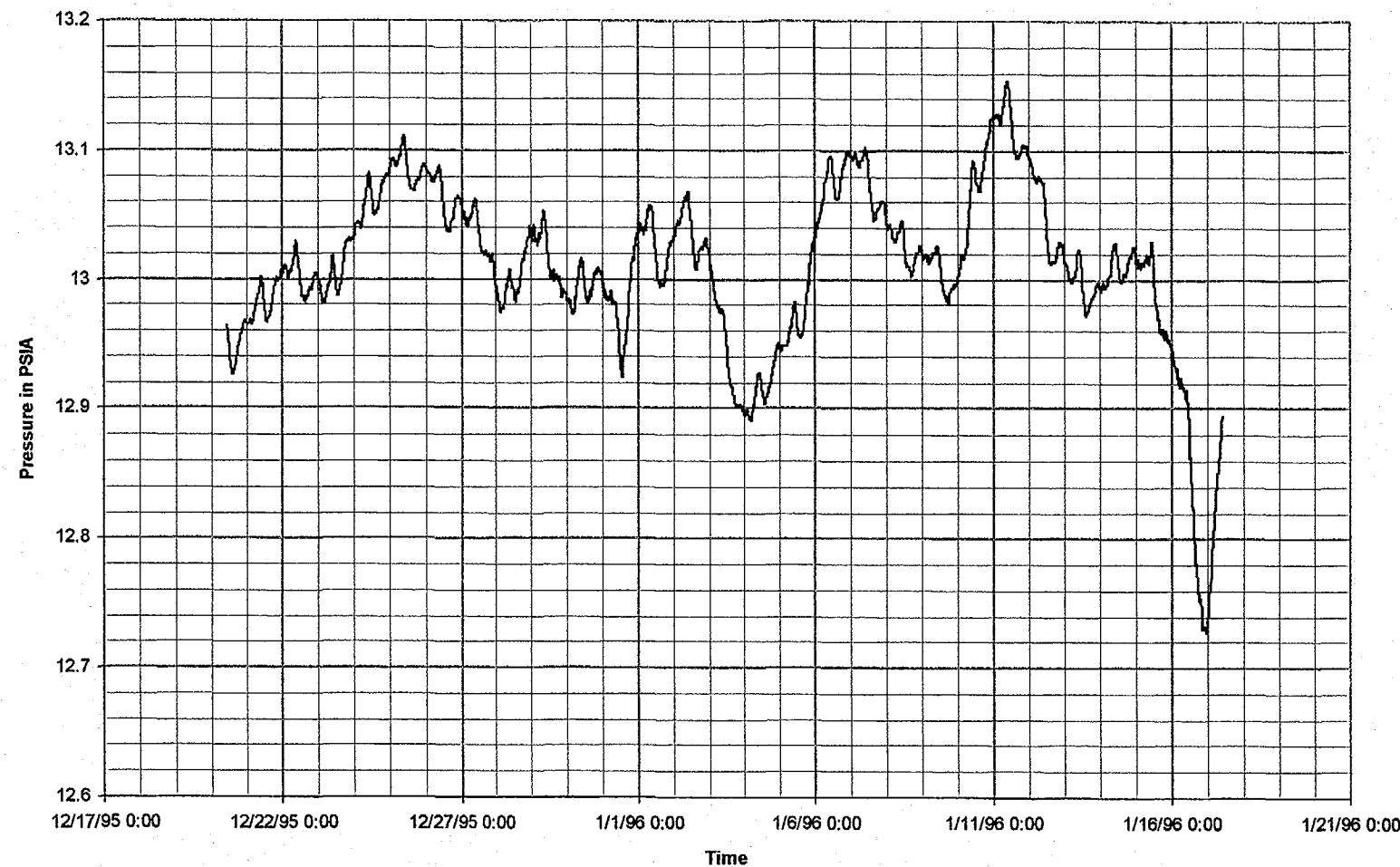


Figure 4-16f Pressure fluctuation with time in ESF Tunnel

FEBRUARY 1996

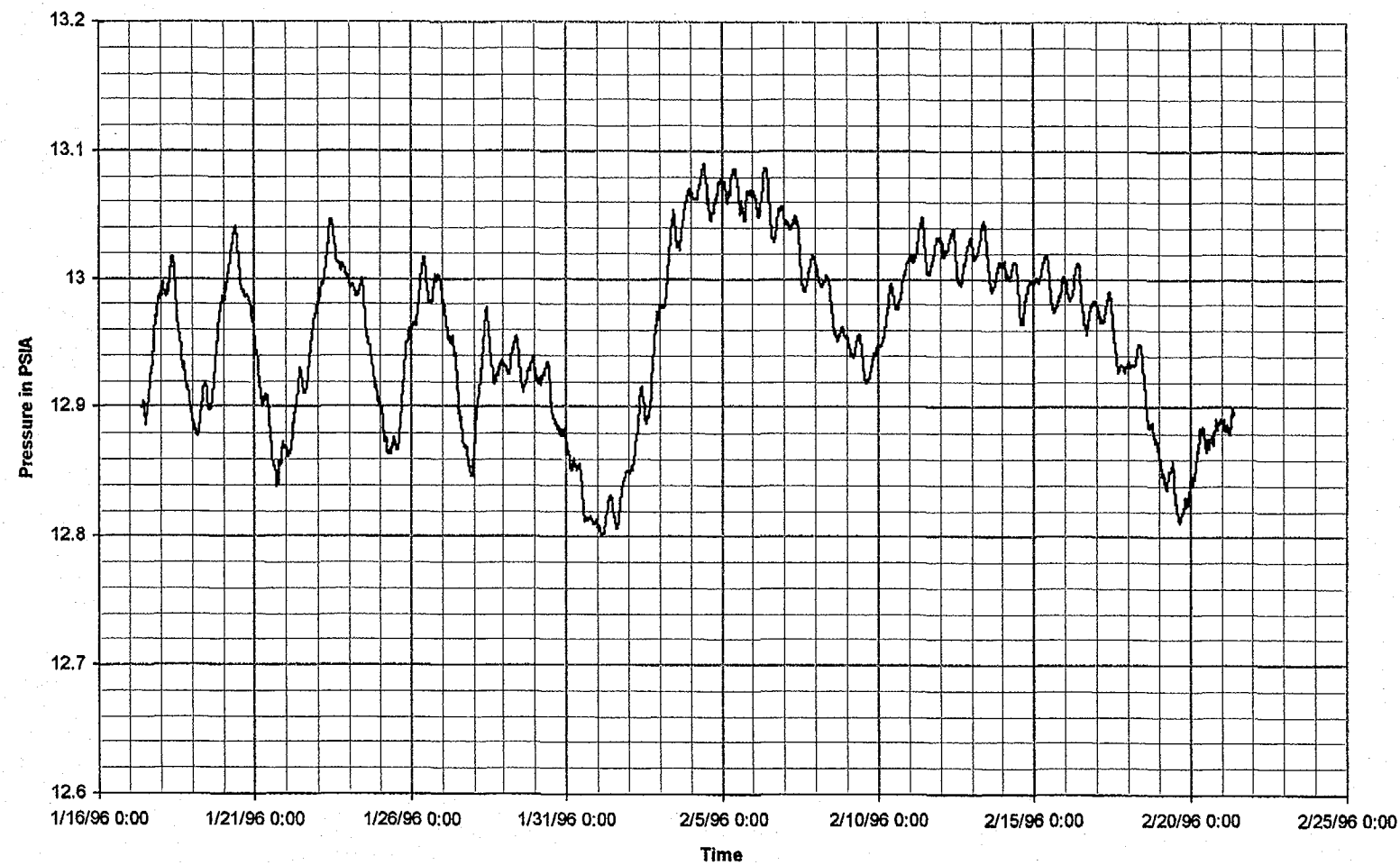


Figure 4-16g Pressure fluctuation with time in ESF Tunnel

August 24, 1996
P266:D:\user\projects\Nye County\annrep96\figures

Prepared for:
Nye County Nuclear Waste Repository Project Office

Prepared by:
Multimedia Environmental Technology, Inc.
Newport Beach, CA

MARCH 1996

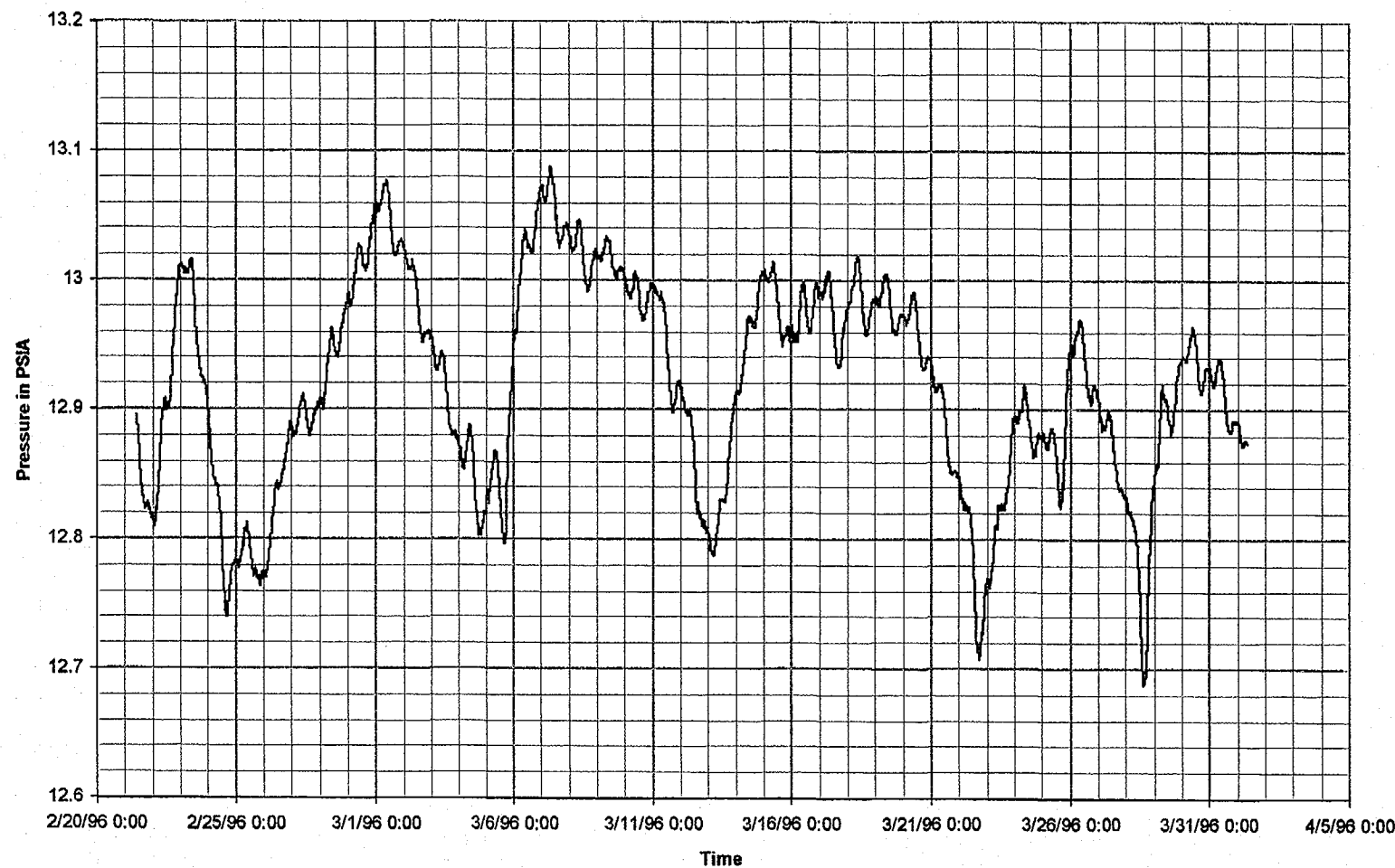


Figure 4-16h Pressure fluctuation with time in ESF Tunnel

August 24, 1996
P260:D:\user\proj0ct\Nye\county\annrep96\figures

Prepared for:
Nye County Nuclear Waste Repository Project Office

Prepared by:
Multimedia Environmental Technology, Inc.
Newport Beach, CA

APRIL 1996

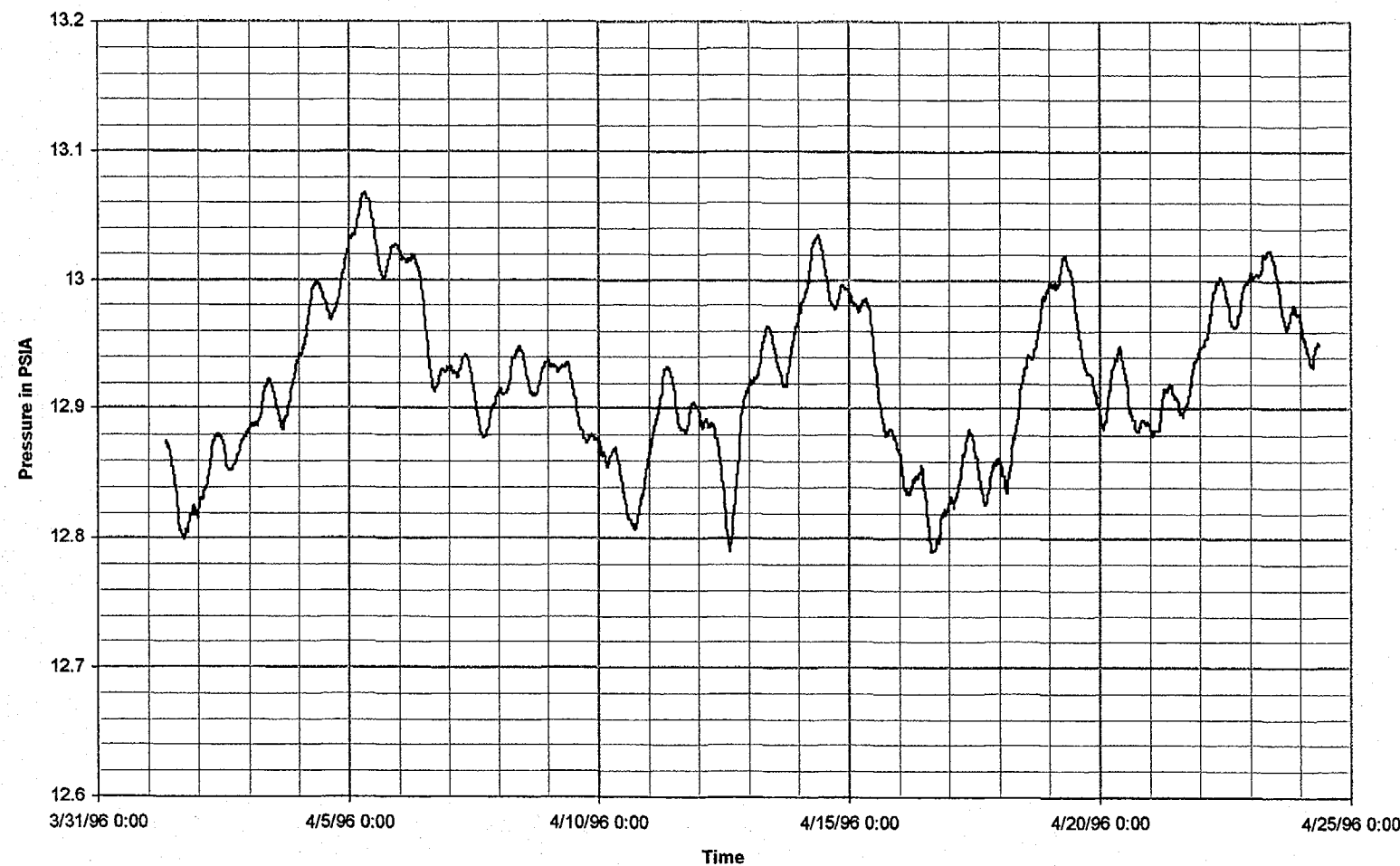


Figure 4-16i Pressure fluctuation with time in ESF Tunnel

MAY 1996

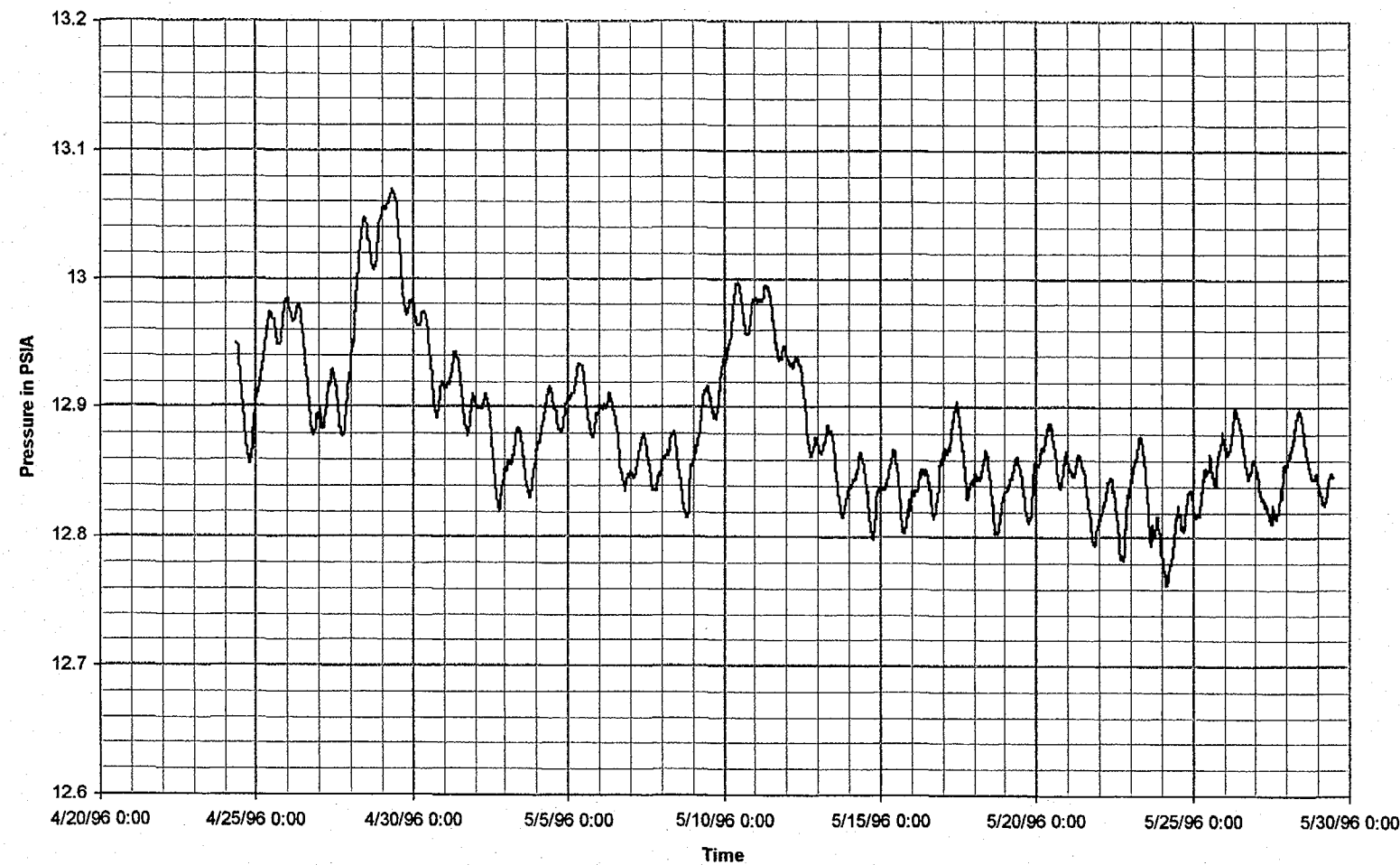


Figure 4-16 Pressure fluctuation with time in ESF Tunnel

August 24, 1996
P266:D:\uacr\projects\Nye\county\annrep96\figures

Prepared for:
Nye County Nuclear Waste Repository Project Office

Prepared by:
Multimedia Environmental Technology, Inc.
Newport Beach, CA

JUNE 1996

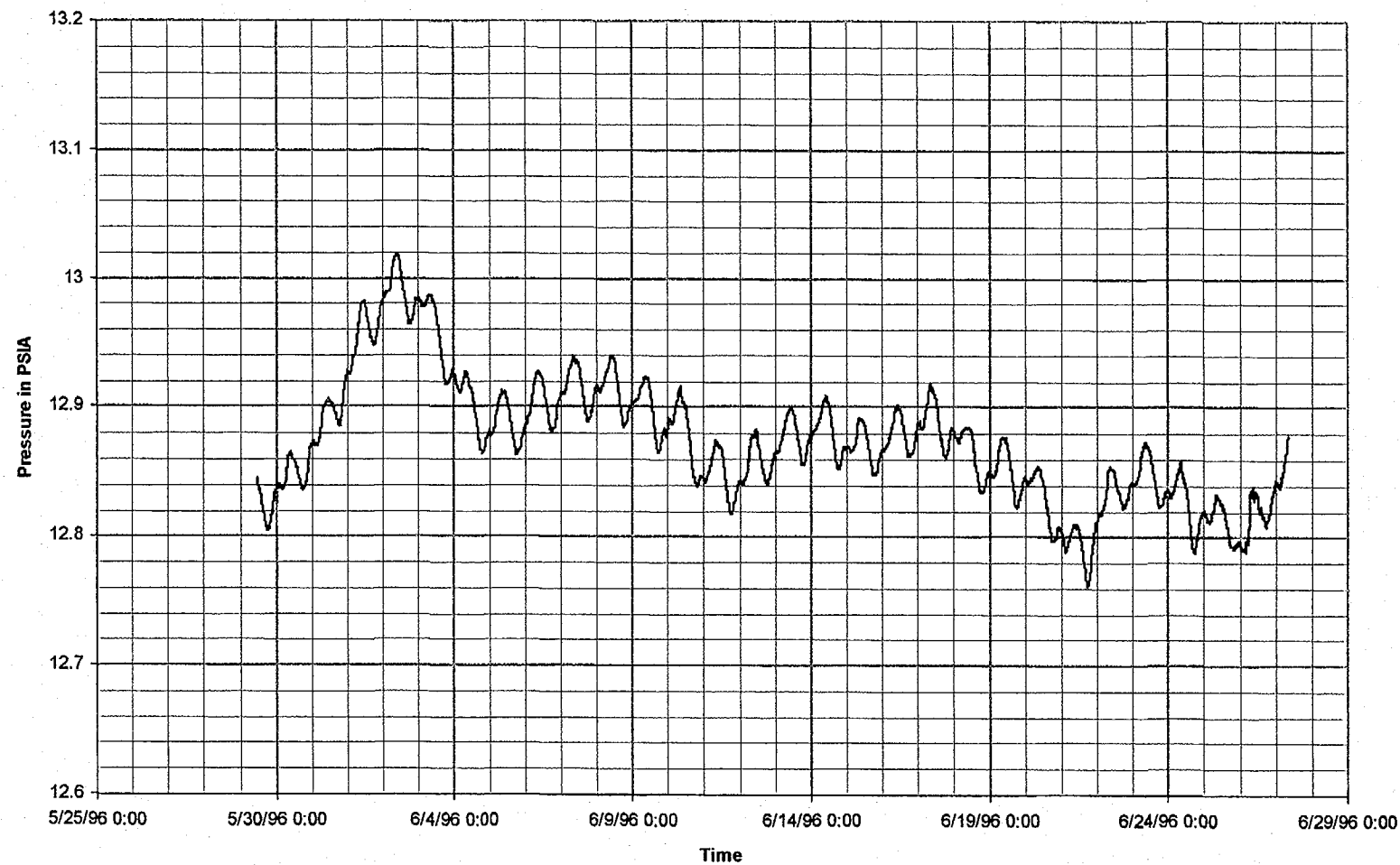


Figure 4-16k Pressure fluctuation with time in ESF Tunnel

August 24, 1996
P266:D:\user\projects\Nye county\annrep96\figures

Prepared for:
Nye County Nuclear Waste Repository Project Office

Prepared by:
Multimedia Environmental Technology, Inc.
Newport Beach, CA

JULY 1996

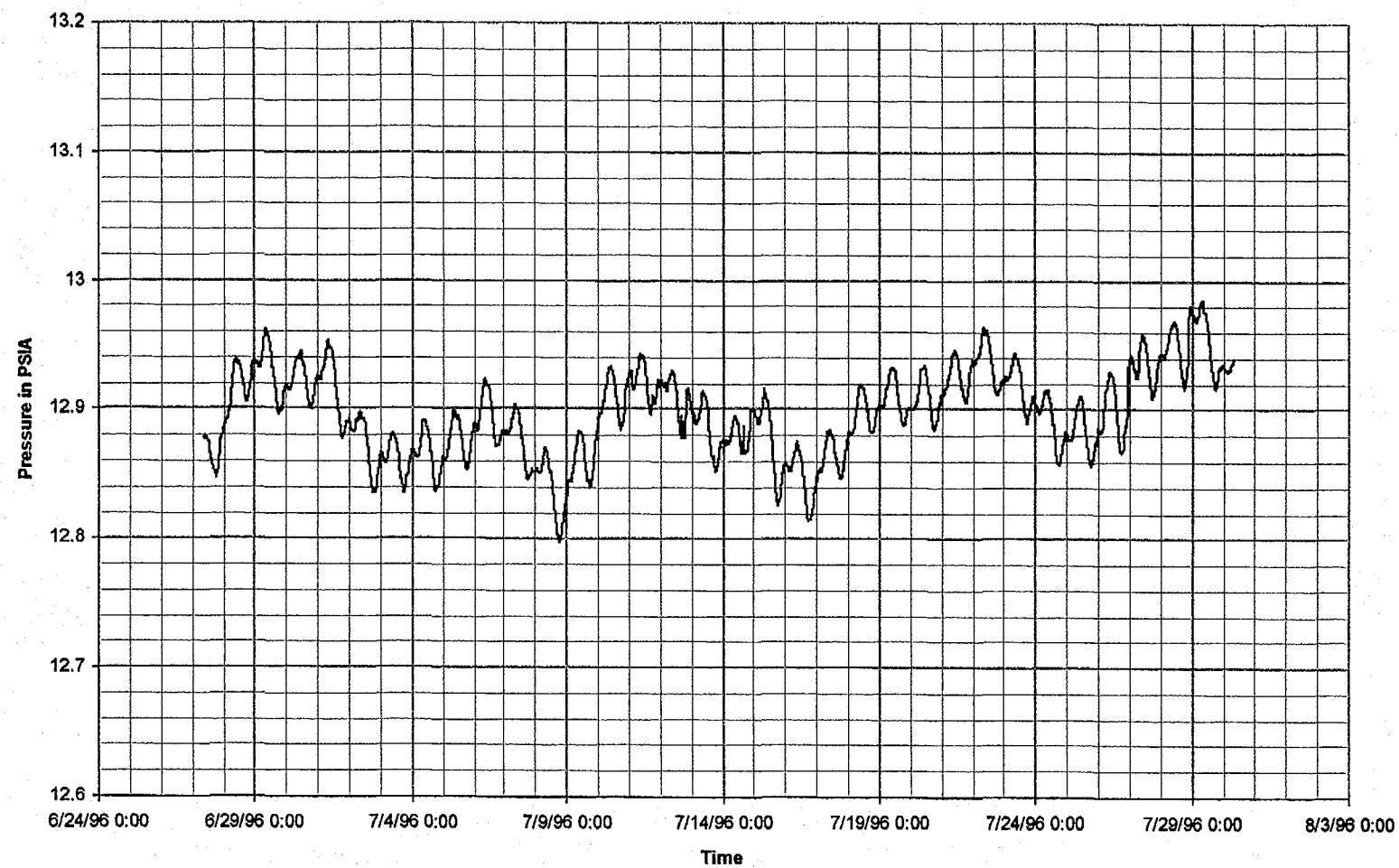


Figure 4-16L Pressure fluctuation with time in ESF Tunnel

August 1996

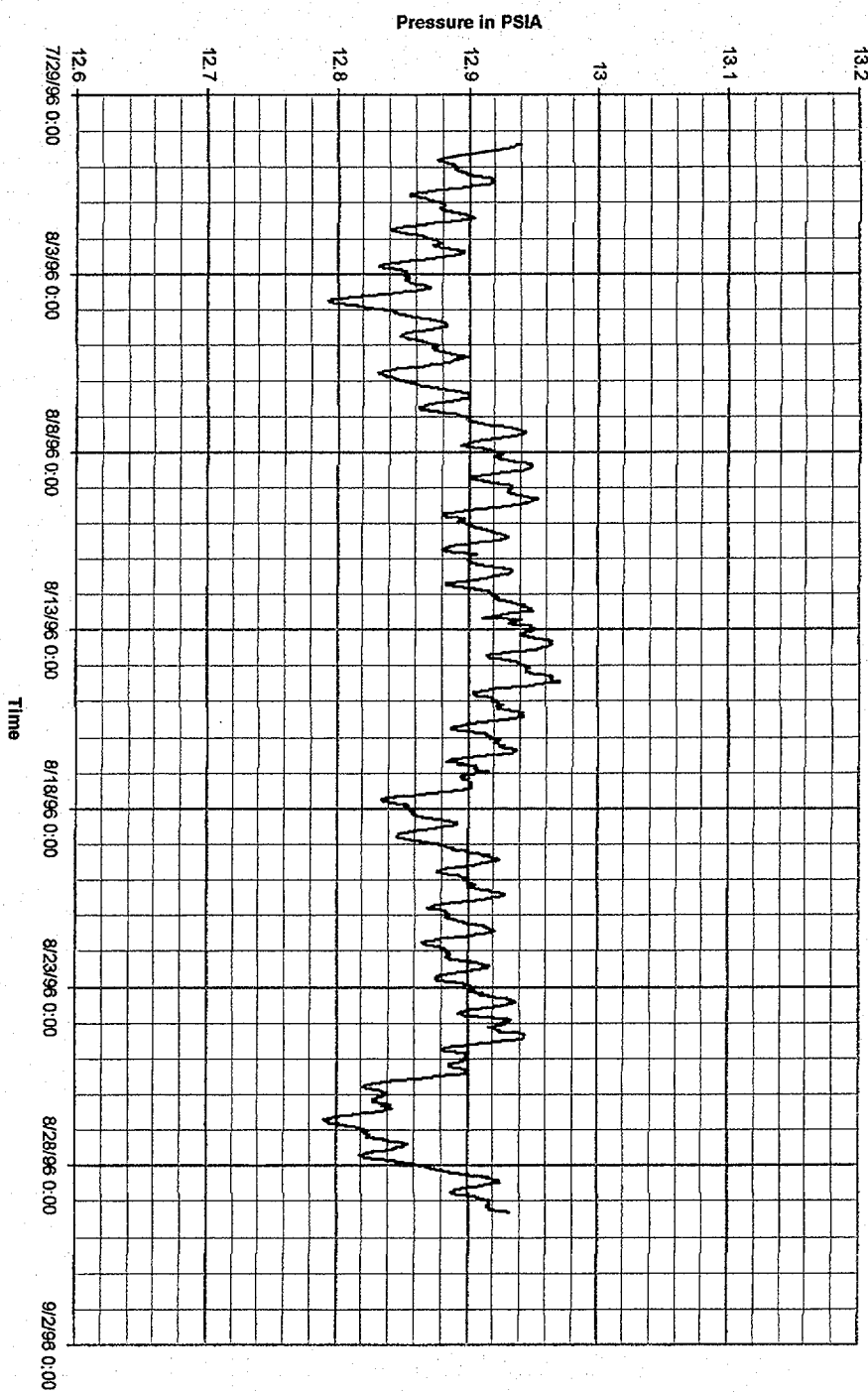


Figure 4-16m Pressure fluctuation with time in ESF Tunnel

August 24, 1996
P2467-59 AMD:usw:project:NyeCountyEnvmp80Migra

Prepared for:
Nye County Nuclear Waste Repository Project Office

Prepared by:
Multimedia Environmental Technology, Inc.
Newport Beach, CA

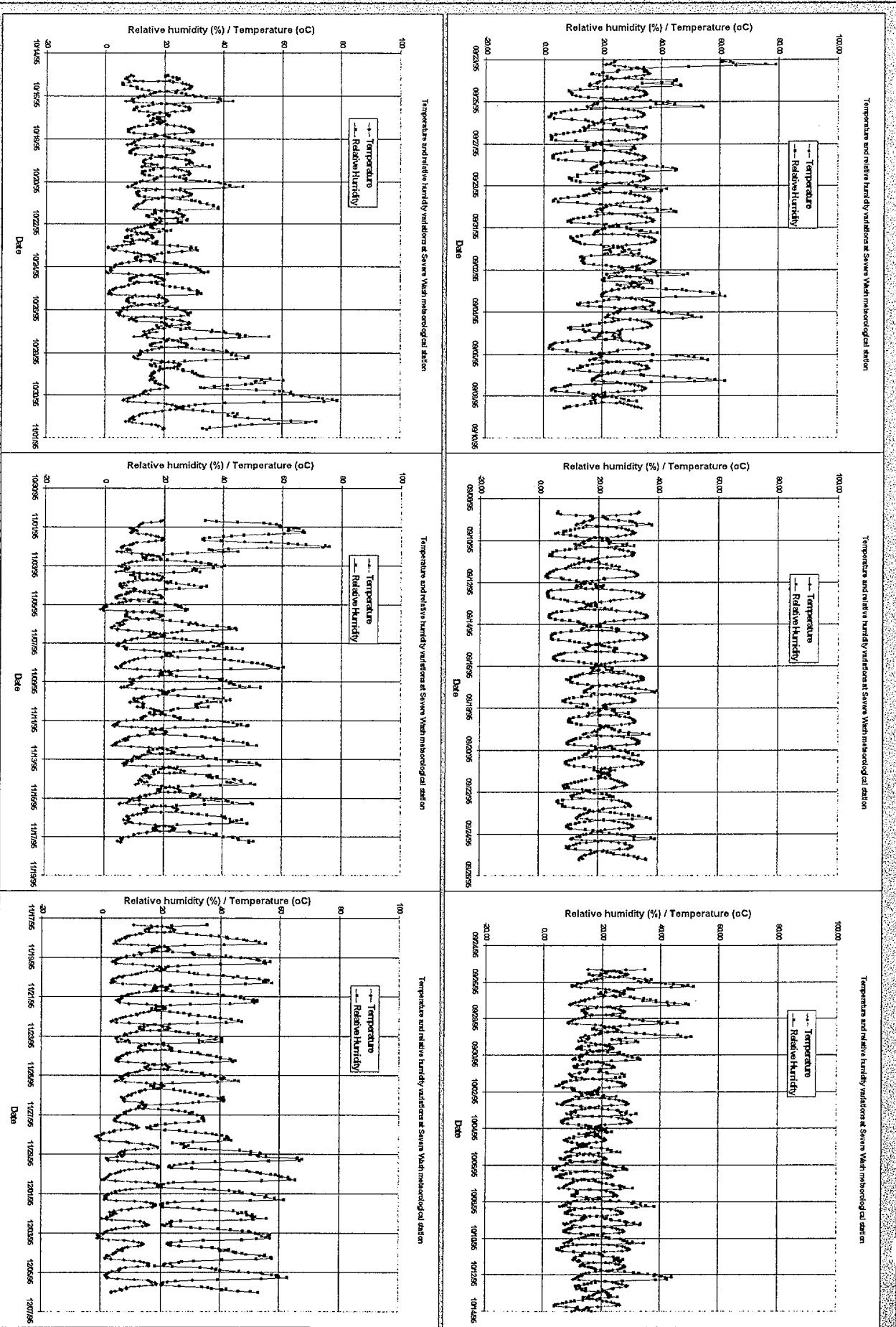


Figure 4-17 - Temperature and humidity variation at Severe Wash meteorological station.

August 24, 1996
P26607-07 PMD user\proj\sevewash\temp\ppg\Figures

Prepared for:
Nye County Nuclear Waste Repository Project Office

Prepared by:
Multimedia Environmental Technologies, Inc.
Newport Beach, CA

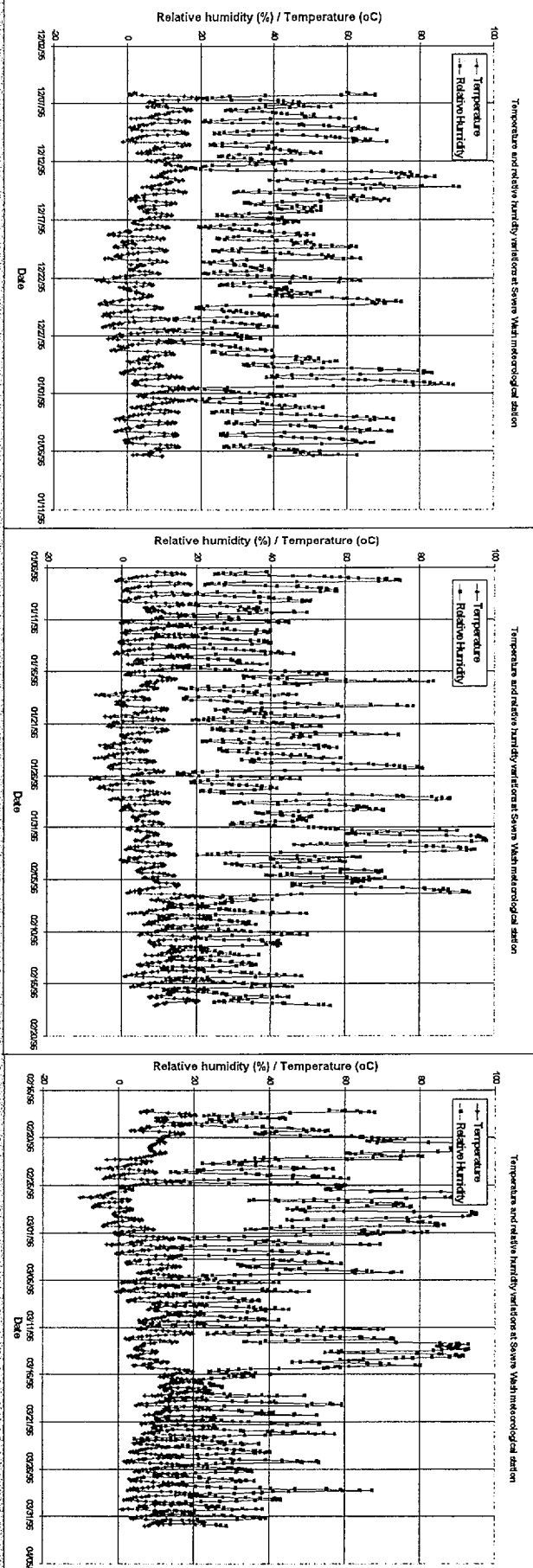


Figure 4-17(Cont.) - Temperature and humidity variation at Severe Wash meteorological station.

August 24, 1996
P2607-07 PMD:due\projects\Nye\count\annapp\figures

Prepared for:
Nye County Nuclear Waste Repository Project Office

Prepared by:
Multimedia Environmental Technology, Inc.
Newport Beach, CA

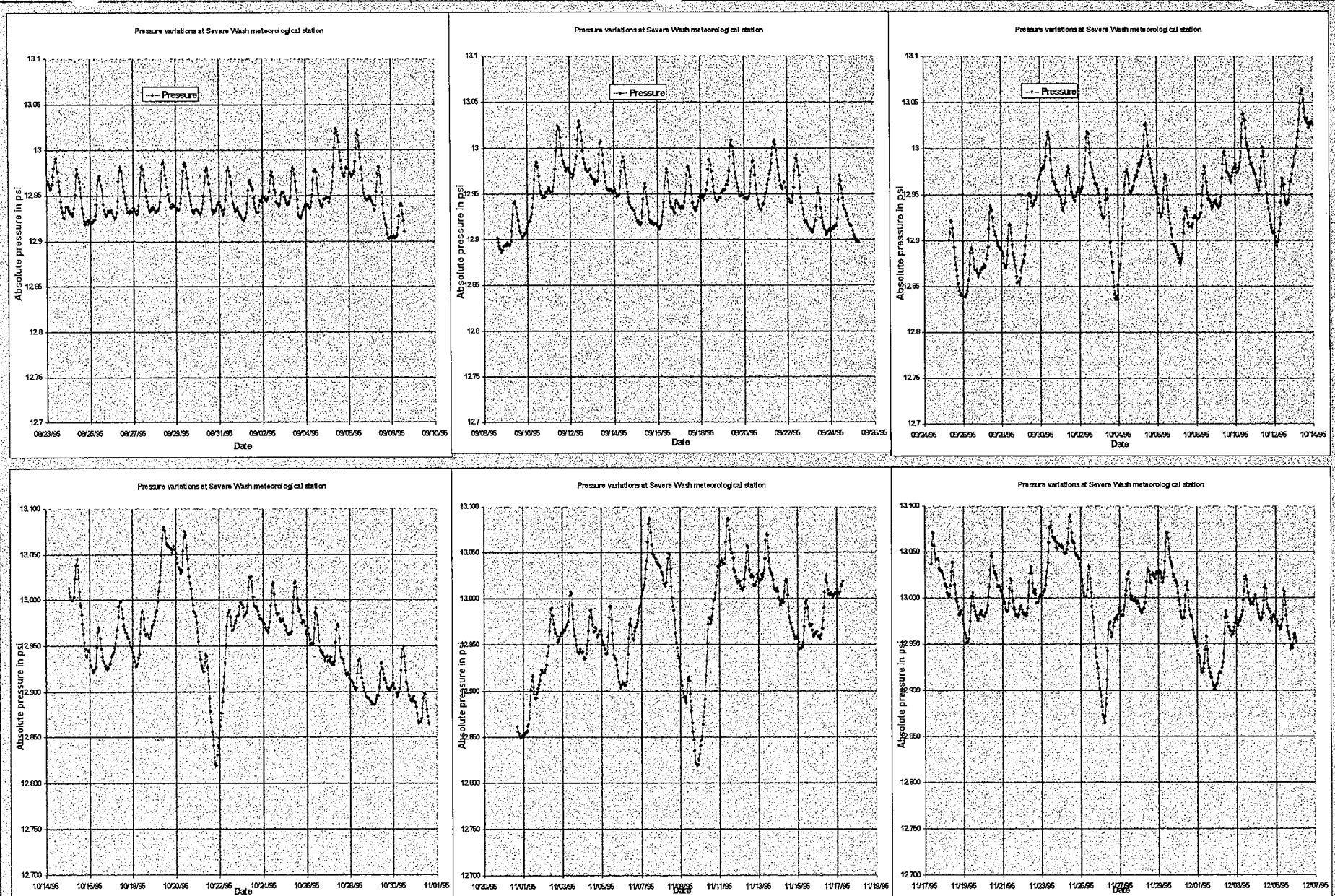


Figure 4-18 - Pressure variation at Severe Wash meteorological station.

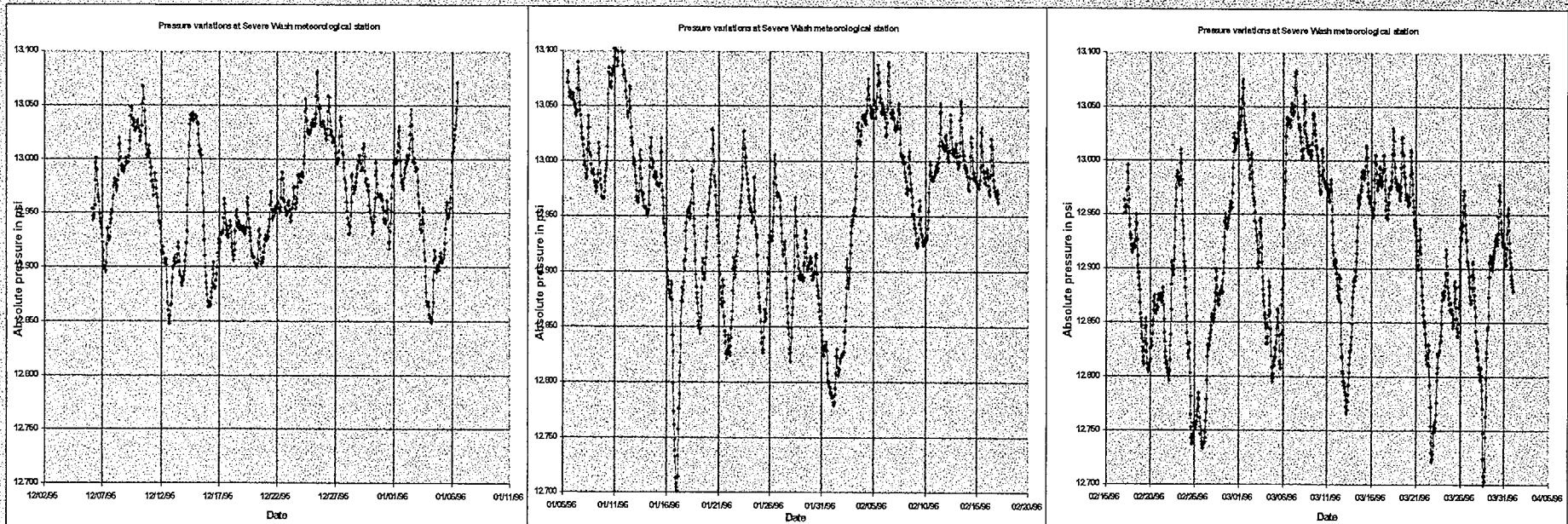


Figure 4-18 (Cont.) - Pressure variation at Severe Wash meteorological station.

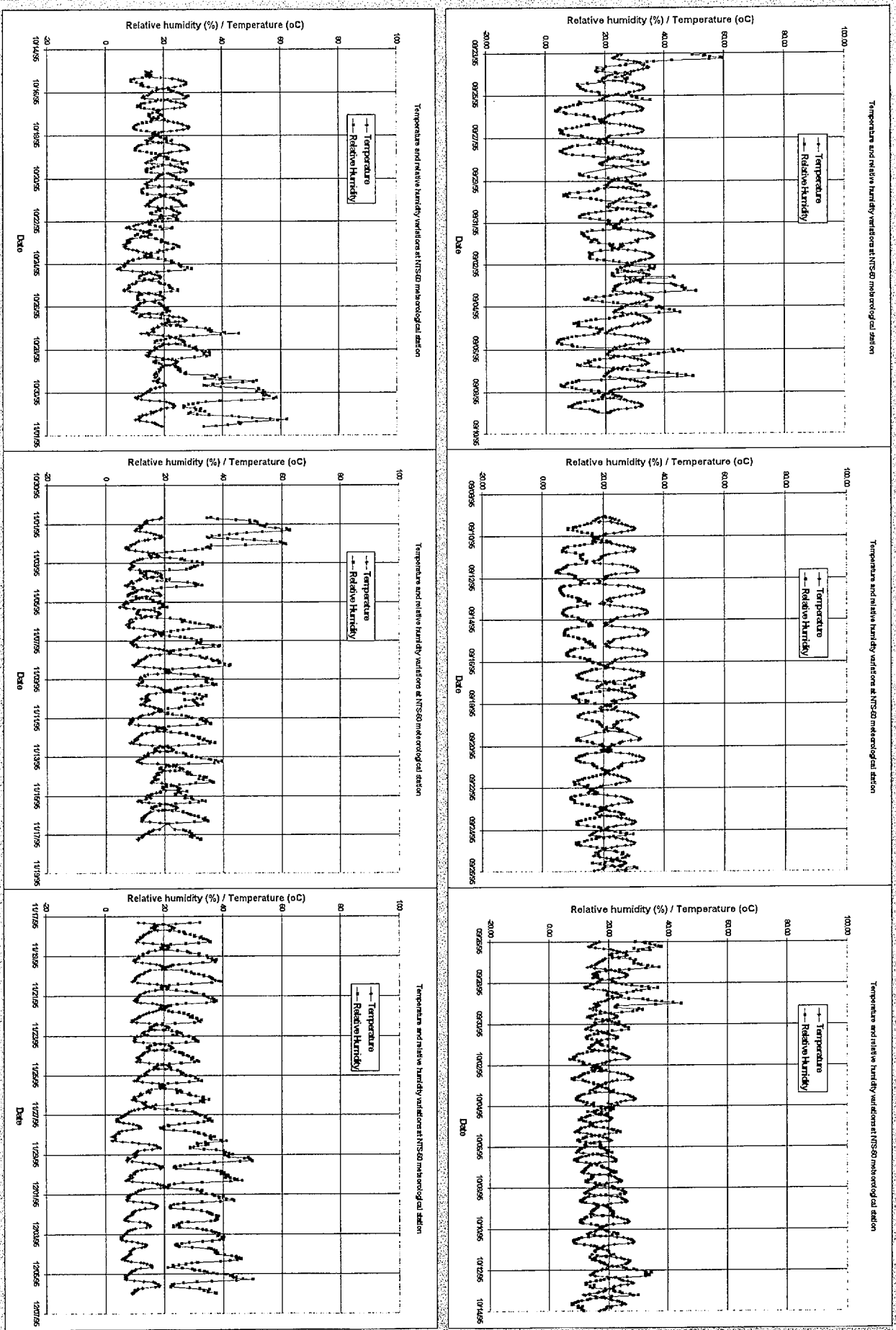


Figure 4-19 - Temperature and humidity variation at NTS-60 meteorological station.

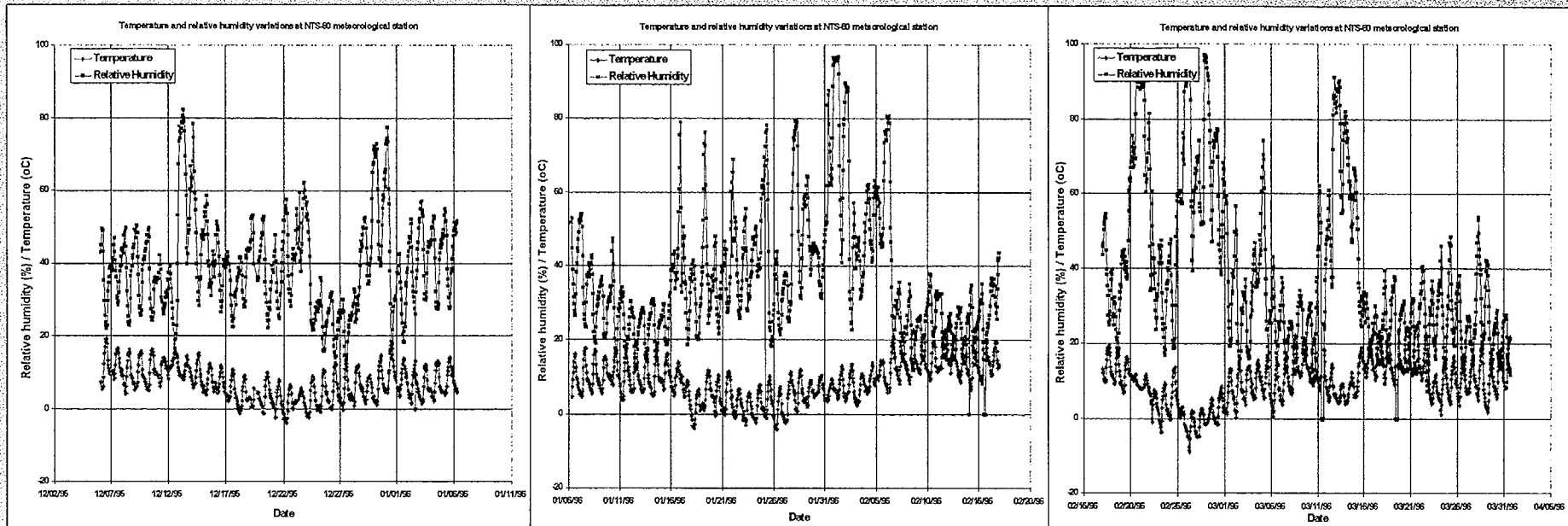


Figure 4-19 (Cont.) - Temperature and humidity variation at NTS-60 meteorological station.

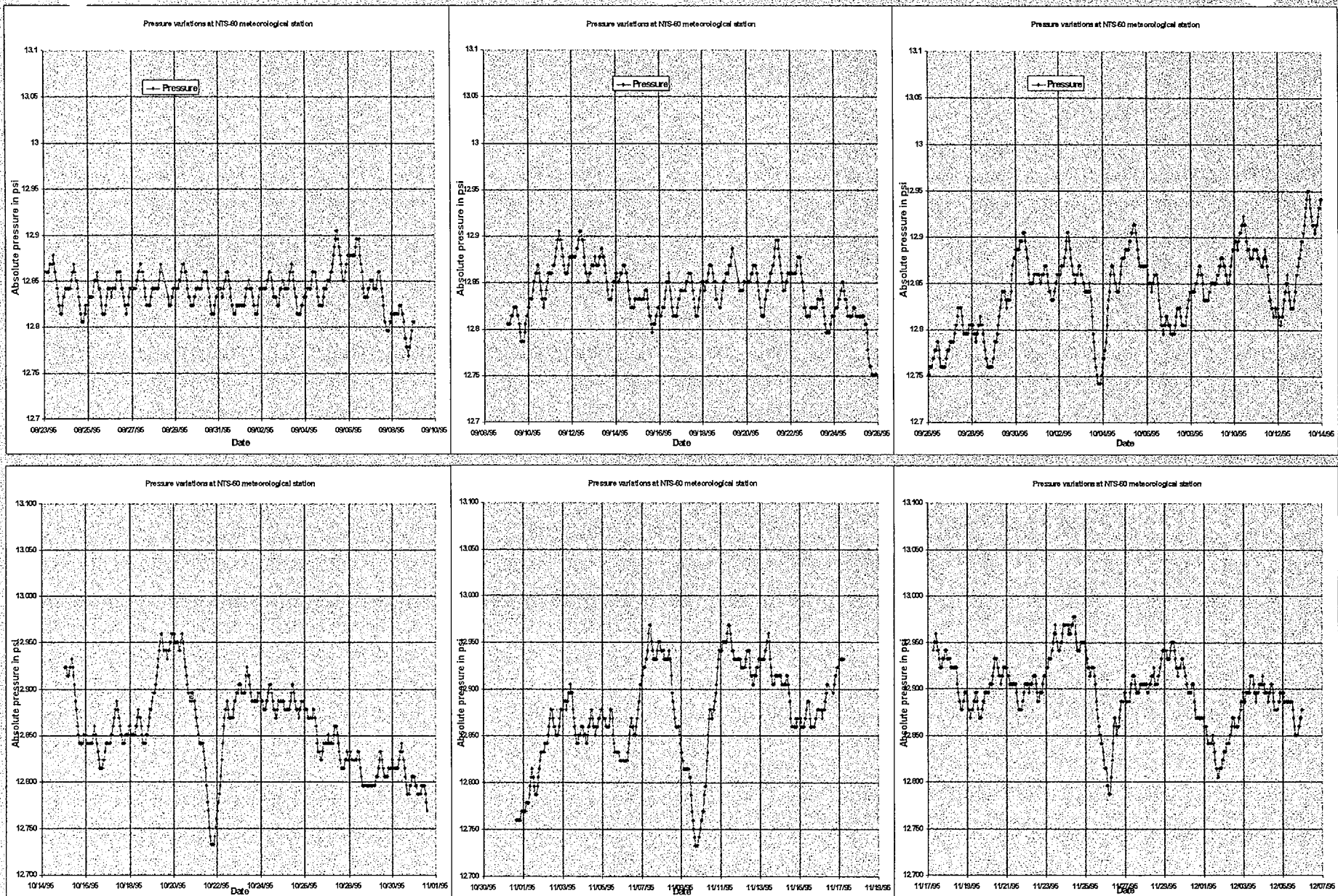


Figure 4-20 - Pressure variation at NTS-60 meteorological station.

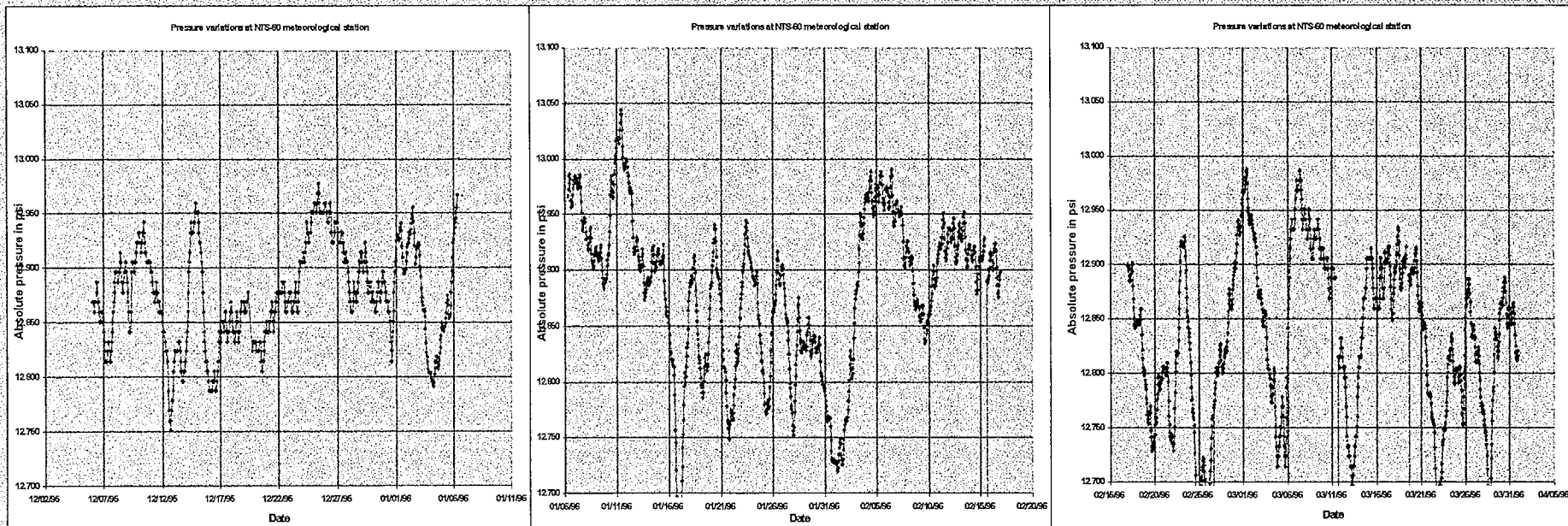


Figure 4-20 (Cont.) - Pressure variation at NTS-60 meteorological station.

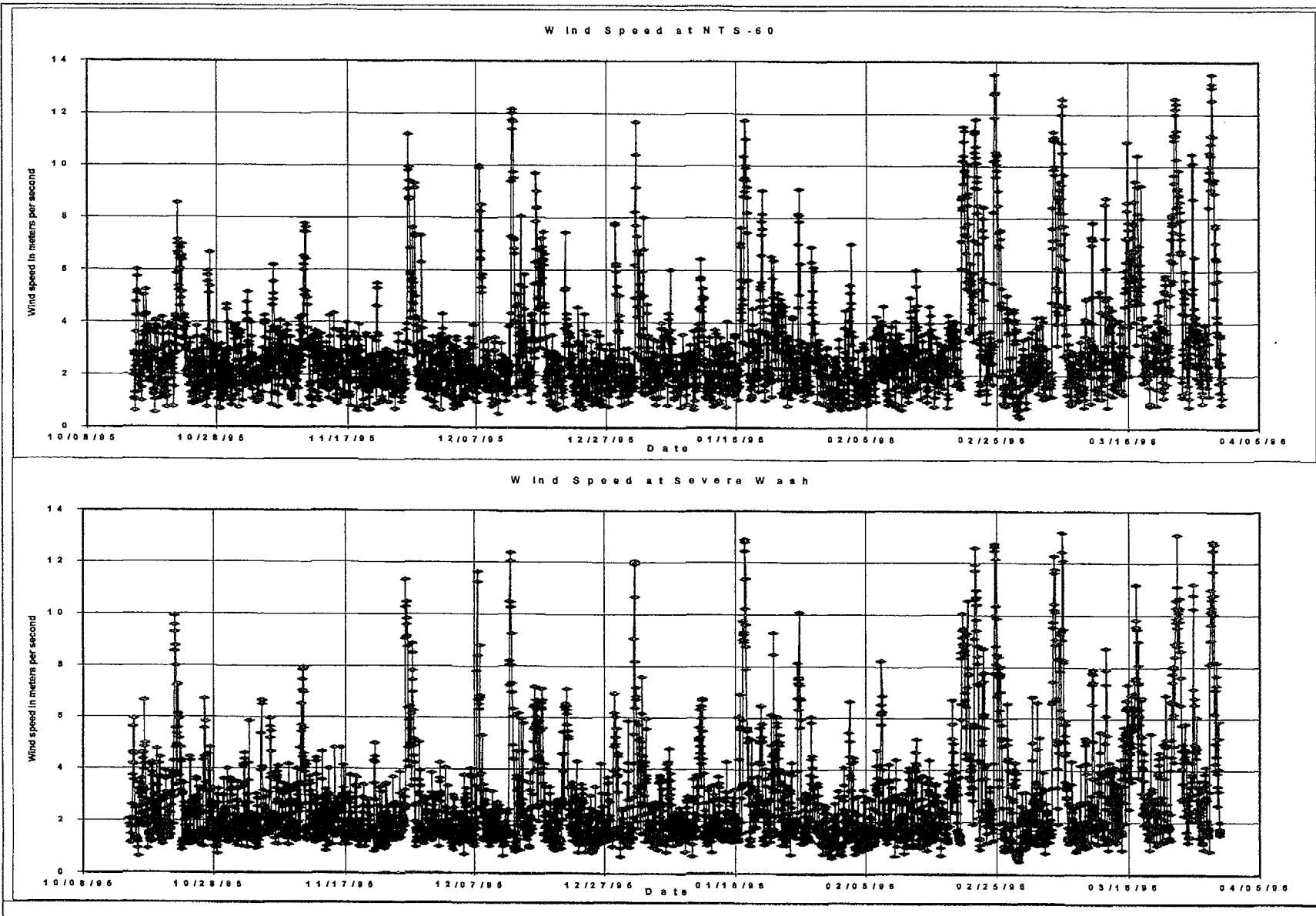
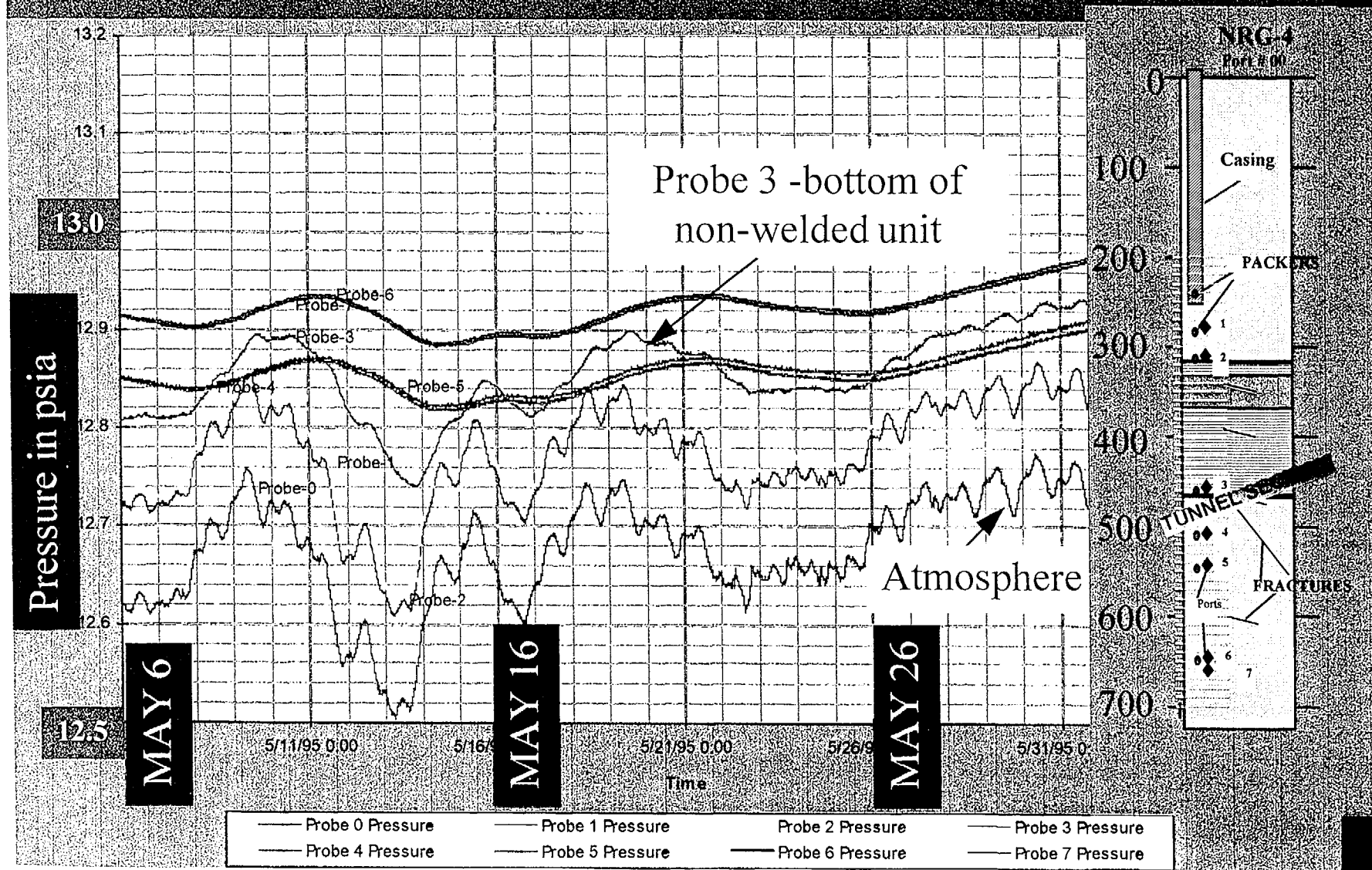


Figure 4-21 - Wind speed variation at NTS-60 meteorological station.

PRESSURE FLUCTUATION WITH TIME IN NRG-4 DURING MAY 1995

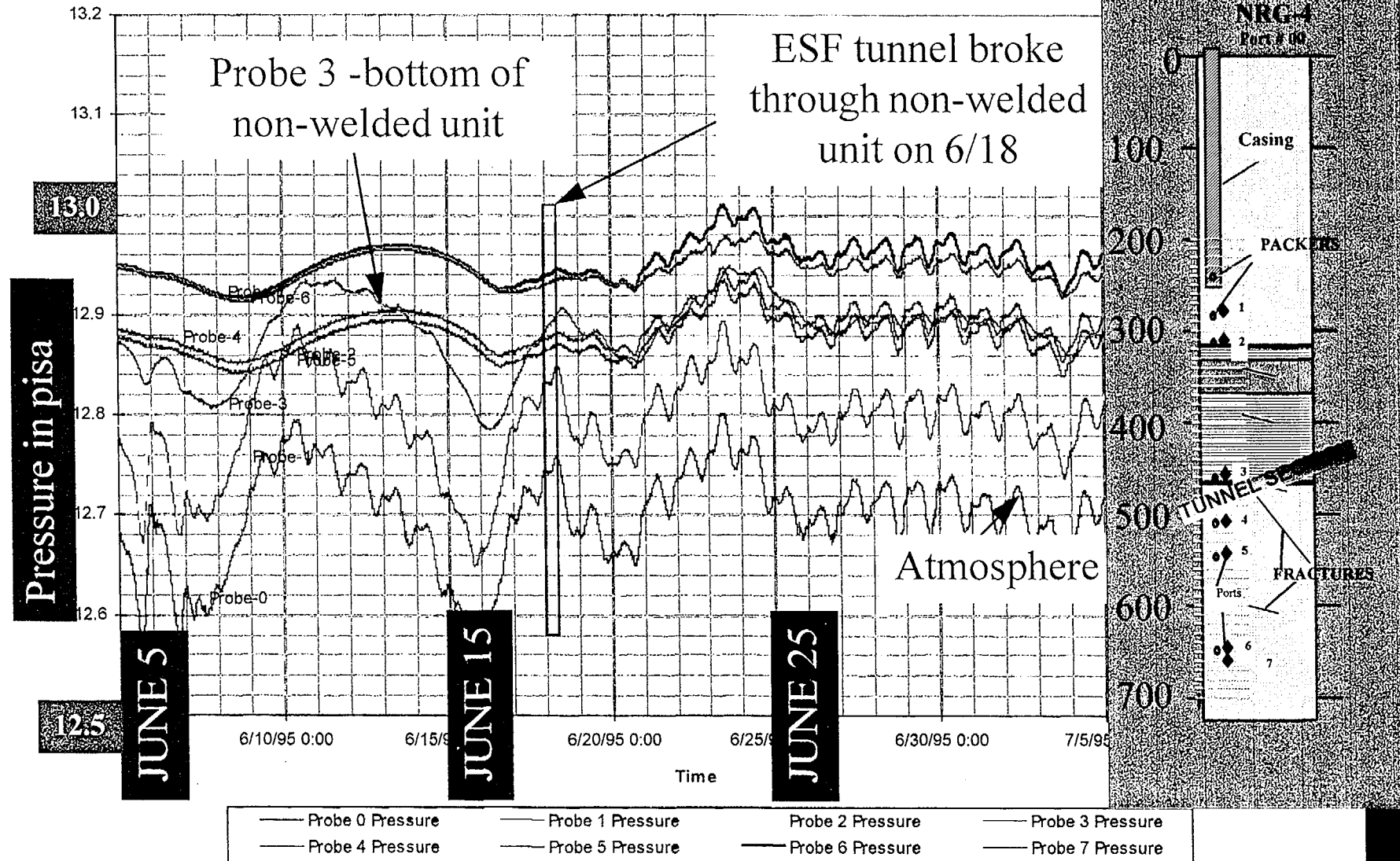


Prepared for:
Nye County Waste Repository Project Office

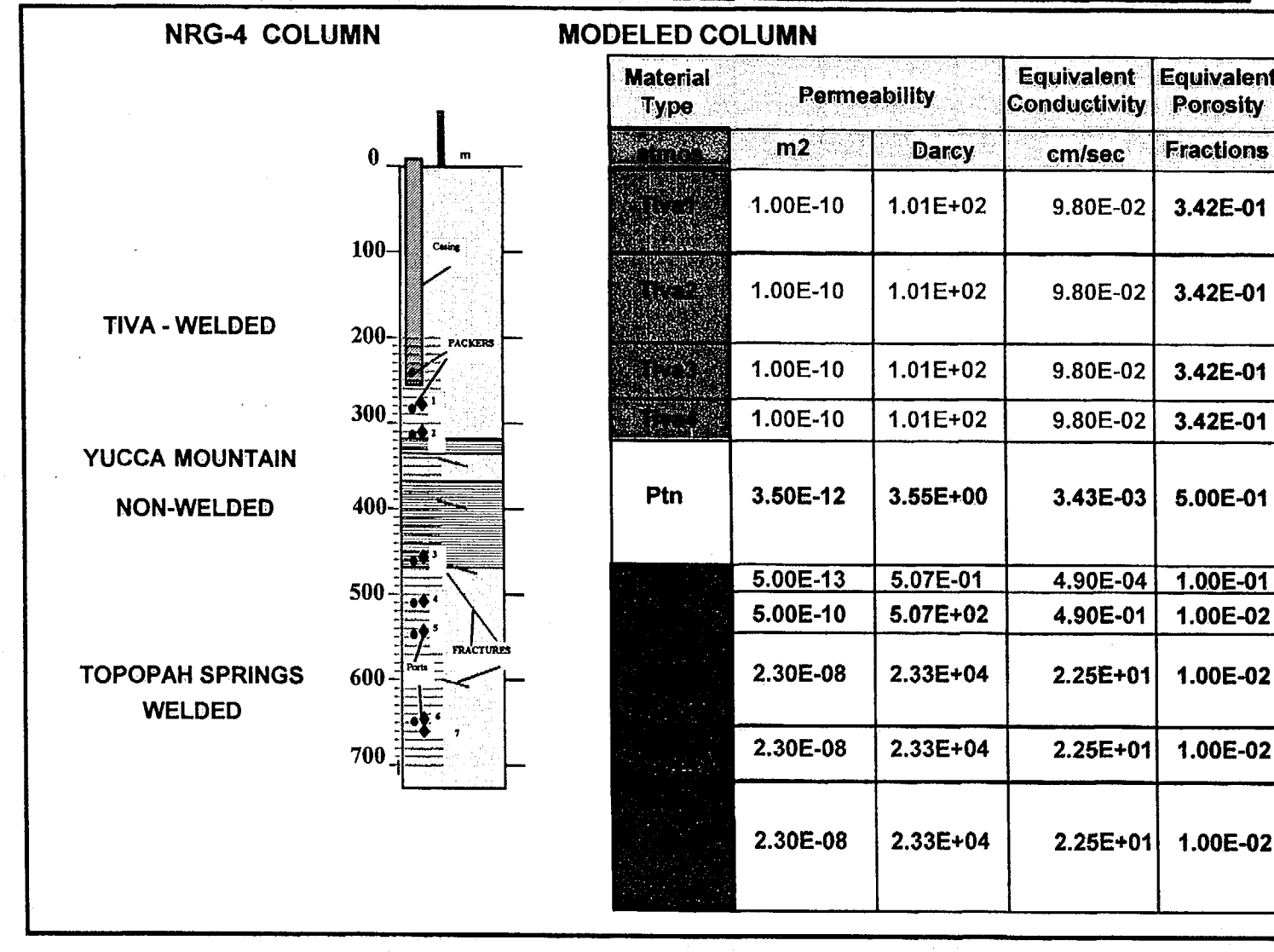
Figure 5-1

Prepared by:
Multimedia Environmental Technology, Inc.
Newport Beach, CA

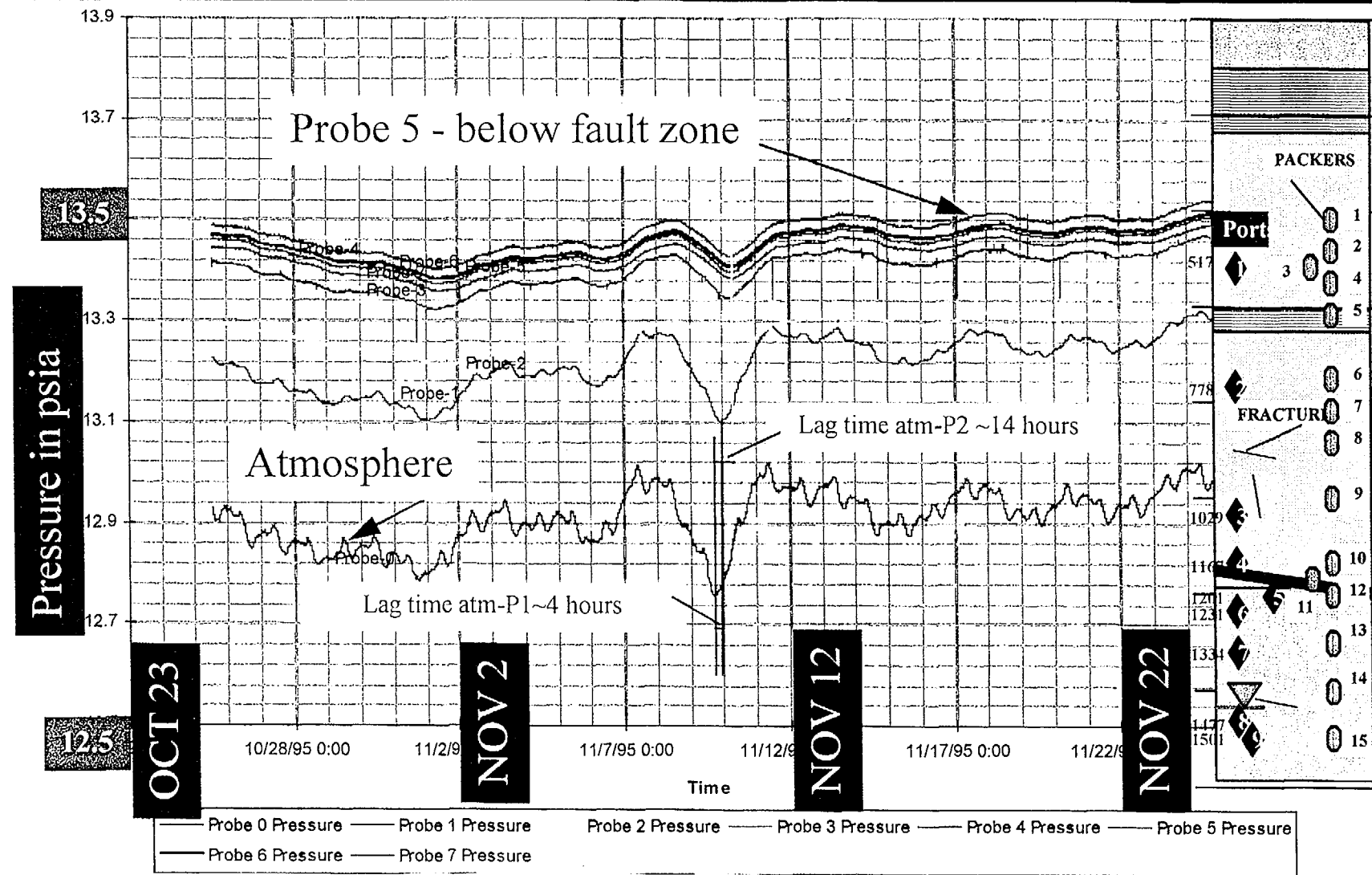
PRESSURE FLUCTUATION WITH TIME IN NRG-4 DURING JUNE 1995



ONE-DIMENSIONAL GRID AND THE RESULTS OF PERMEABILITY CALCULATIONS FOR USW NRG-4



PRESSURE FLUCTUATION WITH TIME IN ONC #1 DURING NOVEMBER 1995

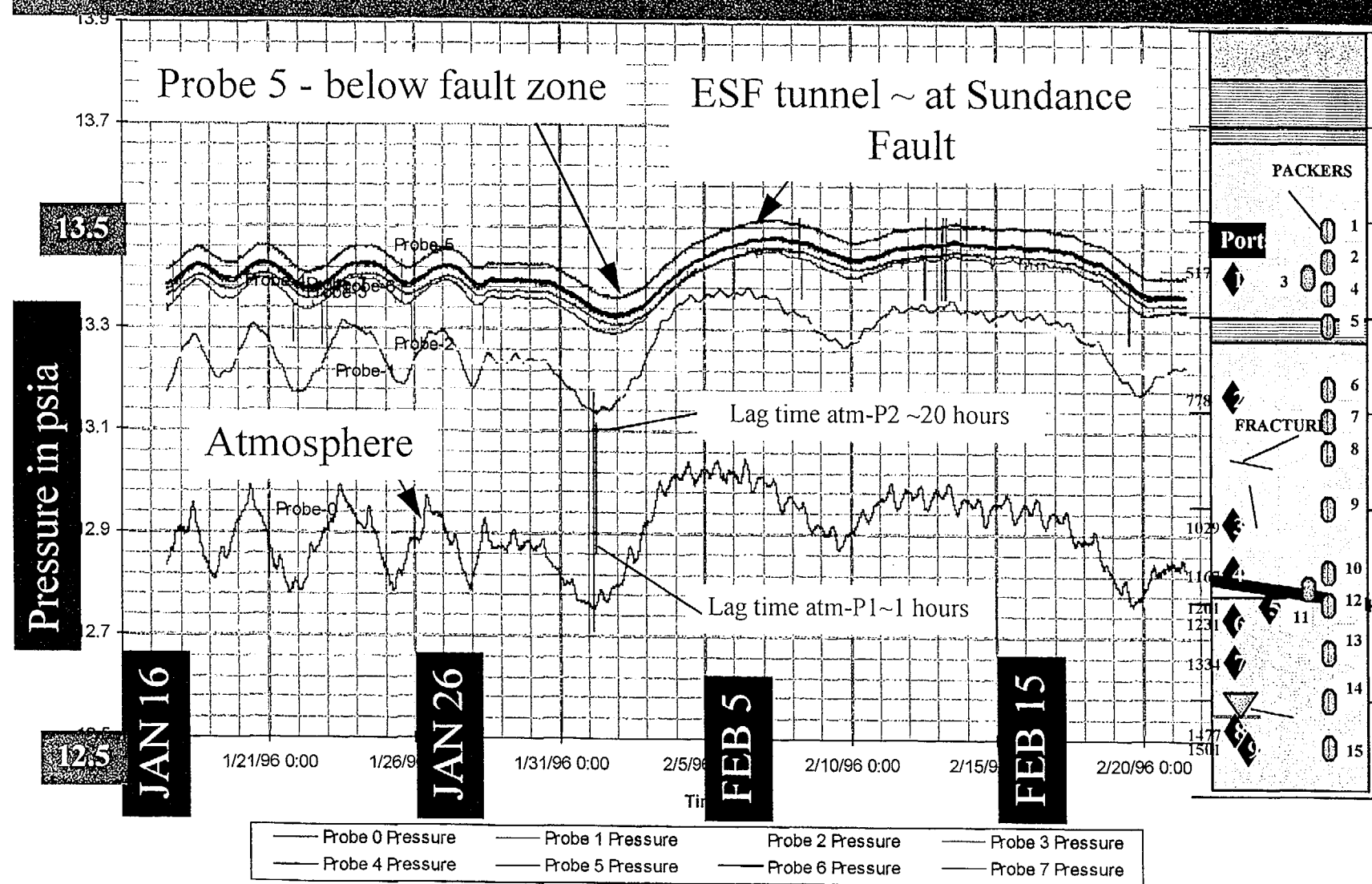


Prepared for:
Nye County Waste Repository Project Office

Figure 5-4

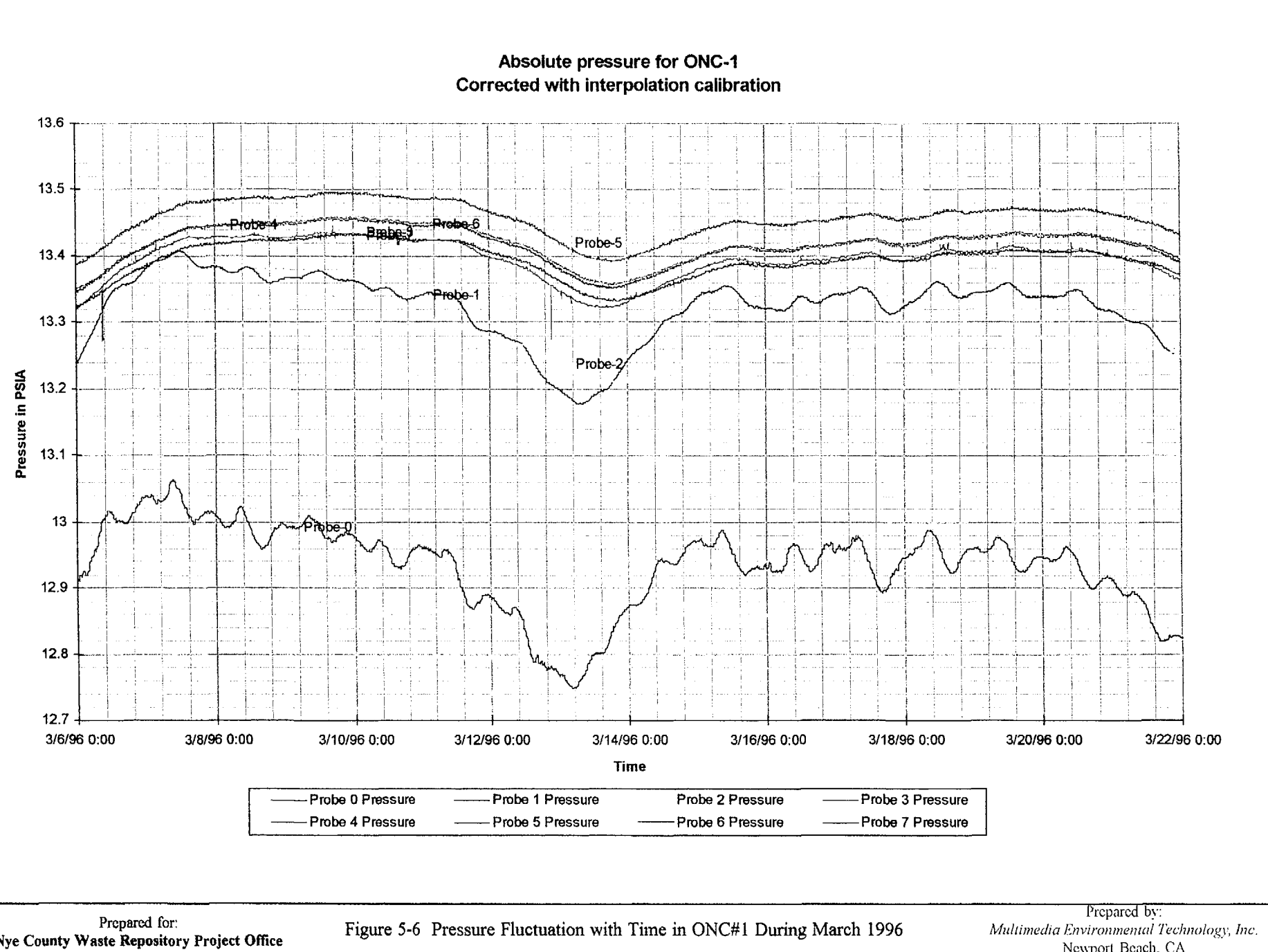
Prepared by:
Multimedia Environmental Technology, Inc.
Newport Beach, CA

PRESSURE FLUCTUATION WITH TIME IN ONC #1 DURING JANUARY 199



(

)



**MODELED COLUMN FOR NYE
COUNTY BOREHOLE ONC#1**

<u>DEPTH IN FEET</u>	<u>ONC-#1</u>	<u>Thickness in m</u>	<u>Rock Type</u>	<u>Depth feet tb</u>	<u>Depth in m tb</u>	<u>PERMEABILITY (m²)</u>	<u>PERMEABILITY (darcy)</u>	<u>Equivalent Conductivity cm/sec</u>	<u>Equivalent Porosity</u>
0		2	atmos						
200	ALLUVIUM RAINIER MESA	60.96	tiva1	200.00	60.96	5.00E-11	5.07E+01	4.90E-02	3.42E-01
400	PACKERS	60.96	tiva2	400.00	121.92	5.00E-11	5.07E+01	4.90E-02	1.00E-03
517	Ports	30.48	tiva3	500.00	152.40	5.00E-11	5.07E+01	4.90E-02	3.42E-02
517	1 2 3 4 5	30.48	tiva4	600.00	182.88	5.00E-13	5.07E-01	4.90E-04	3.42E-03
600	NONWELDED	101.92		934.38	284.80	8.00E-10	8.11E+02	7.84E-01	3.00E-02
778	FRACTURES	20				8.00E-10	8.11E+02	7.84E-01	3.00E-02
800	TOPOPAH SPRINGS	30.48		1034.38	315.28	5.00E-10	5.07E+02	4.90E-01	3.00E-02
1000		30.48		1198.36	365.26	1.00E-10	1.01E+02	9.80E-02	3.00E-02
1029		49.98		1206.36	367.76	5.00E-09	5.07E+03	4.90E+00	1.00E-03
1167	4	49.98		1239.37	377.76	5.00E-09	5.07E+03	4.90E+00	4.92E-01
1200	FAULT ZONE	50.00	cal01	1403.35	427.74	5.00E-09	5.07E+03	4.90E+00	4.92E-01
1231	5 6 7 8 9 10 11 12	49.98	cal02	1485.37	452.74	2.31E-08	2.35E+04	2.27E+01	4.92E-01
1334	CALICO HILLS	25	pro01	1613.65	491.84	2.31E-18	? Saturated	2.27E-09	4.92E-01
1400		39.1	pro02	1813.65	552.80	2.31E-18	? Saturated	2.27E-09	4.92E-01
1477		60.96	pro03						
1501	8 9			Sundance Fault in 3-D connection		8.00E-11	8.11E+01	7.84E-02	1.00E-05

Prepared for:
Nye County Waste Repository Project Office

Figure 5-7

Prepared by:
Multimedia Environmental Technology, Inc.
Newport Beach, CA

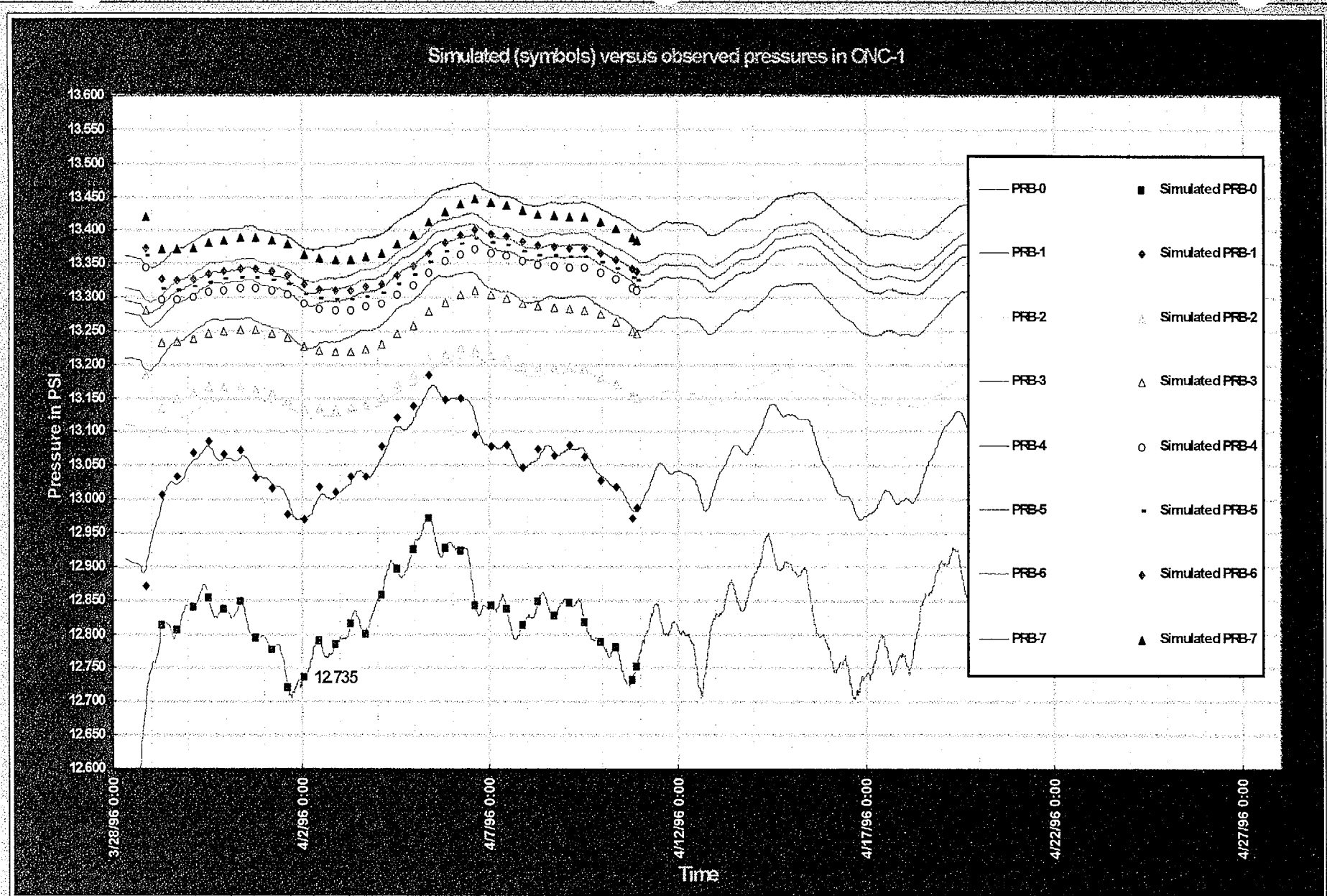


Figure 5-8 - Comparison of the simulated and observed barometric pressure responses in ONC #1 borehole using one-dimensional vertical column of nodes. Only probes 2 and above can be matched.

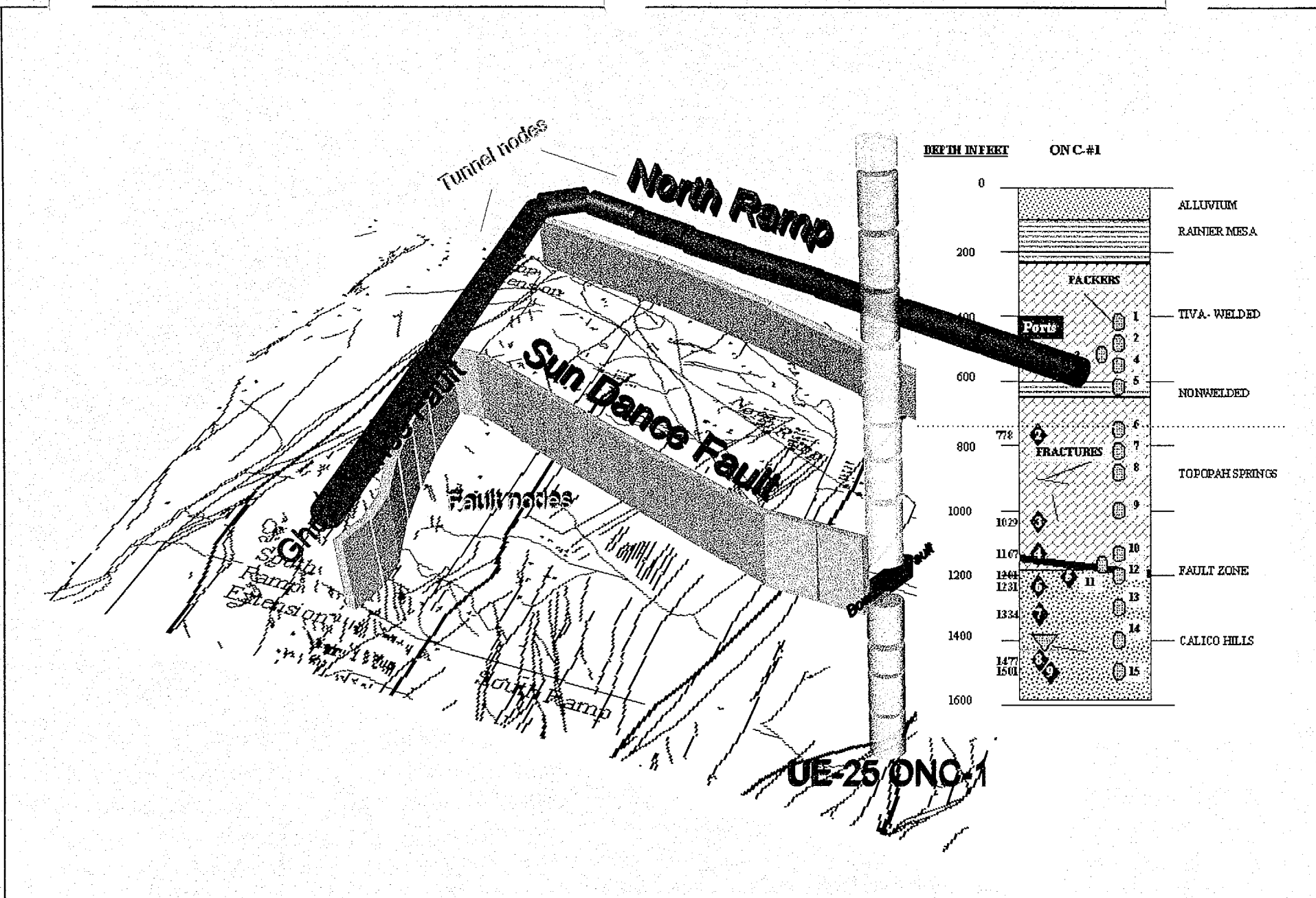


Figure 5-9. Detail of UE-25 ONC#1

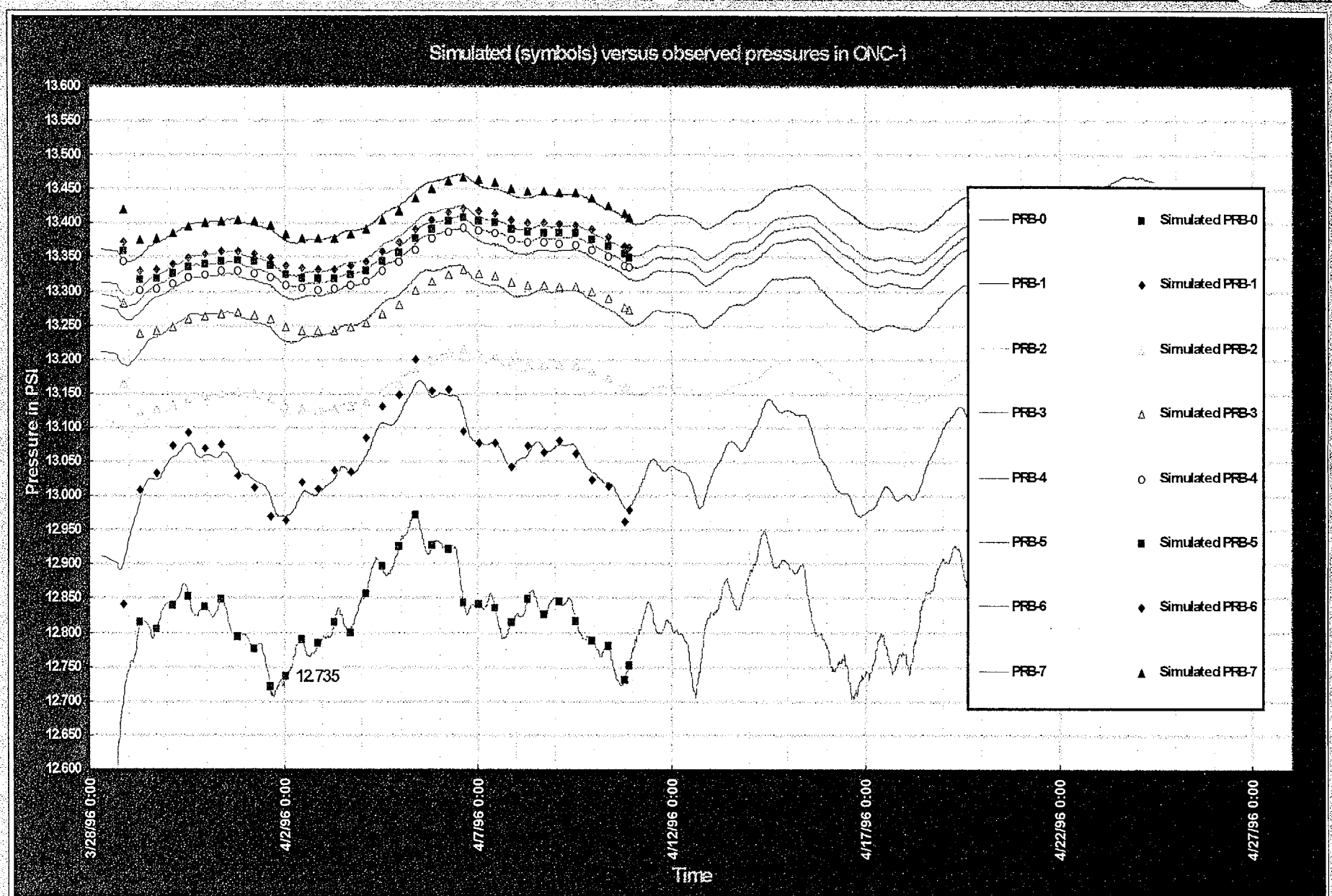


Figure 5-10 - Comparison of the simulated and observed barometric pressure responses in ONC #1 borehole using tunnel and a one-dimensional mesh. An almost perfect match at all probes is evident.

MESH FOR SIMPLE SIMULATIONS WITH A-TOUGH

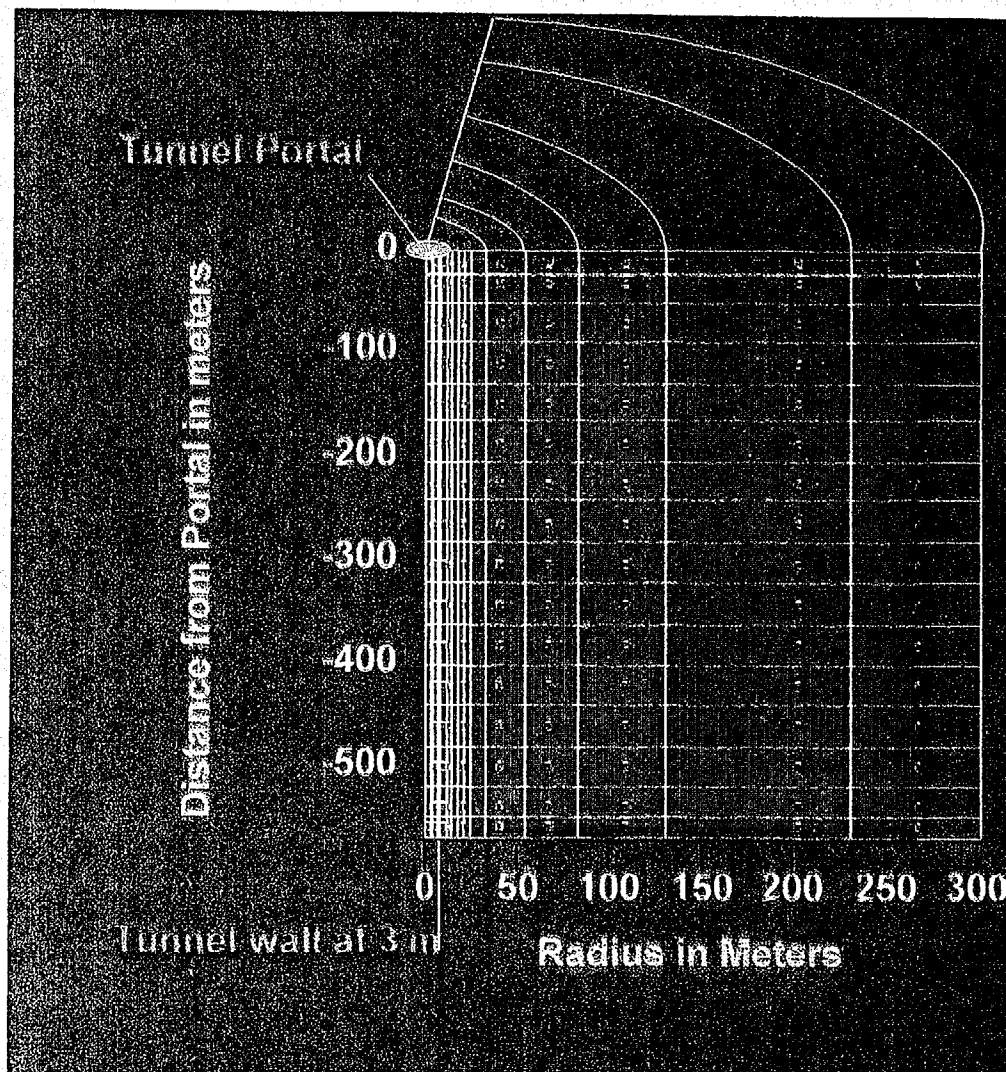


Figure 6-1 - Plan view of the axi-symmetric mesh used for simulations of tunnel ventilation.

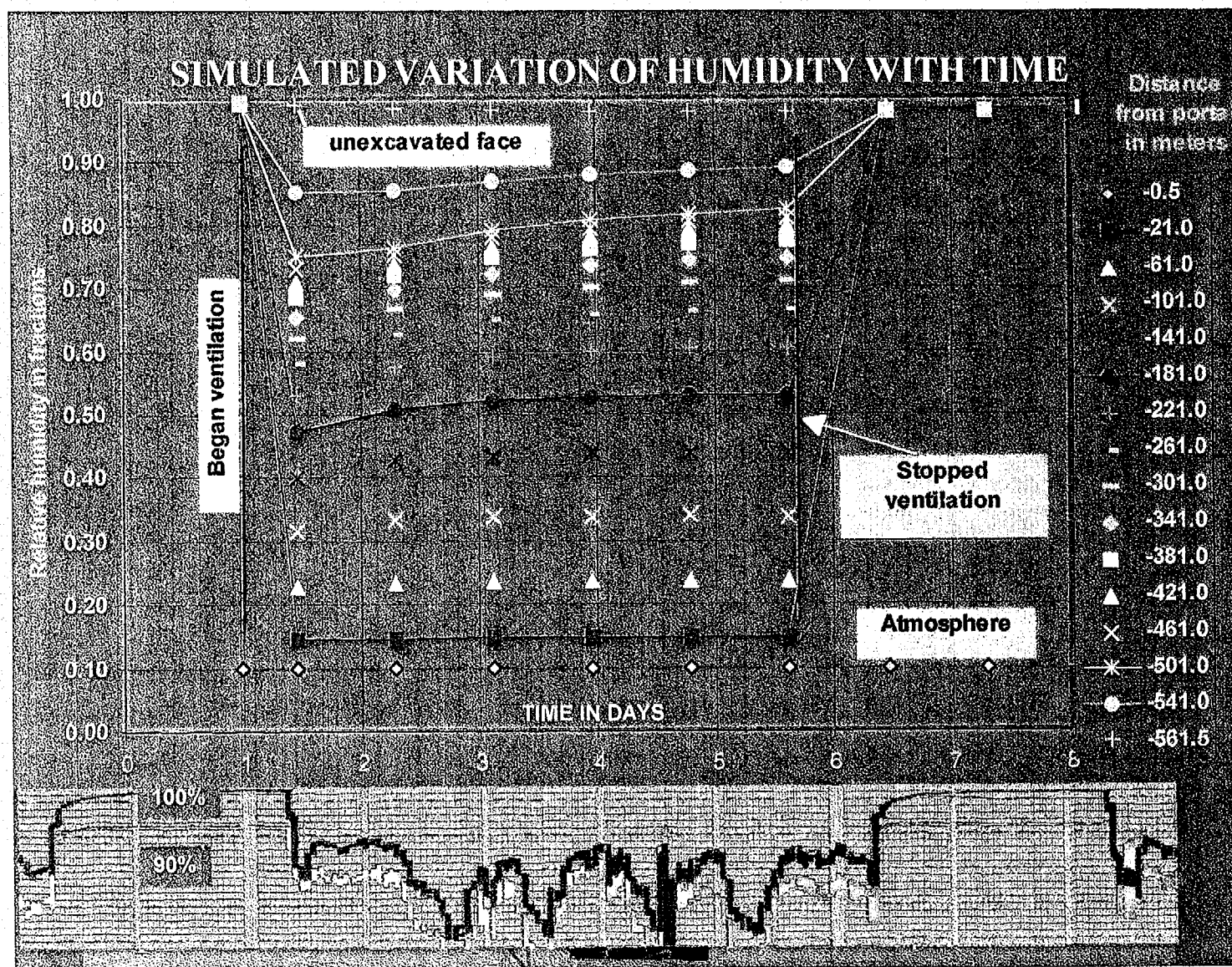


Figure 6-2 - Simulated humidity for one week of ventilation. The inset at the bottom of figure shows the measured humidity during the same period.

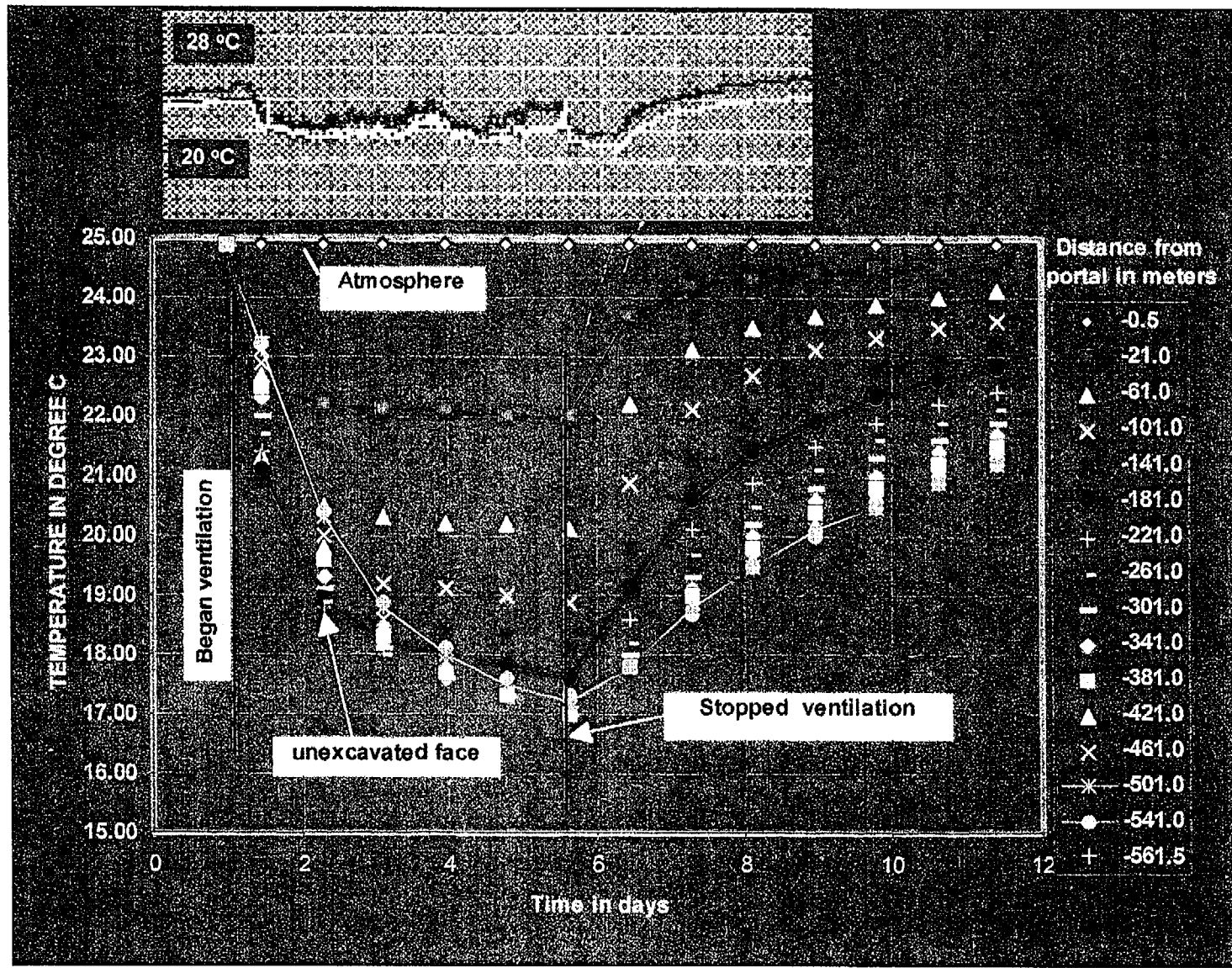


Figure 6-3 - Simulated temperature for one week of ventilation. The inset at the top of figure shows the measured temperatures during the same period.

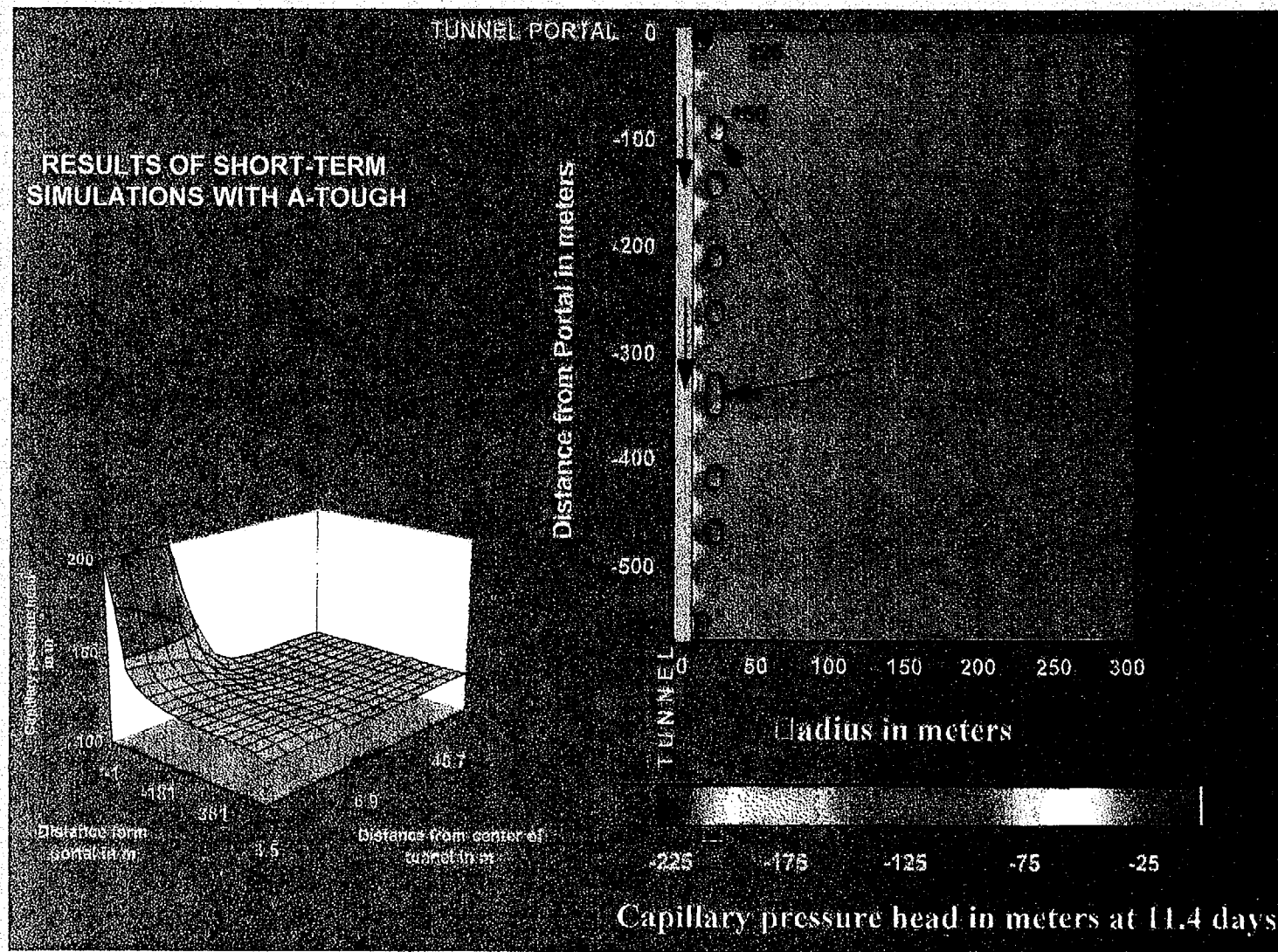
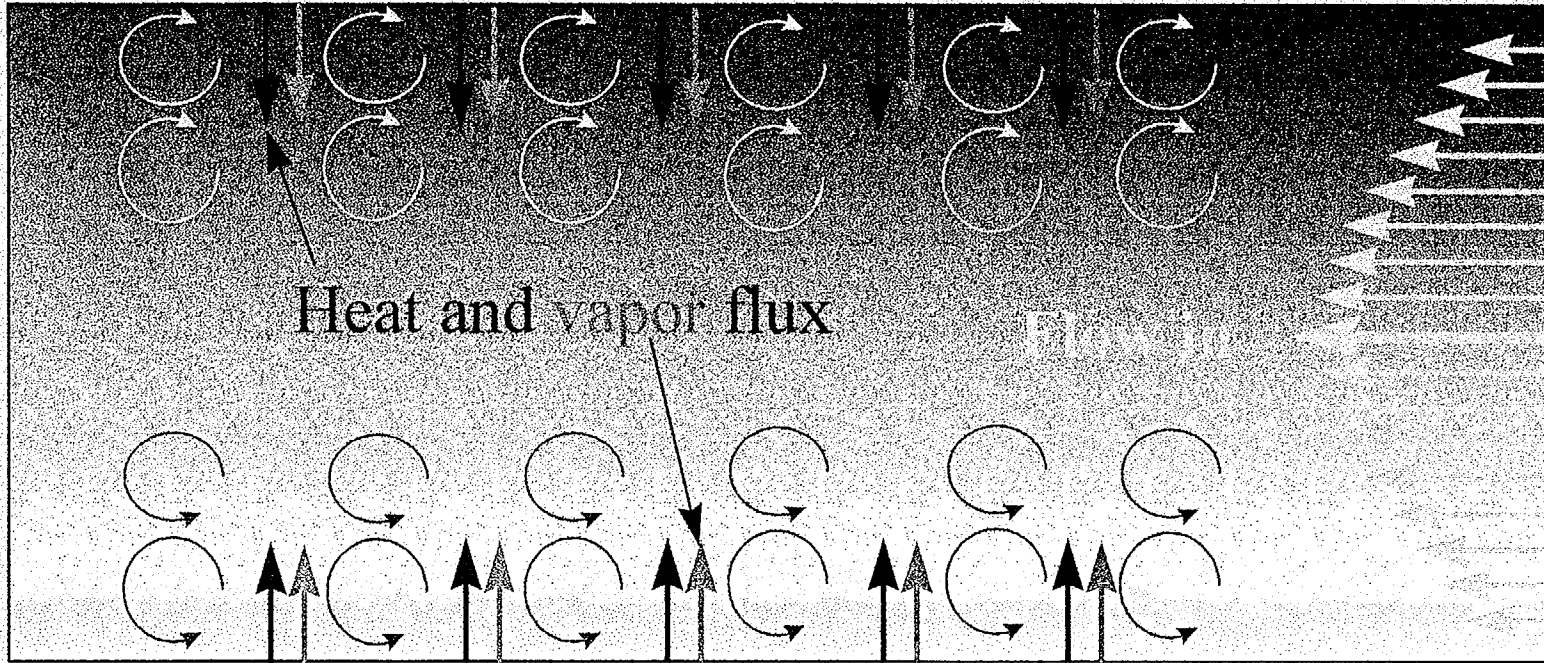


Figure 6-4 - Simulated distribution of capillary pressure around the tunnel for at 11.4 days after start of ventilation. The isometric surface on the lower left shows the values of capillary pressure.



LONGITUDINAL CROSS SECTION

Figure 6-4a - Schematic diagram of flow through a tunnel (eddy diffusivity concept).

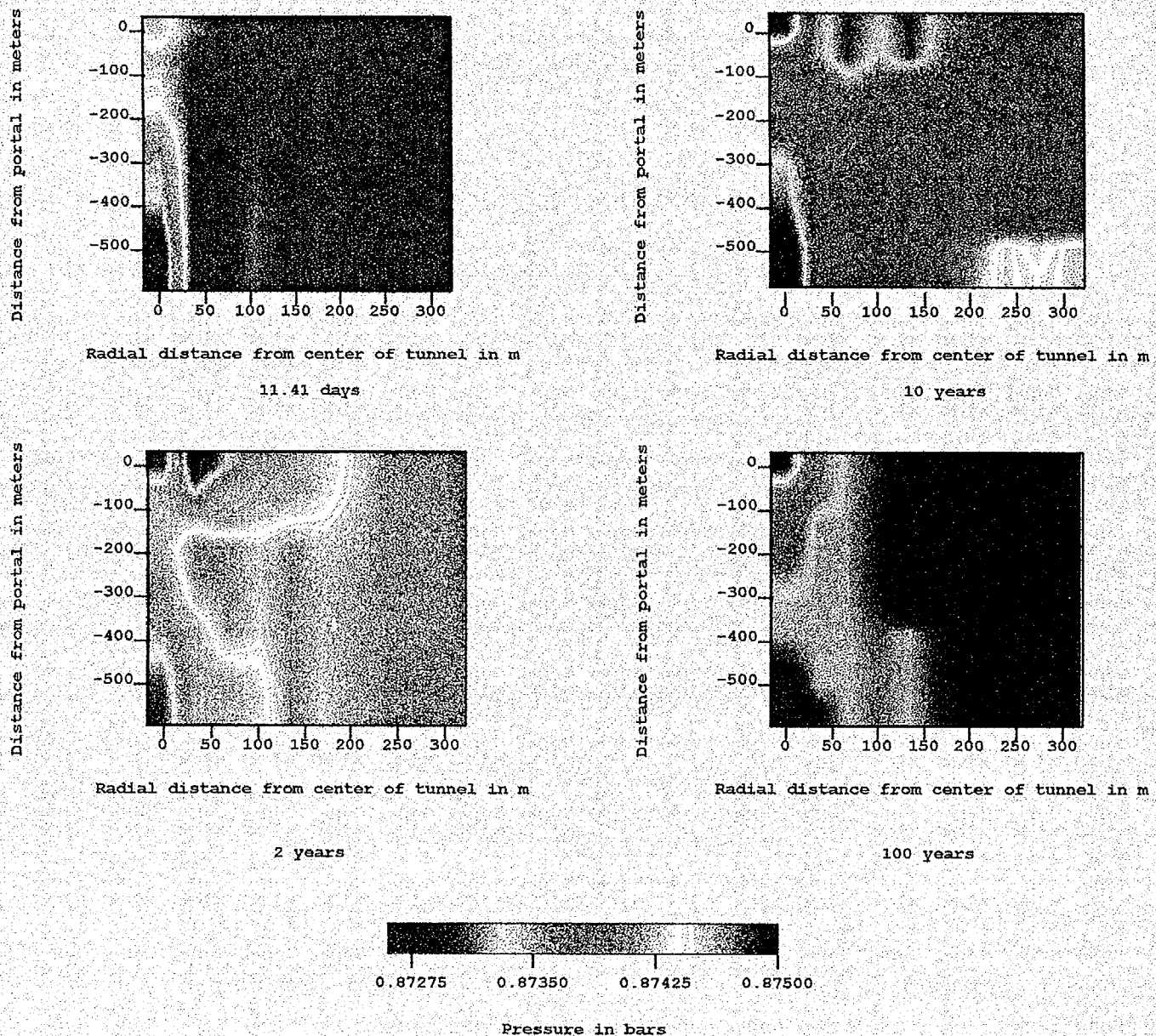


Figure 6-5 - Simulated pressures around the tunnel for various times. Case 1, eddy diffusivity = 0.01, atmosphere temperature = 15 °C.

Case 1
Pressure versus time for $D_{atm} = 0.01$ and atmosphere temperature = 15 C
Distance from portal = 261 m

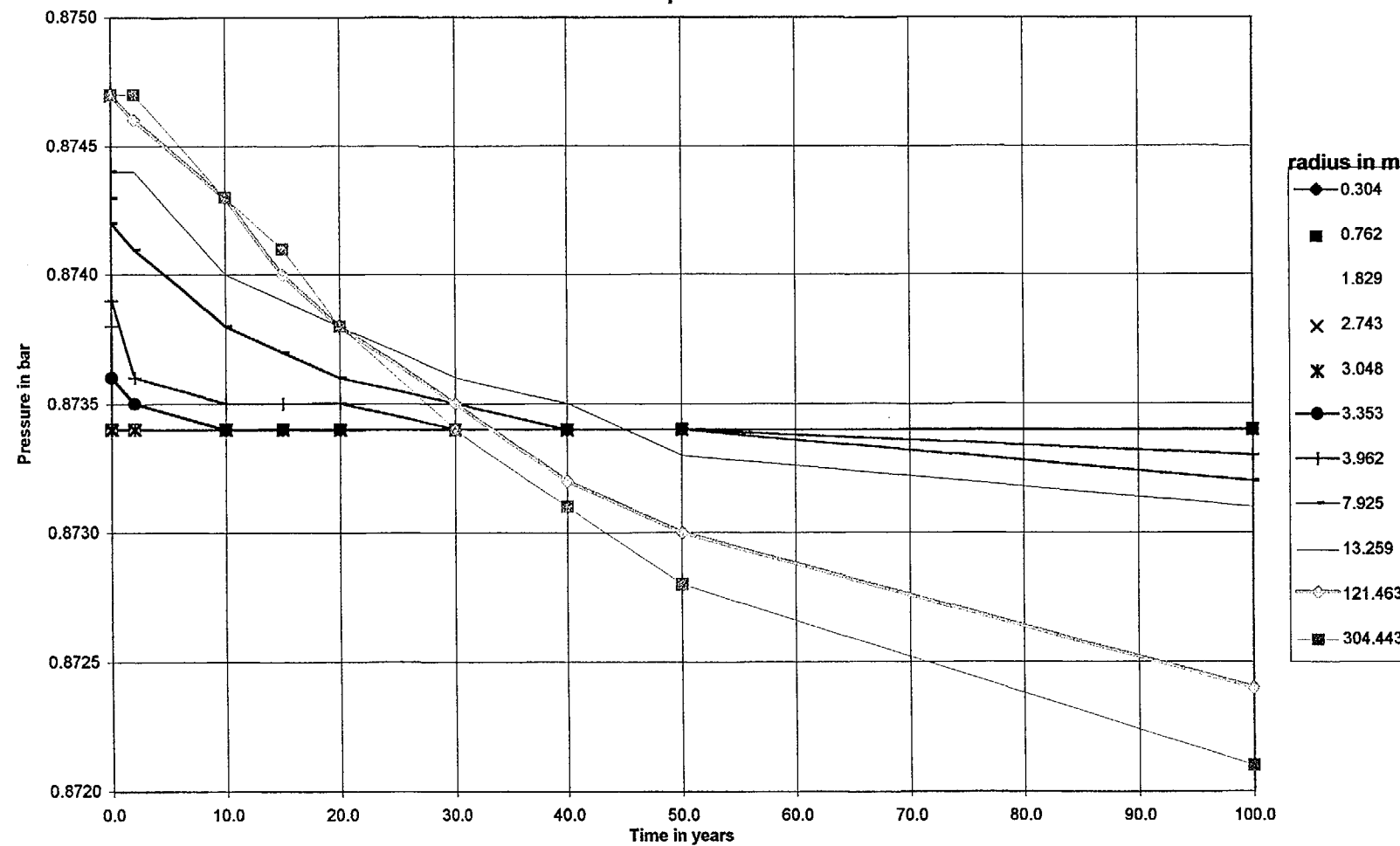


Figure 6-5a

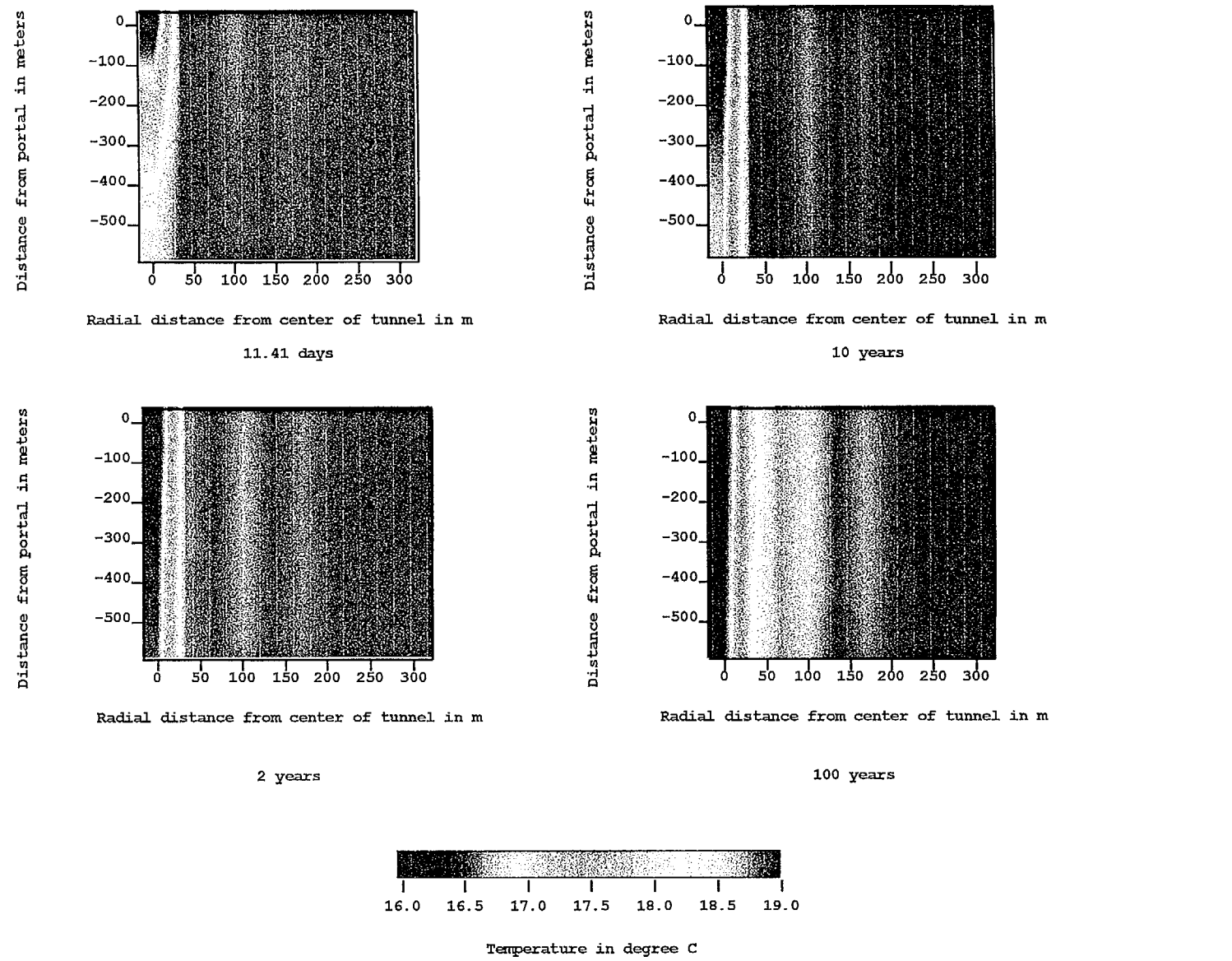


Figure 6-6 - Simulated temperature around the tunnel for various times. Case 1, eddy diffusivity = 0.01, atmosphere temperature = 15 °C.

Case 1

Temperature versus time for $D_{atm} = 0.01$ and atmosphere temperature = 15 C
Distance from portal = 261m

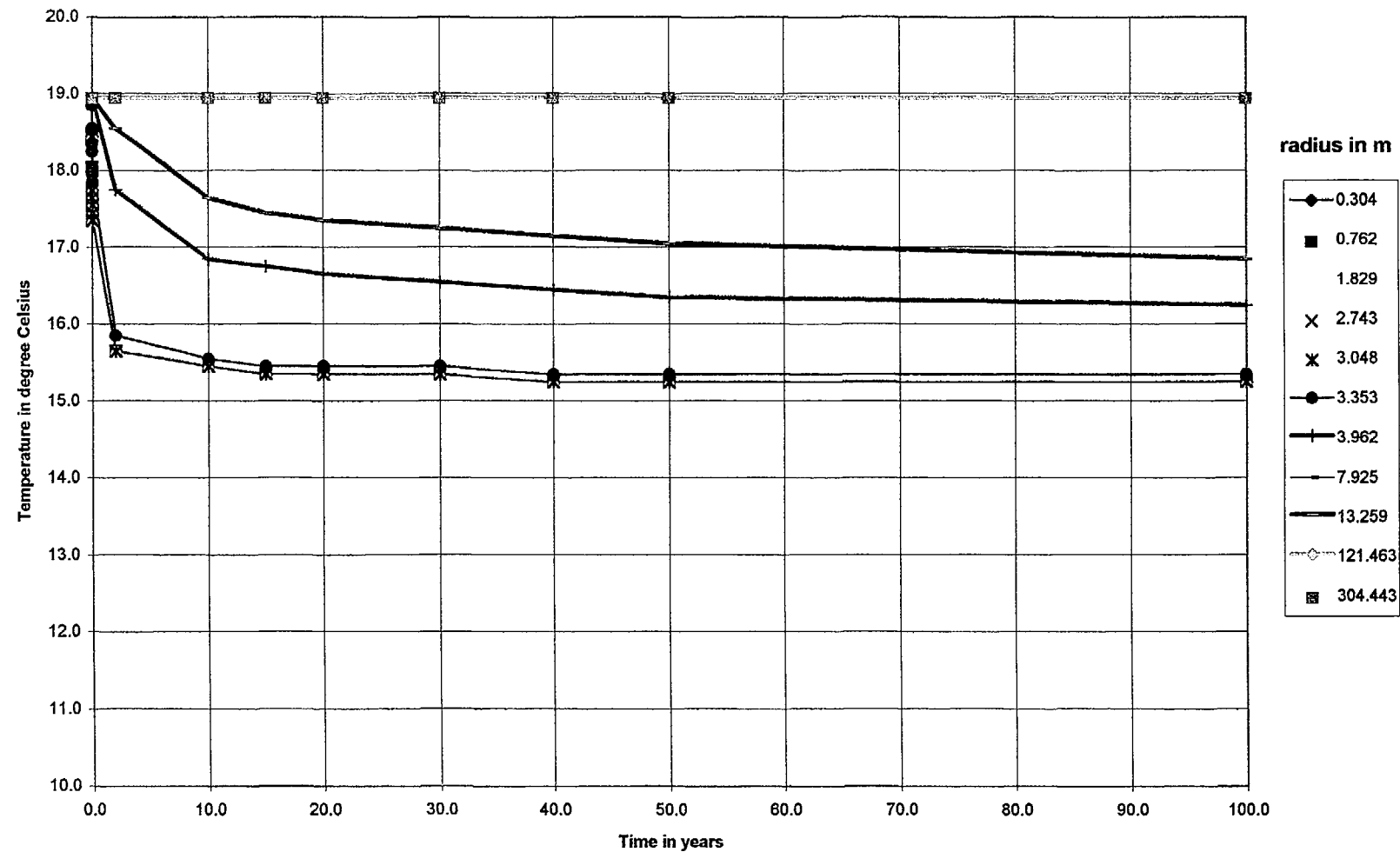


Figure 6-6a

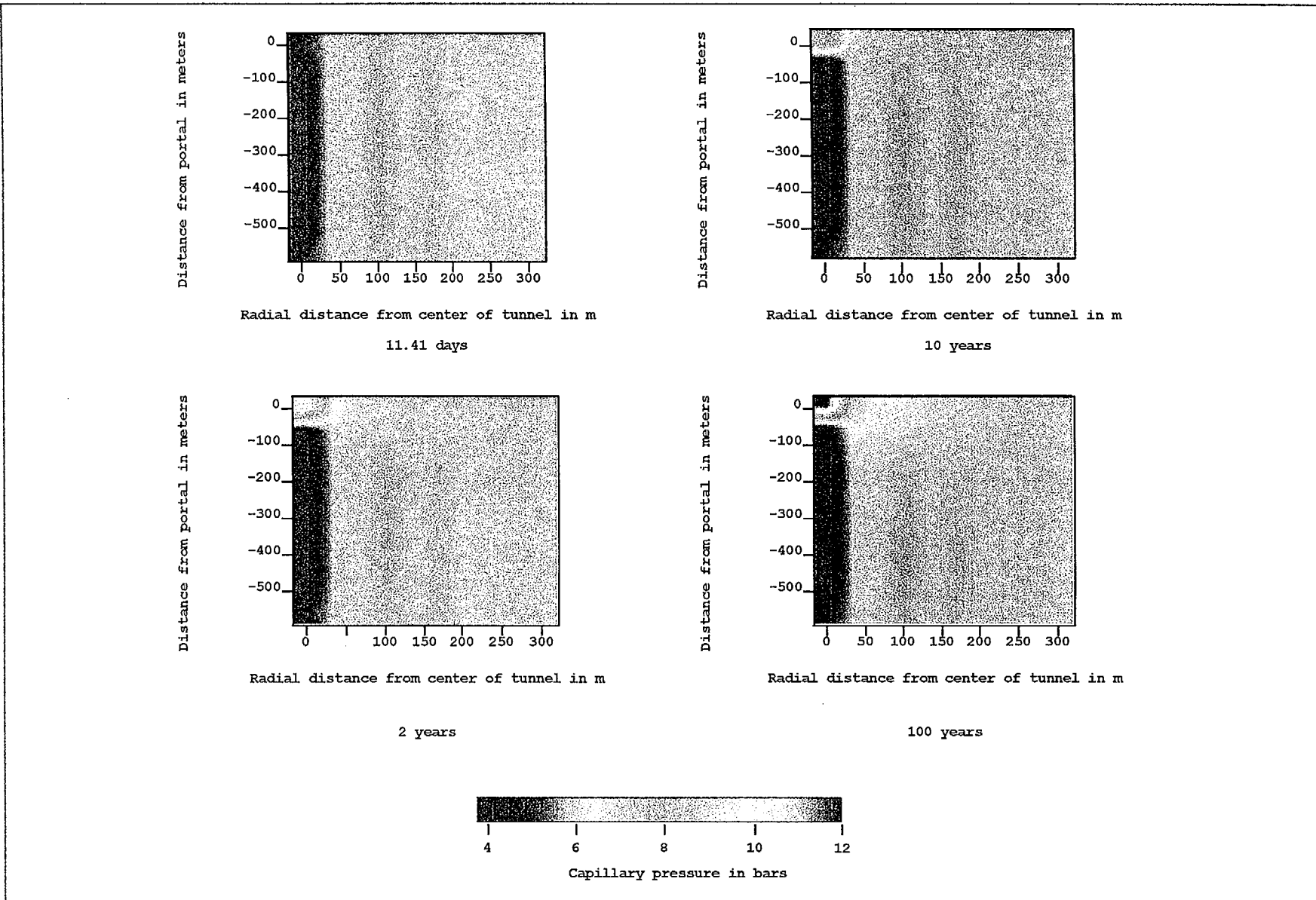


Figure 6-7 - Simulated capillary pressure around the tunnel for various times. Case 1, eddy diffusivity = 0.01, atmosphere temperature = 15 °C.

Case 1

**Capillary Pressure versus time for $D_{atm} = 0.01$ and atmosphere temperature = 15 C
Distance from portal = 261 m**

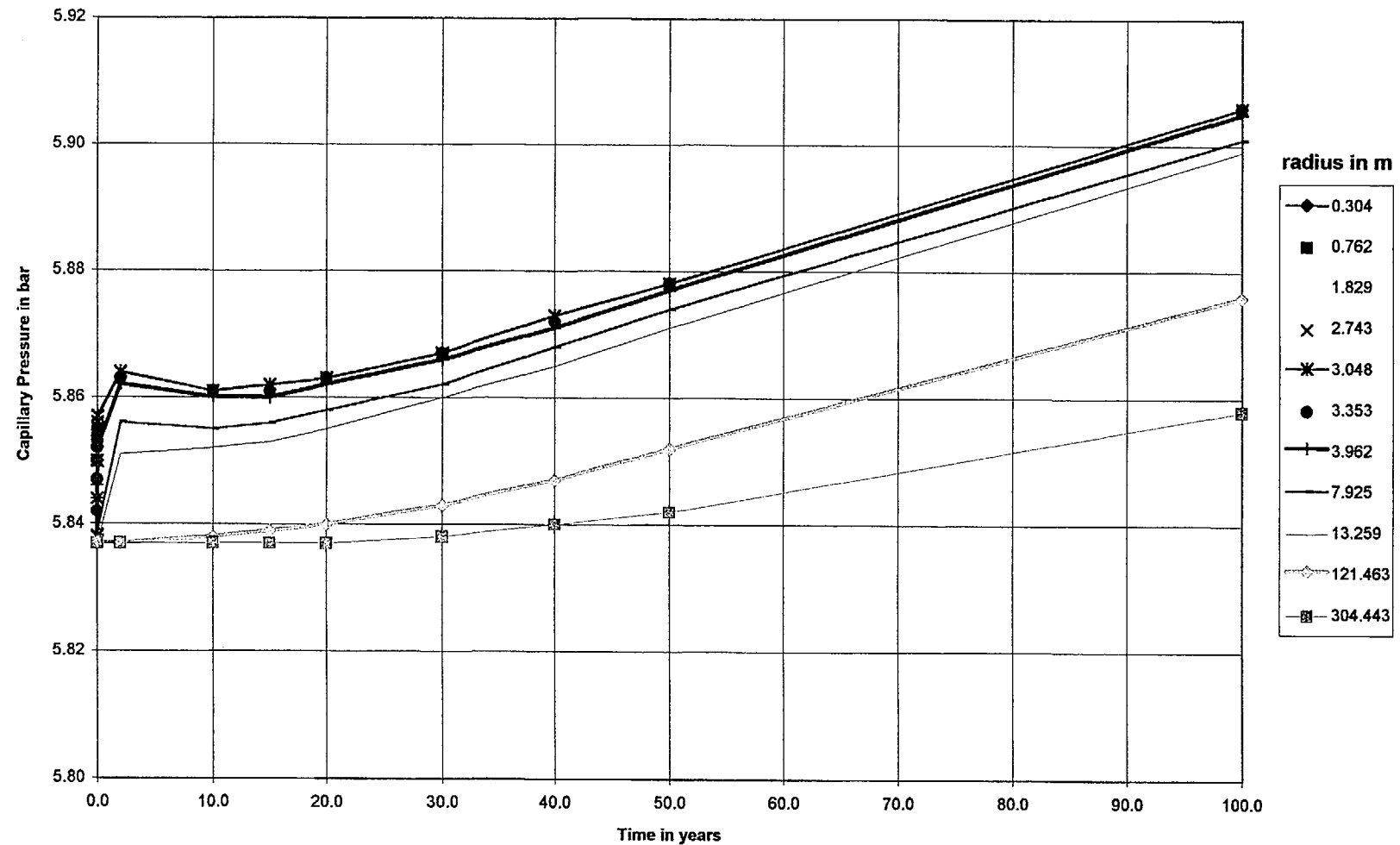


Figure 6-7a

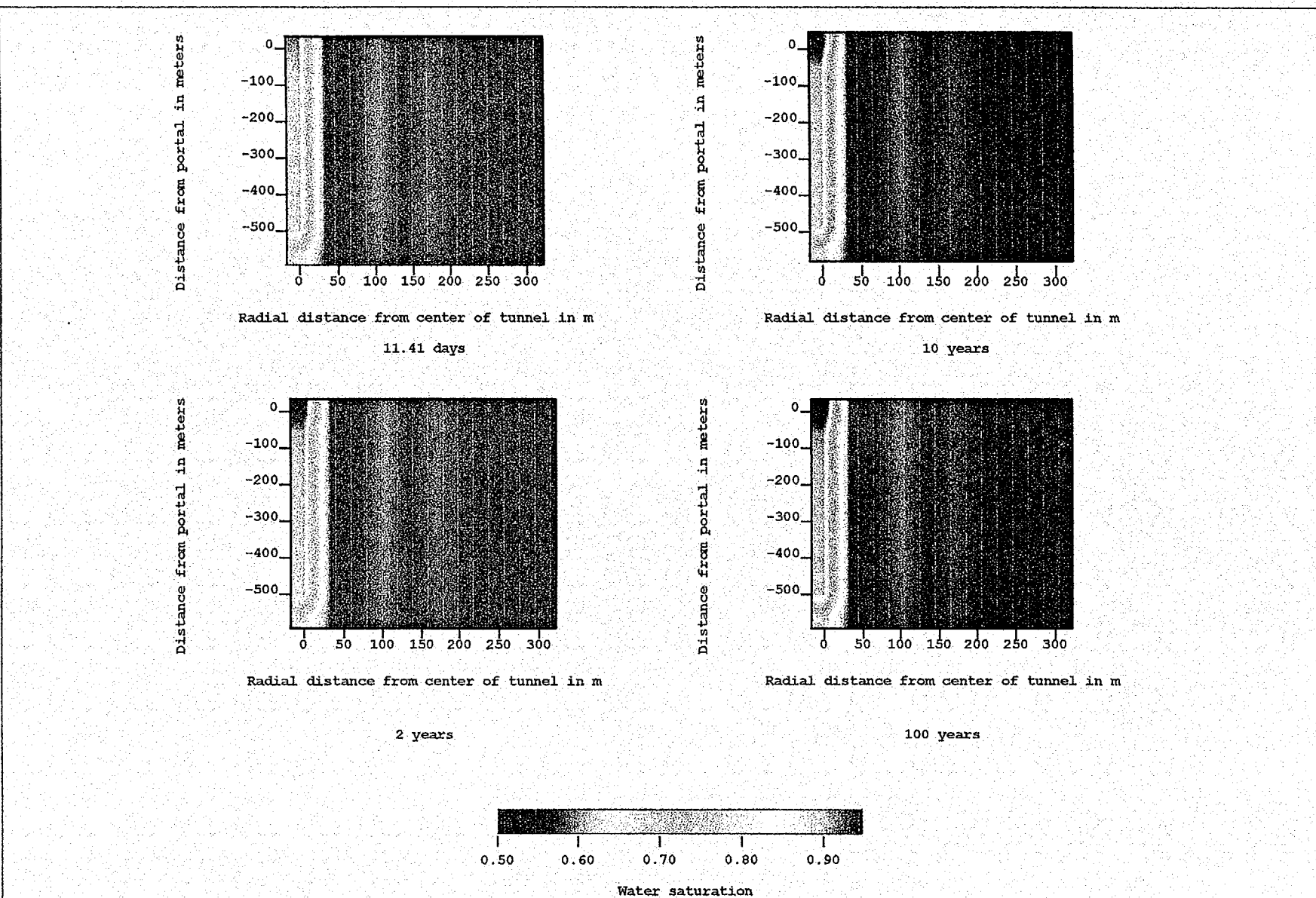


Figure 6-8 - Simulated saturation around the tunnel for various times. Case 1, eddy diffusivity = 0.01, atmosphere temperature = 15 °C.

Case 1

**Water saturation versus time for $D_{atm} = 0.01$ and atmosphere temperature of 15 C
Distance from portal = 261 m**

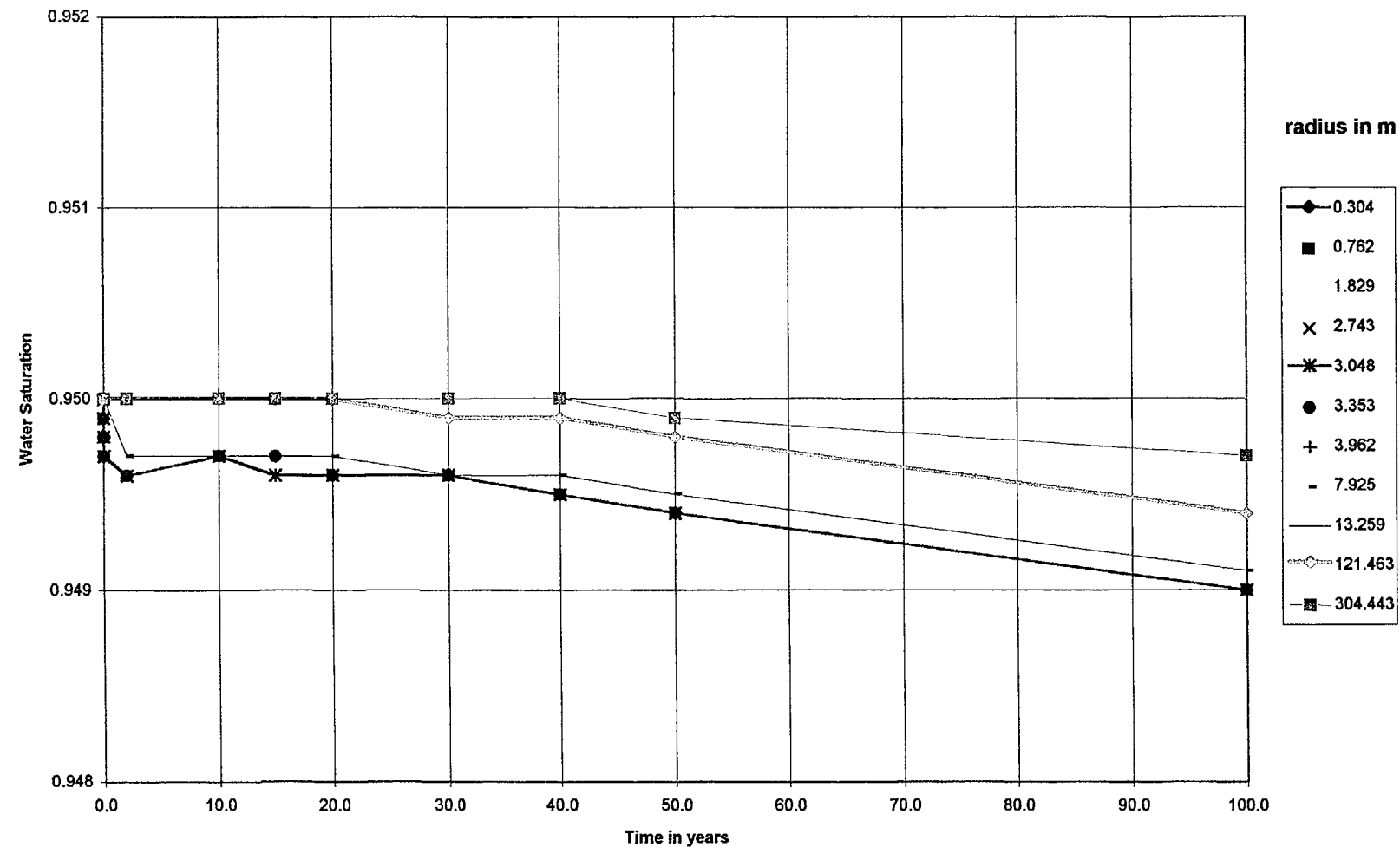


Figure 6-8a

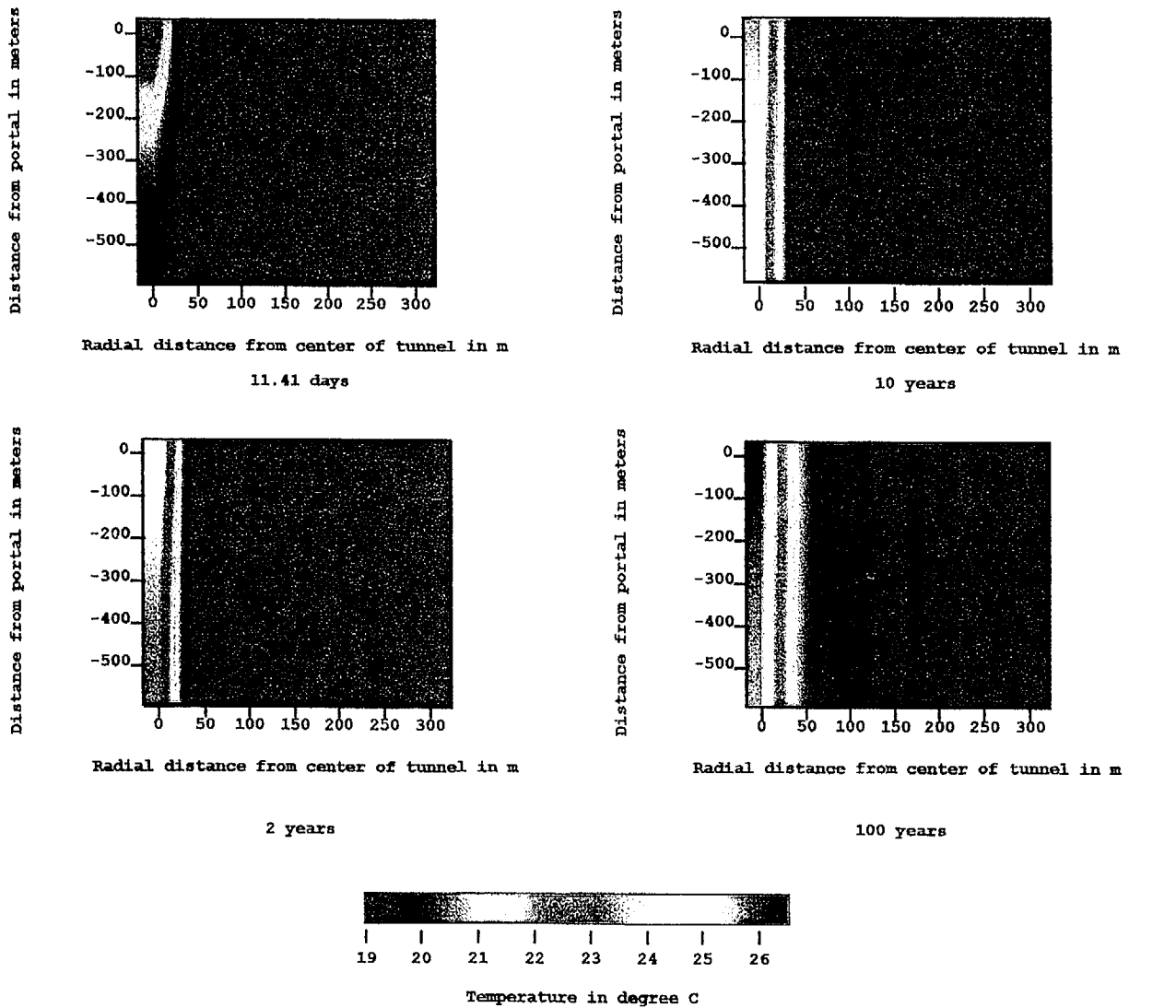


Figure 6-9 - Simulated temperature around the tunnel for various times. Case 2, eddy diffusivity = 0.01, atmosphere temperature = 28 °C.

August 24, 1996
P26609:54 AMD:\user\projects\NyeCounty\amrep\96\figures

Prepared for:
Nye County Nuclear Waste Repository Project Office

Prepared by:
Multimedia Environmental Technology, Inc.
Newport Beach, CA

Case 2

**Pressure versus time for $D_{atm} = 0.01$ and atmosphere temperature = 28 C
Distance from portal = 261 m**

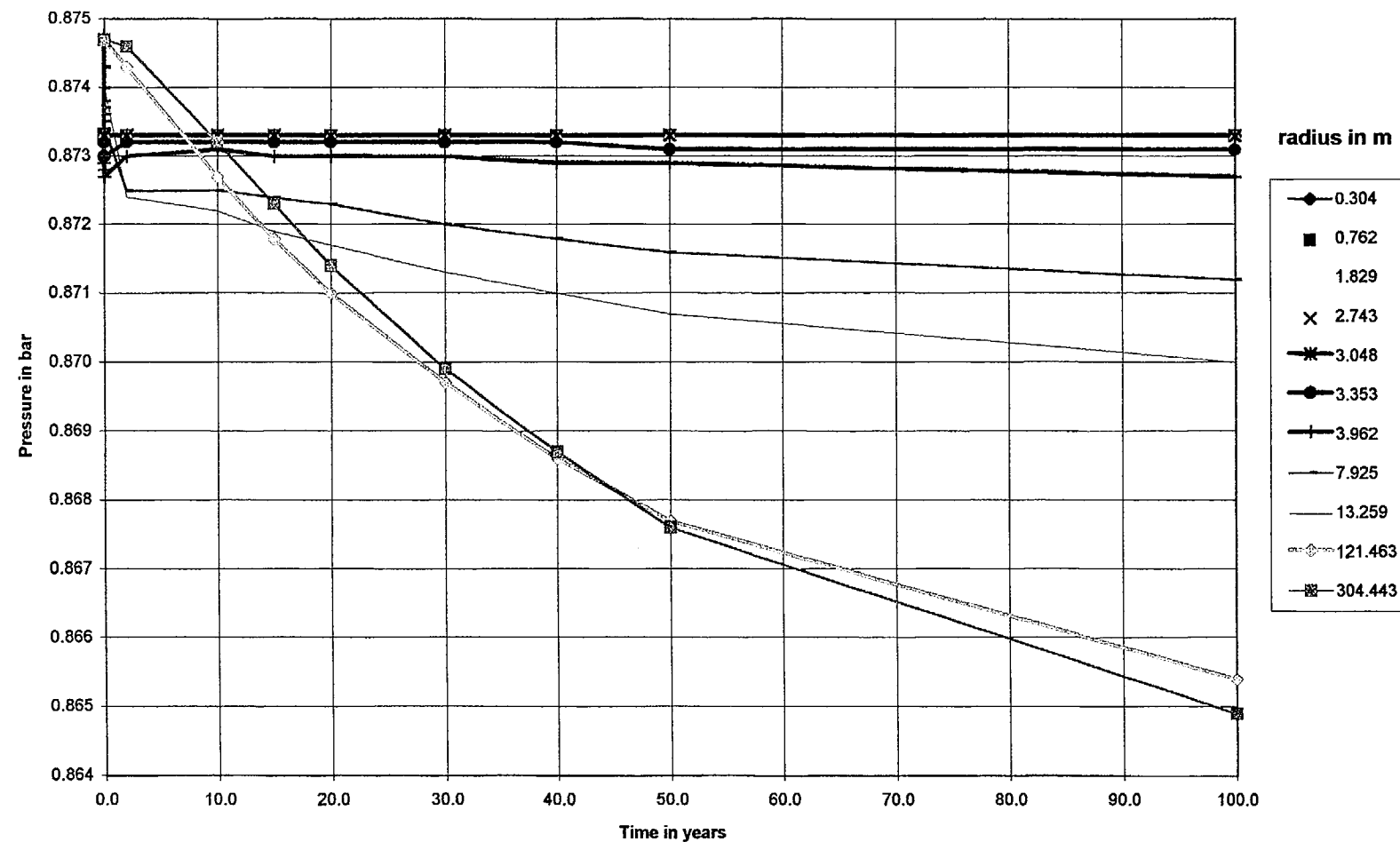


Figure 6-9a

Case 2

Temperature versus time for $D_{atm} = 0.01$ and atmosphere temperature = 28 C
Distance from portal = 261m

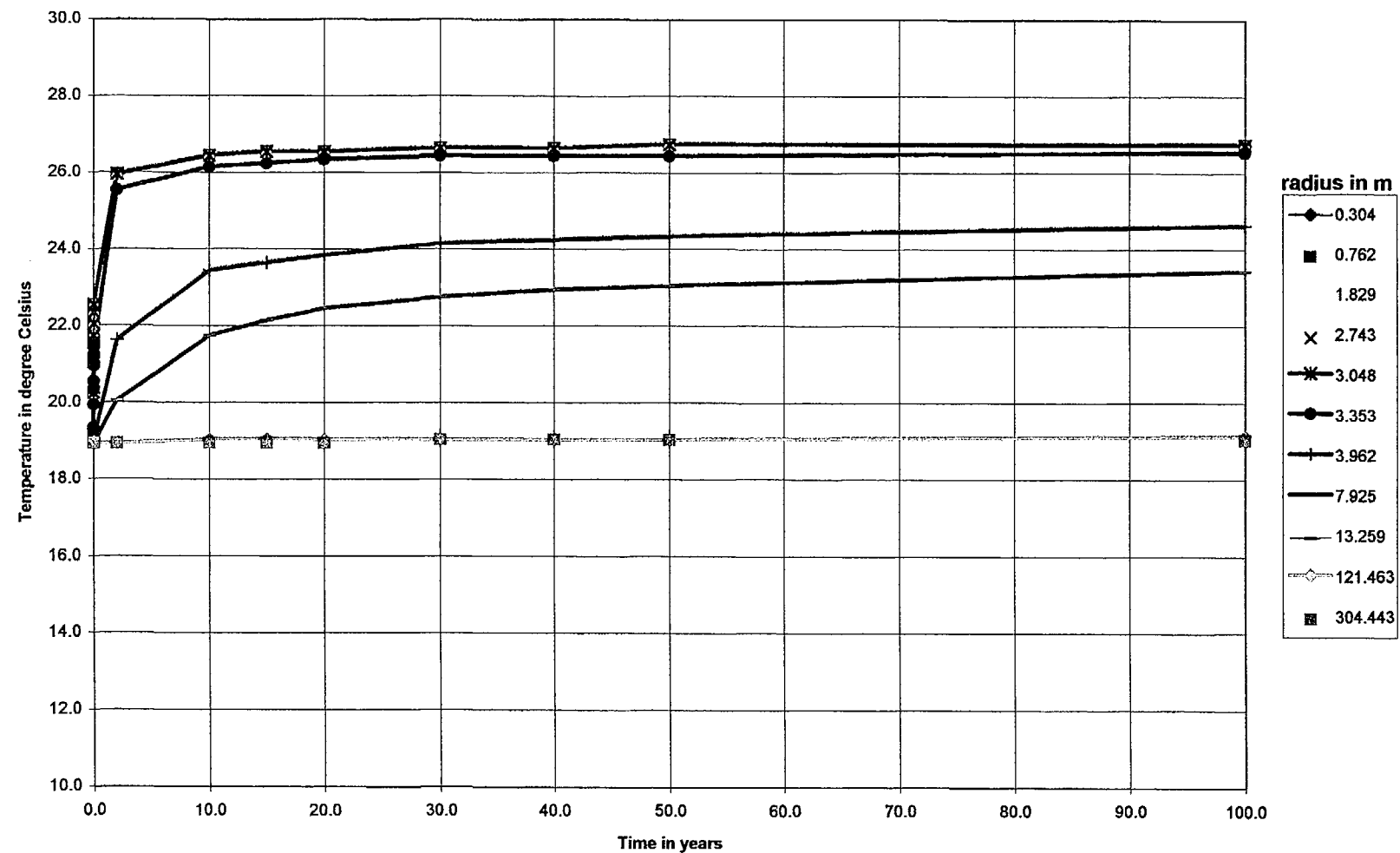


Figure 6-9b

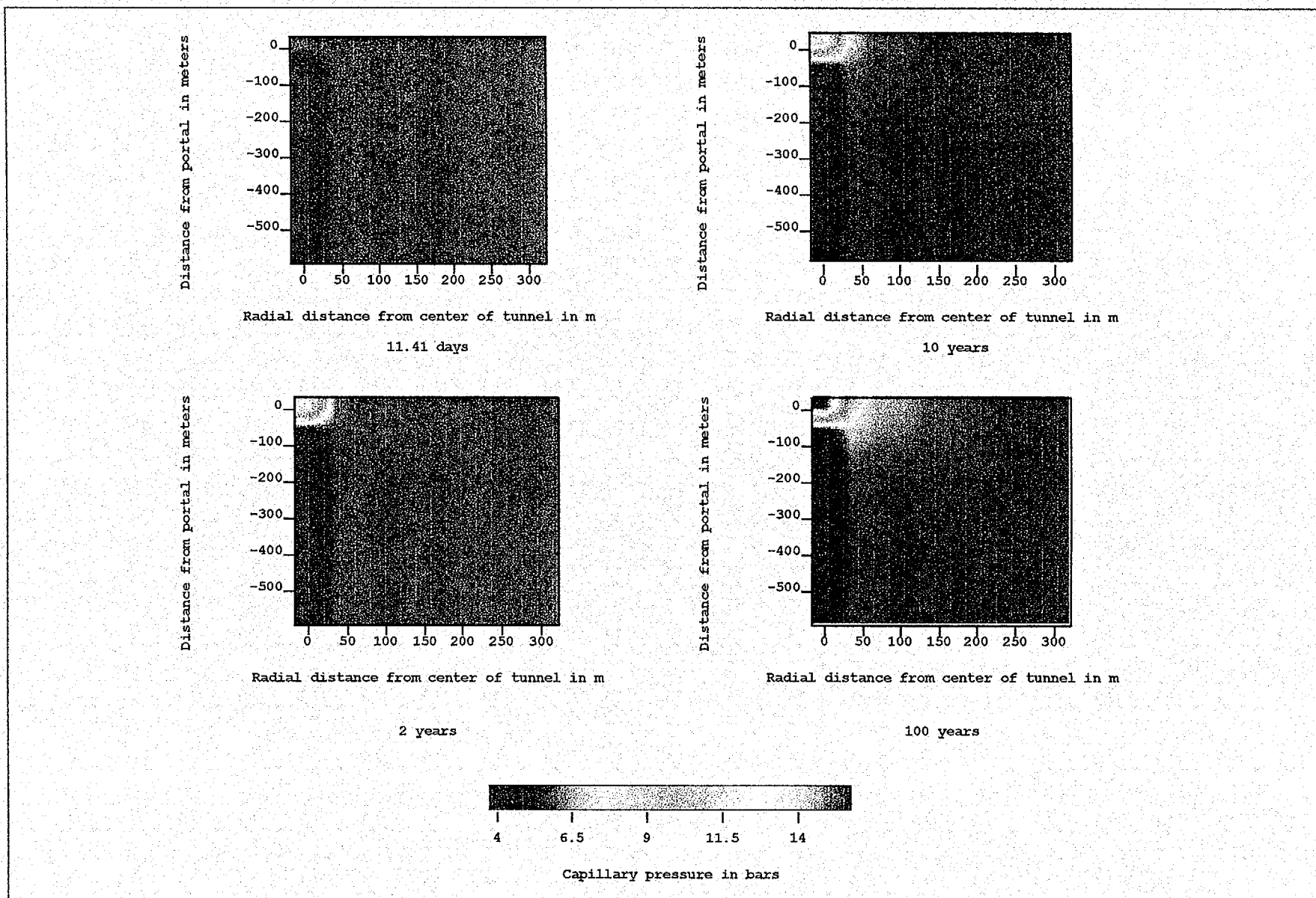


Figure 6-10 - Simulated capillary pressure around the tunnel for various times. Case 2, eddy diffusivity = 0.01, atmosphere temperature = 28 °C.

Case 2

Capillary Pressure versus time for $D_{atm} = 0.01$ and atmosphere temperature = 28 C
 Distance from portal = 261 m

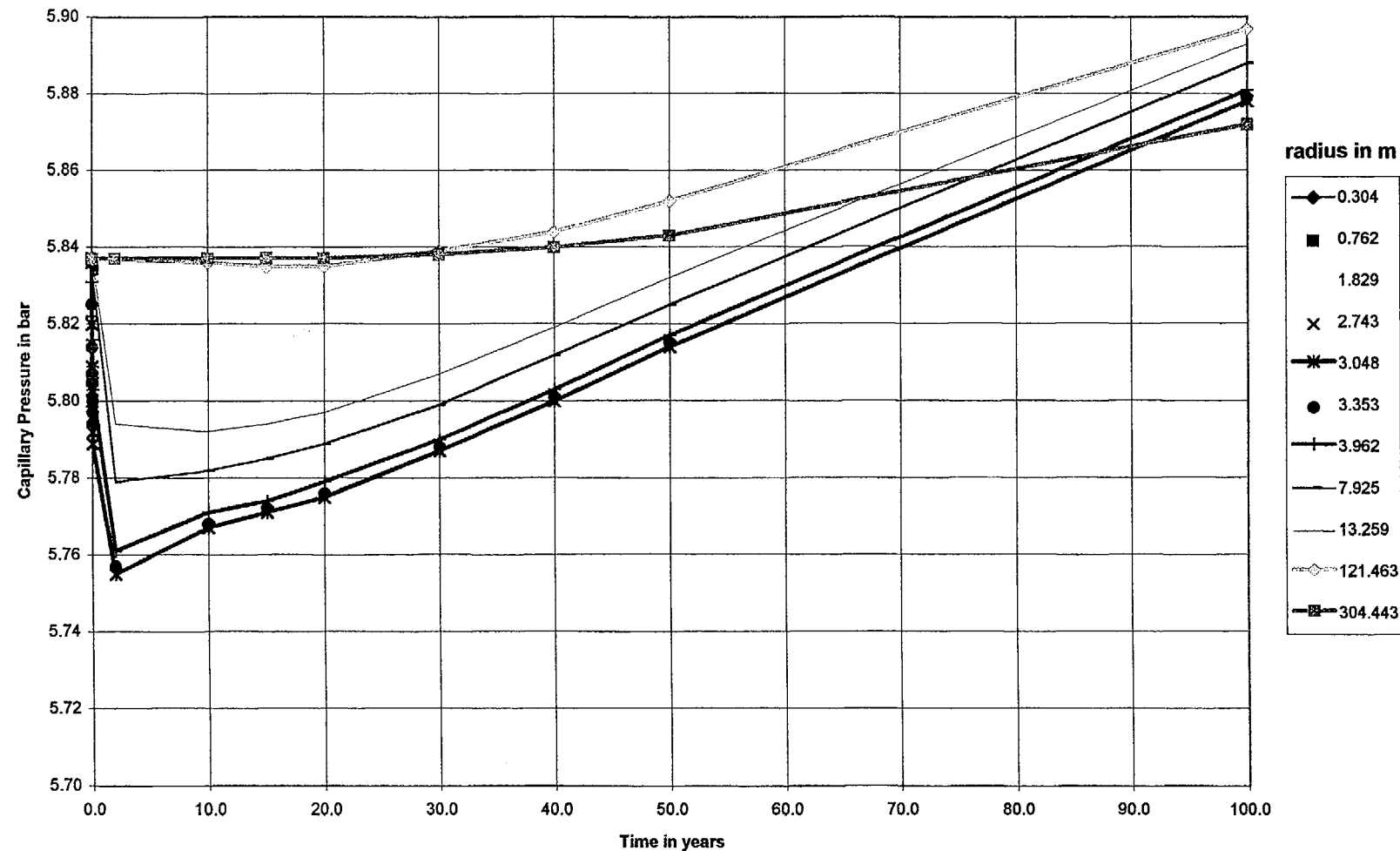


Figure 6-10a

Case 2

**Water saturation versus time for $D_{atm} = 0.01$ and atmosphere temperature = 28 C
Distance from portal = 261 m**

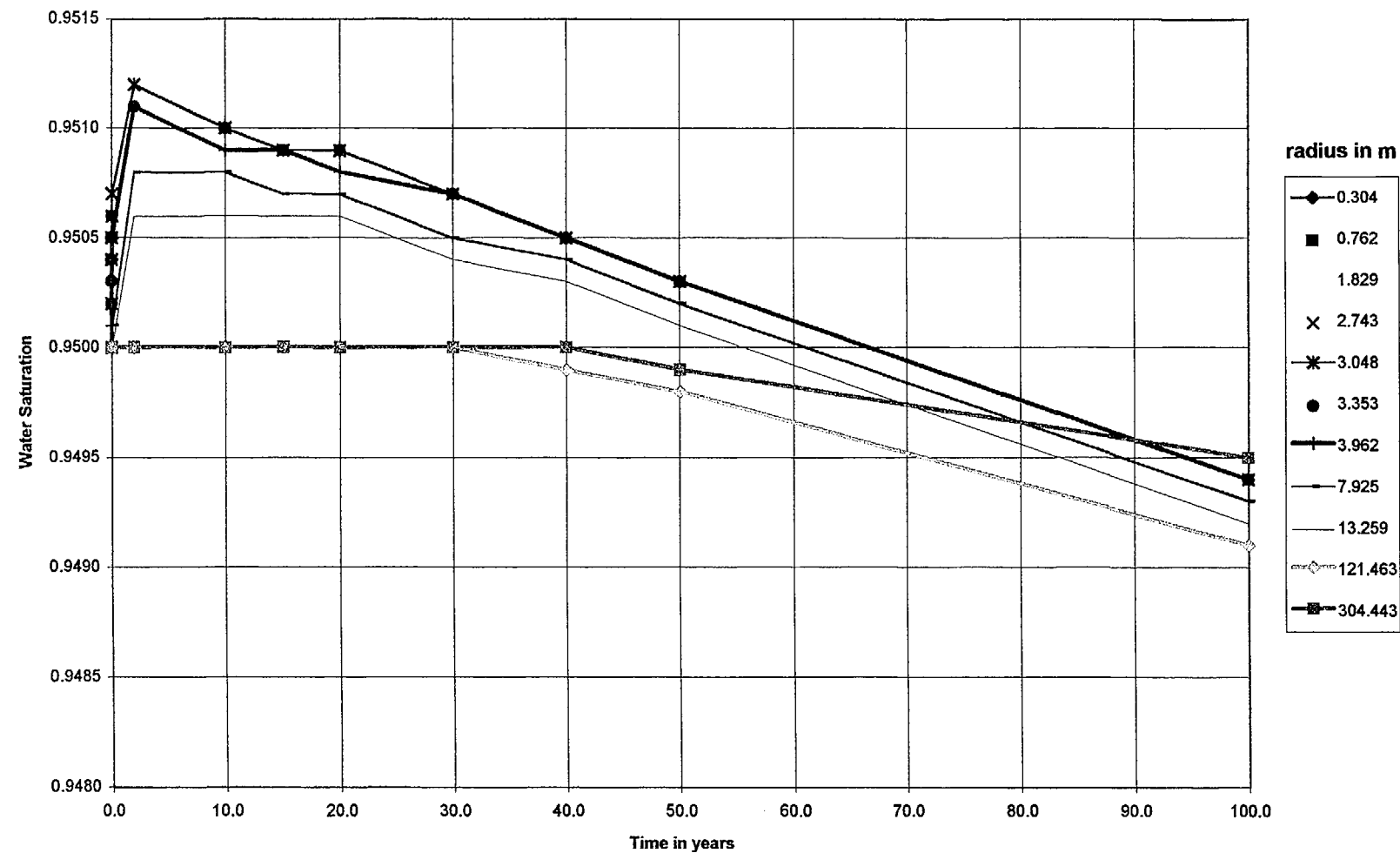


Figure 6-10b

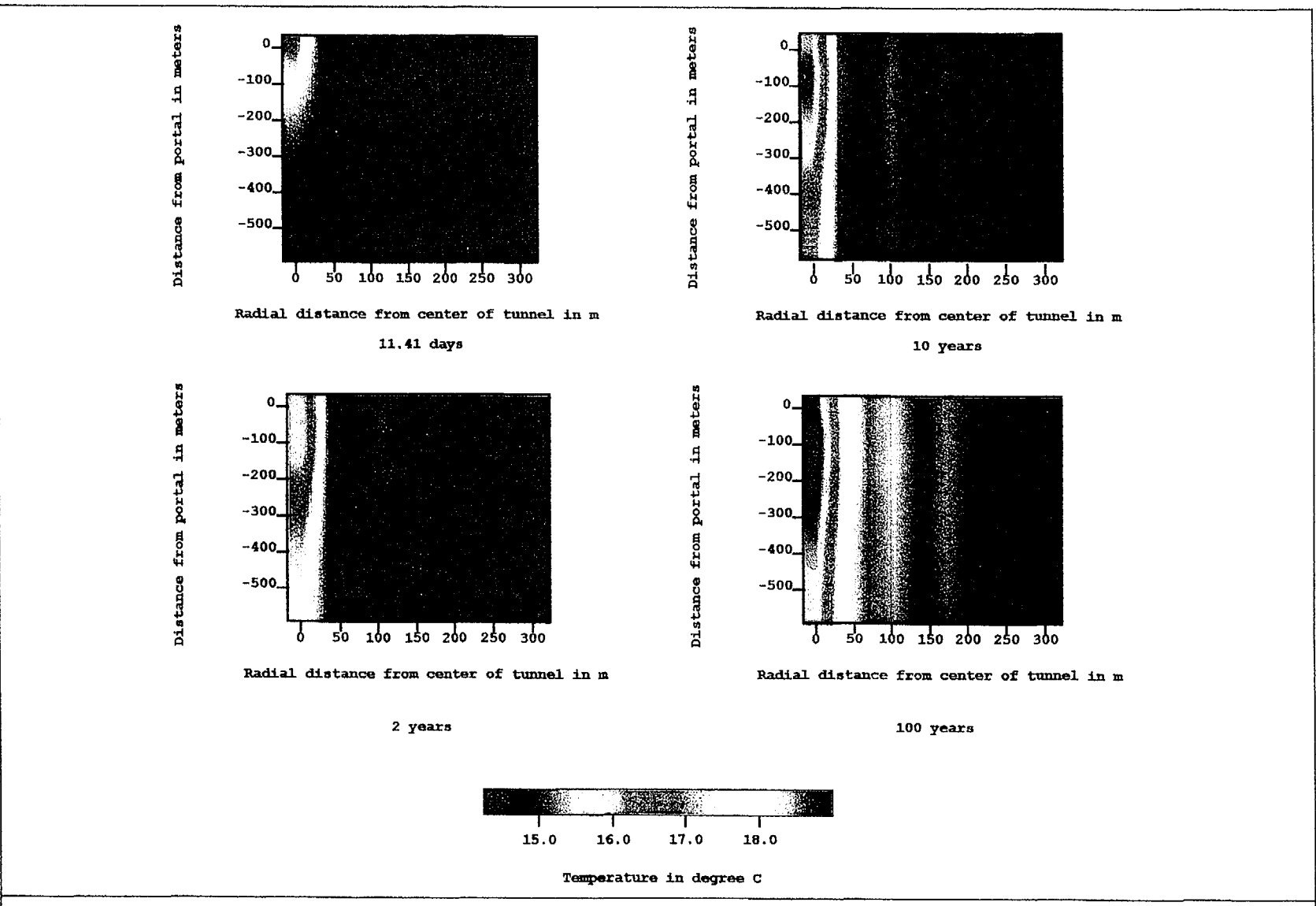


Figure 6-11 - Simulated temperature around the tunnel for various times. Case 3, eddy diffusivity = 0.001, atmosphere temperature = 15 °C.

Case 3

Temperature versus time for $D_{atm} = 0.001$ and atmosphere temperature = 15 C
Distance from portal = 261m

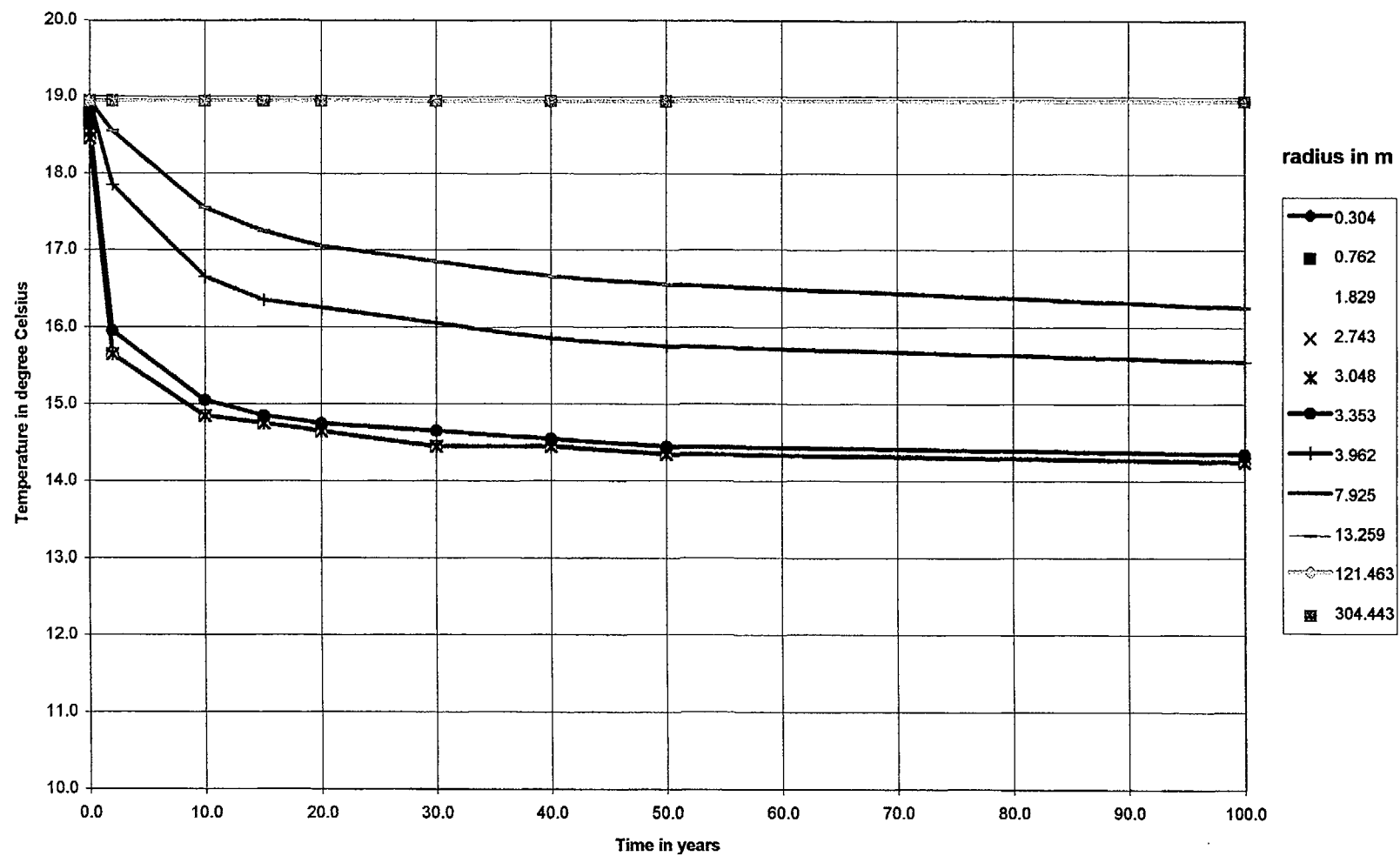


Figure 6-11a

Case 3

**Pressure versus time for $D_{atm} = 0.001$ and atmosphere temperature = 15 C
Distance from portal = 261 m**

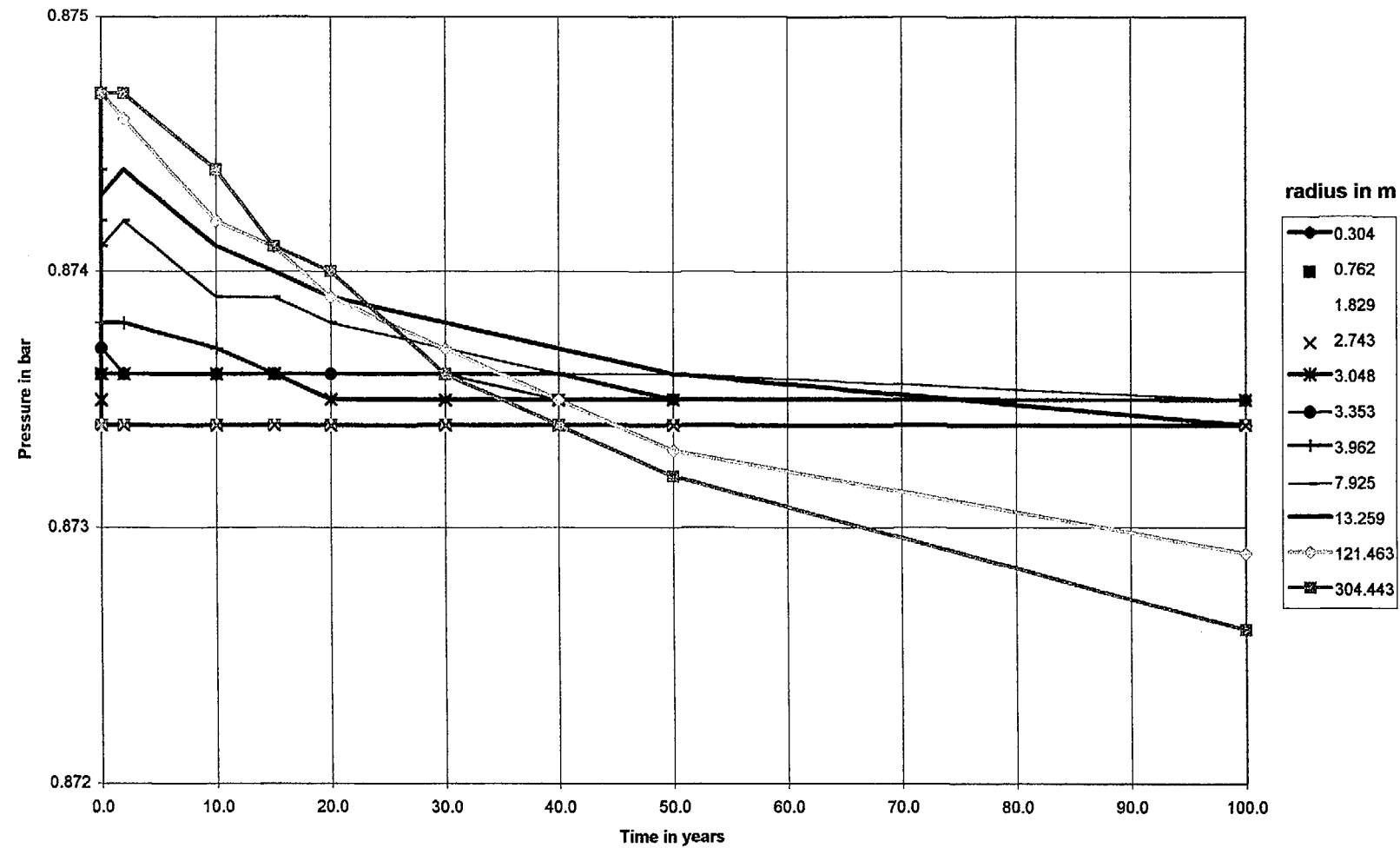


Figure 6-11b

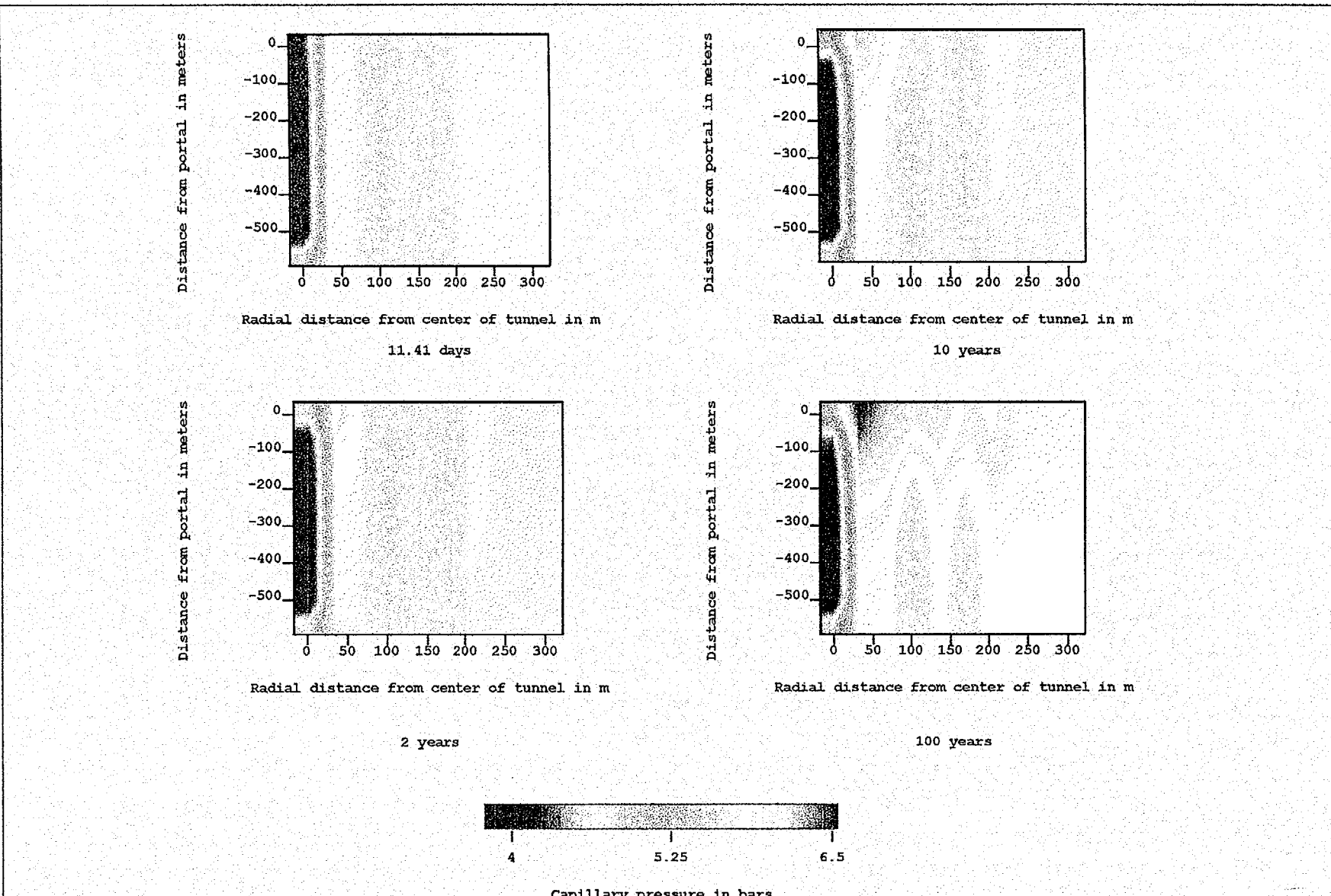


Figure 6-12 - Simulated capillary pressure around the tunnel for various times. Case 3, eddy diffusivity = 0.001, atmosphere temperature = 15 °C.

Case 3

Capillary Pressure versus time for $D_{atm} = 0.001$ and atmosphere temperature = 15 C
Distance from portal = 261 m

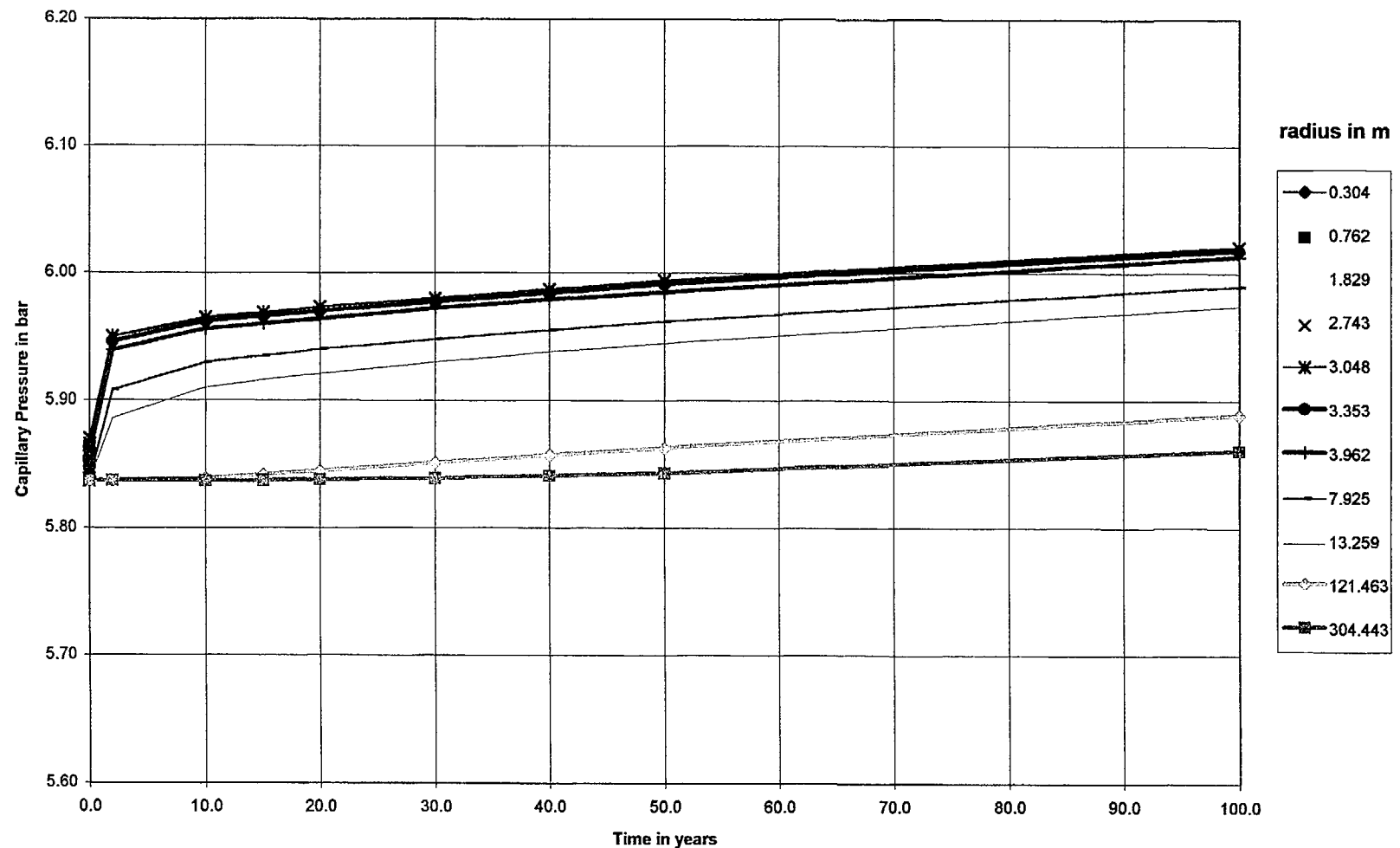


Figure 6-12a

Case 3

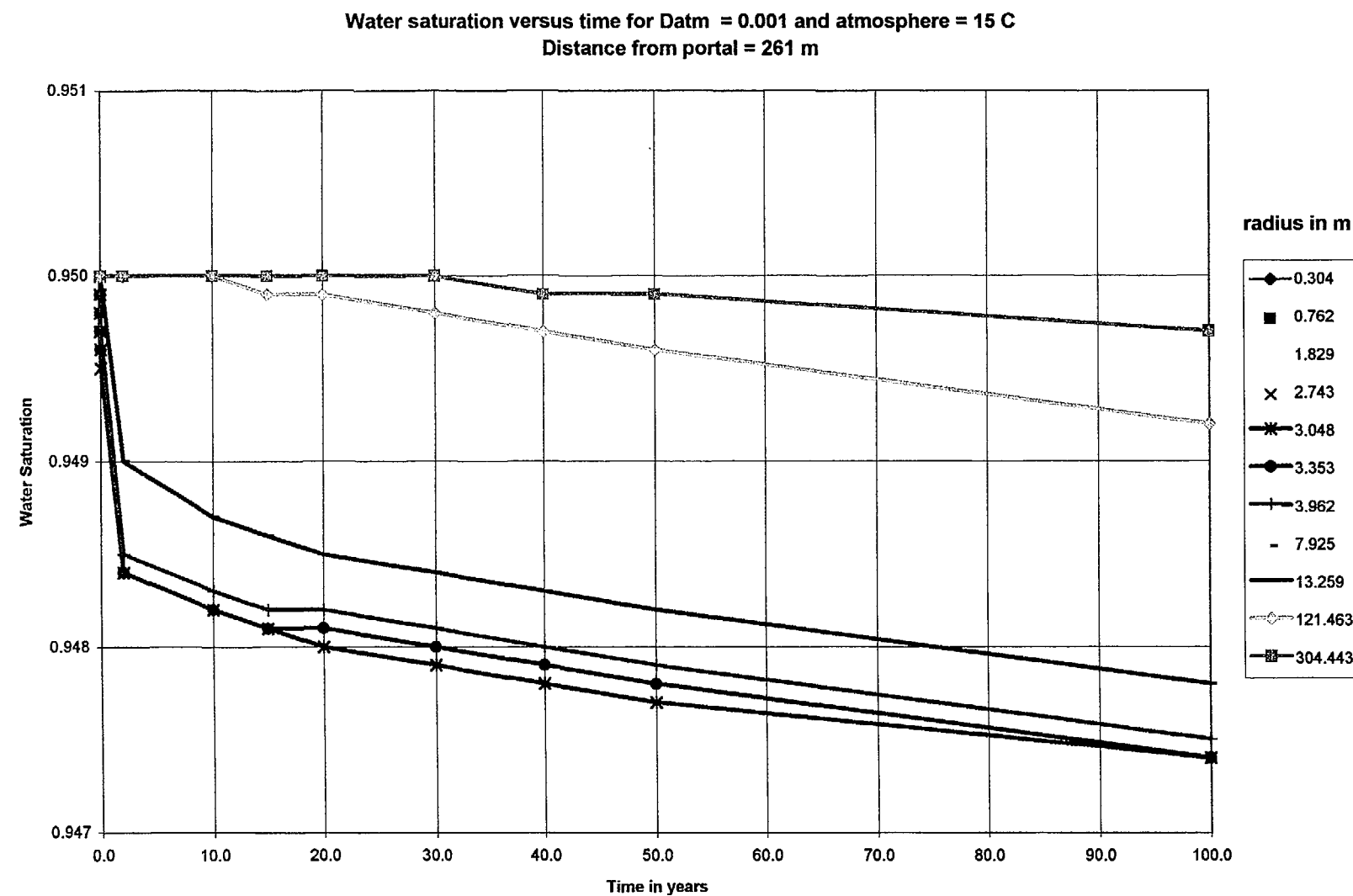


Figure 6-12b

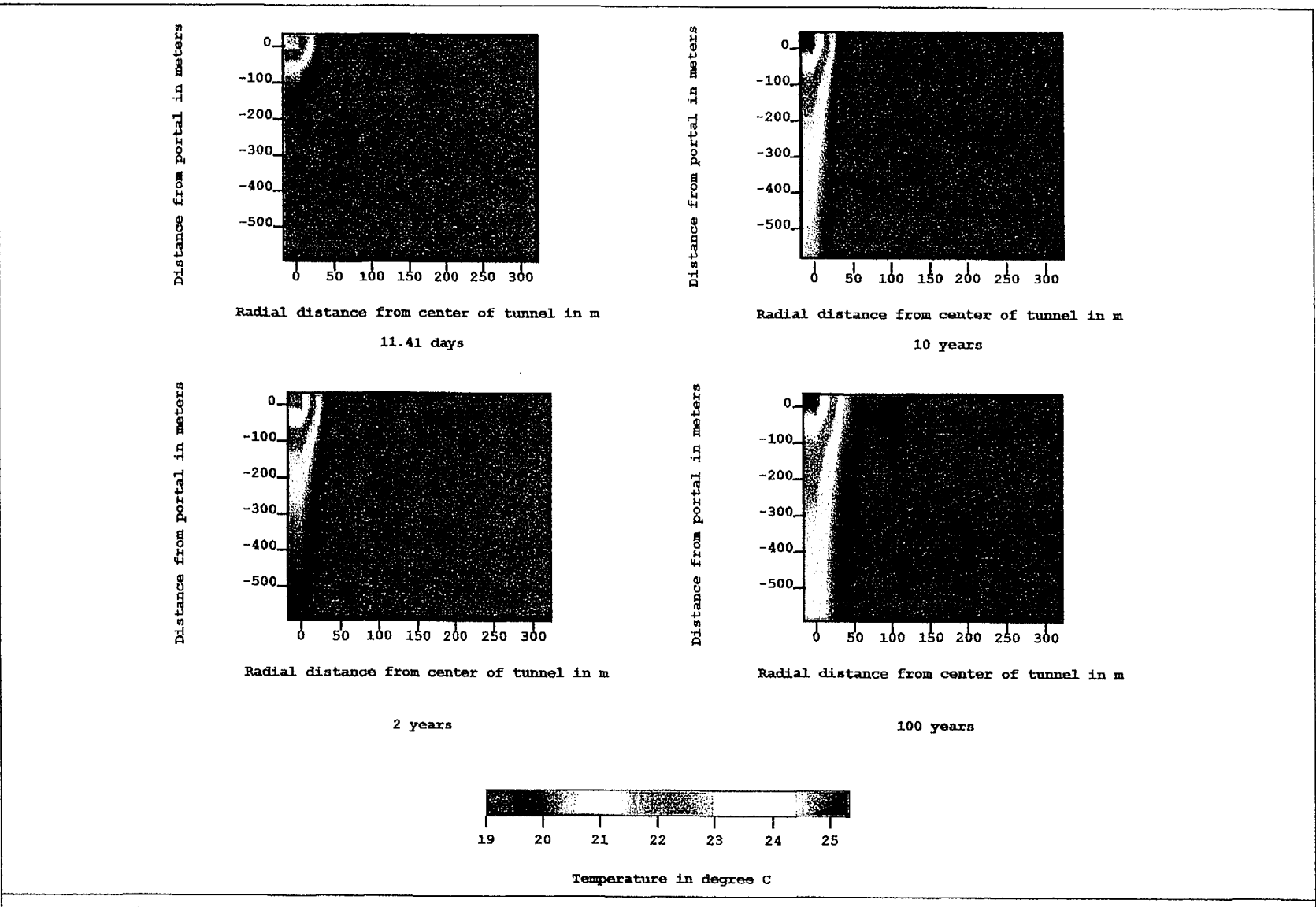


Figure 6-13 - Simulated temperature around the tunnel for various times. Case 4, eddy diffusivity = 0.001, atmosphere temperature = 28 °C.

Case 4

Temperature versus time for $D_{atm} = 0.001$ and atmosphere temperature = 28 C
Distance from portal = 261m

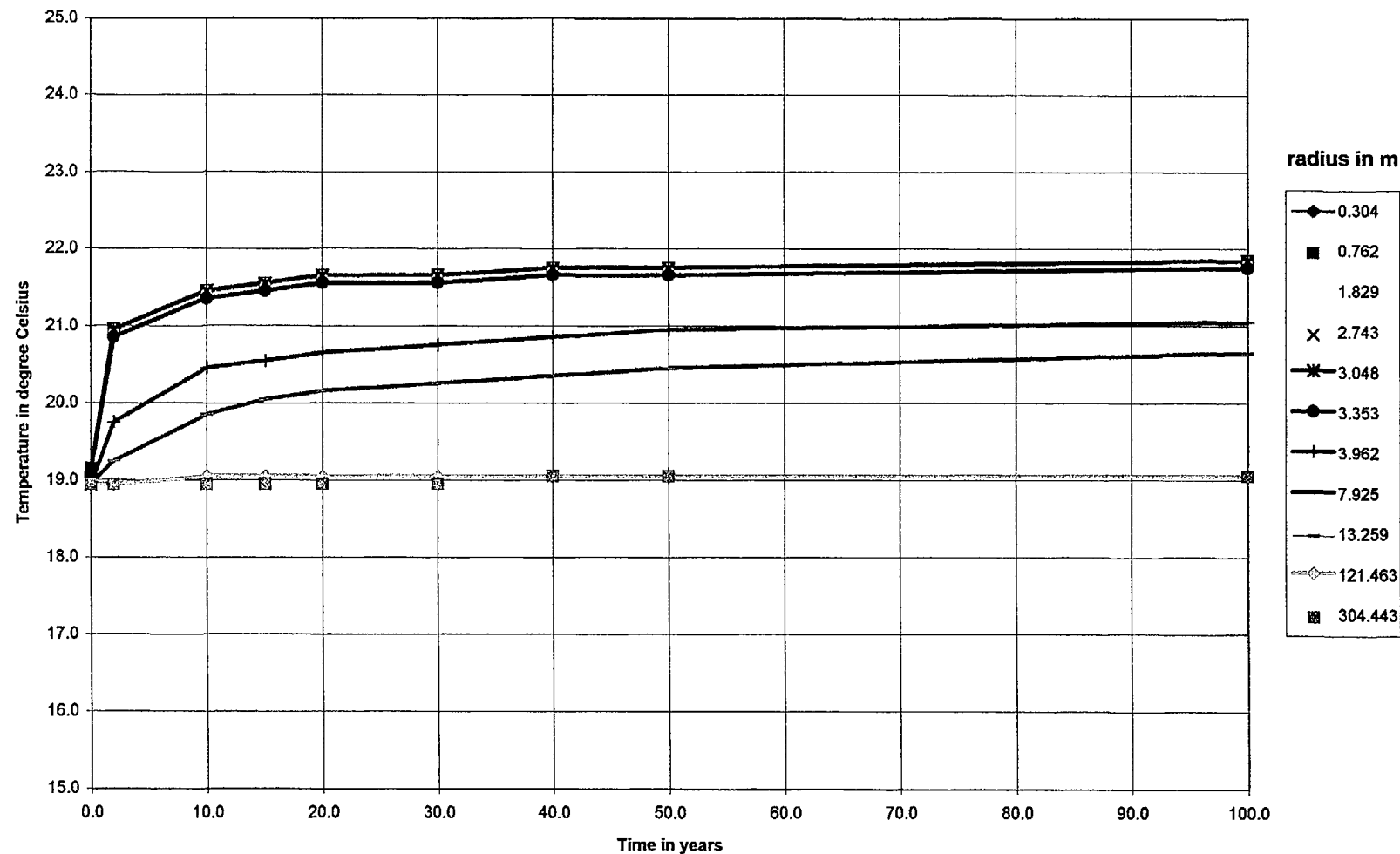


Figure 6-13a

Case 4

Pressure versus time for $D_{atm} = 0.001$ and atmosphere temperature = 28 C
Distance from portal ≈ 261 m

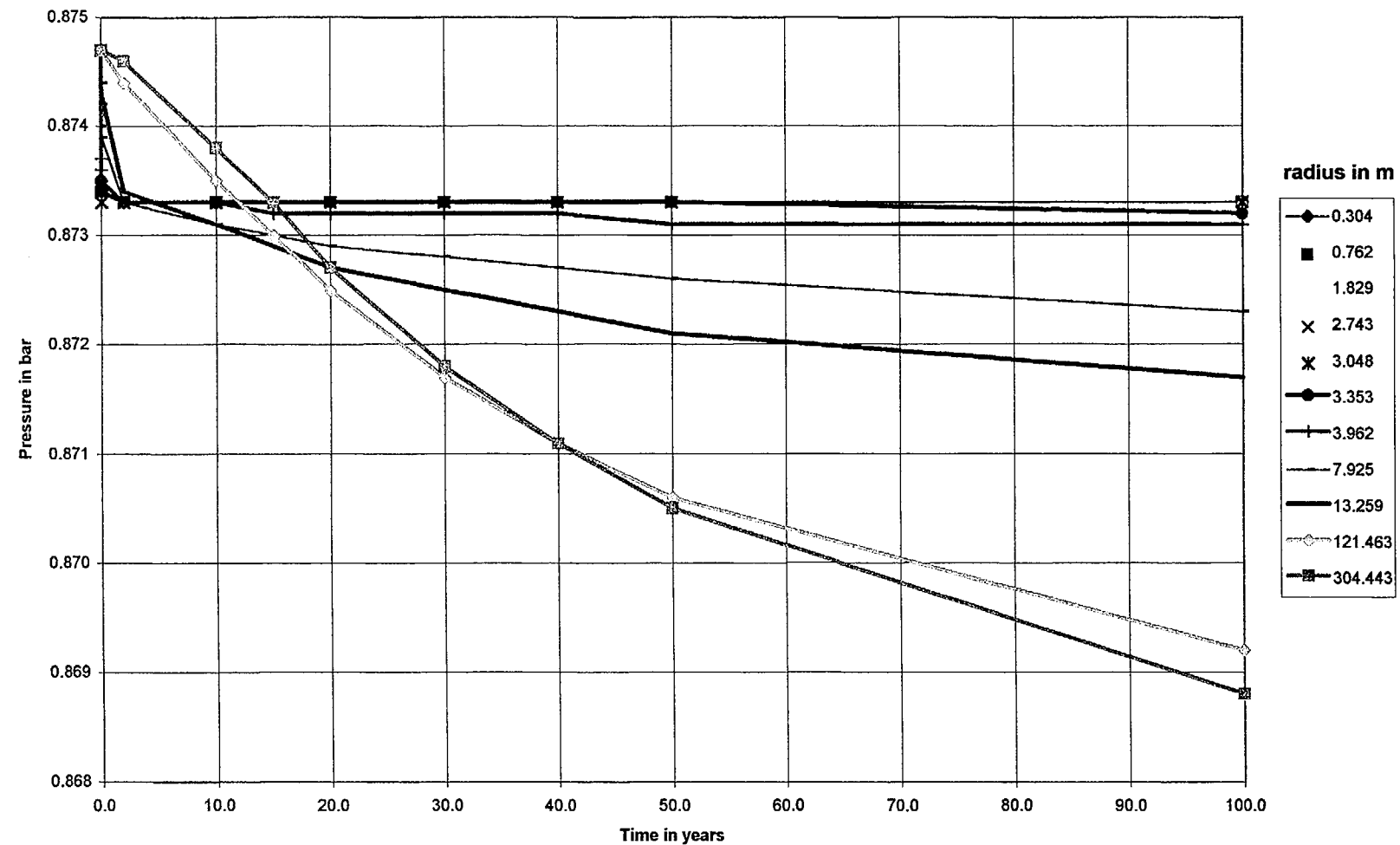


Figure 6-13b

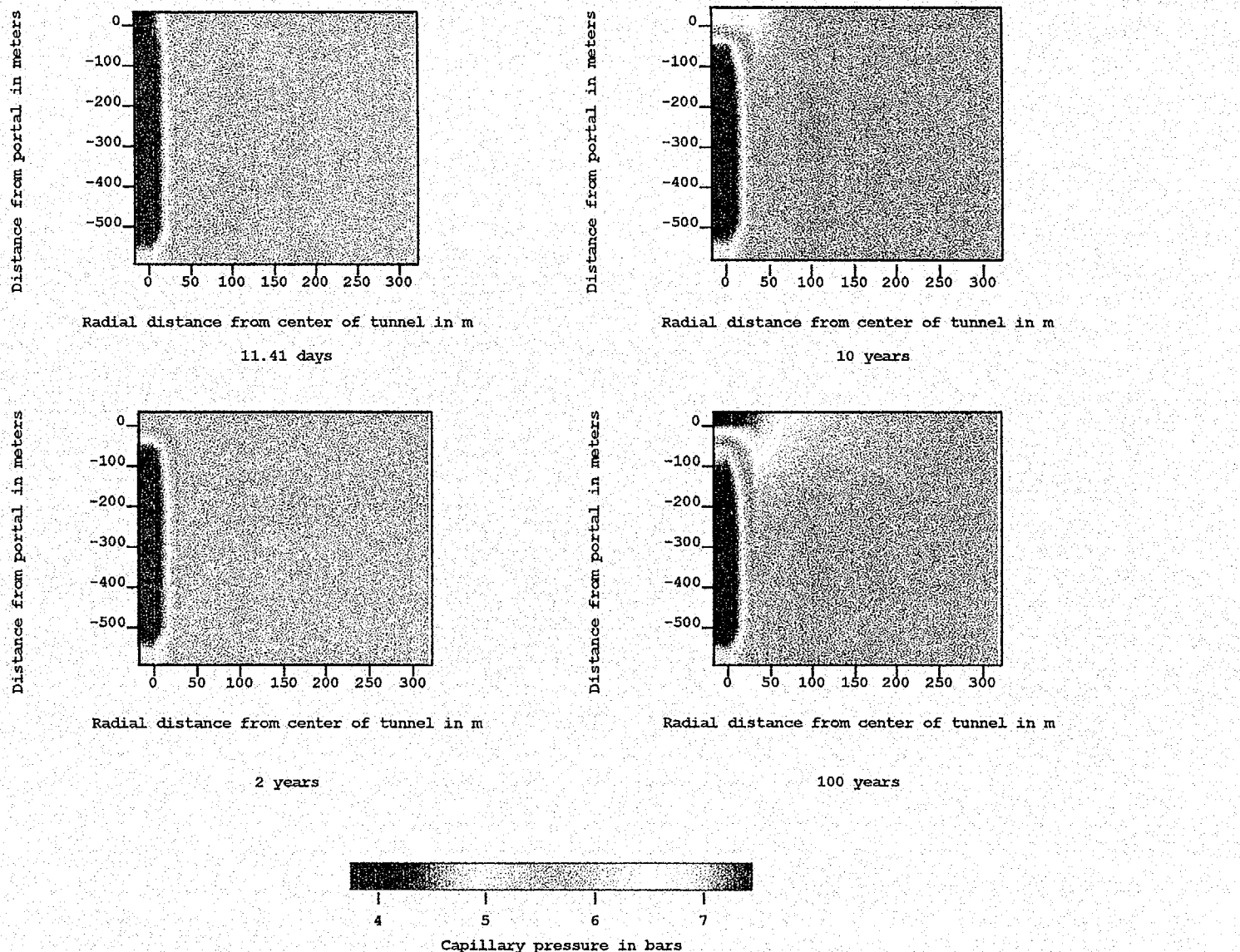


Figure 6-14 - Simulated capillary pressure around the tunnel for various times. Case 4, eddy diffusivity = 0.001, atmosphere temperature = 28 °C.

Case 4

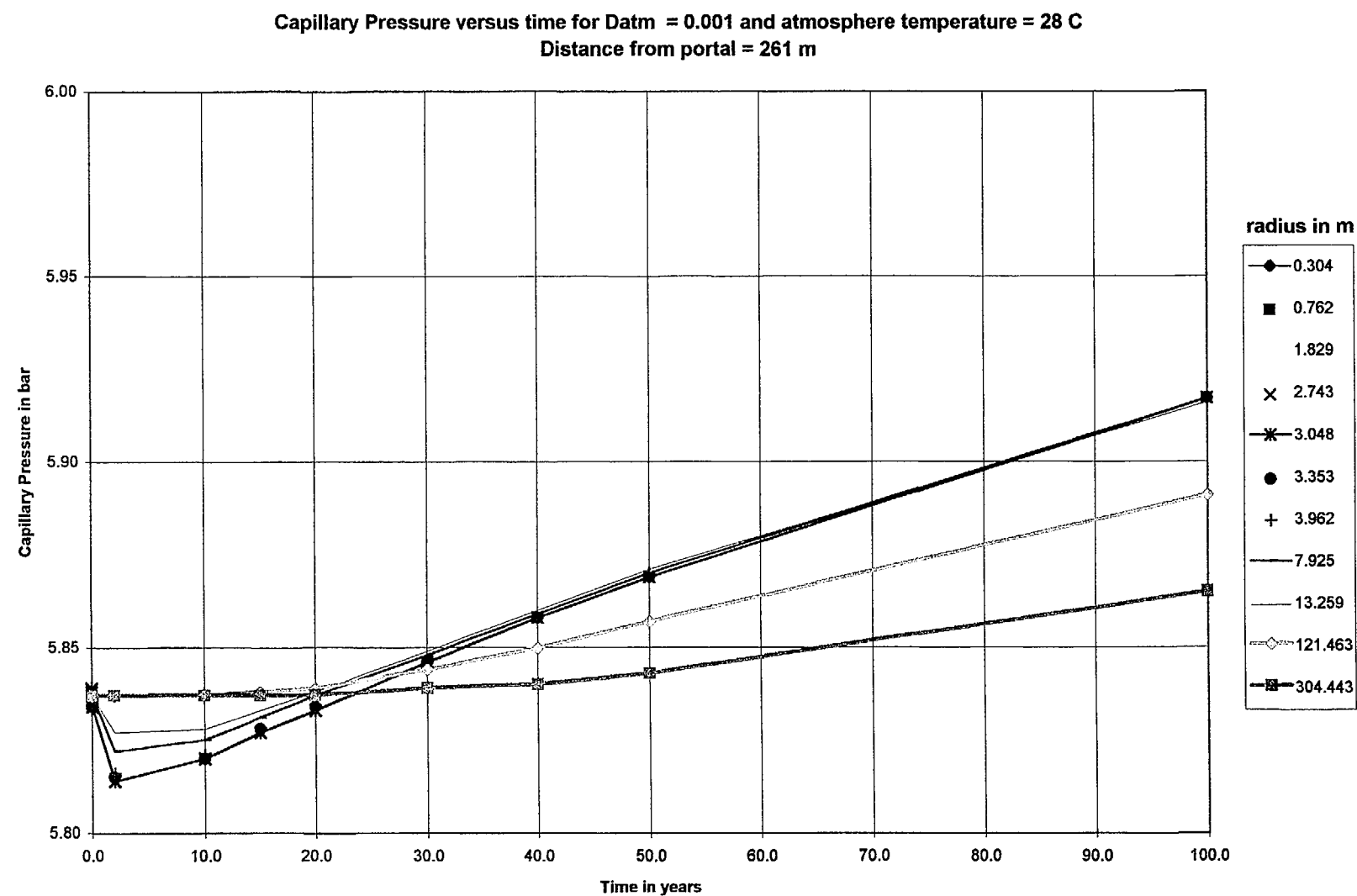


Figure 6-14a

Case 4

**Water saturation versus time for $D_{atm} = 0.001$ and atmosphere temperature = 28 C
Distance from portal = 261 m**

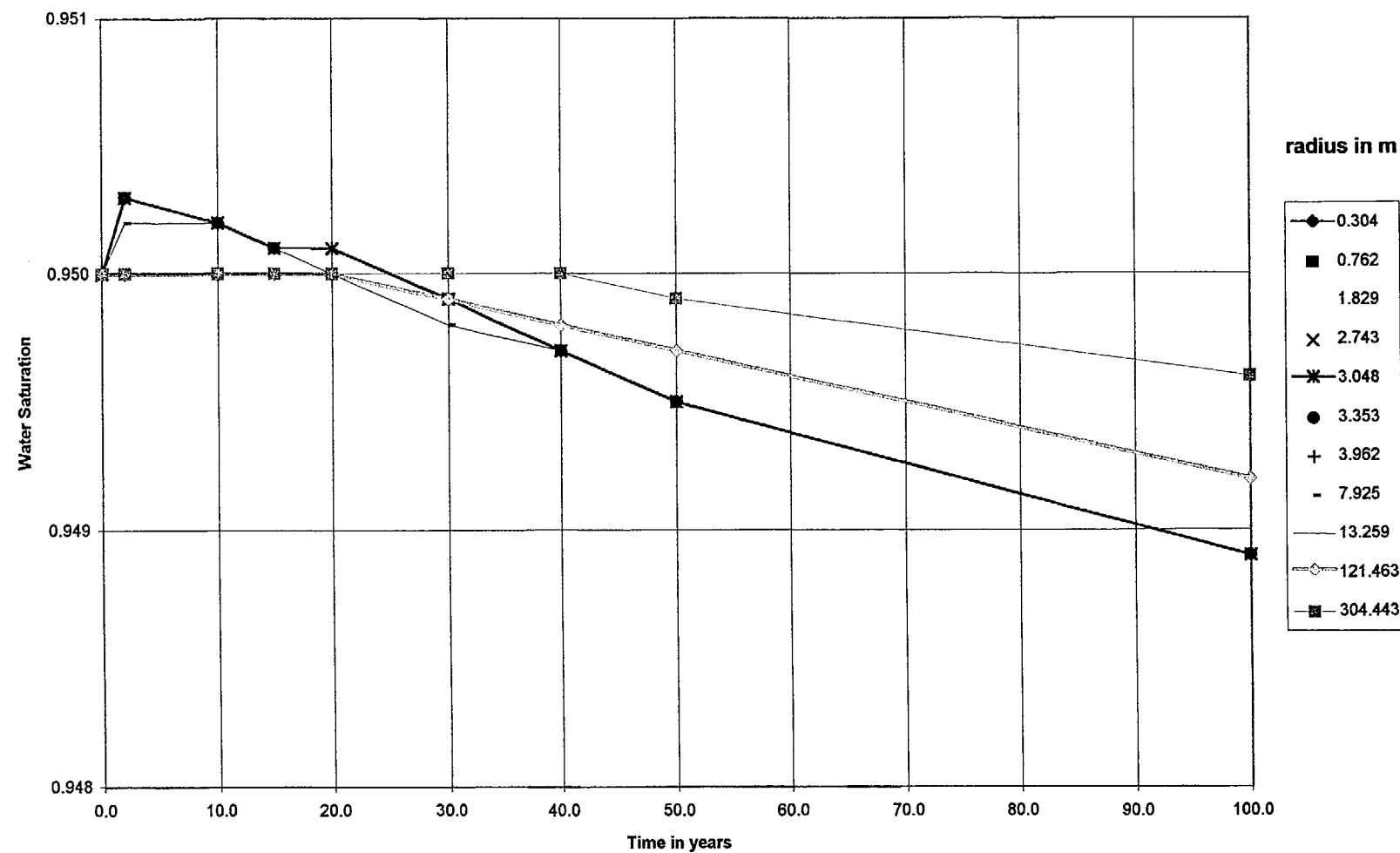


Figure 6-14b

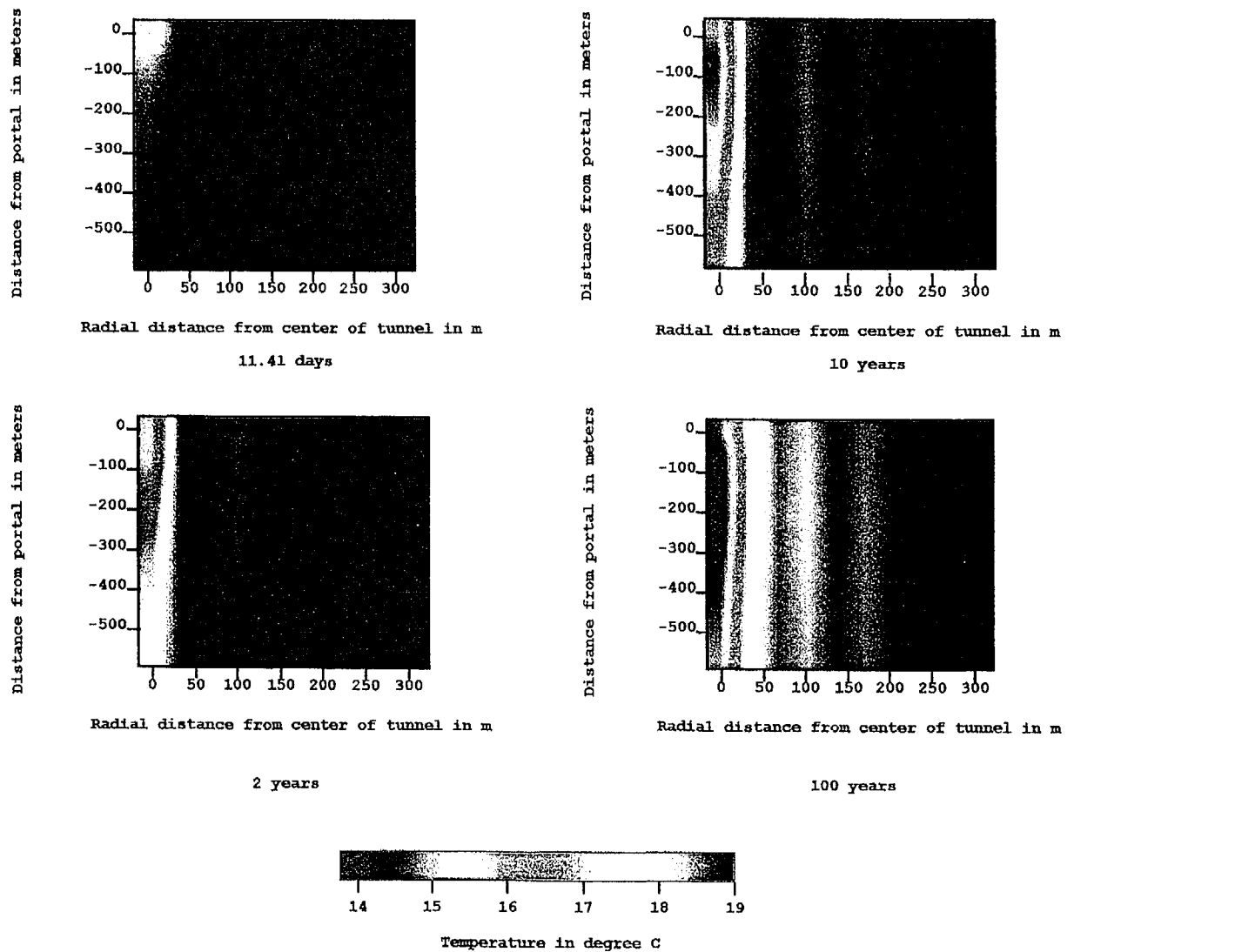


Figure 6-15 - Simulated temperature around the tunnel for various times. Case 5, eddy diffusivity = 0.0001, atmosphere temperature = 15 °C.

Case 5

Temperature versus time for $D_{atm} = 0.0001$ and atmosphere temperature = 15 C
Distance from portal = 261m

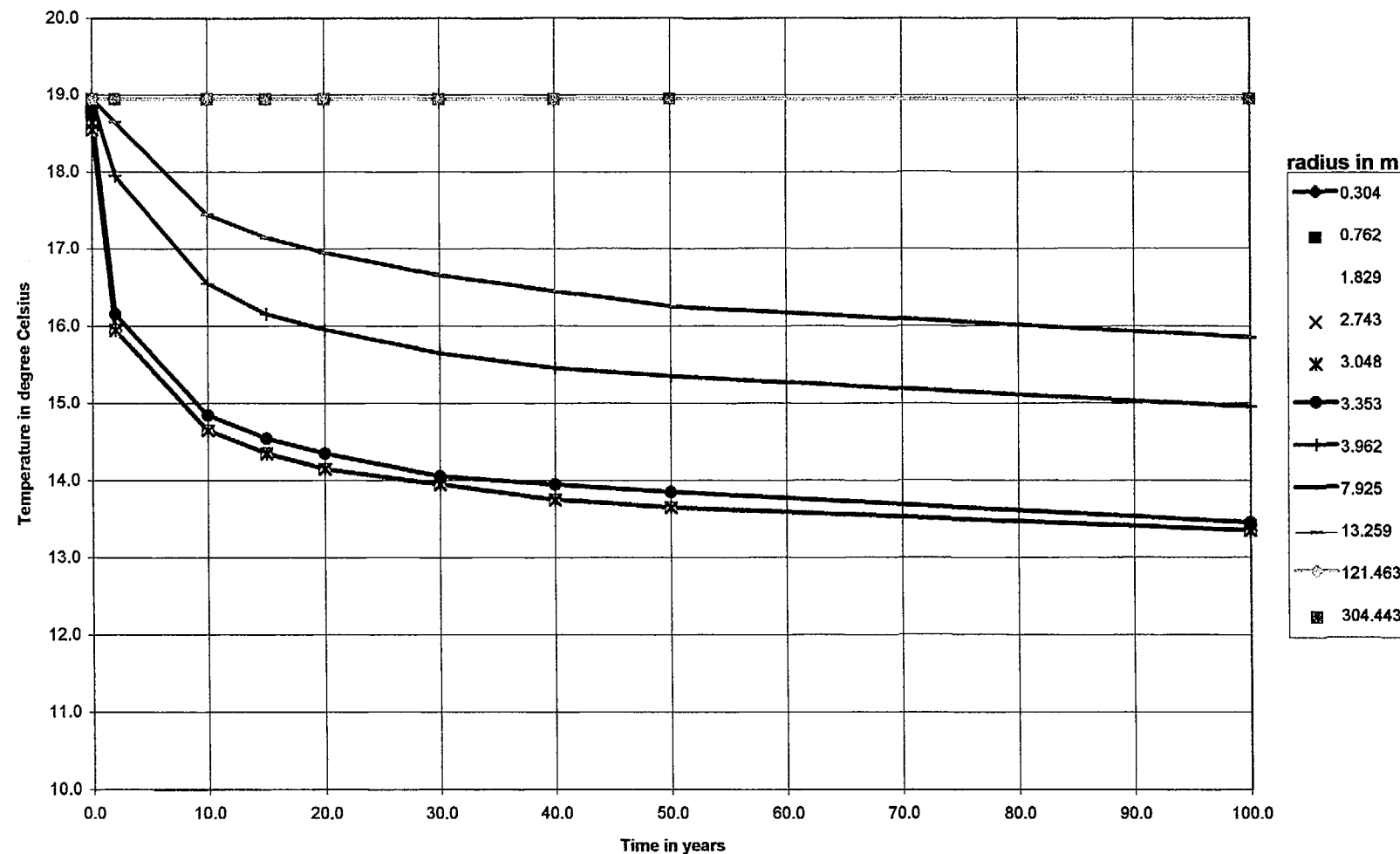


Figure 6-15a

Case 5

Pressure versus time for $D_{atm} = 0.0001$ and atmosphere temperature = 15 C
Distance from portal = 261 m

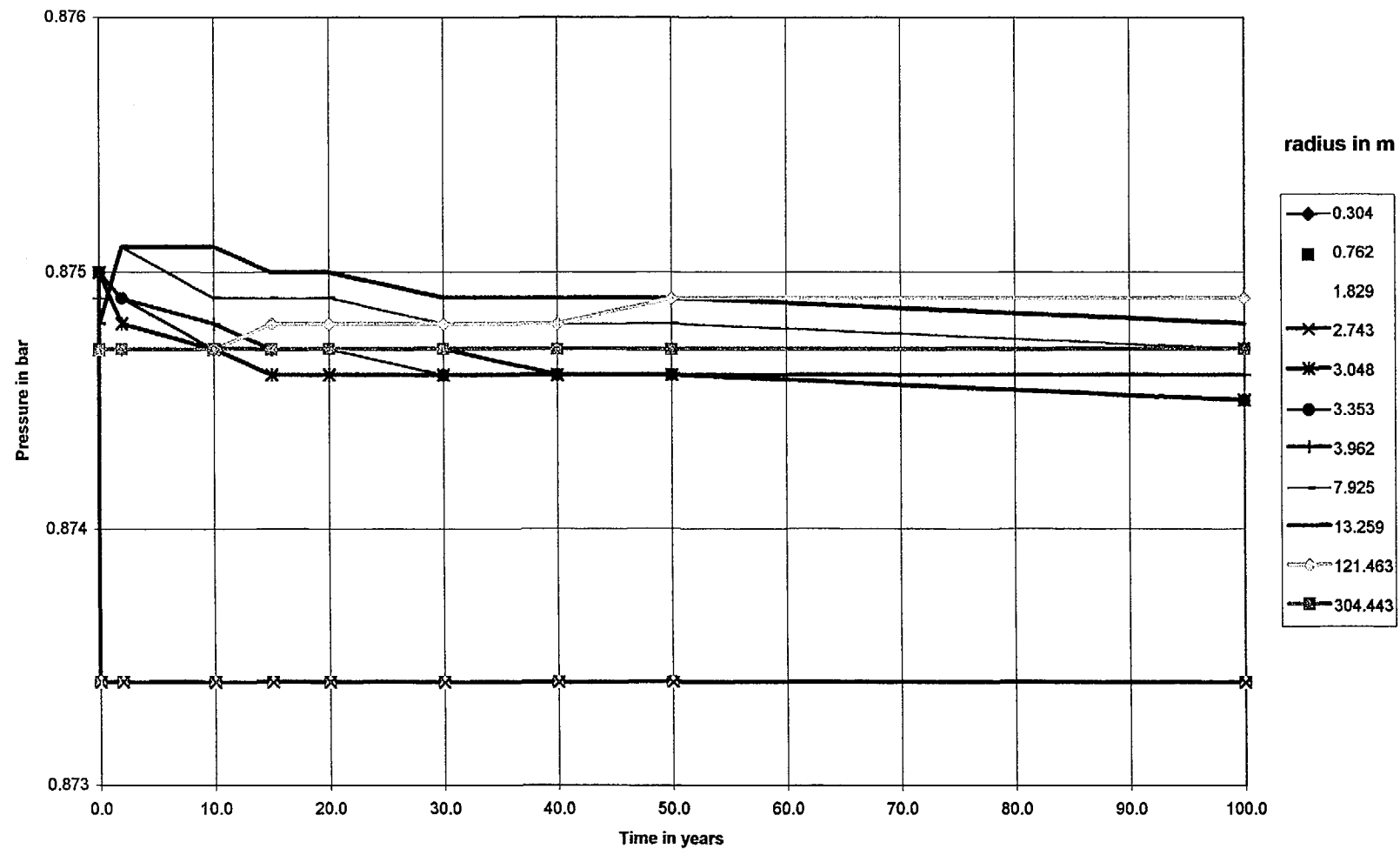


Figure 6-15b

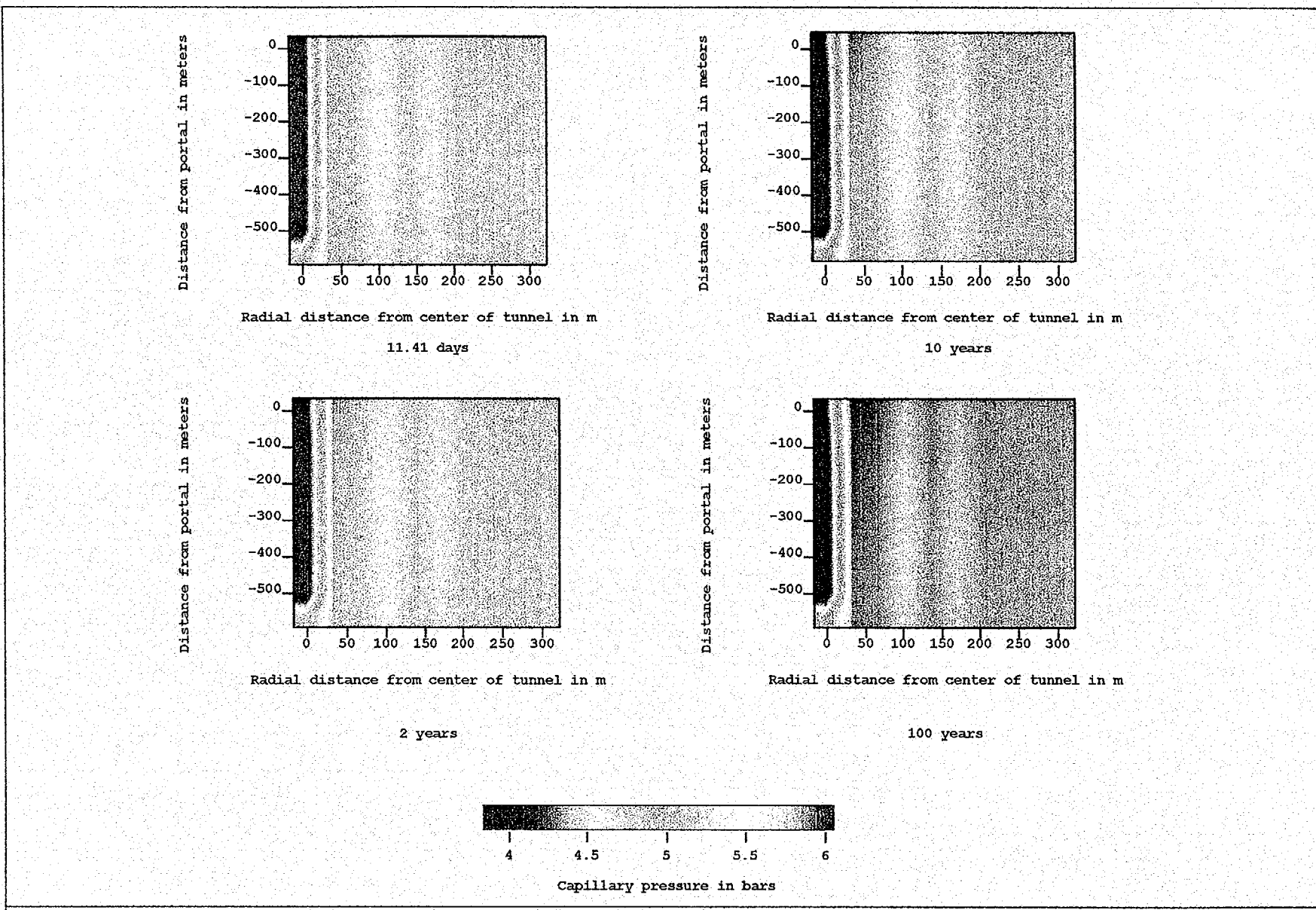


Figure 6-16 - Simulated capillary pressure around the tunnel for various times. Case 5, eddy diffusivity = 0.0001, atmosphere temperature = 15 °C.

Case 5

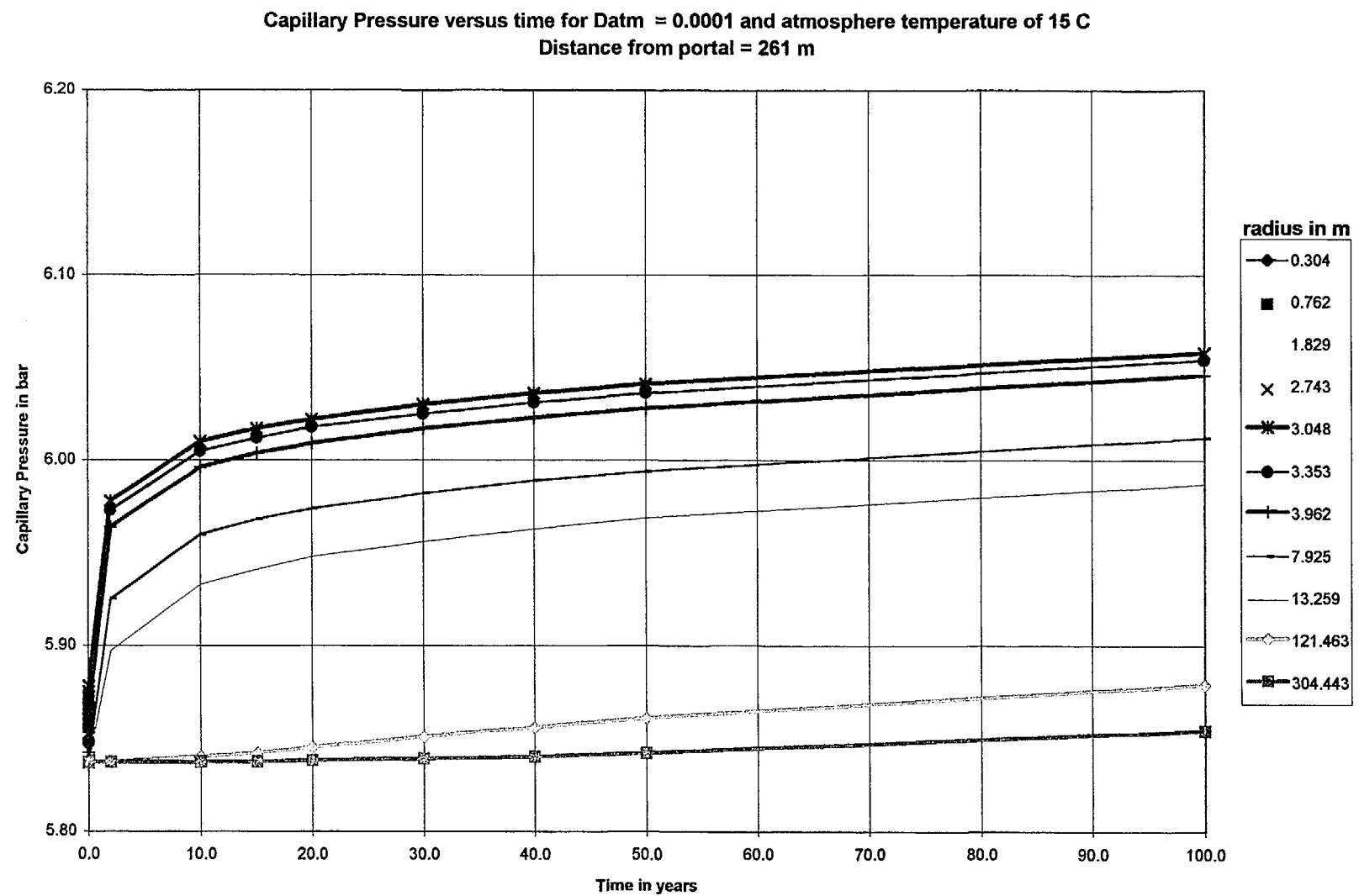


Figure 6-16a

Case 5

**Water saturation versus time for $D_{atm} = 0.0001$ and atmosphere temperature = 15 C
Distance from portal = 261 m**

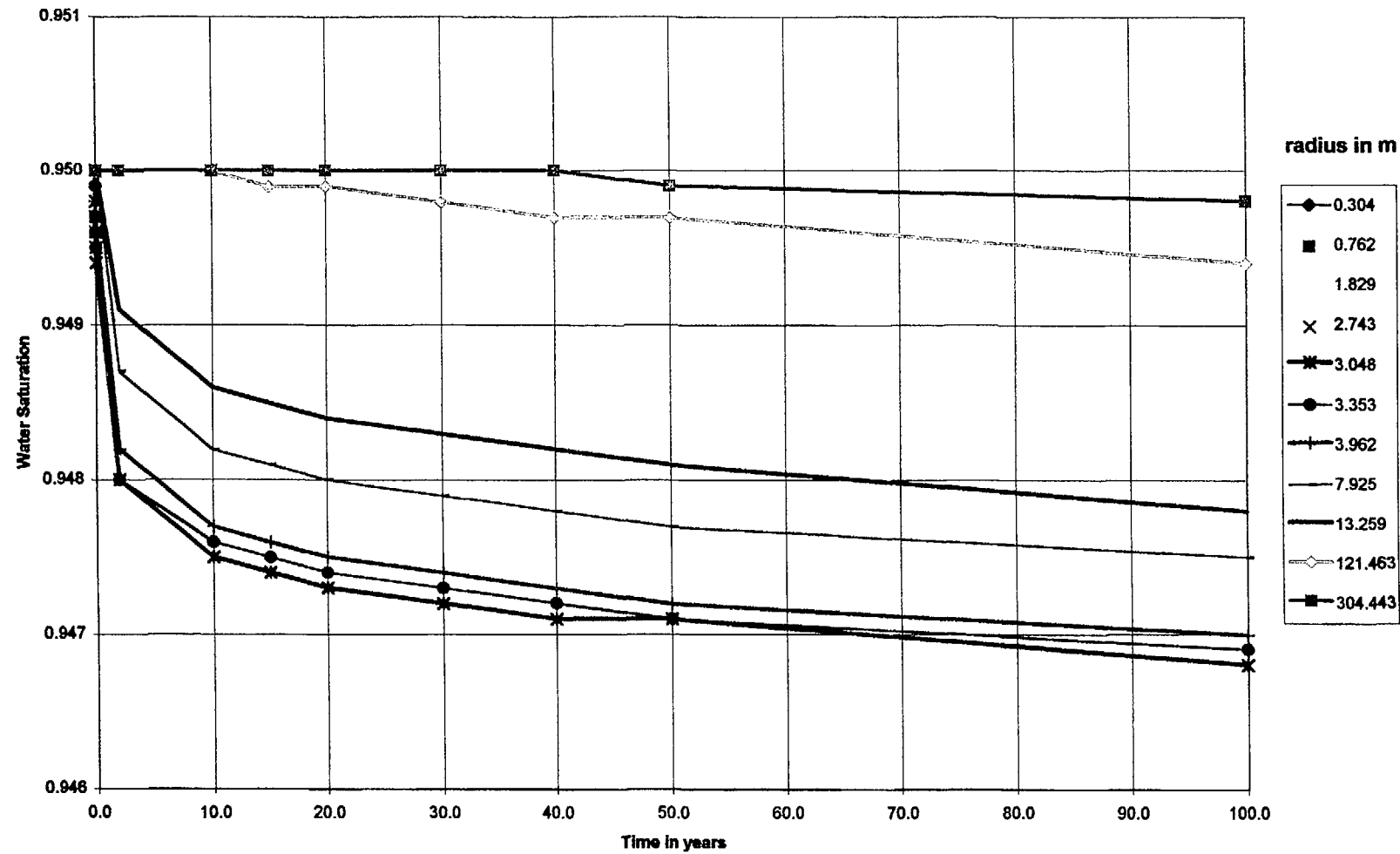


Figure 6-16b

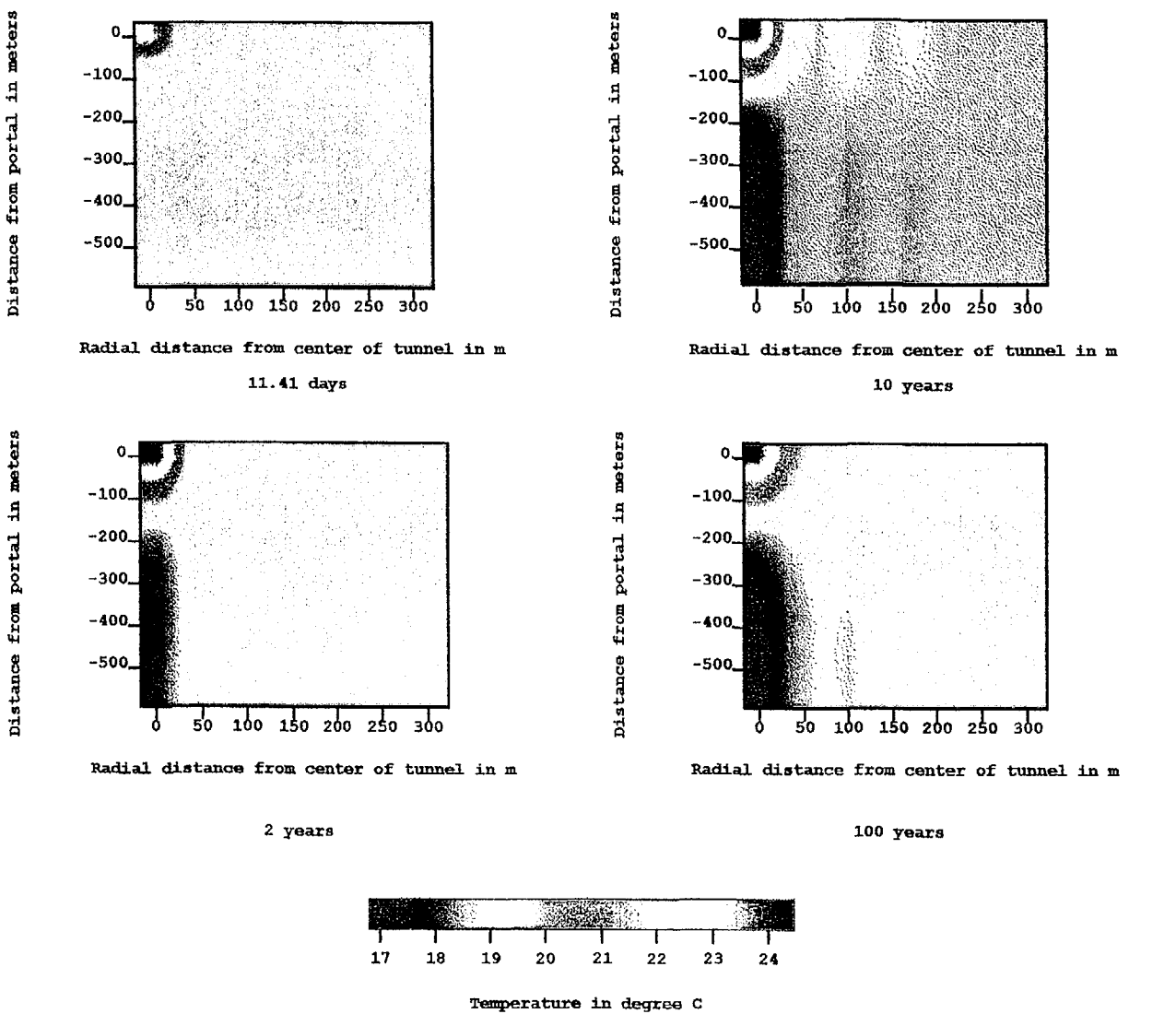


Figure 6-17 - Simulated temperature around the tunnel for various times. Case 6, eddy diffusivity = 0.0001, atmosphere temperature = 28 °C.

Case 6

**Temperature versus time for $D_{atm} = 0.0001$ and atmosphere temperature = 28 C
Distance from portal = 261m**

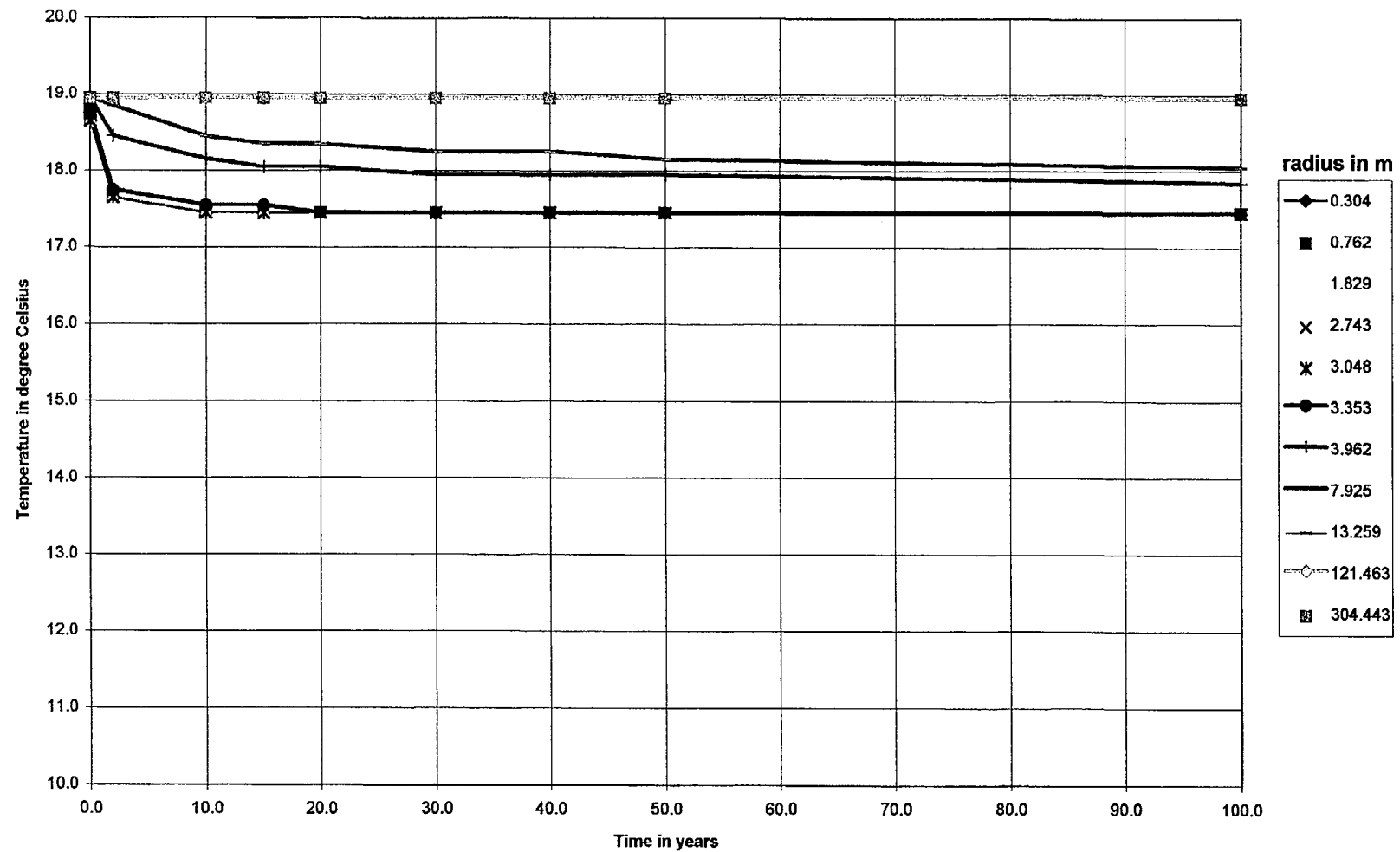


Figure 6-17a

Case 6

Pressure versus time for $D_{atm} = 0.0001$ and atmosphere temperature = 28 C
Distance from portal = 261 m

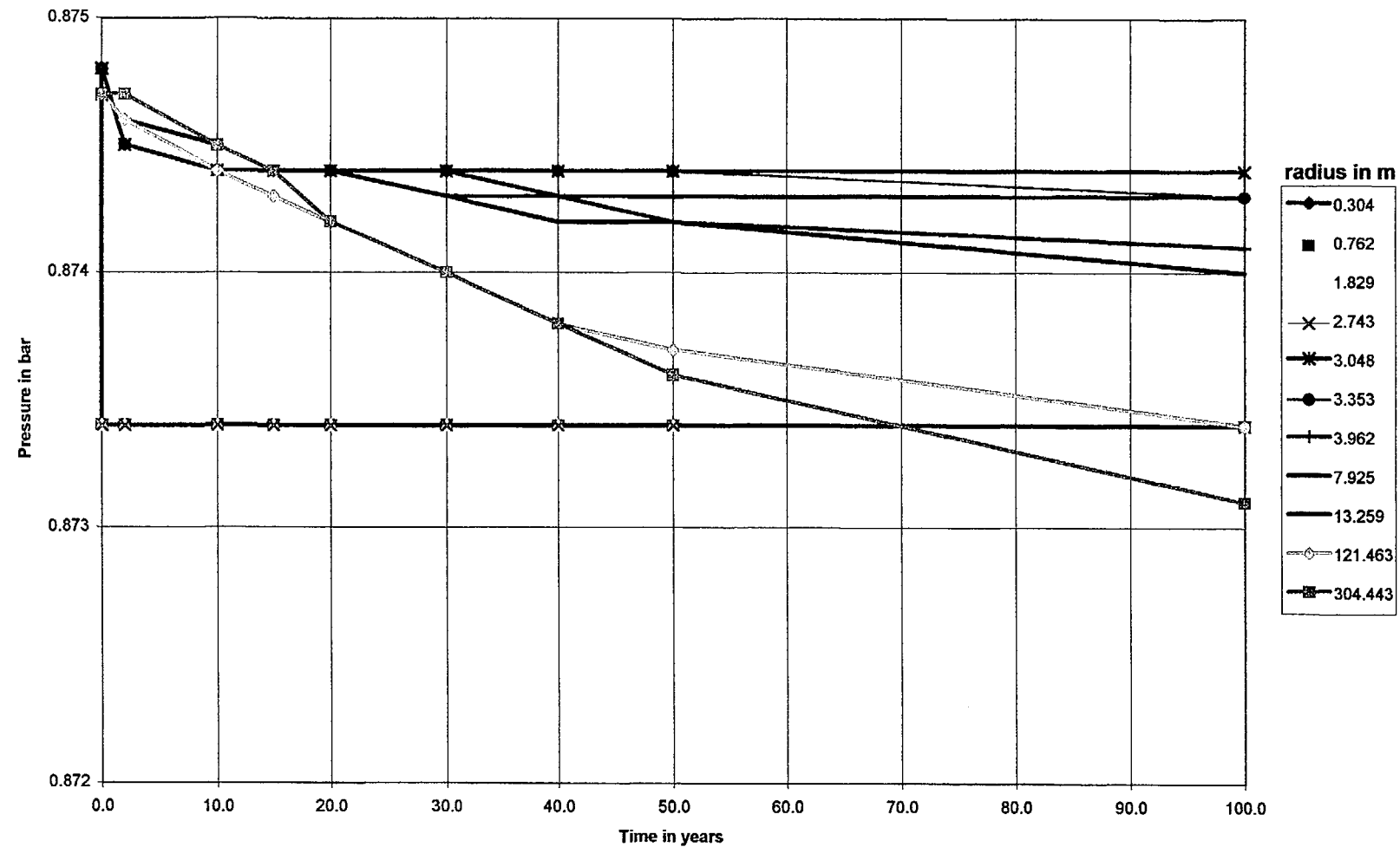


Figure 6-17b

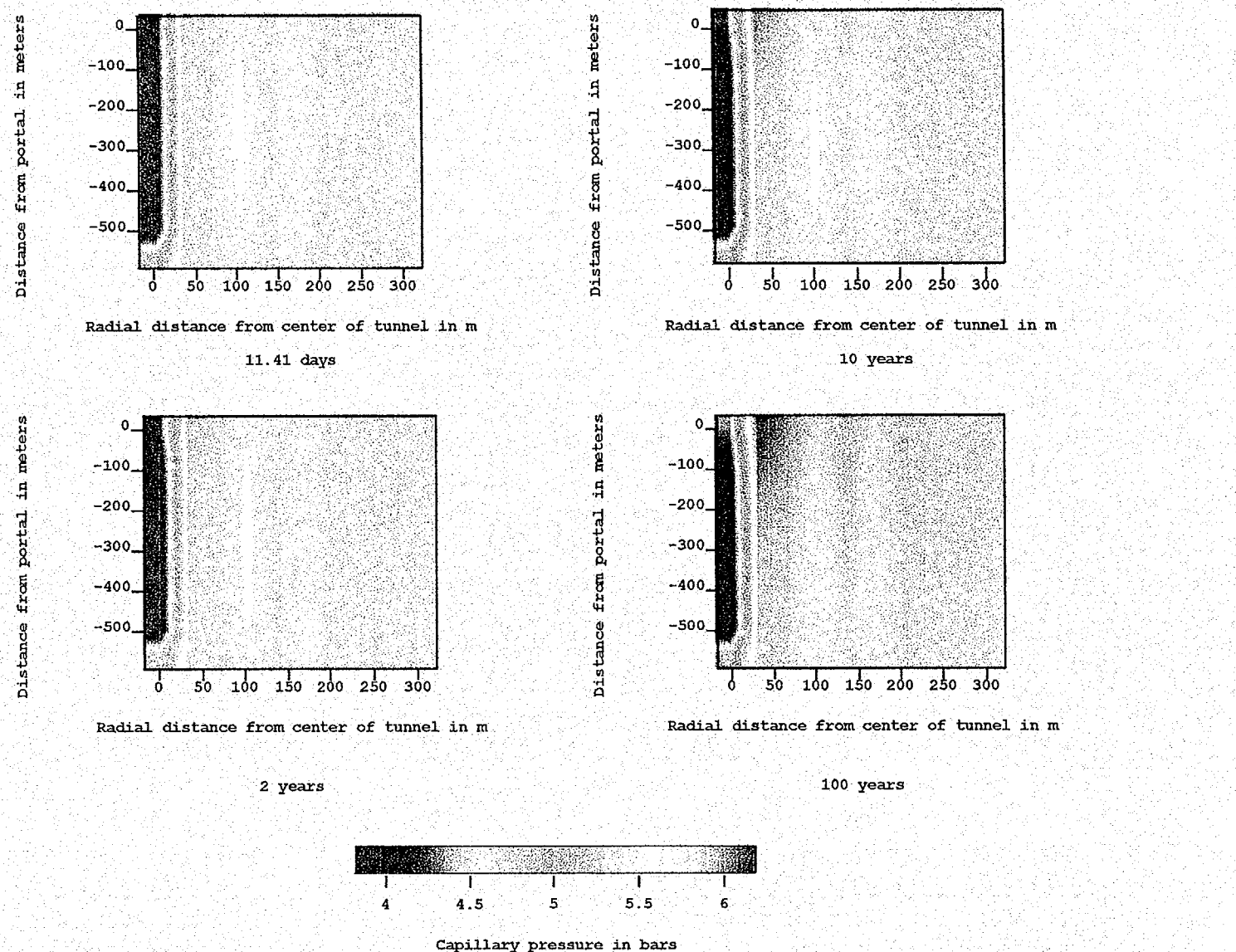


Figure 6-18 - Simulated capillary pressure around the tunnel for various times. Case 6, eddy diffusivity = 0.0001, atmosphere temperature = 28 °C.

Case 6

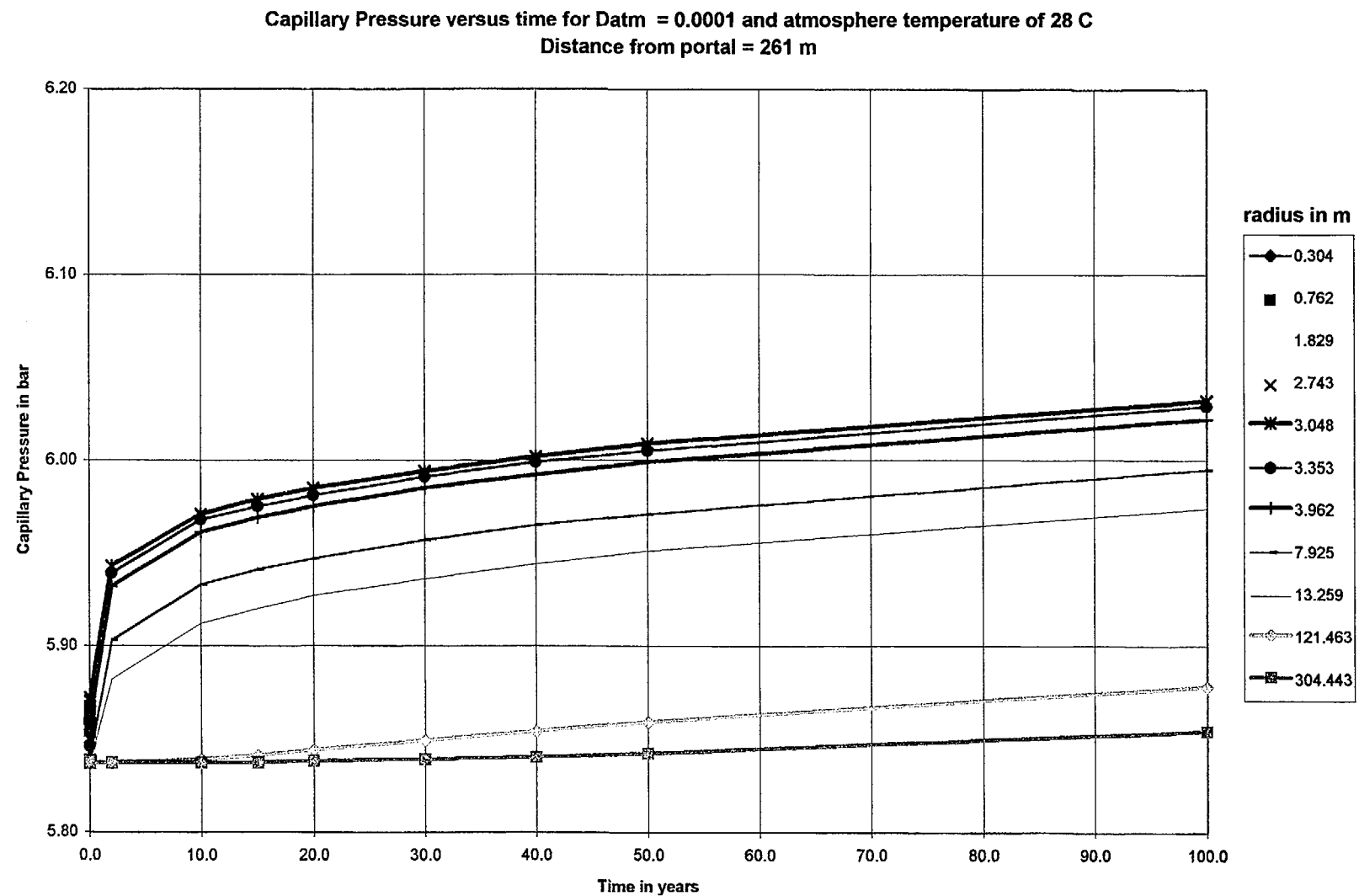


Figure 6-18a

Case 6

**Water saturation versus time for $D_{atm} = 0.0001$ and atmosphere temperature = 28 C
Distance from portal = 261 m**

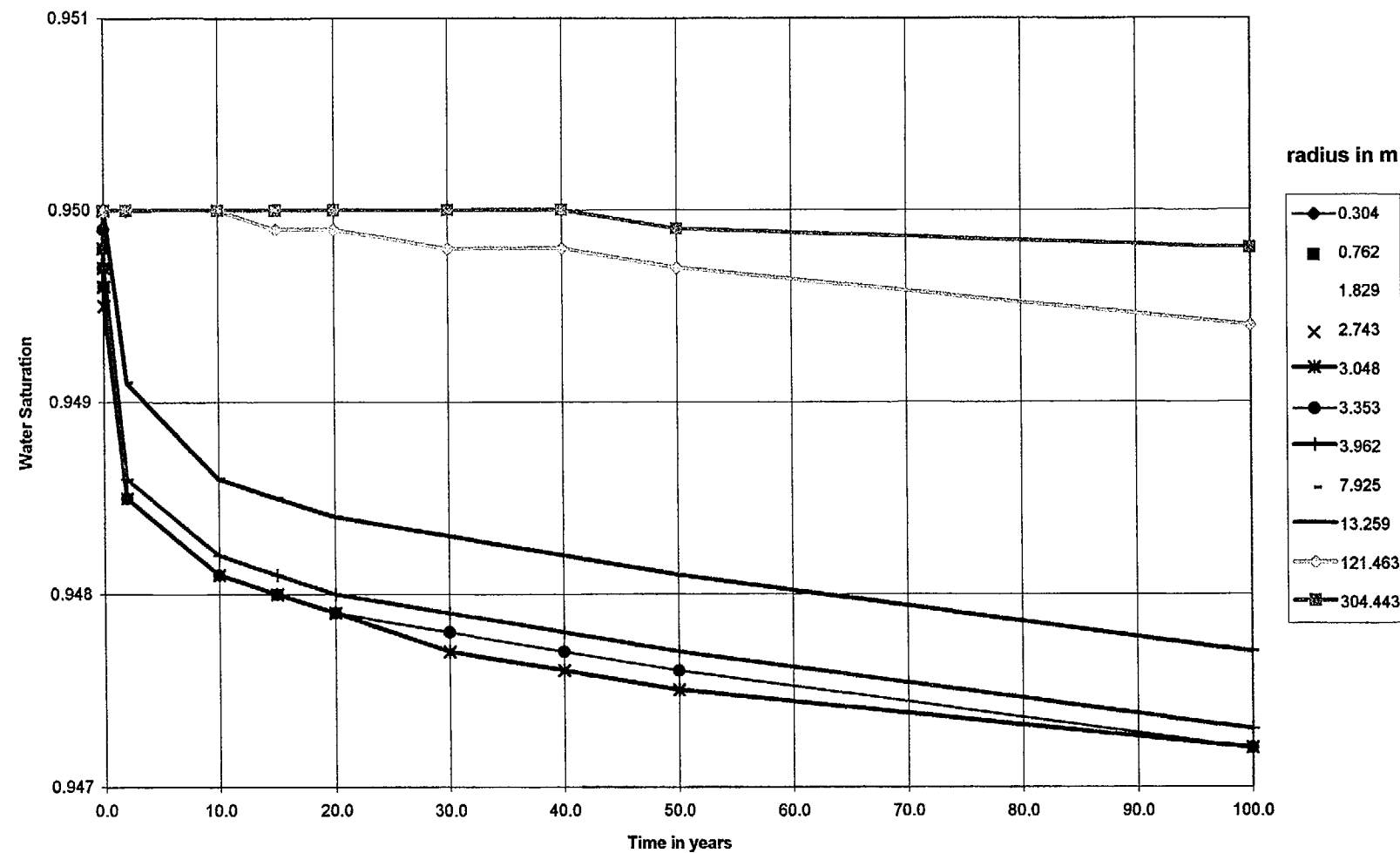


Figure 6-18b

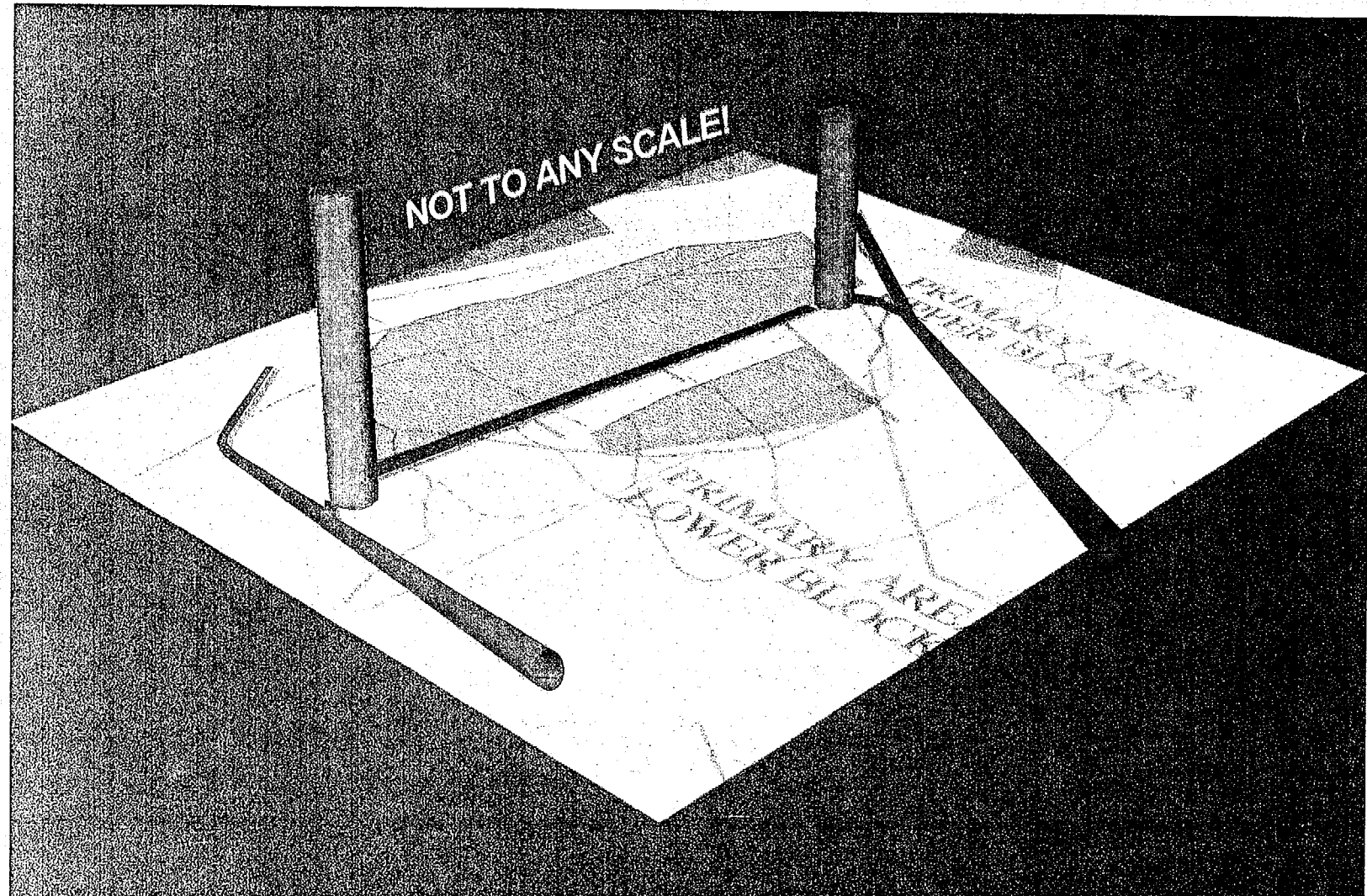


Figure 6-19 - Conceptual model of ventilation shafts relative to the ESF tunnel.

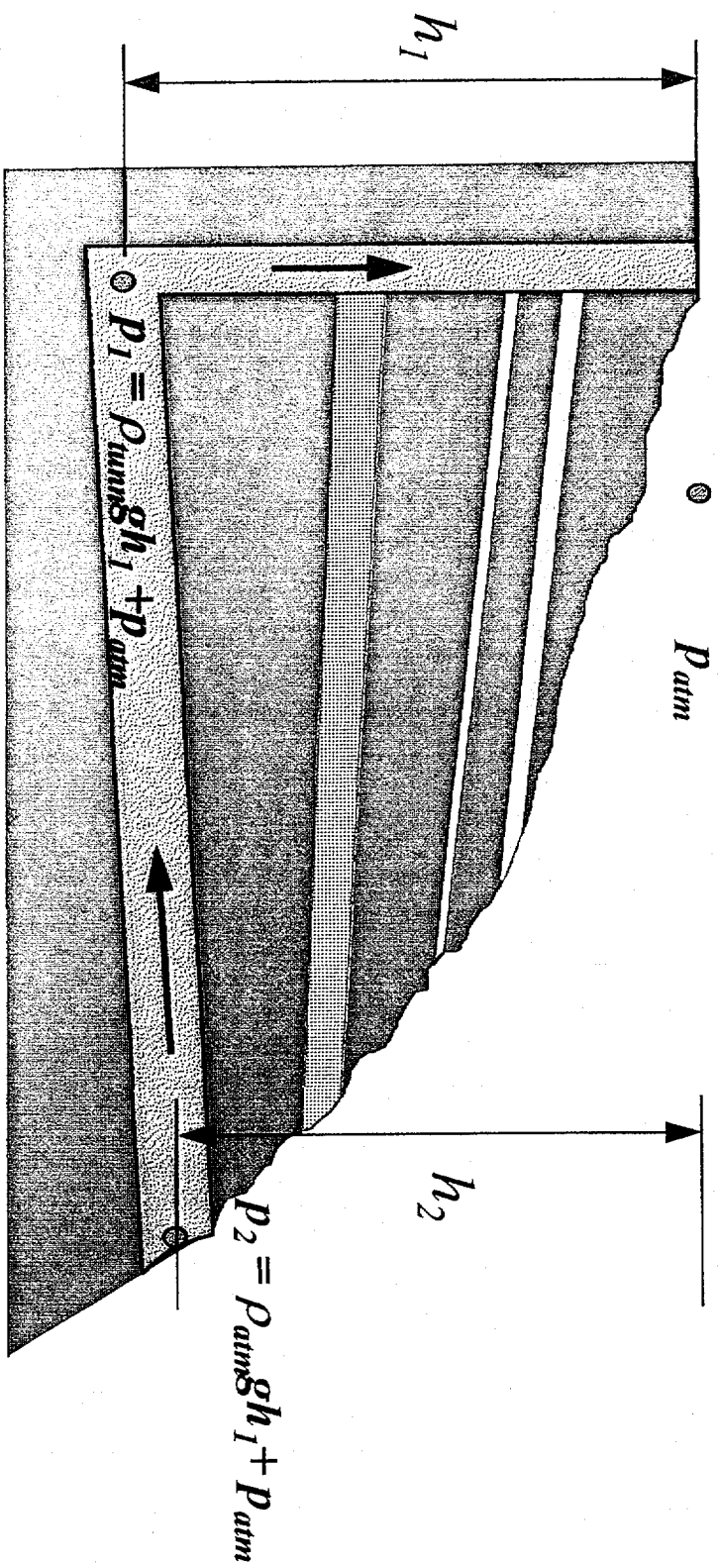
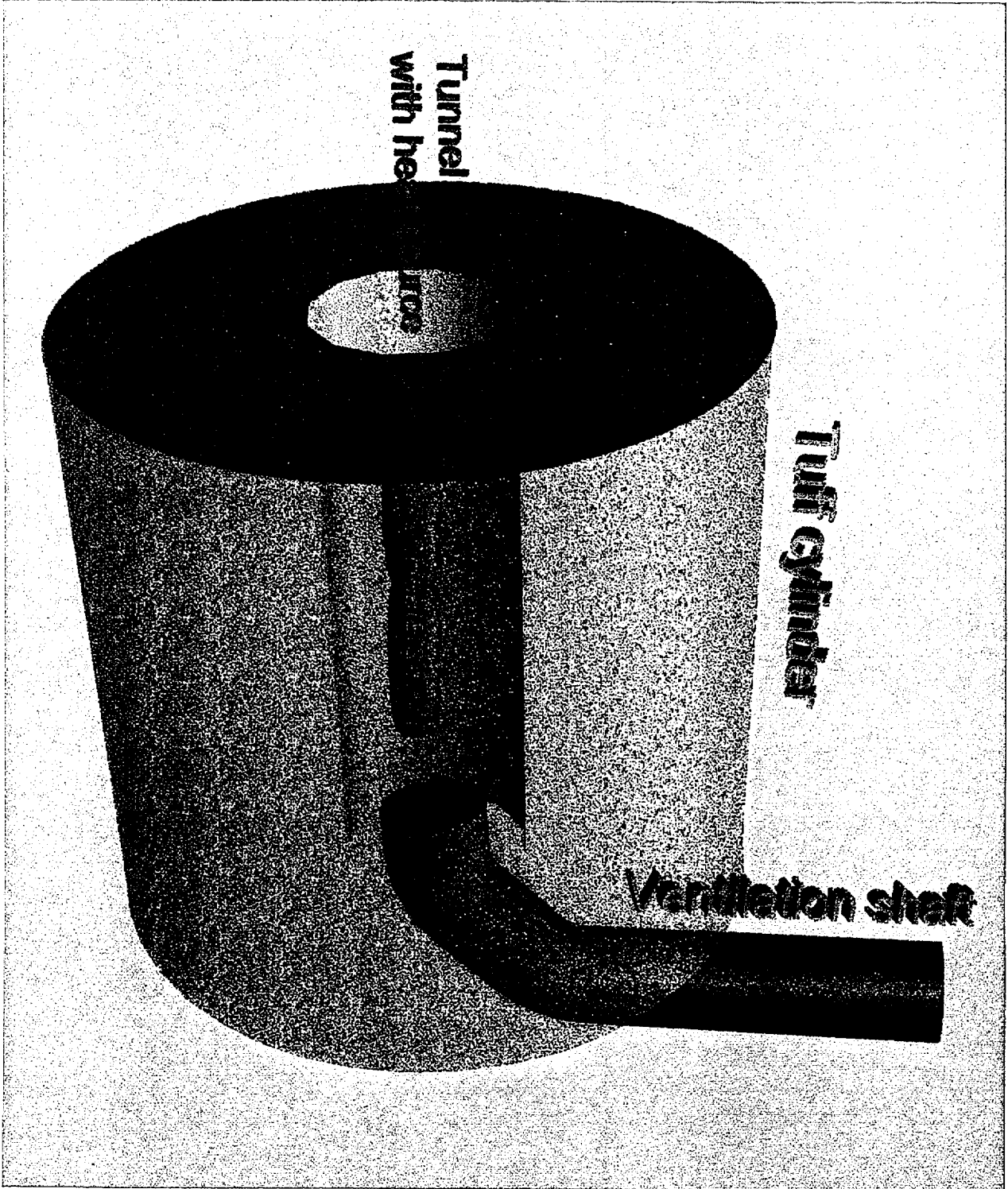


Figure 6-19a- Conceptualization of natural ventilation.

August 24, 1996
AMD:User\proj01\Nyecounty\unmc\99\figures
P260837

Prepared for:
Nye County Nuclear Waste Repository Project Office

Prepared by:
Multimedia Environmental Technology, Inc.
Newport Beach, CA



Prepared for:
Nye County Waste Repository Project Office

Figure 6-19b Conceptualization of Tuff Cylinder

Prepared by:
Multimedia Environmental Technology, Inc.
Newport Beach, CA

Cases 7-9

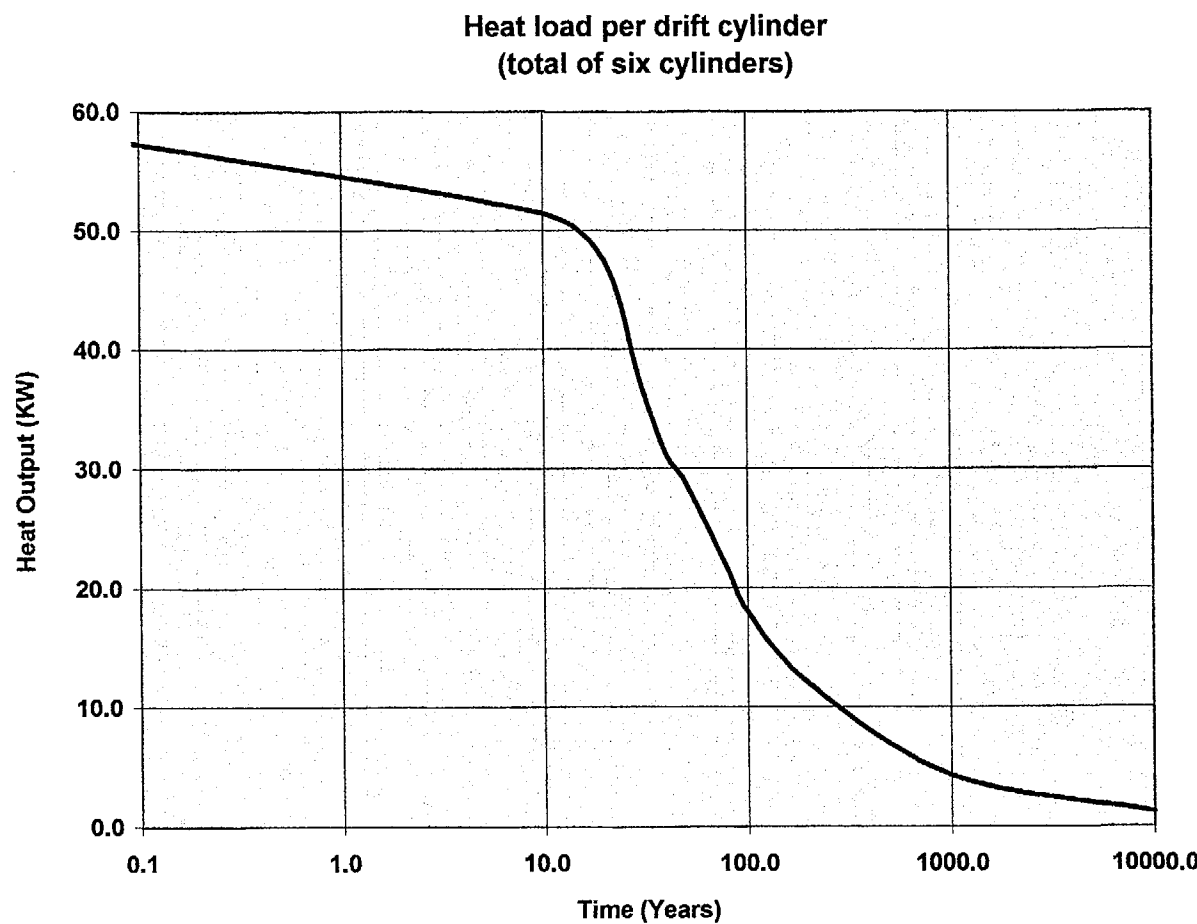


Figure 6-19c

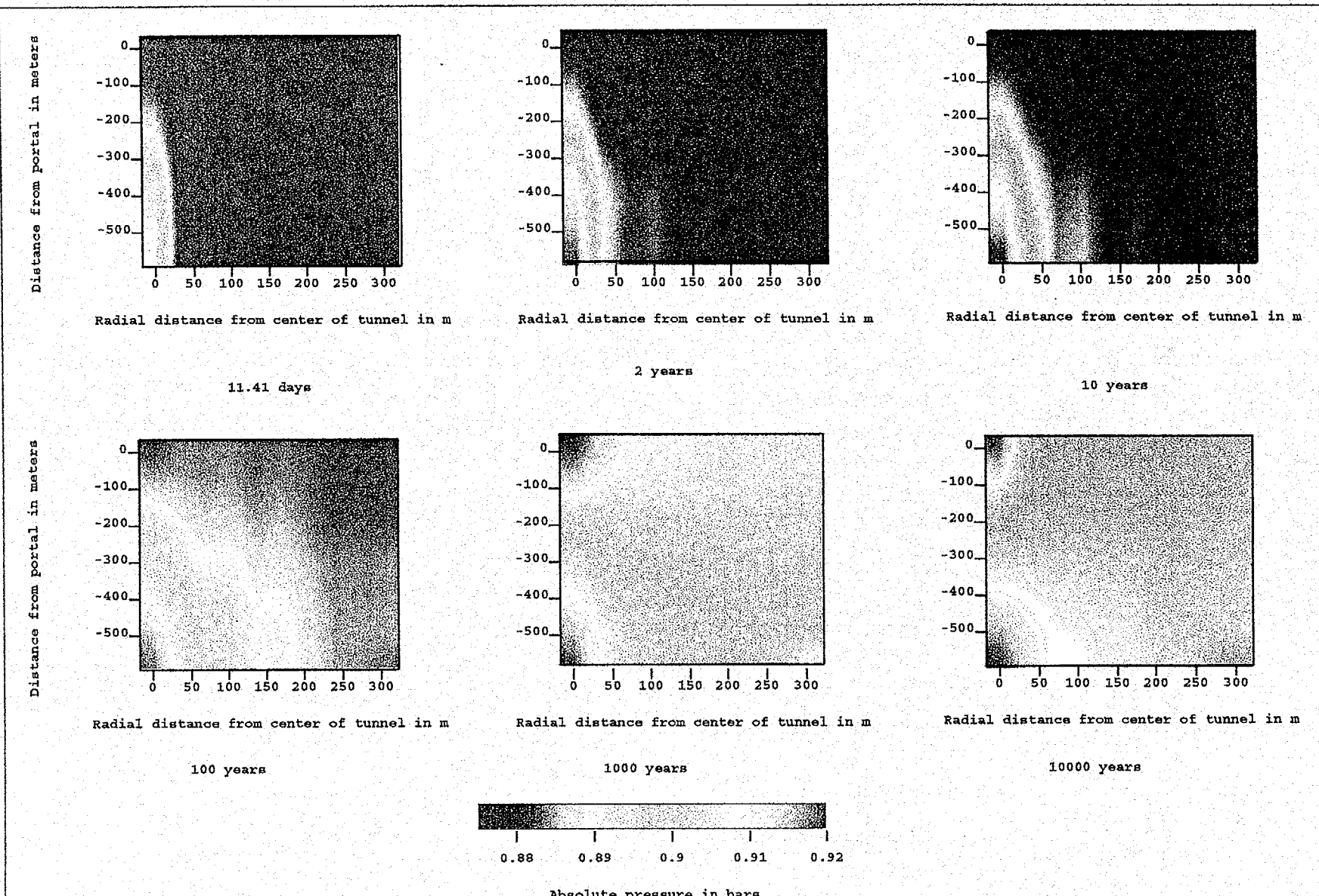


Figure 6-20 - Simulated pressure around the tunnel for various times. Case 7, with decaying heat load. Eddy diffusivity = 0.01, atmosphere temperature = 15 °C.

Case 7

Pressure versus time for $D_{atm} = 0.01$ and atmosphere temperature = 15 C
 Distance from portal = 261 m

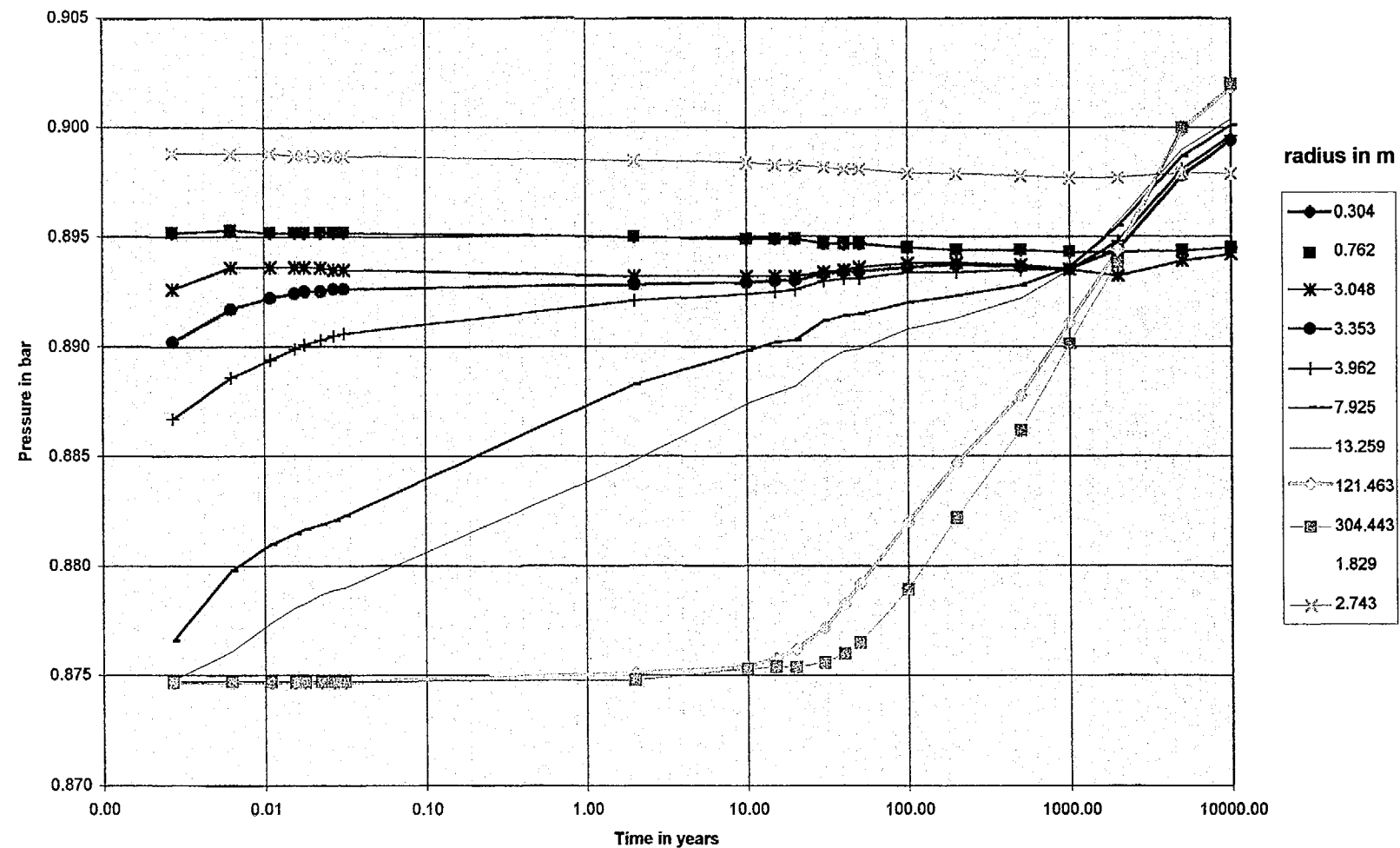


Figure 6-20a

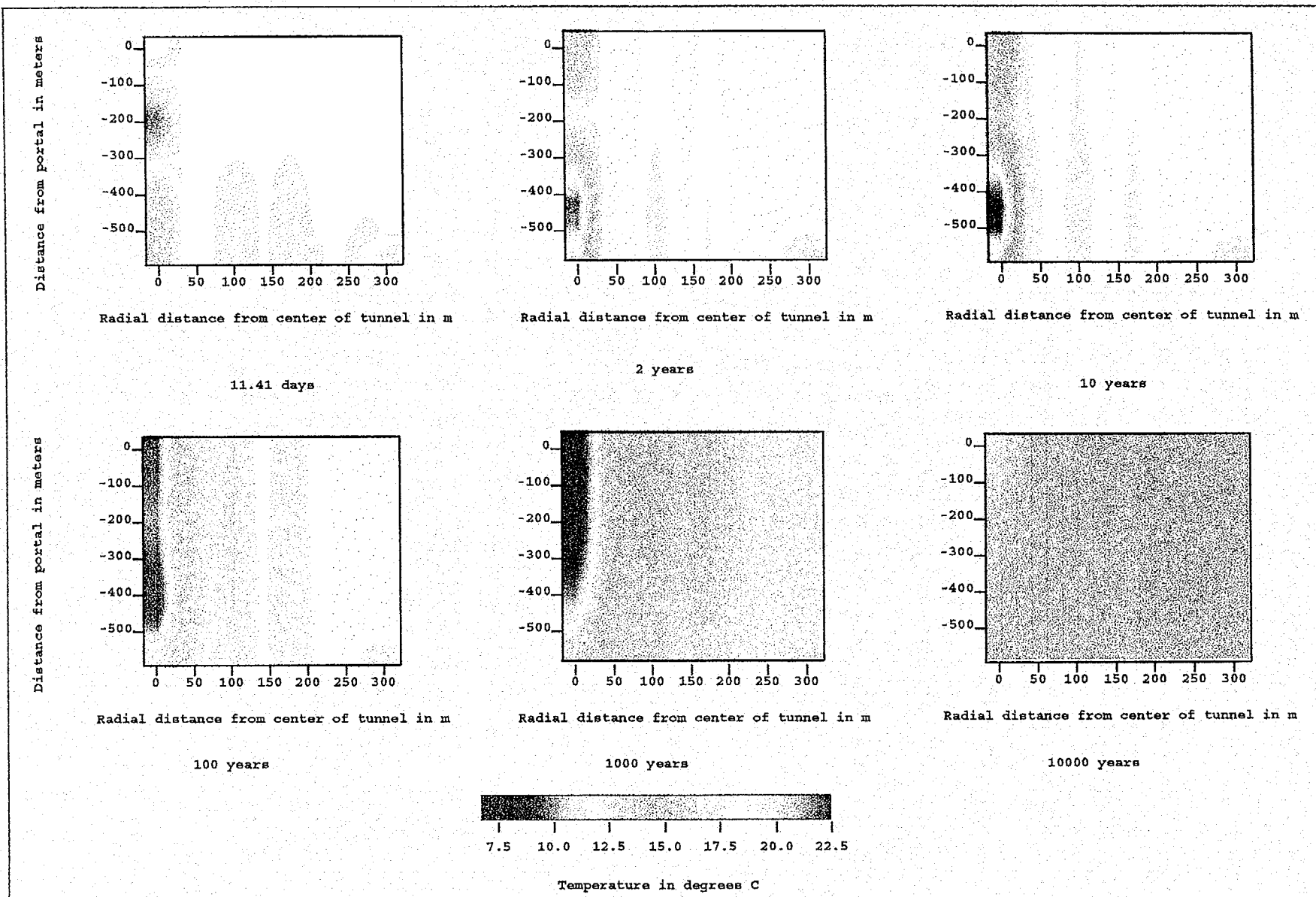


Figure 6-21 - Simulated temperature around the tunnel for various times. Case 7, with decaying heat load. Eddy diffusivity = 0.01, atmosphere temperature = 15 °C.

Case 7

Temperature versus time for $D_{atm} = 0.01$ with decayed heat load
 Distance from portal = 261 m

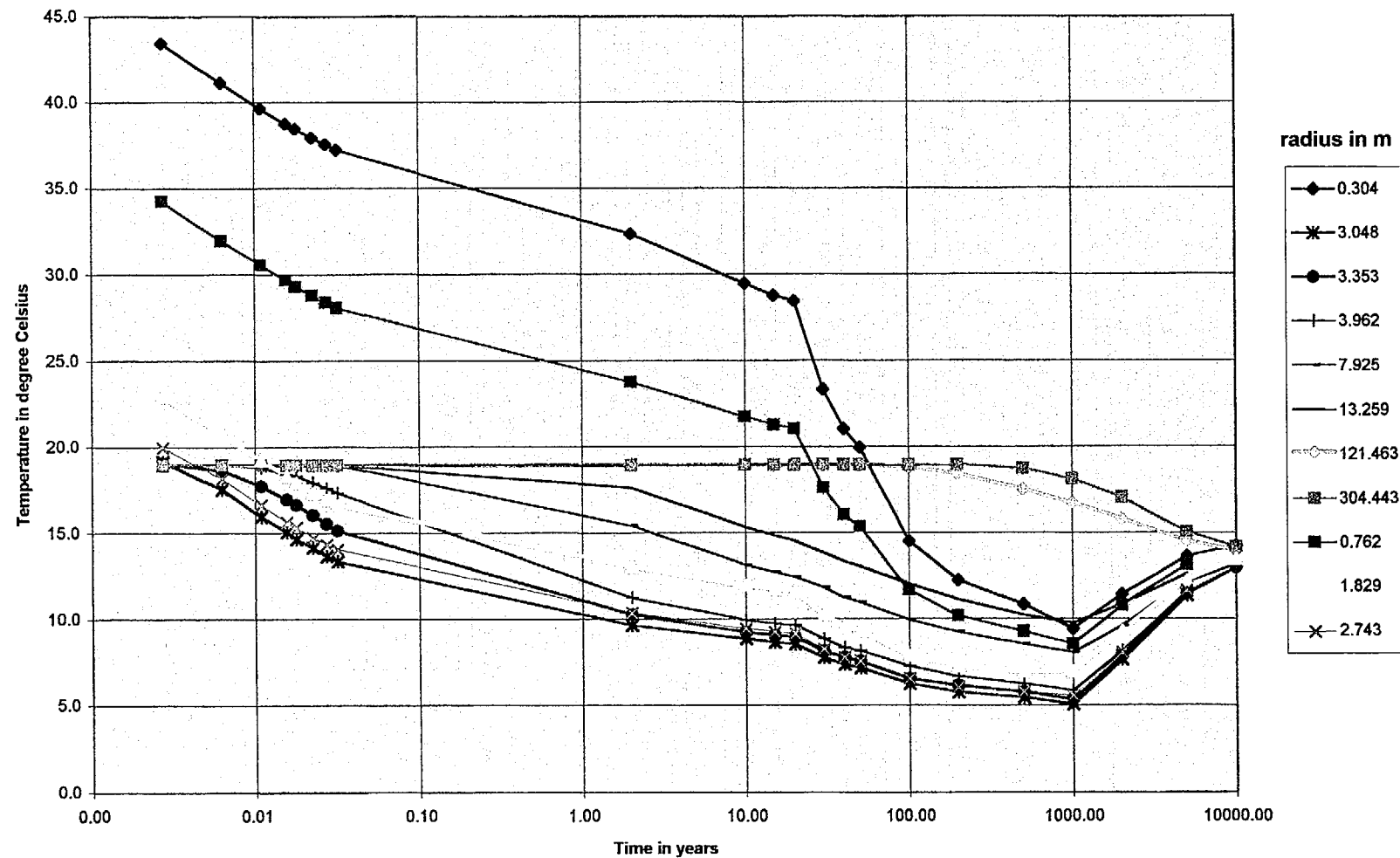


Figure 6-21a

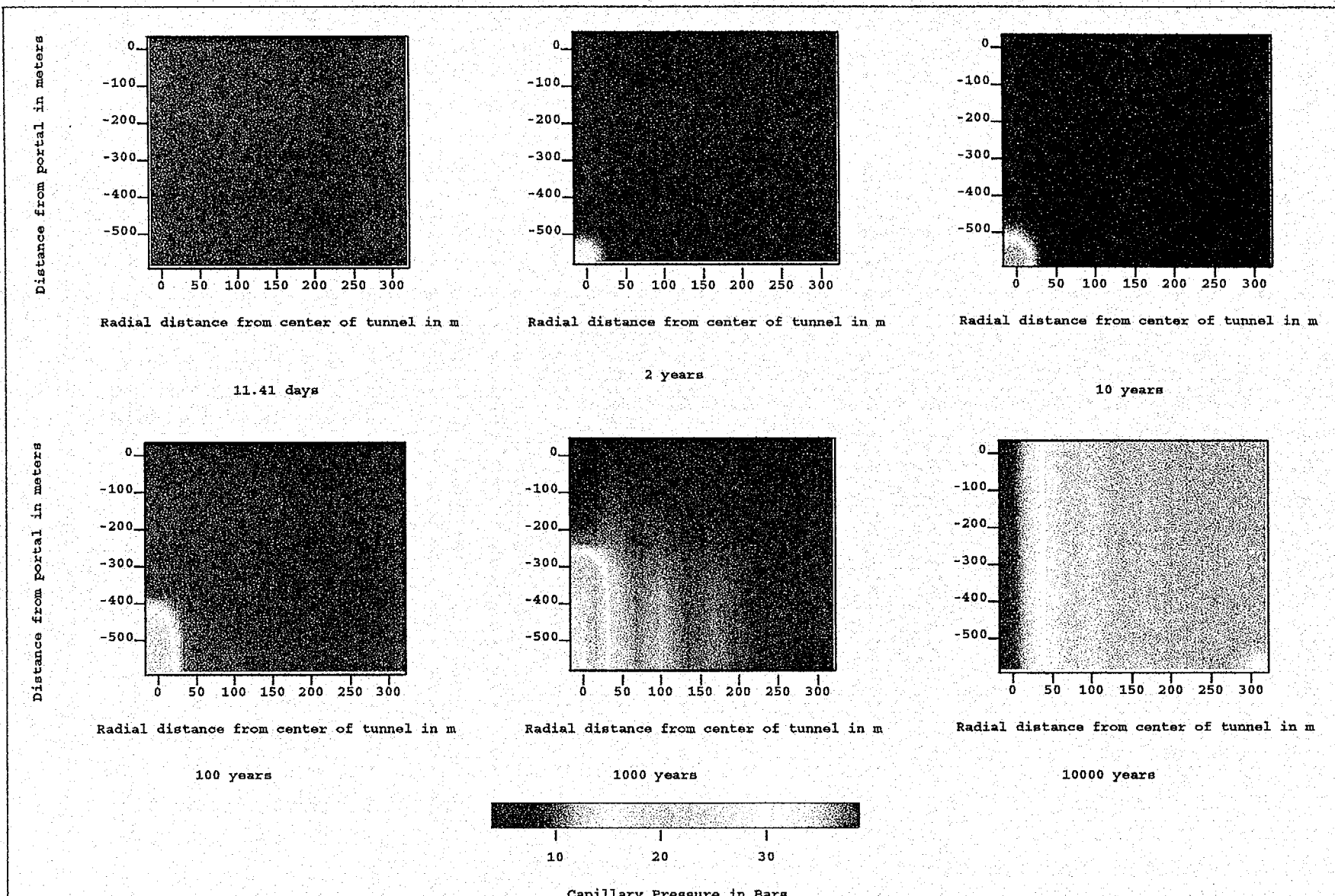


Figure 6-22 - Simulated capillary pressure around the tunnel for various times. Case 7, with decaying heat load.
Eddy diffusivity = 0.01, atmosphere temperature = 15 °C.

Case 7

Capillary Pressure versus time for $D_{atm} = 0.01$ and atmosphere temperature = 15 C
Distance from portal = 261 m

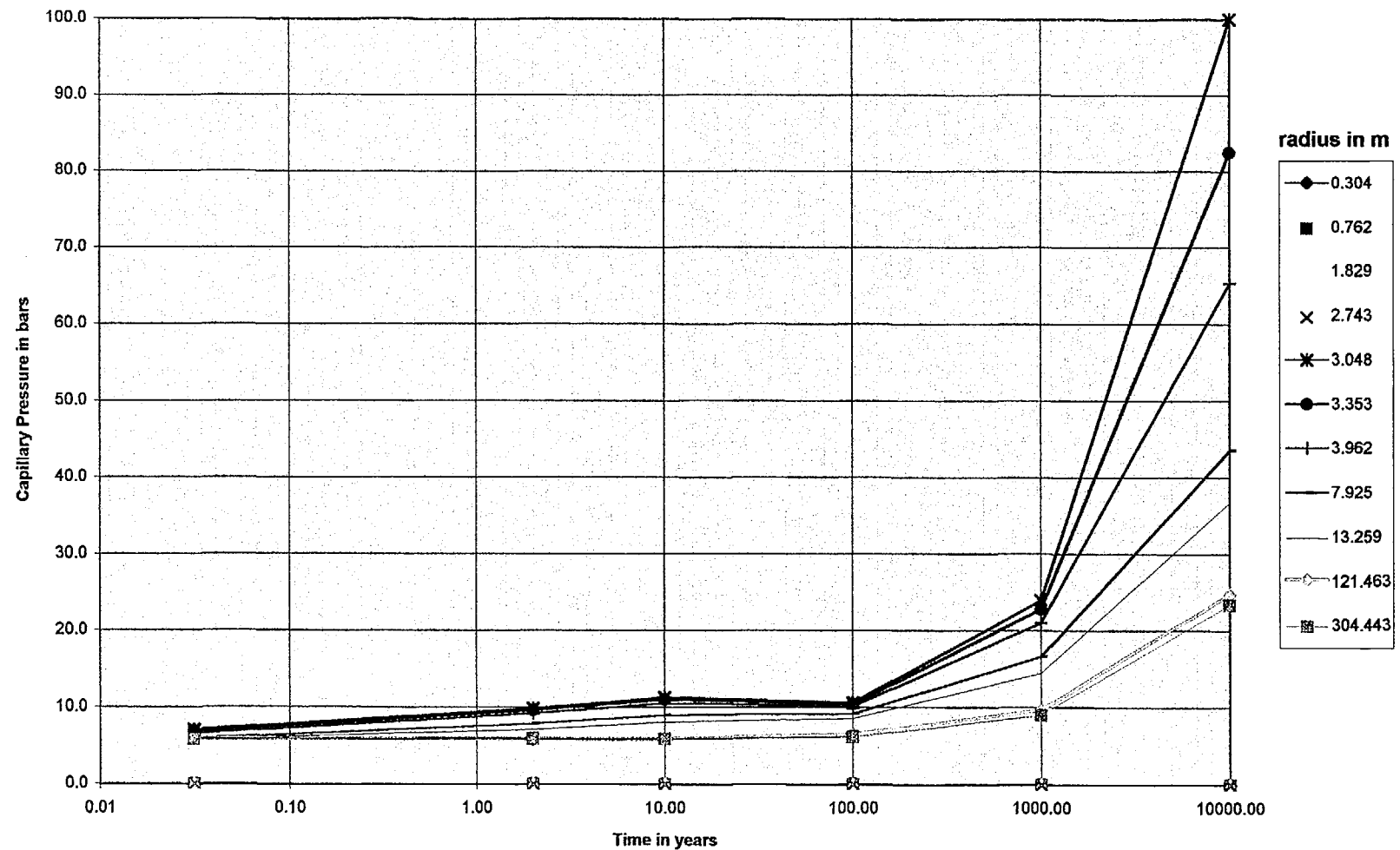


Figure 6-22a

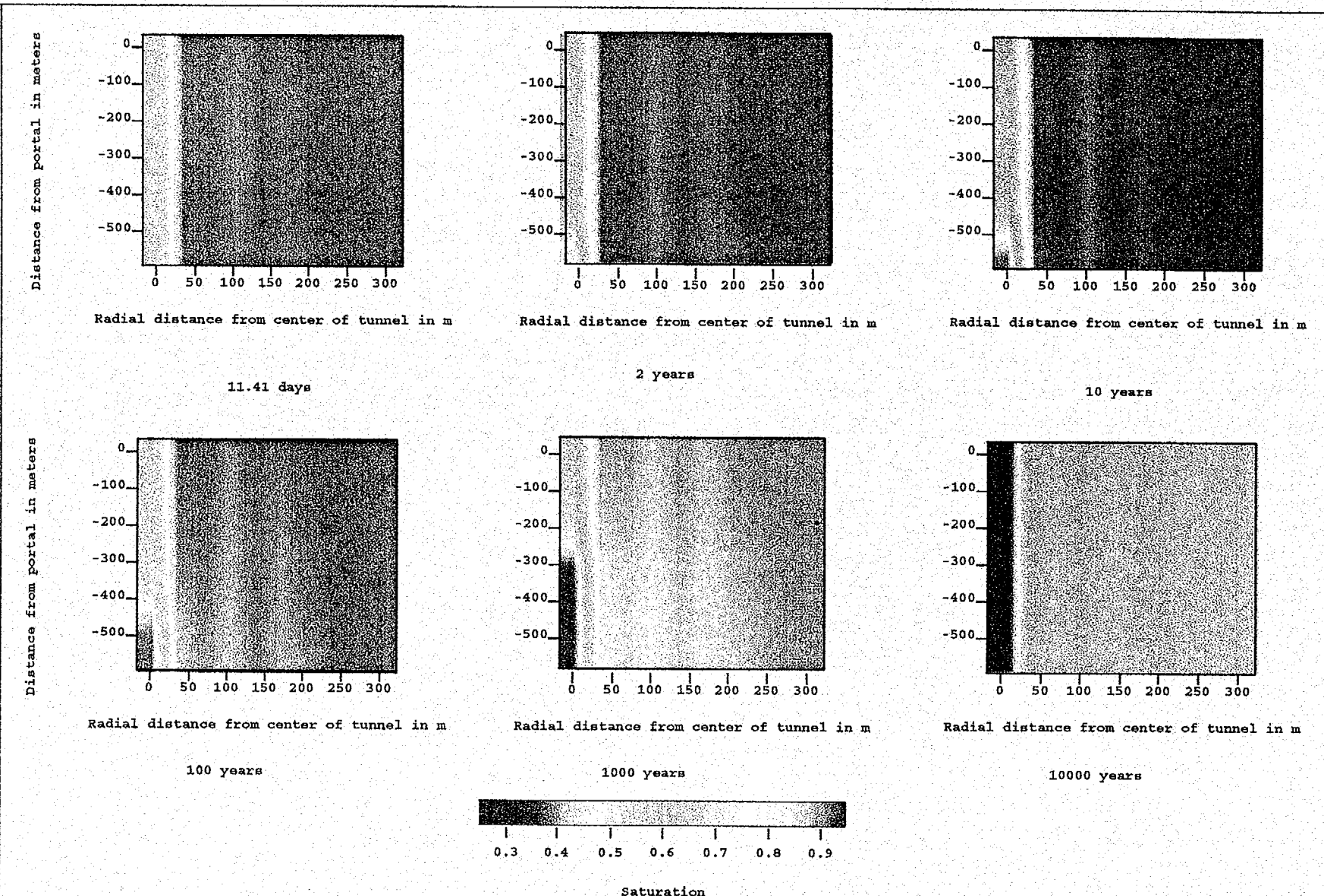


Figure 6-23 - Simulated saturation around the tunnel for various times. Case 7, with decaying heat load. Eddy diffusivity = 0.01, atmosphere temperature = 15 °C.

Case 7

Water saturation versus time for $D_{atm} = 0.01$ and atmosphere temperature of 15 C
Distance from portal = 261 m

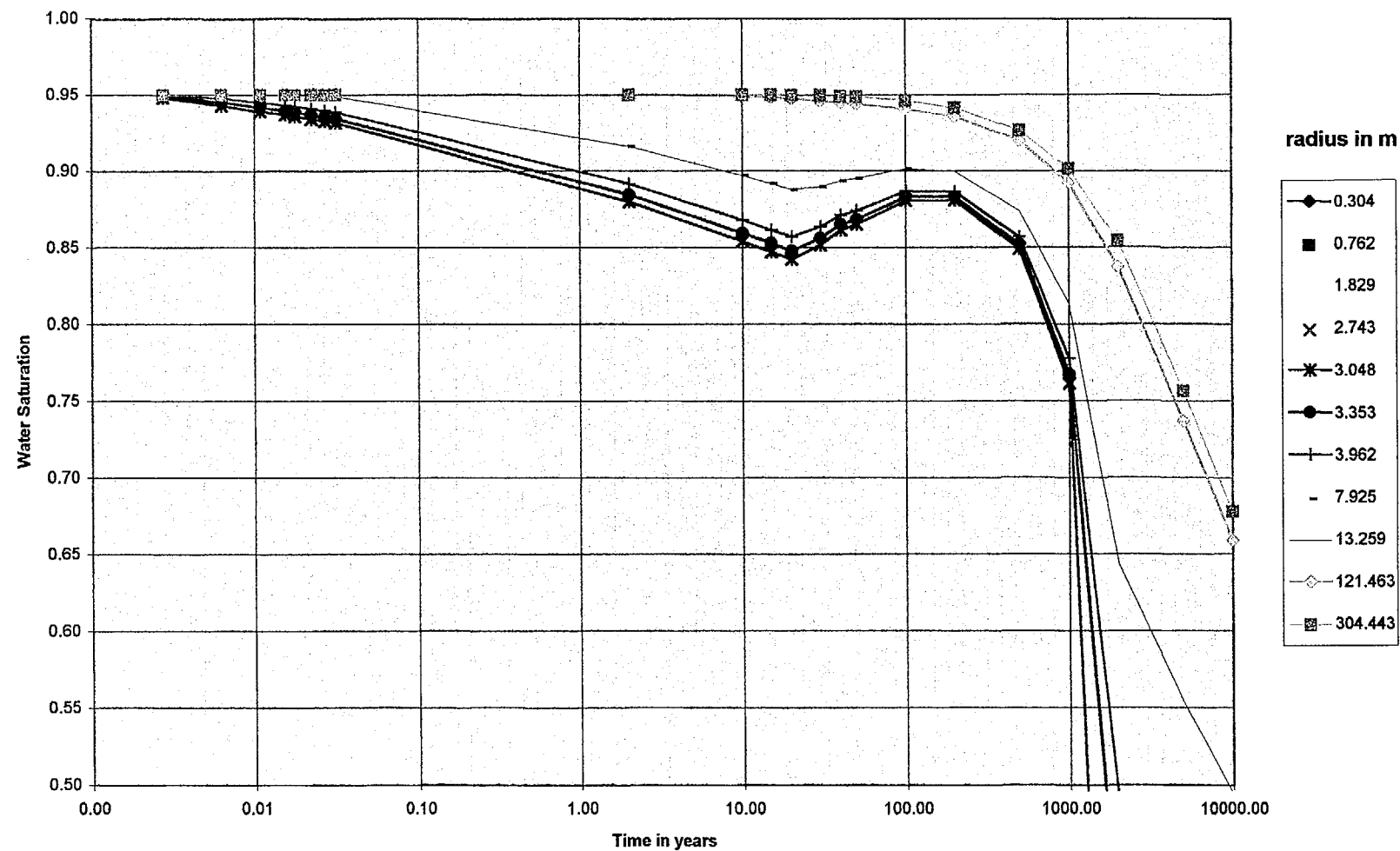


Figure 6-23a

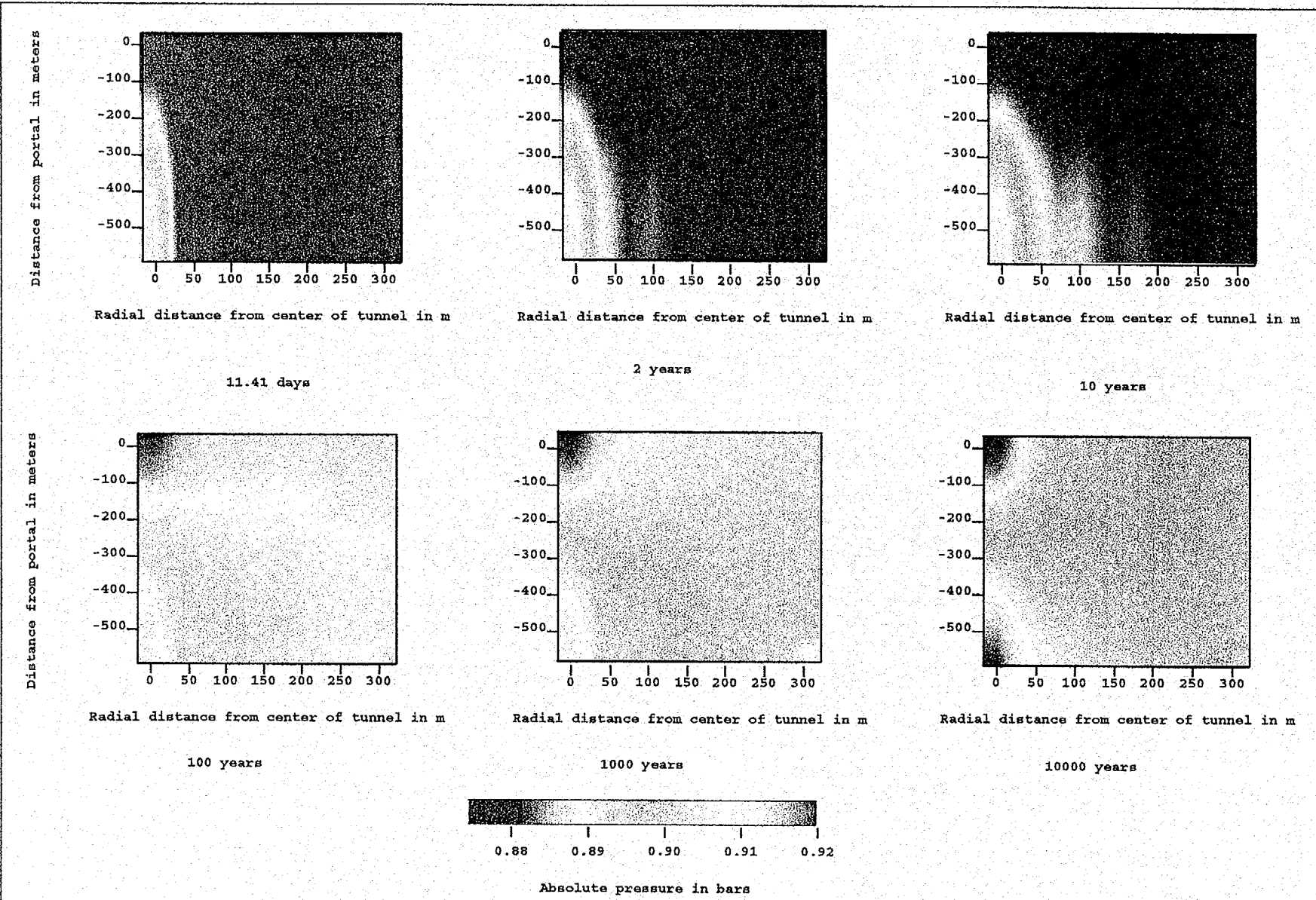


Figure 6-24 - Simulated pressure around the tunnel for various times. Case 8, with decaying heat load. Eddy diffusivity = 0.001, atmosphere temperature = 15 °C.

Case 8

**Pressure versus time for Datm = 0.001 and atmosphere temperature = 15 C
Distance from portal = 261 m**

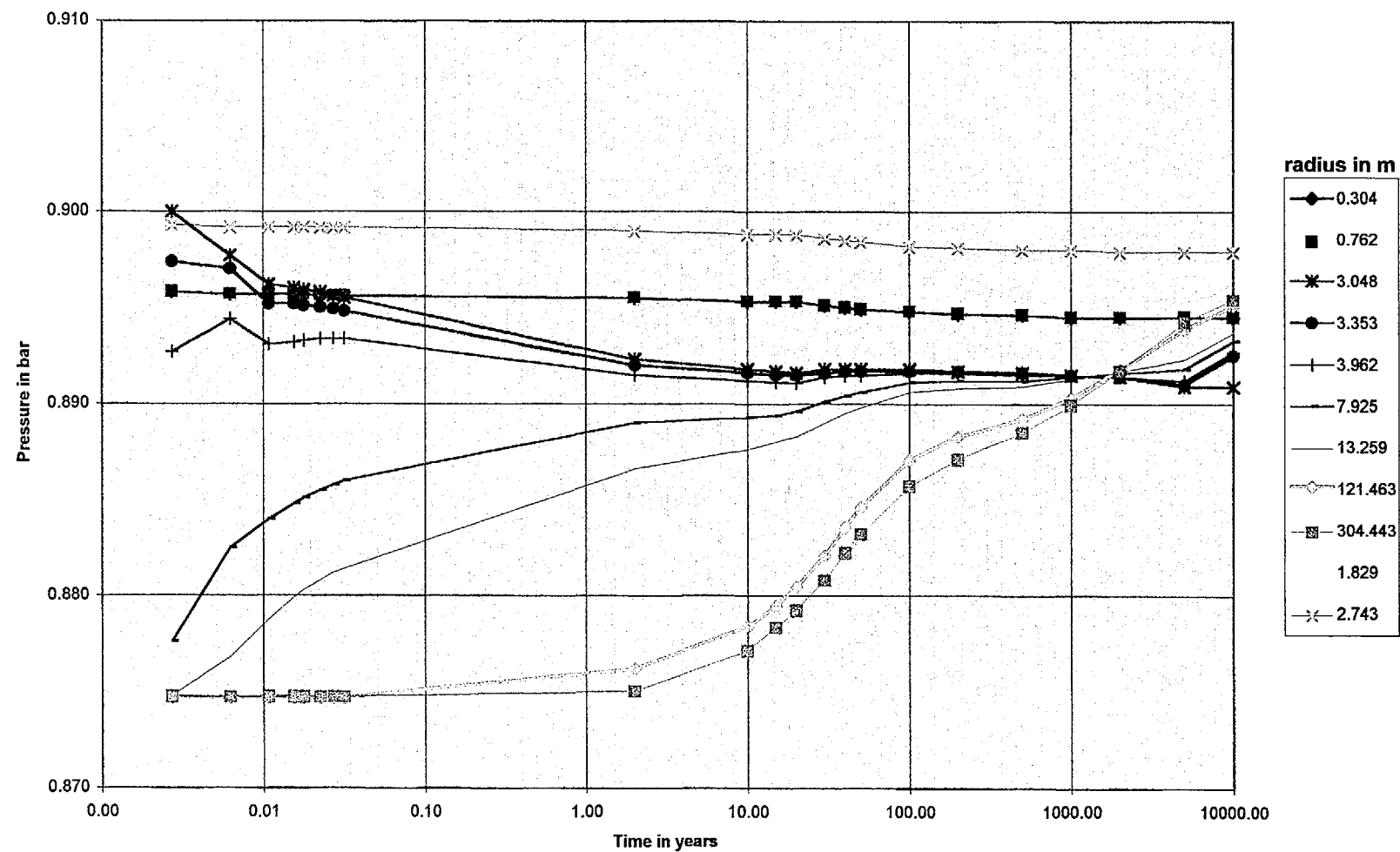


Figure 6-24a

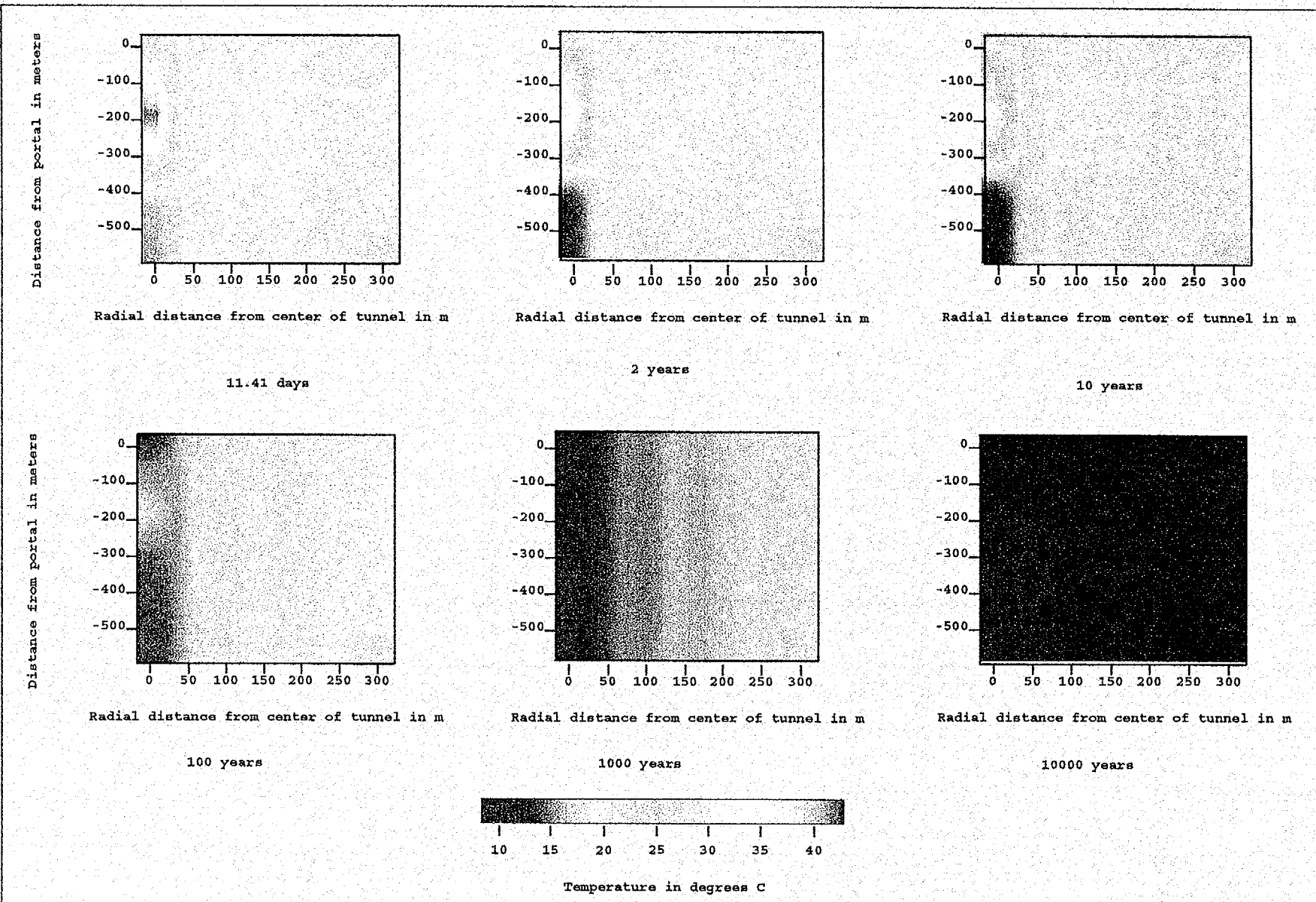


Figure 6-25 - Simulated temperature around the tunnel for various times. Case 8, with decaying heat load. Eddy diffusivity = 0.001, atmosphere temperature = 15 °C.

Case 8

Temperature versus time for $D_{atm} = 0.001$ with decayed heat load
Distance from portal = 261 m

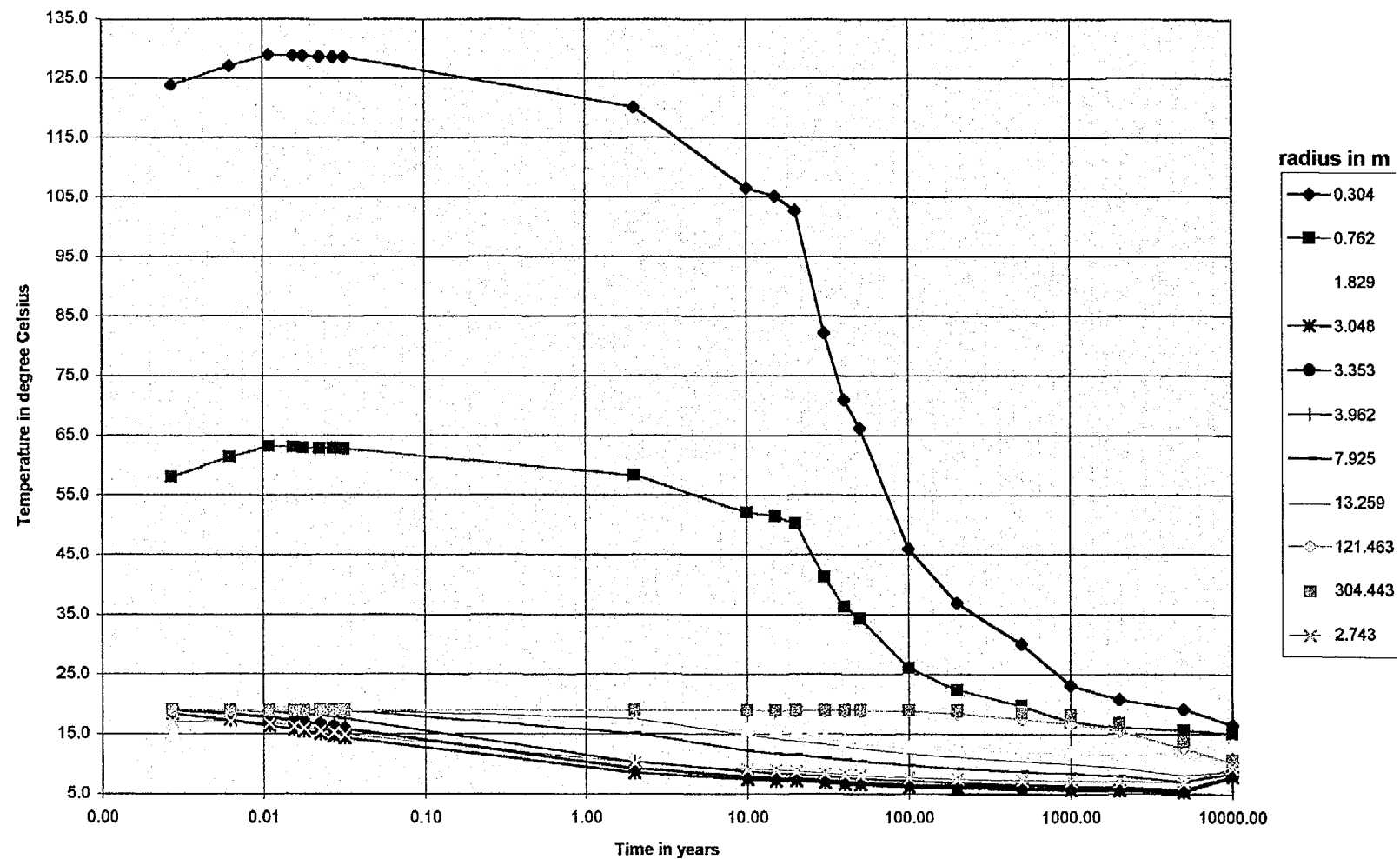


Figure 6-25a

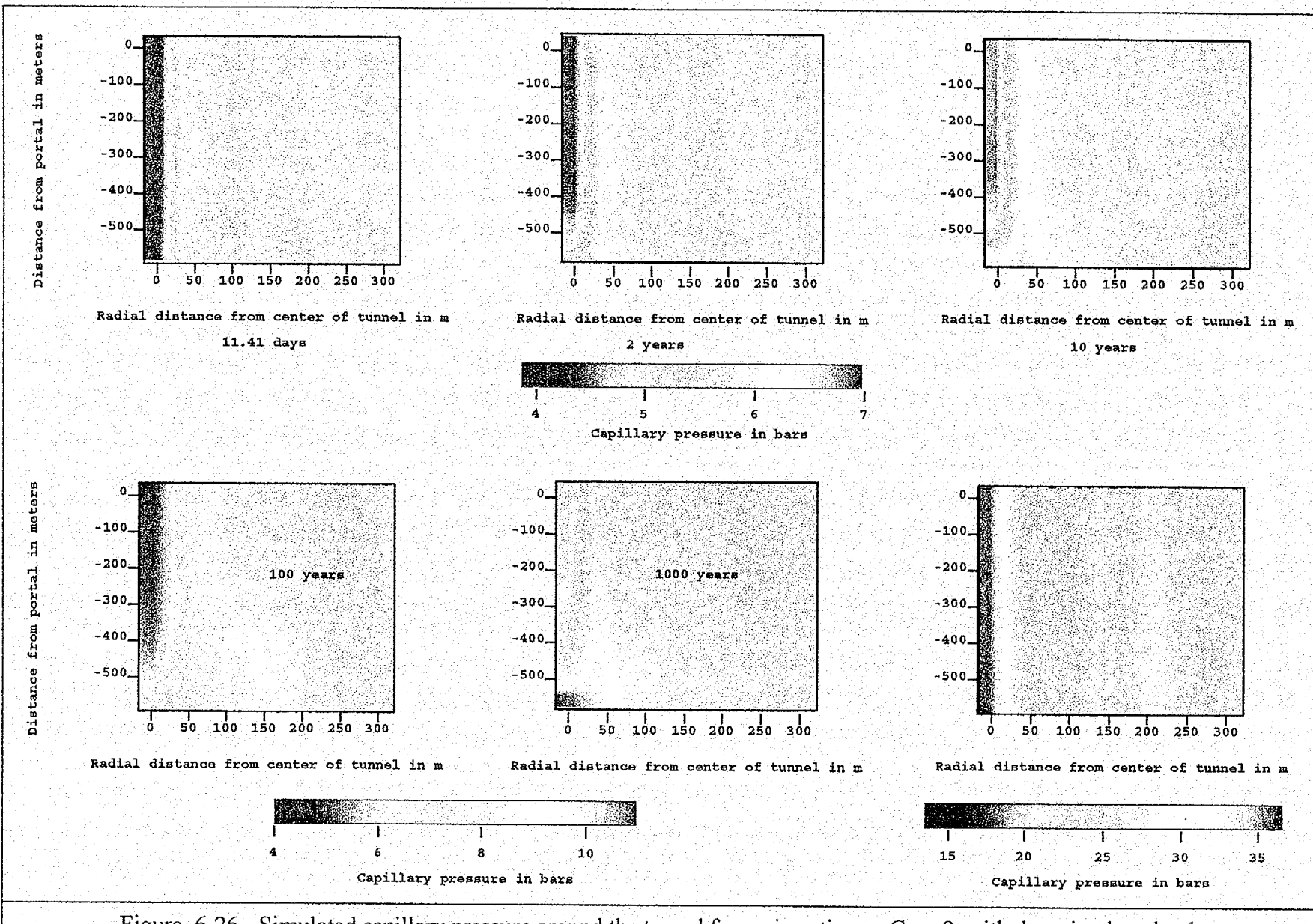


Figure 6-26 - Simulated capillary pressure around the tunnel for various times. Case 8, with decaying heat load.
Eddy diffusivity = 0.001, atmosphere temperature = 15 °C. Note: scale changes among graphs.

Case 8

Capillary Pressure versus time for $D_{atm} = 0.001$ and atmosphere temperature = 15 C
Distance from portal = 261 m

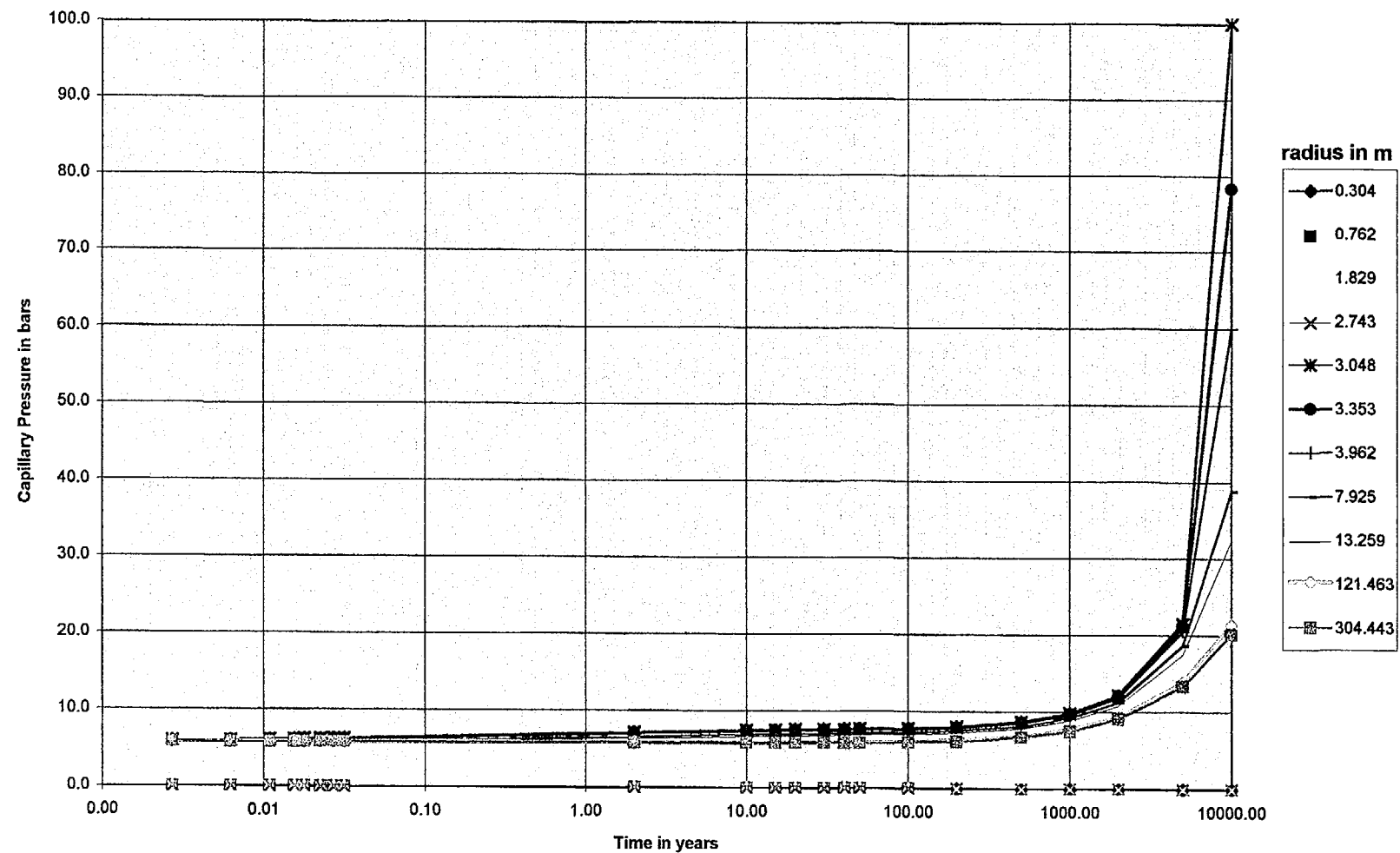


Figure 6-26a

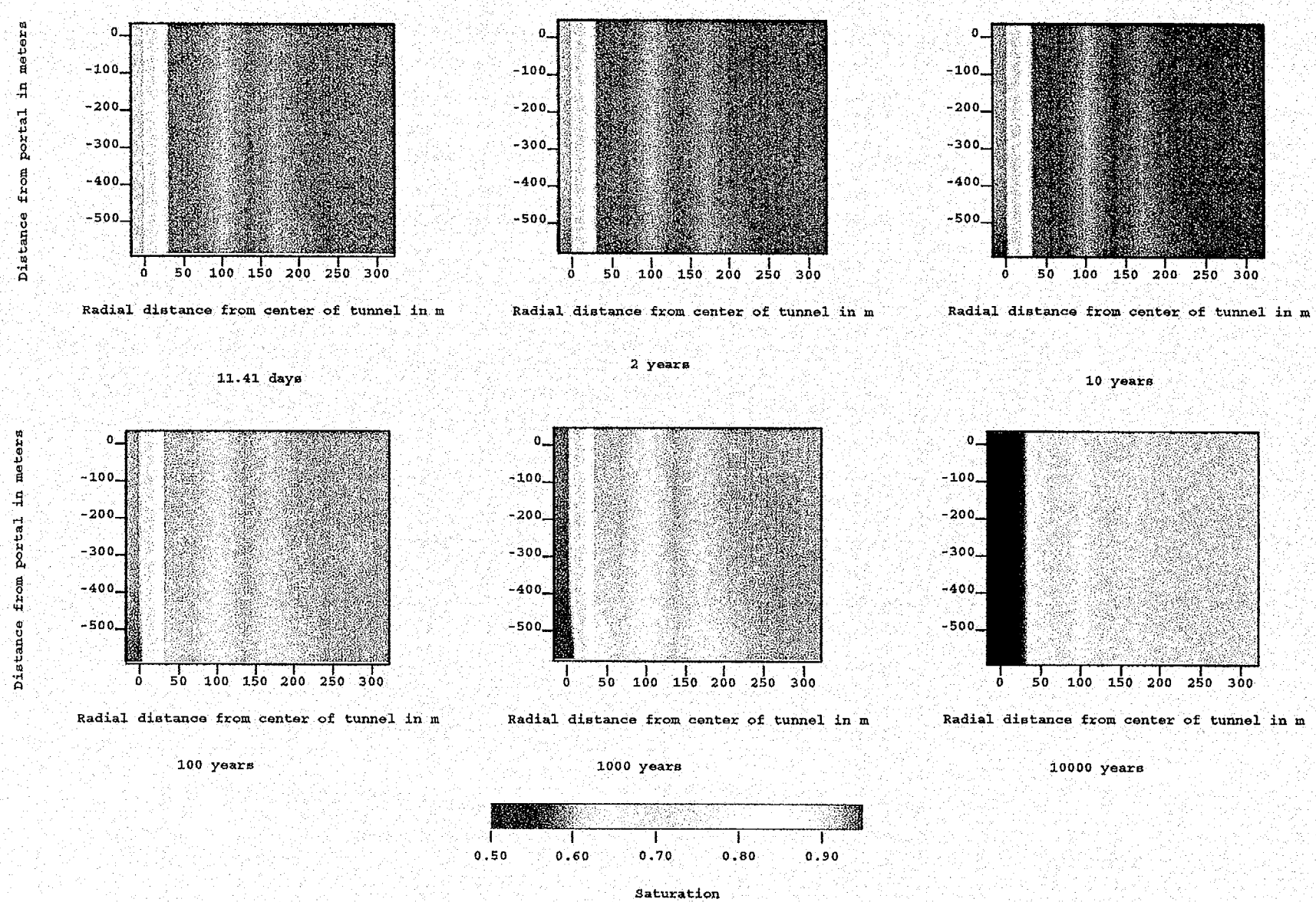


Figure 6-27 - Simulated saturation around the tunnel for various times. Case 8, with decaying heat load. Eddy diffusivity = 0.001, atmosphere temperature = 15 °C.

Case 8

**Water saturation versus time for $D_{atm} = 0.001$ and atmosphere temperature of 15 C
Distance from portal = 261 m**

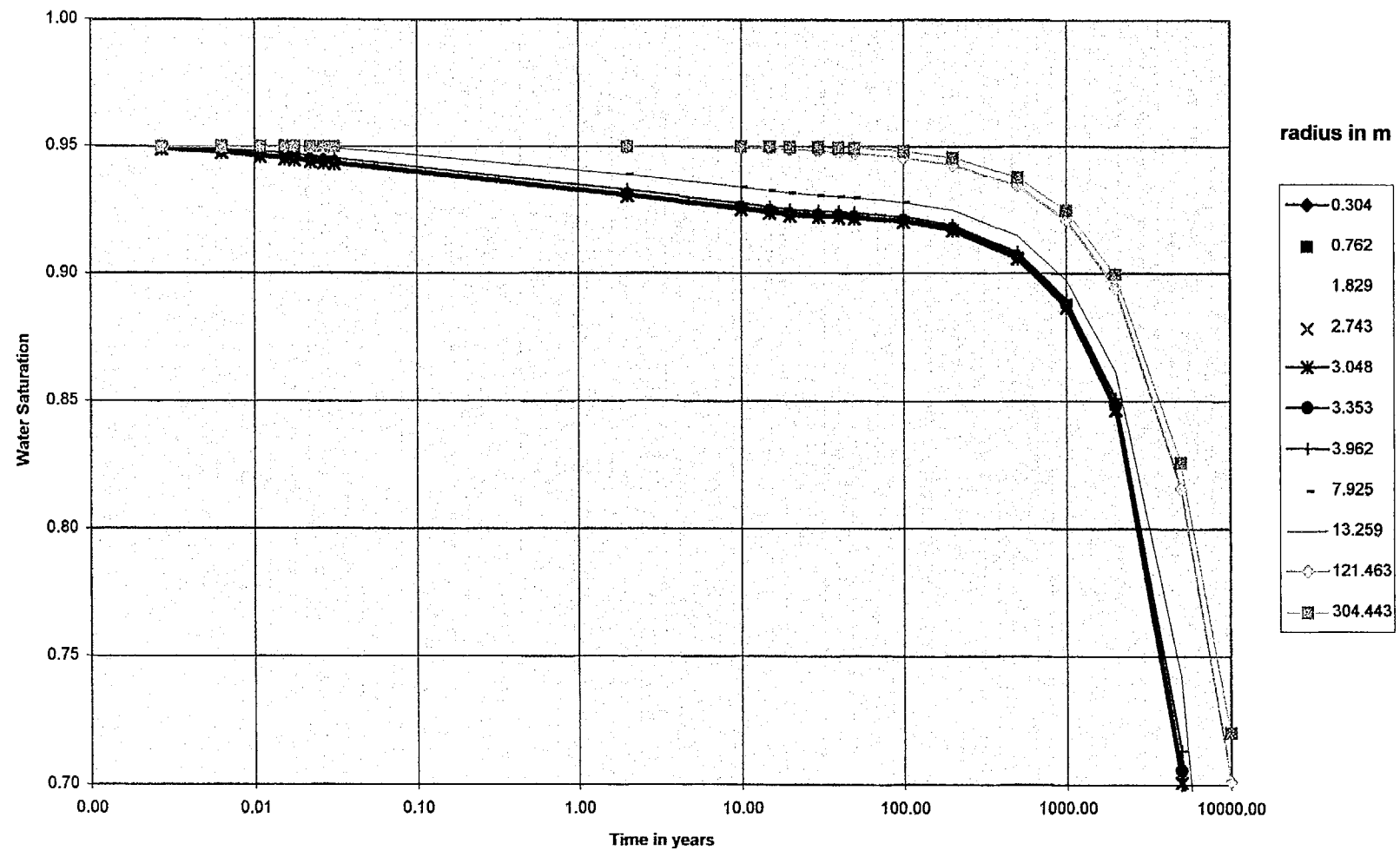


Figure 6-27a

Note: Figures 6-28 through 6-31 (Case 9) have been intentionally removed

Cases 10 and 11

Heat Load per Gridblock
(Total of ten gridblocks 40 m long)

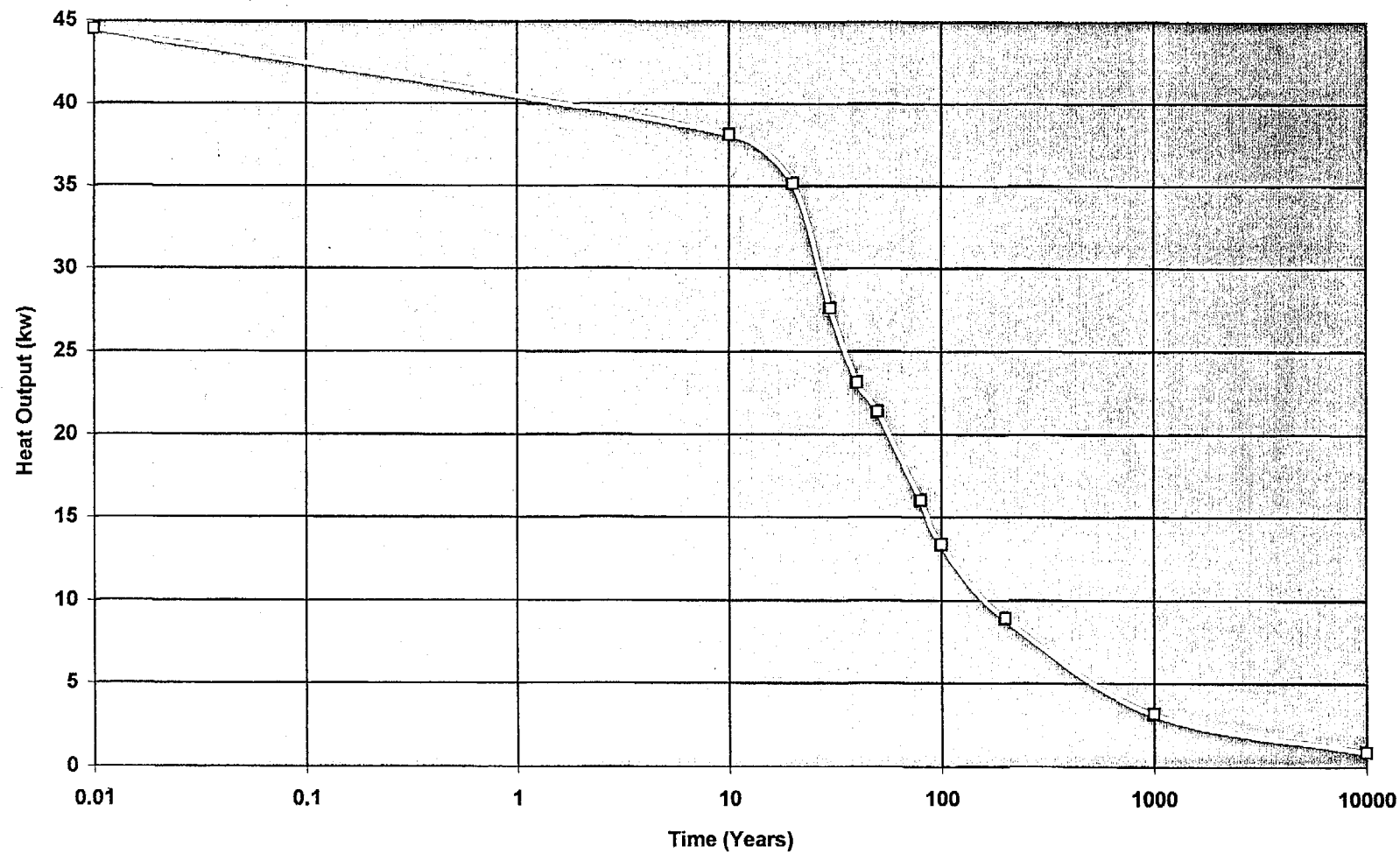


Figure 6-32

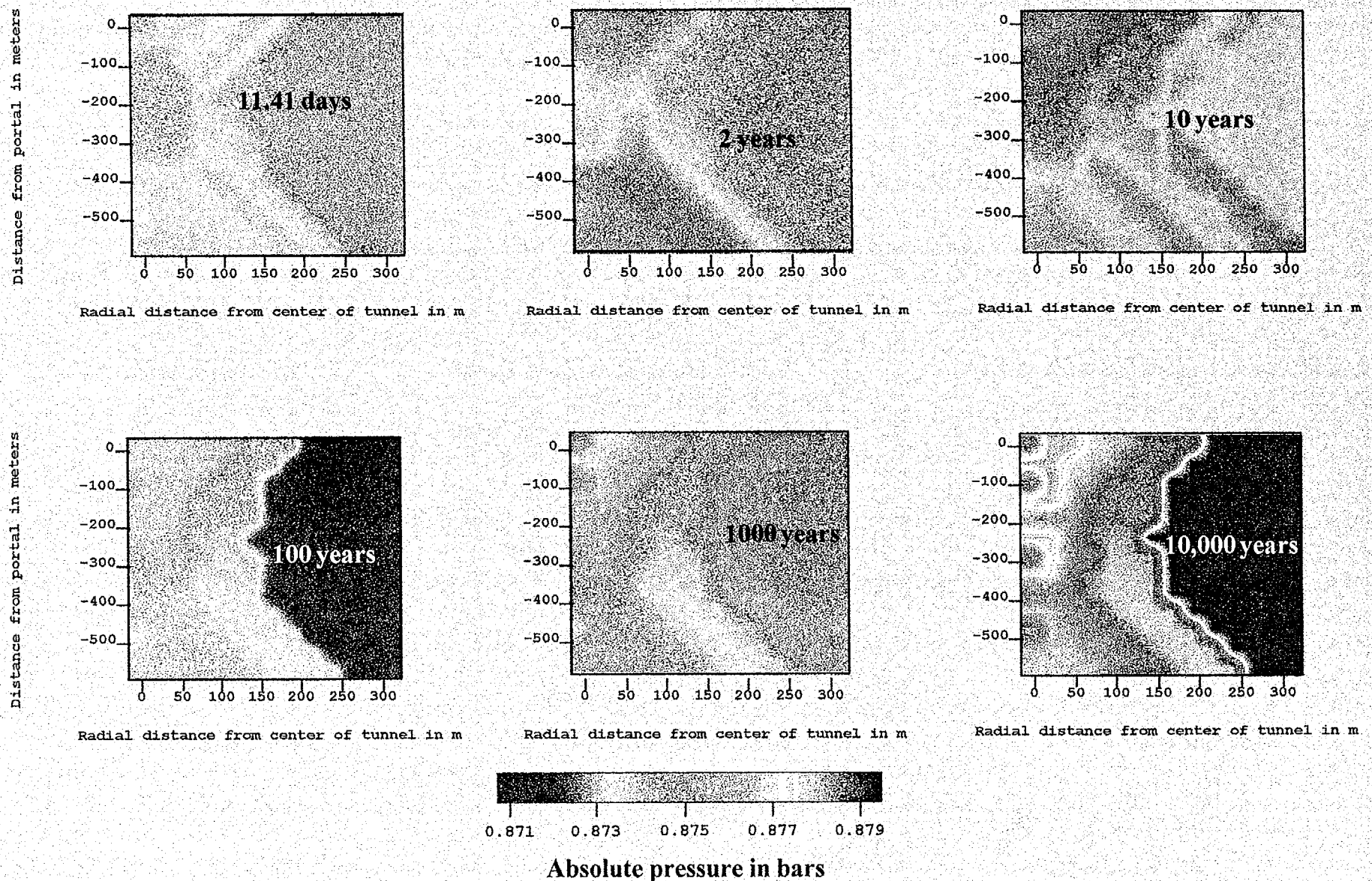


Figure 6-33 - Simulated pressure around the tunnel for various times. Case 10, with decaying heat load. Eddy diffusivity = 0.01, atmosphere temperature = 15 °C.

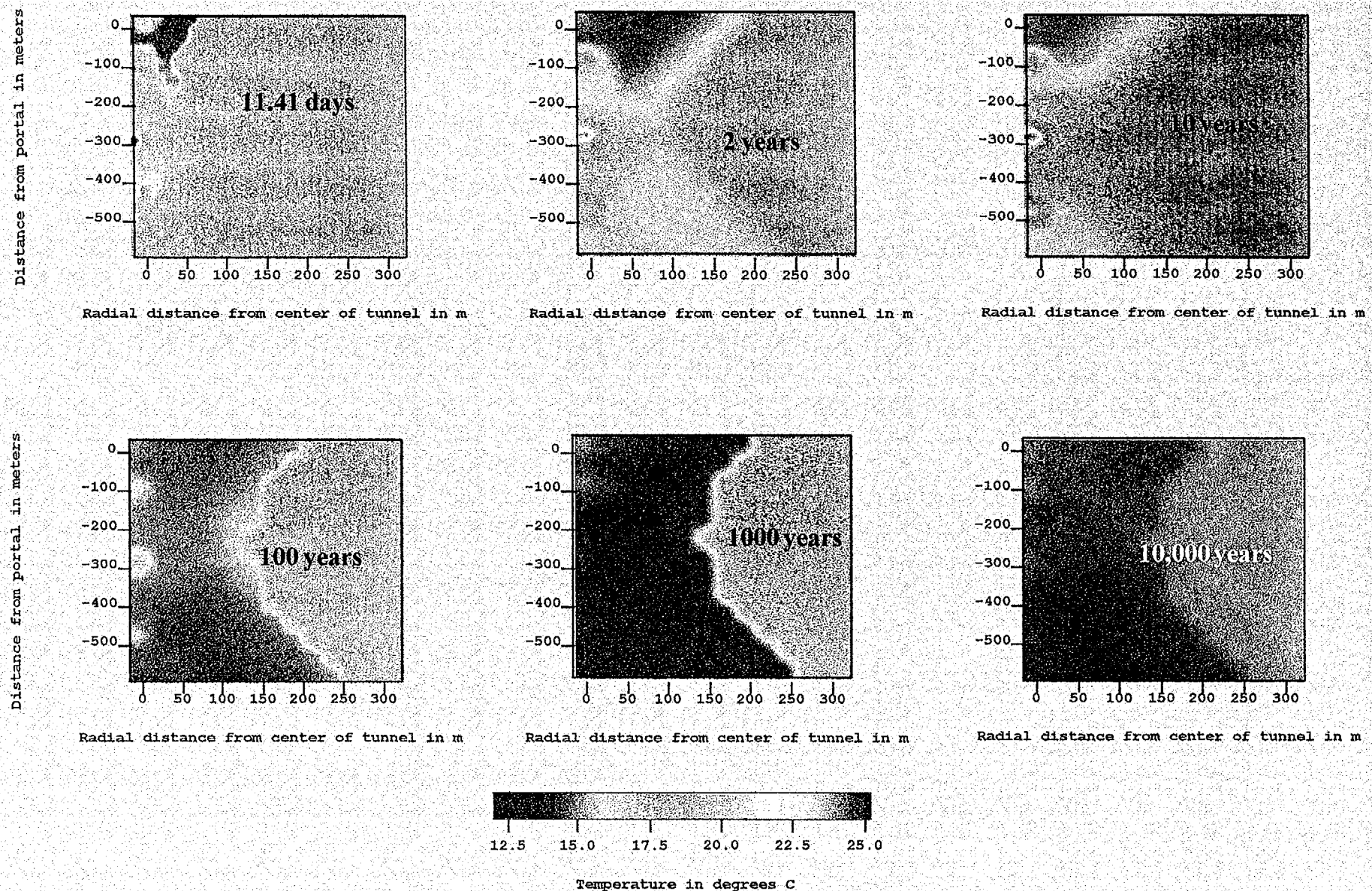


Figure 6-34 - Simulated temperature around the tunnel for various times. Case 10, with decaying heat load. Eddy diffusivity = 0.01, atmosphere temperature = 15 °C.

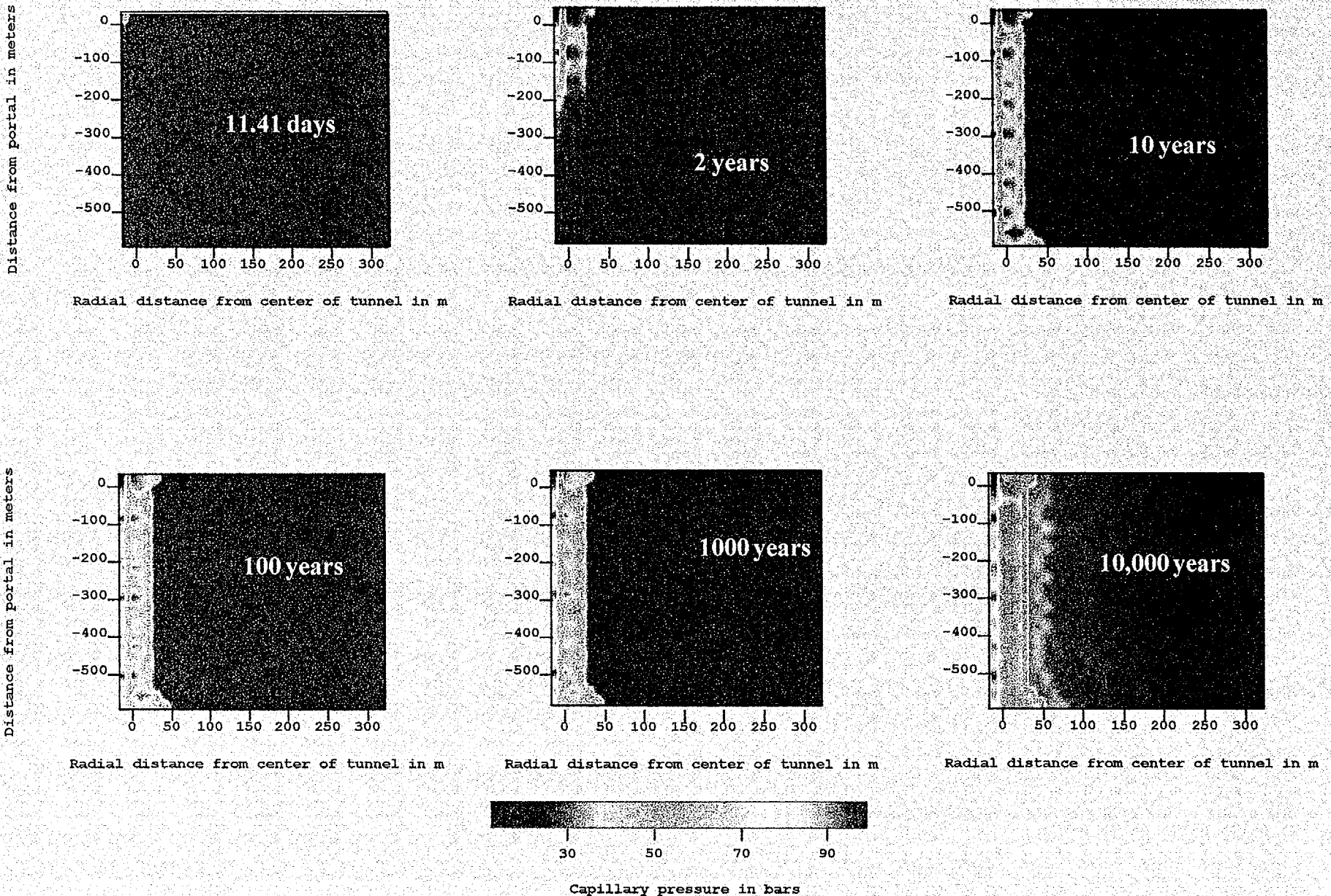


Figure 6-35 - Simulated capillary pressure around the tunnel for various times. Case 10, with decaying heat load. Eddy diffusivity = 0.01, atmosphere temperature = 15 °C. Note: scale changes among graphs.

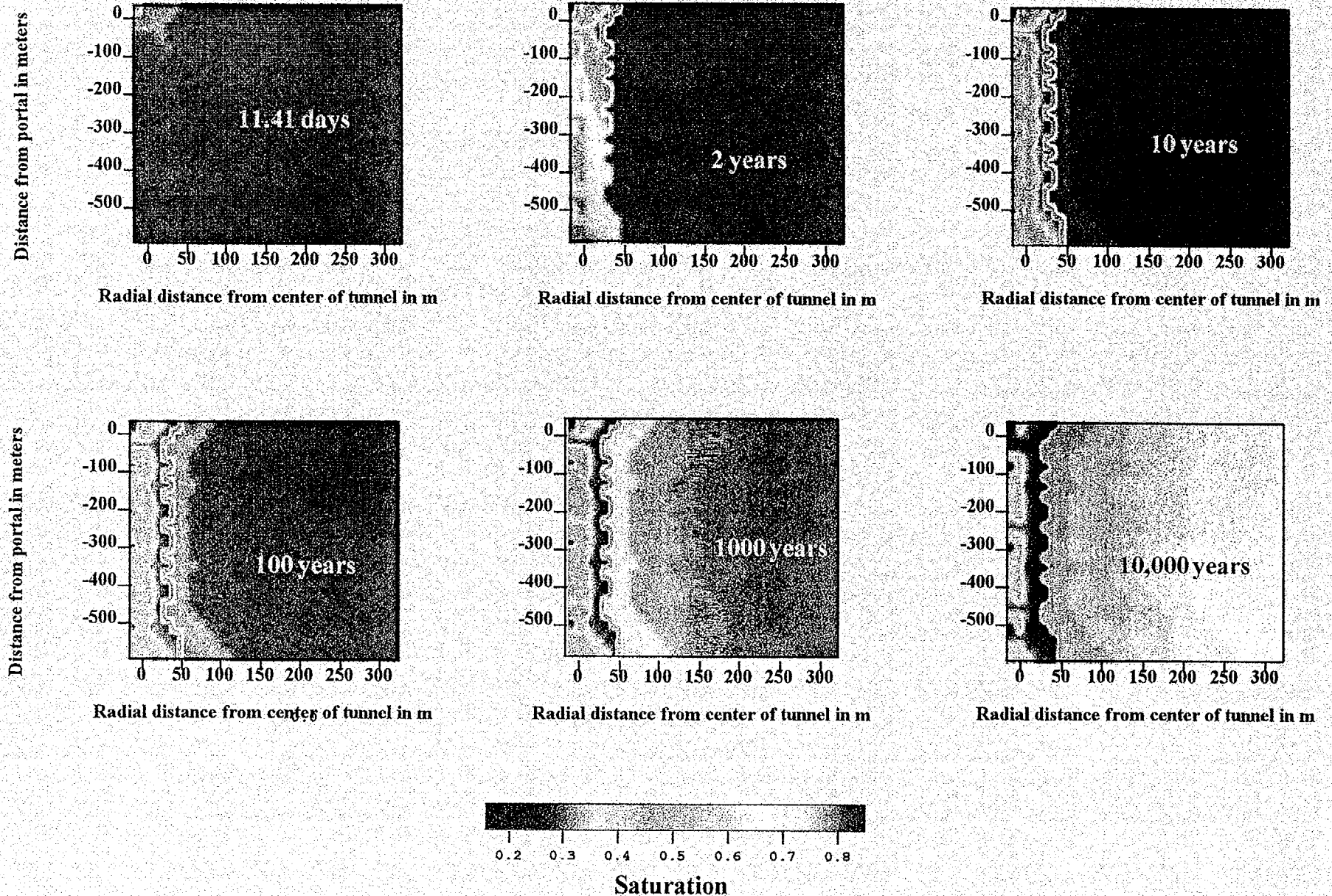


Figure 6-36 - Simulated saturation around the tunnel for various times. Case 10, with decaying heat load. Eddy diffusivity = 0.01, atmosphere temperature = 15 °C.

Case 10

Simulated variation of temperature with time for selected nodes perpendicular to the center of heat load (Eddy Diff = 0.01 Case)

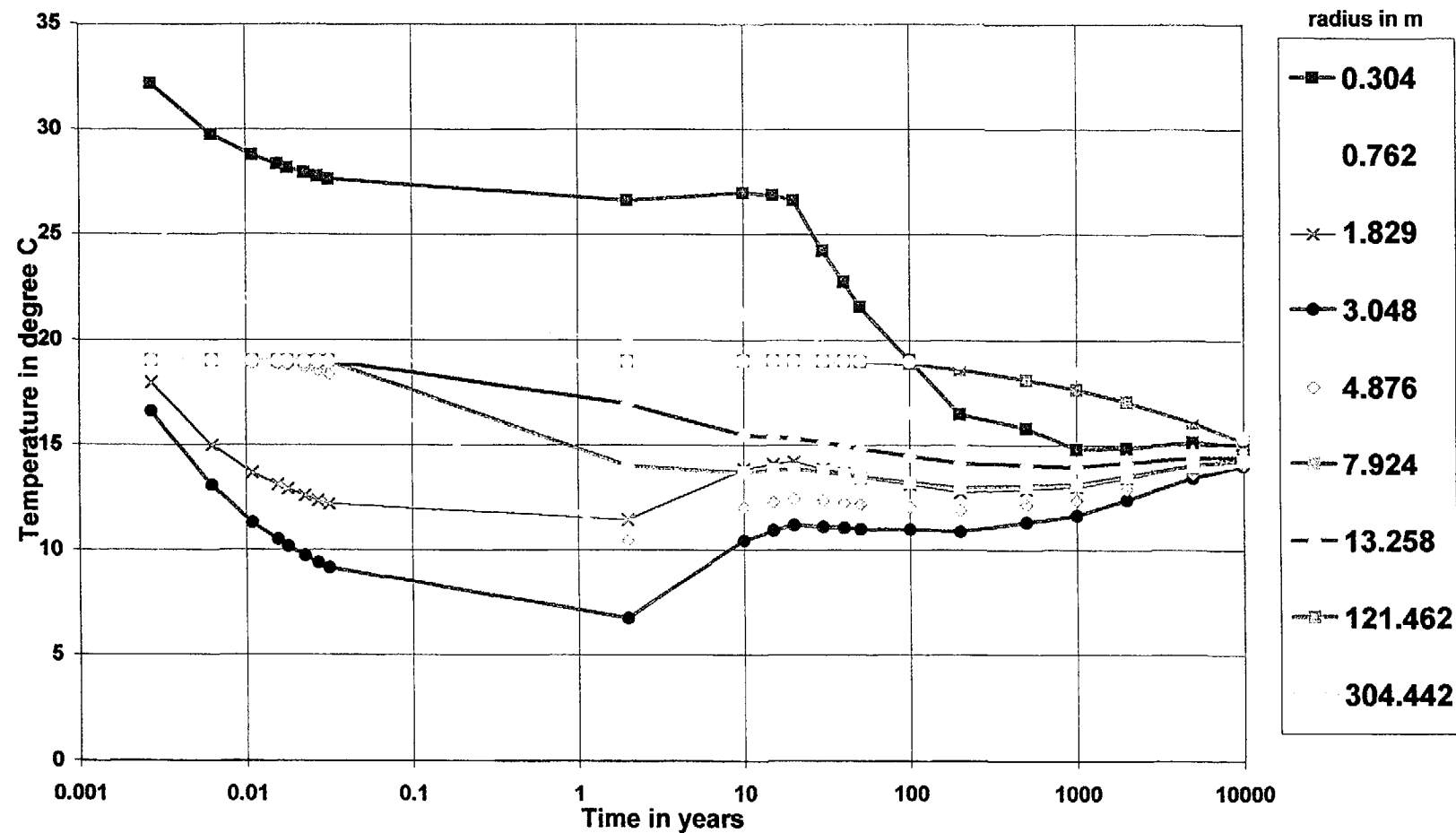


Figure 6-37

Case 10

Simulated variation of saturation with time for selected nodes perpendicular to the center of heat load (Eddy Diff = 0.01 Case)

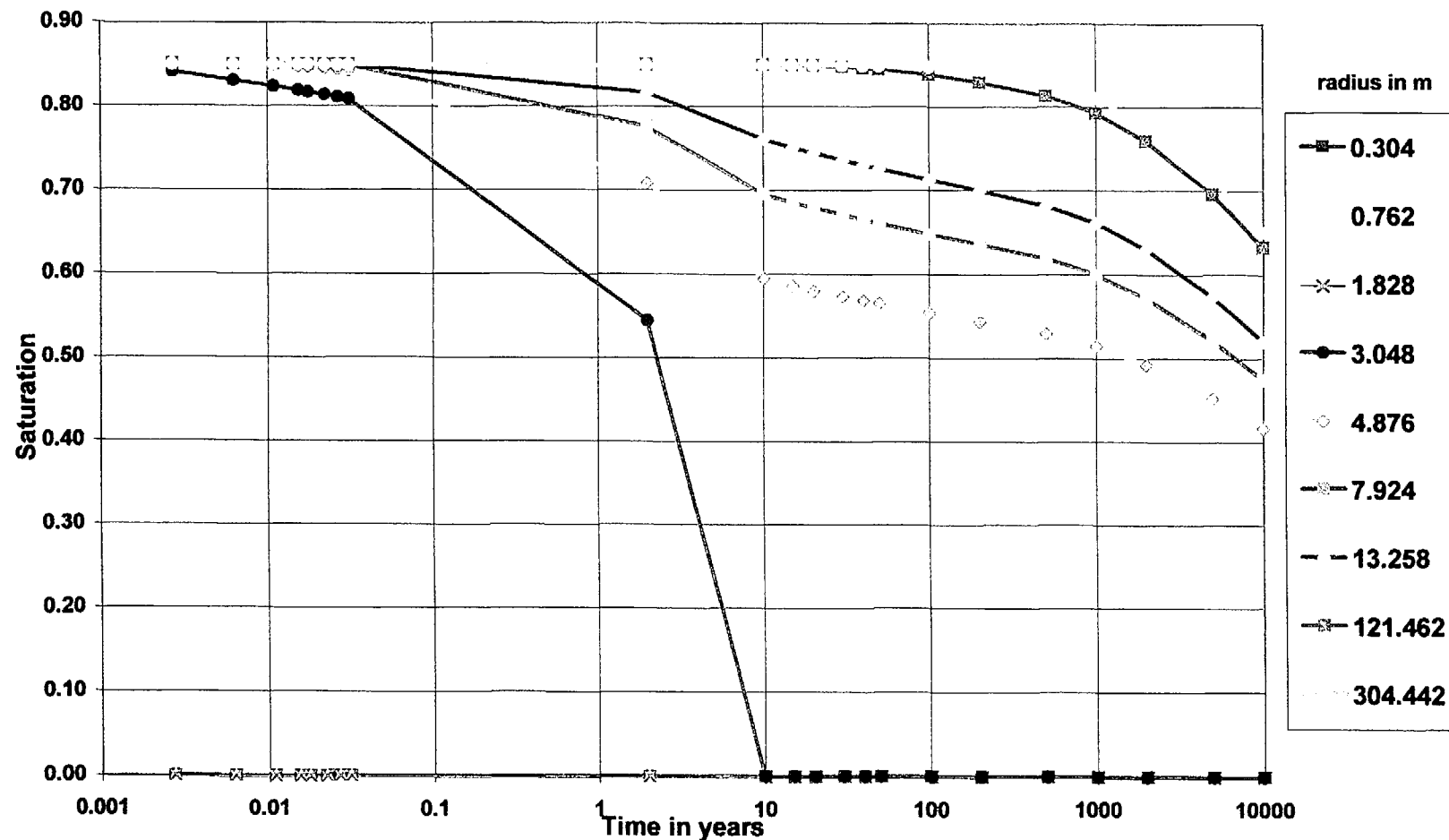


Figure 6-38

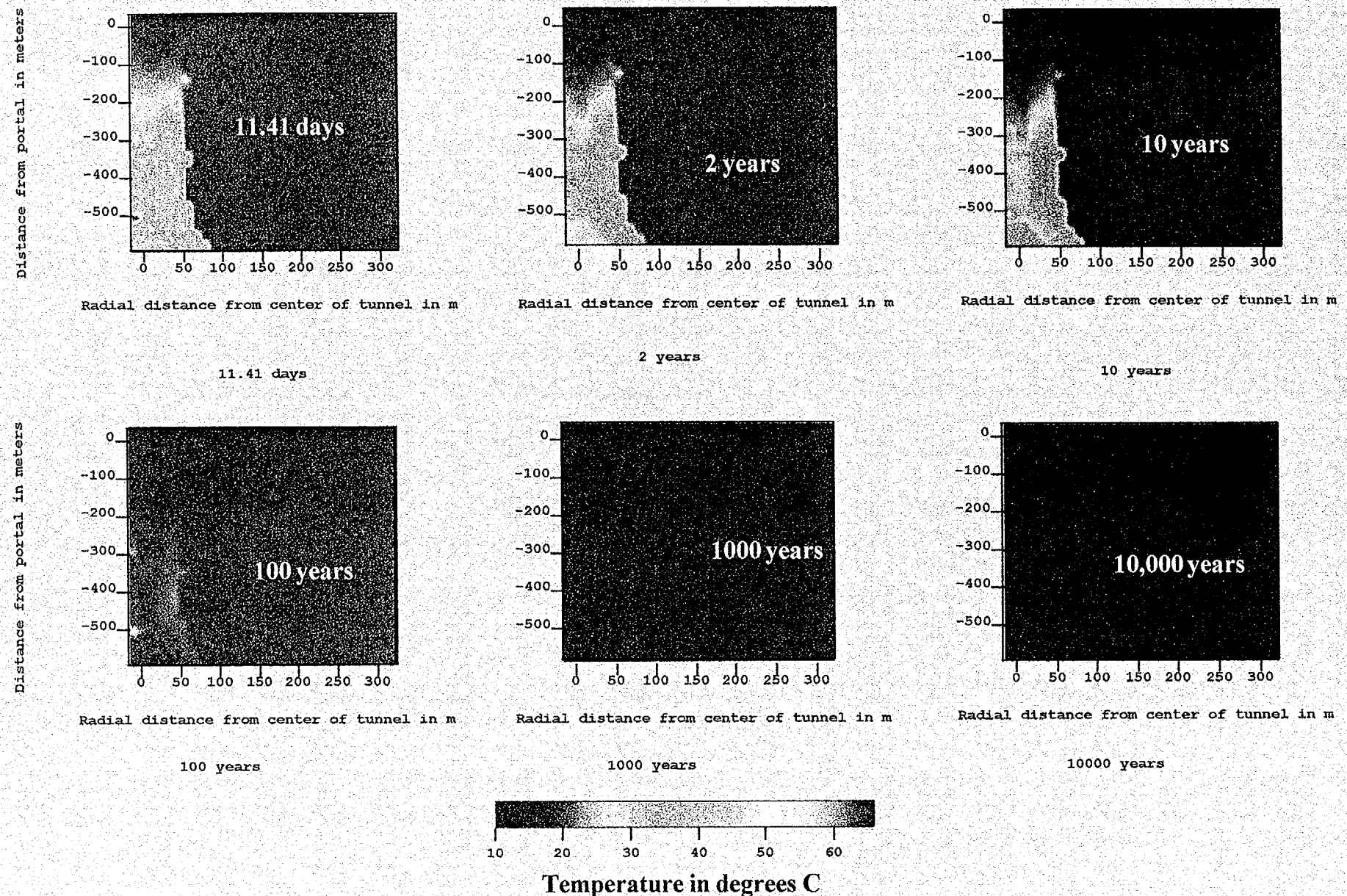


Figure 6-39 - Simulated temperature around the tunnel for various times. Case 11, with decaying heat load. Eddy diffusivity = 0.001, atmosphere temperature = 15 °C.

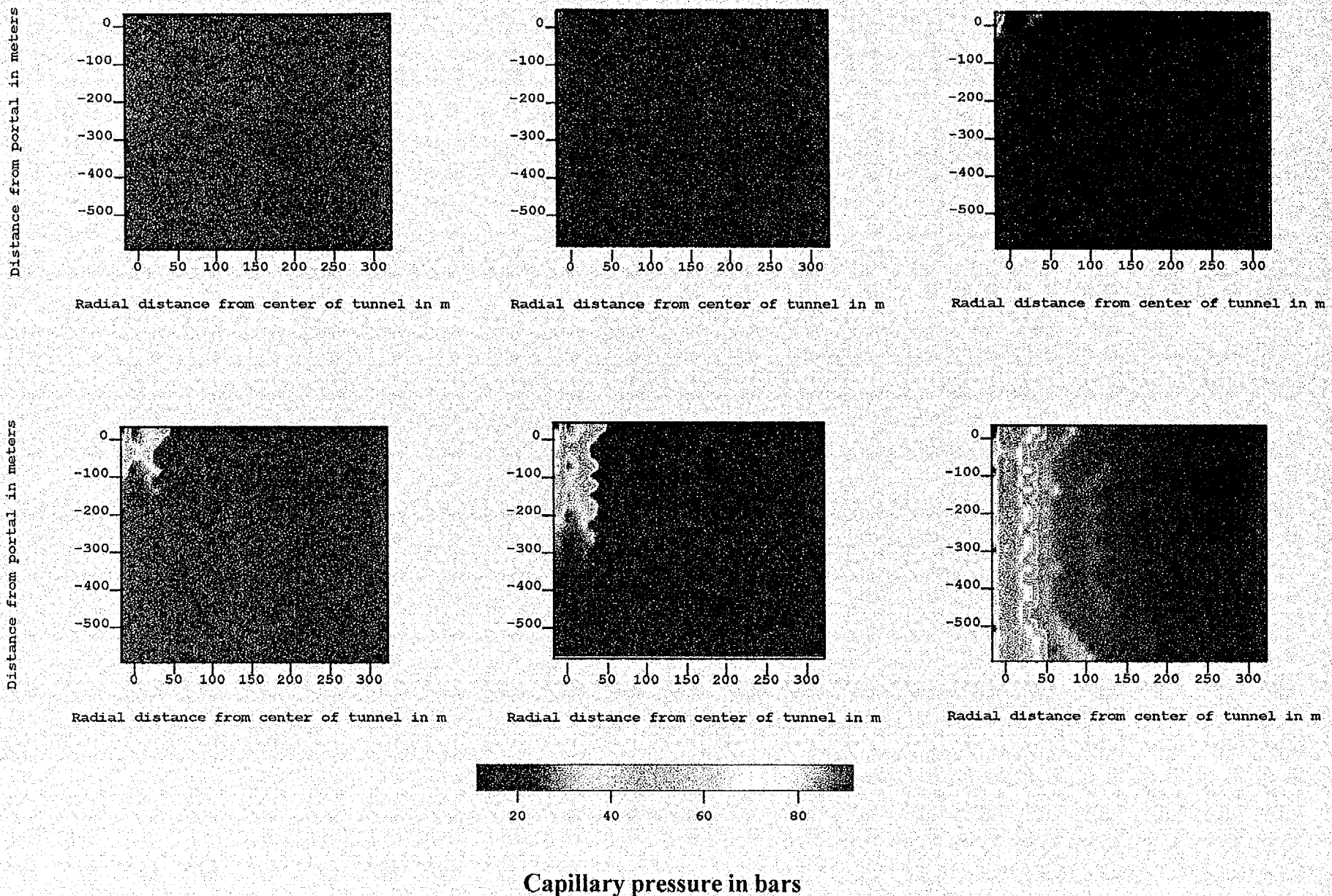
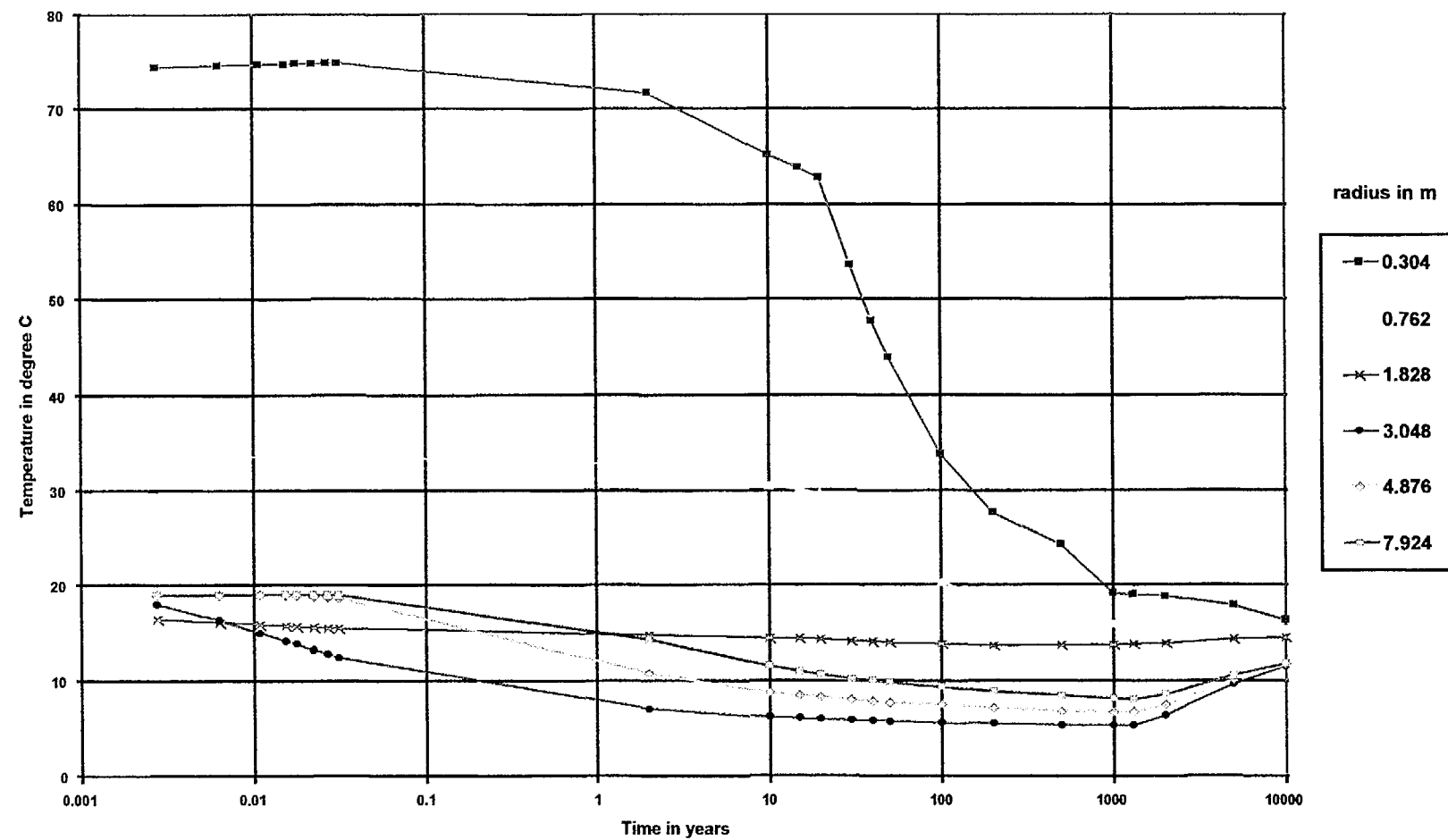


Figure 6-40 - Simulated capillary pressure around the tunnel for various times. Case 11, with decaying heat load.
Eddy diffusivity = 0.001, atmosphere temperature = 15 °C.

Simulated variation of temperature with time for selected nodes perpendicular to the center of heat load
(Eddy Diff = 0.001 Case)



**Simulated variation of saturation with time for selected nodes perpendicular to the center of heat load
(Eddy Diff = 0.001 Case)**

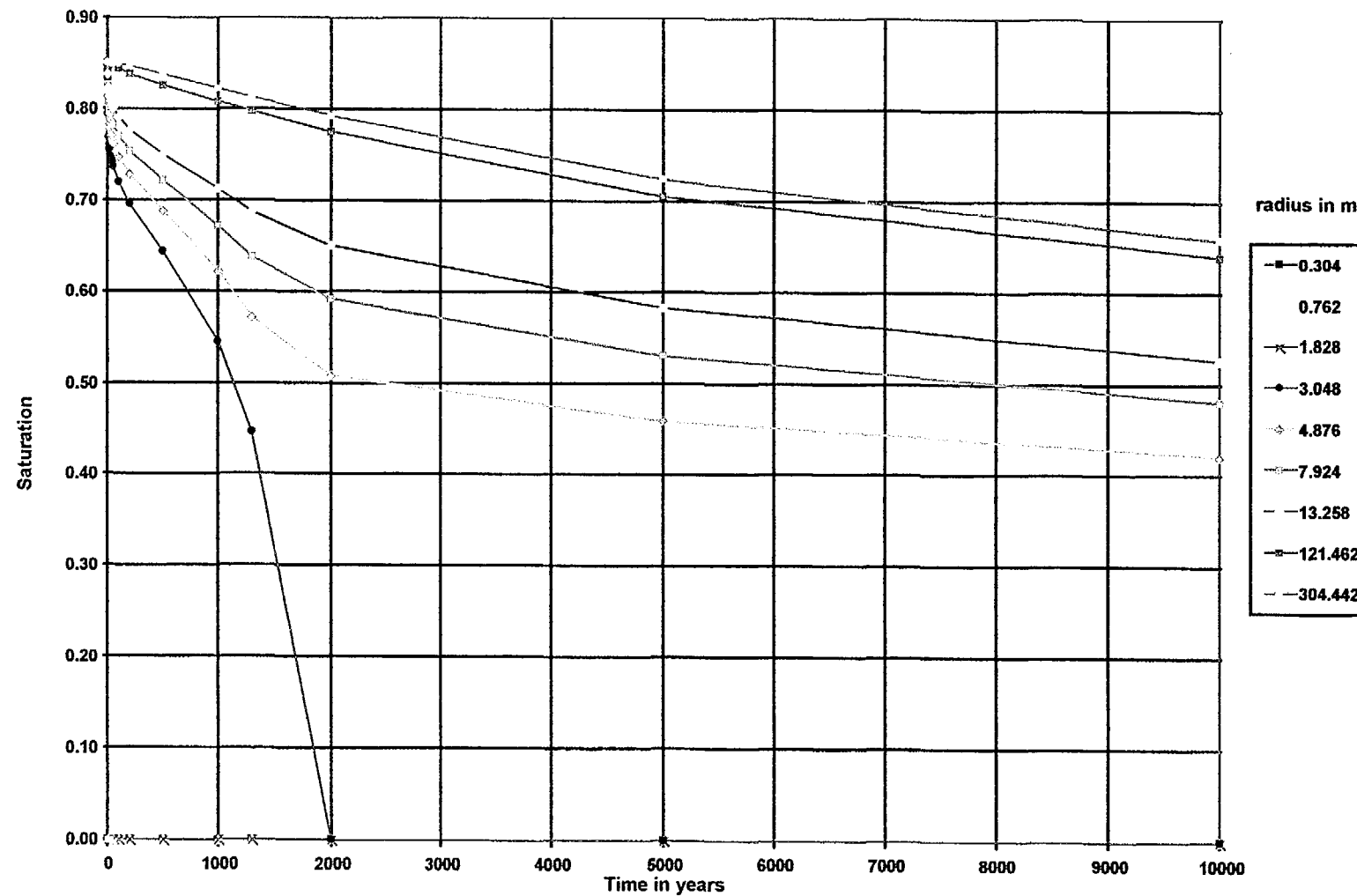
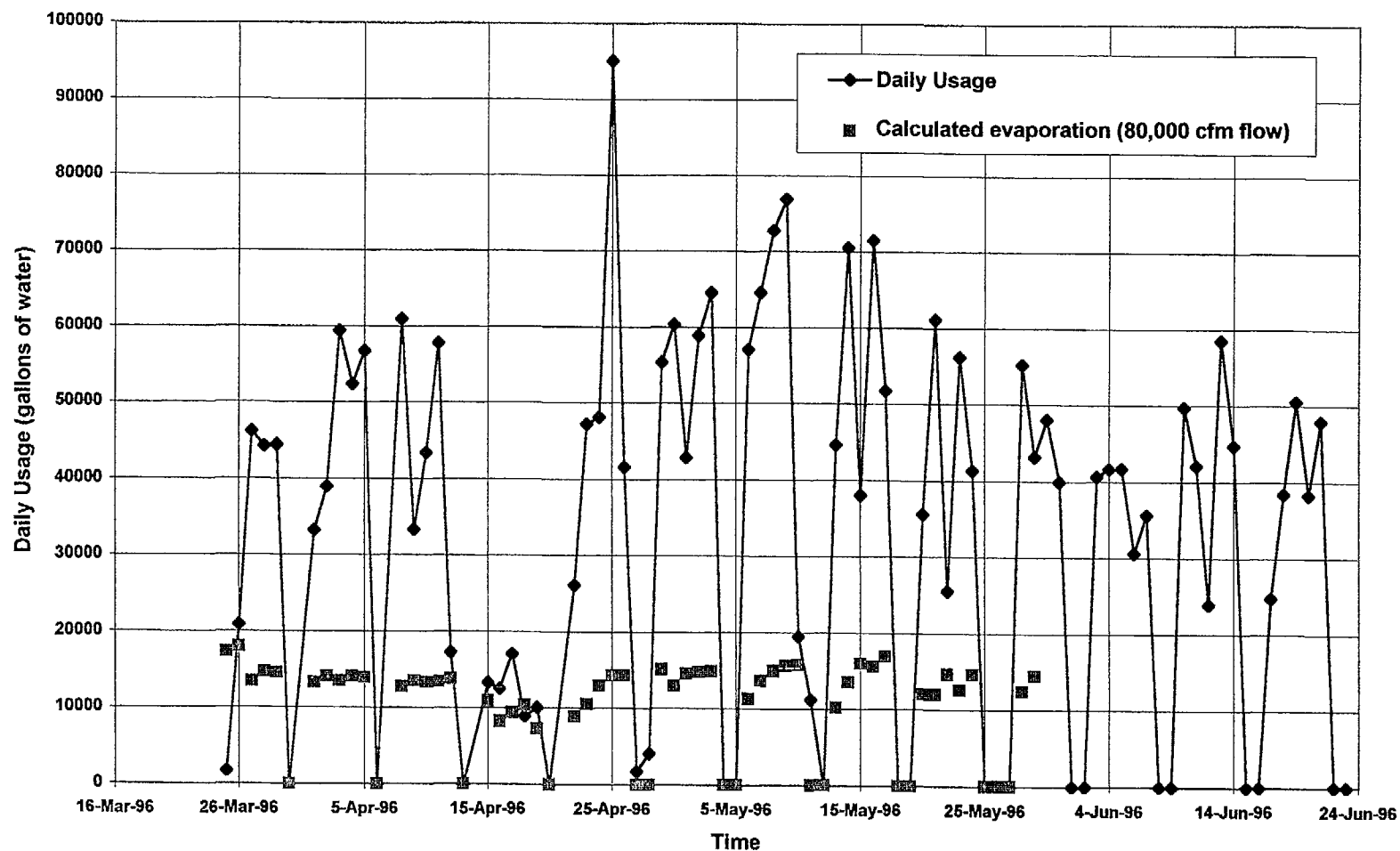


Figure 7-1 - Comparison of Daily Water Usage with Calculated Ventilation-Induced Evaporation



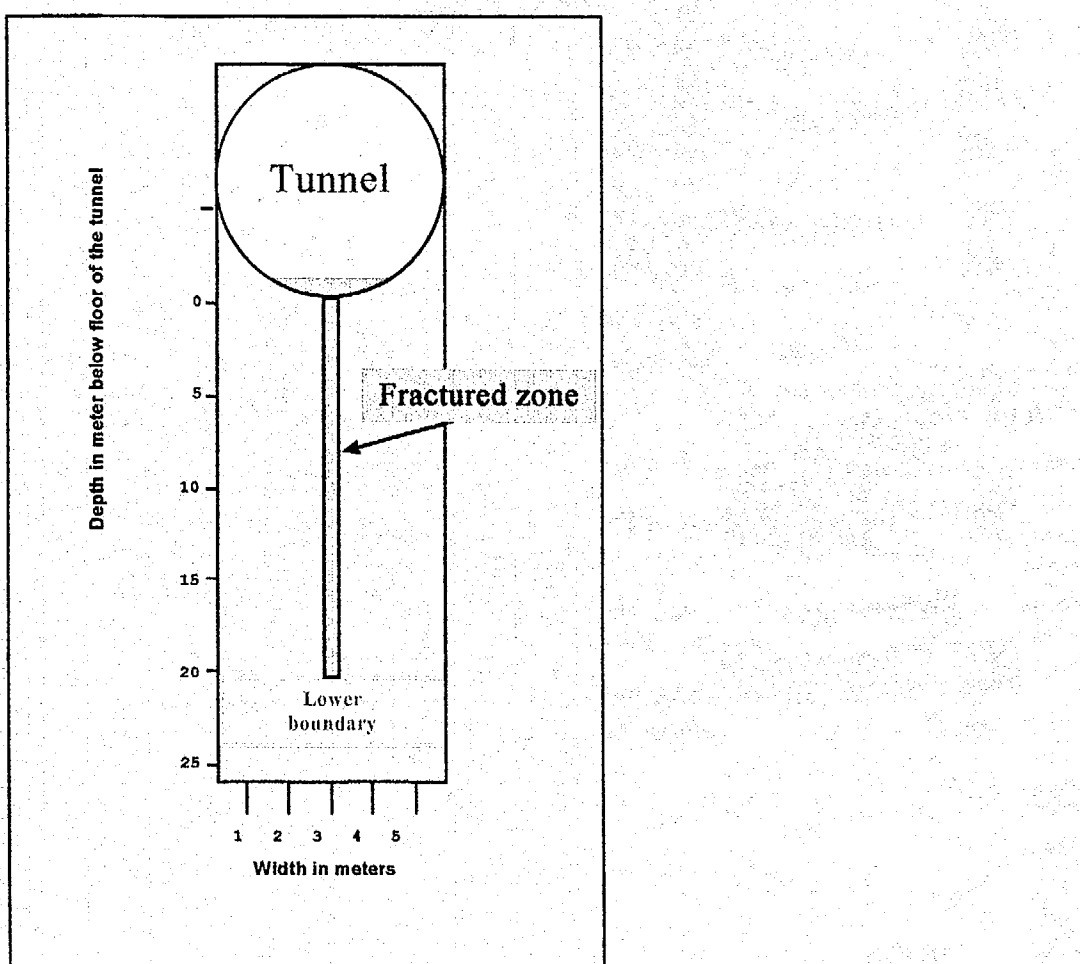


Figure 7-2 - Conceptual model of infiltration into a fractured zone exposed in a wet tunnel floor.

August 24, 1996
P26623:36D:\user\projects\Nye county\annrep96\figures

Prepared for:
Nye County Nuclear Waste Repository Project Office

Prepared by:
Multimedia Environmental Technology, Inc.
Newport Beach, CA

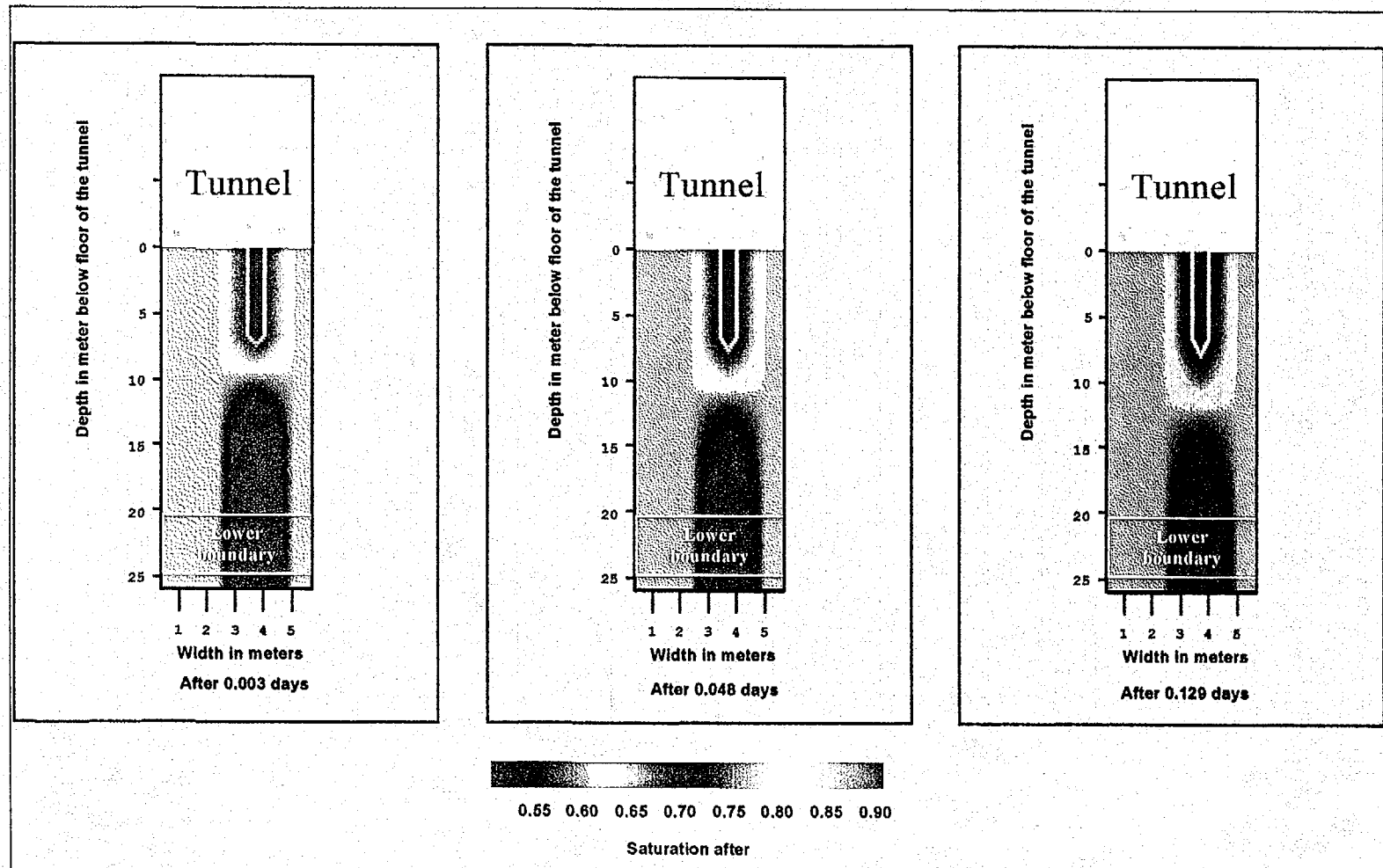


Figure 7-3 - Simulated saturation profile for a wet tunnel surface.

August 24, 1996
P2661:25D:\user\projects\NyeCounty\unrep96\figures

Prepared for:
Nye County Nuclear Waste Repository Project Office

Prepared by:
Multimedia Environmental Technology, Inc.
Newport Beach, CA

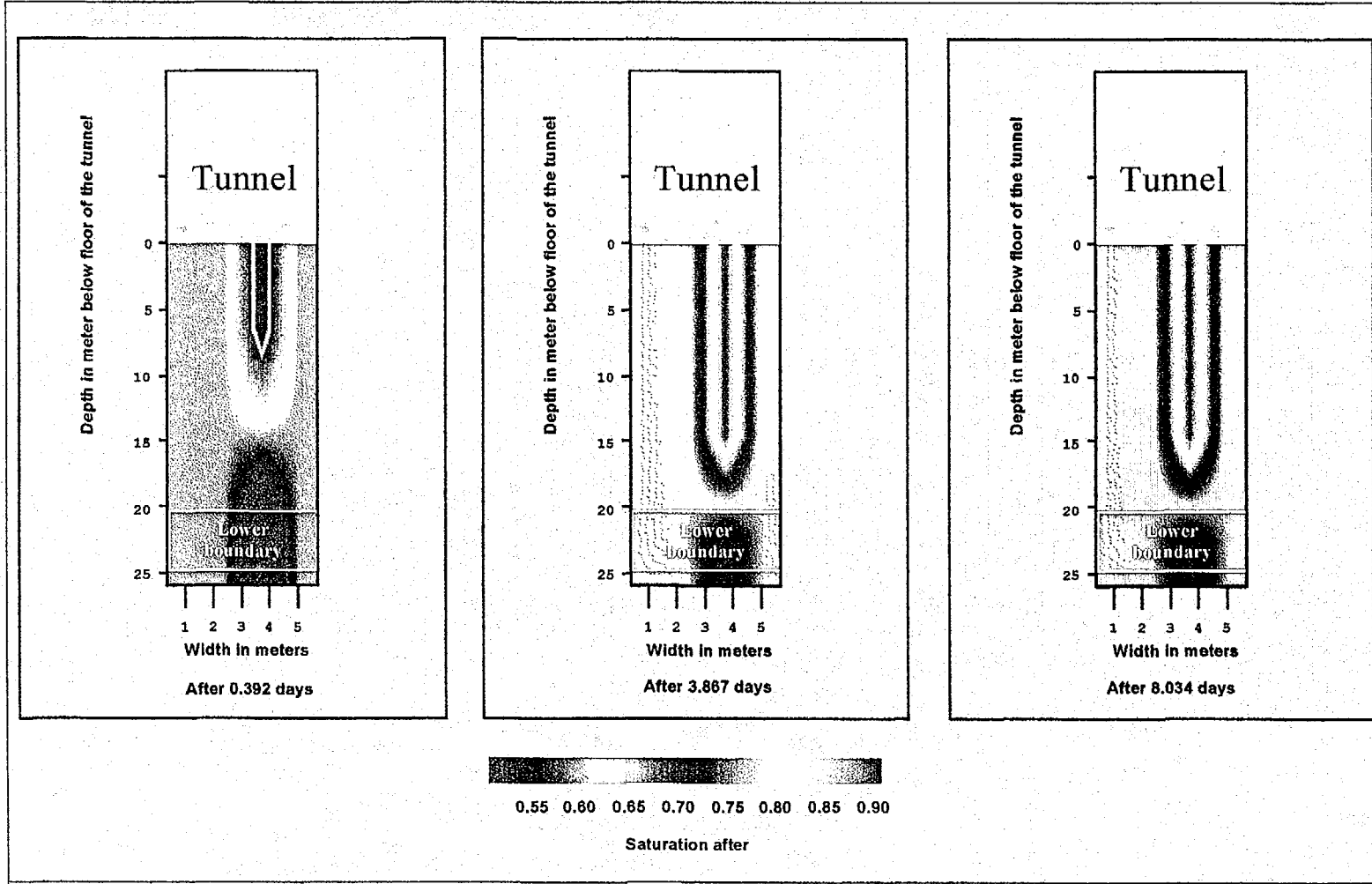


Figure 7-3 (Cont.) - Simulated saturation profile for a wet tunnel surface.

August 24, 1996
P26623:39D:\user\projects\Nye county\annrep96\figures

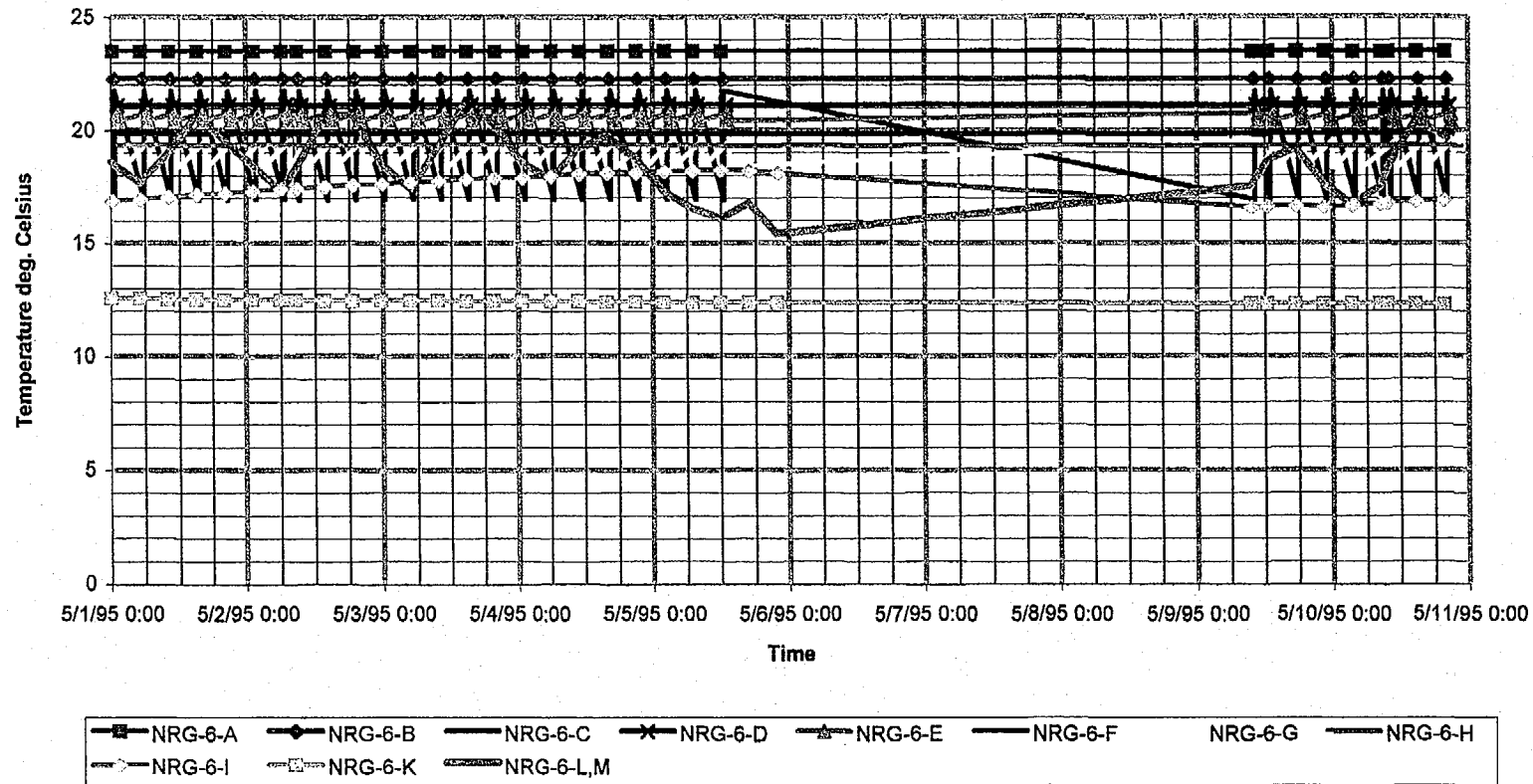
Prepared for:
Nye County Nuclear Waste Repository Project Office

Prepared by:
Multimedia Environmental Technology, Inc.
Newport Beach, CA

Appendix A

USGS Borehole Data

May 1 - May 10 1995



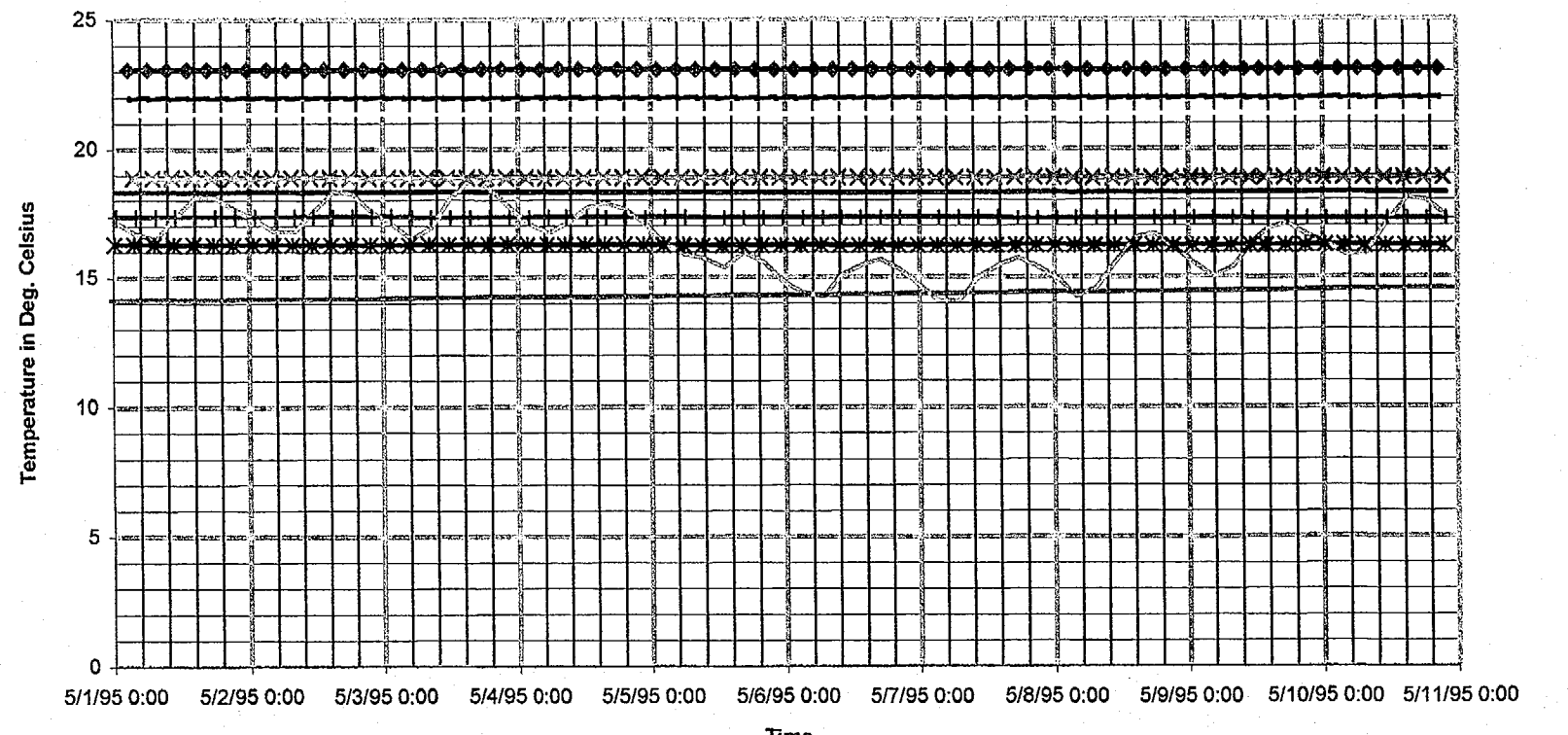
Temperature vs. time for NRG-6

August 24, 1996
P266:D:\user\projects\NyeCounty\annrep96\figures

Prepared for:
Nye County Nuclear Waste Repository Project Office

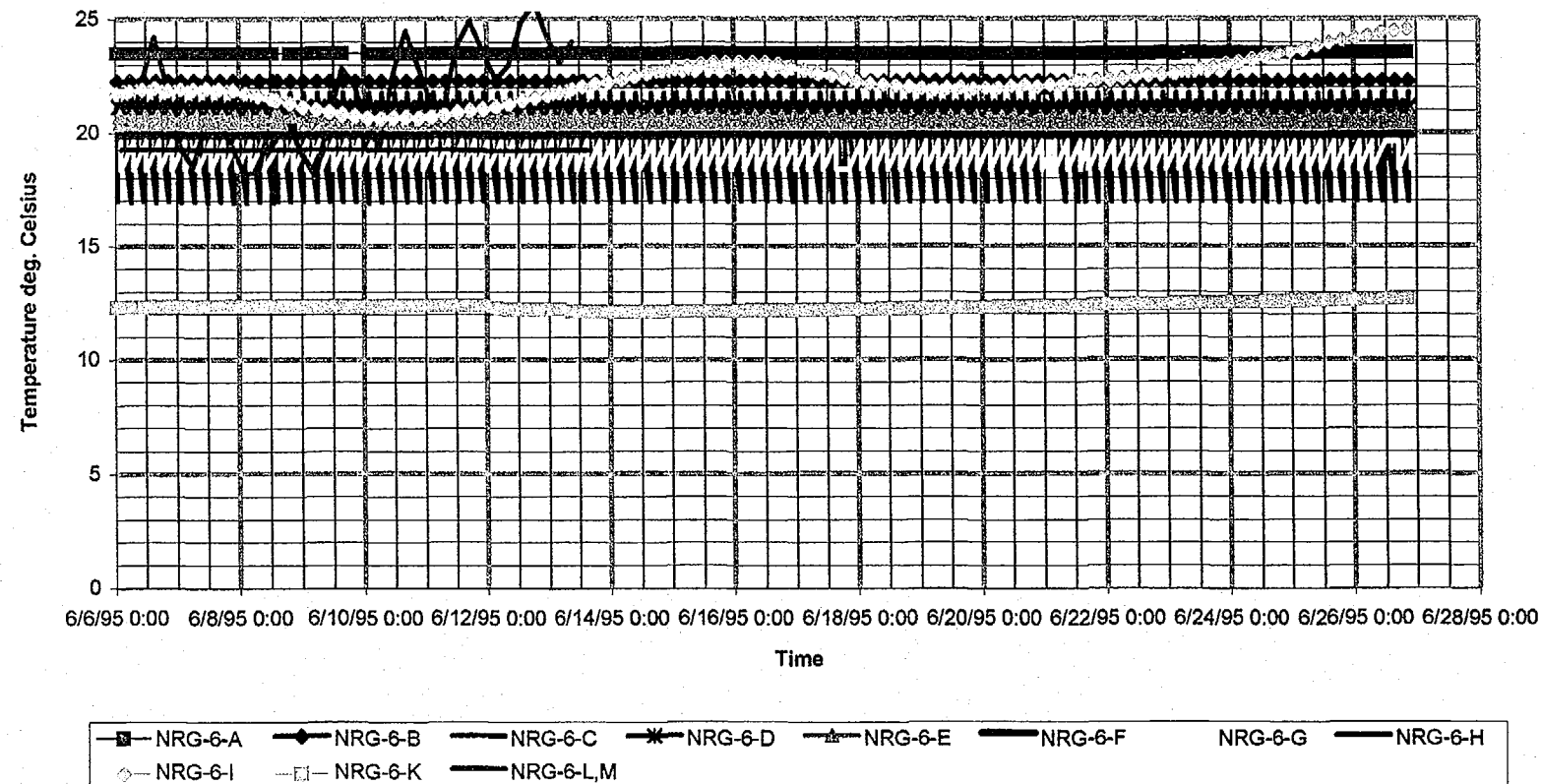
Prepared by:
Multimedia Environmental Technology, Inc.
Newport Beach, CA

May 1 - May 10 1995



Temperature vs. time for NRG-7a

June 6 - June 26 1995



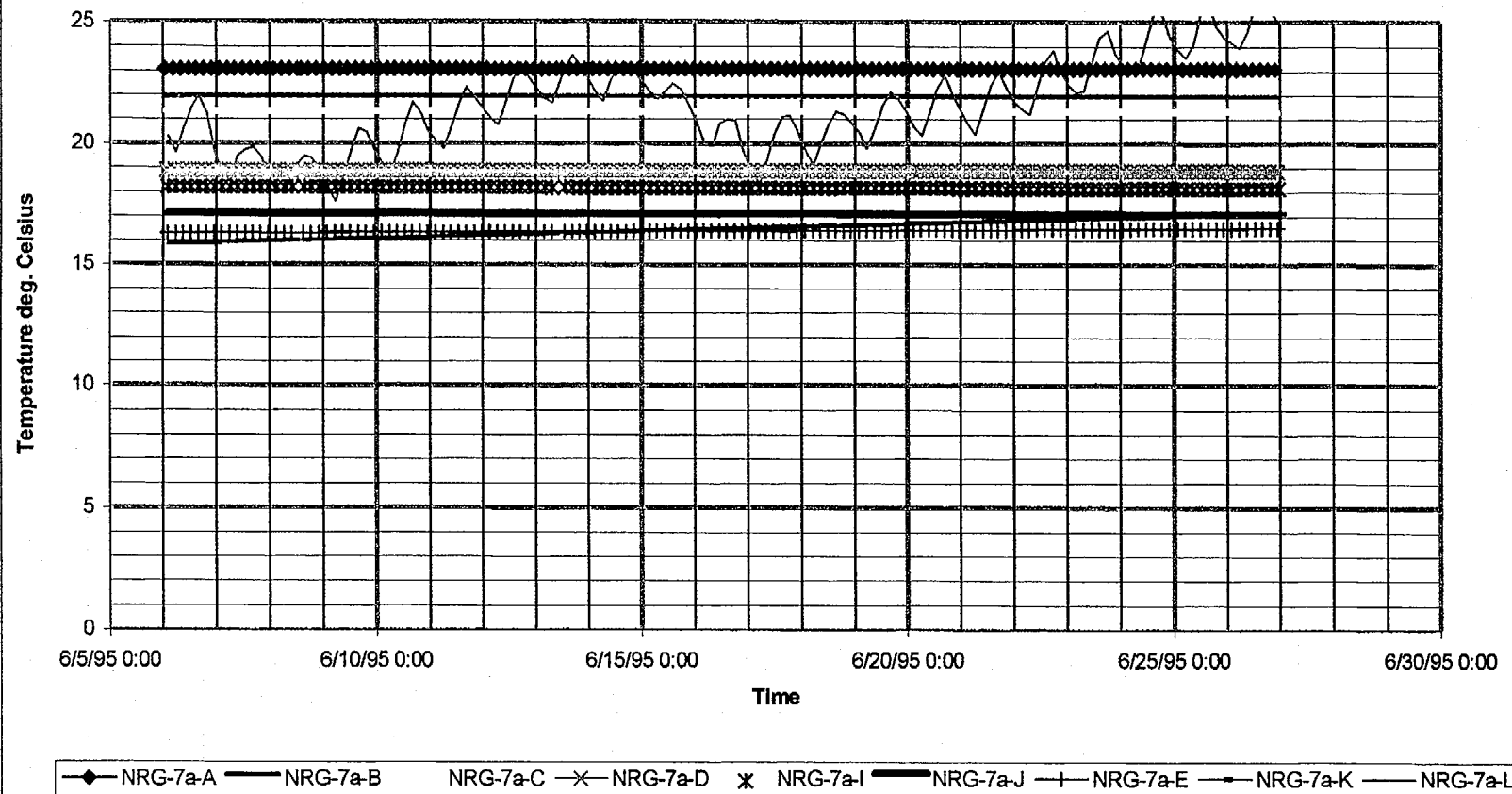
Temperature vs. time for NRG-6

August 24, 1996
P266:D:\user\projs\NyeCounty\annrep96\figures

Prepared for:
Nye County Nuclear Waste Repository Project Office

Prepared by:
Multimedia Environmental Technology, Inc.
Newport Beach, CA

June 6 - June 26 1995



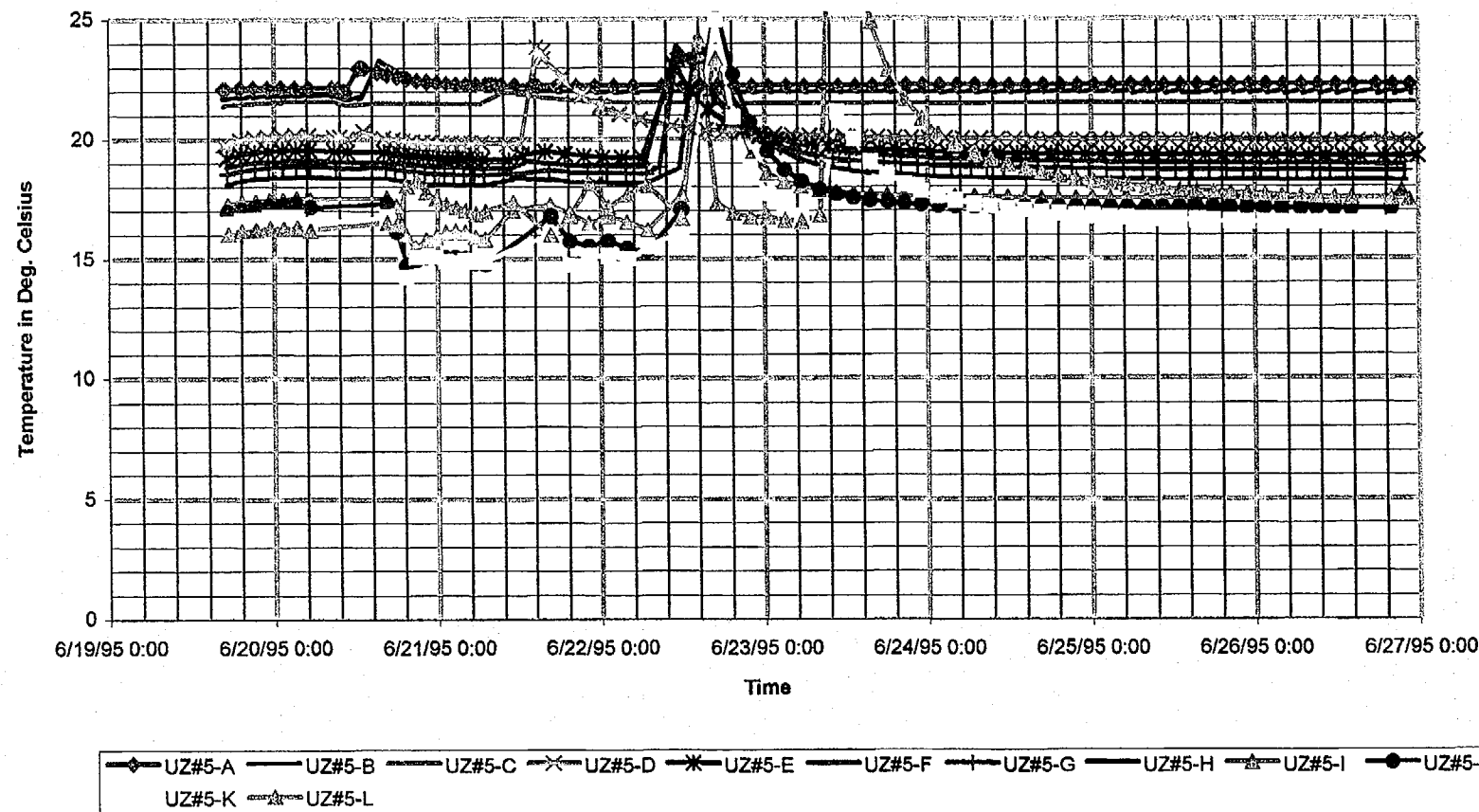
Temperature vs. time for NRG-7a

August 24, 1996
P266:D:\user\projects\NyeCounty\annrep96\figures

Prepared for:
Nye County Nuclear Waste Repository Project Office

Prepared by:
Multimedia Environmental Technology, Inc.
Newport Beach, CA

June 6 - June 26 1995



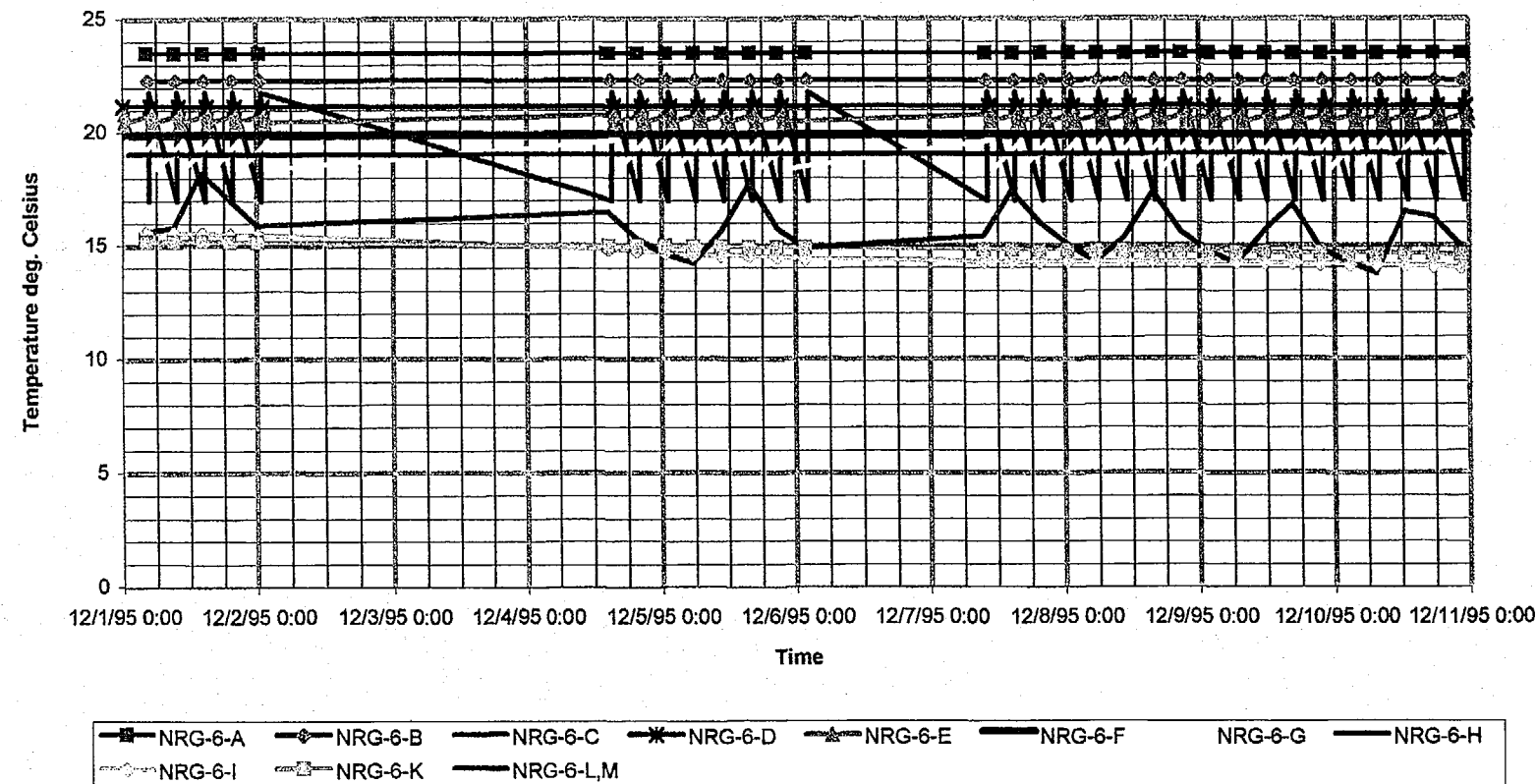
Temperature vs. time for UZ#5

August 24, 1996
P266:D:\user\projects\NyeCounty\annrep96\figures

Prepared for:
Nye County Nuclear Waste Repository Project Office

Prepared by:
Multimedia Environmental Technology, Inc.
Newport Beach, CA

December 1 - December 12 1995



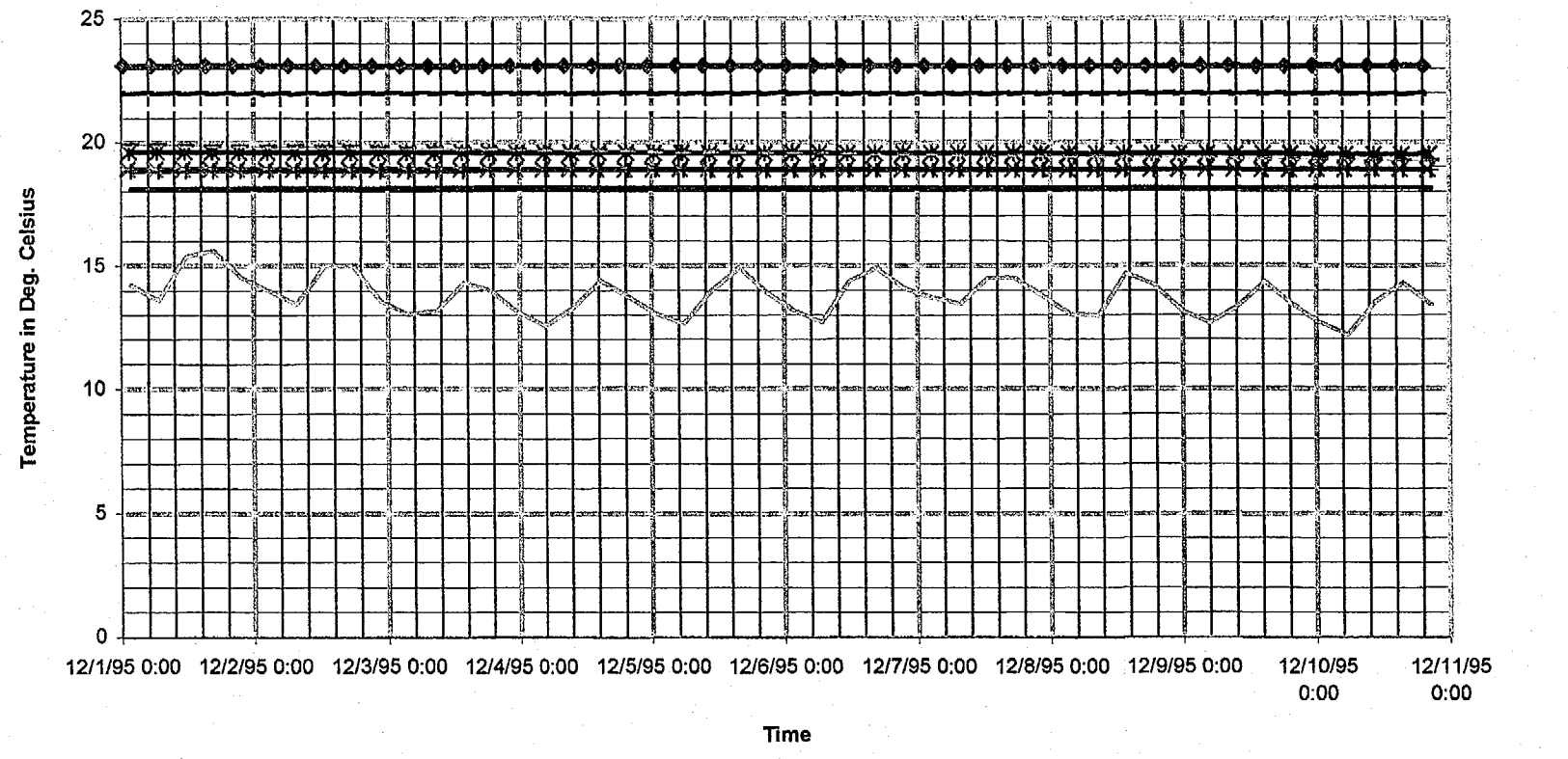
Temperature vs. time for NRG-6

August 24, 1996
P266:D:\user\project\NyeCounty\annrep96\figures

Prepared for:
Nye County Nuclear Waste Repository Project Office

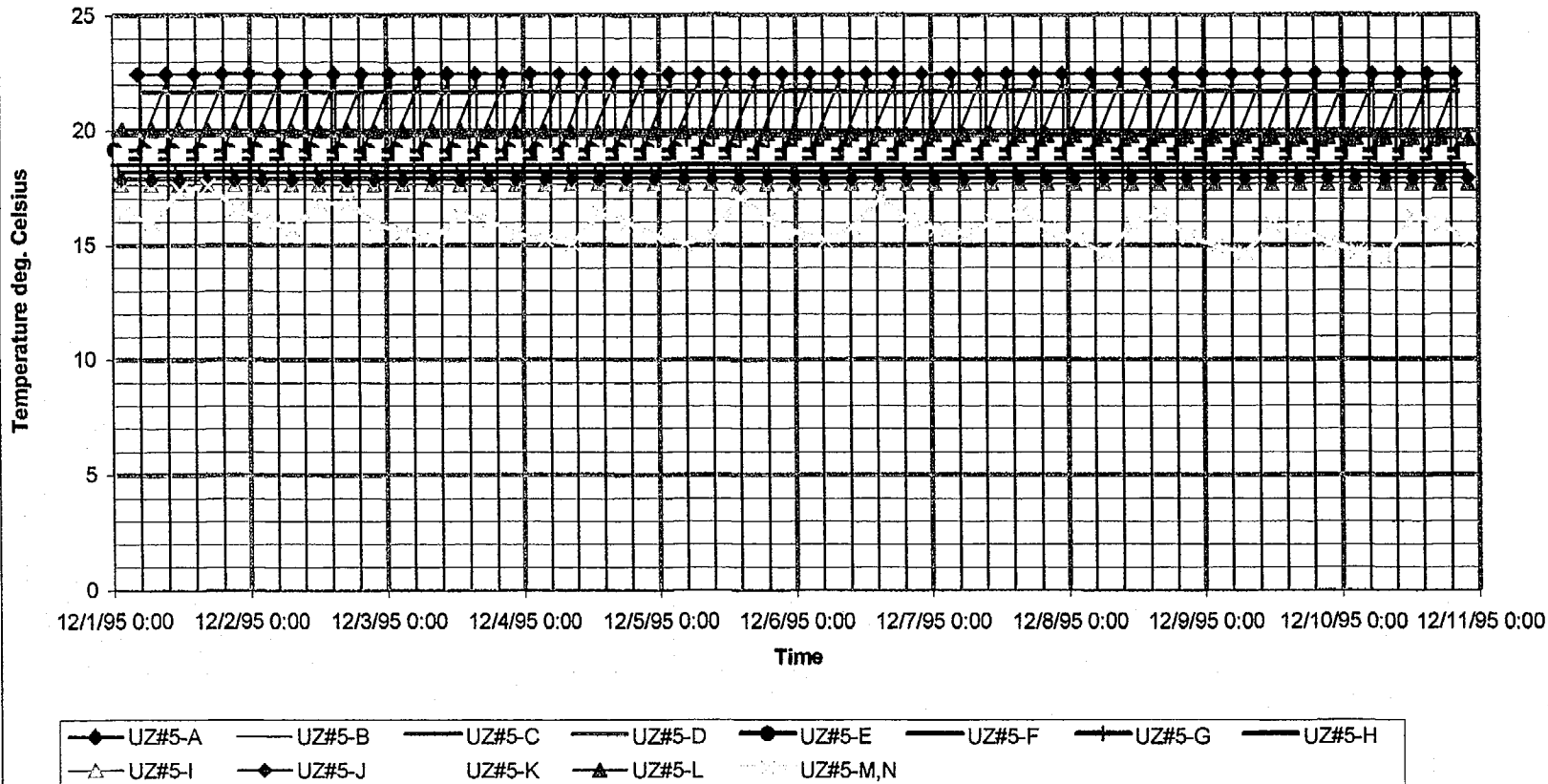
Prepared by:
Multimedia Environmental Technology, Inc.
Newport Beach, CA

December 1 - December 12 1995



Temperature vs. time for NRG-7a

December 1 - December 12 1995



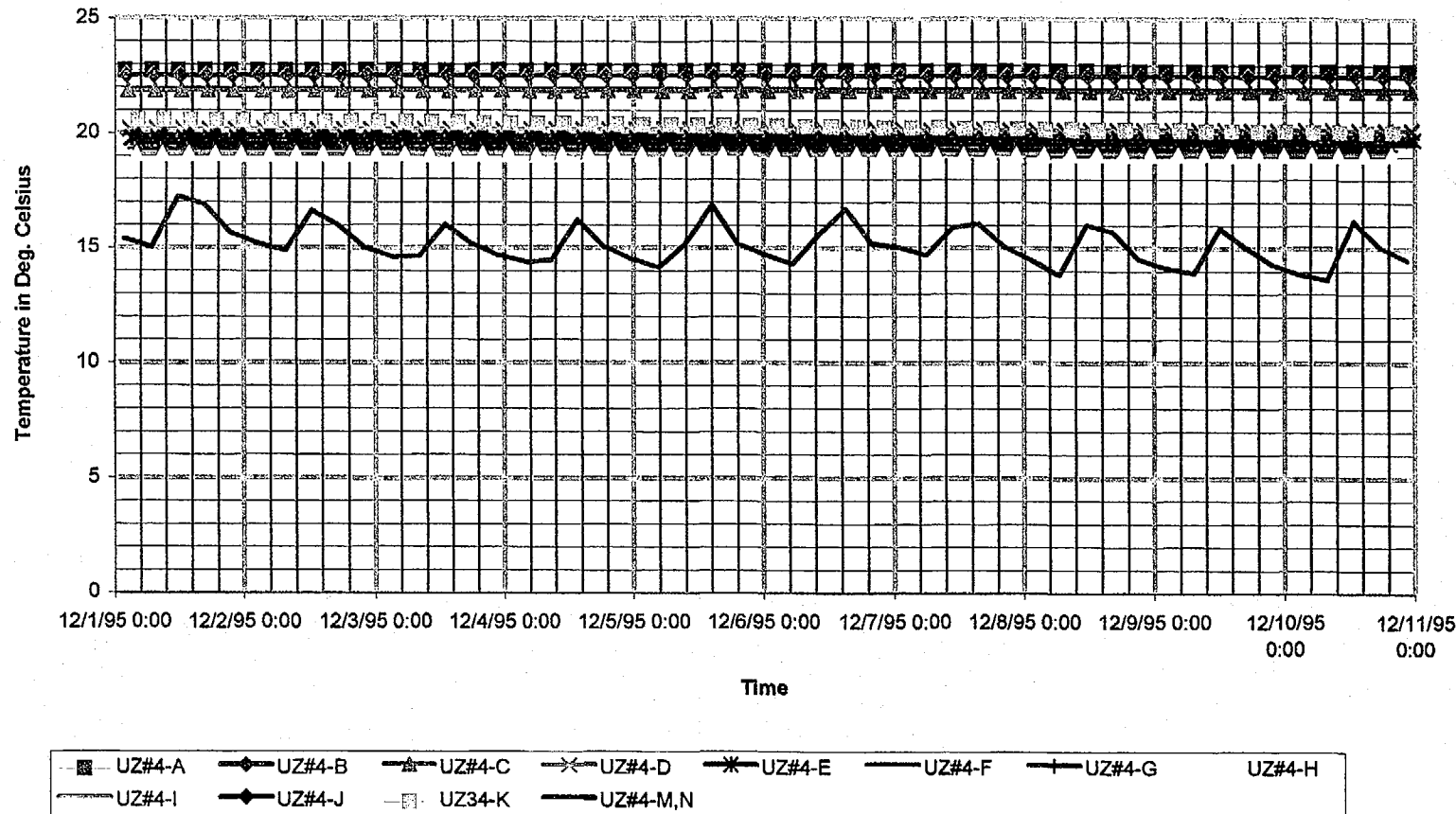
Temperature vs. time for UZ#5

August 24, 1996
P266:D:\user\projects\NyeCounty\annrep96\figures

Prepared for:
Nye County Nuclear Waste Repository Project Office

Prepared by:
Multimedia Environmental Technology, Inc.
Newport Beach, CA

December 1 - December 12 1995



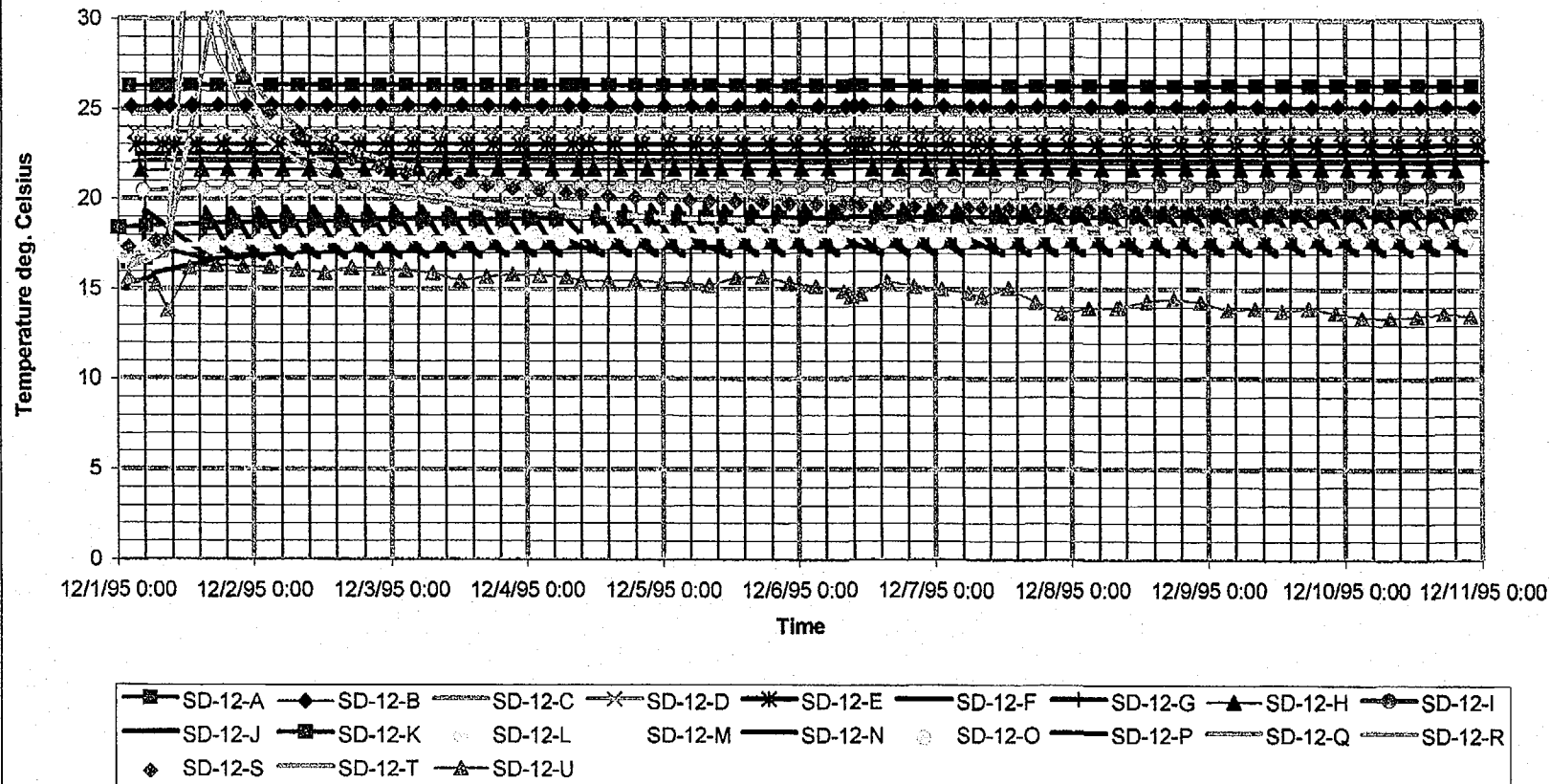
Temperature vs. time for UZ#4

August 24, 1996
P266:D:\user\projects\NyeCounty\annrep96\figures

Prepared for:
Nye County Nuclear Waste Repository Project Office

Prepared by:
Multimedia Environmental Technology, Inc.
Newport Beach, CA

December 1 - December 12 1995



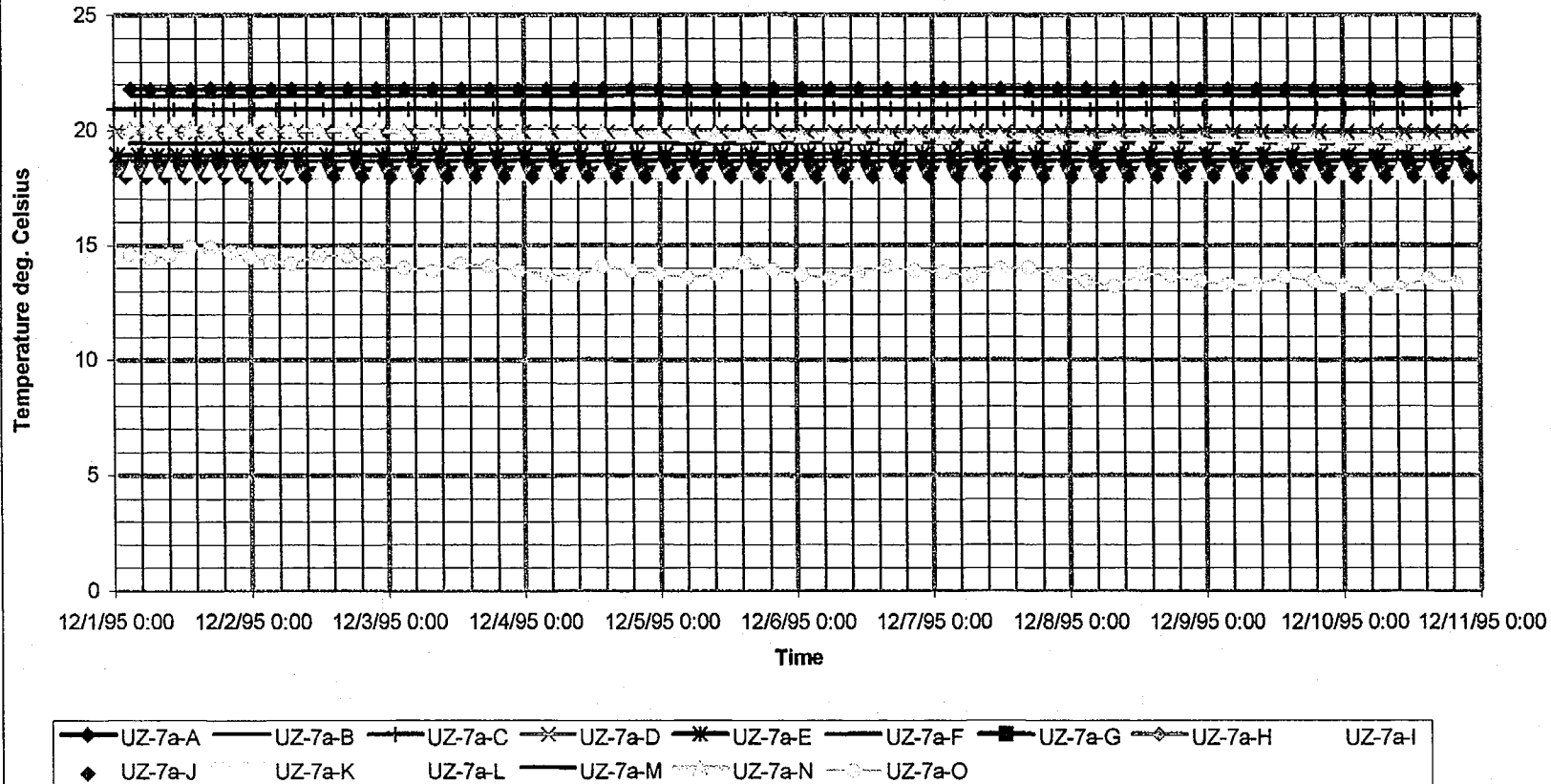
Temperature vs. time for SD-12

August 24, 1996
P266:D:\user\projcts\NyeCounty\annrep96\figures

Prepared for:
Nye County Nuclear Waste Repository Project Office

Prepared by:
Multimedia Environmental Technology, Inc.
Newport Beach, CA

December 1 - December 12 1995



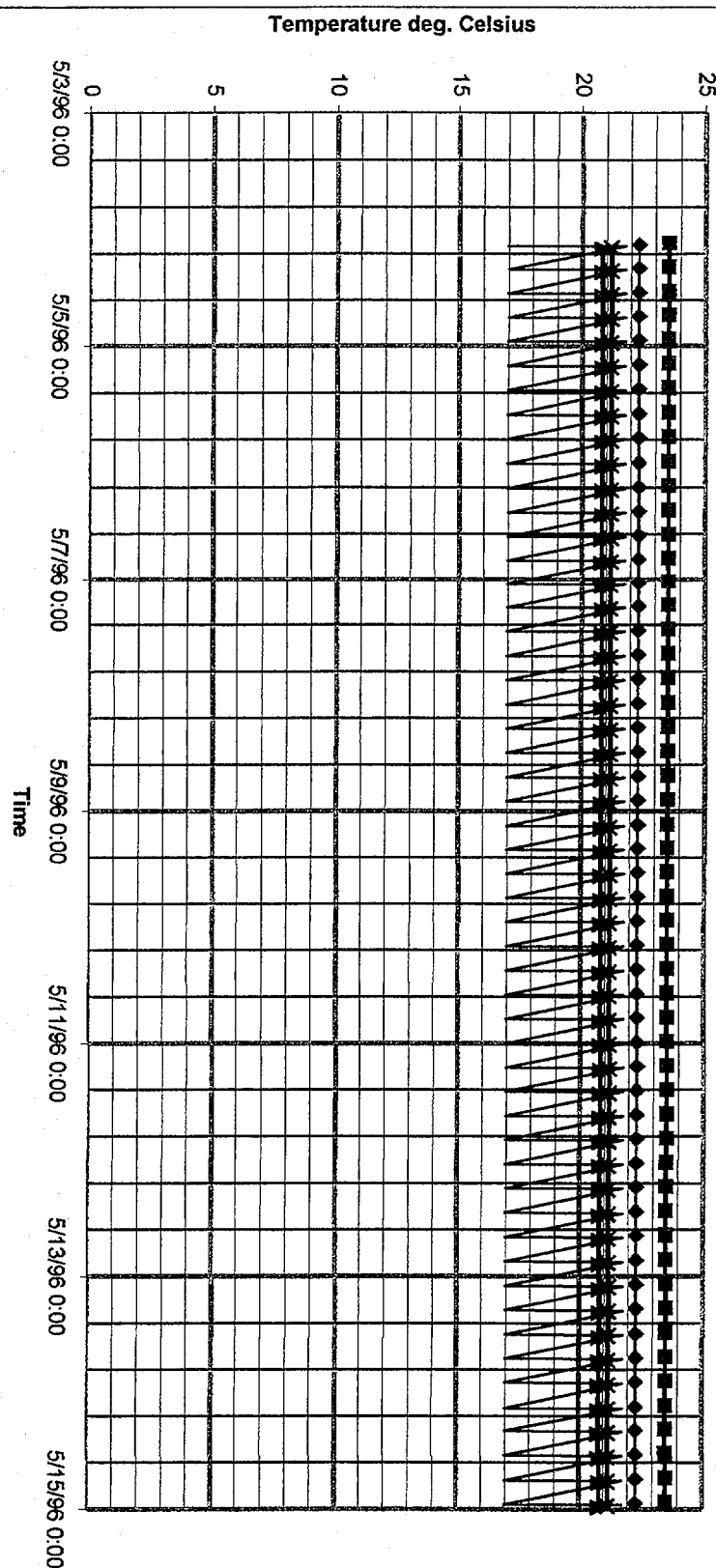
Temperature vs. time for UZ-7a

August 24, 1996
P266:D:\user\projext\NyeCounty\annrep96\figures

Prepared for:
Nye County Nuclear Waste Repository Project Office

Prepared by:
Multimedia Environmental Technology, Inc.
Newport Beach, CA

May 4 - May 15 1996



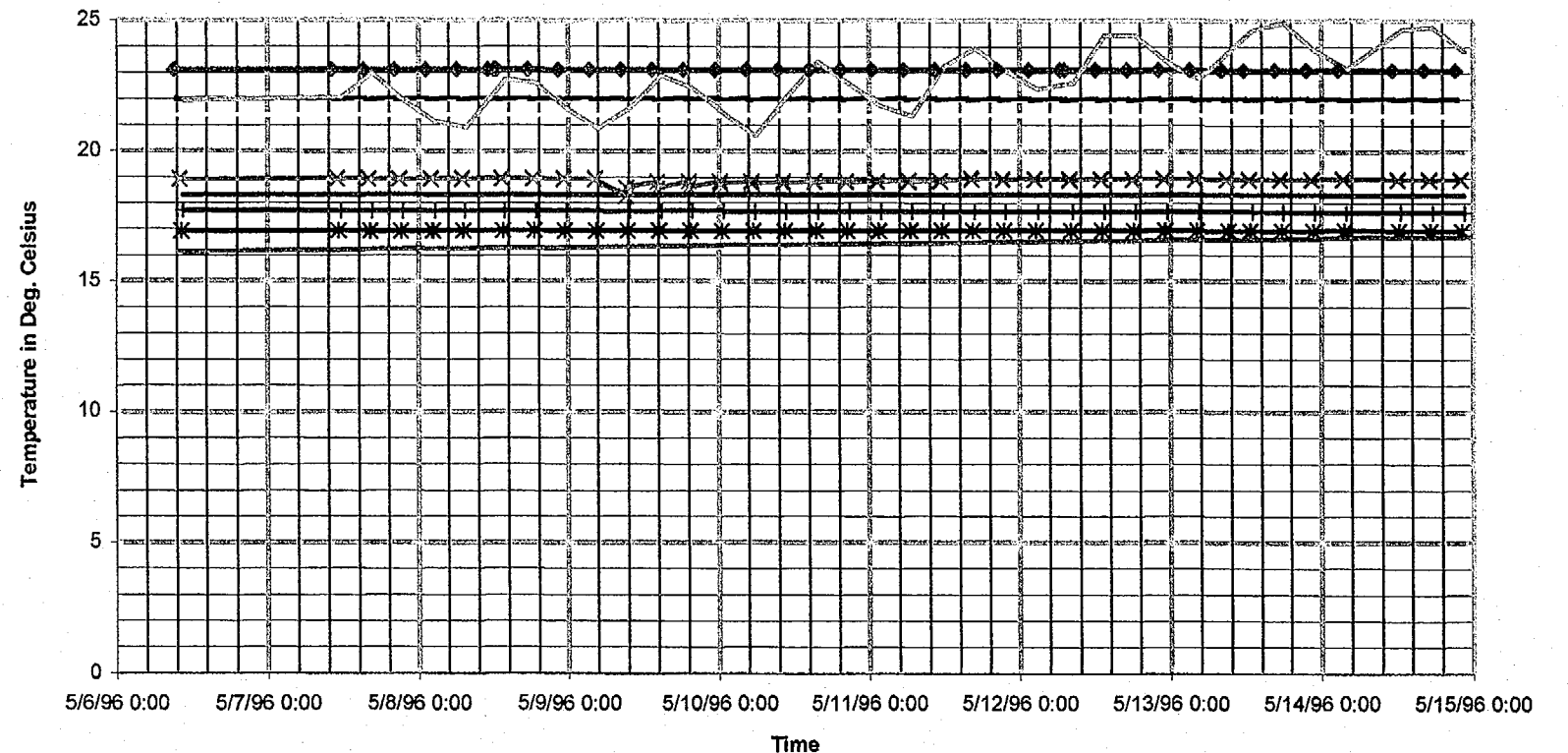
Temperature vs. time for NRG-6

August 24, 1996
P:\265\3D\user\proj\Nye\county\anar96\figures

Prepared for:
Nye County Nuclear Waste Repository Project Office

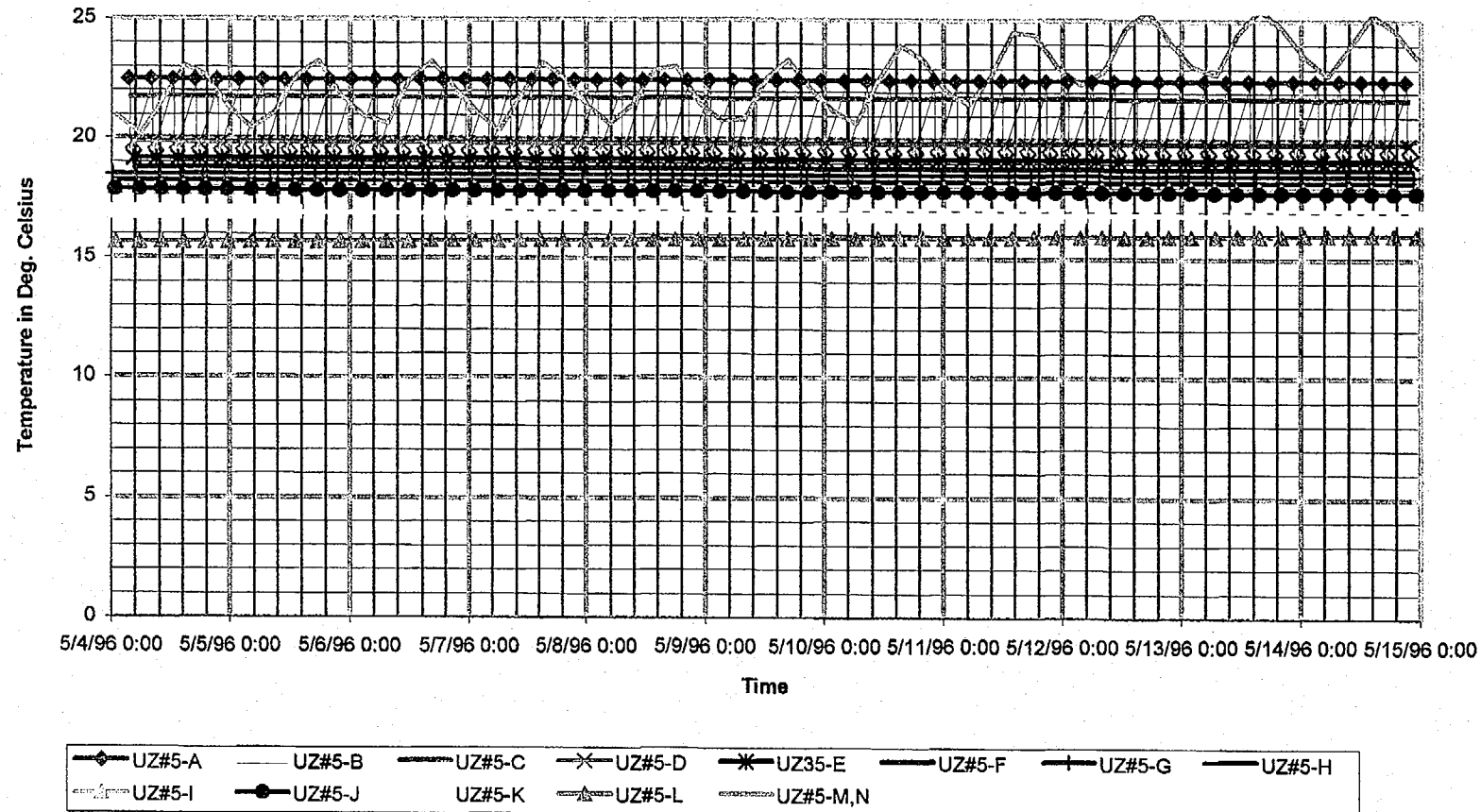
Prepared by:
Multimedea Environmental Technology, Inc.
Newport Beach, CA

May 4 - May 15 1996



Temperature vs. time for NRG-7a

May 4 - May 15 1996



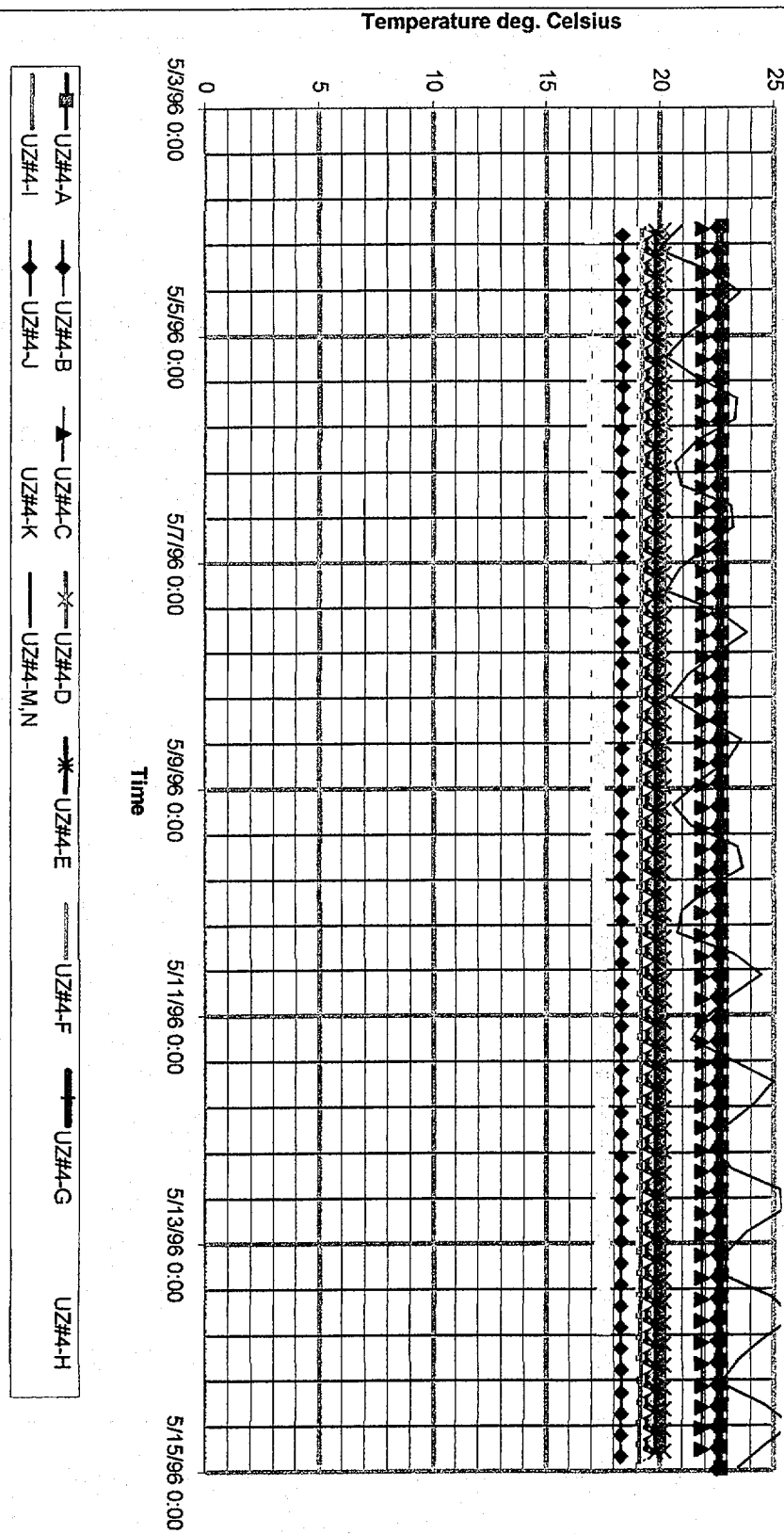
Temperature vs. time for UZ#5

August 24, 1996
P266:D:\user\projects\Nye county\annrep96\figures

Prepared for:
Nye County Nuclear Waste Repository Project Office

Prepared by:
Multimedia Environmental Technology, Inc.
Newport Beach, CA

May 4 - May 15 1996



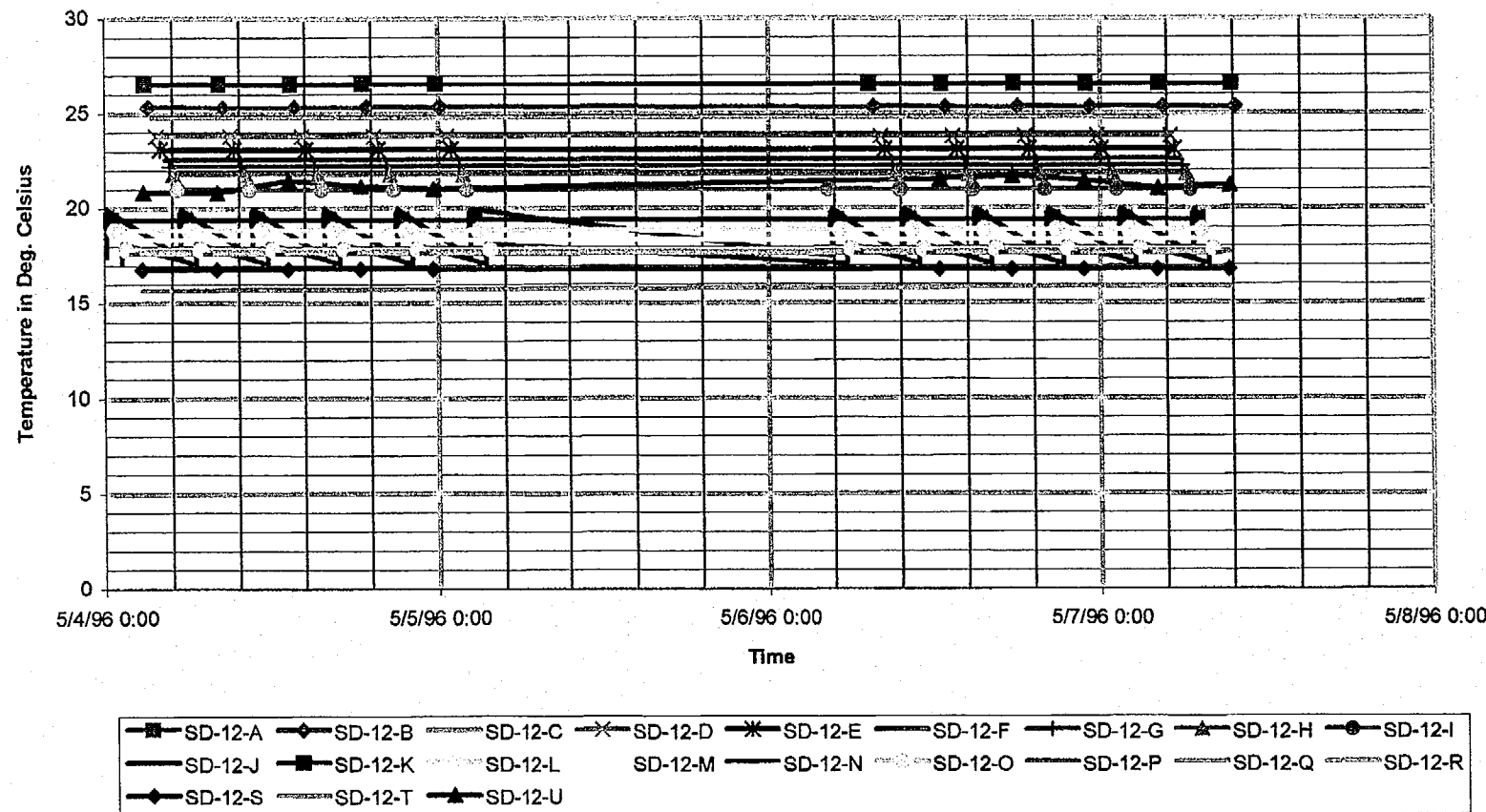
Temperature vs. time for UZ#4

August 24, 1996
Project: Nye County Waste Repository
Prepared for:

Nye County Nuclear Waste Repository Project Office

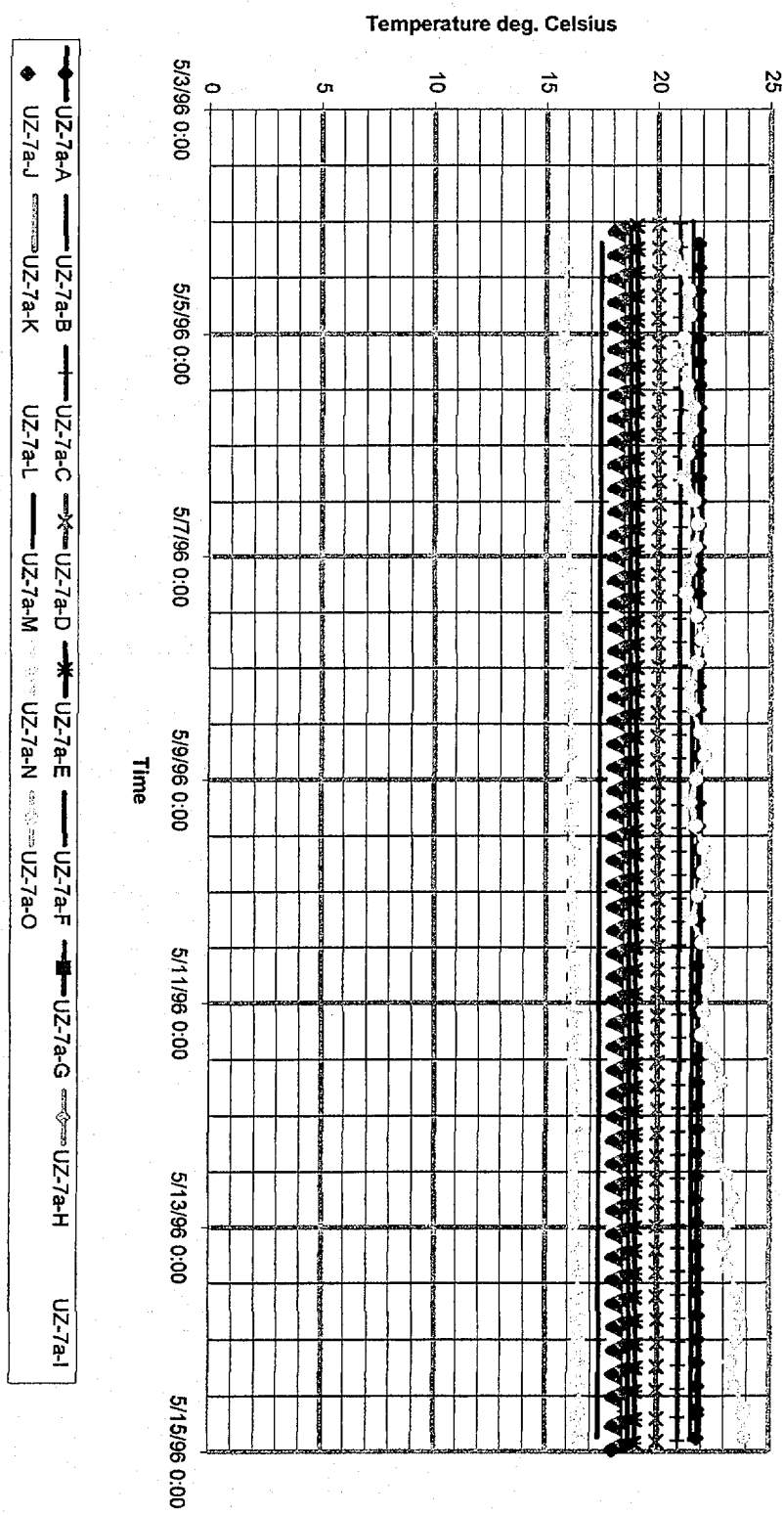
Prepared by:
Multimedia Environmental Technology, Inc.
Newport Beach, CA

May 4 - May 15 1996



Temperature vs. time for SD-12

May 4 - May 15 1996



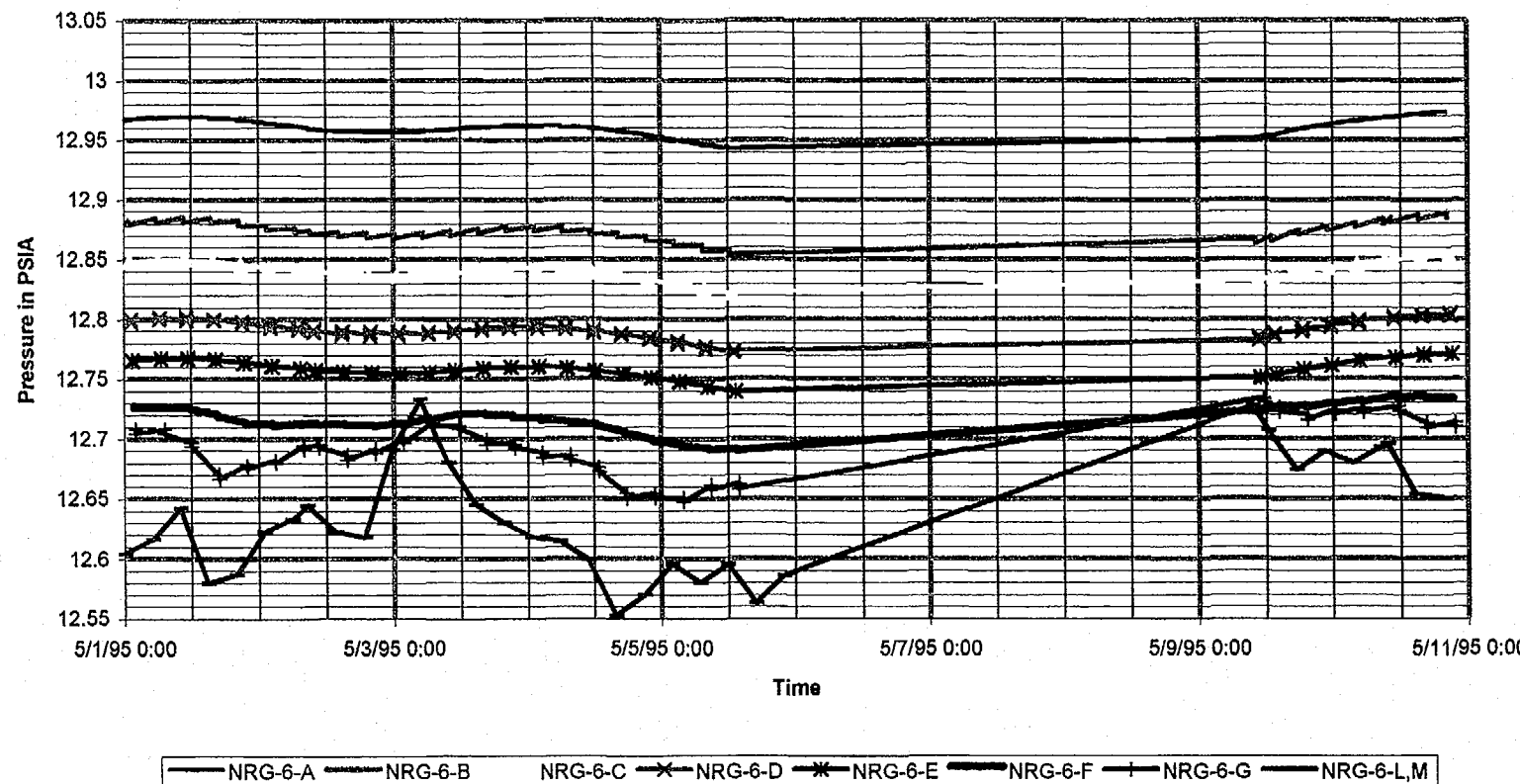
Temperature vs. time for UZ-7a

August 24, 1996
P26512; user\george\Nyecounty\unpub\96Figures

Prepared for:
Nye County Nuclear Waste Repository Project Office

Prepared by:
Multimedia Environmental Technology, Inc.
Newport Beach, CA

May 1 - May 10 1995



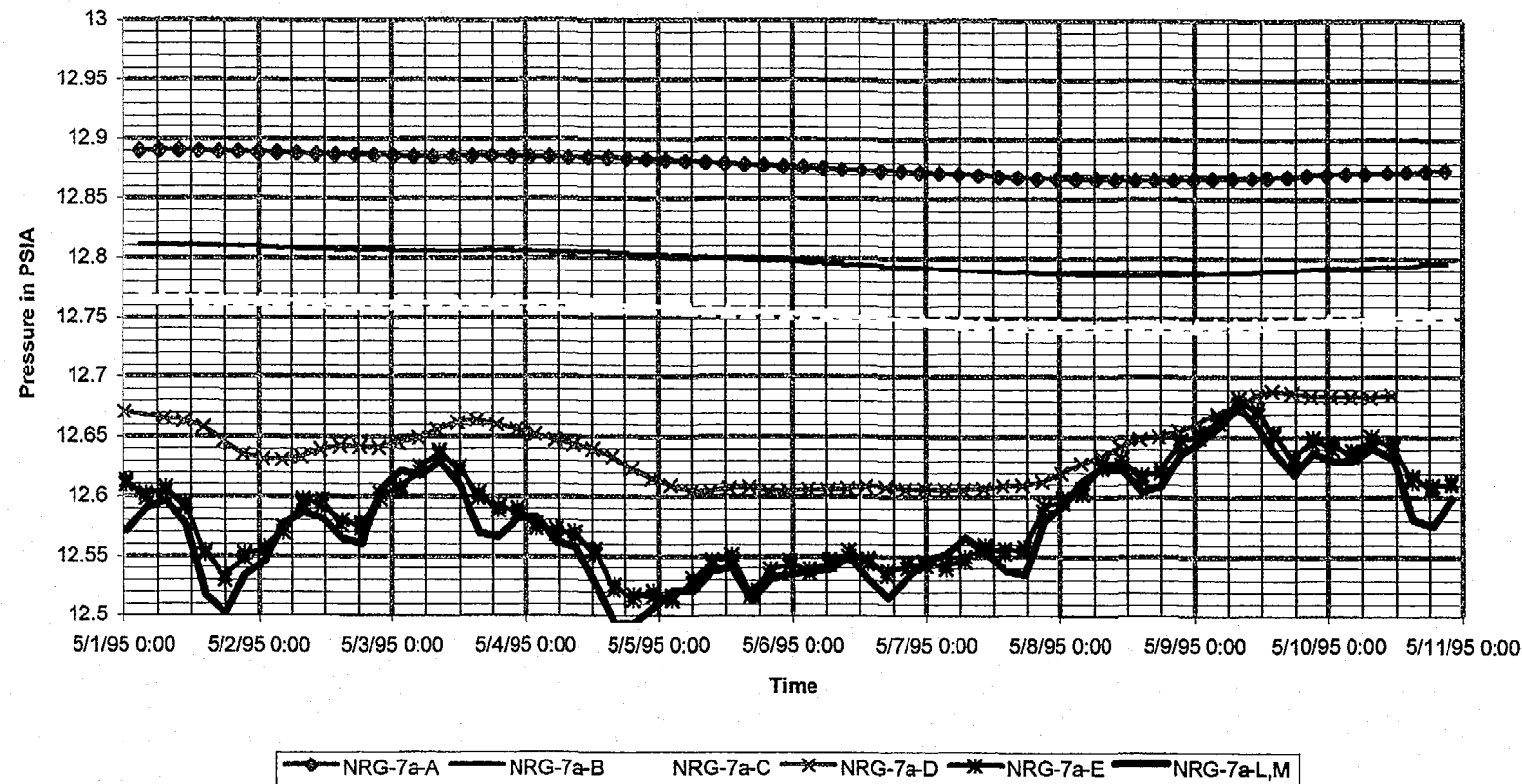
Absolute pressure vs. time for NRG-6

August 24, 1996
P266:D:\user\projects\Nyecounty\annrep96\figures

Prepared for:
Nye County Nuclear Waste Repository Project Office

Prepared by:
Multimedia Environmental Technology, Inc.
Newport Beach, CA

May 1 - May 10 1995



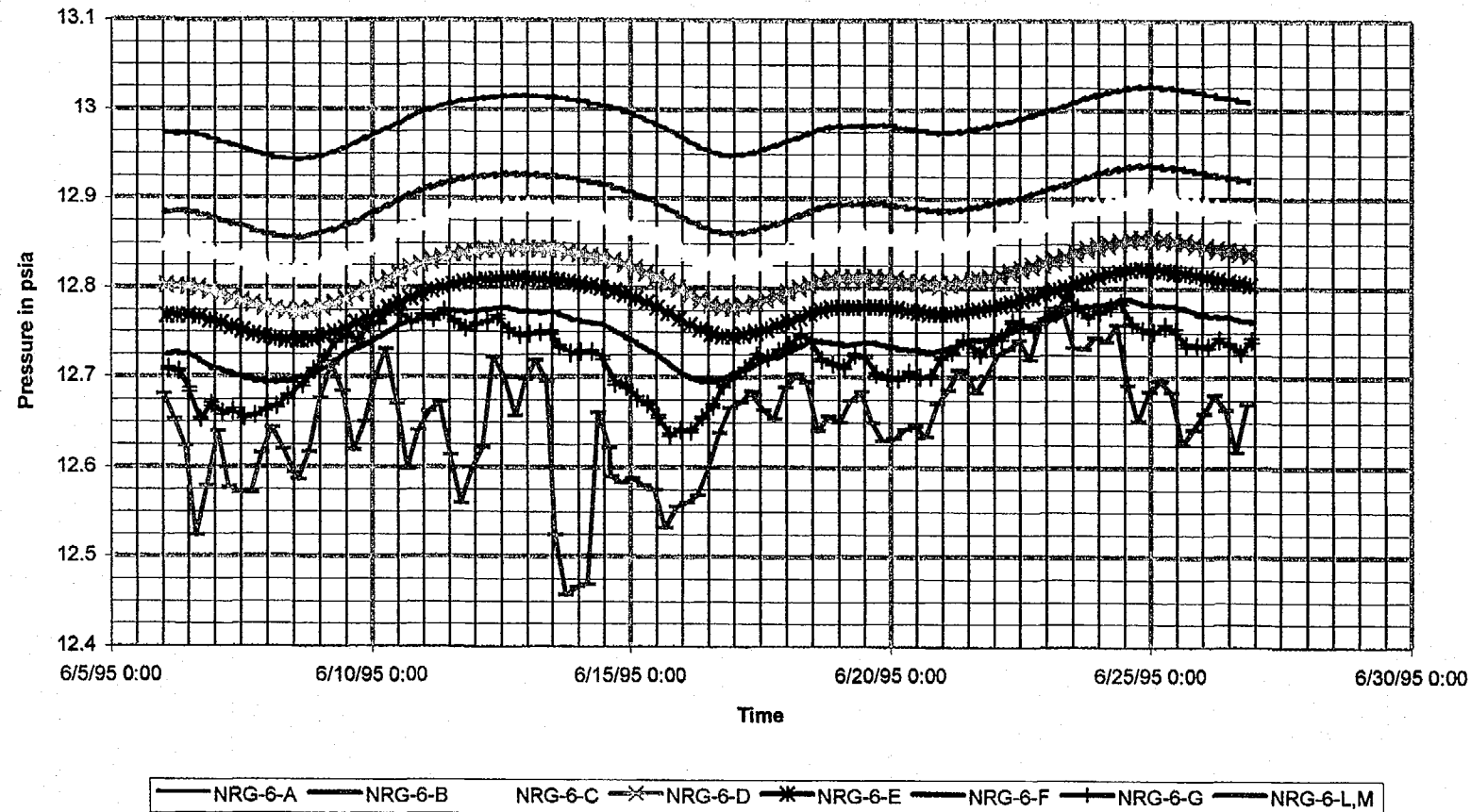
Absolute pressure vs. time for NRG-7a

August 24, 1996
P266:D:\user\projects\NyeCounty\ennrep96\figures

Prepared for:
Nye County Nuclear Waste Repository Project Office

Prepared by:
Multimedia Environmental Technology, Inc.
Newport Beach, CA

June 6 - June 26 1995



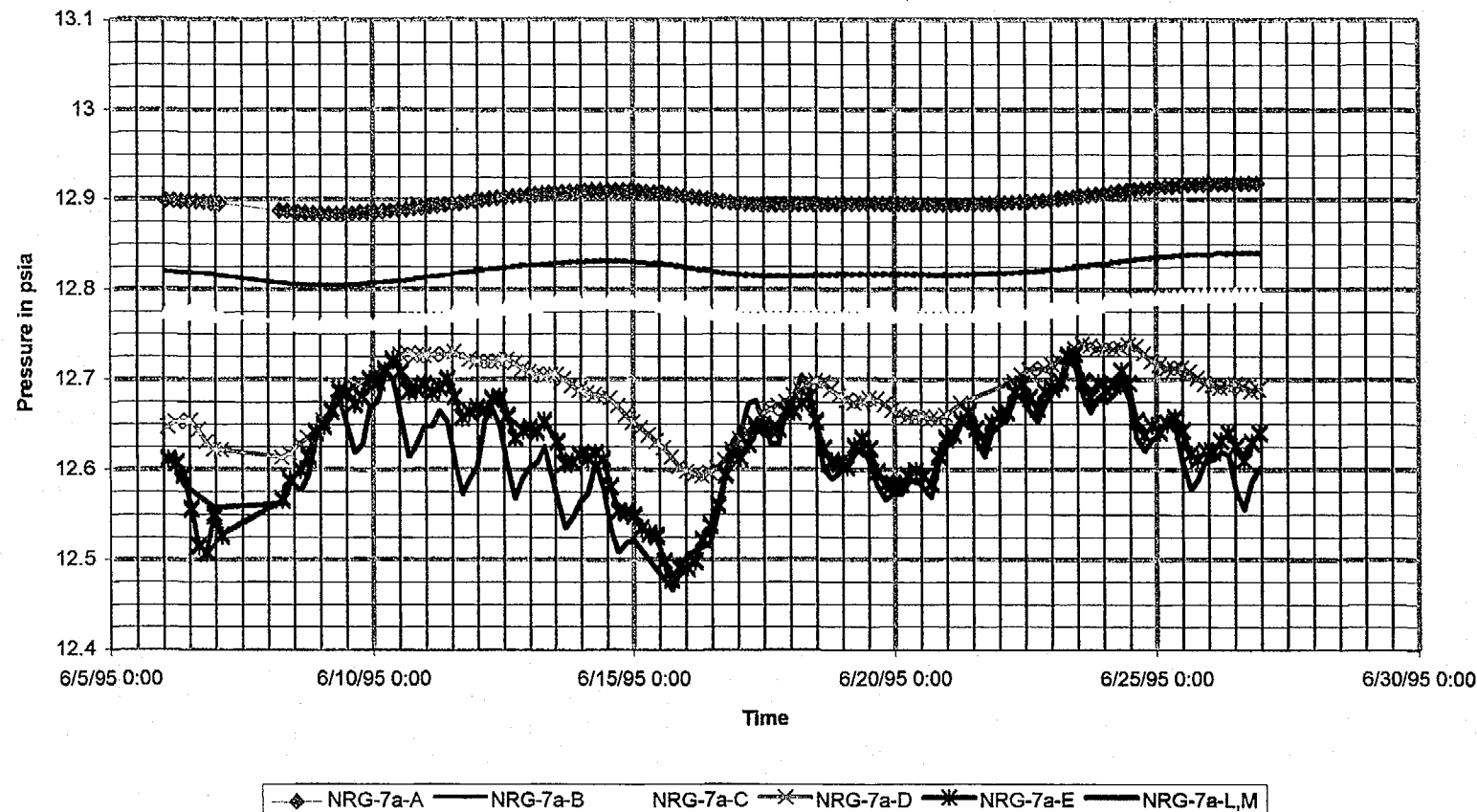
Absolute pressure vs. time for NRG-6

August 24, 1996
P266:D:\user\projects\NyeCounty\annrep96\figures

Prepared for:
Nye County Nuclear Waste Repository Project Office

Prepared by:
Multimedia Environmental Technology, Inc.
Newport Beach, CA

June 6 - June 26 1995



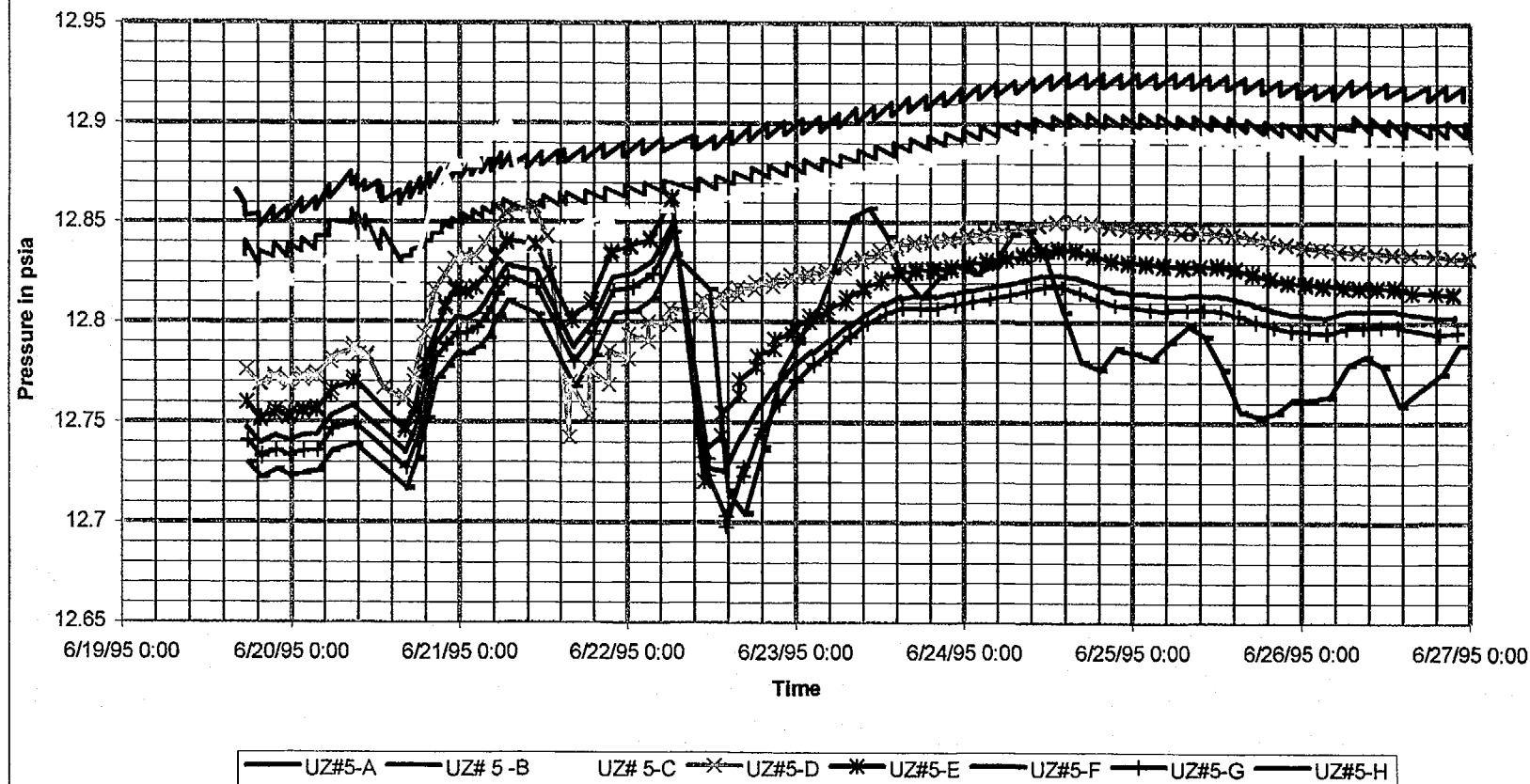
Absolute pressure vs. time for NRG-7a

August 24, 1996
P266:D:\user\projects\NyeCounty\annrep96\figures

Prepared for:
Nye County Nuclear Waste Repository Project Office

Prepared by:
Multimedia Environmental Technology, Inc.
Newport Beach, CA

June 6 - June 26 1995



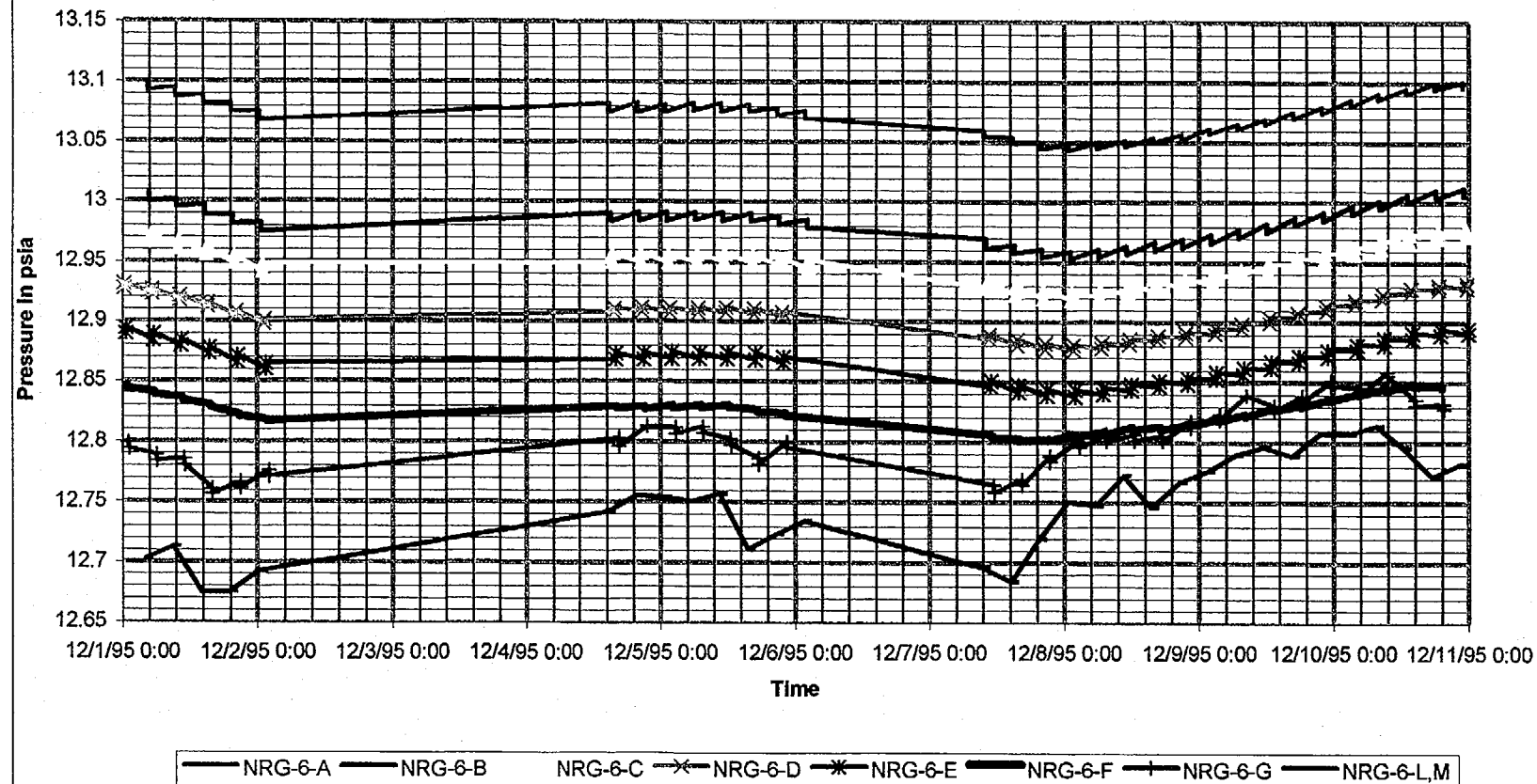
Absolute pressure vs. time for UZ#5

August 24, 1996
P266:D:\user\projects\NyeCounty\annrcp96\figures

Prepared for:
Nye County Nuclear Waste Repository Project Office

Prepared by:
Multimedia Environmental Technology, Inc.
Newport Beach, CA

December 1 - December 12 1995



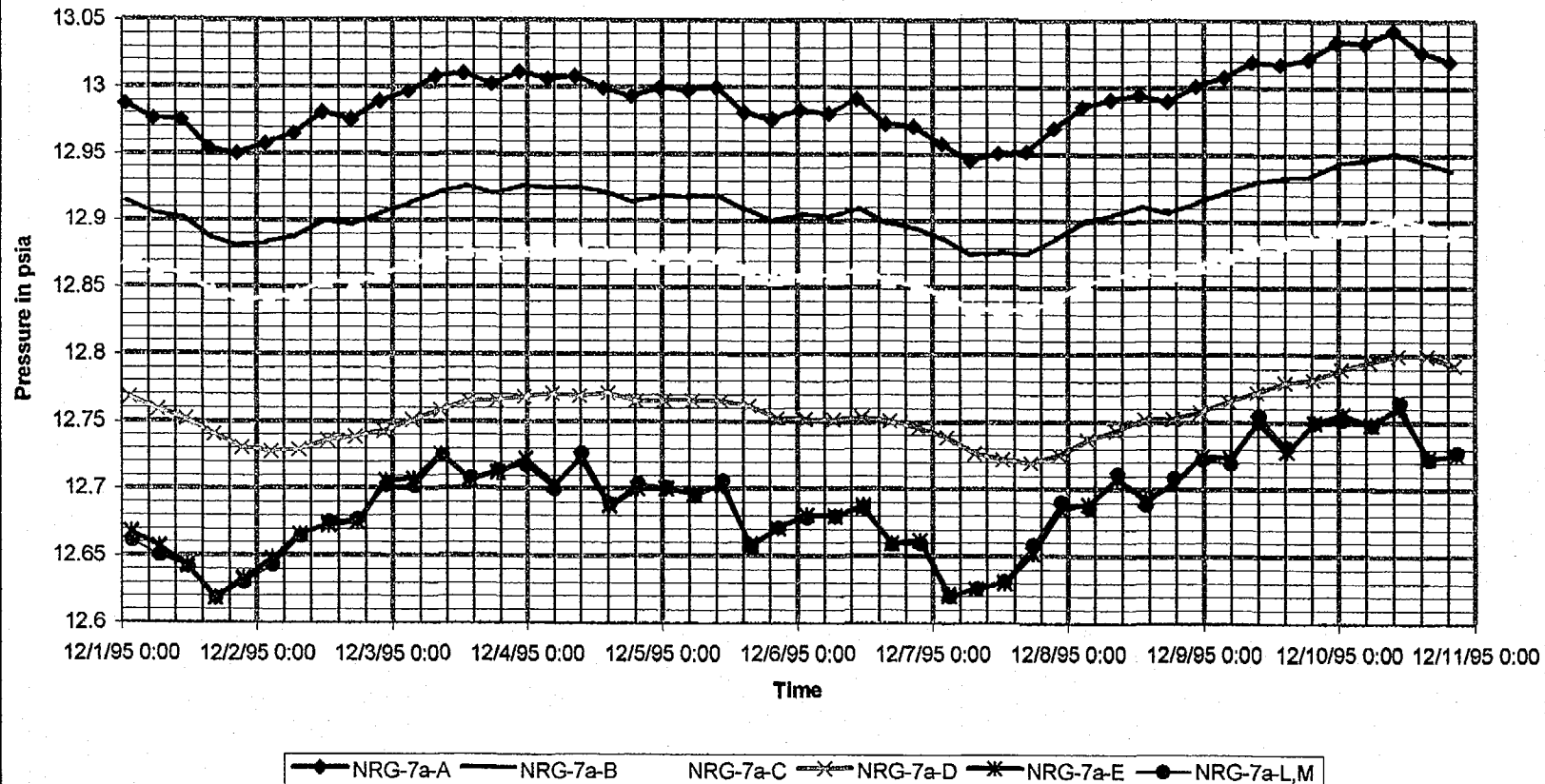
Absolute pressure vs. time for NRG-6

August 24, 1996
P266:D:\user\projects\NyeCounty\annrep96\figures

Prepared for:
Nye County Nuclear Waste Repository Project Office

Prepared by:
Multimedia Environmental Technology, Inc.
Newport Beach, CA

December 1 - December 12 1995



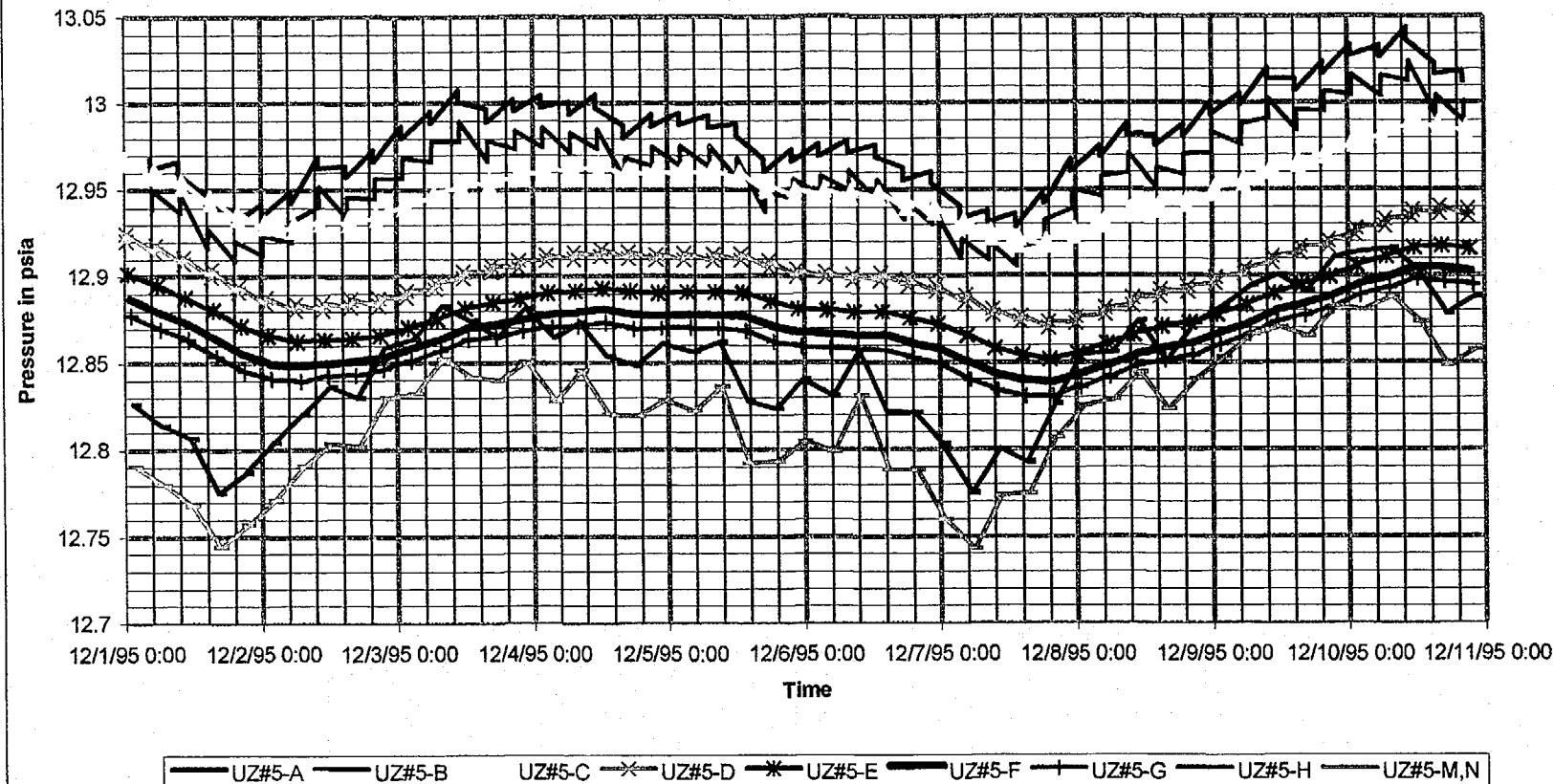
Absolute pressure vs. time for NRG-7a

August 24, 1996
P266:D:\user\projects\Nye county\anrep96\figures

Prepared for:
Nye County Nuclear Waste Repository Project Office

Prepared by:
Multimedia Environmental Technology, Inc.
Newport Beach, CA

December 1 - December 12 1995



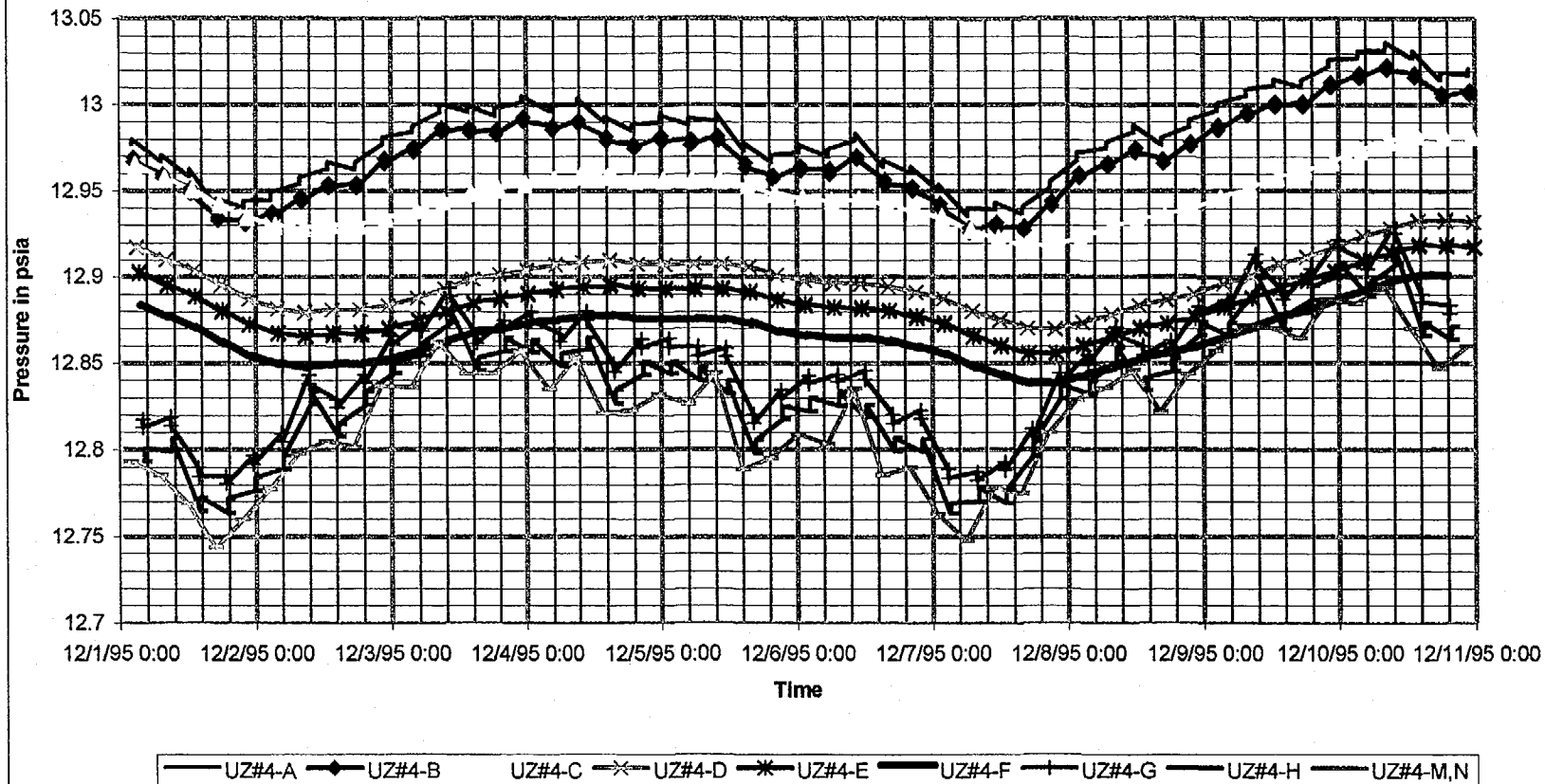
Absolute pressure vs. time for UZ#5

August 24, 1996
P266:D:\user\projects\Nye county\annrcp96\figures

Prepared for:
Nye County Nuclear Waste Repository Project Office

Prepared by:
Multimedia Environmental Technology, Inc.
Newport Beach, CA

December 1 - December 12 1995



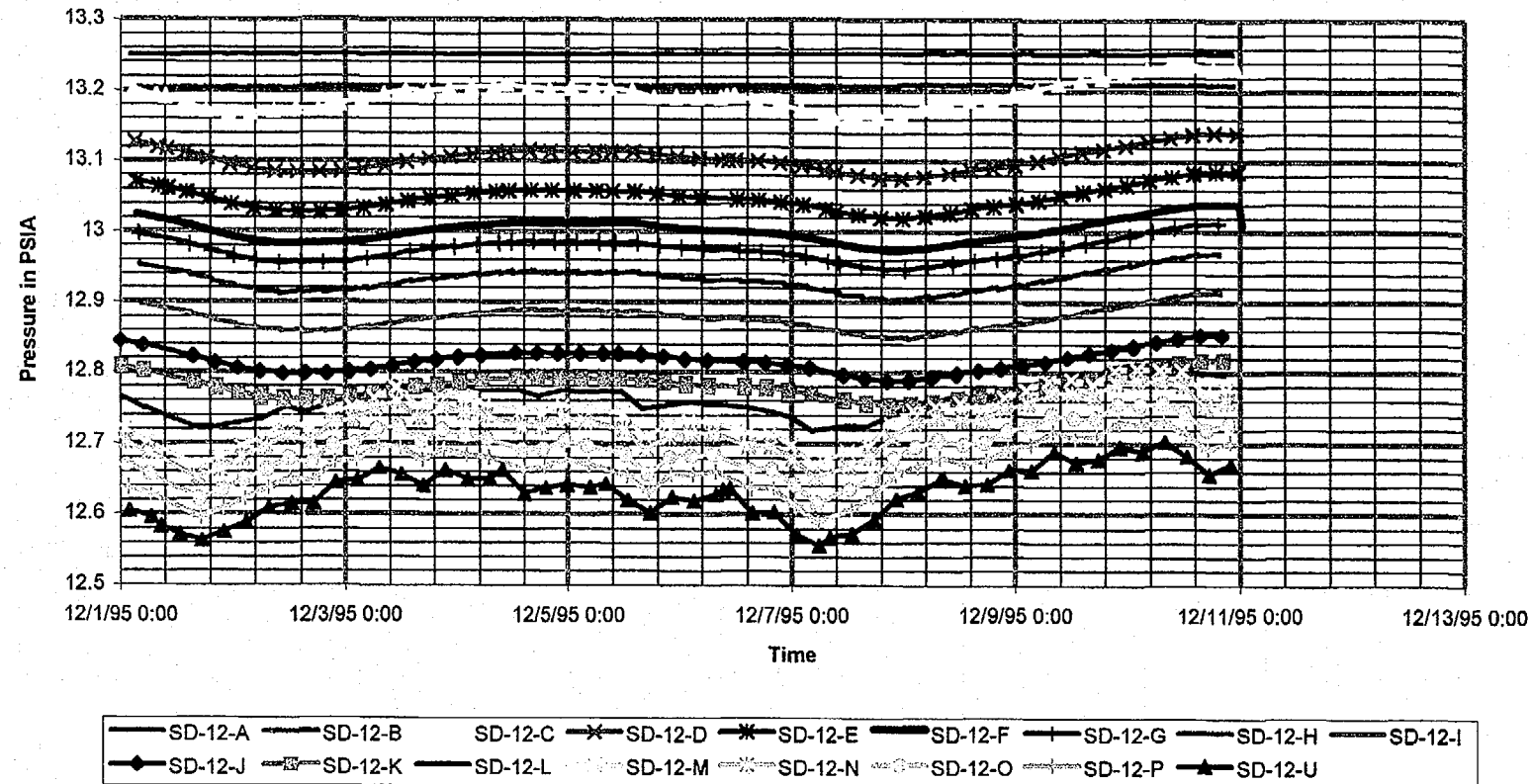
Absolute pressure vs. time for UZ#4

August 24, 1996
P266:D:\user\projects\Nye county\annrep96\figures

Prepared for:
Nye County Nuclear Waste Repository Project Office

Prepared by:
Multimedia Environmental Technology, Inc.
Newport Beach, CA

December 1 - December 12 1995



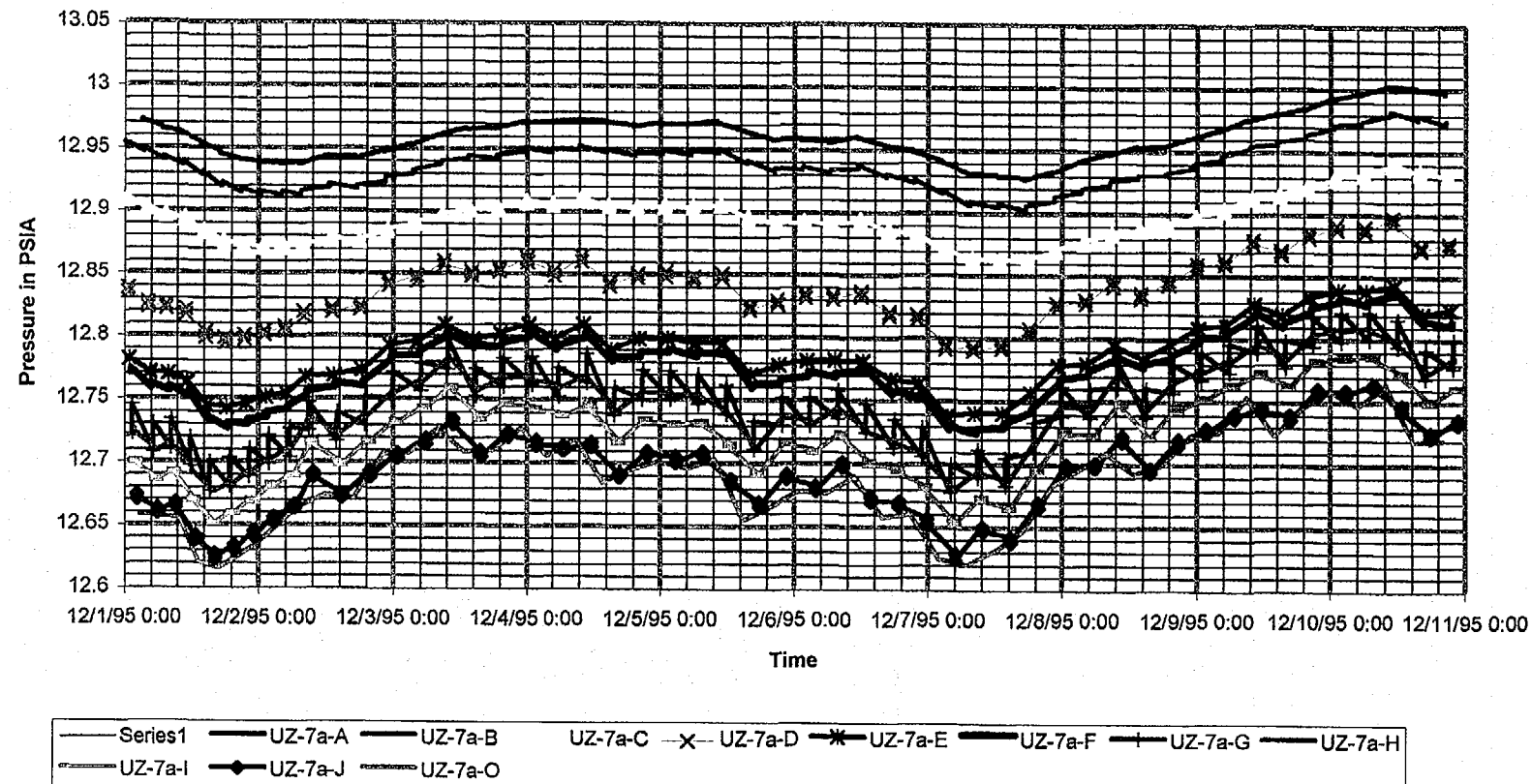
Absolute pressure vs. time for SD-12

August 24, 1996
P:\user\projects\NyeCounty\mineRep96\figures

Prepared for:
Nye County Nuclear Waste Repository Project Office

Prepared by:
Multimedia Environmental Technology, Inc.
Newport Beach, CA

December 1 - December 12 1995



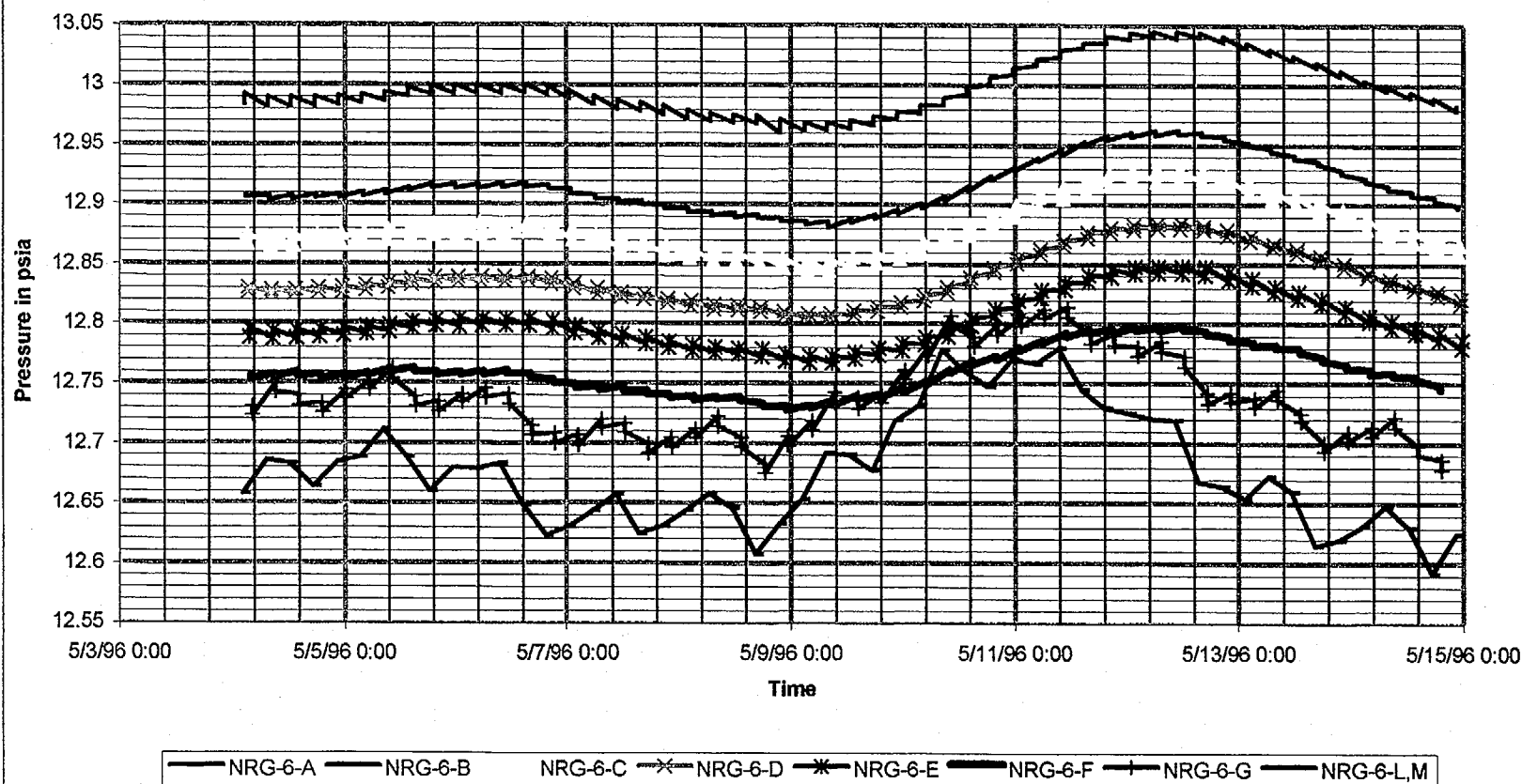
Absolute pressure vs. time for UZ-7a

August 24, 1996
P266:D:\user\projects\NyeCounty\annurep96\figures

Prepared for:
Nye County Nuclear Waste Repository Project Office

Prepared by:
Multimedia Environmental Technology, Inc.
Newport Beach, CA

May 4 - May 15 1996



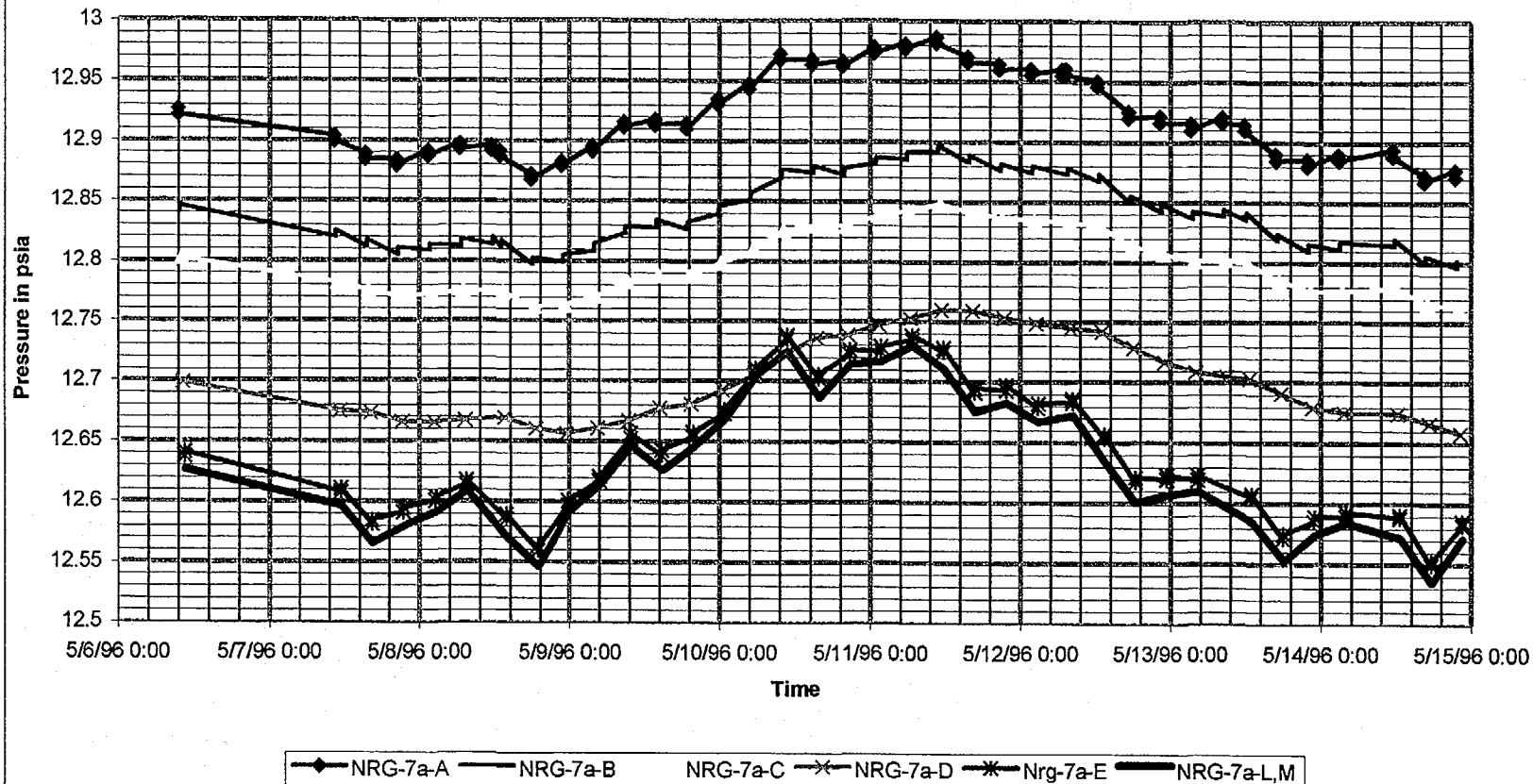
Absolute pressure vs. time for NRG-6

August 24, 1996
P266::D:\user\projects\Nyeoounty\annurep96\figures

Prepared for:
Nye County Nuclear Waste Repository Project Office

Prepared by:
Multimedia Environmental Technology, Inc.
Newport Beach, CA

May 4 - May 15 1996



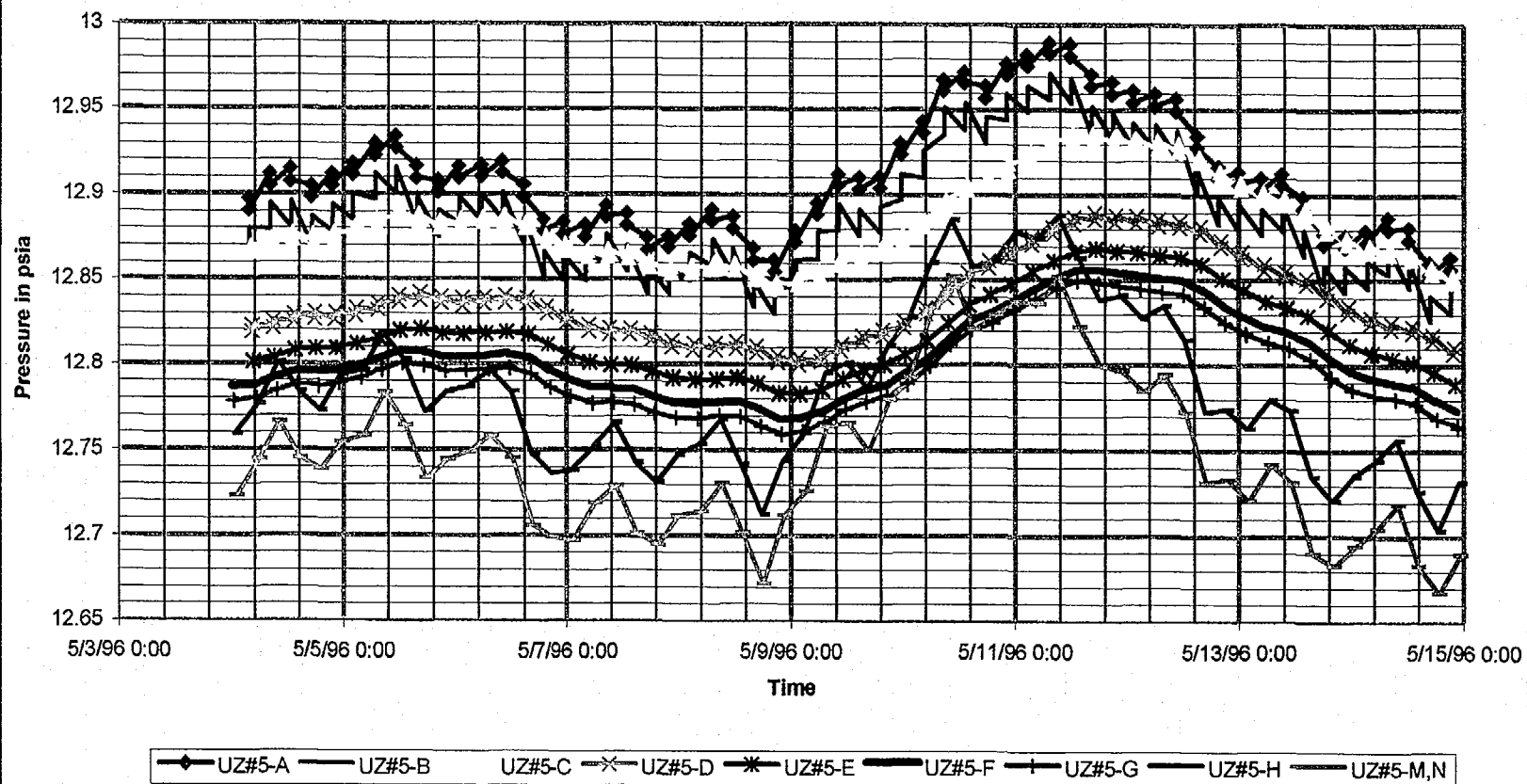
Absolute pressure vs. time for NRG-7a

August 24, 1996
P266::D:\user\projects\Nyeoounty\annrep96\figures

Prepared for:
Nye County Nuclear Waste Repository Project Office

Prepared by:
Multimedia Environmental Technology, Inc.
Newport Beach, CA

May 4 - May 15 1996



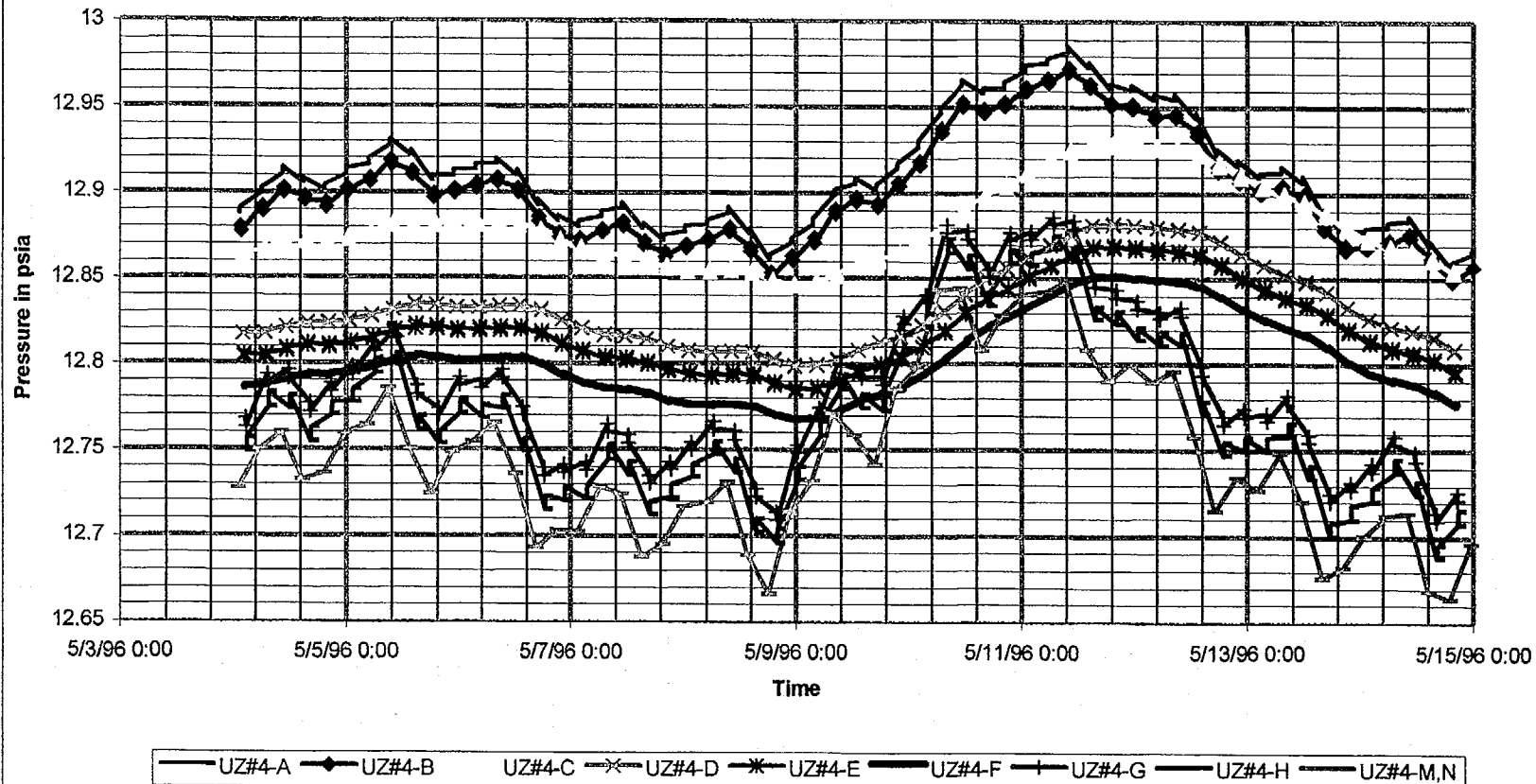
Absolute pressure vs. time for UZ#5

August 24, 1996
P266:D:\user\projects\Nye county\annrep96\figures

Prepared for:
Nye County Nuclear Waste Repository Project Office

Prepared by:
Multimedia Environmental Technology, Inc.
Newport Beach, CA

May 4 - May 15 1996



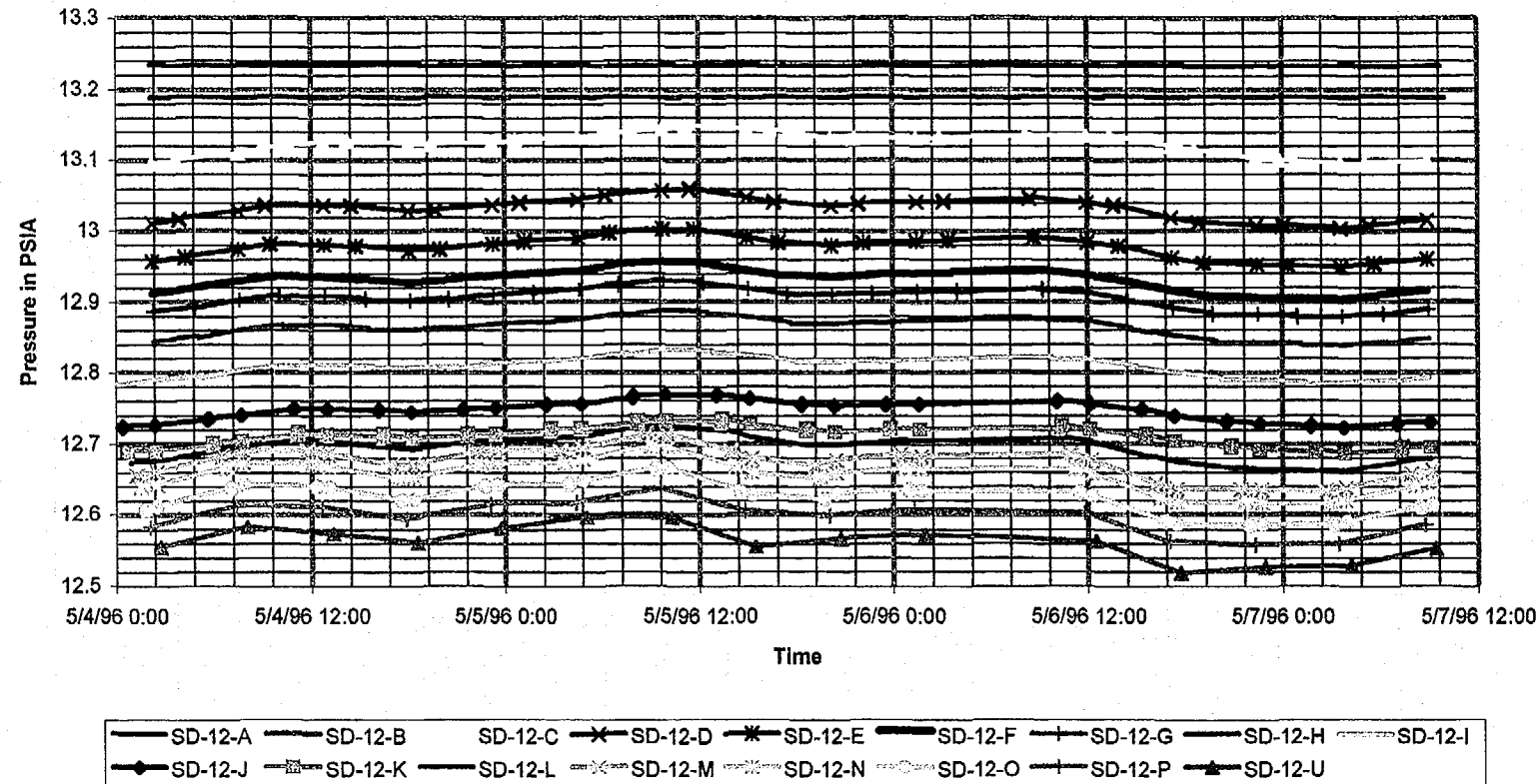
Absolute pressure vs. time for UZ#4

August 24, 1996
P266:D:\user\projects\NyeCounty\annrep96\figures

Prepared for:
Nye County Nuclear Waste Repository Project Office

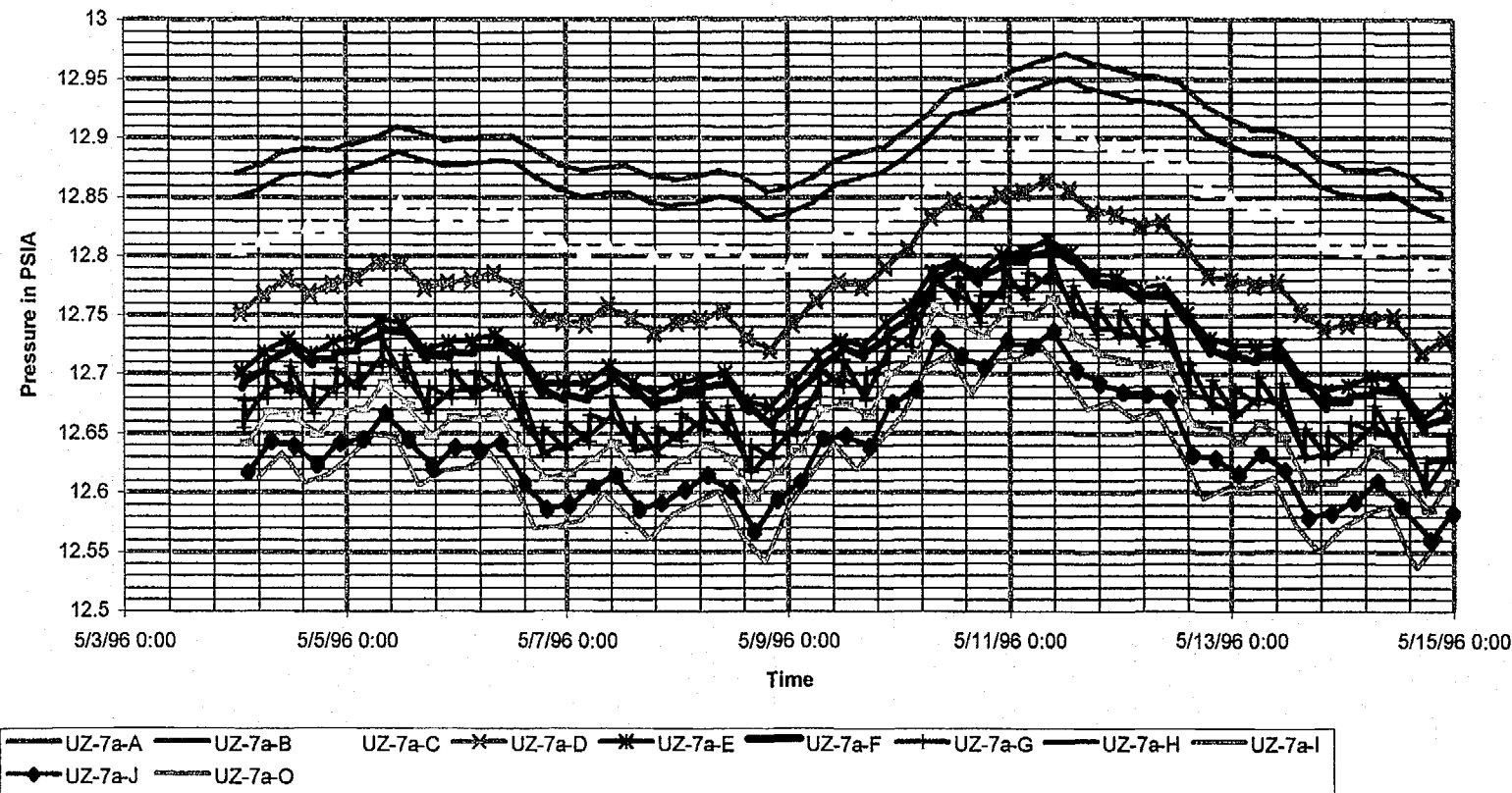
Prepared by:
Multimedia Environmental Technology, Inc.
Newport Beach, CA

May 4 - May 15 1996



Absolute pressure vs. time for SD-12

May 4 - May 15 1996



Absolute pressure vs. time for UZ-7a

August 24, 1996
P266:D:\user\projects\NyeCounty\annrep96\figures

Prepared for:
Nye County Nuclear Waste Repository Project Office

Prepared by:
Multimedia Environmental Technology, Inc.
Newport Beach, CA